

AD

USAAVLABS TECHNICAL REPORT 68-32

TILT PROP-ROTOR COMPOSITE RESEARCH AIRCRAFT

By

Kenneth G. Wernicke

November 1968

U. S. ARMY AVIATION MATERIEL LABORATORIES
FORT EUSTIS, VIRGINIA

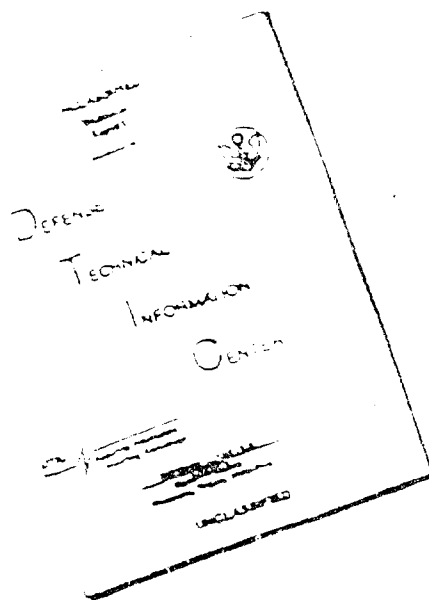
CONTRACT DA 44-177-AMC- 373(T)
BELL HELICOPTER COMPANY
FORT WORTH, TEXAS

*This document has been approved
for public release and sale; its
distribution is unlimited.*



AD 684317

DISCLAIMER NOTICE



THIS DOCUMENT IS BEST
QUALITY AVAILABLE. THE COPY
FURNISHED TO DTIC CONTAINED
A SIGNIFICANT NUMBER OF
PAGES WHICH DO NOT
REPRODUCE LEGIBLY.

REPRODUCED FROM
BEST AVAILABLE COPY

THIS DOCUMENT CONTAINED
BLANK PAGES THAT HAVE
BEEN DELETED

Disclaimers

The findings in this report are not to be construed as an official Department of the Army position unless so designated by other authorized documents.

When Government drawings, specifications, or other data are used for any purpose other than in connection with a definitely related Government procurement operation, the United States Government thereby incurs no responsibility nor any obligation whatsoever; and the fact that the Government may have formulated, furnished, or in any way supplied the said drawings, specifications, or other data is not to be regarded by implication or otherwise as in any manner licensing the holder or any other person or corporation, or conveying any rights or permission, to manufacture, use, or sell any patented invention that may in any way be related thereto.

Trade names cited in this report do not constitute an official endorsement or approval of the use of such commercial hardware or software.

Disposition Instructions

Destroy this report when no longer needed. Do not return it to the originator.

ACCESSION INFO		
CFSTI	WHITE SECTION <input checked="" type="checkbox"/>	
DOC	BUFF SECTION <input type="checkbox"/>	
UNANNOUNCED	<input type="checkbox"/>	
JUSTIFICATION		
BY		
DISTRIBUTION/AVAILABILITY CODES		
DIST.	AVAIL.	and/or SPECIAL
/		



DEPARTMENT OF THE ARMY
U. S. ARMY AVIATION MATERIEL LABORATORIES
FORT EUSTIS, VIRGINIA 23604

This report is a summary of the preliminary design study of a Tilt Prop-Rotor Composite Research Aircraft (CRA) concept. The general objective of the CRA was to combine into one research aircraft the efficient hovering characteristics of a helicopter and the high-speed cruise characteristics of fixed-wing aircraft.

This study presents one approach to meeting the above objective. This report is published for the dissemination of information and the stimulation of new ideas.

Task 1F163204D15704
Contract DA 44-177-AMC-373(T)
USAAVLABS Technical Report 68-32
November 1968

TILT PROP-ROTOR COMPOSITE RESEARCH AIRCRAFT

By

Kenneth G. Wernicke

Prepared by

Bell Helicopter Company
Fort Worth, Texas

for

U.S. ARMY AVIATION MATERIEL LABORATORIES
FORT EUSTIS, VIRGINIA

This document has been approved for public
release and sale; its distribution is unlimited.

SUMMARY

A preliminary design study for a composite research aircraft has been conducted in accordance with Contract DA 44-177-AMC-373(T). The primary objectives were to define the optimum design and to prepare a program for the follow-on development of a VTOL rotary-wing composite research aircraft embodying the low disc loading and low-speed maneuverability of the helicopter and the high speed and lift/drag ratios of fixed-wing aircraft. The D266 Composite Research Aircraft design that has resulted is based on the demonstrated and proved tilting-rotor concept.

This report discusses the selection of the design concept, summarizes the results of the preliminary design effort, describes the D266, and summarizes its performance and flight characteristics. It also shows how experience with the XV-3 permitted Bell Helicopter Company to focus the design study on the solution of known problems and on the refinement of the design to include operational features.

Design gross weight of the D266 is 23,000 pounds. Power is provided by two General Electric T64-GE-12 free-turbine engines. Design complexity is no greater than that of a twin-engine dual-rotor helicopter. All flight procedures are simple and straightforward and may be performed by one pilot. The cargo compartment, which exceeds the requirements, provides space for 24 troops.

The performance of the D266 substantially exceeds all the requirements in the schedule of the study contract. Maximum speed is 345 knots at sea level and 383 knots at 10,000 feet. Single-engine maximum speed is 259 knots at sea level and 288 knots at 10,000 feet. The hovering ceiling, out of ground effect on a 95°F day, is 11,050 feet with both engines operating and sea level with one engine operating. Maximum rate of climb in helicopter mode is 6160 feet per minute and in the fixed-wing mode, 6800 feet per minute.

The aircraft may be converted from helicopter to high-speed flight during maneuvering, climbing, descending, or level flight. The broad conversion airspeed corridor eliminates the requirement for scheduling conversion with airspeed and power requirements. There are no restrictions on the steep descents at low power settings which are typical of Army tactical flight operations. Flight tests of the XV-3 Convertiplane, conducted by Army, Air Force, and NASA pilots, demonstrated that in the event of total power failure, power-off reconversions could easily be made, permitting entry into autorotation from any mode of flight.

CONTENTS

	<u>Page</u>
SUMMARY	iii
LIST OF ILLUSTRATIONS	vii
LIST OF TABLES	xxii
LIST OF SYMBOLS	xxiv
I. DESIGN CONCEPT	1
A. INTRODUCTION	1
B. BACKGROUND	6
C. DESIGN DESCRIPTION AND SELECTION	16
II. PROPULSION DATA	57
A. POWERPLANT	57
B. POWER TRAIN	71
C. LIFT AND THRUST SYSTEMS	83
III. STRUCTURES	96
A. CRITERIA	96
B. STRUCTURAL DESIGN LOADS	110
C. FATIGUE CONSIDERATIONS	128
D. VERIFICATION OF MAJOR STRUCTURE	131
E. DYNAMIC ANALYSIS	145
IV. WEIGHT AND BALANCE	192
V. PERFORMANCE DATA	201
A. SUMMARY	201
B. LIFT AND DRAG	201
C. ENGINE PERFORMANCE	224
D. HOVERING	237
E. HELICOPTER FORWARD FLIGHT	245
F. CONVERSION	253
G. FIXED-WING FLIGHT	257
H. SINGLE-ENGINE AND POWER-OFF FLIGHT	289
VI. ELECTRICAL, HYDRAULIC, AND MECHANICAL SYSTEMS	305
A. FLIGHT CONTROLS	305
B. HYDRAULIC SYSTEM	323
C. FLIGHT ASSIST SYSTEMS	331
D. LANDING GEAR	341

	<u>Page</u>
E. CONVERSION SYSTEM	344
F. ELECTRICAL SYSTEM	347
G. HEATING, VENTILATION, AND ICE PROTECTION SYSTEM	349
VII. STABILITY AND CONTROL	353
A. INTRODUCTION	353
B. HELICOPTER FLIGHT	354
C. FIXED-WING FLIGHT	377
D. CONVERSION FLIGHT	395
VIII. COCKPIT ARRANGEMENT	416
A. SEATS	416
B. FLIGHT CONTROLS	416
C. POWER-MANAGEMENT CONTROLS	419
D. SUPPORT SYSTEM CONTROLS	421
E. ENVIRONMENTAL CONTROLS	422
F. INSTRUMENTS	422
G. WARNING AND CAUTION SYSTEMS	424
H. VISIBILITY	425
IX. EMERGENCY SYSTEMS AND PROCEDURES	427
A. POWERPLANT	427
B. FUEL SYSTEM	429
C. FLIGHT CONTROLS	430
D. EGRESS	432
E. CRASH PROTECTION	433
REFERENCES	434
APPENDIX, DRAWINGS	437
DISTRIBUTION	449

ILLUSTRATIONS

<u>Figure</u>		<u>Page</u>
1	D266 Composite Research Aircraft	2
2	D266 - Front and Rear Views	3
3	D266 - Conversion Procedure	4
4	XV-3 Tilt-Rotor Aircraft	7
5	Various BHC Multibladed Rotor Systems	10
6	Examples of VTOL Composite Aircraft Configurations Examined During Preliminary Studies	12
7	Six Low-Disc-Loading VTOL Designs Resulting from BHC Comparative Design Study Program	13
8	Variation of Wing Weight With Thickness	27
9	Effect of Wing Thickness on Range	27
10	Wing-Pylon Geometry	28
11	Effect of Twist on Hovering Power Required	41
12	Effect of Solidity on Power Required to Hover	43
13	Effect of Twist on Propeller Efficiency, Tip Speed of 400 Ft/Sec	44
14	Effect of Twist on Propeller Efficiency, Tip Speed of 600 Ft/Sec	45
15	Effect of Solidity on Propeller Efficiency in Forward Flight	47
16	Swashplate-Pylon Coupling Schematic	51
17	Effect of Swashplate-Pylon Coupling Ratio	53
18	Dynamic Stability Model	54
19	Rotor-Pylon Stability at Sea Level	56

<u>Figure</u>		<u>Page</u>
20	Engine Mounting	61
21	Fuel System Schematic	62
22	Engine Lubrication Schematic	64
23	Power-Management Schematic	66
24	Power Control Shaft Schedule	67
25	Engine Cooling Provisions	69
26	Exhaust Wake Temperature Profile	70
27	Drive System Schematic	72
28	Engine Gearbox Oil System	75
29	Main Transmission Oil System	77
30	Rotor Figure of Merit	87
31	Propeller Efficiency 198 RPM, Sea Level	89
32	Propeller Efficiency 248 RPM, Sea Level	90
33	Propeller Efficiency 297 RPM, Sea Level	91
34	Collective Pitch Range, Helicopter Mode	92
35	Collective Pitch Range, Fixed-Wing Mode	93
36	D266 Conversion Corridor	99
37	D266 V-n Diagram (Sea Level) Design Gross Weight = 23,000 Lb	100
38	D266 V-n Diagram (Sea Level) Minimum Flying Weight = 16,710 Lb	101
39	Ultimate Fuselage Shears	111
40	Ultimate Fuselage Bending Moments	112
41	Ultimate Fuselage Torsion, Gust on Vertical Tail	113

<u>Figure</u>		<u>Page</u>
42	Wing Ultimate Vertical Shear (V_z)	115
43	Wing Ultimate Spanwise Bending Moment (M_x) Referred to Direction of Elastic Axis	116
44	Wing Ultimate Torsion About Rear Spar (M_y) Referred to Direction of Elastic Axis	117
45	Wing-Pylon Intersection Notation and Geometry	119
46	Landing-Gear Notation	121
47	Rotor Blade Limit Static Beamwise and Chordwise Bending Moment Distribution for 3g, 372-RPM Helicopter Maneuver	122
48	Limit Centrifugal Force Distribution for 3g, 372-RPM Helicopter Maneuver	123
49	Rotor Blade Oscillatory Beamwise Bending Moment Distribution for 150 Knots and Various Mast Angles	125
50	Pylon Loads - Fixed-Wing Flight	126
51	Pylon Loads - Helicopter Flight	127
52	Wing Total Upper Surface Skin Gage	132
53	Wing Ultimate Compression Stress and Allowable Compression Stress	133
54	Wing Ultimate Front Spar Shear Flows and Allowable	134
55	Wing Ultimate Rear Spar Shear Flows and Allowable	135
56	Cross Section of Rotor Blade at 50- Percent Span	136
57	Beamwise and Chordwise EI Distribution	140
58	Modified Goodman Diagram of Allowable Stress in an Aluminum Main Rotor Blade Basic Section Outboard of Doublers	141

<u>Figure</u>		<u>Page</u>
59	Blade Applied and Allowable Oscillatory Beam-Bending Moment Distributions for 150 Knots and 30° Mast Angle	143
60	Rotor Mean Beam-Bending Moment and Centrifugal Force Distributions	144
61	Airframe Natural Frequencies, Helicopter Mode	147
62	Airframe Natural Frequencies, Fixed-Wing Mode	148
63	Helicopter-Mode Crew-Compartment Response to 1000-Pound Vertical Shear at Hub	149
64	3/Rev Crew-Compartment Vertical Vibration Level	150
65	Gust Response Time History 196-Knot Airspeed - 66-FPS Sharp-Edged Gust	152
66	Time History of Encounter With Horizontal Gust at 350 Knots	153
67	Jump-Takeoff Time History	154
68	Steady-State Flapping, Fixed-Wing Flight	156
69	350-Knot Pullup Time History	157
70	Rotor Natural Frequencies - Collective Mode	158
71	Rotor Natural Frequencies - Cyclic Mode	159
72	Blade Bending Moments - Helicopter Mode, 90 Knots	162
73	Blade Beam-Bending Moments - Helicopter Mode, 150 Knots	163
74	Blade Chord-Bending Moments - Helicopter Mode, 150 Knots	164
75	Blade Beam-Bending Moments - Fixed-Wing Mode	165

<u>Figure</u>		<u>Page</u>
76	Blade Chord-Bending Moments - Fixed-Wing Mode	166
77	Blade Bending Moments, 250-Knot Pullup	167
78	Blade Bending Moment Time History, 66-FPS Gust	168
79	Aeroelastic Analytical Models	171
80	$dH/d\dot{\alpha}$ Versus Airspeed	172
81	$dH/d\dot{\alpha}$ Versus Frequency	173
82	Symmetric Free-Free Wing Flutter, One-Half Fuel	174
83	Wing Asymmetric Flutter, One-Half Fuel	175
84	Origin of the Destabilizing H-Force Moment	177
85	Swashplate-Pylon Coupling	179
86	Illustration of Swashplate Retardation and δ_3	180
87	Model Correlation With Calculated Damping	182
88	Model Correlation With Calculated Frequency	183
89	Rotor-Pylon Stability, Sea Level	185
90	Rotor-Pylon Stability, 15,000 Feet	186
91	Rotor-Pylon Stability, 30,000 Feet	187
92	Relative Effect of Precone on Blade Motion Stability	189
93	Blade Motion Stability, Fixed-Wing Level Flight	191
94	Center-of-Gravity Limits	193
95	Synthesized Rotor Airfoil Lift Data, 7% to 20% Radius	204

<u>Figure</u>		<u>Page</u>
96	Synthesized Rotor Airfoil Drag Data, 7% to 20% Radius	205
97	Synthesized Rotor Airfoil Lift Data, 20% to 50% Radius	206
98	Synthesized Rotor Airfoil Drag Data, 20% to 50% Radius	207
99	Synthesized Rotor Airfoil Lift Data, 50% to 100% Radius	208
100	Synthesized Rotor Airfoil Drag Data, 50% to 100% Radius	209
101	Rotor Airfoil Data Comparison	211
102	Lift Coefficient Versus Angle of Attack	212
103	Lift Distribution Between Rotor and Airframe in Level Flight, Helicopter Configuration	214
104	Lift Distribution Between Rotor and Airframe in Autorotation	215
105	Lift Distribution Between Rotor and Airframe in a 2g Pullup, Helicopter Configuration	216
106	Lift Distribution Between Rotor and Airframe During Conversion	217
107	Drag Coefficient Versus Angle of Attack	223
108	Lift Coefficient Versus Drag Coefficient	223
109	Vertical-Flight Power Available Per Engine, 16,600 Engine RPM, Twin-Engine Operation	225
110	Rotor Shaft Horsepower Available Per Engine, Military Rated Power, 16,600 Engine RPM, Twin-Engine Operation	226
111	Rotor Shaft Horsepower Available Per Engine, Normal Rated Power, 16,600 Engine RPM, Twin-Engine Operation	227

<u>Figure</u>		<u>Page</u>
112	Rotor Shaft Horsepower Available Per Engine, Military Rated Power, 12,100 Engine RPM, Twin-Engine Operation	228
113	Rotor Shaft Horsepower Available Per Engine, Normal Rated Power, 12,100 Engine RPM, Twin- Engine Operation	229
114	Rotor Shaft Horsepower Available Per Engine, Military Rated Power, 10,075 Engine RPM, Twin-Engine Operation	230
115	Rotor Shaft Horsepower Available Per Engine, Normal Rated Power, 10,075 Engine RPM, Twin- Engine Operation	231
116	Rotor Shaft Horsepower Available Per Engine, Military Rated Power, 8050 Engine RPM, Twin- Engine Operation	232
117	Rotor Shaft Horsepower Available Per Engine, Normal Rated Power, 8050 Engine RPM, Twin- Engine Operation	233
118	Fuel Flow Per Engine, Sea Level, Twin-Engine Operation	234
119	Fuel Flow Per Engine, 10,000 Feet, Twin- Engine Operation	235
120	Fuel Flow Per Engine, 25,000 Feet, Twin- Engine Operation	236
121	Net Jet Thrust Per Engine, Sea Level, Twin- Engine Operation	238
122	Net Jet Thrust Per Engine, 10,000 Feet, Twin- Engine Operation	239
123	Net Jet Thrust Per Engine, 25,000 Feet, Twin- Engine Operation	240
124	Nondimensional Hovering Power Required	241
125	Rotor Figure of Merit	242
126	Dimensional Power Required to Hover	243

<u>Figure</u>		<u>Page</u>
127	Hovering Ceiling	244
128	Excess Rotor Shaft Horsepower Available for Vertical Climb	246
129	Helicopter Power Required, Flaps Up	247
130	Helicopter Power Required, Flaps Down	248
131	Maximum Rate of Climb, Military Rated Power, Single-Engine Operation, Helicopter Con- figuration	249
132	Maximum Rate of Climb, Military Rated Power, Twin-Engine Operation, Helicopter Configu- ration	250
133	Maximum Rate of Climb, Normal Rated Power, Single-Engine Operation, Helicopter Con- figuration	251
134	Maximum Rate of Climb, Normal Rated Power, Twin-Engine Operation, Helicopter Configu- ration	252
135	Maximum Speed, Helicopter Configuration	254
136	Conversion Power Required	255
137	Conversion Corridor	256
138	Propeller Efficiency, 297 RPM, Sea Level	258
139	Propeller Efficiency, 248 RPM, Sea Level	259
140	Propeller Efficiency, 198 RPM, Sea Level	260
141	Propeller Efficiency, 297 RPM, 10,000 Feet	261
142	Propeller Efficiency, 248 RPM, 10,000 Feet	262
143	Propeller Efficiency, 198 RPM, 10,000 Feet	263
144	Propeller Efficiency, 297 RPM, 25,000 Feet	264
145	Propeller Efficiency, 248 RPM, 25,000 Feet	265
146	Propeller Efficiency, 198 RPM, 25,000 Feet	266

<u>Figure</u>		<u>Page</u>
147	Propeller Efficiency Correlation	267
148	Thrust Horsepower Required, Sea Level	268
149	Thrust Horsepower Required, 10,000 Feet	269
150	Thrust Horsepower Required, 25,000 Feet	270
151	Net Jet Thrust Horsepower Versus Thrust Horsepower, Sea Level, Twin-Engine Operation	272
152	Net Jet Thrust Horsepower Versus Thrust Horsepower, 10,000 Feet, Twin-Engine Operation	273
153	Net Jet Thrust Horsepower Versus Thrust Horsepower, 25,000 Feet, Twin-Engine Operation	274
154	Rotor Shaft Horsepower Versus Total Thrust Horsepower, Sea Level	275
155	Rotor Shaft Horsepower Versus Total Thrust Horsepower, 10,000 Feet	276
156	Rotor Shaft Horsepower Versus Total Thrust Horsepower, 25,000 Feet	277
157	Engine Shaft Horsepower Required	278
158	Overall Lift/Drag Ratio	279
159	Maximum True Airspeed, Fixed-Wing Configu- ration	281
160	Specific Range, Sea Level, Single-Engine Operation	282
161	Specific Range, Sea Level, Twin-Engine Operation	283
162	Specific Range, 10,000 Feet, Single-Engine Operation	284
163	Specific Range, 10,000 Feet, Twin-Engine Operation	285

<u>Figure</u>		<u>Page</u>
164	Specific Range, 25,000 Feet, Single-Engine Operation	286
165	Specific Range, 25,000 Feet, Twin-Engine Operation	287
166	Payload Range	288
167	Maximum Rate of Climb, Military Rated Power, Single-Engine Operation, Fixed-Wing Configuration	290
168	Maximum Rate of Climb, Military Rated Power, Twin-Engine Operation, Fixed-Wing Configuration	291
169	Maximum Rate of Climb, Normal Rated Power, Single-Engine Operation, Fixed-Wing Configuration	292
170	Maximum Rate of Climb, Normal Rated Power, Twin-Engine Operation, Fixed-Wing Configuration	293
171	Rate of Descent in Autorotation	294
172	Single-Engine Flight Capability, Helicopter Configuration	295
173	Single-Engine Flight Capability, Fixed-Wing Configuration	296
174	Time History of Power Failure in Hover, 8-Foot Wheel Height	298
175	Time Histories of Power-Off Flare and Landing	299
176	Time History of Power Failure in Out-of-Ground-Effect Hover	300
177	150-Knot Power-Off Reconversion Time History, Rotor Governor On	302
178	350-Knot Throttle-Chop Time History, Rotor Governor On	303
179	Height-Velocity Diagram	304

<u>Figure</u>		<u>Page</u>
180	Control Relationship - Pitch and Roll	308
181	Control Relationship - Directional and Thrust	309
182	Cyclic-and-Differential-Cyclic Mixing	312
183	Longitudinal Control Phasing Levers	313
184	Swashplate-Pylon Coupling Control	315
185	Collective Range-Shift Phase Control	317
186	Lateral Control Phasing Levers	318
187	Rudder Pedal Phase Control	319
188	Collective-and-Differential-Collective Mixing Levers	321
189	Hydraulic Systems I and II, Schematic	324
190	Hydraulic System III, Schematic	326
191	SAS Hydraulic System, Schematic	329
192	Force-Gradient Actuator, Schematic	330
193	APU Hydraulic Subsystem, Schematic	332
194	Rotor-Pitch Governor, Schematic	333
195	Rotor-Pitch Governor, Block Diagram	334
196	Force-Gradient System, Schematic	336
197	Force-Gradient System, Block Diagram	338
198	Variations in Force Gradient With Dynamic Pressure and Airspeed	339
199	Stick Force Gradient Versus Frequency Of Motion	340
200	Stability Augmentation System, Schematic	342
201	Stability Augmentation System, Block Diagram	343

<u>Figure</u>		<u>Page</u>
202	Electrical System, Block Diagram	348
203	Heating and Ventilation System, Schematic	350
204	Heat Requirements Versus Ambient Temperature for 40°F Cabin Temperature	352
205	Control Sensitivity Throughout Flight Regime . .	359
206	Control Power and Damping Characteristics . . .	360
207	Pitch Response in Hovering to F/A Stick Input	362
208	Control Positions for Trimmed Flight	364
209	Collective-Stick-Fixed Speed Stability	365
210	Handling Quality Boundaries Affected by Lateral-Directional Coupling	367
211	Roll and Yaw Response at 85 Knots to Pedal Input, Helicopter Mode	368
212	Sideslip Characteristics	369
213	Roll and Yaw Response at 85 Knots to Lateral Control-Stick Input, Helicopter Mode	370
214	Longitudinal Dynamic-Stability Characteristics	372
215	Normal Acceleration and Pitch-Rate Characteristics at 70, 98, and 120 Knots - Analog	373
216	Normal Acceleration Response to Pulse Input at 70, 98, and 120 Knots - Analog	374
217	Time History of Power Failure in Out-of- Ground-Effect Hover	375
218	Time History of Power-Off Flare and Landing . .	376
219	Longitudinal Stick Position in Trimmed Fixed- Wing Flight	378

<u>Figure</u>		<u>Page</u>
220	F/A Control-Stick Displacement Per g	379
221	Fuselage Angle of Attack Versus Speed at Various Levels of Normal Acceleration	380
222	Longitudinal Stick Force Per g	381
223	Fixed-Wing Lift Coefficient	382
224	Time History of Normal Accelerations for a Pull-and-Hold and a Pull-and-Return at 250 Knots	383
225	Steady Roll Rate Performance	385
226	Roll and Yaw Response to Lateral Control Stick Input at 150 Knots	387
227	Roll and Yaw Response to Lateral Control Stick Input at 280 Knots ($0.8 V_H$)	388
228	Roll and Yaw Response to Lateral Control Stick Input at 350 Knots	389
229	Lateral Control Displacement and Stick Force in Sideslips	390
230	Time History of Speed Reduction Due to Aft Stick Displacement	392
231	Yawing Moment Coefficient in Sideslips	393
232	Pedal Displacement and Pedal Force in Sideslips	394
233	Time History of Short-Period Longitudinal Oscillation	396
234	Longitudinal Short-Period Damping at 350 Knots	397
235	Roll and Yaw Response to Pedal Input at 350 Knots	398
236	Conversion Corridor	400
237	Conversion Time History to Fixed-Wing Mode at 120 Knots	401

<u>Figure</u>		<u>Page</u>
238	Conversion Time History to Helicopter Mode at 120 Knots	402
239	Time History of Conversion to 45 Degrees and Abort	403
240	Static Trim at Partial Mast Angles - 90 Knots	405
241	Static Trim at Partial Mast Angles - 120 Knots	406
242	Static Trim at Partial Mast Angles - 150 Knots	407
243	Sideslip Characteristics at 30-Degree Mast Angle	408
244	Pitch Response to F/A Control Input	410
245	Normal Acceleration and Pitch Response to an Aft Control Displacement 30-Degree Mast Angle	411
246	Lateral-Directional Response to Pedal Input at 30-Degree Mast Angle at 120 Knots	412
247	Lateral-Directional Response to Lateral Control Input at 30-Degree Mast Angle at 120 Knots	413
248	Lateral-Directional Response to Pedal Input at 60-Degree Mast Angle at 120 Knots	414
249	Lateral-Directional Response to Lateral Control Input at 60-Degree Mast Angle at 120 Knots	415
250	D266 Pilot Visibility	426
251	General Arrangement	437
252	Inboard Profile	439
253	Hub Assembly	441

<u>Figure</u>		<u>Page</u>
254	Blade Assembly	443
255	Control System Schematic	445
256	Cockpit Arrangement	447

TABLES

<u>Table</u>	<u>Page</u>
- Dimensional Data	18
II T64-GE-6A and T64-GE-12 Engine Comparison	33
III T64-GE-12 Engine - Performance Ratings at Sea-Level-Static Conditions, $T_2 = 59^\circ\text{F}$	58
IV T64-GE-12 Engine - Performance Data at 20,000 Ft, 370 Knots True Airspeed	59
V Engine Installation Losses Per Engine	60
VI RPM and Gear Ratios	73
VII Elemental Power Loss at 3110 HP and 12,100 RPM (1350 ft-lb)	78
VIII Total Power Loss and Efficiency	79
IX Total Power Loss and Efficiency - Single Engine Operation.	79
X Total Power Loss and Efficiency - Reduced-Power Operation	79
XI Accessory Power Requirements	80
XII Design Criteria - Power Train	81
XIII Gear-Tooth Stresses	82
XIV $L_{B_{10}}$ Bearing Life at 75-Percent Maximum Continuous Torque	83
XV Design Conditions for Helicopter Flight	102
XVI Design Conditions for Fixed-Wing Symmetrical Flight	103
XVII Design Conditions for Landing	105
XVIII Design Conditions for Taxiing	106
XIX Design Conditions for Ground Handling	107
XX Crash Load Factors (Ultimate - Acting Separately)	108

<u>Table</u>	<u>Page</u>
XXI Engine and Transmission Design Speeds and Torques	109
XXII Ultimate Loads Applied by Pylon to Outboard Wing Ribs	118
XXIII Ultimate Main-Gear and Nose-Gear Reactions . . .	120
XXIV Ultimate Conversion Actuator and Support Loads	124
XXV Fatigue Life Determination of Wing Joint at B.L. 42.0	137
XXVI Performance Summary - Helicopter Mode	202
XXVII Performance Summary - Fixed-Wing Mode	203
XXVIII D266 Drag Summary	219
XXIX D266 Drag Breakdown	220
XXX D266 Drag Analysis Using Skin-Friction Coefficients	221
XXXI 1/10-Scale Model Drag Analysis Using Skin-Friction Coefficients	222
XXXII Substantiation of Climb Efficiency Factor	253
XXXIII Flight-Control-System Travels	306
XXXIV Static and Dynamic Stability, Helicopter Mode	355
XXXV Static and Dynamic Stability, Fixed-Wing Mode	357
XXXVI Handling Qualities	367

SYMBOLS

A	area, rotor-disc area, effective structural area
AR	aspect ratio
a_w	slope of lift curve
b	span
C	theoretical chord
c	blade chord
\bar{c}	mean aerodynamic chord
C_D	drag coefficient
$C_{f_{WET}}$	wetted drag-area coefficient
C_L	lift coefficient
$C_{N_{A_{max}}}$	maximum airplane normal force coefficient
C_P	power coefficient
C_T	thrust coefficient
$\frac{dH}{d\alpha}$	change in rotor in-plane force with angle of attack
$\frac{dH}{d\dot{\alpha}}$	change in rotor in-plane force with rate of change of angle of attack
$\frac{d\epsilon}{d\alpha}$	rate of change of wing downwash with angle of attack
E	modulus of elasticity (Young's modulus)
e	Oswald's airplane efficiency factor
EI	bending stiffness

f	equivalent flat-plate drag area
F/A	fore and aft
f_B	bending stress
f_{BS}	blade stress due to mean beam bending moment
F_{be}	endurance limit
f_i	induced-drag area
f_t	tension stress
f_{total}	total stress
F_{tu}	ultimate allowable tension stress
F_{zB}	allowable oscillatory beam bending moment for infinite life
H-force	an in-plane aerodynamic force
h	mast length
h_p	vertical distance from thrust line to cg in fixed-wing mode
I	moment of inertia
I_B	beamwise moment of inertia
I_b	moment of inertia of one blade about flapping axis
I_C	chordwise moment of inertia
i_w	angle between wing zero-lift line and fuselage waterline
K_h	longitudinal hub restraint per rotor
K_l	longitudinal hub restraint per blade
l	length

M	applied moment
M_B	blade beamwise bending moment
M_{BS}	mean blade beamwise bending moment
M_C	blade chordwise bending moment
M_H	time-averaged H-force moment
M_x	bending moment about the longitudinal axis, spanwise bending moment
M_y	bending moment about the lateral axis, wing torsional bending moment
M_z	bending moment about the vertical axis
N	number of cycles to failure
n	number of cycles per 1000 flight hours, number of blades per rotor
n/N	damage fraction
n_x	fore-and-aft load factor
n_y	lateral load factor
n_z	vertical load factor, design load factor
P	load
R	rotor radius
\bar{R}	mean rotor radius
RN	Reynolds number
SHP	shaft horsepower available
S_{WET}	total wetted skin area
S_y	side shear
s_z	vertical shear

T	time
THP_{FN}	net jet-thrust power
V	airspeed
V_F	maximum allowable speed with flaps down
V_G	maximum speed for 66-fps gust
V_H	high speed
V_L	limit speed
W	weight
Z_B	beamwise section modulus
α_M	rotor-mast angle of attack
ΔH	in-plane force
ΔT	aerodynamic flapping force
δ_α	aileron deflection
δ_3	pitch-flap coupling angle
ϵ	swashplate retardation angle
η	propeller efficiency
θ	blade or fuselage pitch angle
θ_1	blade twist

Λ	leading-edge sweep
$\Lambda_{.25}$	sweep at 1/4-chord
$\frac{\rho_{ac} R^4}{I_b}$	rotor Lock number
σ	rotor-disc solidity
ϕ_x	pylon-deflection velocity
$(\dot{\phi}_x + \dot{a}_1)$	rotor-plane rotational velocity
ω	angular pitching velocity
$\dot{\omega}$	pitching acceleration
ΩR	rotor-blade tip speed

Subscripts

b	rotor blade
e	elevator
i	inboard
o	outboard
r	root
s	horizontal stabilizer
t	tip
u	up-going
v	vertical stabilizer
w	wing
x	longitudinal axis

y lateral axis
z vertical axis

SECTION I. DESIGN CONCEPT

A. INTRODUCTION

1. BASIC OBJECTIVE

The basic objective of the Bell D266 Composite Aircraft design is to achieve efficient vertical flight and efficient fixed-wing cruise flight with the simplest possible mechanical systems and pilot-control procedures. The tilt-rotor configuration makes it possible to avoid duplicating systems--such as dual powerplants, one kind for lift and another for cruise; or dual propulsion elements, such as rotors for low speed and propellers, shrouded fans, or jets for fixed-wing flight, each with its associated drive gearing and clutching or diverter-valve arrangements.* This approach is a factor in designing an aircraft with a low empty weight and therefore a high useful-load-to-gross-weight ratio--a key factor that determines the effectiveness of any aircraft.

2. DESIGN REQUIREMENTS

The following design requirements were specified by the Statement of Work of the Design Study contract:

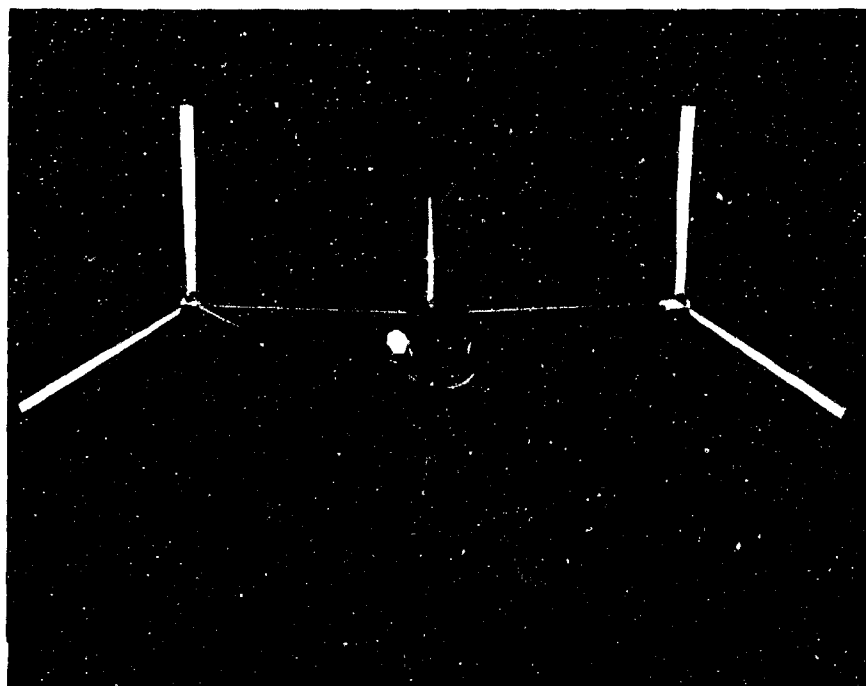
- Payload - 3000 pounds
- Fuel - 3000 pounds
- Vertical takeoff and landing
- Hover OGE at 95°F and 6000-foot pressure altitude
- Disc loading - 10 psf or less
- Speed - 300 knots required (400 knots desired)
- L/D ratio - at least 10
- Cargo-compartment - 5.5 feet wide, 6 feet high, 14.5 feet long

The weights of fuel (3000 pounds), payload (3000 pounds), and equipment and furnishings (2550 pounds), and the dimensions of the cargo compartment strongly influenced the general arrangement of the D266. The arrangement of the aircraft is shown in Figures 1, 2, and 3. The weight requirements were met at a gross weight of 23,000 pounds, which includes a growth contingency of 440 pounds. The design disc loading at this weight is 9.88 pounds per square foot, which is below the maximum disc loading permitted.

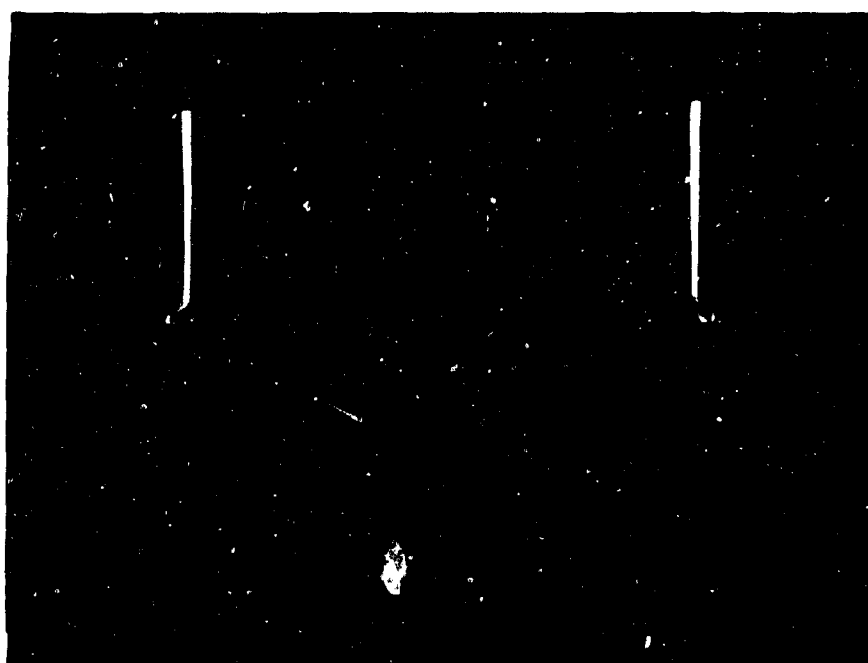
*Throughout this report "helicopter mode" describes the flight condition in which the rotor masts are vertical to 15 degrees forward, "conversion mode" refers to the condition in which the masts are between 15 and 90 degrees forward, and "fixed-wing mode" refers to the condition where the masts are fully converted.



Figure 1. D266 Composite Research Aircraft.

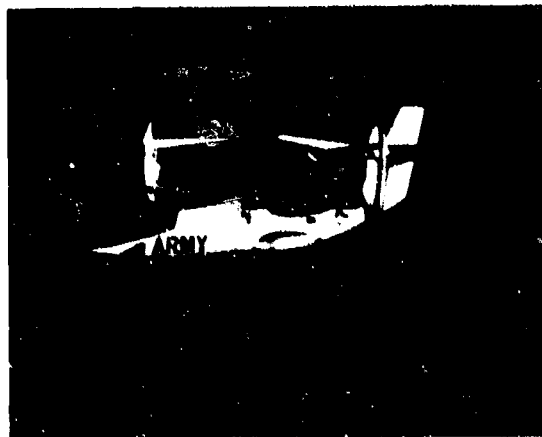


Front View



Rear View

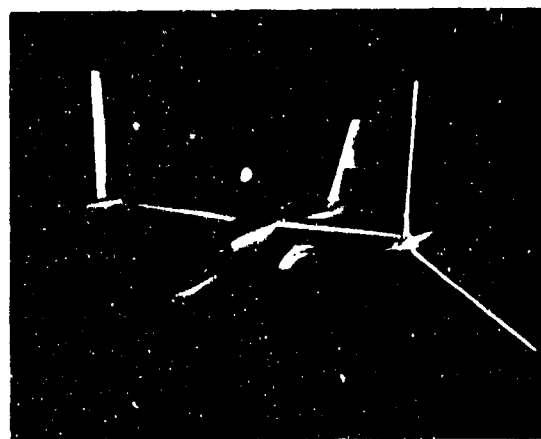
Figure 2. D266 - Front and Rear Views.



Helicopter Configuration



Conversion



High-Speed Configuration

Figure 3. D266 - Conversion Procedure

By properly proportioning the specified fuselage cross section (5-1/2 feet wide, 6 feet high) to the overall airframe and tail surfaces, the required length of the cargo compartment was exceeded by approximately 7 feet. The result is a cargo compartment 5-1/2 feet wide by 6 feet high by 21-1/4 feet long.

If the requirement of 300 to 400 knots and the desired L/D of 10 were to be met, airframe drag, propeller efficiency, and drive-system efficiency must be carefully considered. Low airframe drag was achieved by careful fairing of the fuselage lines, with special attention to the cockpit enclosure and the landing gear fairings. Other drag-producing components, such as the engine nacelles and pylon fairings, were also configured for minimum drag.

3. VERTICAL FLIGHT

The low VTOL disc loading of 10 pounds per square foot specified for the composite research aircraft, together with the relatively small amount of blockage of the rotor downwash in the D266 configuration with wing flaps and ailerons dropped for hover, results in good hover performance. The D266, with twin T64-GE-12 engines, exceeds the hot-day 6600-foot hovering requirement by more than 5000 feet with the specified payload of 3000 pounds, and it meets the requirements with a payload of over 8000 pounds.

4. FIXED-WING FLIGHT

To enter fixed-wing flight, the aircraft is accelerated into forward flight as a helicopter, and then the pilot uses the conversion switch on the control-stick grip to tilt the rotors forward through 90 degrees. The entire process may be accomplished in less than ten seconds, and the pilot may switch from power-turbine to blade-pitch rpm governing either during or after the conversion. Rotor rpm is reduced for best efficiency in fixed-wing flight to about one-half the hover rpm setting. The result is a propeller efficiency comparable to that of conventional propellers, and a maximum cruise speed up to 350 knots, depending on cruise altitude. With one engine cut, the D266 will still cruise at 260 knots.

5. CONVERSION FEATURES

The conversion procedure is relatively uncomplicated. No special skills are required, and the pilot enjoys increased flight versatility and freedom of choice. The more significant conversion features are:

- No rigid programming is required. Conversion can be made in climbing, descending, or turning flight.

- The process is not critical. There are no narrow envelopes or other restrictive limitations.
- The conversion can be stopped at any point in the cycle, and the aircraft can be operated and maneuvered continuously in that configuration.
- Stability and control are excellent throughout the entire conversion cycle.
- Power-off reconversion is possible in the event of total powerplant failure.

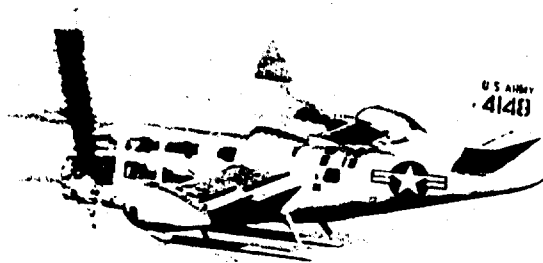
B. BACKGROUND

1. TILT-ROTOR EXPERIENCE

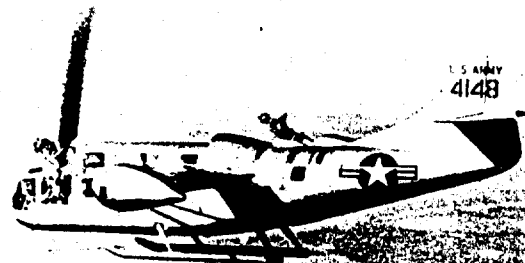
Bell's initial efforts in using a helicopter rotor as a propeller for forward propulsion began in 1941 under the direction of Arthur M. Young, almost at the same time as the early Bell helicopter work. Following initial design studies which indicated the feasibility of the concept, a tethered flight model was constructed and flown in 1943. This program demonstrated that steady flight could be maintained with the rotor shaft axis in any attitude from vertical to horizontal, and that adequate propulsion for airplane flight could be obtained in propeller configuration. No abnormal rotor behavior was found. At this point a prototype aircraft was begun but subsequently dropped in order to allow concentration on helicopter development.

In 1949, work in the low-disc-loading VTOL area was resumed with the initiation of a program directed toward the development of an aircraft which would combine the vertical takeoff and landing, hovering, and low-speed maneuvering abilities of the helicopter with the high-speed and long-range performance of the airplane. Company-sponsored analytical and preliminary design studies were continued for more than two years; and in 1951, Bell, as one of the three winners of the Joint U.S. Air Force-U.S. Army convertiplane competition, began work on the XV-3 development. The three contract awards were for the tilt-rotor, stopped-rotor, and compound helicopter configurations.

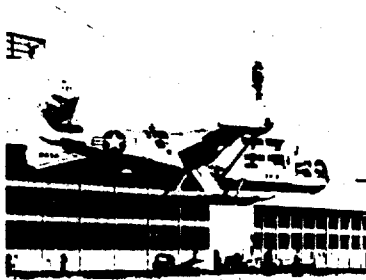
The first Government-sponsored program involved the detailed design of the tilt-rotor machine and extensive model tests and analytical investigations of the concept. The predesign program was essentially completed in 1953, and in the latter part of that year, BHC was awarded a contract for the construction and test of two aircraft designated the XV-3. This program was sponsored and supported by the U.S. Army Transportation Corps. Approximately \$10,000,000 of Government funding was invested in this program. Figure 4 shows the XV-3 in its final configuration, undergoing flight and full-scale wind-tunnel tests.



AIRPLANE CRUISE FLIGHT



MANEUVERS AT INTERMEDIATE ANGLES



NASA FLIGHT EVALUATION



WIND-TUNNEL TESTS



STOL TESTS-FULL AUTOROTATION LANDING

Figure 4. XV-3 Tilt-Rotor Aircraft

Following its initial development and flight testing by Bell, the XV-3 was put through an extensive series of flight tests by U.S. Air Force, NASA, and U.S. Army test groups. The total test program has included over 500 hours of flight, wind-tunnel, and ground-run time, including over 250 test flights in 125 hours of flight time. The test aircraft was flown by ten Government test pilots as well as two Bell pilots, who made over 110 full conversions to fixed-wing configuration and over 30 gear shifts to low-rpm cruise operation. Five of the Government test pilots made power-off reconversions from cruise flight to helicopter autorotation.

In addition to the basic XV-3 program, several related Government-sponsored R&D programs have been conducted. These include a preliminary design study of an 80,000-pound gross weight machine for the USAF, two series of wind-tunnel tests of powered quarter-scale tilt-rotor models, and extensive computer studies of the aerodynamics of rotors in axial flight operation.

Since 1961, work has been intensified to expand the tilt-rotor design base established by the XV-3 program. This work has included several detailed design studies of tilt-rotor aircraft for a variety of military and civil applications. A specific

example is Bell's D252 Tri-Service Transport Aircraft, designed for a 4-ton payload.

Extensive dynamic model testing and analytical work have been conducted to explore characteristics of rotor-pylon systems operating at speeds up to 500 knots. As a result of the model and analytical programs, design tools are now available which should lead to development of tilt-rotor aircraft more nearly free of dynamic problems.

All of this work, especially the XV-3 program, where full-scale problems have been encountered and solved, is directly applicable to the composite research aircraft.

2. RELATED ROTOR EXPERIENCE

Production aircraft of the Bell Helicopter Company incorporate the two-bladed, semirigid, "seesaw"-type rotor system; however, many types of rotors have been investigated under the company's IR&D programs. These investigations have included analytical studies, model tests, and full-scale fabrication and flight tests of articulated, semirigid, and rigid systems with wide variations of design concepts and parameters.

The first multibladed rotor system was designed and evaluated on a Model 47 (H13-H) helicopter in 1956-1957. This rotor had a three-bladed, gimbal-mounted configuration employing mast-moment springs for hub restraint. Since this initial flight investigation, the merits of the multibladed, semirigid configuration have been studied further, and more than a dozen full-scale systems have been evaluated by flight tests. These configurations have included gimbal-mounted (with and without hub restraint), flex-beam, and rigid systems. The most recent system designed, a four-bladed flex-beam type, has been flown to a power-limited true airspeed of 196 knots (with an advancing-tip Mach number of 0.935) on the AVLABS-Bell High-Performance Helicopter. The rotor has since been reconfigured with low-twist, tapered-tip blades for continued high-speed development. It is currently on flight status.

a. Early Developments

During the development of the first semirigid, multibladed rotors, there were two prominent dynamic problem areas. The first involved providing sufficient in-plane stiffness to place the first in-plane frequency higher than one per rev. The other problem was concerned with three-per-rev resonance near the second beam-bending mode of the blade. In several instances, alteration of blade stiffness and/or spanwise mass distribution was necessary before acceptable configurations were achieved. However, with present blade-construction methods, which result in very stiff, lightweight blades, obtaining satisfactory mass

balance and chordwise frequencies is no longer a problem. Also, the present computer programs predict quite accurately the various blade frequencies up through six to eight per rev, so that mass and stiffness variations can be altered during the design stages to eliminate some of the higher-order resonance problems.

b. Experimental Rotors

Figure 5 shows some of the multibladed rotor systems that have been developed and flown by Bell Helicopter Company.

The first multibladed rotor system built by Bell is shown in Figure 5a. After its inadequate chordwise stiffness was corrected, this rotor operated quite satisfactorily and was evaluated throughout the speed range of the test vehicle. Figure 5b shows a rigidly mounted version of the first system which has been mounted on a 47G-2 helicopter for investigation of IFR flight capability. This system was also evaluated by the NASA-Langley Research Center. Figure 5c shows a flex-beam configuration mounted on a Model 47J helicopter. This system was also quite successful, and it was demonstrated with a cg excursion more than twice that normally allowable for the vehicle.

Figure 5d shows the first XH-40 three-bladed rotor after modification with 15-inch-chord blades. This rotor proved to have superior performance and vibration characteristics when compared to the standard rotor for the XH-40. It was flown in 1959 to speeds above 120 knots and to altitudes above 18,000 feet. The same rotor is shown in Figure 5f installed on a UH-1 helicopter, where it was further evaluated. The rotor had a diameter of 40.25 feet, with three 15-inch-chord blades for a rotor solidity of 0.06. Normal rotor speed was 314 rpm (tip speed, 662 fps), and operation was conducted with and without hub-restraint springs. This configuration closely resembles the proposed D266 rotor in most of the significant dynamic parameters, and it provides an excellent base for the new design.

A gimbal-mounted, three-bladed rotor system was designed and flight-tested on the AVLABS High-Performance Helicopter. This rotor, which was flown to speeds above 150 knots as a pure helicopter, also represents quite closely the dynamic system selected for the D266 rotor.

Figures 5g and 5h show the latest multibladed, rigid-rotor system being developed at Bell Helicopter Company. This rotor is scheduled for evaluation at speeds above 250 knots on a forthcoming high-speed compound-helicopter test program.



a. Original Semirigid Multibladed Rotor - Gimbal-Mounted.



b. Rigid-Rotor Test of IFR Flight Capability.



c. Model 47J Experimental Flex-Beam Rotor System.



d. XH-40 Three-Bladed Rotor With Hub-Restraint Springs.



e. High-Performance UH-1 With Three-Bladed Rigid Rotor.



f. Three-Bladed, Gimbal-Mounted Rotor on UH-1.



g. Four-Bladed Rigid Rotor on Model 204B Helicopter.



h. AVLABS-Bell Compound HPH With Four-Bladed Rotor.

Figure 5. Various BHC Multibladed Rotor Systems..

3. COMPARATIVE DESIGN STUDY

The company's in-house technical effort has been expanded since 1963, and a number of analytical model-test and design-study efforts have been authorized to investigate the characteristics and performance of a variety of possible VTOL vehicle configurations, such as those illustrated in Figure 6. In particular, model and full-scale test programs were started on the tilt-rotor, trail-rotor, stopped-rotor, retractable-blade rotor, and unloaded-slowed-rotor composite helicopter configurations.

The preliminary results of these programs indicated that all of these, and several other low-disc-loading VTOL configurations, were feasible with sufficient development effort. It was realized that a choice would have to be made of the one or two best configurations for intensive engineering development.

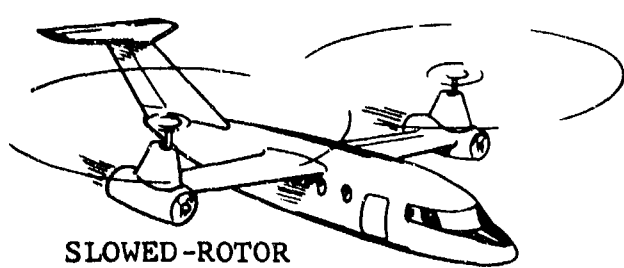
Accordingly, five of the most promising configurations were subjected to a thorough comparative design and mission-effectiveness study. A low-disc-loading version of what appeared to be the most promising of the current generation of high-disc-loading VTOL test aircraft, the tilt wing, was also included in the study for comparison. Aircraft designs of all six configurations were laid out, using the common design factors of 10 pounds per square foot disc loading, two T55-L-7 engines (5300-shp total), hover OGE at 6000 feet, 95°F, and with performance objectives of 3000 pounds payload and 300 knots maximum speed. Sketches of the resulting designs are shown in Figure 7.

The comparative design study was made for the following low-disc-loading composite aircraft configurations:

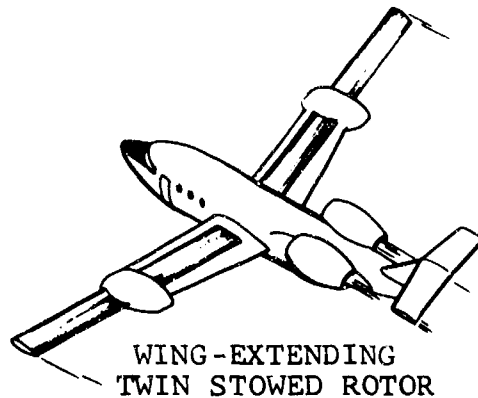
- Slowed-rotor compound
- Stopped rotor
- Stowed rotor
- Tilt rotor
- Trail rotor
- Tilt wing (low-disc-loading version)

Each of these configurations, illustrated in Figure 7, was designed for a disc loading of 10 pounds per square foot.

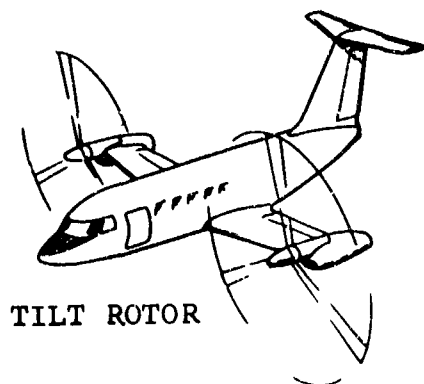
Transport-effectiveness comparisons of the six configurations show that the tilt rotor, tilt wing, and trail rotor have useful loads, productivities, and payload delivery efficiencies



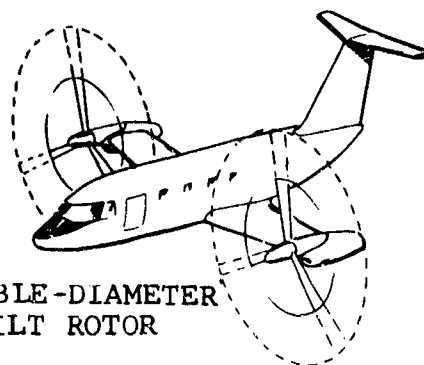
SLOWED-ROTOR
TWIN COMPOUND



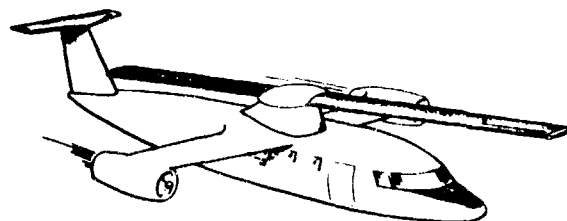
WING-EXTENDING
TWIN STOWED ROTOR



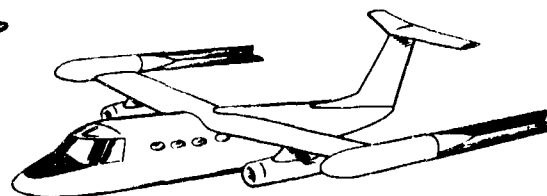
TILT ROTOR



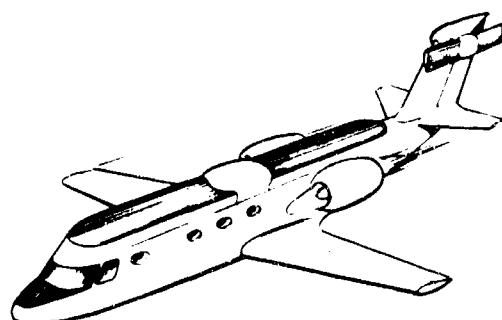
VARIABLE-DIAMETER
TILT ROTOR



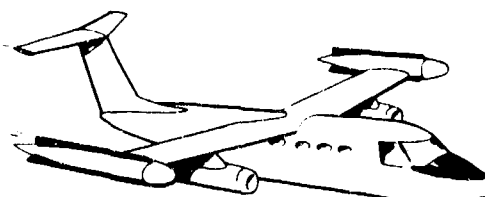
STOPPED ROTOR



TRAIL ROTOR



STOWED ROTOR



FOLDED ROTOR

Figure 6. Examples of VTOL Composite Aircraft Configurations Examined During Preliminary Studies.

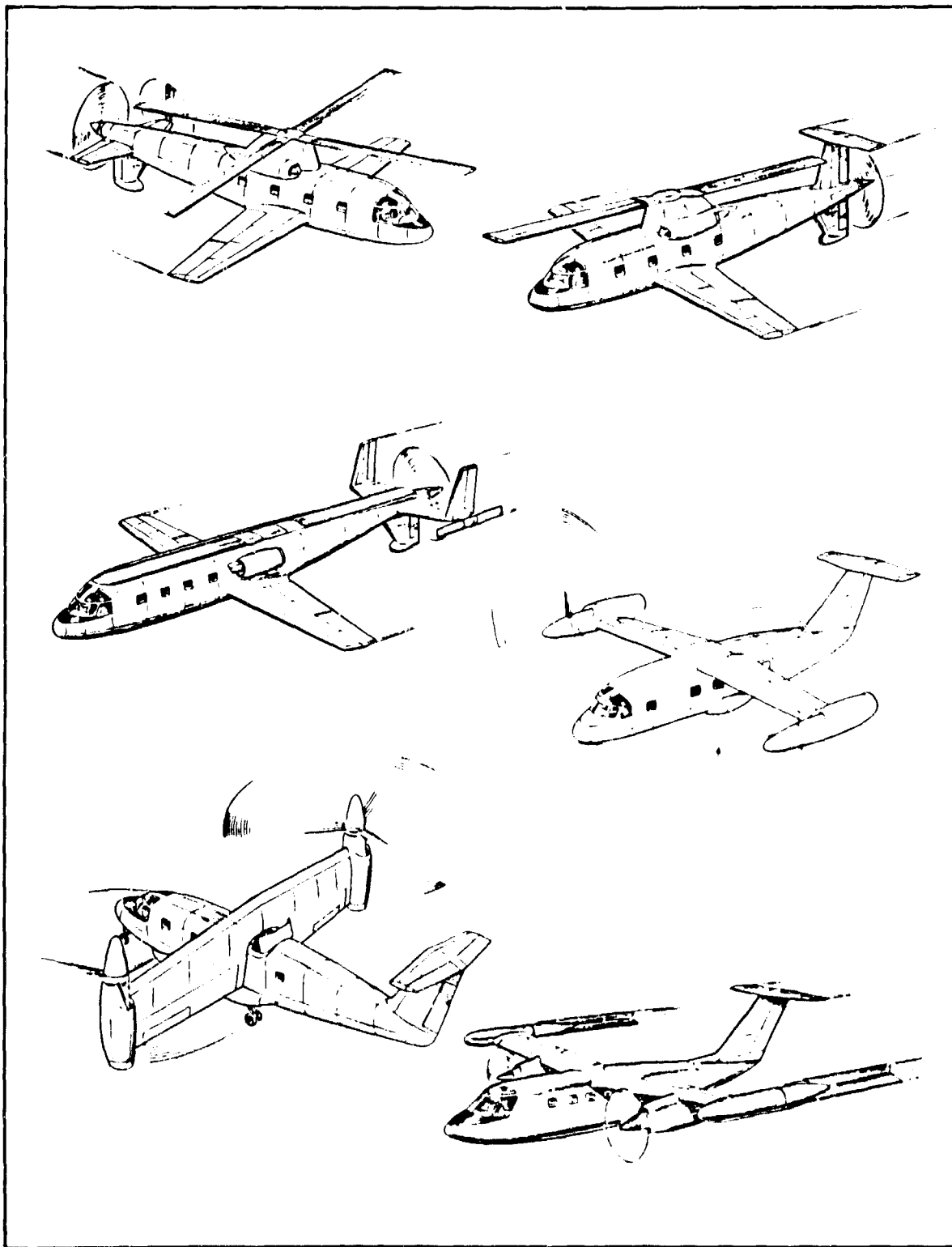


Figure 7. Six Low-Disc-Loading VTOL Designs
Resulting From BHC Comparative Design Study Program.

considerably greater than the other types. The tilt-rotor configuration has the highest transport effectiveness of the six configurations examined.

The twin-rotor VTOL configurations with their high hovering efficiency and high design gross weight can lift 50 percent more useful load than the single-main-rotor aircraft. The difference in hovering efficiency between the twin-rotor and single-rotor aircraft is due primarily to the tail-rotor power loss, and the higher "download" on the fuselage and wing, of the single-rotor aircraft.

Empty weight to gross weight ratios are higher for configurations requiring redundant cruise propellers. Additional increases result from the added fuselage length and complexity required for stowing the pylon and rotor on the stowed-rotor aircraft, and from the larger and more complicated wing required to avoid stalling during transition of the tilt-wing configuration. The tilt-wing and tilt-rotor configurations have approximately the same useful load capability. The tilt wing has considerably more drag, and hence a lower cruise efficiency, than the tilt rotor. The stowed rotor has the lowest drag and is the fastest configuration, but it also has the lowest payload-range capability. The slowed-rotor compound, although it has the highest drag of all, is faster than the tilt wing because of its higher propulsive efficiency.

Payload-range capability, productivity, and payload-delivery efficiency are useful indicators of the mission suitability and transport effectiveness of each design. Comparisons of these indices lead to the following conclusions:

- All six of the low-disc-loading VTOL's examined can carry payloads of at least 3000 pounds to a range of 200 nautical miles. A helicopter with the same power can carry 6000 pounds of payload to the same range, as can the tilt-rotor, trail-rotor, and tilt-wing configurations. Because of the higher delivery efficiency and productivity of the latter three, as well as their outright speed advantage, they are superior to the helicopter and suitable for performing its mission.
- The slowed-rotor, stopped-rotor, and stowed-rotor configurations have less payload-range capability, but higher productivity and payload-delivery efficiency, than the helicopter. This superiority alone would not justify their replacing the helicopter, unless tactical requirements should demand an aircraft with 220- to 330-knot cruise speed capability.

- The tilt-rotor, trail-rotor, and tilt-wing aircraft can carry the design payload of 3000 pounds on a mission of 400 nautical miles or more.
- The productivity and payload-delivery efficiency indices of the low-disc-loading tilt-rotor, tilt-wing, and trail-rotor VTOL types are more than twice as high as those for an equivalent transport helicopter operating at approximately one-half the speed.
- Operation of the low-disc-loading VTOL at a moderate cruise altitude of 20,000 feet increases range by as much as 60 percent, making it suitable for long-range missions. Cruise speed for maximum payload-delivery efficiency increases from 210 knots at sea level to 250 knots at 20,000 feet.
- The tilt rotor has the highest productivity and the highest payload-delivery efficiency of all the configurations studied.

4. CONCEPT SELECTION

The results of the comparative design study show a definite cost-effectiveness superiority of the tilt-rotor configuration, with the trail rotor somewhat less cost effective. This finding, coupled with the very extensive background of Bell Helicopter in tilt-rotor VTOL aircraft development, led to the selection of the tilt rotor as the preferred vehicle configuration for the composite research aircraft.

In addition to good cost effectiveness, it is important that the selected composite research aircraft have characteristics compatible with the Army's operating environment, manpower skill levels, and mission requirements. Design of the aircraft must therefore include such considerations as:

- Reliable components
- Mechanical systems similar to those of current helicopters
- Avoidance of high downwash velocities and hot exhaust impingement on personnel or vegetation
- Ability to make controlled steep descents and climbouts for operation into confined landing zones
- A quick and safe procedure for conversion from one flight mode to the other

- Ability to quickly enter power-off, rotor-supported descent for combat emergency landings.

C. DESIGN DESCRIPTION AND SELECTION

1. GENERAL DESCRIPTION

The D266 is a twin-engine aircraft which combines vertical takeoff, hovering, and low-speed helicopter performance with high-speed cruise efficiency. A tilting, three-bladed, semi-rigid rotor is mounted on each wingtip. Power is provided by two General Electric T64-GE-12 engines, which are mounted one on each side of the fuselage aft of the rear wing spar. Each engine has a military rating of 3435 shp. The aircraft has a high, forward-swept wing.

The design gross weight is 23,000 pounds, and the weight empty is 15,995 pounds. The D266 will hover out of ground effect on a hot day at sea level at design gross weight on a single engine, or at 11,050 feet with both engines operating. A STOL takeoff may be accomplished at an alternate gross weight of 41,500 pounds. The payload at the alternate gross weight is over 24,000 pounds, which, if used for fuel, provides a ferry range of 4275 nautical miles (with 10-percent reserve).

The D266 has a maximum speed of 345 knots at sea level and can maintain 288 knots in single-engine operation at 8500 feet.

The limit design load factors in helicopter flight are +3.0g and -0.5g. These load factors are standard for Class II transport-type helicopters and exceed the aerodynamic capabilities of the rotors by a safe margin. The limit design load factors in the fixed-wing configuration are +4.5g and -1.0g and exceed those used by turboprop utility transport aircraft.

The fuselage sections are the nose section, which includes the nose landing gear, the crew compartment, and the forward structure; the cargo compartment, which includes the main landing gear, the wing-fuselage intersection, and the personnel/cargo doors; and the aft section, which supports the empennage. The fuselage is a conventional nonpressurized semimonocoque structure. The wing is a two-spar single-cell cantilever structure which is swept forward 5-1/2 degrees. Three fuel cells in each wing form the two fuel tanks. The empennage has a large vertical stabilizer and rudder, and a horizontal stabilizer with the elevator mounted near the half spar. The landing gear is of tricycle configuration, with dual nose wheels and tandem main wheels. The wide tread provides a 35-degree turnover angle.

Power for the D266 is supplied by two T64-GE-12 engines, which require no modification to the basic engine. Each engine and reduction gearbox is located in a fuselage-mounted nacelle; the gearbox drives forward to interconnect drive shafting and then outboard to two main transmissions at the wingtips. The main transmissions are attached to spindle-type mounts, which permit rotation from the vertical to the horizontal. The pylons are hydraulically powered and mechanically interconnected. The drive shafts are also interconnected through an accessory gearbox.

The 38.5-foot-diameter rotors are three-bladed, semirigid rotors, which are mounted on universal joints to permit rotor tilt (flapping) relative to the rotor masts. The rotors are provided with hub-restraint springs, which permit increased center-of-gravity travel and which augment control power in pitch and yaw.

The flight-control system includes conventional helicopter controls, fixed surface controls, and cockpit controls. Three independent transmission-driven hydraulic systems, one of which may be powered by the auxiliary power unit, supply redundant hydraulic flight-control power. One system also provides hydraulic power for flight-assist functions and landing-gear operation.

Pertinent basic data are summarized in Table I. The overall dimensions are shown in Figures 251 and 252 in the Appendix.

2. AIRFRAME

a. Fuselage

The fuselage of the D266 aircraft is a conventional, non-pressurized, semimonocoque structure. It is composed of three sections, which are manufactured as separate subassemblies and then joined in a final-mating fixture. The basic structure consists of four main longerons to carry bending, while shear is carried by the external skins. Circumferential frames and stiffeners form the stiffening for the shear-carrying system, and major bulkheads are located at points of concentrated loads.

Heat-treated 7075-T6 aluminum alloy is used for the skins and longerons. Where the structural loads are low and the contours are of single curvature, magnesium alloy skins are used to save weight--but only where the structure is readily visible for routine inspection and where pockets of moisture cannot accumulate. Aluminum honeycomb sandwich construction is used in a few locations. Most prominent among these is the area adjacent to that swept by the tip of the rotor. Sandwich is used here to minimize the effects of the sonic loadings that emanate from the rotor tip.

TABLE I
DIMENSIONAL DATA

Definition	Symbol	D266 Value
<u>ROTOR</u>		
Direction of Rotation (View Looking Down)		
Left		Clockwise
Right		Counterclockwise
Precone Angle		2.5 deg
Number of Blades per Rotor	n	3
Rotor Radius	R	19.25 ft
Disc Area per Rotor	A	1164.00 ft ²
Blade Area per Rotor	A _b	96.00 ft ²
Blade Chord	c	20.00 in.
Blade Taper		0
Solidity	σ	0.0825
Design C _T / σ at 825 fps		0.0745
Design Lift/Rotor		11,500 lb
Design Limit Load Factor:		
Helicopter		3.0 g
Fixed-Wing Mode		4.5 g
Design Limit Torque		88,200 lb-ft
Total Blade-Pitch-Change Range		68.0 deg
Blade Airfoil		
Root (theoretical)		NACA 64A030
Tip		NACA 64A206 a = 0.3
Spinner Extends from Center to 0.07R		
Streamlined Blade Cuff Extends from 0.07R to 0.26R		
Blade Twist	θ_1	
Centerline to 0.20R (-90° Twist Rate)		-18.0 deg
0.20R to 0.35R (-50° Twist Rate)		-7.5 deg

TABLE I - Continued

Definition	Symbol	D266 Value
0.35R to Tip (-27.7° twist rate)		-18.0 deg
Overall (centerline to tip)		-43.5 deg
Tip-Speed Range	ΩR	
VTOL		750-825 fps
Fixed-Wing Mode		400-600 fps
Disc Loading (design gross weight)		9.88 lb/ft ²
Power Loading at Military Rating		3.35 lb/shp
Rotor rpm		
VTOL		372-409 rpm
Fixed-Wing Mode		198-297 rpm
Vertical Distance from Thrust Line to cg in Fixed-Wing Mode, Positive for Thrust Line Below cg	h_p	2.5 ft
Moment of Inertia of One Blade About Flapping Axis	I_b	570 slug-ft ²
Longitudinal Hub Restraint per Rotor	K_h	1500 ft-lb/deg
Lateral Hub Restraint per Rotor		0 ft-lb/deg
Longitudinal Hub Restraint per Blade	K_l	1000 ft-lb/deg
Rotor Lock Number, $\frac{\rho a c R^4}{I_b}$		5.73
Pitch-Flap Coupling	δ_3	30 deg
Maximum Flapping Angle		±8 deg
<u>WING</u>		
Area	A_w	330.5 ft ²
Span (rotor hub to rotor hub)	b	46.8 ft
Wing loading at design gross weight)		70 lb/ft ²

TABLE I - Continued

Definition	Symbol	D266 Value
Aspect Ratio	AR_W	7.44
Lift Curve Slope of the Wing	a_w	4.50/rad
Theoretical Root Chord (B.L. 0)	C_r	87.5 in.
Airfoil Section		NACA 64A423 modified
Theoretical Tip Chord (B.L. 297.5)	C_t	72.5 in.
Airfoil Section		NACA 64A419 modified
Mean Aerodynamic Chord (B.L. 144.1)	\bar{c}	80.2 in.
Root Chord (B.L. 42)		85.4 in.
Chord at Mast Centerline (B.L. 281.0)		73.3 in.
Taper Ratio (C_r/C_t)		1.2
Wing Twist		0
Angle of Incidence (Chord line to W.L.)		1.5 deg
Angle Between Wing Zero Lift Line and Fuselage Waterline	i_w	4.5 deg
Dihedral (1/4-chord line)		2 deg
Forward Sweep (1/4-chord line)	$\Lambda_{.25}$	6.25 deg
Forward Sweep of Wing Leading Edge	Λ	5.5 deg
Aileron-Flap		
Area/Side		13.82 ft ²
Span		103.4 in.
Chord/Wing Chord		0.25
Flap		
Area/Side		13.75 ft ²
Span		85.5 in.
Chord/Wing Chord		0.285

TABLE I - Continued		
Definition	Symbol	p256 Value
<u>HORIZONTAL STABILIZER</u>		
Span	b_s	20.1 ft
Area	A_s	90 ft ²
Aspect Ratio	AR_s	4.5
Stabilizer Lift Curve Slope	a_s	4.0/rad
Root Chord	C_{rs}	66.1 in.
Tip Chord (B.L. 120.7)	C_{ts}	41.4 in.
Mean Aerodynamic Chord (B.L. 55.7)	\bar{c}_s	54.7 in.
Airfoil Section		NACA 64A012
Angle of Incidence (stick neutral)		0 deg
Sweep (1/4 chord)	$\Lambda_{.25s}$	15 deg
Taper Ratio (C_{rs}/C_{ts})		1.6
<u>Elevators</u>		
Total Area	A_e	25 ft ²
Chord/Stabilizer Chord		0.30
Tail Length (1/4 \bar{c}_s to 1/4 \bar{c})	l_s	27 ft
<u>VERTICAL STABILIZER</u>		
Span	b_v	13.15 ft
Area	A_v	100 ft ²
Aspect Ratio	AR_v	1.73
Lift Curve Slope	a_v	2.24/rad
Root Chord (W.L. 123.0)	C_{rv}	121.4 in.
Tip Chord (W.L. 281.0)	C_{tv}	60.7 in.
Mean Aerodynamic Chord	\bar{c}_v	94.4 in.
Taper Ratio (C_{rv}/C_{tv})		2
Sweep (1/4 chord)	$\Lambda_{.25v}$	29 deg
<u>Airfoil Section</u>		
Root		NACA 65A015
Tip		NACA 64A009

TABLE 1 - Continued		
Definition	Symbol	D266 Value
Angle Between Vertical Stabilizer Zero Lift Line and Fuselage Waterline	i_v	0 deg
Rudder		
Area		18 ft ²
Chord/Vertical Stabilizer Chord		0.20
Tail Length, ($\bar{c}_{l/4v}$ to $\bar{c}_{l/4}$)	l_f	24.92 ft
ENGINE		
Designation		T64-GE-12
Power Ratings		
Military at 13,600 rpm		3435 hp
Normal Rated Power at 13,600 rpm		3230 hp
Maximum Power for Structural Design		Based on derated engine torque limit of 1350 ft-lb or 3435 hp
Engine Speeds		
Helicopter Mode		15,100-16,600 rpm
Fixed-Wing Mode		8,050-12,100 rpm
TRANSMISSION DRIVE RATIOS		
Engine to Main Drive Shaft		1.788:1
Overall Reduction from Engine to Rotor		40.613:1
PYLON		
Mast Length (conversion axis to flapping axis)		74 in.
Conversion Axis Location		36.8 % MAC
Conversion Axis Sweep		5 deg

(1) Nose Section

The nose section extends from Station 34 to Station 176. It includes the nose landing gear, nose landing-gear beams, crew compartment, structure for mounting electronic equipment, nose cone, windshield, and side and overhead panels.

The major load-carrying structure of the nose section consists of two nose landing-gear support beams that are symmetrically located about the fuselage centerline at B.L. 10.8 and extend from Station 64 to Station 176. These two beams are supported by bulkheads at Stations 151 and 176. The beam depth is from lower contour to W.L. 73.75. All structure in this section is made of 7075-T6 aluminum alloy. The nose-gear doors, which are located between the beams, are nonstructural.

The crew ejection seats are attached to a bulkhead that is canted 13 degrees aft. Shelves between the canted bulkhead and the frame at Station 176 support the electronic equipment. The nose cone is fiber glass and is hinged for quick access to equipment.

The windshield is made from 0.30-inch-thick stretched acrylic material. A section of the fuselage forward of and below the pilot's compartment has a stretched acrylic windshield to provide downward visibility during vertical landings. The panels above the ejection seats are "as cast" acrylic to permit emergency ejection through them.

(2) Cargo Compartment

The cargo compartment extends from Station 176 to Station 431.5. It contains the main landing gear, the wing-fuselage intersection, two personnel/cargo doors, and the cargo floor with tie-downs. The minimum clear cross-sectional dimensions for cargo are 5-1/2 feet wide by 6 feet high. The length is 21 feet 3 inches, giving a volume of 695 cubic feet, which can easily accommodate 24 passengers.

The basic structure in this section consists of four extruded 7075-T6 longerons, external skins, and circumferential stiffening. The stiffening consists of formed frames at approximately 20-inch spacing with light angles spaced midway between them. In addition to the conventional ultimate design conditions, the external skins are designed to be nonbuckling at one g in flight and on the ground at design gross weight.

The main landing-gear oleo, in the retracted position, nests inside the mold line of the fuselage between Stations 343.5 and 369.5, thereby creating a landing-gear well in this region. In order to obtain the maximum possible volume for this well,

without encroaching into the clear cargo space in the fuselage, an aluminum honeycomb sandwich structure is used.

The cargo floor extends the full length of the compartment. It is an aluminum honeycomb sandwich with conventional cargo tiedowns imbedded in it. The inner face is of rigidized aluminum sheet. The floor is supported at approximately 20-inch intervals by the fuselage circumferential frames. The sides are continuously tied to the lower longerons, which act as the floor-edge member in this section. The floor is designed for a cargo density of 175 pounds per square foot.

Personnel and cargo loading doors are located at the forward and aft ends of the cargo compartment. The forward door, on the right side, is 40 inches wide and 69.5 inches high. The rear door, on the left side, is 40 inches wide and 60 inches high.

The tip of the rotor can sweep from approximately Station 216 to 306.5 and is 12 inches outboard of the fuselage contour as it flaps through its travel of ± 8 degrees. To minimize the possible effects of sonic loadings emanating from the rotor tip, the side skins in this area are made from honeycomb sandwich. A titanium skin adjacent to the engine acts as a fire-wall.

(3) Aft Section

The aft section extends from Station 431.5 to Station 664.5, which is the extreme aft end of the fuselage. Its major structural function is support of the empennage, and it is built integrally with the lower portion of the vertical fin. All structural material is aluminum alloy.

b. Wing

The D266 wing is a two-spar, cantilever structure with a span of 595 inches and a forward sweep of the leading edge of $5\frac{1}{2}$ degrees. Its thickness ratio varies from 23 percent at the root to 19 percent at the tip, and it has a taper ratio of 0.83. Ailerons and flaps occupy the aft 25 percent and 28.5 percent, respectively, of the wing chord.

Optimization of the wing planform was the subject of numerous studies. It was necessary to provide for rotor flapping (with minimum mast length), maximum flap and aileron area, straight-forward drive system, and very high torsional rigidity of the wing. Another very important consideration was the location of the conversion axis with respect to the MAC so that both helicopter and fixed-wing flight requirements were satisfied. The following specific objectives were established for the wing configuration:

- Locate the elastic axis as far forward as possible to minimize the bending-torsion coupling resulting from vertical rotor oscillations.
- Provide as much torsional stiffness as possible without an undue weight penalty.
- Provide the maximum possible flap and aileron areas, and design them to deflect to the maximum possible angle, in order to minimize the projected wing area (and hence the aircraft download) during hover.
- Provide one or more unobstructed passages through which controls and the rotor drive shaft may be routed.

A study of these objectives shows that it is highly desirable to locate the main structural box as far forward as possible. A forward structural box provides a favorable forward location for the elastic axis. The location can then be further refined by optimum usage of shear-carrying structure.

The conversion shaft is set just aft of the rear spar so that it does not infringe upon the main structural box. By keeping the structural box forward, and by sweeping the wing forward, the desired relationship between the wing's center of pressure and the conversion axis is maintained. By placing the conversion axis at 36.8 percent of the MAC, it is possible to maintain normal helicopter cg limits and, because of the moment change after conversion, to shift to a normal airplane cg range of 6.9 to 32.6 percent of MAC.

The main wing box is constructed of aluminum honeycomb sandwich skins to carry all bending. Shear is carried by two spars at 8 and 50 percent of the wing chord. The front spar is a beaded channel section, while the rear spar is a stiffened tension field beam with extruded caps. The box formed by the spars and the sandwich skins gives the wing torsional rigidity. All structure in the main wing box is made of aluminum alloy.

The use of a singlecell, with the rear spar going only as far aft as 50 percent chord, permits two additional design objectives to be met: the aft 50 percent of the wing provides clear space for the controls and rotor drive, and relatively large flap and aileron chords may be used. The lower surface aft of the rear spar can then be a series of nonstructural doors that hinge downward to permit immediate access to the equipment in this region.

A torsionally efficient, lightweight structure is obtained by using sandwich construction for the skins of the structural box. With this structure, all skins are effective both in

bending and in torsion; whereas with a plate-stringer combination, the skins may be in a buckled state under load, and the stringers may provide no torsional stiffness. Since all of the bending material in the sandwich structure carries torsion, a high ratio of torsional stiffness to weight is obtained.

In addition to contributing to the torsional rigidity, the high thickness ratio contributes to the wing bending stiffness, which in turn results in a low structural weight. This is especially true for the D266 configuration because the total lift of the aircraft is concentrated at the tips during vertical flight. A study was made to determine the overall effects of wing thickness. The results, shown in Figures 8 and 9, show that weight decreases markedly with increases in thickness, while the decrease in range is almost negligible. On this basis, an average wing thickness of 21 percent is used.

Figure 10 shows the final wing planform. The conversion axis is shown at 36.8 percent of the MAC and is swept aft 5 degrees (95 degrees to the mast). The wing leading edge is swept forward 5-1/2 degrees to provide for rotor flapping and to permit a short mast to be used.

The 5-degree aft sweep of the conversion axis allows the drive shaft to be located aft of the rear spar without requiring the use of offset gearboxes. The 5-degree outboard cant of the engine minimizes exhaust impingement on the fuselage. The 5-degree aft sweep of the conversion axis, coupled with 2 degrees of wing dihedral, results in the pylons' being positioned 3 degrees outboard in the helicopter static position. During one-g helicopter flight, however, wing deflection increases the dihedral, positioning the pylons in a normal vertical direction.

Three fuel cells per side are located between the front and rear spars and extend from B.L. 65.6 to B.L. 195.0. Interspar ribs are located at the extremities of the fuel cells. There are additional interspar ribs forward of each flap and aileron hinge point. These ribs, with the spars, provide support points for the fuel cells. Access to the cells is through a removable upper panel.

The trailing-edge panels are nonstructural and are of double-skinned, beaded construction. The panels extend from the rear spar to a light subspar just forward of the flaps and ailerons. The clear space between the rear spars and the subspars is used for flap and aileron actuators and for the main drive shaft and collective control tubes. Bearing hangers for the main drive shaft are mounted on the rear spar. The lower trailing-edge panels are hinged for access to this equipment.

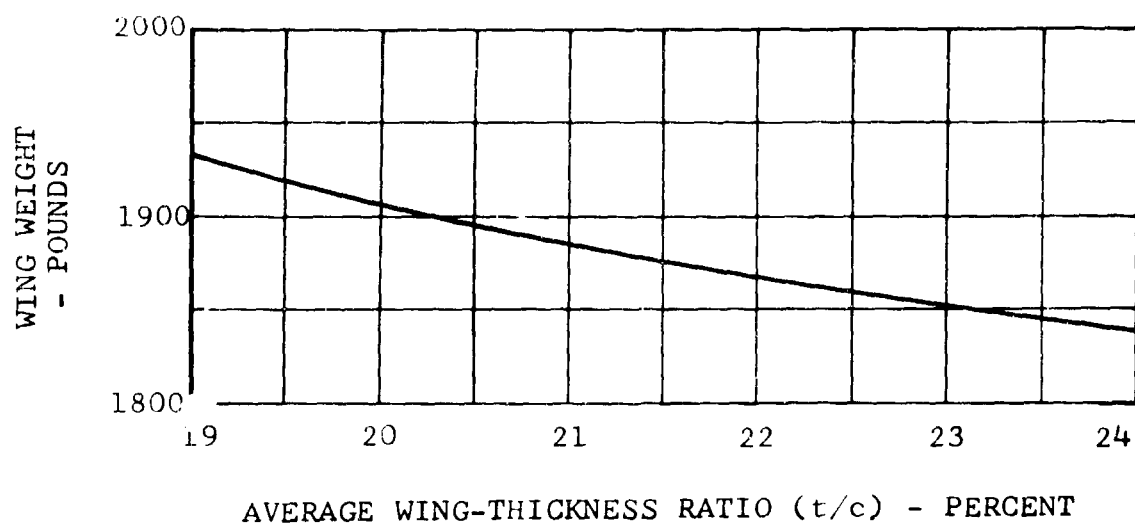


Figure 8. Variation of Wing Weight With Thickness.

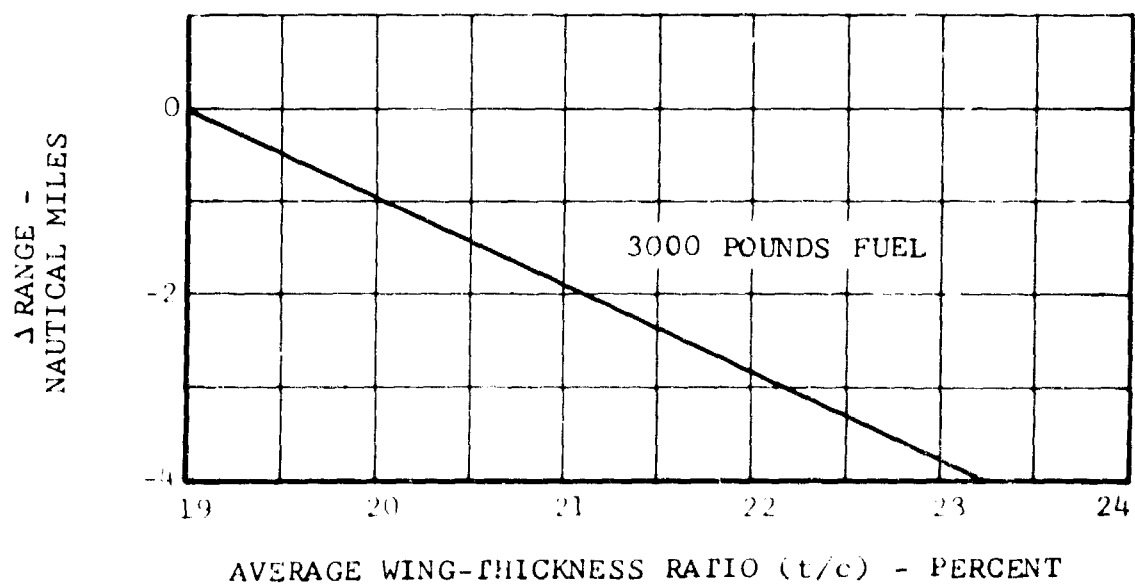


Figure 9. Effect of Wing Thickness on Range.

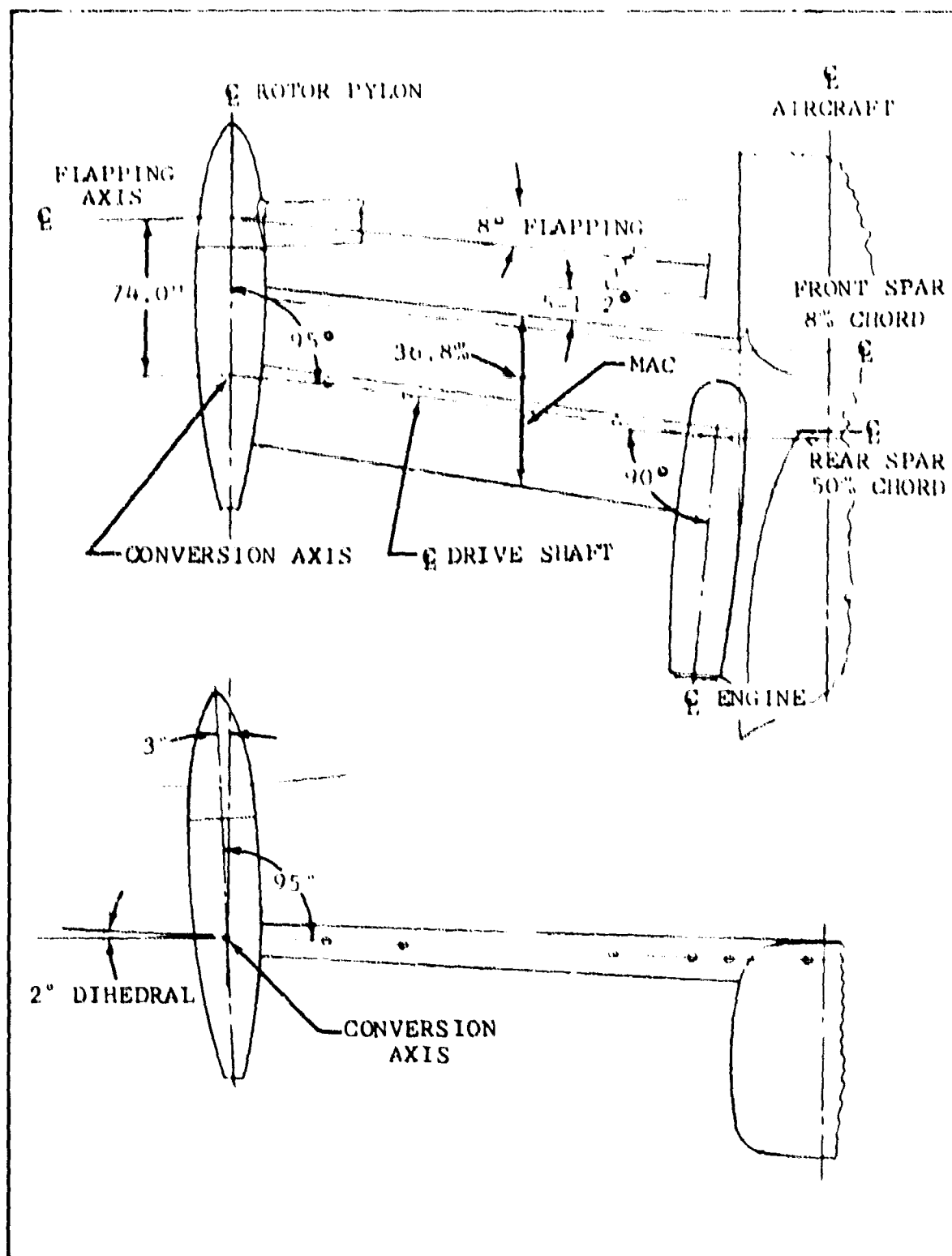


Figure 10. Wing-Pylon Geometry.

The two outboard wing ribs are aluminum forgings which provide structural support for the pylon. These ribs contain the bearing housing for the pylon spindle and are continuous into the main box. The conversion actuator is attached to the rib adjacent to the pylon, which introduces loads from the actuator into the main wing box.

A design objective is to have the minimum possible wing area projecting below the rotor during hovering flight. Accordingly, during helicopter flight the ailerons are deflected symmetrically downward along with the flaps. Maximum deflection of both surfaces is 60 degrees. In fixed-wing mode the ailerons act conventionally to give roll control.

The single-spar flap extends from B. L. 68 to 154, and the hinge line is along the 71.5-percent wing chord. It is attached to the main wing structure at three points and is hydraulically actuated adjacent to the center support point. Skins are formed from magnesium alloy, while the spars and ribs are aluminum alloy. The upper surface skins are thicker than the lower. This is to account for the oscillatory pressures on the upper surface caused by the induced velocity from the rotors in the helicopter mode of flight.

The aileron is hinged at the 75-percent wing chord and extends from B.L. 154 to B.L. 254. At the inboard station it shares a common support point with the outboard end of the flap. It is attached to the wing main structure at three points and is actuated adjacent to the center support. The maximum deflection is ± 15 degrees, with respect to the flap deflection, and is accomplished by dual boost actuators. Because of the redundancy, a servotab is not required on this surface as it is on the elevator. Since the surface is dual-boosted, no mass balance is required.

c. Empennage

The empennage has the horizontal tail attached to the vertical fin slightly below the fin midspan. For transportability, the vertical tail may be disassembled and the horizontal tail may be removed at the intersection of these two surfaces.

The rudder is a conventional, single-spar structure that forms the aft 25 percent of the vertical tail surface. The hinge line is along the 80-percent chord line. It is hinged at four points and is hydraulically actuated at a single point.

A major design consideration is the determination of the optimum vertical location for the horizontal tail. The three most probable locations are on the fuselage, on top of the vertical tail (T-tail), and midway up the vertical tail.

A fuselage-mounted horizontal tail for the D266 is undesirable for several reasons. Some of these are:

- The aft location of the engine adjacent to the fuselage causes a hot wake in the region where a fuselage-mounted horizontal tail would be located. If the tail were fuselage-mounted, it would have to be made of heat-resistant materials, which would be heavy.
- A fuselage-mounted horizontal tail would be directly in the wing wake, due to the high wing configuration of the D266, during cruise and fixed-wing flight. This makes $\frac{dC_L}{d\alpha}$ large. Since the longitudinal stability depends on the product of (Tail Area) $\times (1 - \frac{dC_L}{d\alpha})$, a large horizontal tail area would be required.
- A low horizontal tail is sensitive to the reflected wake of the rotor when in ground effect.

The T-tail was seriously considered during the concept study, but it was felt that the deep stall problem, caused by the wake of a stalled wing blanketing the tail, could be potentially serious.

A good compromise, therefore, is to locate the horizontal tail only sufficiently high on the vertical fin to keep it out of the wake of the engine and wing. The stabilizer is a continuous surface with a span of 241.4 inches. It is a two-spar structure using aluminum honeycomb sandwich construction for the upper and lower surfaces between spars. The sections forward and aft of the spars are of light aluminum construction.

The elevator is similar in construction to the rudder. It is controlled by a single hydraulic boost cylinder. A combined servo/trim tab is located on the left elevator. It provides both trim and control aid in the event of a boost malfunction.

d. Landing Gear

Several design objectives were set forth as guides for the landing gear configuration. Some of these objectives are:

- Obtain a wide main landing-gear tread to provide maximum stability in takeoff and landing.
- Use relatively low-pressure tires to obtain good flotation characteristics for the gear.
- Retract the main gear clear of space allotted for the cargo compartment.

- Configure the gear in such a manner that external fairings (if required) will result in the minimum aircraft drag.

The landing gear is of tricycle configuration, with both nose and main gears being housed in the fuselage. Each gear has two wheels with low-inflation tires. The nose gear is a conventional dual-wheel arrangement, while a tandem arrangement is used on the main gear. The latter configuration maintains the dual-wheel capability; but, when retracted, it affords a low fuselage drag profile comparable to that of a single-wheel gear. Steering is accomplished by differential cyclic-pitch change and by braking. Nose-gear steering is not required.

- The nose wheels are 7.00-6 magnesium alloy castings that mount 7.00-6 Type III 8-ply tube-type tires inflated to 44 psi. Effective ground pressure is 24 psi. A shimmy damper is mounted on the nose-gear strut to permit STOL operation.

The main wheels are 24 x 7.7 magnesium alloy castings that mount 8.50-10 Type III 6-ply tube tires inflated to 61 psi. Effective ground pressure at design gross weight is 37.7 psi. The aft wheel on each side incorporates a single disc-type brake. A four-bar linkage that retracts upward and inward was configured to give a main gear tread of 170 inches, which gives a turnover angle of 35 degrees. Both gears use hydraulic power for extension and retraction. A manual unlocking system permits free-fall of the gears if hydraulic power is lost.

3. PROPULSION SYSTEM

The D266 propulsion system arrangement was selected on the basis of studies of individual component requirements and the integration and interrelation of the major propulsion system components with the basic aircraft arrangement. Parameters such as engine type, engine location, wing geometry (sweep, planform, etc.), and wing structural arrangement and resulting drive-system arrangement were evaluated in terms of aircraft weight and performance. Secondary effects of these parameters on related components, such as structure, controls, and accessories, were also considered. The results of these studies formed the basis on which the T64-GE-12 engine and the shoulder-mounted engine installation aft of the wing were selected. The system is described in detail in Section II.

a. Powerplant

The D266 is powered by two General Electric T64-GE-12 engines. Final selection of the General Electric T64-GE-12 engine for the D266 was made after a comprehensive study of both production and advanced engines by two manufacturers. The T64-GE-6A and the T64-GE-12 have military ratings of 2690 and 3435

horsepower, respectively. Although the T64-GE-6A has the power required to meet the hot-day hover performance and speed requirements, its power margin is inadequate for one-engine-out hover and normal operational growth of the aircraft. It is also heavier by 30 pounds (per engine) than the higher-powered T64-GE-12. The ample power margin of the -12 engine permits lower power levels (turbine temperatures) in the normal operating regimes, which will provide a longer and more trouble-free engine life. A comparison of performance of the T64-GE-6A and the T64-GE-12 is shown in Table II.

The T64-GE-12/AAFSS is the same engine as the T64-GE-12 except for an additional hot-day rating. This higher hot day rating provides an improvement in hovering performance but no improvement in fixed-wing flight because it has the same torque limit as the -12. Because the D266 with the T64-GE-12 engine exceeds the hot-day hovering requirement by a wide margin, no advantage is to be gained by using the T64-GE-12/AAFSS version. Therefore, the T64-GE-12 was selected for the D266 Composite Research Aircraft.

Studies were made of various locations for T55 and T64 engines. Locations considered included: mounting on pylons which rotate during conversion, fixed installations at the wingtip, underwing installations, midwing mounting aft of the wing spar, and fuselage mounting.

The rotating engine installations yielded the lightest and simplest propulsion system arrangement but had the basic disadvantage that the engines were vertical in the helicopter mode. The requirement for retractable exhaust deflectors, to prevent exhaust impingement on the ground and the associated fire hazard, adds complexity to the design of vertical engine installation. An additional disadvantage was the reduced roll-angle clearance of the low engine tailpipes.

The underwing position provides for good mounting and accessibility but imposes an excessive weight penalty. It also necessitates moving the front spar aft, which results in rearward displacement of the wing elastic axis and the fuel center of gravity.

Mounting the engines aft of the wing spars at midwing, or on the centerline at the wingtip, requires an additional complex mounting structure at either location. The drive-system components and weights are basically the same as for the location of engines on the fuselage shoulder aft of the wing-fuselage intersection.

Of the fixed-engine installation, the shoulder location provides the best mounting arrangement, with minimum weight of drive-system components and associated structure. It also affords clearance for routing controls past the engine gearbox.

TABLE II			
T64-GE-6A AND T64-GE-12 ENGINE COMPARISON			
		Engines	
	Units	T64-GE-6A	T64-GE-12
Military Rating	shp	2,690	3,435
Normal Rating	shp	2,270	3,230
Torque Limit	ft-lb	1,350	1,520
Dry Weight	lb	723	693
Hovering Ceiling at DGW-- OGE-95°F - MRP	ft	6,700	11,050
Gross Weight to Hover - OGE-6000 ft-90°F - MRP	ft	23,500	28,100
Hover Ceiling at DGW - One Engine Out-OGE Standard Day - MRP	ft	-	6,200
Maximum Speed at S.L. - 1350 ft-lb Torque Limit	kt	345	345

The installation requires no modifications or changes to the basic engine. Each engine, with a reduction gearbox attached to the output pad, is mounted in a nacelle adjacent to the fuselage behind the aft wing spar. The relationship to the aircraft is shown in Figure 252. The engines are operated over a wide range of speed--from 8050 rpm to 16,600 rpm--for the various modes of flight. This range is well within the operating limitations defined by the engine specifications.

The engine is supplied with oil from a 3-gallon tank in the nacelle aft of the engine gearbox and forward of the engine firewall. Fuel is supplied by two separate systems, one for each engine. Cooling is provided by a turbine-driven bleed-air fan.

b. Drive System

The D266 drive system consists of two engine gearboxes, two main transmissions, and an accessory gearbox which are interconnected by drive shafting. The overall reduction ratio is 40.6:1.

Upon selection of the engine location, studies were conducted to define the arrangement of the drive-system components. These studies included investigations of engine gearbox, accessory drive, drive shafting, and main transmission arrangements.

The use of a 50-percent rear wing spar with a 5-1/2-degree forward sweep allows the conversion axis and the complete power train to be located aft of the wing structure. This arrangement permits the use of direct power drives among all gearboxes and eliminates the offset boxes that would be required if shafting is run down the leading edge, and/or if the conversion axis is between spars. The engine gearbox arrangement studies showed that by using 90-degree gearboxes, the units at the two engines would be identical. The 90-degree angle not only minimized the number of different components but also permitted the engine exhaust to be rotated 5 degrees outboard, to increase its clearance with the fuselage.

The engine gearbox is bolted directly to the engine output pad and has two fittings for attachment to the forward mounts. Engine power is delivered to the gearbox at power-turbine speed (16,600-rpm maximum) and is reduced to 9284-rpm maximum at the output drive shaft flanges. A freewheeling unit permits autorotation in the event of engine failure and allows single-engine operation.

Each main transmission is attached at the wingtip to a spindle-type mount, which permits the transmission to rotate for conversion between the vertical and horizontal positions. Hydraulically powered and mechanically interconnected ball screw actuators support, power, and control the conversion of the pylons. Each transmission also has a self-contained lubrication and cooling system that includes a shaft-driven oil-cooler blower and a hydraulic-pump drive.

Different gearing, shafting, and mounting arrangements for the main transmissions were studied. The use of a low-reduction bevel-gear stage to bend the power through a 95-degree angle, and two stages of high-reduction planetary units, each having six planets, provided the lightest gear-stage arrangement. The mast length was made short by extending the basic gear housing to provide a support point as close as possible to the

rotor hub. This arrangement was found to be lighter and more rigid than one in which the mast extends through the transmission.

Various arrangements of accessories were studied. They included mounting of the principal units at the main transmissions, at the engine gearboxes, or on a separate accessory box. A separate box, between the engines, was selected because it could provide the drive for most of the accessories - two generators, two tachometers, and a hydraulic pump - at minimum weight, and with ample space for accessibility and future accessory requirements. At the other locations, duplicate gear drives for the accessories would be required, and space is limited. This center box is also used as a support for the interconnect drive shafting.

The main drive shafts transmit torque from the engine gearboxes to the main transmissions. The interconnect drive shaft connects the two engine gearboxes through the accessory gearbox.

The arrangement of the drive shafting was selected on the basis of minimizing the number of components and maximizing their operating speed to achieve a lightweight system. A maximum drive shaft operating speed of approximately 9000 rpm was found to afford a shaft size that required only three supports between the engine box and the main transmission to meet the critical speed requirement, and it has a good strength-to-weight ratio to carry the maximum operating torque. This drive shaft speed also provides a good balance of gear-stage reductions in the main transmission and engine gearboxes.

Each main drive shaft consists of two floating sections and a long, straight section supported in bearing hangers. Each end of the supported section is attached to one of the floating shafts through a spherical gear type coupling that permits misalignment and axial freedom.

The interconnect shafting between the engine gearboxes consists of two floating shaft sections with spherical gear-type couplings on each end. Except for size, it is similar to the main drive shafts.

Design features include interchangeable bevel-gear assemblies, flexible drive shaft couplings, and modular major components.

Construction is rugged; no shimming or alignment is required during maintenance. All components are readily accessible, a minimum number of special tools are required, and interchangeable parts are used throughout.

4. ROTOR SYSTEM

a. Description

The 38.5-foot-diameter rotors, which provide both lift for helicopter operation and thrust for fixed-wing flight, are of the multibladed, semirigid type. They are mounted on universal joints to permit rotor tilt (flapping) relative to the drive shafts. The principal components of the rotors are shown in Figures 253 and 254.

Extensive rotor design studies, including design layouts and rotor load and vibration analyses, were conducted on three basic rotor configurations prior to the selection of the rotor for the D266. The results of these studies indicated that the multibladed, semirigid rotor system best satisfied the basic requirements of the helicopter and fixed-wing operating modes. The final refinement in the design of the rotor system resulted from integrating specific considerations of aerodynamic efficiency, oscillatory blade loads, mechanical simplicity, and maintenance and reliability. The design and configuration of the D266 rotor system embody advanced engineering concepts; yet the system is similar to, and retains features of, multibladed rotor systems that have been proved successful by flight-test evaluation.

Considerable attention was given throughout the design study to the achievement of low vibration levels in the D266. Because the rotor is the primary source of vibration, both in helicopter and in fixed-wing flight, minimizing vibration was of paramount concern in the configuration selection and design of the rotor system.

In the helicopter mode, rotor vibrations arise from asymmetry of the airflow that is produced by forward flight. In fixed-wing flight, with the masts fully converted, the rotors also operate in an asymmetrical condition, because the gravity field excites the blades in the chord-bending direction as they rotate. In both flight modes, a two-bladed rotor transmits in-plane shear forces to the pylon at a two-per-rev frequency. These two-per-rev vibrations arise from gravity excitation in the fixed-wing flight mode and from first-order aerodynamic forces in the helicopter flight condition.

In a rotor with three or more blades, however, in-plane shear forces resulting from gravity and the first-order effects are not transmitted to the pylon, because they are cancelled among the blades. The lowest vibratory frequencies to be transmitted to the pylon would be at a three-per-rev frequency for a three-bladed rotor. Basic excitations at this frequency are due to small, higher-order aerodynamic effects. Because a multibladed rotor offers the potential advantage of essentially eliminating all vibration in the fixed-wing mode, where the aircraft would spend most of its flight time, and in consideration of additional requirements described below, the three-bladed rotor configuration was selected for the D266. Four-bladed configurations were also considered but were found to impose a weight penalty, with no advantages over the three-bladed rotor.

Early in the design study, it became apparent that the feasibility of some of the configurations depended upon the blade-flapping amplitude that would be encountered in various modes of flight. Calculations were made to predict the amount of flapping that would take place during conversion, in steady fixed-wing flight, and in maneuvers during forward flight, as well as for control in hovering. The conditions were found to be critical for maneuvers in fixed-wing flight and for hovering with full control displacement of the rudder pedals and the control stick. Pitch and yaw control in hover require tilting of the rotor disc, i.e., flapping. The rotors are tilted differentially for yaw control and in the same direction for pitch control. The amount of flapping which takes place in fixed-wing maneuvers depends on the pitch-flap coupling ratio, $\delta-3$. High values of $\delta-3$ reduce flapping. Early in the design study, a pitch-flap coupling angle of 30 degrees was selected. From the requirements for fixed-wing flight and hovering maneuvers, it was established that 8 degrees of flapping clearance would be required to accommodate the flight conditions which would be encountered. For normal, steady, level-flight conditions, however, an angle of 4 degrees would rarely be exceeded.

The type of articulation to be used also had to be determined. The flex-beam rotor offered a significant weight advantage because of the lack of mechanical joints. It can generate high control moments by the elastic deflection of the flex-beam plates that fasten the blades to the rotor mast. After examination of many design approaches and many different materials, it was concluded that extensive work would be required to develop a "flex-plate" with adequate fatigue life for the flapping angles that would be encountered.

A rotor configuration using offset flapping hinges was then examined. The rotor hub with its three flapping hinges was found to be quite heavy. These hinges not only had to carry

the centrifugal load but also had to carry high chord bending moments that resulted from Coriolis loads produced by the flapping of the semirigid blades. Classically, this problem has been avoided in fully articulated rotor systems by the use of lead-lag hinges. It was desired, however, to avoid the complexity and the mechanical instability problem of fully articulated rotor systems.

With three-bladed, gimbaled rotors, there are no restrictions on the flapping amplitude, and Coriolis loading is essentially zero. From a weight standpoint, the configuration was promising, so means for providing hub restraint were investigated. Several design approaches for attaching springs on the hub were explored. Systems which had adequate fatigue life were all found to be excessively heavy.

Systems were then investigated for placing the hub-restraint springs in the fixed, nonrotating system. This approach eliminated the fatigue loading, as the springs were deflected only statically by blade flapping. Several feasible mechanical arrangements were found for the application of this principle. From the study, it became apparent that the three-bladed, semirigid, gimbal-mounted rotor, with hub restraint in the fixed system, offered the best approach for the rotor system of the D266.

The precone angle of 2.5 degrees, which is built into the yoke spindles, minimizes the steady beamwise bending moments on the hub and reduces spindle bearing loads and blade deflections. This reduction, in turn, helps to lower control system loads. The angle selected is a compromise between the ideal precone required for helicopter operation and that desired for fixed-wing flight. The thrust of the rotor is quite different for the two conditions, as is the blade centrifugal force, because of the difference in operating speeds; therefore, the precone angle is close to optimum for all flight conditions.

With a complete universal-joint mounting, as is used on multi-bladed, semirigid rotors, undersling is not necessary because the rotor cg will not be forced to oscillate; the blades will rotate as elements of a true cone even when the tip-path plane is at an angle to the mast. In the D266 design, this feature has allowed the rotor-mounting universal joint to be located inside the center of the hub yoke, which results in a compact, lightweight system. Secondary benefits accrue in the control system and in clearance requirements due to blade pitch and rotor flapping--especially for nonoperating conditions such as ground clearance checks.

Each rotor has three highly twisted blades, which are bonded assemblies made primarily of aluminum alloy materials. The blades must be aerodynamically clean and must incorporate a high degree of twist in order to maintain good aerodynamic efficiency at high speeds. As shown in Figure 254, the blades have a constant 20-inch chord and a constant twist rate, but they are tapered in thickness.

The materials selected for the various components of the rotor hub are, for the most part, similar to current production items; but titanium alloys have been chosen for several important components. Although stiffness is a primary requirement for the rotor hub yoke, it was found that a forged titanium part would be quite satisfactory and would result in the lightest weight. The hub is mounted on its driving shaft (mast) by means of a universal joint of conventional design.

The D266 rotors are provided with hub-restraint springs to permit increased center-of-gravity travel and to augment control power for pitch and yaw. The configuration selected places the springs in the nonrotating system, where they are not subjected to one-per-rev oscillatory loads, as would be the case if they were rotating with the hub. While this arrangement requires the use of a large, moment-loaded bearing, it is light and permits the use of asymmetrical spring rates.

The hub fairing, or spinner, is made of fiber glass stiffened with an aluminum honeycomb core. The nose is spun aluminum. Spherical surfaces on the basic spinner match the inboard end of the blade root cuffs to cover the spinner openings during high-speed operation.

The blade cuff fairings are also made of fiber glass and aluminum honeycomb. They are shaped to fair the blade doublers and the blade grip forging and to provide helical twist for the inboard portion of the rotor blade.

b. Aerodynamic Considerations

The selected rotor design parameters favored efficient hover and cruise performance equally and did not unduly penalize either flight mode.

From consideration of the operating conditions, a highly twisted, low-solidity rotor would be optimal for fixed-wing flight; but a low-twist, high-solidity rotor would be best for helicopter flight. The effect of these opposing requirements is minimized by reducing rotor rpm in the cruise condition. The wide range of operating rpm of the T64 engines

used in the D266 permits the use of a cruise rpm which is less than one-half that of the hovering value; it thus affords an acceptable design compromise. The differing requirements for blade twist are satisfied by using a combination of linear twist on the outboard part of the blade and helical twist on the inboard part.

A parametric performance study was made of the effects of tip speed, blade twist and twist distribution, and rotor solidity.

(1) Hovering Efficiency

Rotor performance in hover was analyzed for a wide range of parameter variations before the final design was selected. Major items varied were solidity, tip speed, and blade twist. This comparison study was made with Bell Helicopter Company IBM Computer Program F35 using NASA 0012 airfoil data. To determine the effect of blade twist, radius and solidity were held constant and data were obtained for several different twist values through a range of tip speeds. For the computer analysis, the blade was divided into four segments and a linear twist rate was used for each segment. The blade was divided into the following segments:

- Segment 1 $r/R = 0.10$ to 0.20
- Segment 2 $r/R = 0.20$ to 0.35
- Segment 3 $r/R = 0.35$ to 0.50
- Segment 4 $r/R = 0.50$ to 1.00

Figure 11 shows the rotor horsepower required to hover for several of the twist configurations studied. This figure shows the effect of both tip speed and twist. Each blade configuration is designated in terms of the twist rate for each of the four blade segments. The twist rate value for the inboard segment is given first and is in terms of twist rate for the full blade radius. Figure 11 shows that a linear twist of -30 degrees gives the best hovering performance. A higher-than-normal twist rate (in terms of helicopter practice) is optimal, because of the high disc loading of 10 pounds per square foot. The requirement for high propulsive efficiency in the fixed-wing flight mode, however dictates an even more highly twisted blade. A twist of -40 degrees is near optimum in fixed-wing flight but is seen in Figure 11 to be very poor from a hovering-power-required standpoint. The necessary high twist for fixed-wing flight is effectively achieved by the blade with the -60, -45, -30, -30 twist rate. As shown in Figure 11, this twist rate also gives acceptable hovering performance.

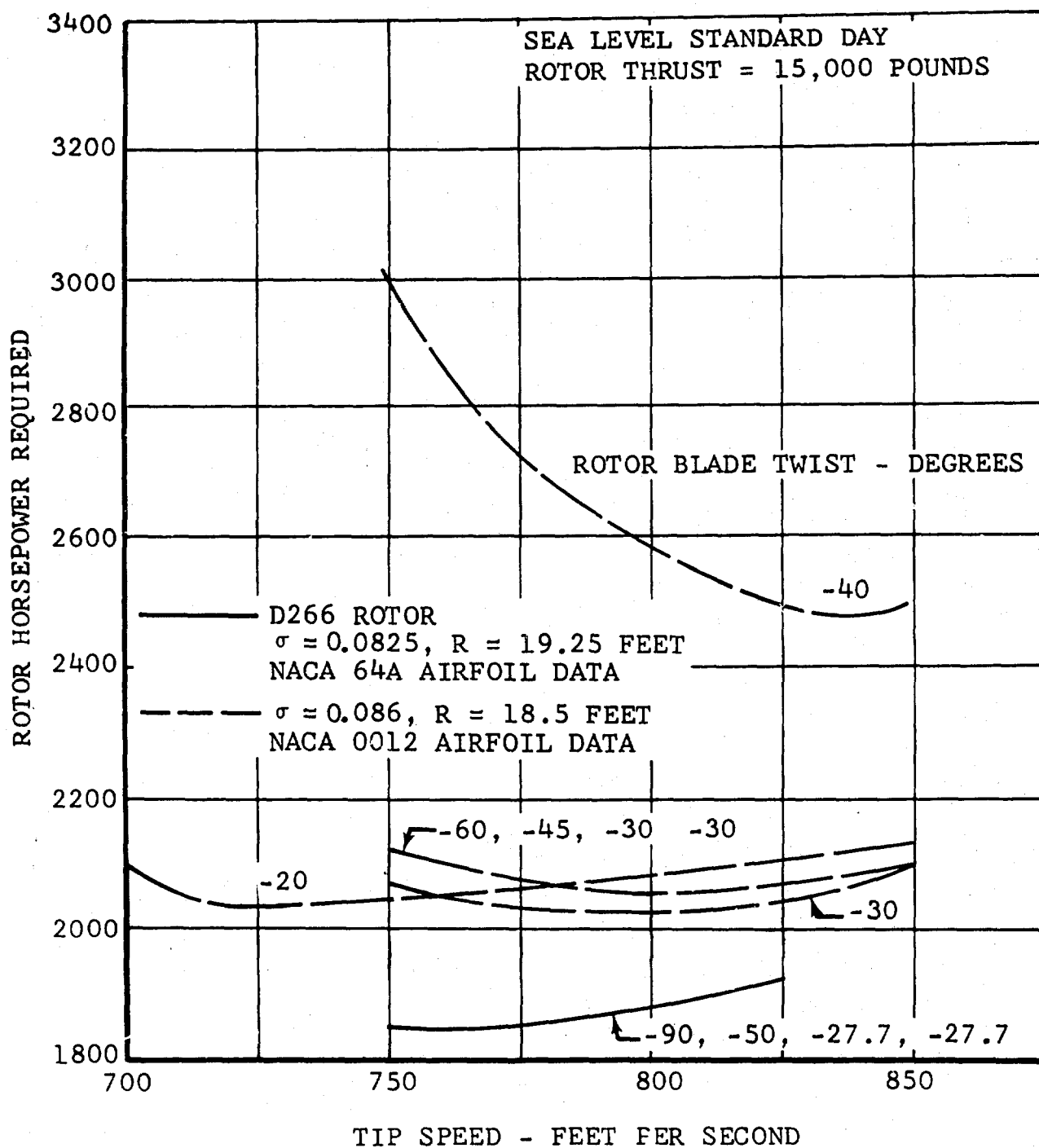


Figure 11. Effect of Twist on Hovering Power Required.

The effect of rotor solidity variation is shown in Figure 12. Rotor power required to hover is shown for one twist-rate distribution and three tip speeds. This figure illustrates that the higher the tip speed, the lower the solidity required. The hovering power required increases somewhat with lower solidity and higher tip speed, but the cruise efficiency improvements make this a worthwhile compromise.

Hovering power for the selected design parameter of the D266 rotor is shown in Figure 11, but the data are not directly comparable with the results of the parametric study, as they include the effect of the larger rotor diameter of the D266. The helical twist in the D266 blade cuff is approximated in the computer analysis by the different linear twist rates in blade segments 1 and 2. Data for the D266 rotor using NASA 64A series airfoils are also included in Figure 11 to show the improved performance obtained with low-drag airfoil sections.

(2) Propeller Efficiency

The propeller efficiency was calculated for a range of values of tip speed, blade twist, and solidity. The range of values of twist and solidity was the same as that used for the hovering study. For fixed-wing flight, tip speed was reduced to a range more desirable for propeller operation. Efficiencies are shown in Figures 13 and 14 for tip speeds of 400 and 600 feet per second.

Also shown in Figures 13 and 14 are lines of ideal efficiency. The ideal efficiency is defined as being that condition under which the profile drag coefficient for all blade elements is 0.010. Because the minimum drag coefficient of the 0012 airfoil data being used for this study was 0.010, this was a limiting value on the maximum obtainable efficiency. Induced drag is calculated for each element based on angle of attack.

With optimum twist distribution, efficiencies equal to the ideal efficiency are obtained. Figures 13 and 14 show that the linear -40-degree twist produced very high efficiencies throughout the airspeed range at both 400- and 600-feet-per-second tip speed. This high twist, however, is completely unacceptable from the hovering-power-required standpoint. Studies of different twist distribution showed that propeller efficiency was quite sensitive to the rate of twist on the inboard 35 percent of the blade. This sensitivity was due to stalling of the inboard segments in the negative angle-of-attack direction for low twist rates. Efficiency for the basic -30-degree twist distribution is increased appreciably when the inboard twist rate is increased as shown in Figures 13 and 14 for the -60, -45, -30, -30 twist distribution.

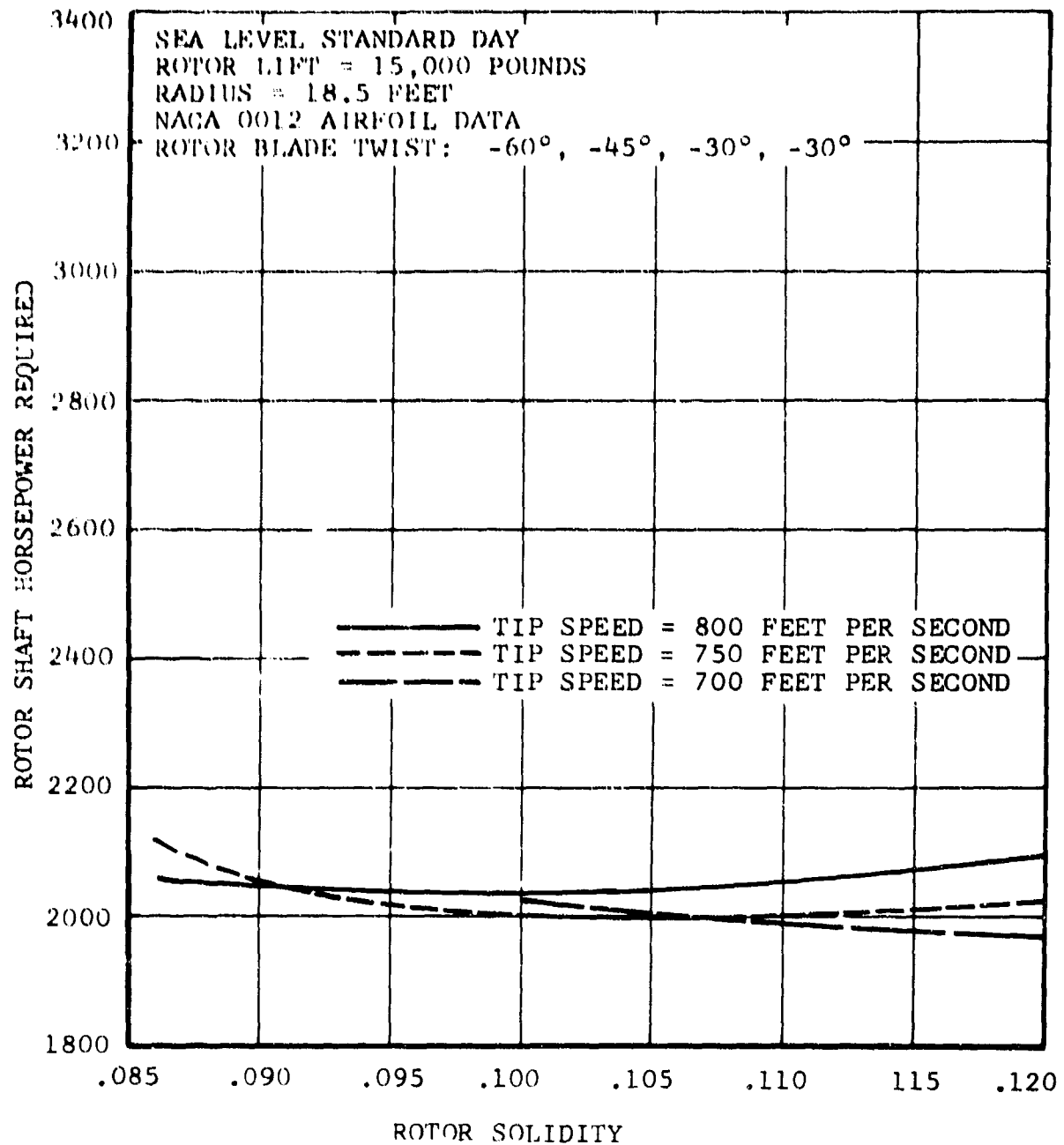


Figure 12. Effect of Solidity on Power Required to Hover.

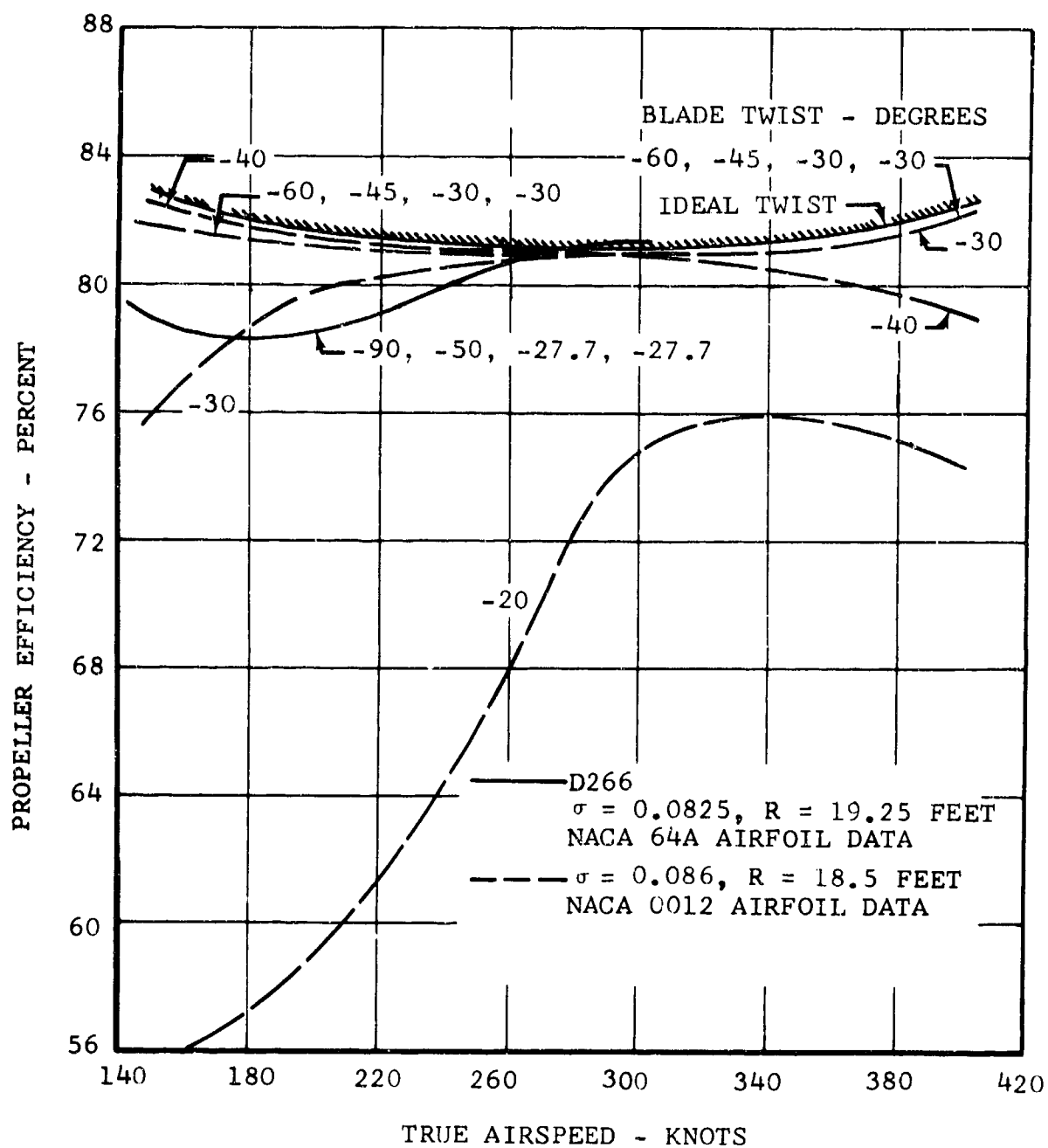


Figure 13. Effect of Twist on Propeller Efficiency, Tip Speed of 400 Ft/Sec.

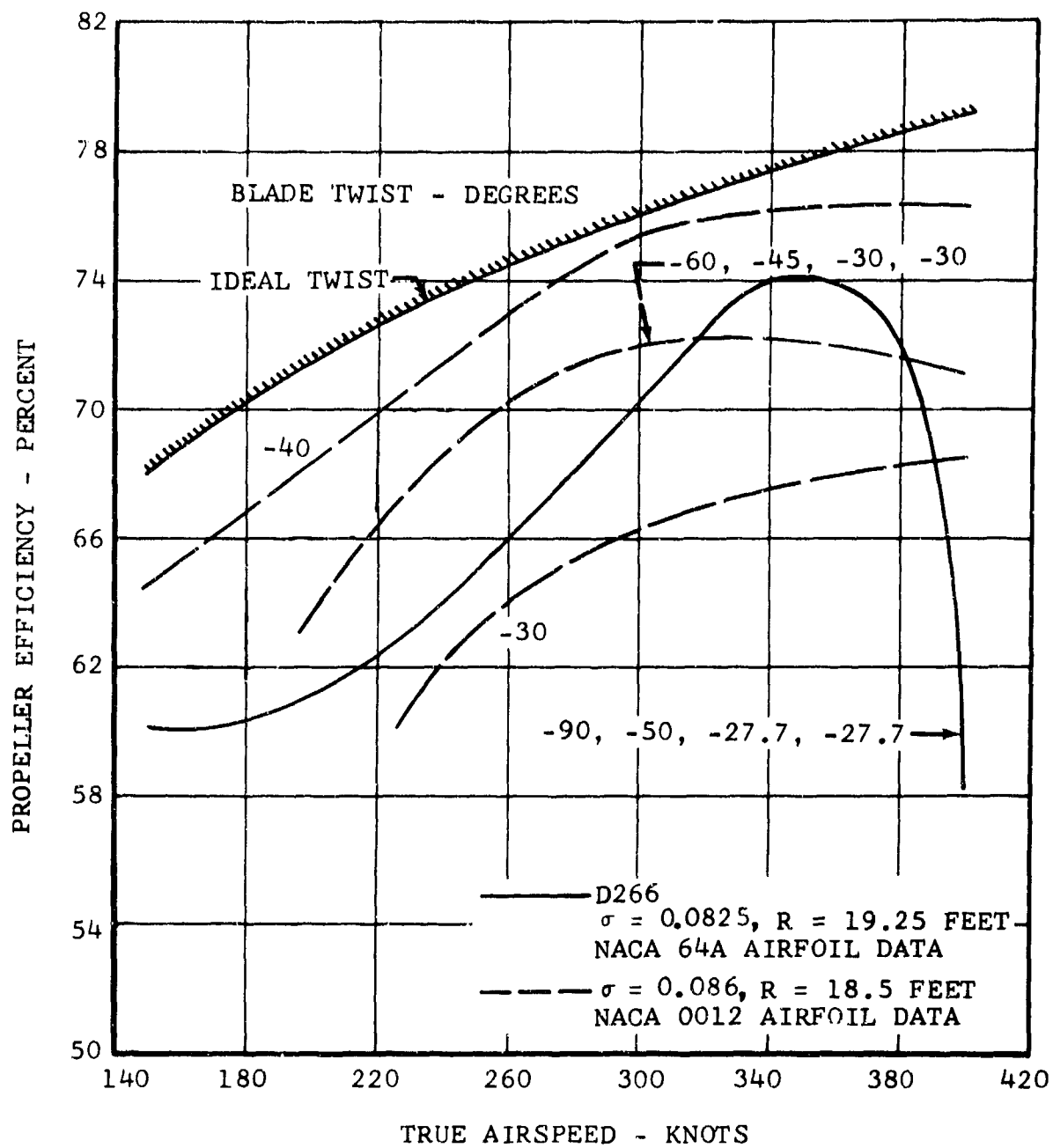


Figure 14. Effect of Twist on Propeller Efficiency, Tip Speed of 600 Ft/Sec.

Figure 11 shows that this twist distribution is also acceptable for hovering.

The final selection of blade twist was made after evaluation of the effects of twist on blade loads and stresses. High twist rates on the outboard portion of the blade increased blade stresses during fixed-wing helicopter flight. The twist distribution for the D266 rotor of -90 , -50 , -27.7 , -27.7 is based on consideration of rotor loads, as well as performance, in helicopter and fixed-wing flight.

The effect of increasing solidity is seen in Figure 15 to have a pronounced adverse effect on propeller efficiency. The final selection of solidity was a compromise between the two flight conditions but resulted in only a small loss of efficiency for either condition.

Data for the final configuration selected for the D266 are included in Figures 11 through 14. These are not directly comparable with the data from the study, because of the increase in diameter and the difference in airfoil sections. Low-drag 64A-series airfoils, with a minimum drag coefficient of 0.008, are used on the D266. These plots show that an increase of approximately 5 percent in efficiency can be obtained with the low-drag airfoils. In addition to these differences, the computed results for the D266 include a modification to the computer program to include the swirl losses in the slipstream, which amount to about a 3-percent loss in propeller efficiency.

c. Rotor/Pylon Stability

Wing-mounted propeller systems are susceptible to whirl instabilities at the high airspeeds typical of modern turboprop airplanes and current VTOL designs. This phenomenon is called nacelle whirl flutter. It is caused by the gyroscopic and aerodynamic moments on the propeller. A flapping rotor mounted on a flexibly supported pylon may encounter similar phenomena. The blade flapping and pitch-change degrees of freedom introduce additional considerations, other than pylon damping and elastic restraint, which govern the stability of these rotor-ptyon systems.

During the past three years, Bell Helicopter Company has conducted an extensive analytical and experimental research program to explore this problem area. A complete understanding of the stability mechanism and the effects of the important controlling parameters has been attained. Several analytical methods have been derived and programmed for the IBM computer which have given excellent correlation with data from wind tunnel tests of scale models and the full-scale XV-3. As a

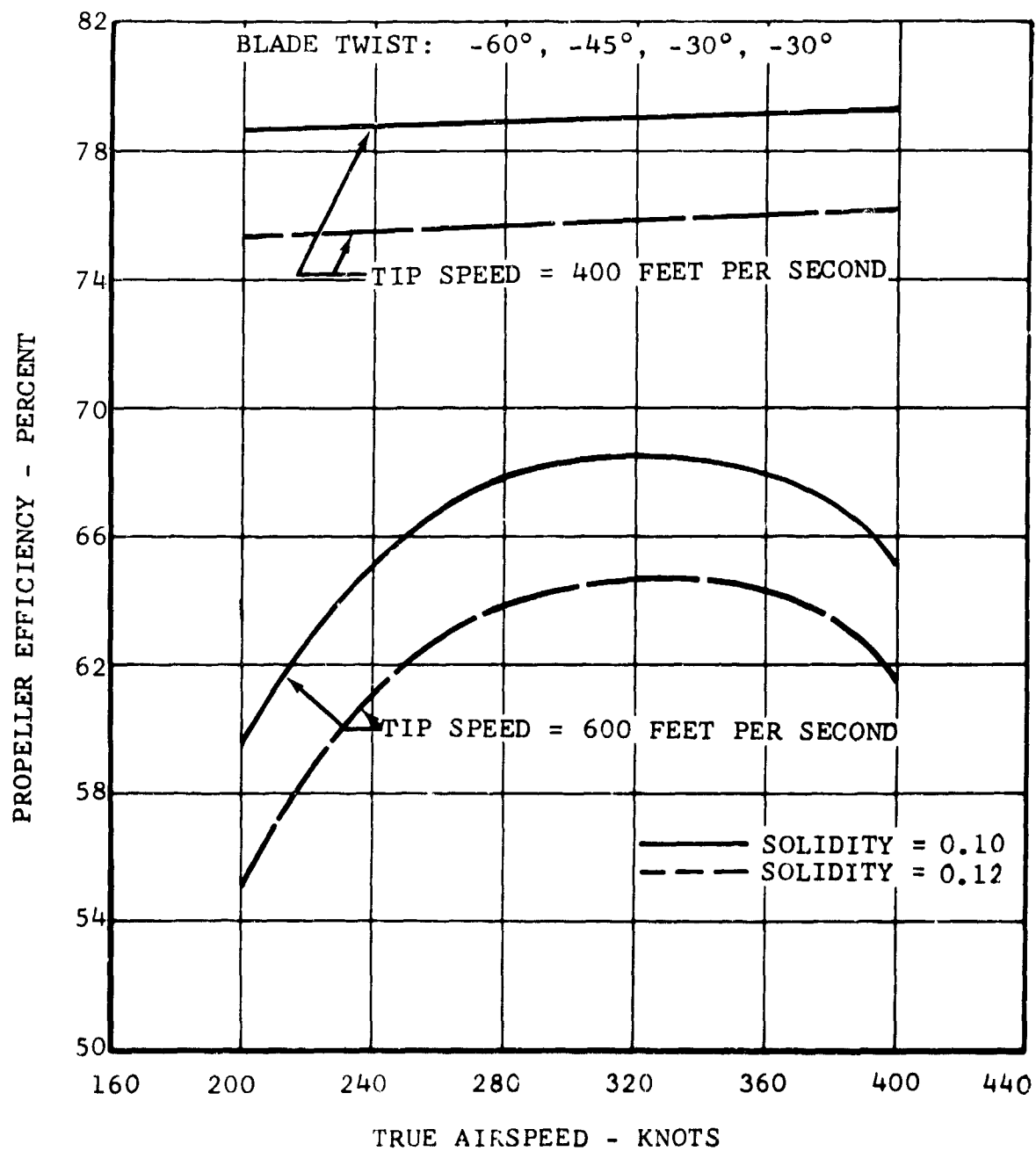


Figure 15. Effect of Solidity on Propeller Efficiency in Forward Flight.

result of this research effort, analytical and model test techniques are now available that permit the design of aircraft that will be completely free of rotor/pylon stability problems.

Tests of the full-scale XV-3 Convertiplane in the NASA-Ames 40-by-80-foot wind tunnel during 1966 have verified the accuracy of these techniques. Tests were conducted to evaluate variations of the major controlling parameters and to establish the effectiveness of several design solutions. All predicted trends were confirmed, and the predicted levels of stability and speeds for instability showed good agreement with the test results.

The work described above has revealed that several design approaches will provide a satisfactory solution to the rotor-pylon stability problem. During the design study of the D266, these approaches have been evaluated both analytically and experimentally. The more promising of these approaches, and the design study results that led to the final selection of the design used in the D266, are described and discussed below.

(1) Basic Considerations

Rotor-pylon instabilities can occur at the high blade inflow angles (i.e., high advance ratios) encountered at advanced aircraft speeds. These motions may be of a limit-cycle nature, or they may be undamped whirling instabilities of the rotor and/or pylon. The principal cause of this behavior is the aerodynamic in-plane shear force generated by or accompanying rotor precession. The phase of the force is such as to produce a negative damping and/or negative spring effect on the pylon.

Instability of the rotor-pylon system can occur in one of several modes of motion. Like wing flutter, it will occur at some speed. The aircraft must therefore be designed so that the instability speed is outside the flight envelope. The design solution must be compatible with other aircraft and mission requirements. Other aircraft characteristics which depend on rotor behavior must also be considered. Two such problems were discovered during the XV-3 Convertiplane flight-test programs: a decrease in aircraft short-period damping with increased airspeed, and wide rotor-blade flapping during maneuvers.

The short-period airplane stability is decreased by the negative damping contributions of the rotors. This negative damping arises from the in-plane shear force of the rotor and is

the same effect described briefly above for the pylon. Pitch-flap coupling, $\delta-3$, can be used to decrease negative rotor damping at the low frequencies associated with the short-period aircraft motion, but it aggravates the rotor-pylon stability problem. Applying hub restraint to the rotor produces positive damping, which has a beneficial effect on rotor-pylon stability. Decreasing the length of the rotor shaft improves both short-period aircraft and rotor-pylon stability, because it reduces the effective moment arm of the rotor in-plane shear forces.

During maneuvers, high rotor-blade flapping is caused by the asymmetrical flow field resulting from aircraft sideslip and/or angle-of-attack changes. The use of a high pitch-flap coupling ratio, $\delta-3$, very effectively reduces blade flapping; but it must be used with discretion, as high values of $\delta-3$ have adverse effects on rotor-pylon stability.

Another approach for reducing flapping which has been explored by Bell Helicopter Company is the use of a flat-tracking device. The device may take many forms, but essentially it senses rotor-blade flapping and introduces an appropriate signal into the control system to reduce the flapping. In the simplest form this can be done with a direct mechanical linkage; but only small reductions in flapping can be obtained in this way because high coupling ratios lead to rotor instability. By the use of a lagged network or an integrating feedback function which can be accomplished with a hydraulic servo system, flapping may be quite effectively reduced. Such a system was investigated during rotor-pylon stability tests of a scale wind-tunnel model, reported in Reference 1.

(2) Possible Design Approaches

(a) Pylon Restraint

Nacelle whirl flutter investigations by NASA and others have indicated that for stability, a certain level of stiffness and damping in the pylon suspension is required. Increasing damping and stiffness were both beneficial. These same two parameters are also important in controlling rotor-pylon stability. Damping is effective in stabilizing the pylon modes, and the amount of damping required decreases as the pylon frequencies increase. The rotor mode, however, is little affected by damping but is dependent primarily on aircraft speed, pitch-flap coupling ratio ($\delta-3$), and pylon restraint. The higher the $\delta-3$ and the higher the airspeed, the greater the restraint must be to provide stability. Therefore, high pylon restraint is desirable for all modes. High restraint can be achieved in a practical design by mounting the pylons

rigidly to the wingtips of the aircraft. During the D266 design study, this approach was evaluated in analytical calculations and model tests. Its primary advantage was its basic simplicity. It was found that the pylon restraint provided by the wing structure provided the desired level of stability for the D266 for delta-3 angles up to 20 degrees. At higher values of delta 3, structural weight penalties were prohibitive.

(b) Swashplate-Pylon Coupling

Considerable research and development effort has been directed toward evaluating and refining design techniques of what is called swashplate-pylon coupling. This design approach provides stability by mechanically coupling the swashplate to pylon motions. This feedback between pylon and swashplate motions decouples rotor motions from pylon oscillations, causing the rotor in-plane shear force to become small or even stabilizing. The mechanical simplicity of swashplate-pylon coupling is illustrated by the schematic in Figure 16.

(c) Automatic Swashplate Coupling

This approach uses a servo system to introduce swashplate control as determined by inputs from gyros mounted on the pylon and in the aircraft. Basically, the effect is the same as that of mechanical swashplate-pylon coupling. The advantage of automatic coupling is that the high-ylon-restraint approach can be combined with the swashplate-coupling approach. The pylon is locked solidly to the wingtip and is stabilized by the inherent effective stiffness of the wing structure. But since the pylon is now fastened to the wing, there is no mechanical means to obtain a pylon motion signal. The signal is therefore provided by comparing signals from the rate gyros on the pylon and in the aircraft. The automatic swashplate control system can also incorporate flat-tracking provisions so that low values of delta-3 can be employed.

(3) Aircraft Arrangement

Many features of the D266 general aircraft arrangement were based on consideration of rotor/pylon stability, including wing planform geometry, rotor hub arrangement, and rotor mast length. Detailed design features of the rotors, pylon, and wings were also based on stability requirements. It was decided early in the design study of the D266 that the aircraft should be configured to minimize the effects of the rotor in-plane shear force by placing the rotors as close to the aircraft cg and pylon pivot points as possible. To do this, rotor masts were made short, and the wing swept forward slightly to provide the necessary flapping clearance.

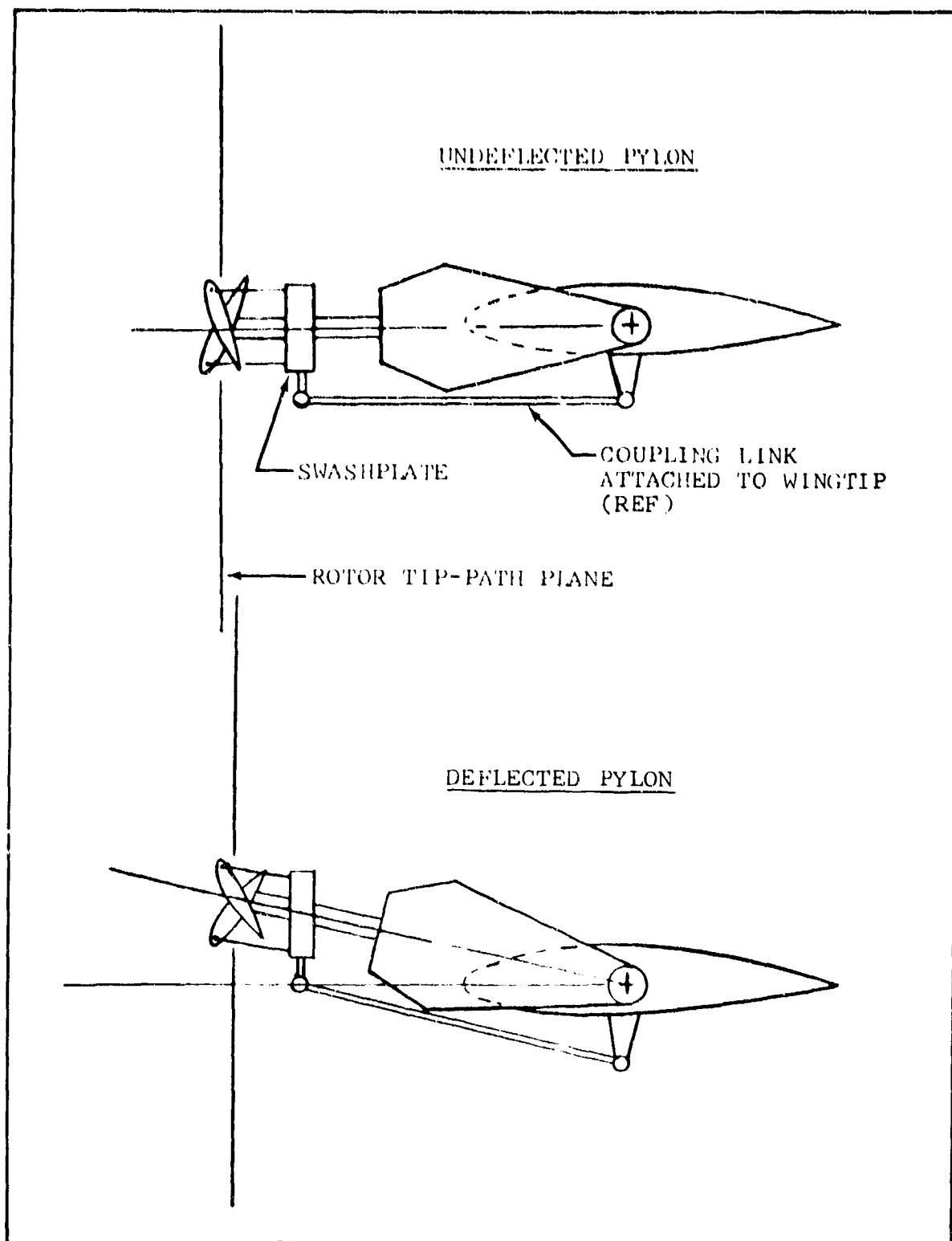


Figure 16. Swashplate-Pylon Coupling Schematic.

The structural arrangement of the wing was also determined by the requirement to provide the wingtip-mounted pylons with as much restraint as possible within weight allowances. The two most important requirements in this regard were to place the elastic axis as far forward (near the rotor hubs) as possible and to provide high torsional stiffness about this axis. The wing torque box was therefore located forward, with spars at 8- and 50-percent chord. In order that the wing bending material could also be fully effective in providing torsional restraint, wing skins consisting of honeycomb panels were selected over the more conventional plate-stringer type of construction.

The design of the D266 results in a basic aircraft that minimizes the rotor-pylon stability problem and permits the selection of any one of the design approaches discussed above.

(4) Selected Design Approach

The final selection of the design approach for the D266 was made after evaluating results from analyses, model tests, and structural and layout design studies. These results indicated that swashplate-pylon coupling was the single most effective controlling parameter and that, by appropriate selection of the coupling ratio and its applied phase angle (swashplate retardation), stability could be provided for almost any combination of the other parameters.

The computer results in Figure 17 show the powerful effect of swashplate-pylon coupling. Increasing the coupling ratio from 1.4:1 to 1.8:1 increases the speed for instability from 270 knots to above 500 knots. The same effects are shown in the model test results obtained with the dynamic stability model shown in Figure 18. The model was dynamically scaled to simulate the D266 rotor and pylon, and it included wing bending and torsion degrees of freedom. Testing was conducted to scale speeds in excess of 450 knots.

Because of its powerful effect and its mechanical simplicity, swashplate-pylon coupling is used in the design of the D266 to insure a high level of stability. Swashplate-pylon coupling about the pylon-pitch axis also increases the longitudinal short-period damping of the aircraft by tilting the rotor in a direction opposing the aircraft pitching rate.

It was found that it is not necessary to apply swashplate-pylon coupling about both pylon axes if it is applied about the axis with the softest pylon restraint and if the other axis is restrained with a very stiff spring. This has been done in the design of the D266 by mounting the pylon solidly

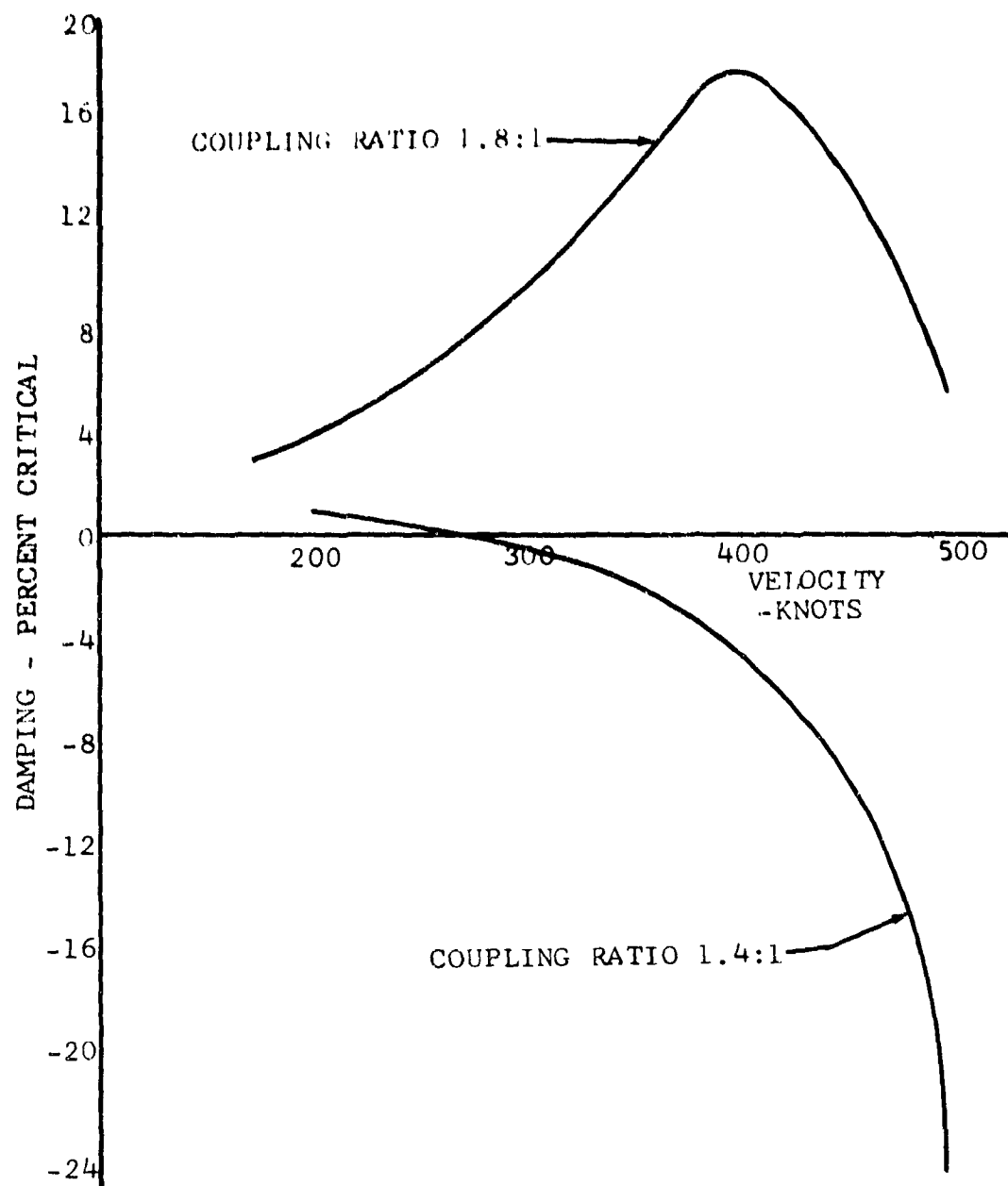


Figure 17. Effect of Swashplate-Pylon Coupling Ratio.

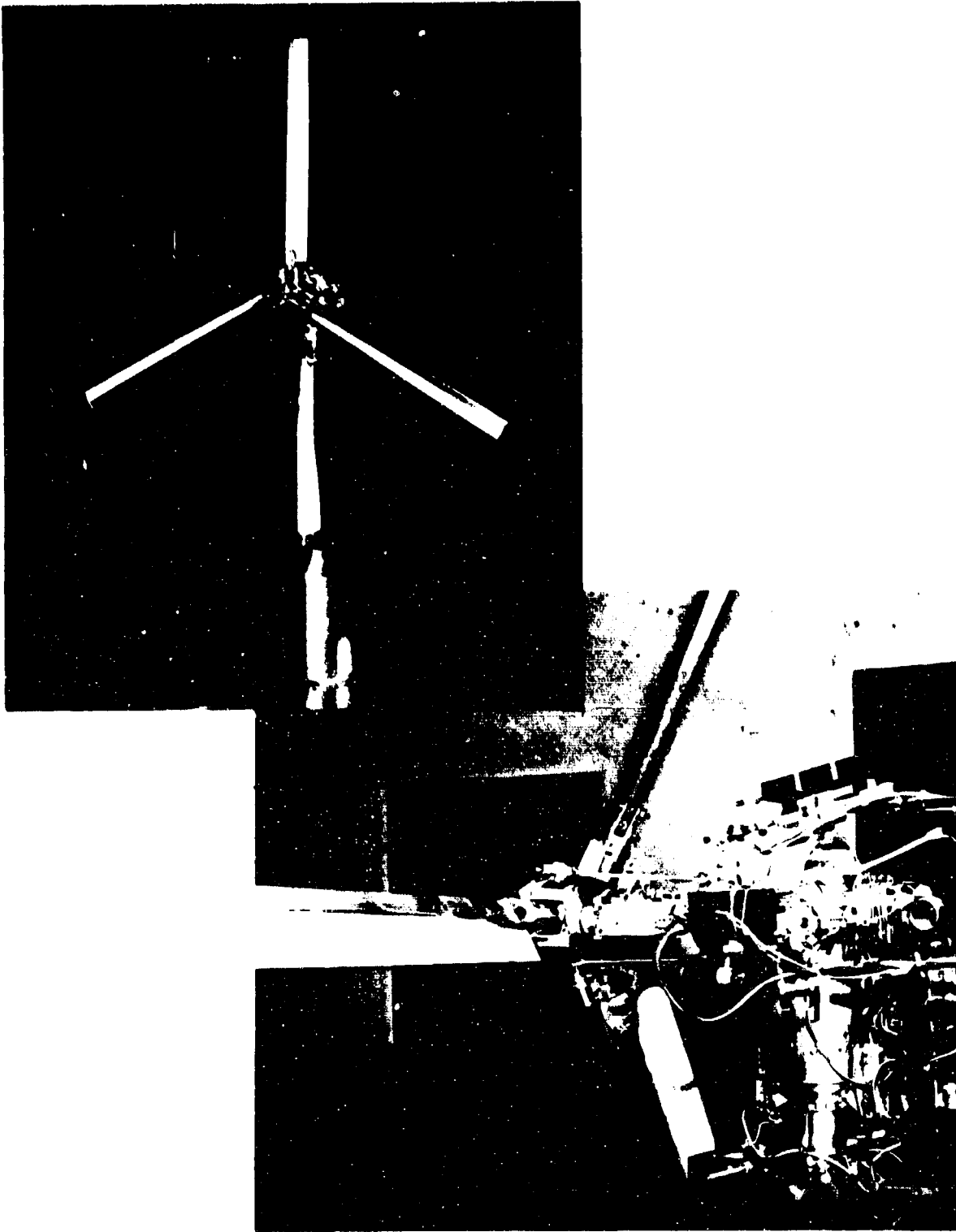


Figure 18. Dynamic Stability Model.

to the wingtip in the lateral direction. Because of the high chord-stiffness of the wing, restraint of the pylon to yawing motion is very high.

The design of the D266 rotor-ptyon system is based on extensive analytical and experimental studies. Predicted rotor-ptyon damping is shown in Figure 19 for the maximum and minimum rpm. Heavy damping is provided to speeds in excess of the "flutter-free" speed of 503 knots (1.15 limit dive speed).

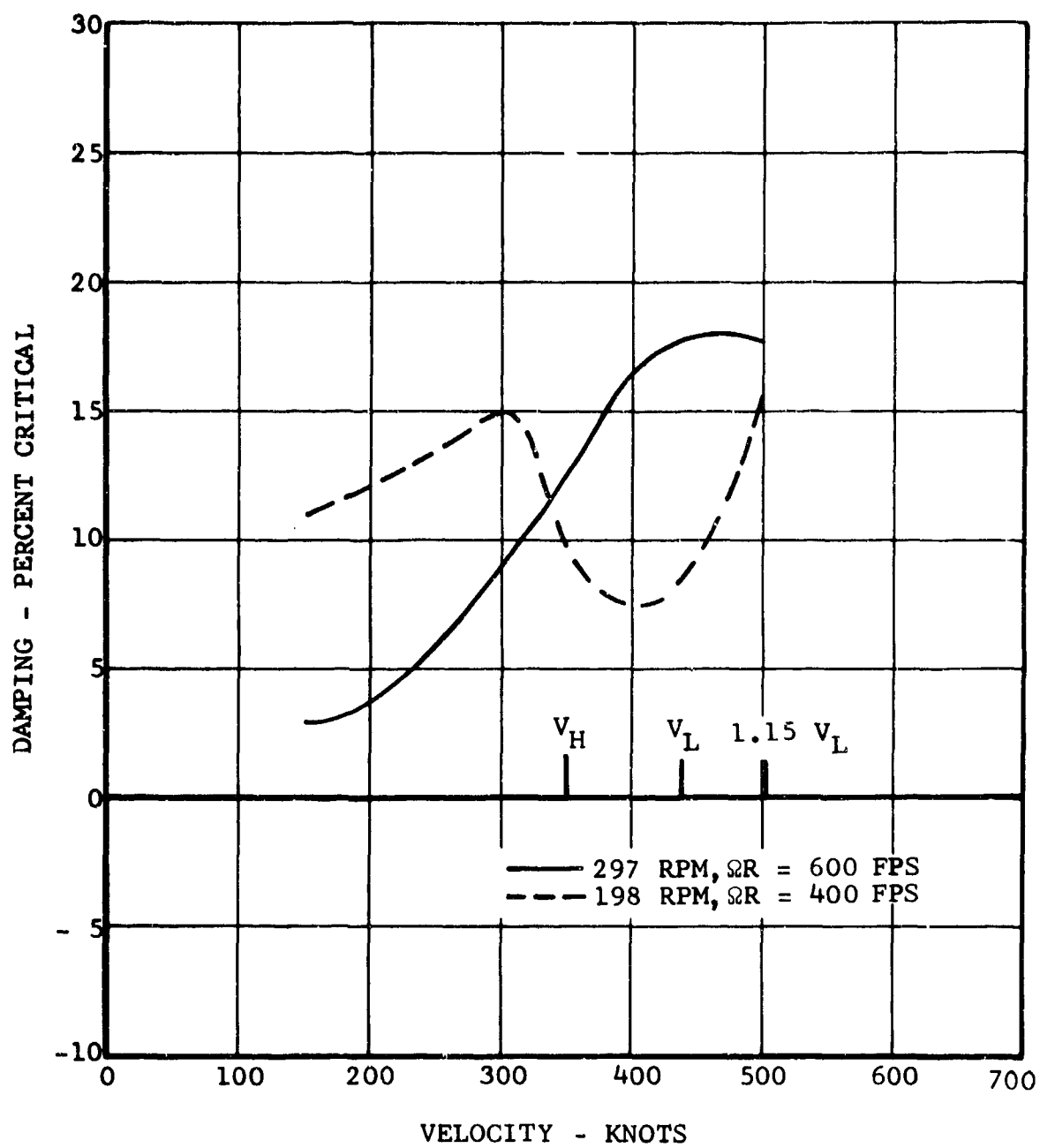


Figure 19. Rotor-Pylon Stability at Sea Level.

SECTION II. PROPULSION DATA

Power is supplied by two General Electric T64-GE-12 engines, mounted in nacelles adjacent to each side of the fuselage aft of the rear wing spars. Power management is accomplished by the engine power-turbine governor in helicopter flight and by a combination of rotor pitch governor and engine power control in fixed-wing flight.

Lift and thrust are provided by rotors mounted on pylons at each wingtip and rotating in opposite directions to cancel torque. Each rotor has a diameter of 38.5 feet, has three blades, and is of semirigid design. The rotor and pylon assembly is vertical or near vertical for the helicopter mode and is tilted forward for operation in the fixed-wing mode.

The power distribution system (power train) consists of engine-mounted gearboxes, main transmissions, an accessory gearbox, and interconnecting shafting.

A. POWERPLANT

Performance ratings for the T64-GE-12 engine are shown in Tables III and IV. These data from the engine manufacturer's specification define the minimum engine power available at sea level standard conditions. Reduction of engine power available to installed power available is accomplished by a summation of the engine installation losses, which are shown in Table V. Compressor bleed and tailpipe losses are calculated from data presented in the engine specification. The tailpipe area has been reduced from the 450 square inches used for engine certification to 300 square inches, in order to obtain positive jet thrust over a broader range of flight speeds. The inlet total pressure losses are estimated from test data supplied by General Electric for similar inlet ducts on other installations. The engines are operated over a wide range of speed from 8050 rpm to 16,500 rpm, with 16,600 rpm considered as 100-percent speed. This is below the 17,000-rpm maximum continuous output shaft speed allowed by the engine specification. In the helicopter mode (16,600 - 15,100 rpm), the power required is below the torque limit of the engine. However, in the fixed-wing mode (12,100 - 8050 rpm), the engine power output is limited to a steady-state torque of 1520 pound-feet by the engine specification. A derated torque limit of 1350 pound-feet is used for the D266. Curves showing power available and fuel flow are presented in Section V. Three mounting fittings support the combined engine-reduction gearbox package. As shown in Figure 20, two fittings on the forward end of the reduction gearbox attach to fittings on the rear wing spar. One fitting reacts to loads in all three directions, while the second transmits only vertical loads. For the third mounting fitting, the engine compressor's rear

TABLE III T64-GE-12 ENGINE PERFORMANCE RATINGS AT SEA-LEVEL-STATIC CONDITIONS, $T_2 = 59^\circ\text{F}$ (Ratings Are At Power-Turbine Output Shaft) Exhaust Area = 450 in. ²						
Rating	Min SHP	Torque For Rated Power And Speed (lb-ft)	Max SFC (lb/shp/hr)	Max Gas-Generator Speed ^a (rpm)	Rated Power-Turbine Speed ^b (rpm)	Max Measured Power-Turbine Inlet Temp (T_4) ^e ($^\circ\text{F}$)
Military (30 min)	3435	1326	0.480	18,230	13,600	1260 (682C)
Normal	3230	1247	0.485	18,010	13,600	1225 (663C)
90% Norm	2905	1122	0.493	-	13,600	-
75% Norm	2420	934	0.514	-	13,600	-
Ground Idle	110 ^c	-	300 lb/hr ^d	-	-	-
NOTES: a Maximum allowable continuous gas-generator speed is 18,230 rpm (100% gas-generator speed). Maximum allowable transient gas-generator overspeed limit shall be 18,500 rpm (101.5% of gas-generator speed) for a period not in excess of 10 sec. b Maximum allowable continuous output speed for T64-GE-12 Engine: 17,000 rpm. c Maximum. d Maximum fuel flow. e For reference purposes, Military (30-min) $T_4 = 1890^\circ\text{F}$; Normal $T_4 = 1846^\circ\text{F}$.						

TABLE IV

T64-GE-12 ENGINE

PERFORMANCE DATA AT 20,000 FT, 370 KNOTS TRUE AIRSPEED
(Ratings Are At Power-Turbine Output Shaft)
Exhaust Area = 450 in.²

Rating	Min Shp	Torque For Rated Power And Speed (lb-ft)	Max SFC (lb/shp/hr)	Max Gas- Generator Speed (rpm)	Rated Power-Turbine Speed (rpm)	Max Measured Power-Turbine Inlet Temp (T ₅)** (°F)
Military (30 min)	2805	1082	0.421	18,230	13,600	1300 (704C)
Normal	2560	990	0.417	18,010	13,600	1225 (663C)
90% Normal	2305	890	0.417	-	13,600	-
75% Normal	1920	741	0.422	-	13,600	-
Flight Idle	185	-	195 lb/hr*	-	-	-

NOTES: *Maximum fuel flow.

**For reference purposes, Military (30-min) T₄ = 1949°F;
Normal T₄ = 1851°F.

TABLE V				
ENGINE INSTALLATION LOSSES PER ENGINE				
Condition	Inlet Temp Rise	Inlet Loss	Compressor Bleed HP Loss	Tailpipe HP Loss (300-in. ² area)
6000 ft 95°F Hover OGE Military Power N _f = 16,600 rpm	0	-0.5% Total Pressure	13.0	48
S.L. Normal Rated Power N _f = 12,100 rpm	0	-1.0% Total Pressure	18.0	62
S.L. 95°F Hover OGE N _f = 16,600 rpm	0	-0.5% Total Pressure	22.0	60
N _f = Free power turbine speed.				

frame mounting pad is attached to the fuselage structure through a bipod, which carries vertical and lateral loads. Spherical bearings are provided at the three support fittings and at the attachment of the bipod to the fuselage. This method of mounting permits thermal expansion of the engine and gearbox without inducing loads into the engine or airframe; it also permits airframe deflection without inducing loads into the engine-gearbox package. Rigid attachment of the reduction gearbox to the engine output pad results in a configuration which is similar to a conventional turboprop installation. General Electric has reviewed and approved this mounting system.

1. FUEL AND LUBRICATION SYSTEMS

Fuel for the D266 is supplied by two separate systems, one for each engine. As shown schematically in Figure 21, each system is composed of three cells interconnected to form a single

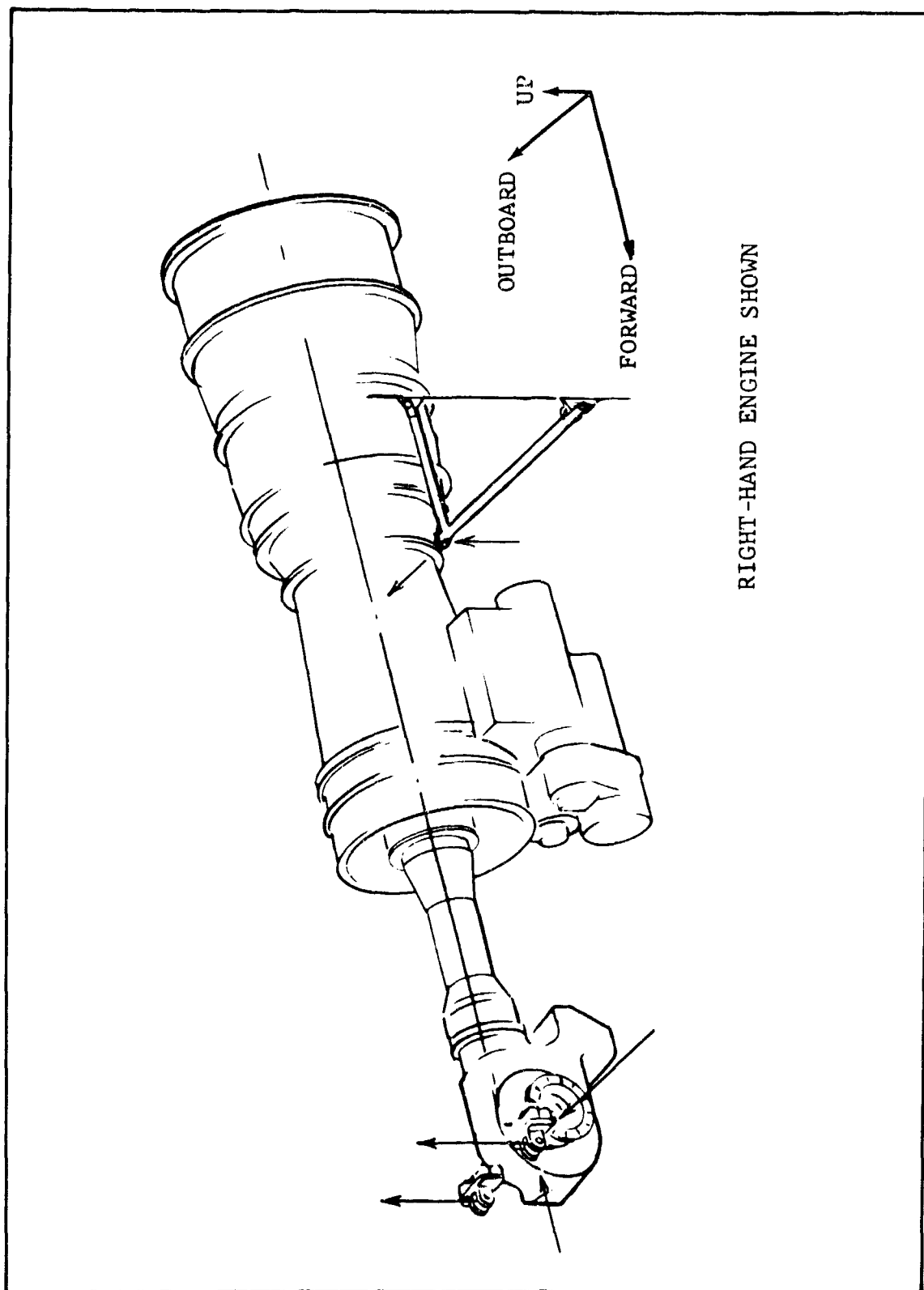


Figure 20. Engine Mounting.

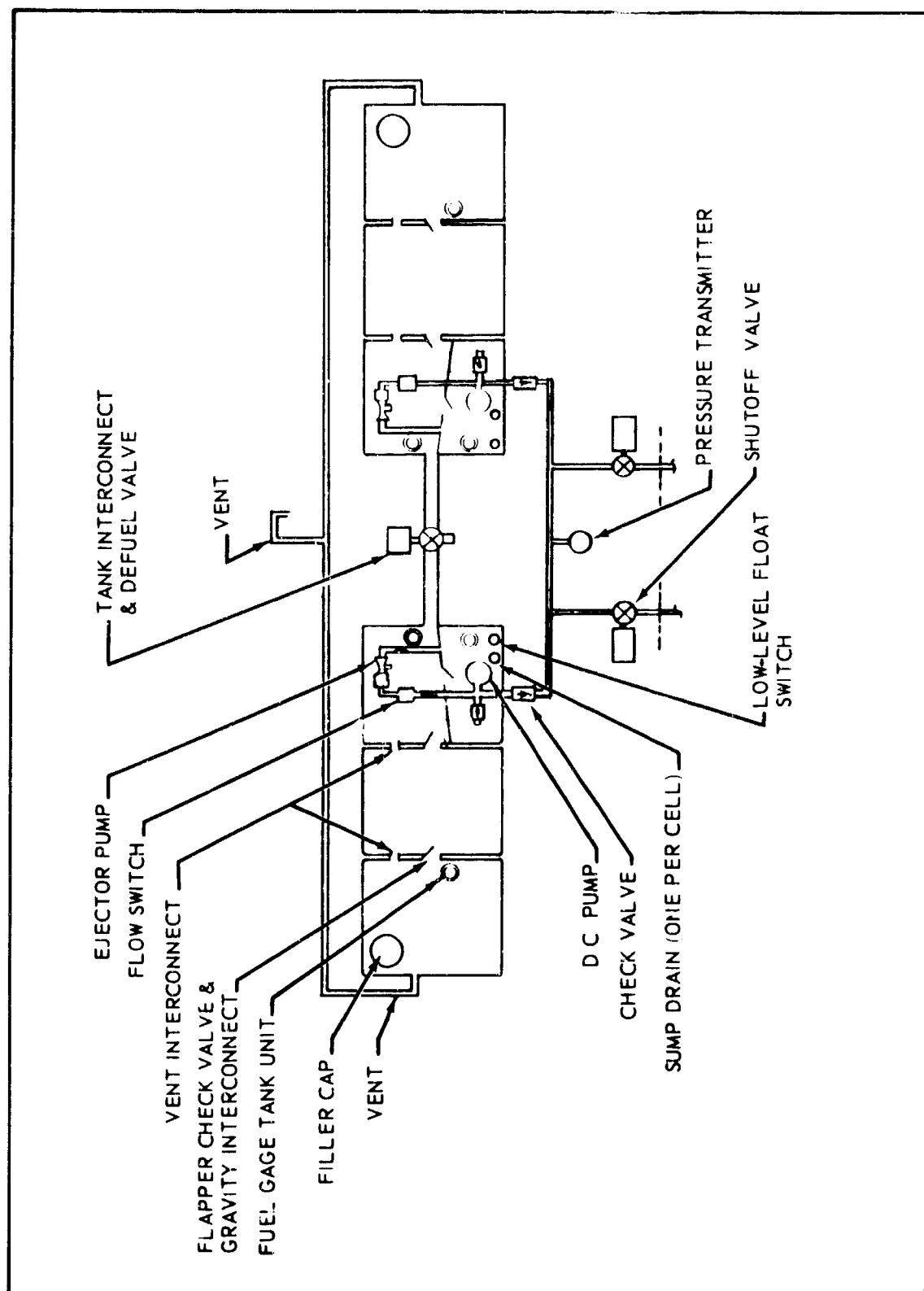


Figure 21. Fuel System Schematic.

tank. The cells are constructed of a flexible non-self-sealing bladder material conforming to MIL-T-6396. Continuous support for each cell is provided by three cavities located between the spars in each wing. Gravity refueling is accomplished through filler caps located in each of the outboard cells. Gravity interconnects between the cells admit fuel to the transfer pump inlets in the inboard cells. Flapper check valves at each interconnect prevent outboard fuel flow during momentary wing-down maneuvers. Venting between the three cells in each tank is accomplished by interconnect fittings at the high points between cells. Vents from the high point in each outboard cell interconnect in the center of the fuselage and route overboard through a single line.

The inboard cell in each system is divided into two compartments by an internal baffle. The portion of the cells aft of the baffles will be maintained full at all times by the ejector transfer pumps forward of the baffles. One dc-driven fuel booster pump is located in each of the inboard cells aft of the baffles. The pumps serve a dual purpose of supplying fuel to the engine and providing motive flow for the ejector transfer pumps. Engine fuel passes from the booster pump discharge through a check valve, firewall shutoff valve, and engine-supplied centrifugal fuel purifier before entering the engine fuel control. A gage in the cockpit indicates booster pump discharge pressure. An interconnect between the two pump discharge lines permits one pump to supply both engines in the event of a single pump failure. Three capacitance-type transmitters in each tank give continuous indication of fuel quantity.

The engine is supplied with oil from a 3-gallon tank in the nacelle aft of the gearbox and forward of the engine firewall. This location, above the engine oil inlet, permits a positive head at all times. Oil flow is shown schematically in Figure 22. The oil cooler is inboard of the engine, forward of the firewall. Forced airflow is provided by a bleed-air-turbine-driven fan. Engine and tank are vented by a single overboard line from the tank. Air is separated from the oil by de-aeration baffles within the tank. Oil level may be checked and the tank serviced through an access door in the cowling. Temperature and pressure instruments in the cockpit give continuous indication of the system's operation.

2. FUEL CONTROL

Power management in the D266 is simple and is designed for straightforward cockpit procedures. Power control is provided by two interrelated control systems. For helicopter flight, the engine power turbine governors maintain selected rotor rpm by increasing or decreasing power as manual changes are made

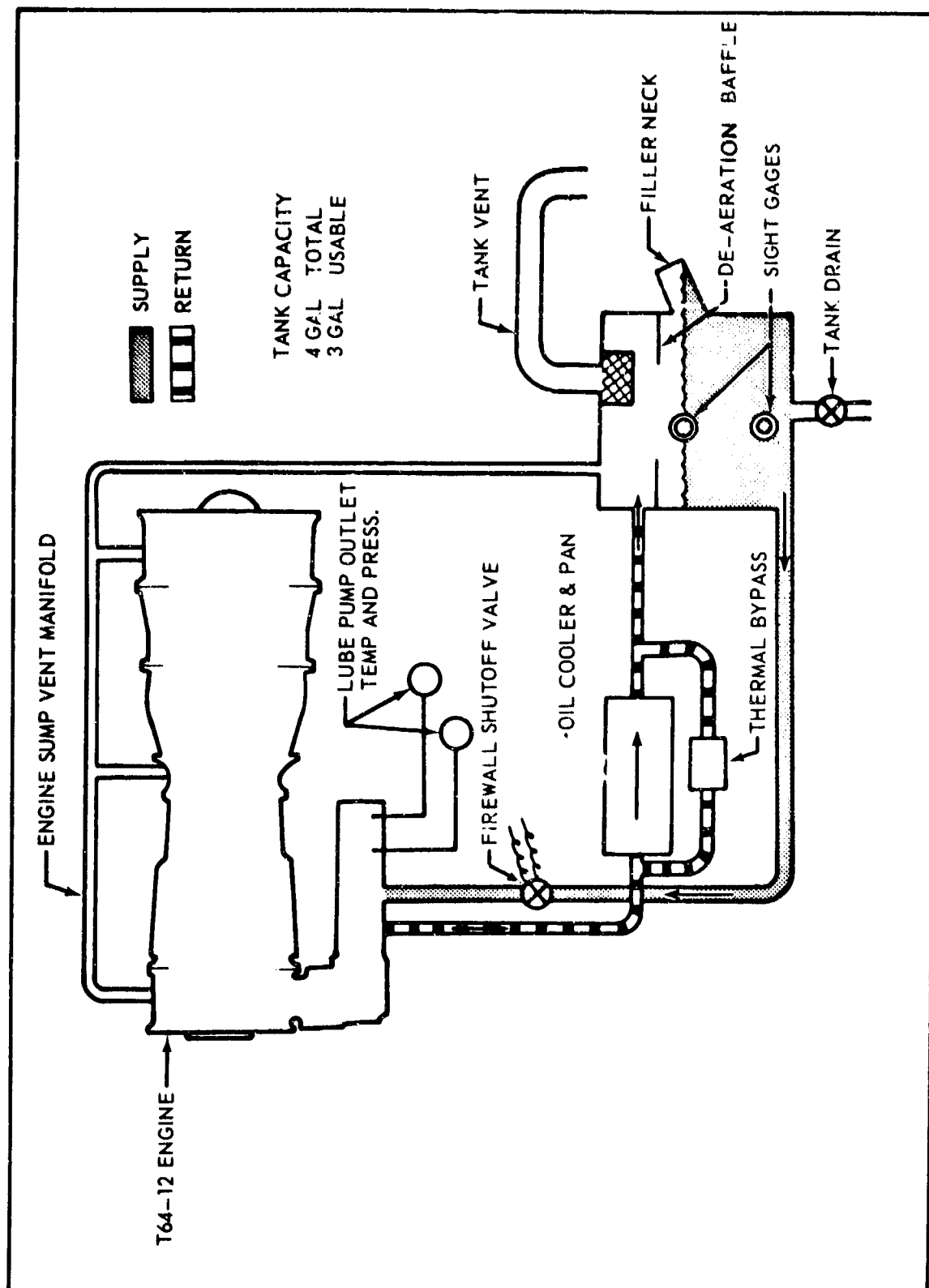


Figure 22. Engine Lubrication Schematic.

in collective pitch. In fixed-wing flight, the rotor pitch governor maintains selected rpm by increasing or decreasing collective pitch as manual power changes are made. Thus, the D266 may be flown in helicopter mode in the same manner as a conventional helicopter and may be flown in fixed-wing mode in the same manner as a conventional turboprop airplane.

The cockpit controls are shown in Figure 256 in the Appendix. The power-management controls and their connection to the system components are shown schematically in Figure 23.

The T64 engines are equipped with hydromechanical fuel controls which schedule fuel flow and compressor-inlet guide-vane position in such a manner as to protect the engine from stall, to provide altitude and temperature compensation, and to maintain the selected power-turbine speed. The engine power control shaft has a 120-degree rotary travel as shown in Figure 24. In the sector between the idle detent and the minimum govern position, the shaft controls fuel flow directly, and hence engine power output. This sector is used for power control in the fixed-wing flight mode. The power turbine governor limits turbine speed to 95 percent. The electro-hydromechanical rotor-pitch governor automatically changes blade pitch to maintain a selected rotor rpm in the range from 48.5 to 95 percent. Above 95 percent, engine speed is controlled by the power management levers. In the sector between minimum govern and 100 percent, the control shaft selects a governed engine power turbine speed between 95 and 100 percent. This constant-rpm operation greatly simplifies helicopter flight, and rpm remains constant while power demands are changed by collective pitch position.

Conventional helicopter rpm droop compensation is provided. The collective lever is connected through the droop compensator linkage to a droop cam on each engine. The droop cams position the load signal shafts on the engine fuel control, which in turn schedule limited rpm changes to compensate for the engine droop characteristics.

3. STARTING SYSTEM

The engines are started on the ground by a self contained hydraulic system with an airborne auxiliary power unit. The hydraulic starter motor, mounted on the aft side of the engine accessory case, drives the engine gas-producer section through a freewheeling unit.

The auxiliary power unit is the Solar T-62T-16B Titan gas turbine, which produces 55 horsepower from sea level to 15,000 feet. It is located just aft of the cargo compartment as

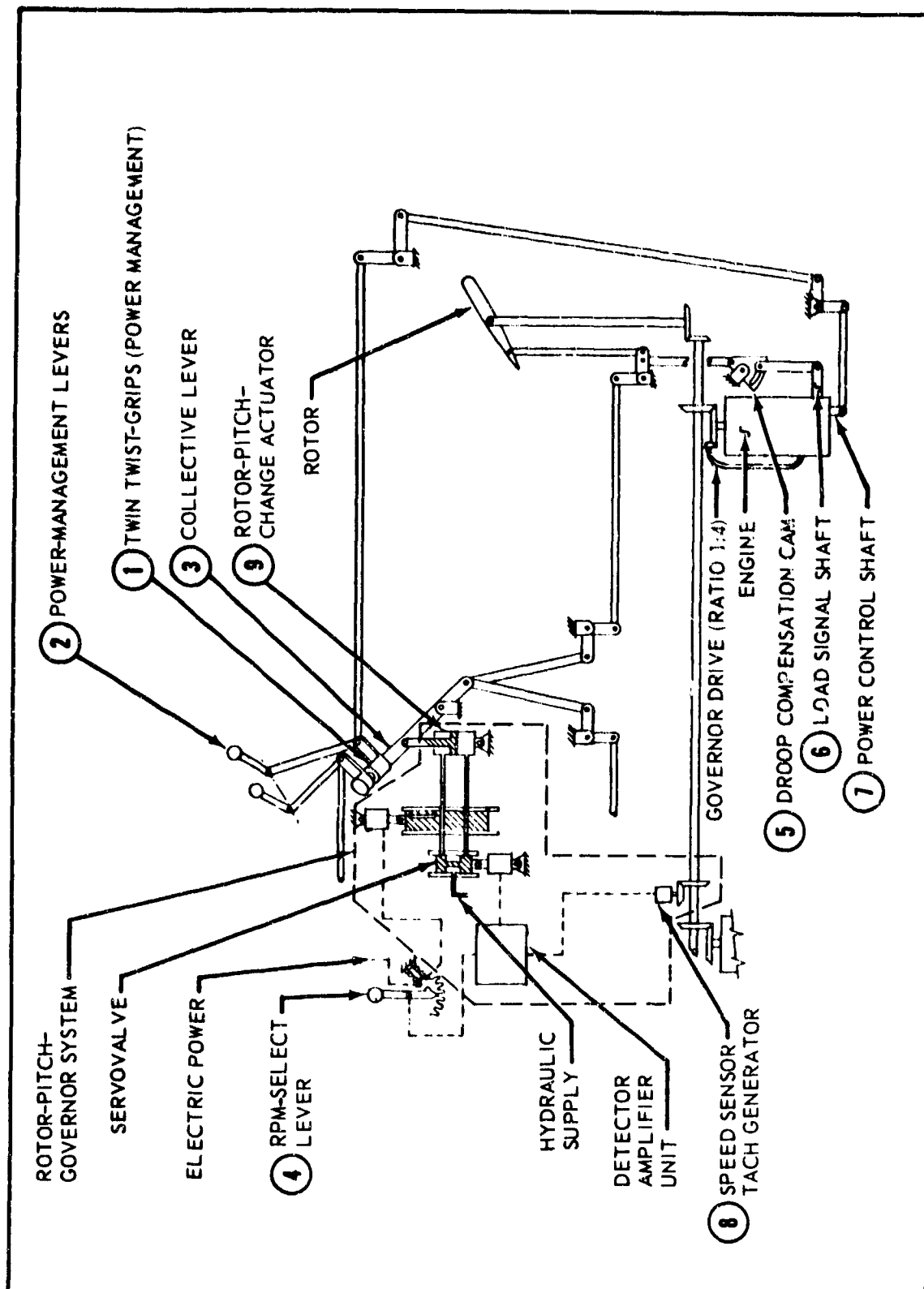


Figure 23. Power-Management Schematic.

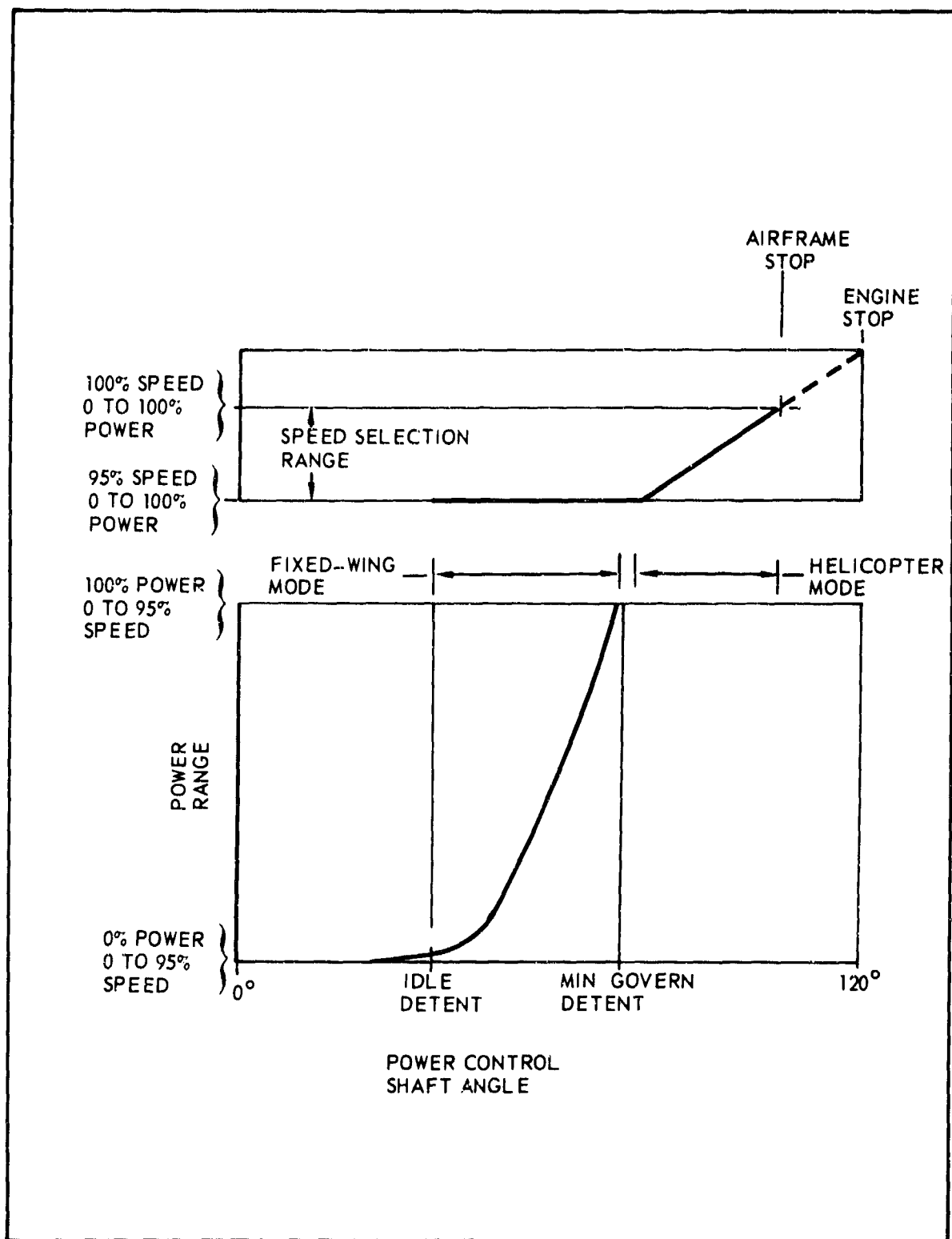


Figure 24. Power Control Shaft Schedule.

shown in Figure 252. This location provides ready access for removal and maintenance, as well as minimum noise isolation problems. Air for the turbine enters at the forward, outside portion of the compartment. The exhaust is directed aft and outboard and provides enough ejector airflow to cool the compartment. Fuel is supplied to the turbine from the main aircraft fuel system. A 20-kva alternator is mounted on the engine centerline pad. The electric APU starter is located on the forward offset accessory pad. It is connected to the aircraft's battery and will start the APU at temperatures down to -25°F . The hydraulic pump for main engine starting is mounted on the aft side of the offset accessory gearbox.

For air starts, the aircraft's hydraulic system is used. It is directly connected to the starting valves. According to the engine manufacturer, the engine does not require any starter assist above 250 knots airspeed at sea level. In the interest of simplicity, and since hydraulic power is available, the pilot will engage the engine starter for all air starts. Hence, he need not decide if sufficient ram power is available.

4. INLET, EXHAUST, COOLING

The engine air inlet, shown in Figure 25, is a single duct that runs forward and down from the round air inlet flange to an elliptical opening below the wing. A boundary-layer air bleed immediately above and inboard of the inlet removes stagnant air to afford more efficient pressure recovery.

The exhaust system consists of a stainless steel tailpipe that terminates approximately twelve inches from the end of the nacelle and forms the nozzle for an ejector used for aft engine compartment cooling. Sufficient clearance has been provided between the nacelle and the fuselage to prevent excessive fuselage skin temperatures caused by engine exhaust gas. Figure 26 shows the exhaust wake temperature profile relative to the fuselage.

Firewalls separate the engine from the remainder of the aircraft. One firewall, also used for fuselage skin, extends fore and aft and separates the engine nacelle from fuselage structure. The second or forward firewall is in the plane of the engine inlet flange and separates the engine from the reduction gearbox and wing structure. A third or aft firewall separates the engine accessory or forward section from the hot or aft section. Both the forward and aft firewalls are supported from the engine and form a portion of the cowl supporting structure. Flexible diaphragms in each firewall permit engine thermal expansion and prevent loads from being imposed on the engine.

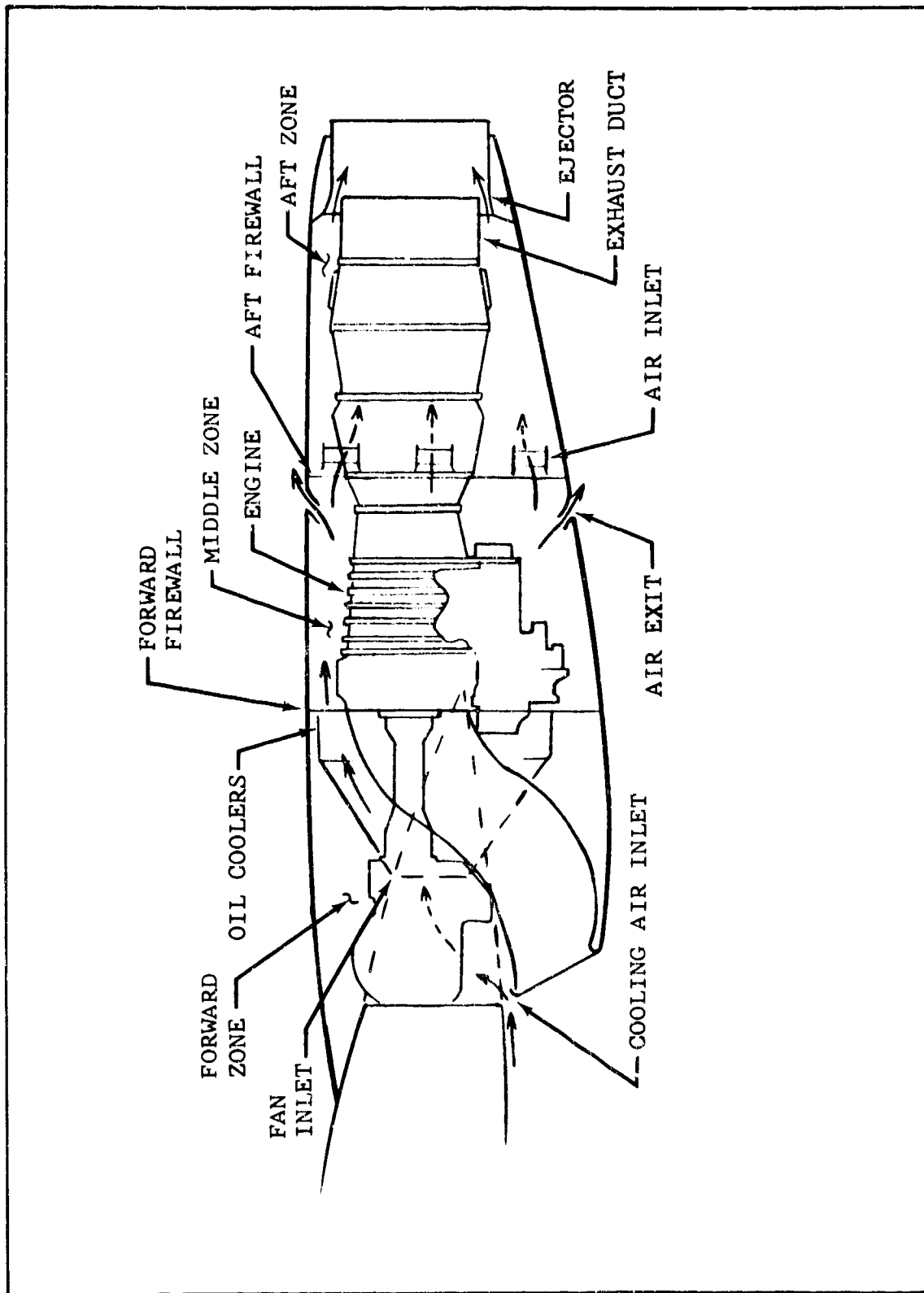


Figure 25. Engine Cooling Provisions.

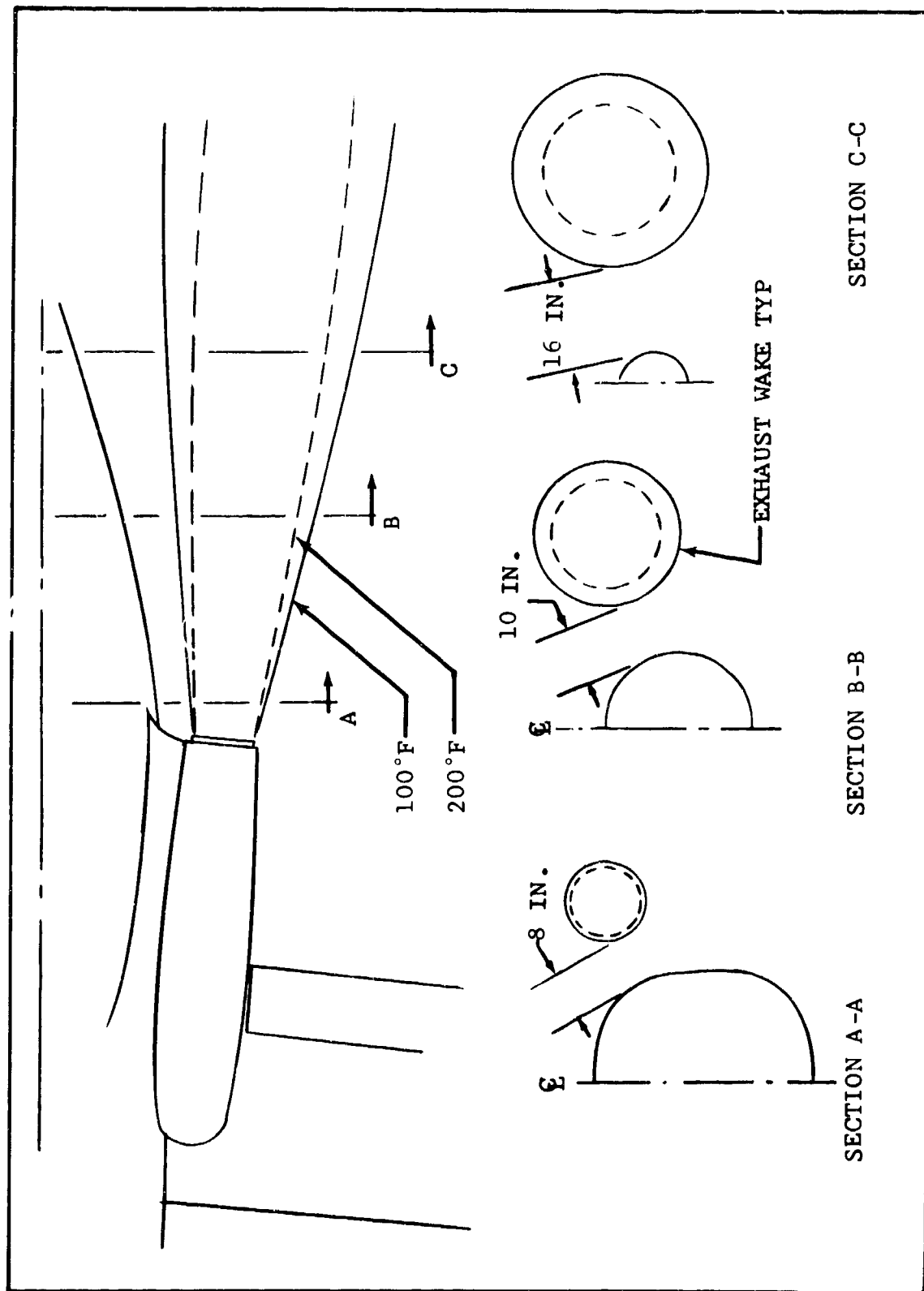


Figure 26. Exhaust Wake Temperature Profile.

The firewalls divide the engine nacelle into three separate zones. Figure 25 shows the nacelle division and the cooling air paths. The first or forward zone serves as a plenum for the oil-cooling air. Air enters the nacelle through an opening between the engine air inlet and the wing. Air is directed from the fan discharge through two oil coolers, one for the engine and one for the engine gearbox. The discharge air from the oil coolers is directed into the second or middle nacelle zone and is discharged overboard through flush outlets forward of the aft firewall. The third or aft nacelle zone contains the engine turbine and exhaust sections. Cooling air for this zone is drawn into the nacelle through flush inlets aft of the aft firewall. These inlets are staggered with the air outlets from the middle zone to prevent reentrance of oil-cooler air. The air drawn into the inlets is pumped overboard by the ejector formed by the engine exhaust duct and nacelle skin.

B. POWER TRAIN

The drive system consists of two engine gearboxes, two main transmissions, and a center accessory gearbox, interconnected by drive shafting. The arrangement of the components is shown in Figure 27. Speeds and reduction ratios of the principal components are shown in Table VI.

1. ENGINE GEARBOX

The engine gearbox is bolted directly to the engine torque-shaft housing. It has a single bevel-gear reduction stage, a freewheeling unit, an engine drive shaft thrust bearing, an engine N_f tachometer drive, a power-turbine governor drive, and a self-contained lubrication system. Engine power is delivered to the gearbox at power-turbine speed and is reduced by a factor of 0.5593 (9284-rpm max helicopter) at the output drive-shaft flanges.

Engine power is delivered to the gearbox through a spline coupling, integral with the overrunning spring clutch and accessory drive gear. The one-way clutch is a taper-wound spring which is energized by a small drag force generated by the slight interference fit of the last two (low-torque) coils with the driven member. This freewheeling unit permits auto-rotation in the event of engine failure and allows single-engine operation.

The bevel-gear stage has a 33-tooth pinion and a 59-tooth gear, which results in a reduction ratio of 0.5593. Both the pinion and the gear are designed with straddle-mounted bearing supports. The use of straddle-mounted bearing supports for the gears, preloaded ball-bearing assemblies, and rigid housing design provides minimum deflections of the gear-tooth mesh in all

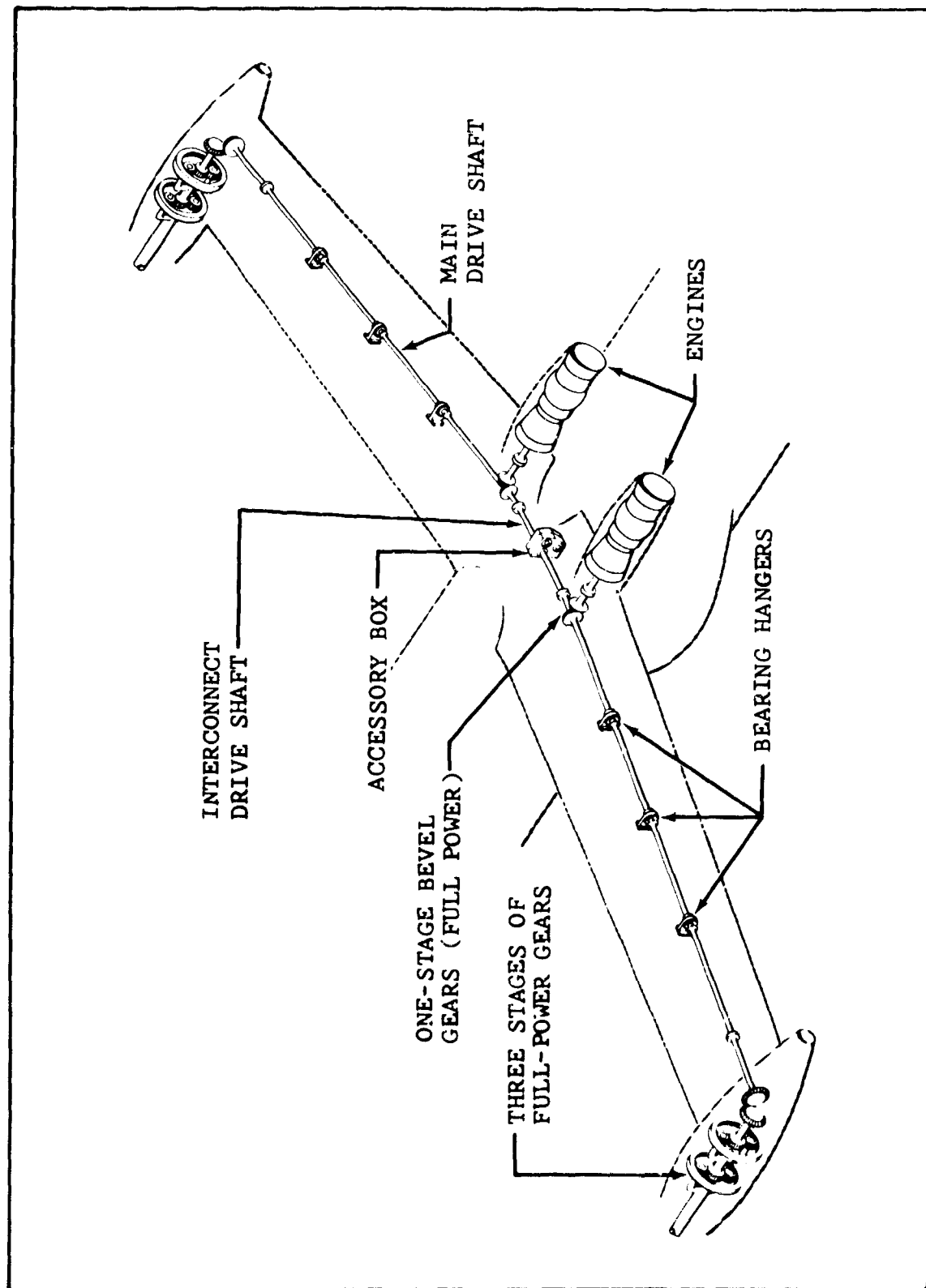


Figure 27. Drive System Schematic.

TABLE VI
RPM AND GEAR RATIOS

	Fixed-Wing Configuration (rpm)		Helicopter Configuration (rpm)		Ratios
	Min	Max	Min	Max	
Engine	8,050	12,100	15,100	16,600	Basic
Main Drive Shaft and Engine Gearbox Oil Pump	4,502	6,768	8,445	9,284	0.5593
Engine Gearbox Tachometers (N _f Engine and Power-Turbine Governor)	2,013	3,025	3,775	4,150	0.2500
Main Transmission Lower Sun Gear	2,976	4,473	5,582	6,137	0.3697
Main Transmission Upper Sun Gear	768	1,154	1,441	1,584	0.0954
Rotor Mast	198	297	372	409	0.0246
Main Transmission Accessories (Hydraulic Pump, Oil Pump and Blower)	2,909	4,373	5,457	6,000	0.3614
Accessory Gearbox Generator Pads	3,973	5,971	7,452	8,192	0.4935
Accessory Gearbox Hydraulic Pump Pad	2,937	4,414	5,508	6,056	0.3648
Accessory Gearbox Tachometers (Rotor and Rotor Governor)	2,046	3,076	3,838	4,219	0.2542

operating regimes. A damping ring is installed in the pinion gear to reduce high-frequency vibrations and to preclude resonant frequencies or harmonics from coinciding with the operating rpm. Provisions are made for a damping ring in the output gear if development indicates its requirement.

The engine gearbox lubrication system is shown schematically in Figure 28. The wet sump system uses MIL-L-7808 oil. The pump is an internal gear type with a capacity of 6 gallons per minute and is partially submerged in the sump. The oil sump, integral to the case, holds 6 quarts of oil. The case has a filler cap and a self-closing magnetic sump drain plug with a removable electric chip detector. The sump has a liquid level sight gage. The oil cooler is adjacent to the engine oil cooler and has a built-in thermostatic bypass and pressure-relief valve. Pressure oil jets are provided for the ball and roller bearings and main gear mesh. The accessory gears and bearings are splash-lubricated.

The cases are magnesium alloy castings. Steel liners for all antifriction bearings preclude wear and looseness caused by creep and/or thermal expansion.

2. DRIVE SHAFTING

All shafting is made of aluminum alloy tubing. The main drive shaft consists of one fixed and two floating sections per side. The fixed section is supported by three oil-lubricated bearing hangers and is located approximately midway between the engine gearbox and the main transmission. The floating sections connect the engine gearbox to the fixed section and the fixed section to the main transmission. Spherical gear-type couplings on each end of the floating shaft allow the freedom required for wing flexure. Each floating shaft is a self-contained unit that may be assembled and grease-packed prior to installation.

The interconnect shafting consists of two floating sections which, with the exception of size, are similar to the floating sections of the main drive shaft.

Shaft critical speeds are calculated for each section including overhang. The longest shaft sections exhibit a minimum of 38-percent margin of critical speed above maximum operating speed. Acceptable practice for existing military aircraft allows a 20-percent margin over shaft critical speeds.

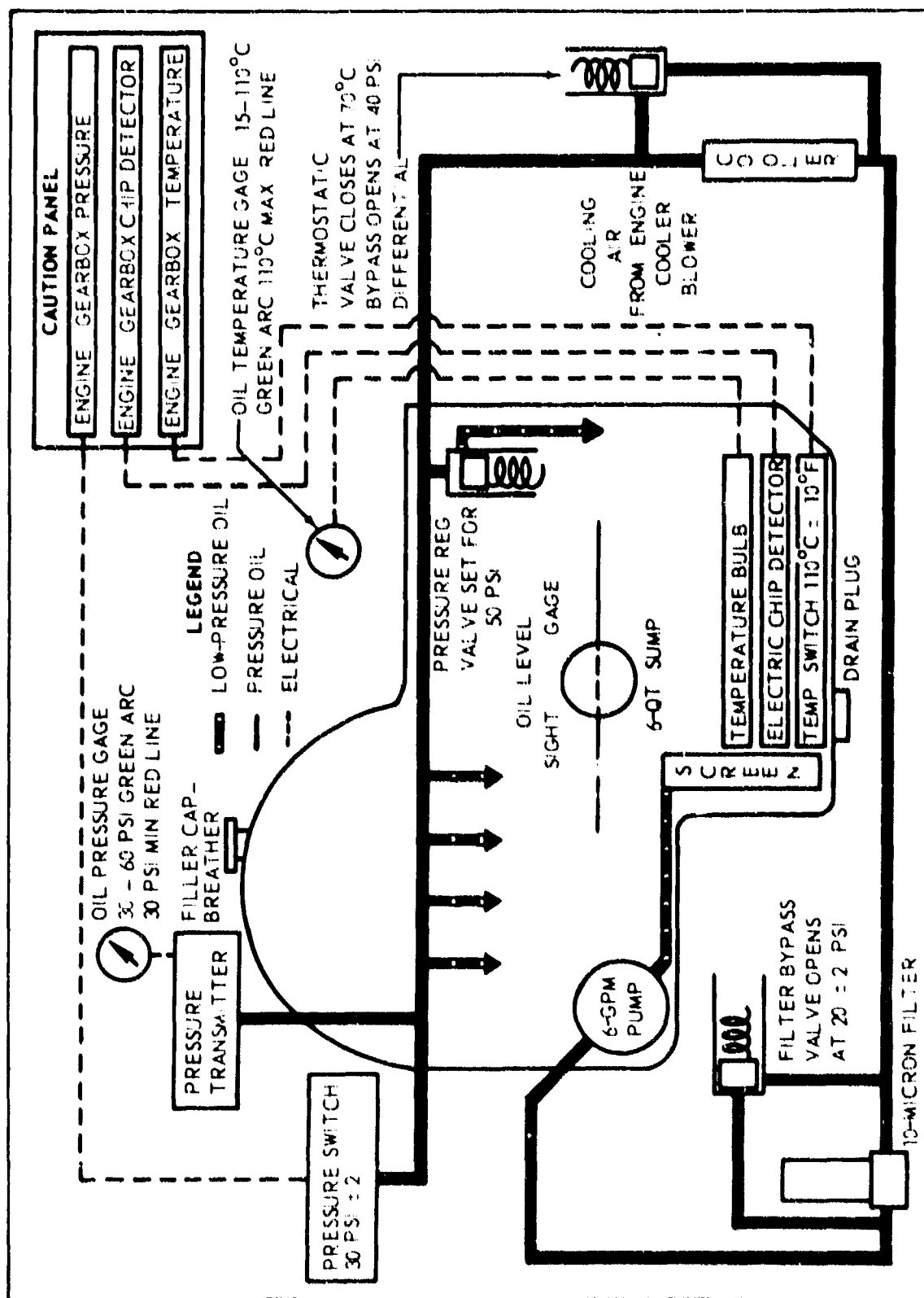


Figure 28. Engine Gearbox Oil System.

3. MAIN TRANSMISSION

Each main transmission is mounted at the wingtip on a spindle, which is free to rotate about the conversion axis on two Teflon support bearings. The transmission consists of a bevel-gear stage, two planetary stages, a self-contained lubrication and cooling system, a shaft-driven oil-cooler blower, and a hydraulic pump drive. Engine power is delivered to the input spiral bevel pinion by the main drive shaft at 9284 rpm (maximum helicopter-mode rpm). The pinion drives the spiral bevel gear and reduces the speed to 6137 rpm. The bevel-gear shaft is the input to the lower-stage planetary sun gear which drives six planetary pinions mounted in a rotating carrier. The ring gear is fixed, and the rotating carrier is the input to the upper-stage planetary sun gear. The upper sun gear turns at 1584 rpm and drives six planetary pinions, also mounted in a rotating carrier. The upper-stage ring gear is fixed to the case, and the rotating carrier drives the rotor mast, a steel tube heat-treated to 180,000 psi, at 409 rpm (maximum helicopter).

The bevel gears, the planet pinion bearings, the planetary gear meshes, and the main rotor mast bearing are pressure-lubricated from jets. The semi-dry-sump lubrication system is shown schematically in Figure 29. The sump is integral with the lower transmission case and contains 4-1/2 gallons of oil. The case is provided with a filler cap and a breather. A self-closing magnetic sump drain plug has a removable electric chip detector. The oil cooler, mounted on the transmission, receives 1000-cfm airflow from a transmission-mounted and -driven centrifugal blower. The cooler has built-in thermostatic bypass and pressure-relief valves.

The gear case is of magnesium alloy for the planetary ring-gear case which is aluminum alloy. Steel liners are used for all antifriction bearing mounts. The main case is bolted to the steel conversion spindle and is rotated from vertical to horizontal by the conversion actuator during conversion from helicopter to fixed-wing flight.

Each pylon is isolated in the pitch direction by a rubber mount between the conversion actuator and the main transmission case. The mount acts in double shear and provides a nominal spring rate of 10,000 pounds per inch, which places the pylon natural frequency at 5.3 cycles per second when coupled with wing beam bending. Stops limit the mount deflection and take crash loads after the pylon exceeds ± 3 degrees of rotation.

4. ACCESSORY GEARBOX

The accessory gearbox at the center of the aircraft serves as a bearing-hanger support for the interconnect drive shaft and

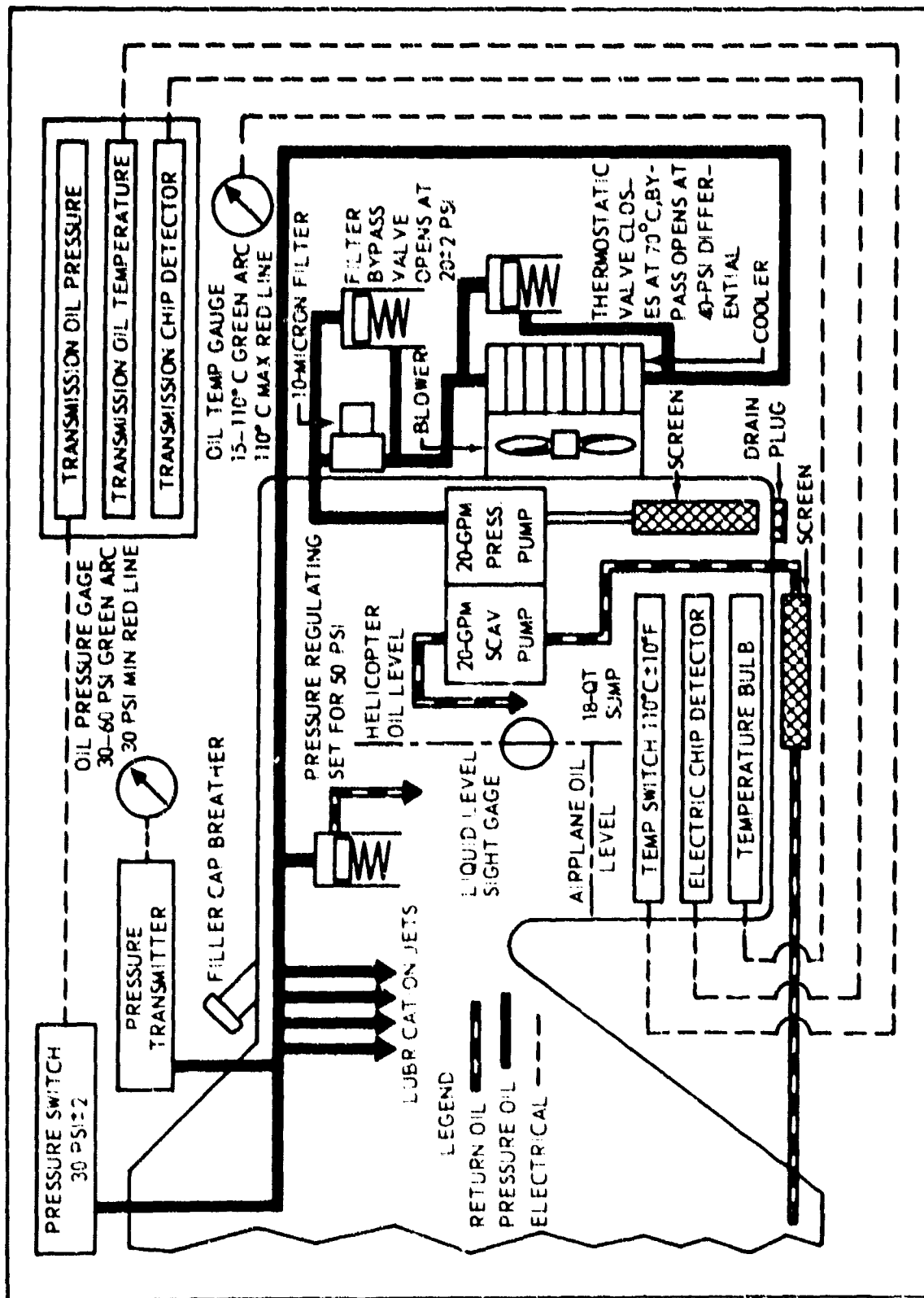


Figure 29. Main Transmission Oil System.

drives two dc generators, two rotor tachometers, and a hydraulic pump. It has an integral oil sump with a capacity of 1 quart. A liquid level sight gage is provided, and a drain plug is located at the low point in the box.

The dc generator pads are in accordance with AND20002, operating at 8192 rpm (corresponding to maximum helicopter rpm); the tachometer pad and governor pad are in accordance with AND20005 operating at 4220 rpm; and the hydraulic pump pad is in accordance with AND 20001 operating at 6056 rpm. The accessories are grouped together above the cabin, where they are easily accessible for maintenance.

5. EFFICIENCY

Power losses and efficiencies are shown in Tables VII through X for various fixed-wing-mode power conditions. Helicopter power conditions were not tabulated because the lower operating power combined with the higher speeds showed negligible differences.

TABLE VII		
ELEMENTAL POWER LOSS AT 3110 HP AND 12,100 RPM (1350 FT-LB)		
Component	Element	HP Loss
Engine Gearbox*	Input Triplex Bearings	8.9
	Bevel Gears	18.0
	Output Duplex Bearings	<u>3.6</u>
	Total =	30.5 (99.01%eff)
Main Transmission*	Input Triplex Bearings	7.3
	Bevel Gears	12.45
	Gear-Shaft Duplex Brgs	2.52
	Planetary Gears	<u>30.0</u>
	Total =	52.27(98.30%eff)
Accessory Gearbox	Negligible Power Loss	
* Roller bearings are not included due to their low fractional horsepower losses.		

Accessory power requirements are defined by Table XI. They are estimated from average accessory loads on the D266 and from efficiencies of similar units on other aircraft.

TABLE VIII TOTAL POWER LOSS AND EFFICIENCY		
Component	HP Loss	Efficiency (%)
Engine Gearboxes*	61.0	99.01
Main Transmissions*	104.54	98.30
Overall efficiency = 97.33%		
*Represents maximum power with both engines at 12,100-rpm output and 3110 hp each.		

TABLE IX TOTAL POWER LOSS AND EFFICIENCY - SINGLE-ENGINE OPERATION		
Component	HP Loss	Efficiency (%)
Powered Engine Gearbox*	30.5	98.97
Unpowered Engine Gearbox*	1.4	
Main Transmissions*	50.72	98.34
Overall efficiency = 97.33%		
*Represents maximum power at 12,100 engine rpm and 3110 hp.		

TABLE X TOTAL POWER LOSS AND EFFICIENCY - REDUCED-POWER OPERATION		
Component	Element	HP Loss
Engine Gearbox*	Input Triplex Bearings	1.02
	Output Duplex Bearings	0.61
	Bevel Gears	2.91
	Total =	4.54 (99.09% eff)
Main Trans- mission*	Input Triplex Bearings	0.637
	Gear-Shaft Duplex Brgs	0.200
	Bevel Gears	2.025
	Planetary Gears	3.68
Total =		6.542 (98.69% eff)
Overall efficiency = 97.79%		
*Represents 500 hp/engine at 8050 engine rpm.		

TABLE XI ACCESSORY POWER REQUIREMENTS		
Accessory	Location	Average Power (hp)
DC Generator (300 amp)	Accessory Gearbox	6
DC Generator (300 amp)	Accessory Gearbox	6
Transmission Oil Cooler Fan	Main Transmission (LH)	1.9
Transmission Oil Cooler Fan	Main Transmission (RH)	1.9
Hydraulic Pump	Main Transmission (LH)	3.5
Hydraulic Pump	Main Transmission (RH)	3.5
Hydraulic Pump	Accessory Gearbox	10.0
Oil Pump Engine Gearbox (RH)	Mounted on Engine Gearbox (RH)	0.50
Oil Pump Engine Gearbox (LH)	Mounted on Engine Gearbox (LH)	0.50
Oil Pump - Main Transmission (RH)	Mounted on Trans- mission	1.6
Oil Pump - Main Transmission (LH)	Mounted on Trans- mission	<u>1.6</u>
Total =		37.0

6. DESIGN CRITERIA

The power train is designed in accordance with MIL-T-5955. The dynamic components are designed for the speeds and loads specified in Table XII. The maximum continuous design loads are based on the military horsepower rating of the T64-GE-12 engine or a torque limit of 1350 foot-pounds from each engine.

The design of the engine gearboxes is based on an input torque limit of 1350 foot-pounds from each engine in the fixed-wing flight mode (12,100-rpm maximum) or 3435 horsepower in the helicopter mode (16,600-rpm maximum).

Loads for the main drive shafts and the main transmissions are based on 55 percent of the maximum continuous torque from both engines (1350 foot-pounds each).

The interconnect drive shaft between the engine gearboxes is designed to 55 percent of the maximum continuous torque of one engine (1350 foot-pounds).

The highest torque condition for design of dynamic components occurs in the fixed-wing flight mode. Therefore, the maximum fixed-wing flight rpm (12,100) was used in conjunction with the maximum continuous torque limit of 1350 foot-pounds to provide loads that will insure satisfactory life margins. Design limit torque is obtained by applying a factor of 1.5 to the maximum continuous torque.

TABLE XII
DESIGN CRITERIA - POWER TRAIN

Component	Speed (rpm)	Design (hp)	Maximum Cont Torque (ft-lb)	Limit Torque (ft-lb)
Engine Output	16,600	3,435	1,090	1,635
	12,100	3,110	1,350	2,025
Main Drive Shaft*	9,284	3,750	2,128	3,192
	6,768	3,394	2,635	3,953
Main Transmission Output*	409	3,684	47,478	71,217
	297	3,335	58,805	88,208
Interconnect Drive Shaft*	9,284	1,875	1,064	1,596
	6,768	1,697	1,317	1,975
* Transmission power losses are included.				

The gears are designed to operate continuously at maximum-torque rpm in fixed-wing flight. Design conditions are 1350 foot-pounds input torque for the engine gearboxes and 2635 foot-pounds input torque for the main transmissions. The design horsepower for the main transmissions is 10 percent higher than the engine gearbox horsepower. This is based on a 55-45-percent power split. That is, both engines are assumed to be capable of delivering 55 percent of the maximum single-engine torque to one pylon simultaneously, thus accounting for a power input of 110 percent of maximum single-engine output.

Gear-tooth bending stress, subsurface shear stress, and k-factors (a design parameter used as a measure of tooth surface durability) are calculated based on maximum continuous torque. Surface compressive stress, pressure velocity products, and Kelly-Blok scoring indexes are calculated based on limit torque.

Allowable stresses are in accord with those values which have shown fatigue reliability in excess of 99.5 percent for all gear products heat-treated and manufactured per Bell Helicopter Company process specifications. Table XIII shows the gear-tooth stresses.

TABLE XIII				
GEAR-TOOTH STRESSES				
Component	Member	Stress		
		Bending (psi)	Compressive (psi)	
Engine Gearbox	Input Bevel Pinion	24,200	168,000	
	Bevel Gear	24,200	168,000	
Main Transmission	Input Bevel Pinion	28,800	169,000	
	Bevel Gear	28,800	169,000	
	Lower Sun Gear	35,800	158,000	
	Lower Planet Idler	32,600	158,000	
	Lower Ring Gear	31,400	95,000	
	Upper Sun Gear	44,000	181,500	
	Upper Planet Idler	44,200	181,500	
	Upper Ring Gear	49,600	109,500	

The bearing design criterion was selected as 75 percent of maximum continuous torque at 12,100 engine rpm. The high-torque conditions determine bearing life more than speed, as ball-bearing life varies as the third power of load ($3\frac{1}{3}$ power for roller bearings), while life varies directly with rpm. It is anticipated from past experience that the selected speed-power spectrum will provide a 1000-hour overhaul period for the drive-system bearings. Table XIV shows the calculated L_{B10} life for each bearing of the power train.

Design of the drive shafts and couplings is based on maximum continuous torque per Table XII. The drive shafts were designed so that the components' yield strengths correspond to the loads at limit torque. The shafts exhibit infinite fatigue life at the maximum continuous torque condition.

TABLE XIV				
$L_{B_{10}}$ BEARING LIFE AT 75-PERCENT MAXIMUM CONTINUOUS TORQUE				
Component	Rotating Member	Bearing	$L_{B_{10}}$ Bearing Life at 12,100-rpr Engine Speed (hrs)	
Engine Gear- box	Input Pinion	7218 Ball Triplex	1,005	
	Input Pinion	309 Roller	4,648	
	Output Gear	7024 Ball Duplex	1,004	
	Output Gear	1924 Roller	19,980	
Main Trans- mission	Input Pinion	7219 Ball Triplex	1,579	
	Input Pinion	312 Roller	4,820	
	Gear Shaft	1928 Ball Duplex	1,600	
	Gear Shaft	1028 Roller	7,752	
	Lower Planet Roller	308 Roller	7,480	
	Upper Planet Roller	20mm Dia	12,720	

C. LIFT AND THRUST SYSTEMS

Rotors, mounted on pylons at each wingtip and rotating in opposite directions so as to cancel torque, provide lift for helicopter operation and thrust for fixed-wing flight. Each rotor has three blades and a diameter of 38.5 feet. Figure 253 shows the details of the design. The semirigid rotors are gimbal-mounted by means of a universal joint in the plane of the rotor. Although the universal joint provides freedom for the hub to tilt in any direction (i.e., blade flapping), this tilt is restrained in the fore-and-aft direction by hub-restraint springs mounted to the pylon assembly. Lateral tilt is unrestrained.

1. ROTOR HUB

a. Yoke

The primary structure of the rotor hub assembly is the forged yoke, which consists of a deep, flanged titanium ring with three integral spindles. The spindles, which mount the blade-pitch-

change bearings, are precone 2.5 degrees to relieve steady beam bending moments due to lift and thrust and are bored to reduce weight and to permit installation of the blade-retention straps within the spindle bores. The inboard ends of the spindles are counterbored to provide a seat for the retention-strap fittings. An index plate, which prevents rotation of the fitting and carries reverse loading when the rotor is inoperative, is attached to the strap fitting and to one of the yoke mounting bolts. To prevent fretting of the titanium yoke, the inner races of the pitch-change bearings and the inboard seal radius rings are separated from the spindle with bonded-in-place Teflon fabric liner.

b. Pitch-Change Bearings

To achieve long life and high reliability, the blade-pitch-change bearings are made of M-50 steel and have oil bath lubrication. In addition, the rollers of the bearings are caged for separation and crowned to reduce the end-loading effect due to structural deflections.

The bearings are located on the spindles by spacer tubes which were selected to achieve low bearing loads and relatively small slope differential across the bearings. The inner race of the inboard bearing seats against a radius ring at the inboard end of the spindle. The radius ring also provides a replaceable wear surface for the inboard oil seal. The inner races and spacer tubes are retained with a sleeve, bolted to the outboard end of the spindle, which also provides a replaceable wearing surface for the outboard oil seal. Shims to adjust axial clamp-up on the races are provided between the sleeve and the spindle. The outer races and needle assemblies are installed in an aluminum pitch-change housing, which is an integral part of the bonded blade assembly. The outer bearing seats against an aluminum radius ring, which also houses the outer oil seal. The bearings are retained in the housing by the pitch horn, which houses the inner oil seal and supports an oil reservoir sight gage. The inner seal is protected by a rubber boot which floats axially with the blade during rotor operation, when blade centrifugal forces cause the multistrand steel wire retention straps to stretch. The boot rubs against a thin steel sheet bonded to the pitch horn and is retained on the spindle by the inner radius ring.

c. Universal Joint

The rotor hub is mounted on the mast by means of a universal joint of conventional design. The universal joint incorporates needle roller bearings, similar to those on the yoke spindles. These bearings, however, are not provided with inner races but roll on carburized journals of a steel cross member. A forged titanium fork, which is splined to the mast and secured with

the rotor split cones and retention nut, picks up one axis of the universal joint cross-member through bearing housings inserted into the open pillow blocks of the fork. The bearings for the second axis are installed in the forged titanium pillow block ring which is bolted to the lower flange of the yoke. This ring has open pillow blocks similar to those of the fork. A common oil reservoir is created by oil passages drilled within the cross-member. Oil level sight gages are installed on the pair of bearing housings mounted in the pillow block ring. All the bearing housings also contain "nylatron" washers which carry the side loads, and Teflon seal rings to retain the oil.

2. BLADES

The rotor blade, shown in Figure 254, is of all-metal bonded construction, having thickness taper but with a constant chord and constant twist in the basic structure. Effective helical twist is provided by means of fairings over the inboard portion of the blade and the blade-root fittings. An integral pitch-change housing, the blade grip, is made from an aluminum forging and is bonded to the blade root. The tangs of the pitch-change housing and several aluminum doublers reinforce the blade root. The airfoil at the theoretical root (centerline of hub) is an NACA 64A030. This changes linearly to an NACA 64A206, $a = 0.3$, at the blade tip.

The basic blade is of hollow construction, with an aluminum spar in the forward part and double aluminum skins, stiffened with honeycomb, in the afterbody. A contoured brass nose block in the outer portion of the blade provides proper section mass balance, while chordwise stiffness is provided as required by a tapered trailing edge made from an aluminum extrusion. Shear between the upper and lower panels is carried by two sheet-metal shear webs, the nose blocks, and the trailing edge. The forward 25 percent of the blade airfoil is protected by a 0.040-inch-thick stainless steel erosion shoe.

A steel pin through the blade near the root of the bonded structure attaches the blade to the rotor hub through the retention strap. Blocks are bonded within the blade to support the pin and to minimize bending. Bushings for the pin, pressed through the structure, provide a mechanical safety for the bond between the grip and the remainder of the blade. Small bolts, outboard of the blade-retention pin, have been added as a safety against bond-failure progression between the blade and the housing. The blade is bonded in a fully enveloping cavity fixture with internal pressure such that all blade elements are pressed outward against the tool during the bonding cycle to maintain ideal contour and alignment of parts. The detail parts are preassembled with a self-tacking adhesive and then cured in an autoclave under heat and pressure. For quality

control of the bond, test panels are taken from the scarfed portions of the root and the tip of the bonded assembly. After bonding, the blades are finished by boring the grip to size and by adding the retention-pin bushings, the peel-prevention safety bolts, the tip caps, the covers, and the balancing provisions.

3. FAIRINGS

Fairings minimize the drag and effectively increase the twist of the blades. The hub fairing, or spinner, is made from fiber glass with an aluminum honeycomb core for stiffening. The nose is spun aluminum with an aluminum ring bulkhead for attachment. The spinner is mounted by slipping it over the hub and attaching it to the forged aluminum spinner support ring. This ring is splined to the mast and is retained between the main rotor-retention nut and the yoke. The cutout areas behind each grip are sealed with separate inserts to provide a continuous ring which closely matches the nonrotating fairing of the pylon. Spherical surfaces on the basic spinner (including part of the inserts) match the inboard end of the blade-root cuffs and maintain a closure over the spinner openings during fixed-wing operation.

The blade cuff fairings are also constructed of fiber glass and aluminum honeycomb. They are shaped to fair the blade doublers and the blade grip forging and, at the same time, to provide helical twist for the inboard portion of the rotor blade. The cuffs are made in two halves which are joined by flush-type quick-disconnect fasteners. The discontinuity between the end of the cuff and the basic blade is faired by a lightweight plastic filler compound. A molded polycarbonate bulkhead, split on the chord plane, seals the inboard end of the cuffs and matches the spherical contours on the spinner fairing.

4. RPM AND PITCH RANGES

The engine and rotor can be operated through a wide speed range without large power losses due to off-optimum engine rpm. In helicopter configuration, the engine operating rpm range is from 15,100 to 16,600. This corresponds to rotor speeds of 372 to 409 rpm. The higher rpm is used at high weights and/or altitudes to obtain best performance. At low weights and/or altitudes, the lower rpm may be used if desired to obtain a slight increase in performance. Figure 30 shows the figure of merit of the rotor in hovering flight.

In the fixed-wing flight mode, the rotor rpm is slowed to obtain better propeller efficiencies. In cruise flight, the engine is operated at 8050 rpm (198 rotor rpm) for airspeeds up to approximately 250 knots. At higher speeds, a torque limit is encountered, but a higher maximum speed can be reached

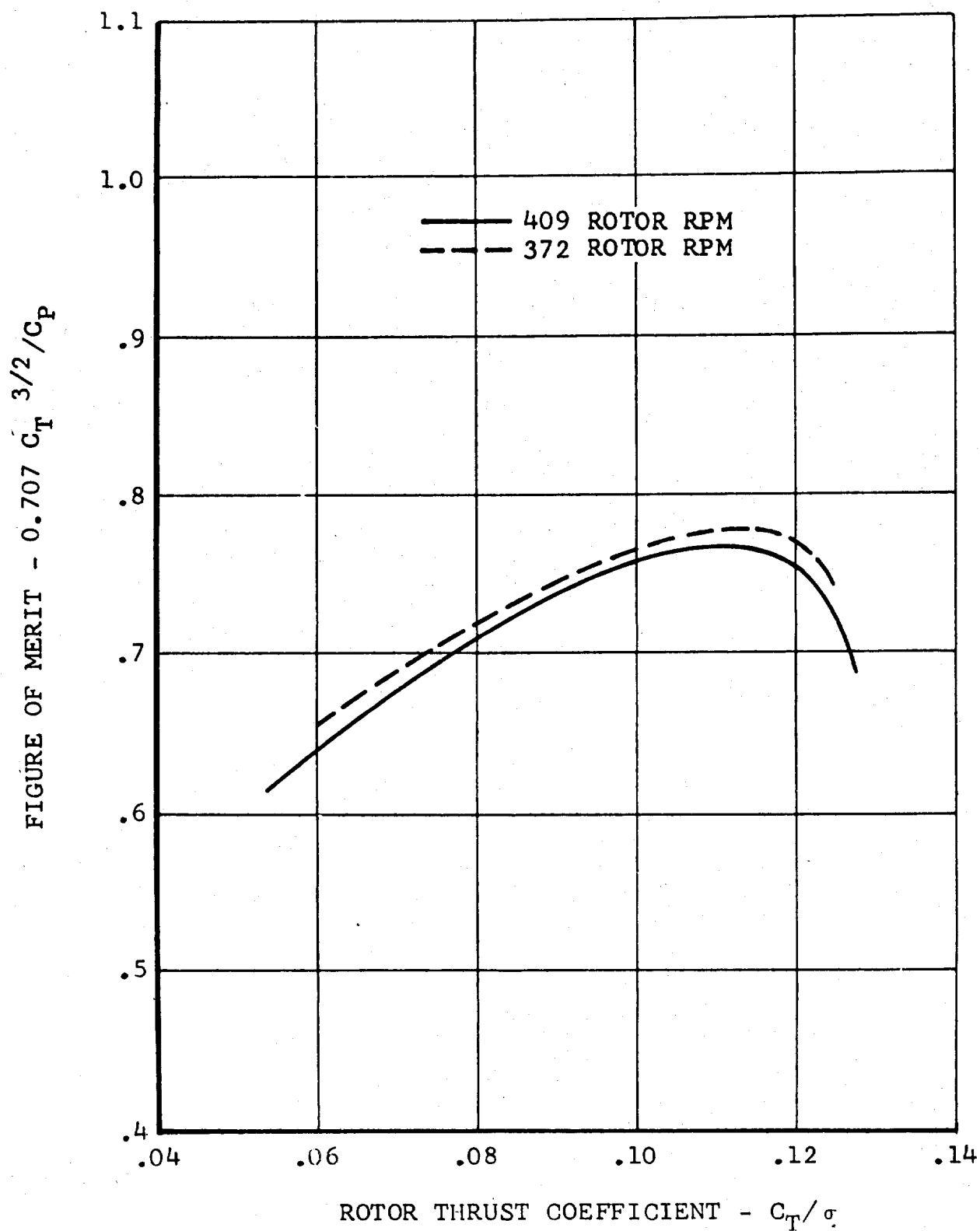


Figure 30 . Rotor Figure of Merit.

by allowing the engine rpm to increase to 12,100 at 340 knots. Although the propeller efficiency is lower at the higher rpm, there is a net gain in thrust horsepower available due to the increase in available shaft horsepower. The propeller efficiencies for speeds from 150 to 400 knots and for engine speeds of 8050, 10,075, and 12,100 rpm (rotor rpm of 198, 248, and 297, respectively) are shown in Figures 31 through 33.

The total available collective-pitch range must be large to operate as both a helicopter rotor and a fixed-wing propeller. The required pitch range in helicopter flight is shown in Figure 34. The minimum pitch is zero degrees (at $3/4$ radius), for autorotation, and the maximum is 18 degrees. For fixed-wing flight, the required pitch range is shown in Figure 35. The minimum pitch required at high rpm (16,600) is 20 degrees. The maximum pitch is 55 degrees. As indicated by the large change in power with collective pitch, the control of collective pitch becomes increasingly sensitive as airspeed is increased in the fixed-wing mode.

Twist and thickness distribution of the blades are shown in Figure 254.

5. ROTATING CONTROLS AND HUB RESTRAINT

a. Rotating Controls

This section is concerned with those controls which are part of the wingtip-mounted pylons and which rotate with the rotors. Controls schematic is shown in Figure 255.

Collective control inputs are introduced by means of a hydraulic cylinder which is attached to the lower end of each main transmission and extends into the rotor mast. The nonrotating collective control tube inside the rotor mast transmits the collective motion to a collective head through a pair of duplexed, grease-packed and sealed, angular-contact bearings. The collective head is bolted to a sleeve which slides on a Teflon bearing attached inside the upper end of the rotor shaft. The sleeve, which is dry-film lubricated, is splined to the mast to cause the upper portion of the collective system to rotate with the mast. Thus, the nonrotating collective input motion of the hydraulic (servo-boost) actuator is transmitted to the rotating crosshead above the rotor. The collective tube travels a total of 5 inches to provide the 55 degrees of collective blade pitch required for both helicopter and high-speed modes.

Cyclic control inputs are introduced through the hydraulic cylinder actuator mounted to the side of the transmission case. The actuator is connected to the nonrotating ring of the

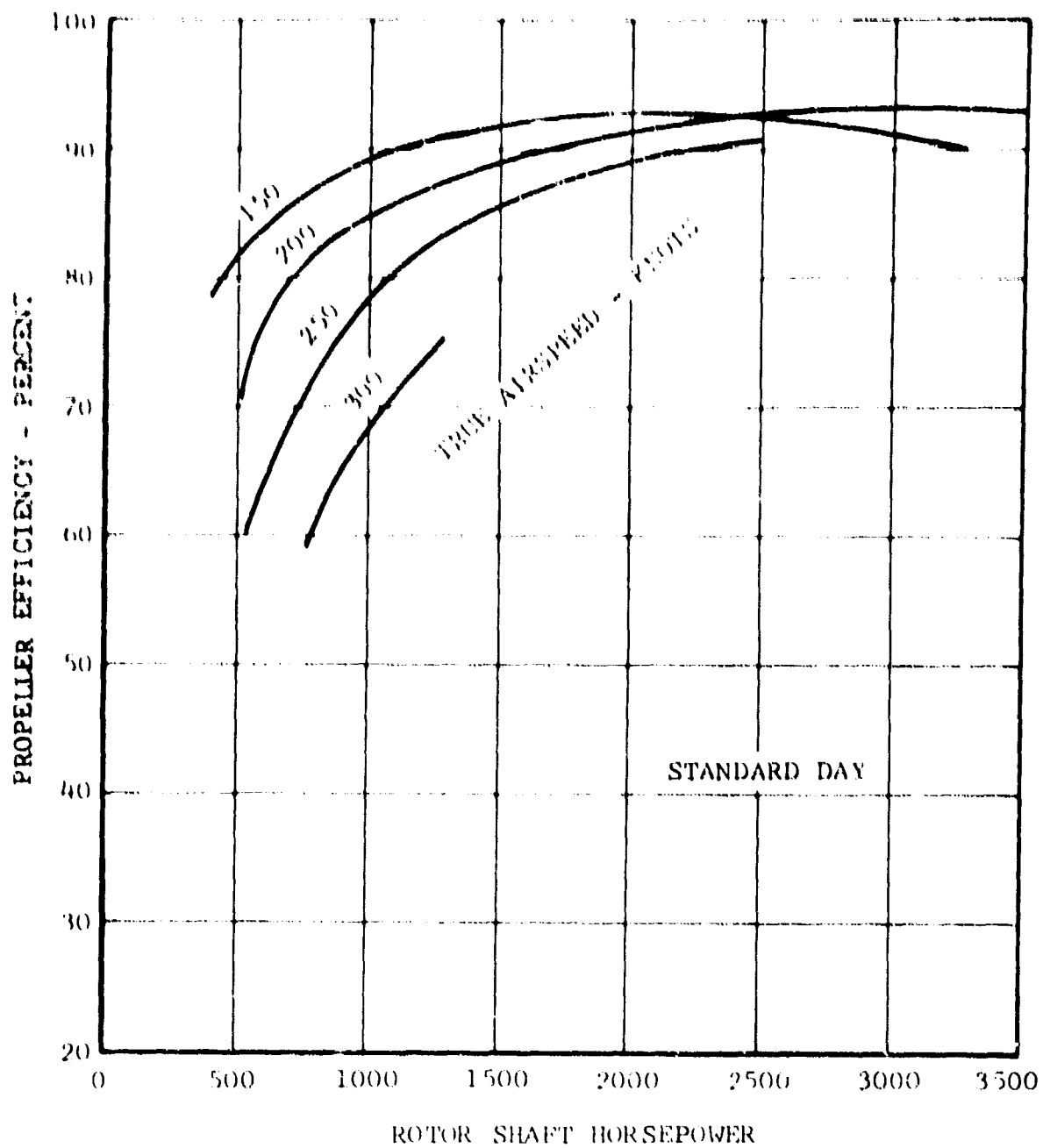


Figure 31. Propeller Efficiency
198 RPM, Sea Level.

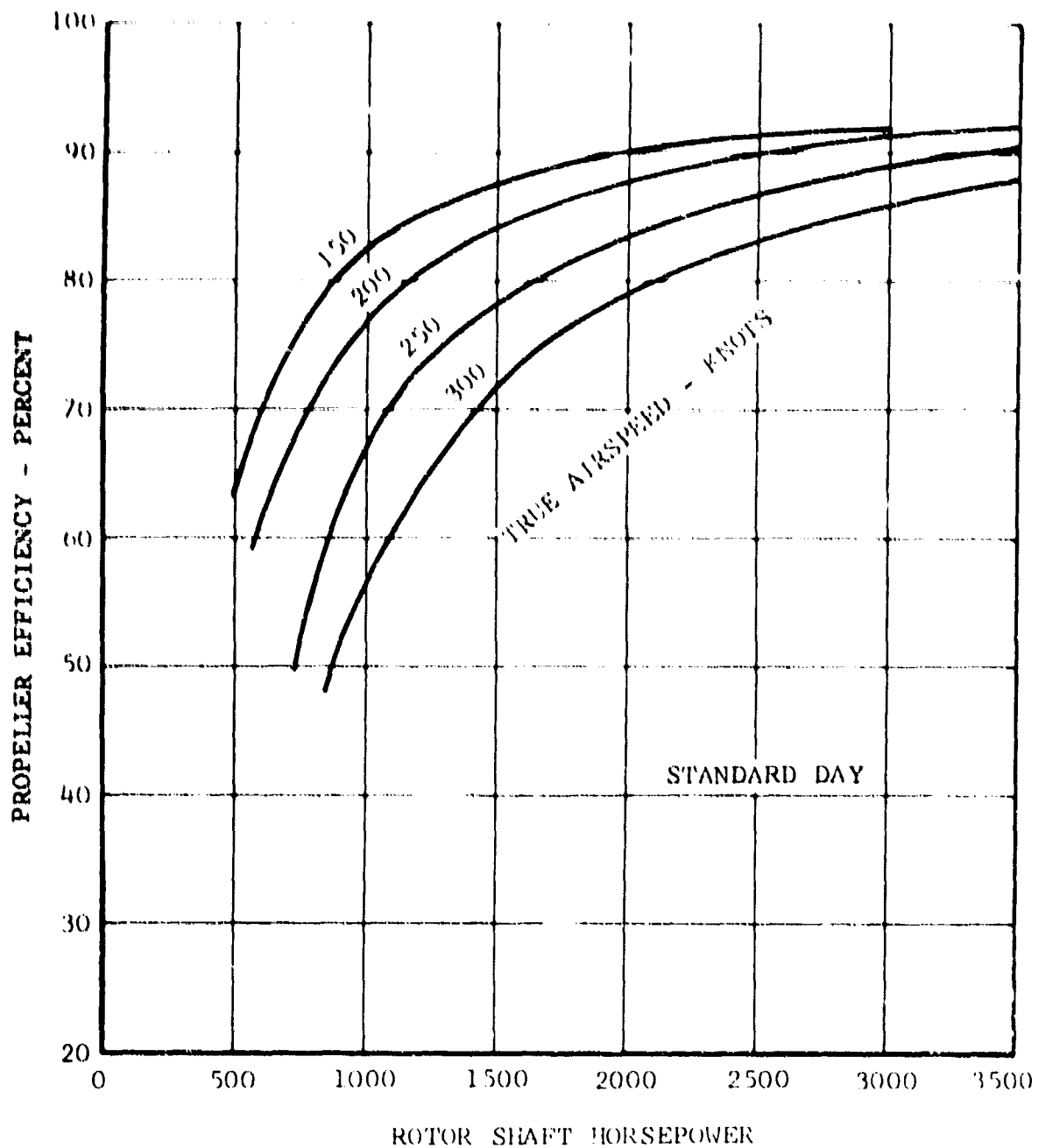


Figure 32. Propeller Efficiency
248 RPM, Sea Level.

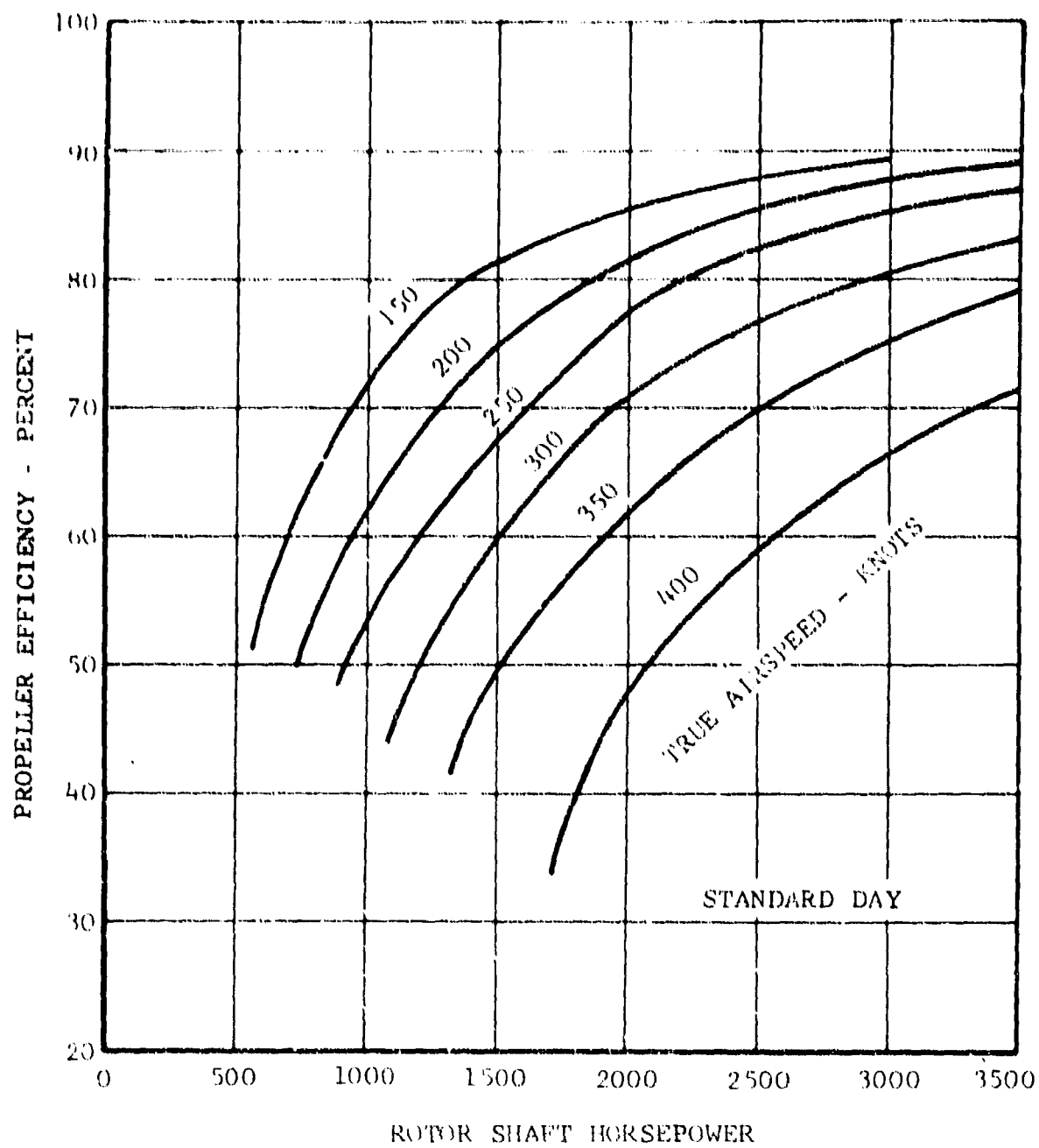


Figure 33. Propeller Efficiency
297 RPM, Sea Level.

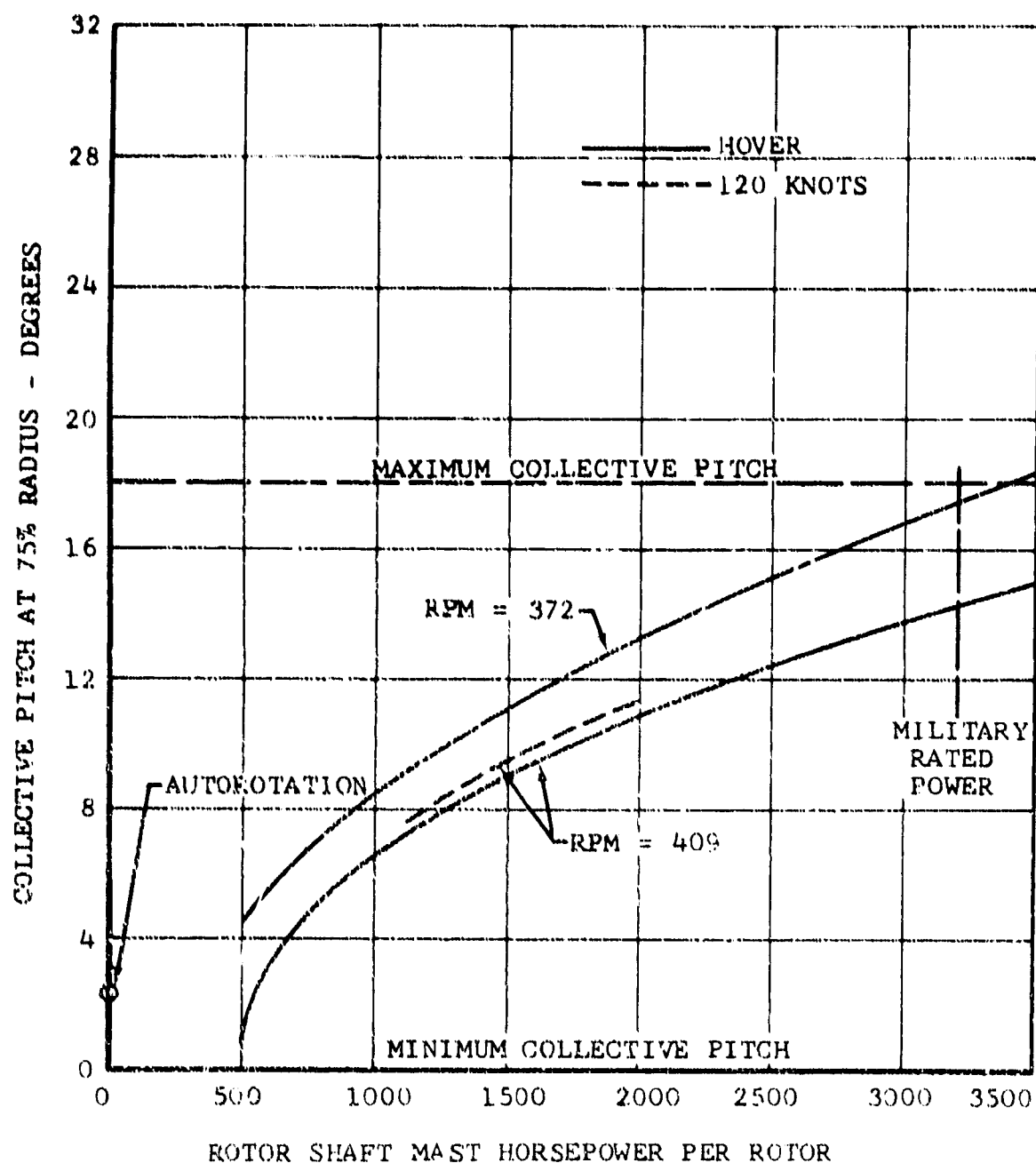


Figure 34. Collective Pitch Range, Helicopter Mode.

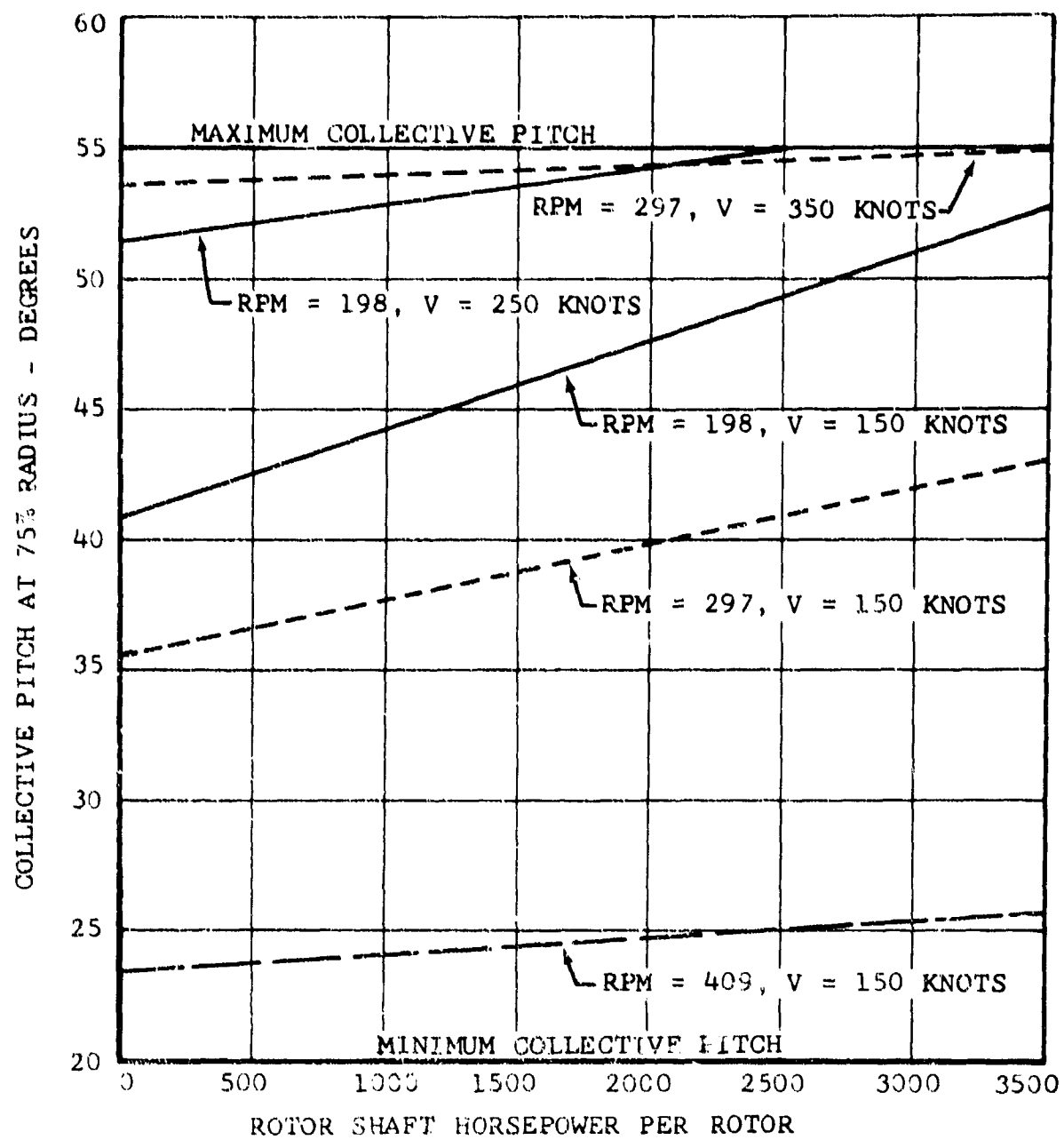


Figure 35. Collective Pitch Range, Fixed-Wing Mode.

swashplate and causes the swashplate assembly to tilt when displaced from its neutral position.

The aluminum forged swashplate is mounted to the swashplate support on caged needle-type bearings which permit the swashplate to tilt ± 10 degrees about one axis for fore-and-aft cyclic inputs. The duplex-mounted swashplate bearings transmit the cyclic input to the rotating ring. Two titanium links, with one end attached to the rotor spinner support ring and the other end attached to the swashplate ring, drive the rotating controls. The spinner support ring is attached to the rotor mast by the main retaining nut of the hub assembly.

Cyclic motion is transmitted from the rotating ring of the swashplate to the mixing levers by fixed-length control tubes. There are three mixing levers, one for each blade, which combine the cyclic and collective motions into one output. They are pivoted to the collective head, with one end attached to the cyclic control tube and the other attached to the pitch-change tube. The pitch-change tube is connected to the blade-pitch horn and is adjustable to provide for tracking the blades. The pickup point of each pitch horn is located 60 degrees ahead of the blade so that 30 degrees of δ_3 (pitch-flap coupling) is effected. The orientation of the swashplate tilt with fore-and-aft cyclic-stick displacement is phased to accommodate this δ_3 .

b. Hub-Restraint Springs

The rotor has hub-restraint springs to increase its moment capability (control power). This allows a greater center-of-gravity range in the helicopter mode. The springs are mounted on the transmission (in the nonrotating system) and are connected to the rotor hub through a pair of grease-lubricated, angular-contact ball bearings which are mounted to the yoke through the pillow-block ring. To counteract the inherent problems of pure moment loading, a preloaded duplex bearing is used. This bearing application is quite similar to that of the swashplate assembly. The retainer plate for the hub-restraint bearings provides a replaceable wear surface for the bearing seal and also serves as the flapping stop for the hub assembly. The rotor hub is free to tilt 8 degrees in any direction, with the hub-restraint springs providing a restoring moment of 18,000 inch-pounds per degree for fore-and-aft tilt, but no restraint to lateral tilt.

Since no moment is required in the lateral direction, the hub springs are mounted on the longitudinal (fore-and-aft) centerline of the rotor-pylon assembly, one forward and one aft. The hub-restraint springs consist of precompressed rubber in metal housings and are loaded in shear by links between the

• springs and the nonrotating ring of the hub-restraint bearing. The spring assemblies are supported from lugs protruding from the transmission case. The links deflect the springs only when the rotor flaps fore or aft, and there are no one-per-rev oscillations of the springs as would be the case for springs mounted in the rotating system. Since the hub-restraint moment is transferred directly from the rotor yoke to the transmission case as a couple, the universal joint and mast bearings do not have to carry any additional loads from the hub springs. A torque tube and linkage, attached to the swashplate support, prevent rotation of the hub-spring bearing housing.

6. CONVERSION SYSTEM

• The conversion unit consists of a hydraulic motor, a nonreversing worm gear and wheel, and a telescoping jack screw. A conversion unit is provided for each pylon. These units are interconnected to provide fail-safe operation. The interconnect shaft transmits no torque unless one of the conversion units fails. In the event of failure of one unit, the other unit would perform the conversion of both pylons. The conversion units are mounted on the outboard end of each wing at the leading edge. The jack screw is attached to a pivoting yoke on the transmission top case. Loads are thus reacted between the transmission top case and the wing outboard rib, with the conversion axis at the center of the spindle in the wing aft section.

SECTION III. STRUCTURES

A. CRITERIA

Because the D266 is, essentially, both a fixed-wing aircraft and a helicopter, it does not completely conform to any of the types of aircraft defined in present structural specifications. Therefore, some improvisation is required to develop basic design criteria.

The basic guideline for the structural design criteria comes from the Statement of Work in Contract DA44-177-AMC-373(T) and applicable military specifications. In the helicopter configuration, the structural loads are in accordance with MIL-S-8698(ASG); in the fixed-wing flight mode, the design loads are in accordance with MIL-S-8861(ASG), MIL-A-8865(ASG), and MIL-A-8870(ASG). Maneuver load factors are specified for both configurations.

In the helicopter configuration, the design load factors and cargo loading conform to those specified for a Class II helicopter in MIL-S-8698(ASG). Therefore, the conditions specified for this class are used throughout in the helicopter configuration.

The fixed-wing configuration of the D266 does not correspond exactly with any of the types referred to in MIL-S-8861(ASG). The nearest type, both in load factor and in eventual mission, is the utility airplane. The utility airplane has a specified maneuver load factor of +4.0 and -2.0, as compared with +4.5 and -1.0 for the D266. Except for maneuver load factor, the design conditions are those specified for the utility airplane.

This aircraft is exposed to two classes of fatigue environment: that of the rotating components which are peculiar to helicopter configuration, and that that is not induced by the rotor system. For the former types of fatigue, emphasis is placed on Bell's experience in the design of rotors and components affected by rotor-induced loads. These loadings are computed using aeroelastic rotor theory. Specific design techniques, using these computed loads, are specified in the section of this report that deals with fatigue. For the structure that is unaffected by rotor cyclic loads, MIL-A-8866(ASG) is used as a guide. The spectra used are those associated with a utility airplane, and the design objective is to obtain the fatigue life specified by MIL-A-8866(ASG).

1. BASIC DESIGN PARAMETERS

a. Helicopter Flight Configuration

Mast Angle	0-15 degrees
Conversion Axis	Fuselage Station 320
Most Forward cg	Station 309.5 at W.L. 125
Most Aft cg	Station 327.5 at W.L. 125
Design Gross Weight	23,000 pounds
Design Load Factor n_z	+3.0, -0.50 limit
Alternate Gross Weight	30,800 pounds
Alternate Gross Weight Load Factor n_z	+2.0 limit
Maximum Sideward and Rearward Velocity	35 knots
Maximum Autorotative Landing Speed	80 knots
Design Sink Speed	8 fps
Sink Speed for Reserve Energy	9.8 fps
Alternate Gross Weight Sink Speed	6.0 fps
Alternate Gross Weight Sink Speed for Reserve Energy	7.35 fps
Design Engine Shaft Horsepower	3435
Rotor Speed	372 to 409 rpm
Transmission Ratio	40.6:1
Yield Factor of Safety	1.0
Ultimate Factor of Safety	1.5
Rotor Speed Limit Factor	1.1

b. Conversion Flight Configuration

Mast Angle	15-90 degrees
Center-of-Gravity Travel During Conversion	10.5 inches
Design Gross Weight	23,000 pounds
Design Load Factor n_z	+3.0, -0.50 limit

c. Fixed-Wing Flight Configuration

Mast Angle	90 degrees
Most Forward cg	Station 296 at W.L. 114.5
Most Aft cg	Station 317 at W.L. 114.5
Design Gross Weight	23,000 pounds
Design Load Factor n_z	+4.5, -1.0 limit
Minimum Flying Weight	16,710 pounds
n_z at Minimum Flying Weight	+4.50, -1.0 limit
Maximum STOL Gross Weight	41,500 pounds
n_z at Maximum STOL Gross Weight	2.50 limit
Maximum Gust Load Factor (n_z) at Design Gross Weight	+3.10, -1.10 limit
at Minimum Flying Weight	+3.82, -1.82 limit

$\dot{\omega}$ at Maximum n_z
 $\dot{\omega}$ at 1/2 Maximum n_z
Rotor Speed

-1.50 radians/second²
+3.0 radians/second²
198 rpm (minimum)
297 rpm (maximum)
1350 foot-pounds

Design Engine Torque

Torque Factor: Transient Factor = 1.50; torque from two engines to be divided 55 percent-45 percent; therefore, total rotor torque factor = $1.5 \times 1.1 = 1.65$ times that of one engine. This is to be carried through spindle bearings. For carry-through structure, torque factor = 1.10.

2. STRUCTURAL DESIGN SPEEDS

The true speeds used for the structural design of the aircraft are defined below. The nomenclature corresponds to MIL-S-8698 (ASG) and MIL-A-8860(ASG).

a. Helicopter and Conversion Flight

In lieu of specifying a single speed for V_H and V_L , these speeds are defined as a function of mast angle. Two maximum speeds are shown to establish the conversion corridor in Figure 36. The lower of these two speeds is the speed at which the rotor is designed for infinite life and is defined as V_H . The higher speed is for noncontinuous operation where the rotor is designed for 10^6 cycles of life and is defined as V_L .

b. Fixed-Wing Flight

The following speeds apply when the aircraft is in the fixed-wing flight configuration with the masts fully converted to 90 degrees.

V_H = High Speed	350 knots
V_L = Limit Speed	437 knots
V_G = Maximum Speed for a 66-fps Gust	196 knots at Design Gross Weight 148 knots at Minimum Flying Weight
V_F = Maximum Allowable Speed With Flaps Down	100 knots for 60° Flap Setting 190 knots for 30° Flap Setting

3. V-n DIAGRAM

V-n diagrams are drawn for the design gross weight and minimum flying weight in Figures 37 and 38. The curves are drawn as

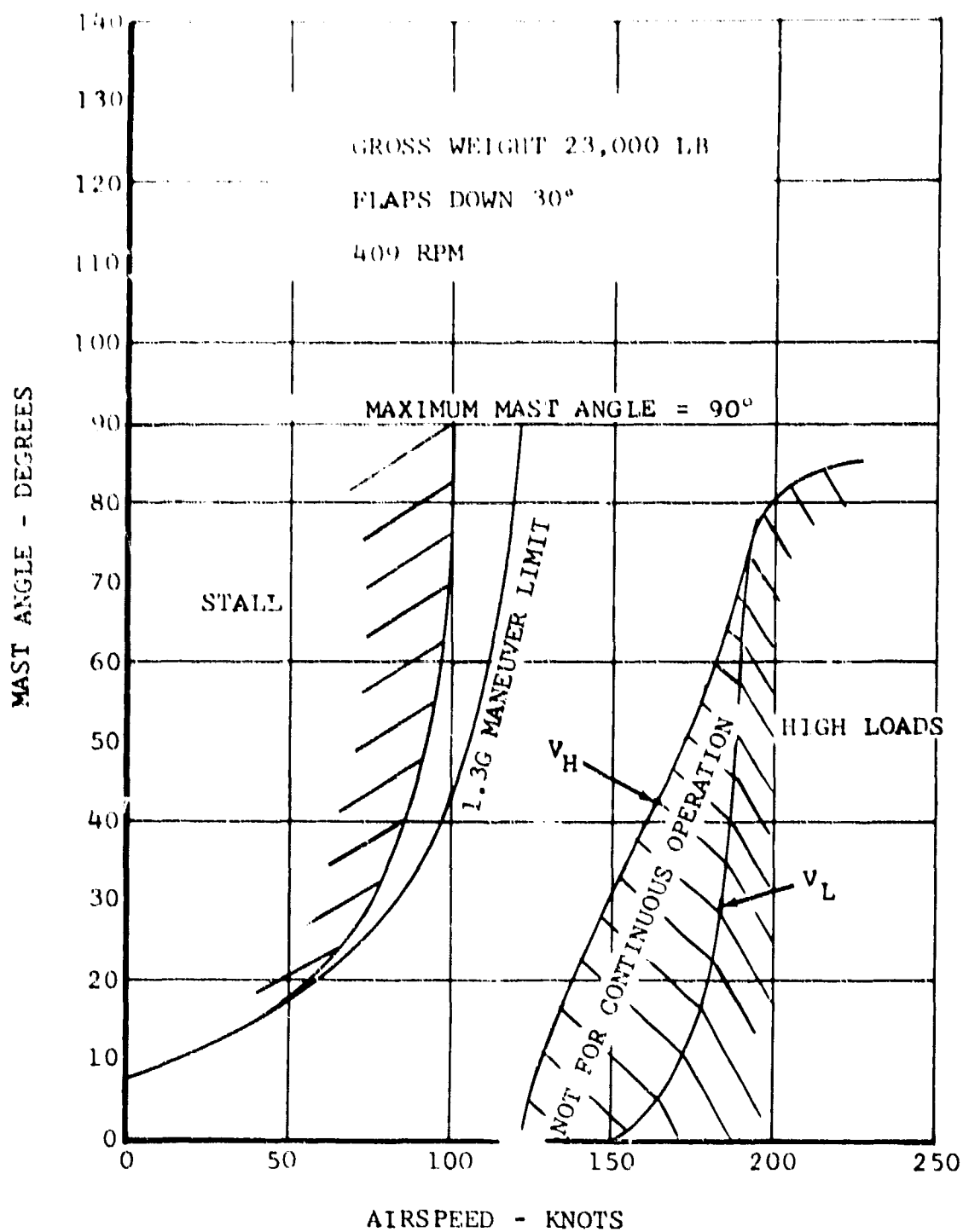


Figure 36. D266 Conversion Corridor.

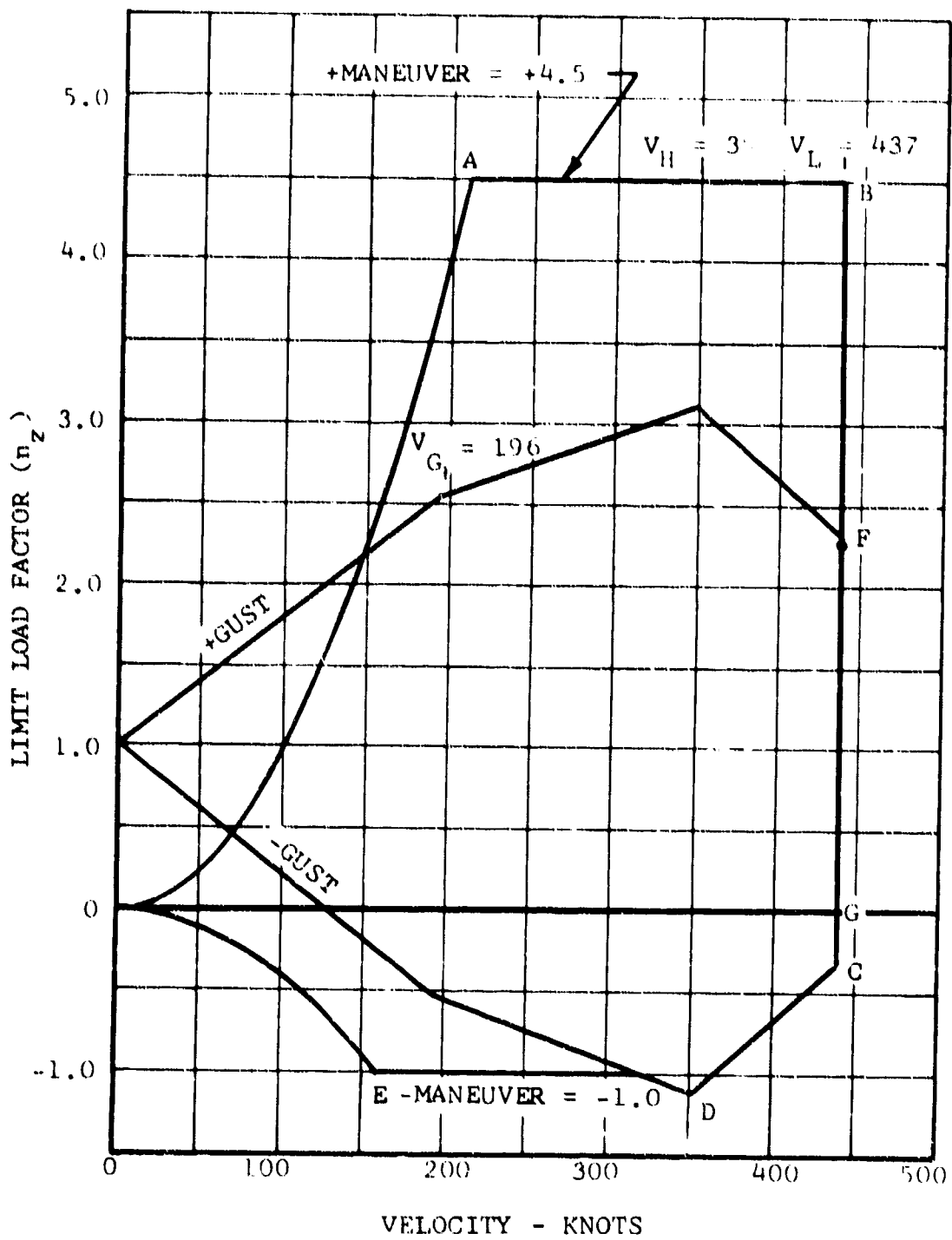


Figure 37. D266 V-n Diagram (Sea Level)
Design Gross Weight = 23,000 Lb.

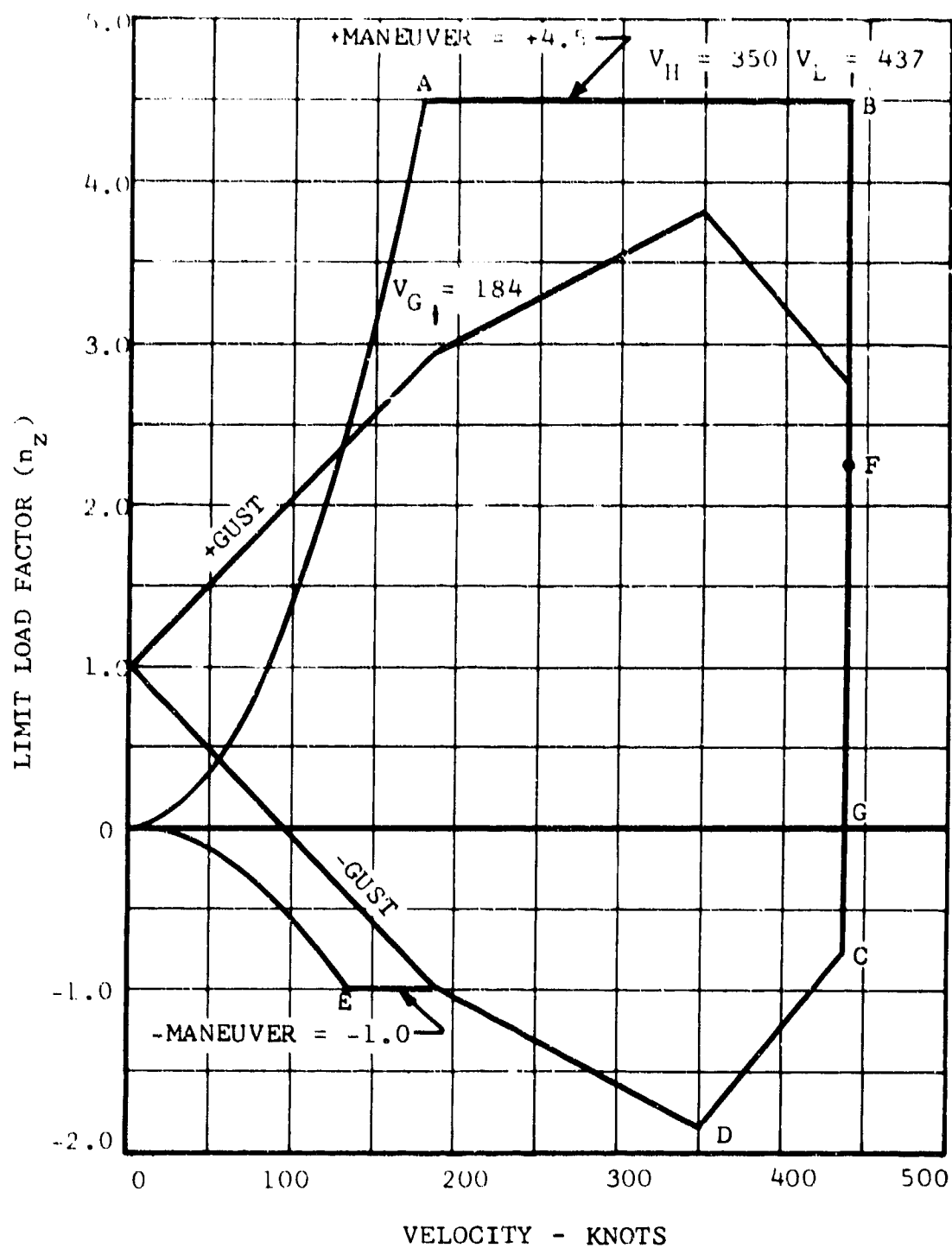


Figure 38. D266 V-n Diagram (Sea Level)
Minimum Flying Weight = 16,710 Lb.

specified in Figure 2 of MIL-S-8861(ASG). A value of 1.65 was used for $C_{N_{Amax}}$ for computing the low-velocity portion of the

diagram. The gust load factors are drawn on the diagrams and where applicable, form part of the envelope of load factor.

The V-n diagram to be demonstrated in flight during the follow-on development program is defined and discussed in the Test Plan Report, Reference 2.

4. GUST LOAD FACTORS

Rigid-body gust load factors are computed for a sharp-edged gust with the gust velocities, alleviation factors, and speeds specified in MIL-S-8861(ASG), paragraphs 3.5, 3.5.1, and 3.5.2. Load factors are computed for both design gross weight and minimum flying weight. These curves are drawn directly on the V-n diagrams of Figures 37 and 38.

5. MAJOR DESIGN CONDITIONS

Some of the major structural design conditions are summarized in Tables XV through XX and the accompanying discussion. These conditions are not to be construed as being the only structural requirements for the aircraft, but rather the ones that are generally critical. All applicable specification requirements will be met unless specific deviations are requested during contract negotiations.

TABLE XV				
DESIGN CONDITIONS FOR HELICOPTER FLIGHT				
Condition	Weight W (lb)	Limit Load Factor n_z	Rotor Speed (rpm)	Airspeed V (kt)
I Maximum Speed	23,000	1.0	372 - 450	125
II Symmetrical Dive and Pullout*	23,000	3.0	372 - 450	150
III Pushover in Forward Flight	23,000	-0.50	372 - 450	125
IV Vertical Takeoff	23,000	3.0	372 - 450	0
	30,000	2.0	372 - 450	0
V Rolling Pullout**	23,000	2.4 & 0	372 - 450	125
VI Yawing***	23,000	1.0	372 - 450	125

TABLE XV - Continued

* Pitching accelerations developed by linear control displacement in 0.30 second to position that results in 3.0g, and return to neutral in 0.30 second.

** Maximum roll rate with full lateral displacement in 0.30 second.

*** Displace controls to maximum attainable sideslip angle, not to exceed 15 degrees; return to neutral.

TABLE XVI

DESIGN CONDITIONS FOR FIXED-WING
SYMMETRICAL FLIGHT

Condition	Weight W (lb)	Limit Load Factor n_z	Airspeed V (kt)	Pitching Angular Velocity $\dot{\omega}$ (rad/sec)	Unit Pitching Acceleration $\ddot{\omega}$ (rad/sec ²)
VII Positive Balanced Maneuver	23,000	4.50	211 to 437	1.5 0.197	0 0
VIII Negative Balanced Maneuver	23,000	-1.0	160 to 360	0.121 0.055	0 0
IX Positive Symmetrical Maneuver With Pitch	23,000	4.50	211 to 350	1.5 $\frac{145}{V}$ fps	-3.0
	23,000	4.50	350 to 437	$\frac{145}{V}$ fps	-1.5
	23,000	2.25	211 to 350	$\frac{217}{V}$ fps	+3.0
	23,000	2.25	350 to 437	$\frac{217}{V}$ fps	+1.50

TABLE XVI - Continued					
Condition	Weight W (lb)	Limit Load Factor n_z	Airspeed V (kt)	Pitching Angular Velocity $\dot{\omega}$ (rad/sec)	Unit Pitching Acceleration $\dot{\omega}$ (rad/sec ²)
X Negative Symmetrical Maneuver With Pitch	23,000	-1.0	160 to 360	$\frac{32.2}{V}$ fps	+3.0
		-0.5	160 to 360	$\frac{48.3}{V}$ fps	-3.0
XI Maneuvers With Specified Control Displacement		As specified in MIL-S-8861(ASG) paragraph 3.2.2.2.			
XII Rolling Pullout	W = 23,00 pounds, V = 437 knots Directional controls in either of two conditions: (1) Fixed for trim with zero rudder. (2) Displaced as necessary to maintain zero sideslip. Displace stick as far as possible with a pilot force of 60 pounds in not more than 0.10 second. Hold until either a 77-degree bank or a roll rate of 270 degrees per second is obtained. Return stick to neutral in no greater than 0.10 second.				
XIII Vertical Gust	W = 16,700 pounds to 23,000 pounds. n_z = per the V-n diagram. (1) Maximum Positive = 3.82 at 16,710 pounds. (2) Maximum Negative = -1.82 at 16,710 pounds.				

TABLE XVII				
DESIGN CONDITIONS FOR LANDING				
Condition	Weight W (lb)	Sink Speed (fps)	Rotor Lift (lb)	Forward Velocity V (kt)
XIV Level Landing, ⁽¹⁾ Three Point	23,000 30,800	8.0 6.0	15,330 20,530	80 80
XV Level Landing, ⁽²⁾ Two Point	23,000 30,800	8.0 6.0	15,330 20,530	80 80
XVI Main Gear ⁽³⁾ Obstruction	23,000 30,800	8.0 6.0	0 0	0 0
XVII Auxiliary Gear ⁽⁴⁾ Obstruction	23,000 30,800	8.0 6.0	0 0	0 0
<p>(1) The main and nose gears shall contact the ground simultaneously.</p> <p>(2) The main wheels shall contact the ground with the nose wheel just clear of the ground.</p> <p>(3) The main landing gear shall contact the ground with the auxiliary gear just clear of the ground. A load equal to one-half the maximum vertical reaction (but not greater than W) shall be applied fore and aft and laterally (but not simultaneously) in combination with the maximum vertical reaction.</p> <p>(4) The auxiliary gear shall contact the ground simultaneously with the main gear. A load equal to seven-tenths of the maximum vertical reaction at the auxiliary gear (but not greater than W) shall be applied fore and aft and laterally (but not simultaneously) in combination with the maximum vertical reaction.</p>				
<p><u>Reserve Energy Requirement</u> - Failure of the structure shall not occur from the sink speeds specified herein times the square root of 1.50.</p>				
<p><u>Spin-Up Requirements</u> - A drag component equal to the force required to accelerate the wheel assembly up to speed during landing impact shall be combined with the vertical ground reaction existing at the time of the spin-up load. A coefficient of friction between the tire and the ground of 0.55 shall be used. The forward velocity at the time of impact shall correspond to the maximum forward velocity during an autorotative descent.</p>				

TABLE XVII - Continued

Dynamic Spring-Back - The loads shall simulate the forward-acting dynamic response of the landing gear during the initial impact.

Maximum Vertical Reaction - The maximum vertical ground reaction shall be combined with a drag load equal to one-quarter of the maximum vertical ground reaction.

TABLE XVIII

DESIGN CONDITIONS FOR TAXIING

Condition	Specification
XVIII Braked Roll, Two Point	W = 23,000 pounds, $n_z = 1.2$ limit. The aircraft shall be in the three-point attitude with the auxiliary gear just clear of the ground. A drag reaction on each wheel in contact with the ground equipped with brakes, equal to 0.8 of the vertical reaction, shall be combined with the vertical reaction. The pitching moment shall be reacted by rotational inertia.
XIX Braked Roll, Three Point	W = 23,000 pounds, $n_z = 1.2$ limit. Same as Condition XVIII except the aircraft is in three-point attitude with all wheels in contact with the ground.
XX Unsymmetrical Braking	W = 23,000 pounds, $n_z = 1.0$ limit. The aircraft shall be in the three-point attitude with one main gear braked and developing a drag load at the ground equal to 0.8 of the vertical reaction of that gear. The aircraft shall be placed in equilibrium as outlined in Paragraph 3.213 of Reference 3.
XXI Reverse Braking	W = 23,000 pounds, $n_z = 1.0$ limit. Same as Condition XIX except drag reaction is acting forward.

TABLE XVIII - Continued	
Condition	Specification
XXII Turning	W = 23,000 pounds, $n_z = 1.0$ limit. The aircraft in the static position shall execute steady turns by means of differential thrust. The gear loads shall be computed per Paragraphs 3.3 and 7.4 of Reference 3.
XXIII Taxiing	W = 23,000 pounds, $n_z = 2.0$ limit. The aircraft shall be in the three-point attitude. No side or drag loads are to be considered.

TABLE XIX	
DESIGN CONDITIONS FOR GROUND HANDLING	
Condition	Specification
XXIV Towing	W = 23,000 pounds, $n_z = 1.0$ limit. The aircraft shall be in the three-point attitude. The following load shall be applied at the tow fitting and shall act parallel to the ground and shall be reacted per Reference 3. The nose-gear tow load shall be 6900 pounds and shall be applied as specified in Paragraph 4.5 of Reference 3.
XXV Jacking	W = 23,000 pounds, $n_z = 2.0$ limit. $n_x = \pm 1.5$ limit, $n_y = \pm 0.5$ limit. The above loads shall be considered in all combinations which include the vertical component. The horizontal loads of the jack points shall be assumed to be reacted in inertia forces in such a manner as to cause no change in vertical loads at the jack points.
XXVI Hoisting	W = 23,000 pounds, $n_z = 2.0$ limit. $n_x = 0$ $n_y = 0$ Loads to be applied at specified helicopter hoist points.

TABLE XIX - Continued	
Condition	Specification
XXVII Mooring	With the aircraft secured in the static attitude, and with the control surfaces locked, the airplane shall be subjected to a 65-knot wind from any horizontal direction.

TABLE XX	
CRASH LOAD FACTORS (ULTIMATE - ACTING SEPARATELY)	
Item	Load Factor
XXVIII Seat Installation, Pilot's and Crew	$n_z = \pm 20.0$ $n_x = 20.0$ forward $n_y = \pm 10.0$
XXIX Cargo, Engine, Rotors, Fuel Tanks, and Other Items, the Failure of Which Would Result in Injury to Personnel	$n_z = \pm 10.0$ $n_x = 20.0$ forward $n_y = \pm 10.0$

The limit pressure for personnel floor shall be 338 psf. The limit pressure for cargo floor shall be 787 psf.

Seventy-five percent of the loads of two pilots shall be applied to the controls where critical. The boost loads shall be considered operative and also inoperative. The loads shall be as specified in Reference 4.

The following are the design criteria for the power train and its associated components:

- The maximum continuous input torque rating of each engine gearbox shall be 1350 foot-pounds.
- The maximum continuous torque rating of the drive system outboard of the engine gearboxes shall be based on 55 percent of the continuous engine output torque rating of both engines.

- The interconnect drive shaft between the engine gearboxes shall be designed to a maximum continuous torque rating based on 55 percent of one engine's output torque rating. Its critical speed shall exceed maximum operating speed by at least 15 percent.
- The limit torque shall be 1.5 times the maximum continuous torque rating.
- The overall reduction as established by gearing arrangement is 40.6 to 1.
- The gear-tooth bending stress, subsurface shear, and K-factors shall be calculated based on the maximum continuous torque with resultant infinite life at this condition.
- Gear-tooth Hertz stresses, Block scoring indices, etc., shall have satisfactory values at limit torque.
- Bearings shall be designed to have a component life of 1000 hours at 75-percent maximum continuous torque and at an engine output speed of 12,100 rpm.

The following table presents the maximum continuous and limit torque design values.

TABLE XXI				
ENGINE AND TRANSMISSION DESIGN SPEEDS AND TORQUES				
Component	Speed (rpm)	Design (hp)	Maximum Cont Torque (ft-lbs)	Limit Torque (ft-lbs)
Engine Output	16,600	3,435	1,090	1,635
	12,100	3,110	1,350	2,025
Outboard Interconnect Drive	9,284	3,750	2,128	3,192
	6,768	3,394	2,635	3,953
Inboard Interconnect	9,284	1,875	1,064	1,596
	6,768	1,697	1,317	1,975
Transmission Output	409	3,684	47,478	71,217
	297	3,335	58,805	88,208

6. FATIGUE REQUIREMENTS

a. Airframe and Landing Gear (Nonoscillatory Structure)

The design objective for the airframe and landing gear shall be a service life of 7500 flight hours and 10,000 landings. The flight maneuver spectrum shall be in accordance with Spectrum C of Reference 5. The distribution of sink speeds shall be in accordance with Table IV of MIL-A-8866(ASG), except that the maximum sink speed shall be 8.0 feet per second. A spectrum of takeoff rotor loads will be developed to supplement the wing loads.

b. Dynamic Components

The design objective for the life of dynamic components shall be 2500 hours. The oscillatory loads shall be those determined both for helicopter and for fixed-wing modes of flight.

B. STRUCTURAL DESIGN LOADS

1. FUSELAGE LOADS

Ultimate loads are shown for three critical flight and two critical landing conditions. These loads were calculated by using unit loadings and balance loads and by multiplying by the appropriate factor.

The following ultimate shears and bending moment curves are shown in Figures 39 and 40.

- Maximum Maneuver Load Factor at $V_L = 437$ knots
- $n_z = 3.375g$, $\dot{\omega} = 4.5$ radians/second², $V = 350$ knots
- Gust on Vertical Tail
- Reserve-Energy Two-Wheel-Landing Spin-Up
- 3.0g Taxiing

Ultimate fuselage torsion curve for vertical tail gust is shown in Figure 41.

2. WING LOADS

Ultimate loads are shown for the following critical conditions:

- 3.0g (limit) jump takeoff
- 4.5g (limit) positive balanced maneuver at 211 knots

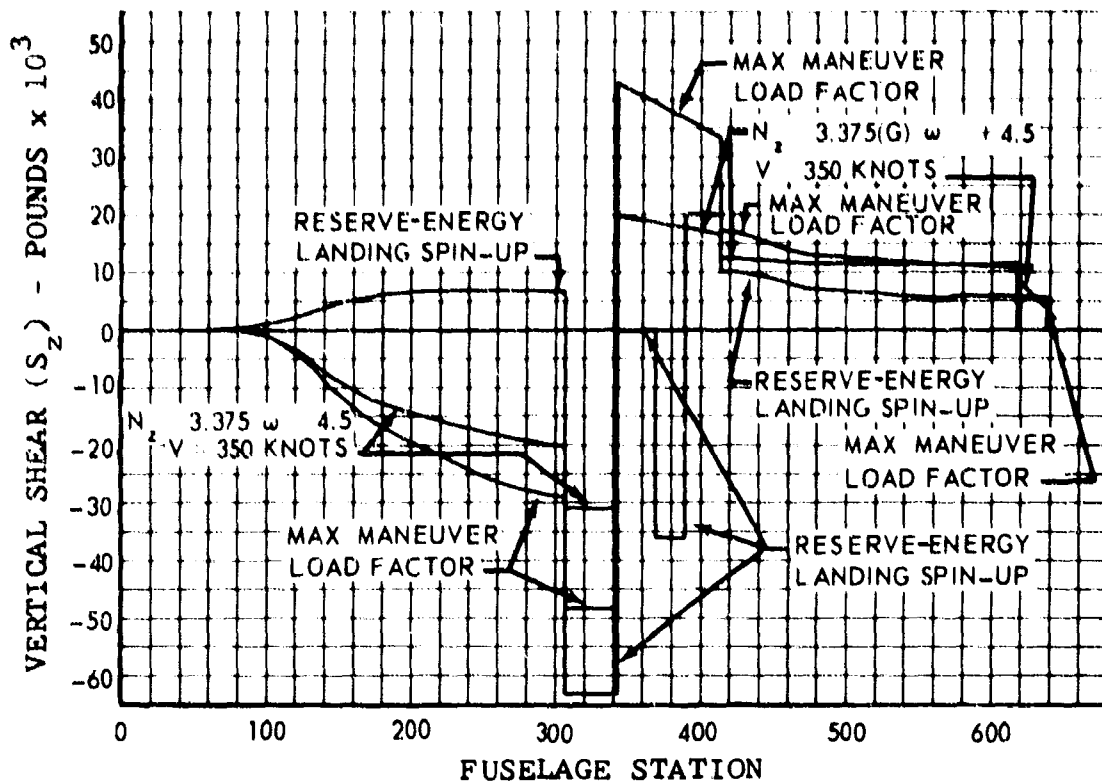
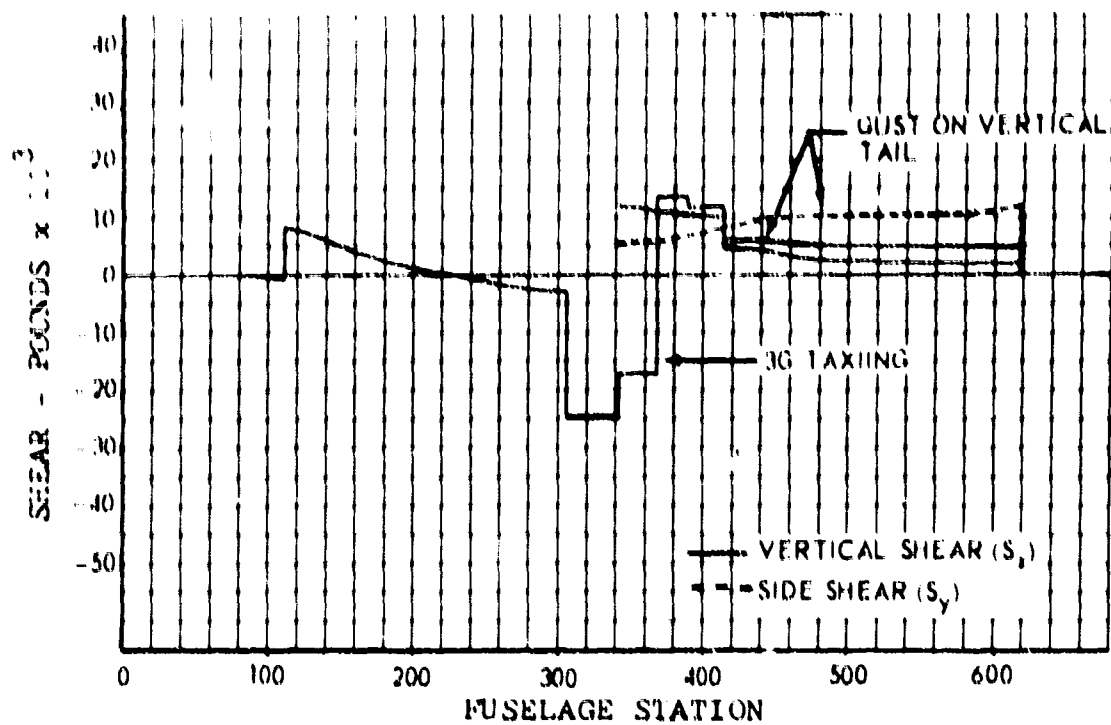


Figure 39. Ultimate Fuselage Shears.

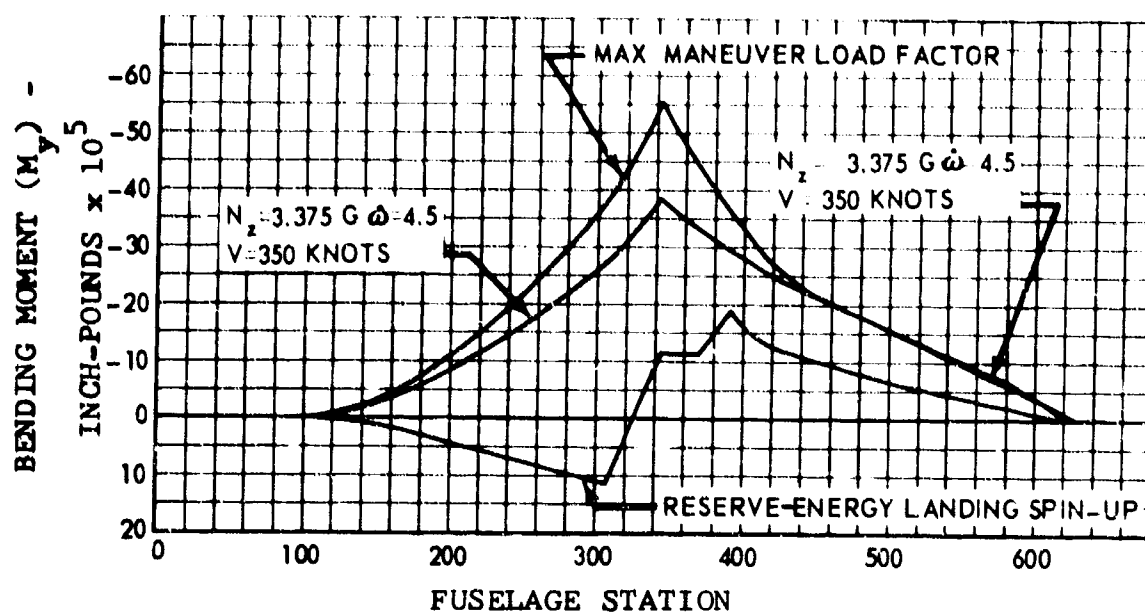
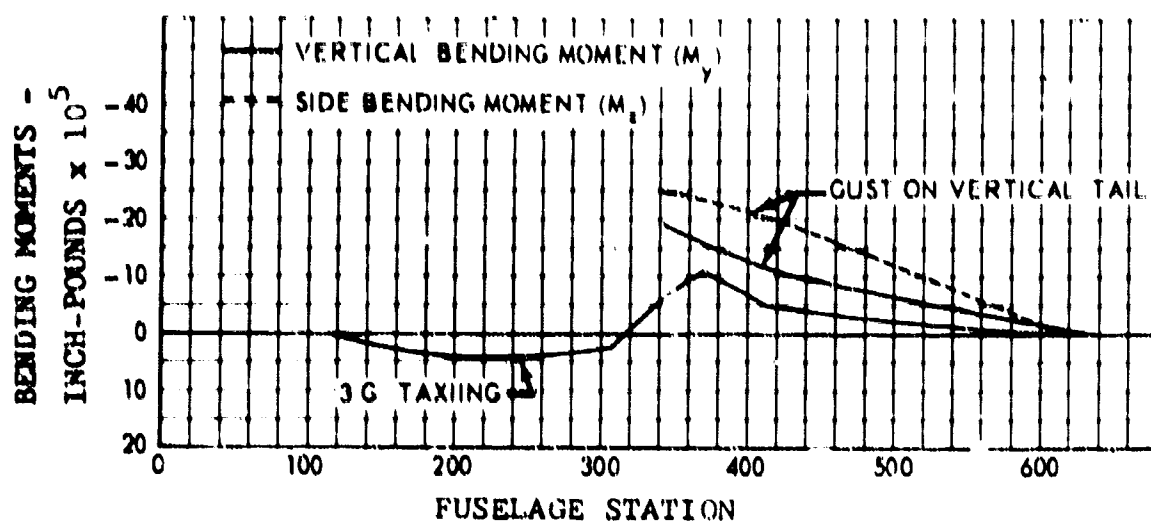


Figure 40. Ultimate Fuselage Bending Moments.

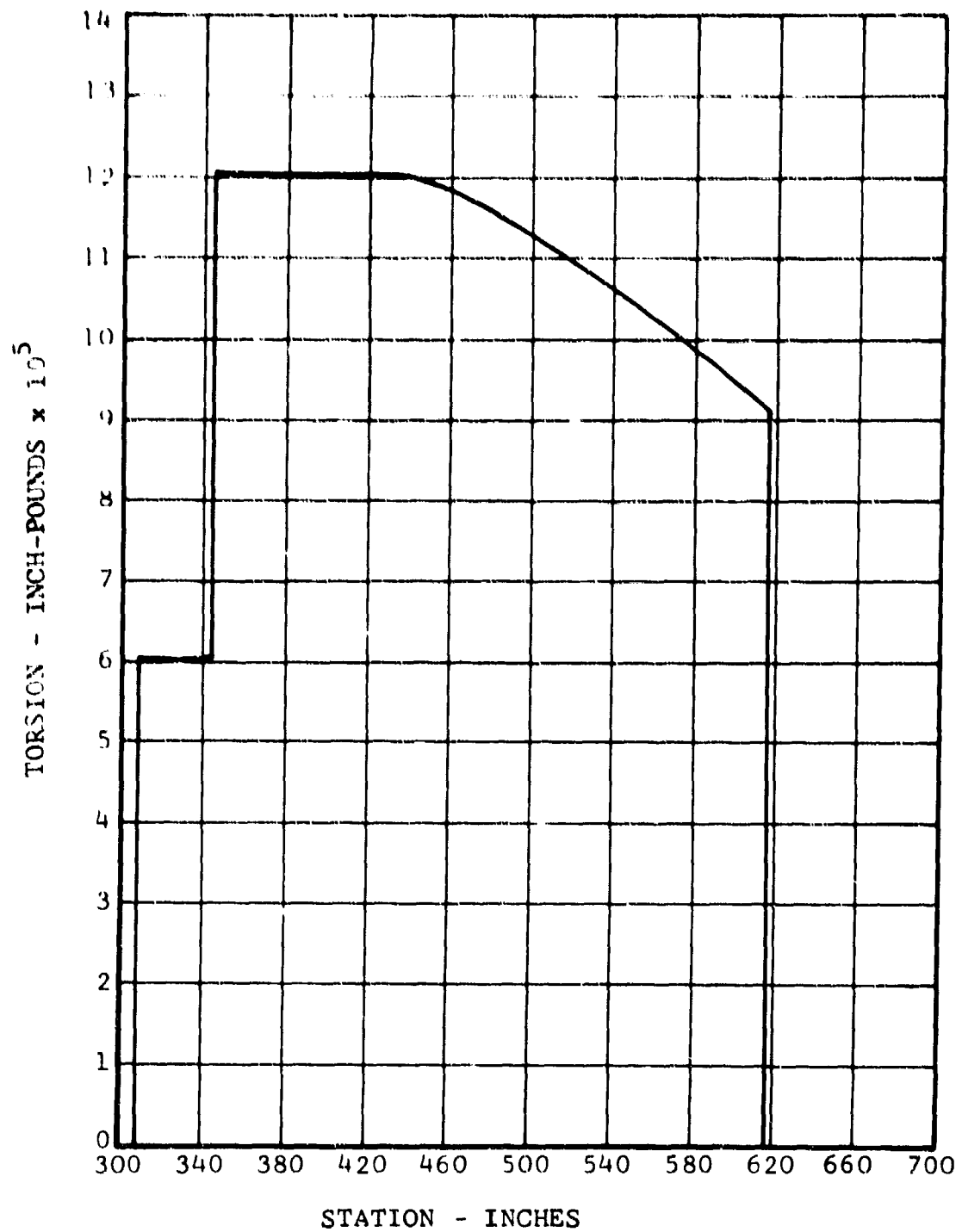


Figure 41. Ultimate Fuselage Torsion,
Gust on Vertical Tail.

4.5g (limit) positive balanced maneuver at 437 knots

-0.3g (limit) negative gust at 437 knots.

The loads, which are shown in Figures 42 through 44, include inertia, air loads, and rotor torque. These values are the results of resolving the moment and torsion into a plane perpendicular and parallel to the elastic axis of the wing.

3. WING-PYLON INTERSECTION LOADS

Actuator and conversion shaft loads for the critical condition are shown in Table XXII. Notation and geometry used are shown in Figure 45. These loads differ somewhat from those shown in Table XXIV since they do not include the 1.65 engine torque factor, which need not be carried beyond the spindle bearings.

4. MAIN-GEAR and NOSE-GEAR LOADS

The main-gear and nose-gear ultimate loads are summarized in Table XXIII. The location of loads is shown in Figure 46.

5. ROTOR LOADS

a. Discussion of Types and Sources of Loads

The rotor and mast are subjected to both static and oscillatory loads and need to be designed for both types. The static loads are those associated with helicopter maneuvers, thrust, and torque. These loads are high in magnitude but occur relatively infrequently during the life of the aircraft. The stresses induced by these loads should be within the limit structural strength of the components. The oscillatory loads are those induced one or more times per rotor revolution and are caused by the cyclic loads on the blades as they traverse their azimuth during helicopter flight. These latter loads, while relatively low in magnitude, have a very high frequency of occurrence, and it is generally necessary to assure that they do not produce stresses in excess of the endurance limit of the structural components. A more detailed discussion of design procedures for oscillatory loads is given in the fatigue section of this report. Bell Helicopter's IBM computer programs were used to generate both static and oscillatory blade and mast loads.

b. Static Blade Loads

The critical loads occur during a 372-rpm, 3g helicopter maneuver. The limit static beamwise and chordwise bending moment distributions on the blade for this condition are shown in Figure 47. The limit centrifugal force distribution is shown in Figure 48. The loads shown in both figures were computed using BHC Program CO2.

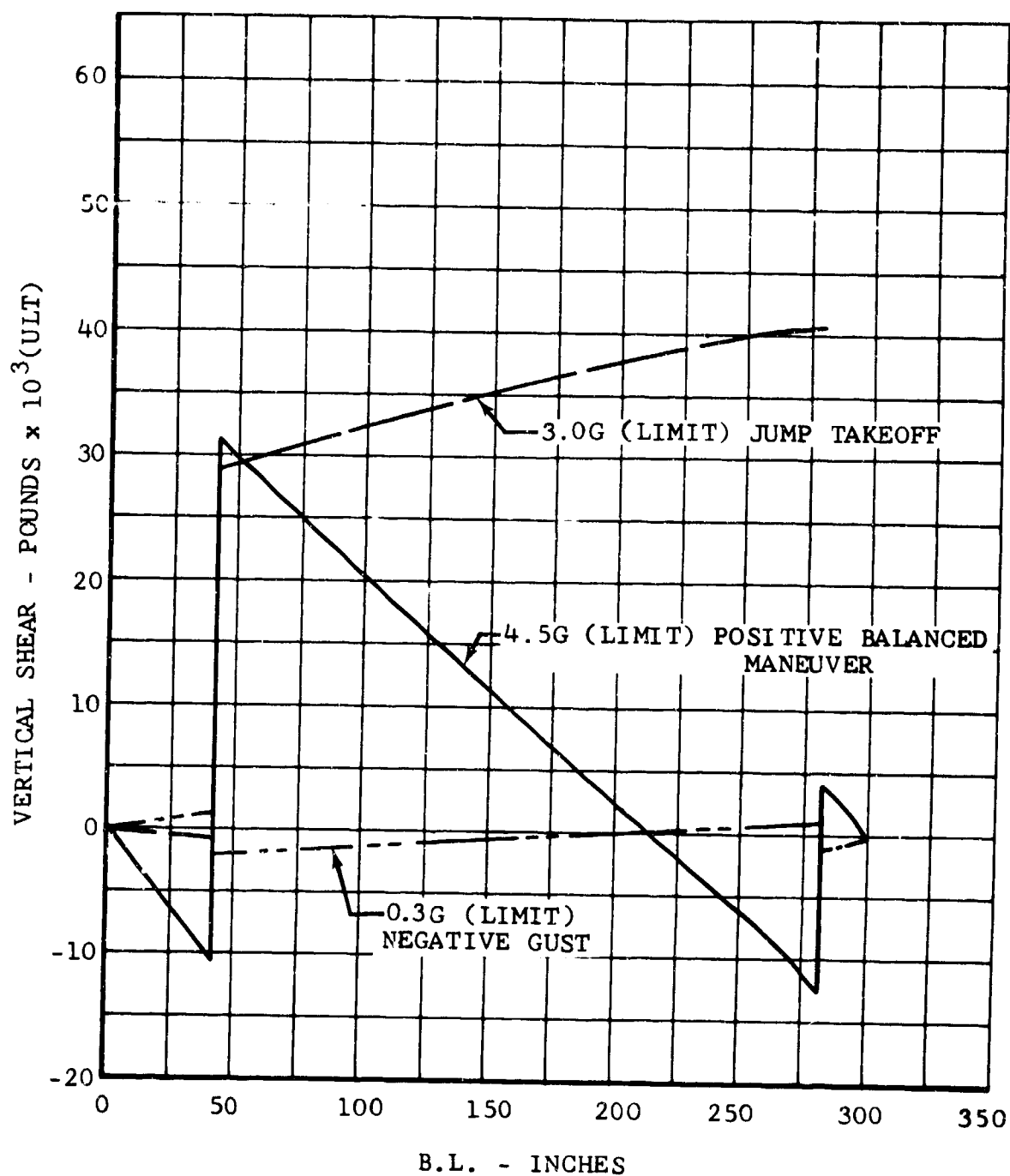


Figure 42. Wing Ultimate Vertical Shear (V_z).

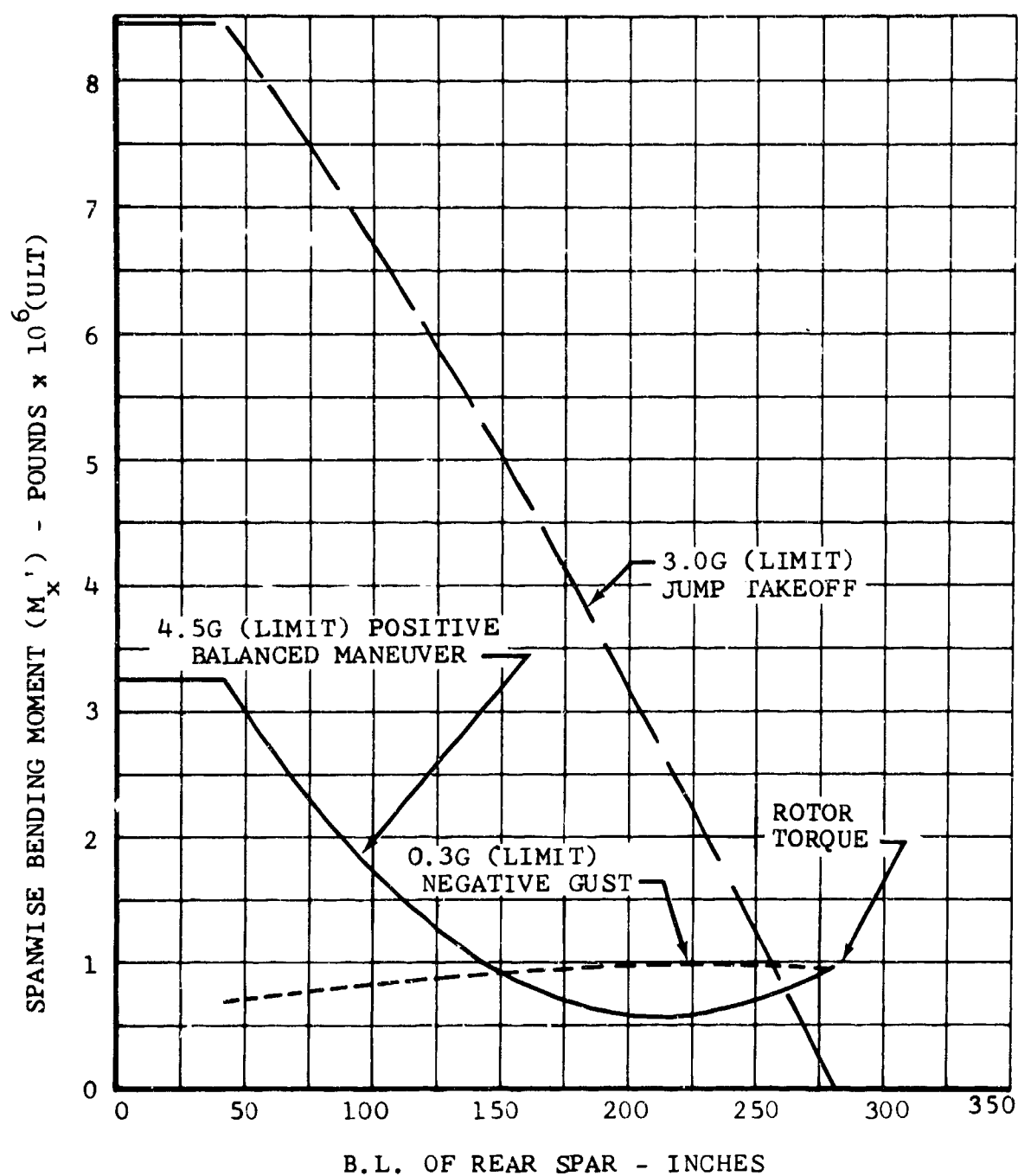


Figure 43. Wing Ultimate Spanwise Bending Moment (M_x) Referred to Direction of Elastic Axis.

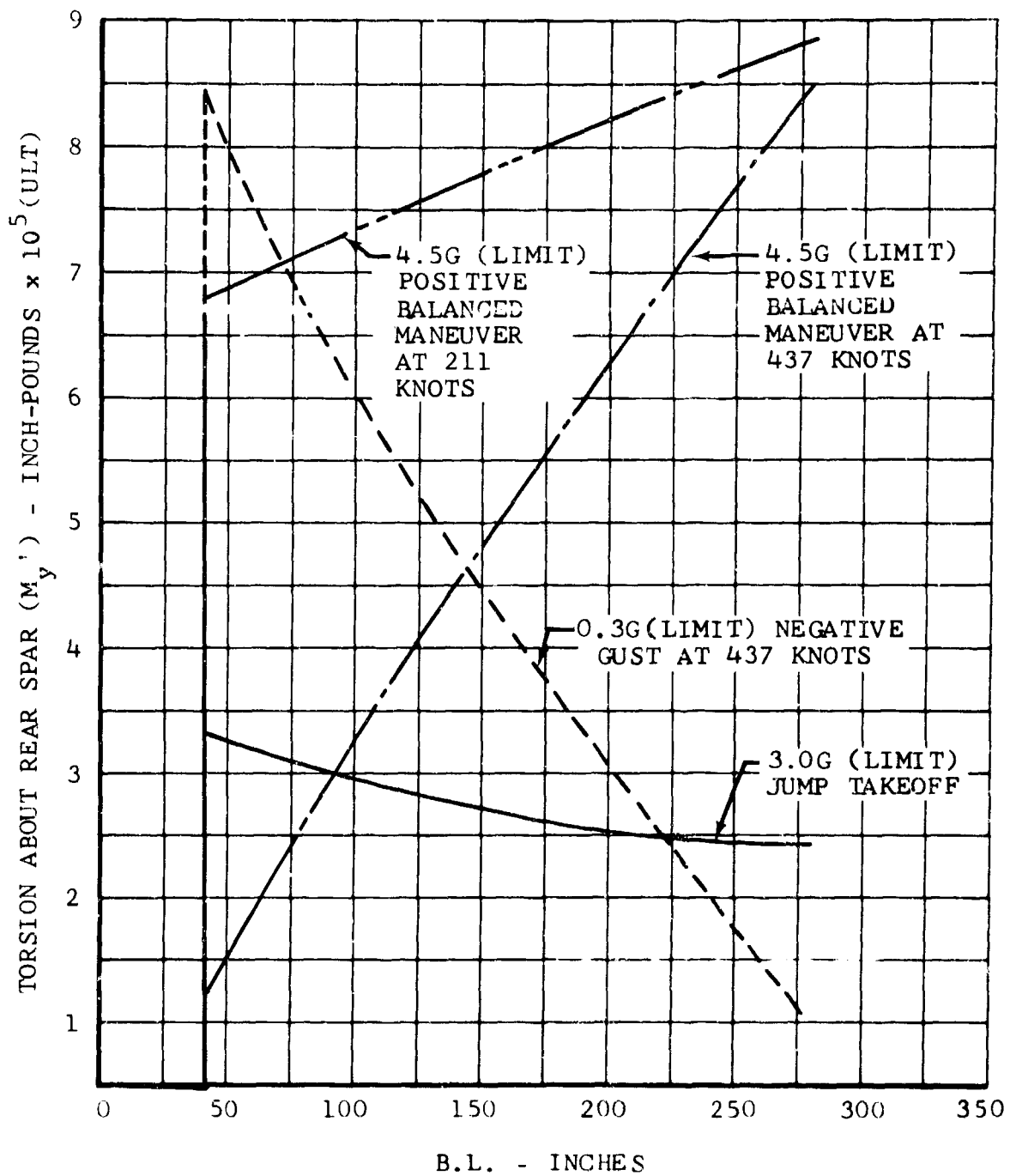


Figure 44. Wing Ultimate Torsion About Rear Spar (M_y) Referred to Direction of Elastic Axis.

TABLE XXII						
ULTIMATE LOADS APPLIED BY PYLON TO OUTBOARD WING RIBS						
Condition	Pounds (Ultimate)					
	P _{az}	P _{ax}	P _{oz}	P _{ox}	P _{iz}	P _{ix}
4.5g (Limit) Fixed Wing (8°-Longitudinal Flapping)	-25,100	33,300	40,700	-28,200	-32,000	1,325
3.0g (Limit) Helicopter No Flapping	-990	2,030	68,900	-44,600	-27,000	42,600
3.0g (Limit) Helicopter (8°-Longitudinal Flapping)	15,100	-31,000	53,900	-22,200	-28,100	46,000
3.0g (Limit) Helicopter (8°-Lateral Flapping)	-1,965	4,030	92,000	-45,200	-48,500	41,500
Note: Loads do not include torque factor.						

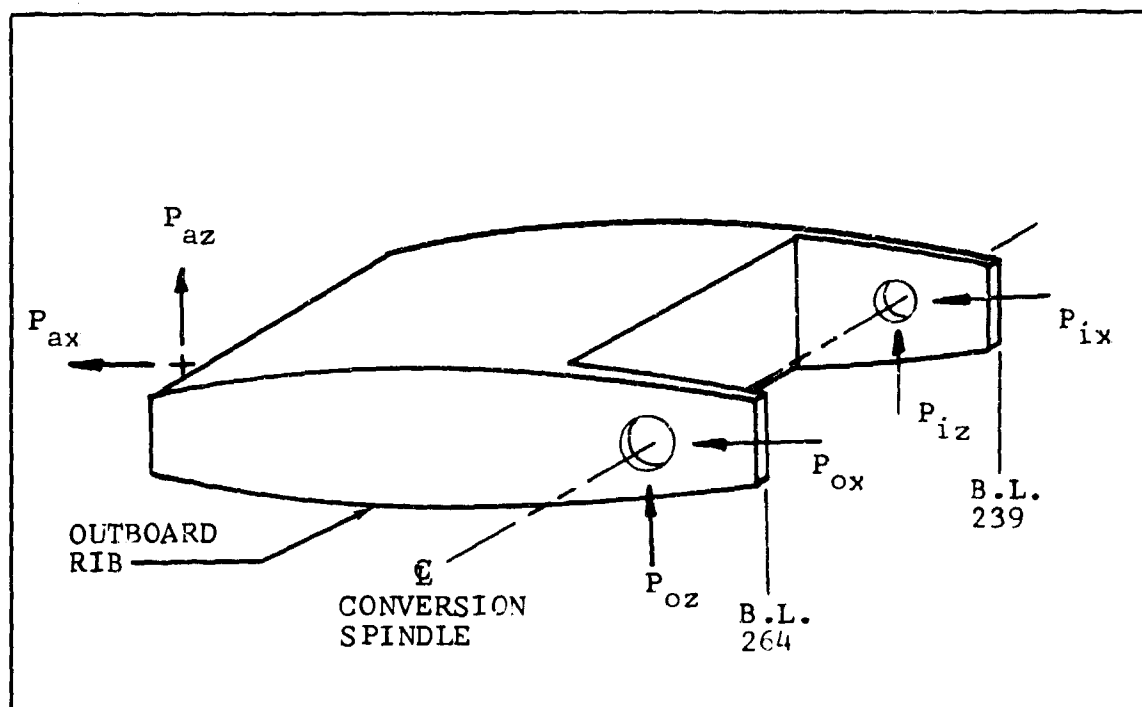


Figure 45. Wing-Pylon Intersection Notation and Geometry.

TABLE XXIII						
ULTIMATE MAIN-GEAR AND NOSE-GEAR REACTIONS						
Condition	Nose Gear			Main Gear		
	P _V	P _D	P _S	P _V	P _D	P _S
Reserve-Energy Landing, Three Point	9000			21200		
Maximum Vertical Reaction	9000	2250*		23800	5950*	
Reserve-Energy Landing, Two Point				23800		
Braked Roll, Two Point				20700	16560	
Braked Roll, Three Point	16300			13800	11040	
Unsymmetrical Braking	10600		±3320	13150	10520	±1830
Reverse Braking				17250	-13800	
Taxiing	13200			20675		
Turning	6540		3270	25815		-12907
Spin-Up	9000	6930*		21650	16700*	
Spring Back	9000	-6190*		23800	-14900*	
Main-Gear Obstruction				23800	±11900*	±11900*
Nose-Gear Obstruction	9000	±6300*	±6300*			
*Defines loads applied at axle.						

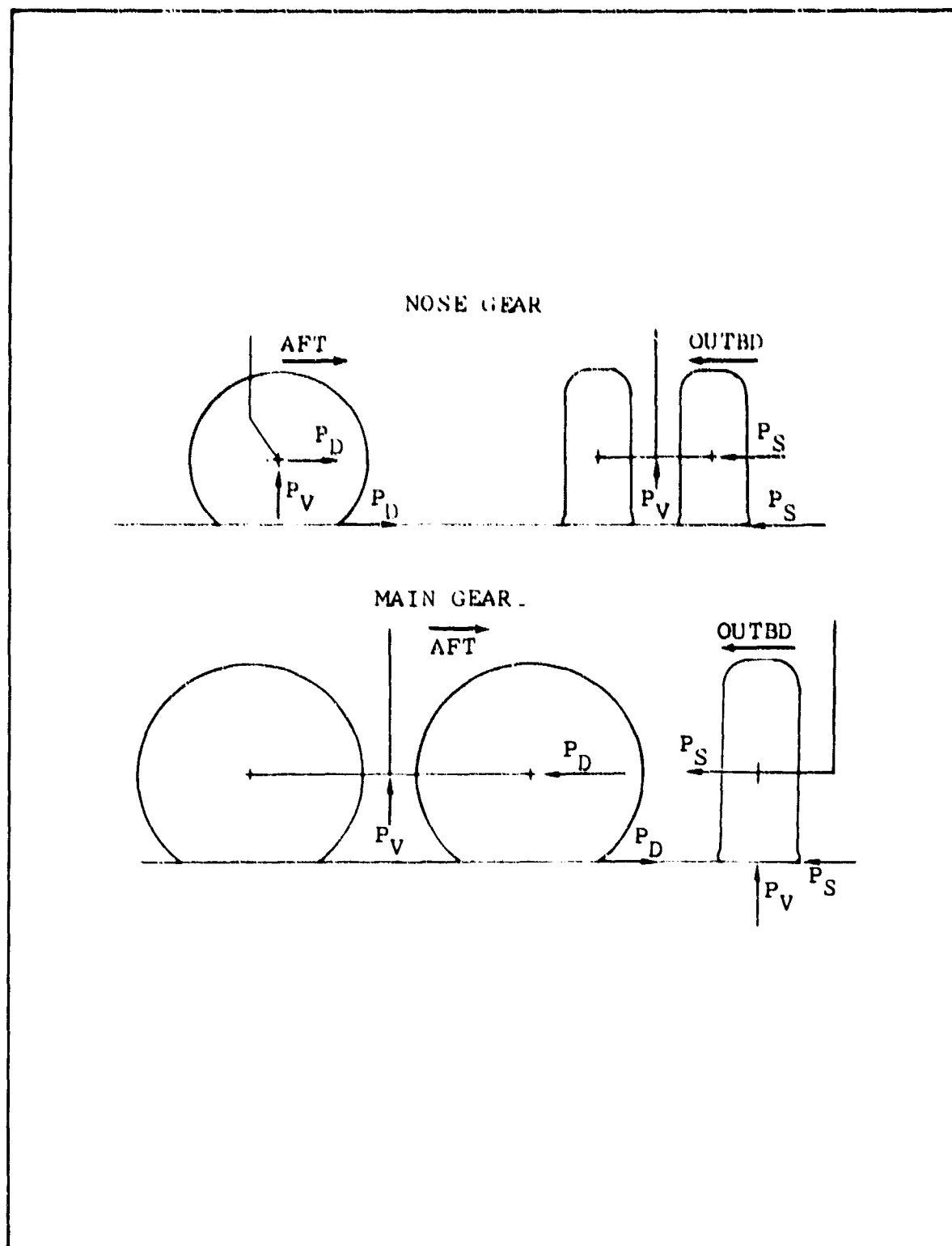


Figure 46. Landing-Gear Notation.

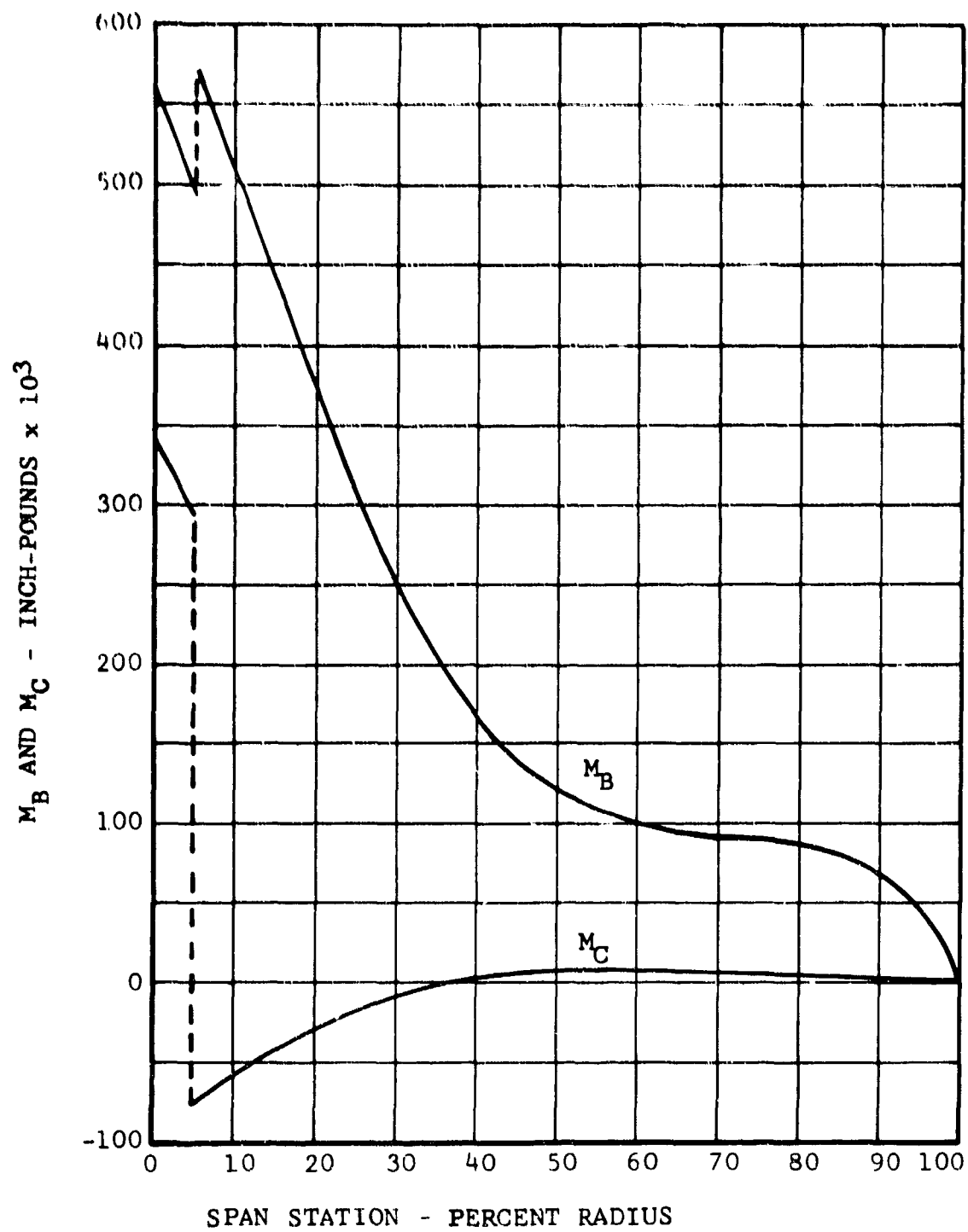


Figure 47. Rotor Blade Limit Static Beamwise and Chordwise Bending Moment Distribution for 3g, 372-RPM Helicopter Maneuver.

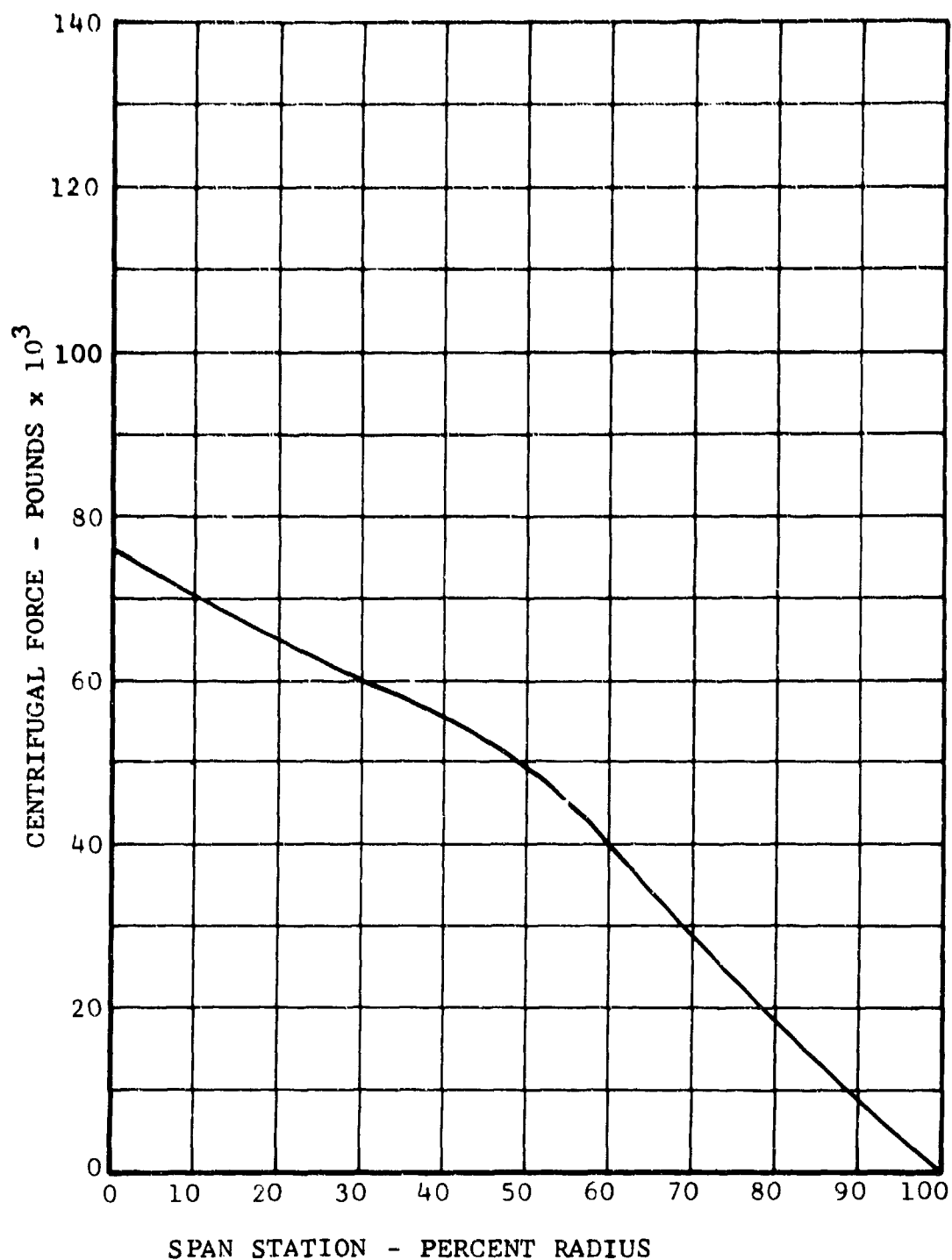


Figure 48. Limit Centrifugal Force Distribution for 3g, 372-RPM Helicopter Maneuver.

c. Fatigue Blade Loads

The loads used for fatigue analysis are the highest loads that exist continuously at VH. Figure 49 shows the oscillatory beam-wise and chordwise bending moment distributions on the blade for various mast angles at 150 knots. Similar curves were developed for a series of speeds in order to establish the curves of Figure 36. A description of the analytical methods used to determine these moments is given in Paragraph E, Dynamic Analysis.

6. TRANSMISSION CASE AND SPINDLE LOADS

The ultimate loads shown in Figures 50 and 51 are used for the design of the conversion actuator, spindle, spindle bearings, and transmission case. The rotor mast torque and drive-shaft torque are obtained from the design criteria. The hub restraint is specified as 1500 foot-pounds per degree, the thrust is estimated as 2500 pounds nominal, and the pylon weight is 2429 pounds per side.

The resultant loads at the conversion actuator attachment point and at the spindle bearings for four conditions are summarized in Table XXIV. The loads resulting from flapping are caused by thrust vector tilt and by hub restraint in the longitudinal direction only. The flapping stops are contacted at 8 degrees of flapping.

TABLE XXIV				
ULTIMATE CONVERSION ACTUATOR AND SUPPORT LOADS				
Condition Load	Fixed-Wing (8°-Long. Flapping)	Helicopter (No Flap- ping)	Helicopter (8°-Long. Flapping)	Helicopter (8°-Lat Flapping)
P_{ax}	34,100	-3,120	29,800	-5,210
P_{az}	25,700	-1,520	14,500	-2,540
P_a	42,600	-3,470	33,200	-5,790
P_{ix}	-1,200	65,400	69,500	65,400
P_{iz}	54,800	27,100	28,400	48,600
P_i	54,800	70,900	74,500	83,400
P_{ox}	29,100	68,600	46,900	70,300
P_{oz}	64,100	69,500	54,600	92,600
P_o	70,500	97,800	72,700	116,200

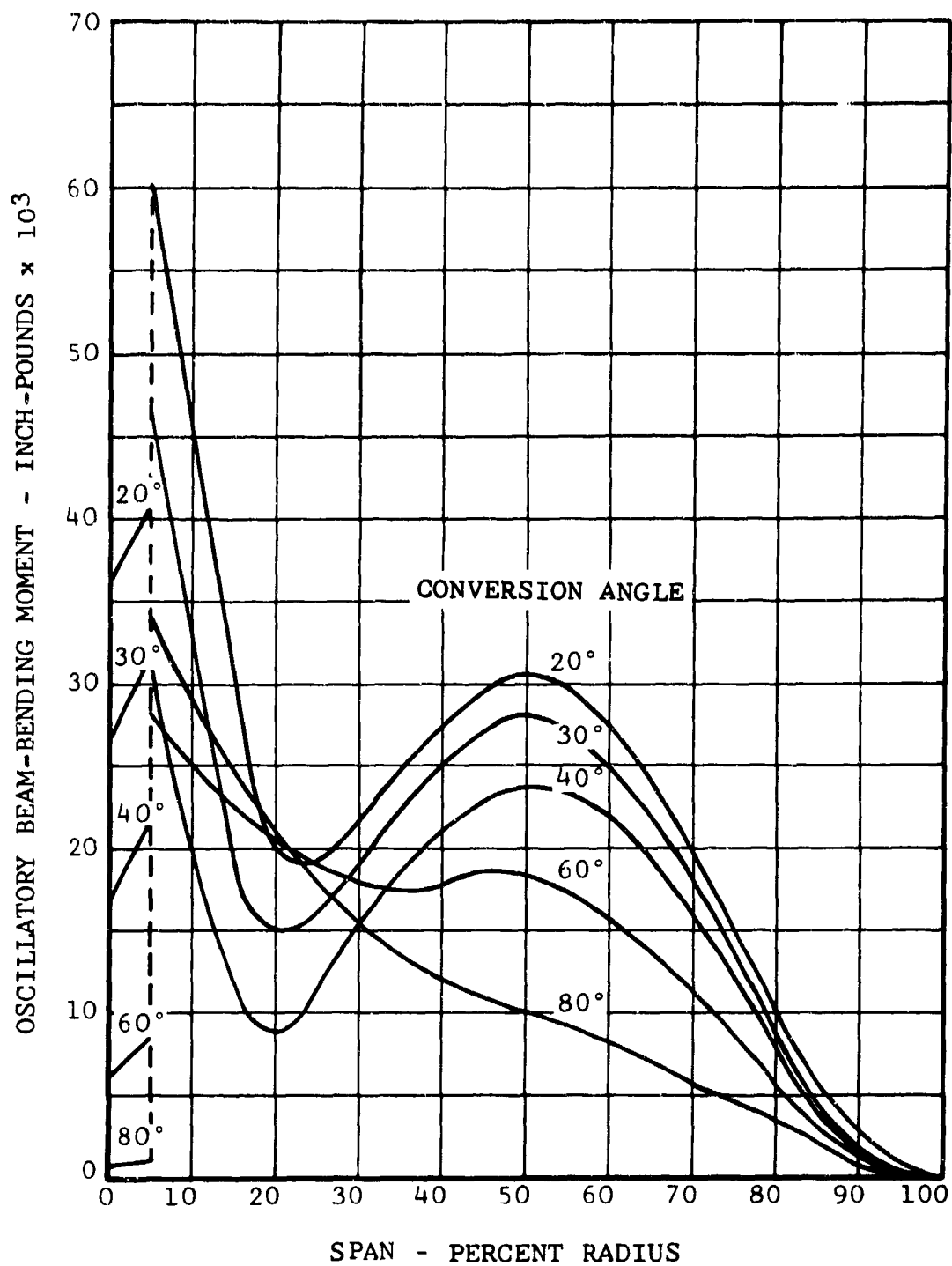


Figure 49. Rotor Blade Oscillatory Beamwise Bending Moment Distribution for 150 Knots and Various Mast Angles.

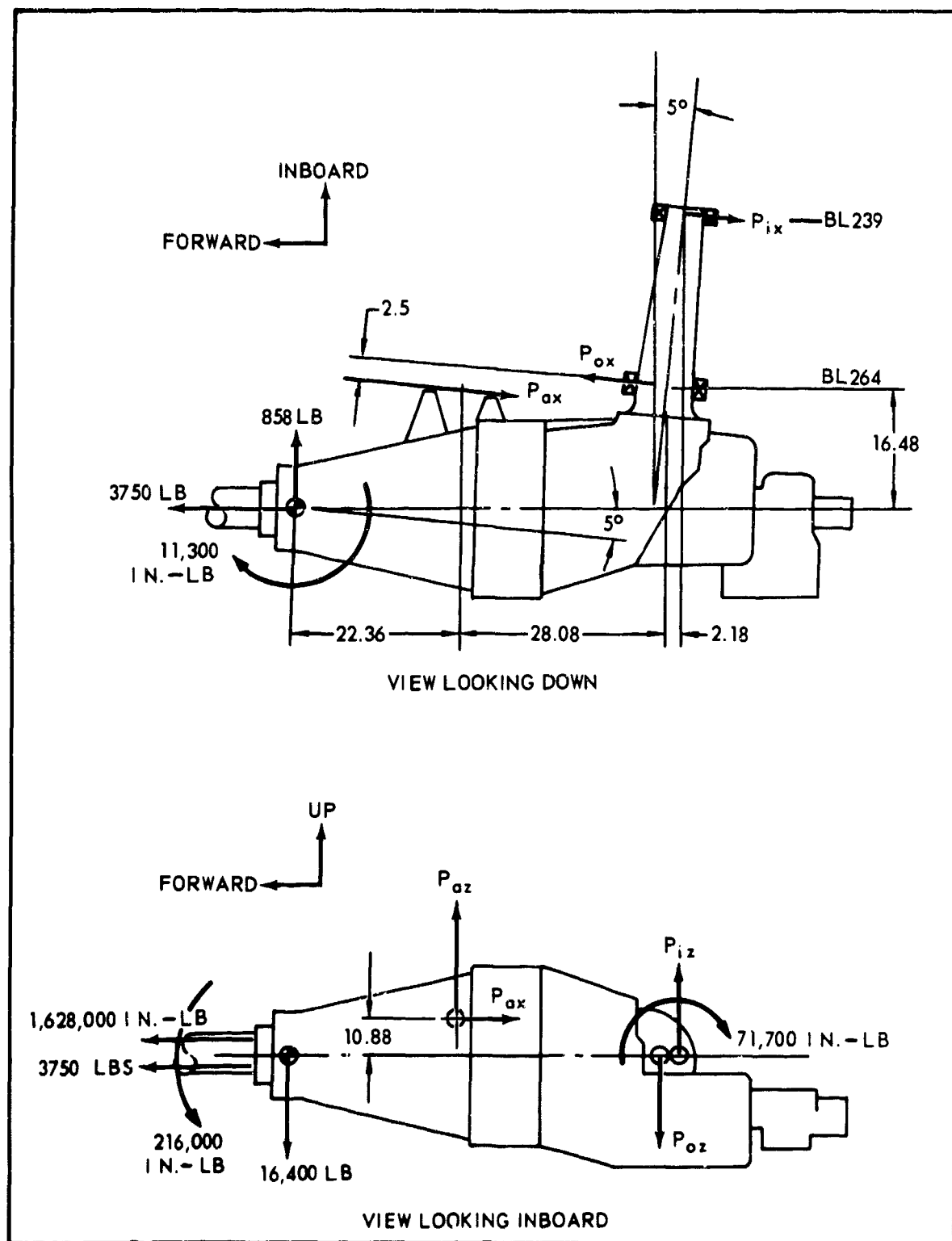


Figure 50. Pylon Loads - Fixed-Wing Flight.

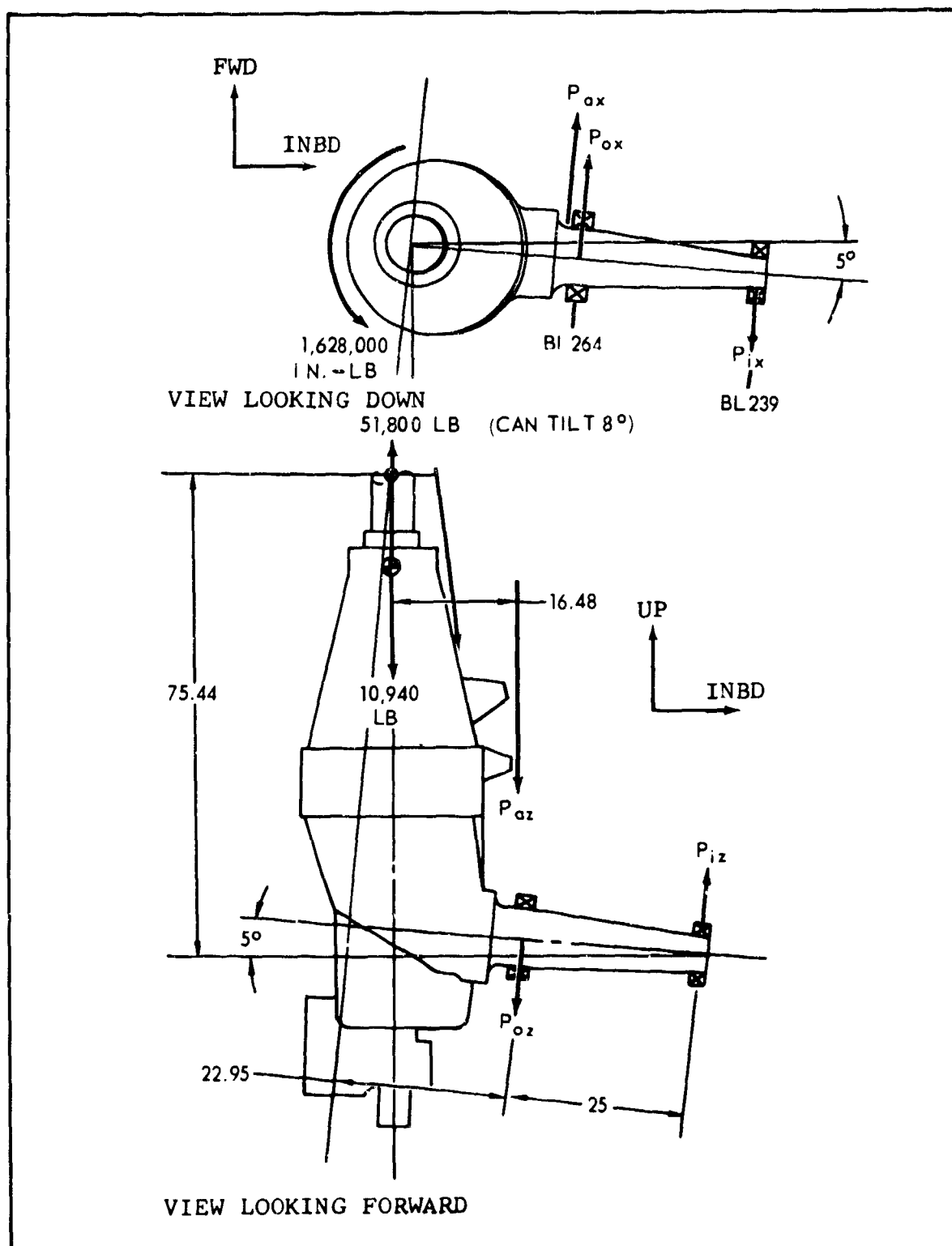


Figure 51. Pylon Loads - Helicopter Flight.

C. FATIGUE CONSIDERATIONS

1. DISCUSSION OF PROBLEM

a. Helicopter Component Loading

Rotary-wing aircraft present problems in fatigue on a much larger scale than do fixed-wing aircraft. This is primarily because of the great number of components that are subject to oscillatory loads and because of the cyclic frequency of these oscillatory loadings. For an aircraft of the D266 type, which is both fixed and rotary wing, special conditions are encountered which encompass the aspects of fatigue of both types of aircraft.

Bell's experience in the design and testing of helicopters has shown that the loads resulting from high-speed level flight are usually the most significant ones affecting the fatigue life for the rotors, pylons, and some portions of the control system. Unlike fixed-wing aircraft, these loads are produced at a constant one-g flight and are essentially a function of forward velocity, being caused by the variation of dynamic pressure and cyclic change in angle of attack of the blades as they sweep the azimuth of rotation. Although the actual magnitudes of these loads are relatively low, the large number of cycles to which the components are subjected makes this condition critical from a fatigue standpoint. Calculations show that these oscillatory loads persist, although they decrease in magnitude, throughout the conversion process until the aircraft is supported by lift of the wings.

The various maneuver and gust conditions in helicopter mode will produce higher loads than the one-g high-speed condition, but these are transient in nature and result in the accumulation of relatively few cycles of high loads during the life of the aircraft.

Design loads for numerous conditions of helicopter flight and transition were derived for this aircraft's main rotors and controls by means of computer programs set up for this purpose. These calculated design loads are then used in accordance with the design criteria.

b. Airframe Loadings

This aircraft, being both rotary and fixed wing, is subject to fatigue loadings peculiar to both types of craft, in addition to loads that occur during conversion from one configuration to the other.

In helicopter configuration, the airframe experiences loads resulting from takeoffs and landings of varying degrees of severity in addition to the usual type of helicopter maneuvers. It should be noted that, because all of the takeoff lift is concentrated at the wingtip, changes in takeoff power directly affect the state of bending stress within the wing. Also, the presence of the large concentrated tip masses will produce dynamic response stresses in the wing due to hard landings.

In fixed-wing configuration, the wing is subjected to the familiar types of loadings common to conventional aircraft. The only difference lies in the fact that rotor torque produces locally high stresses at the tip, and this torque has to be carried through the wing. Variations in power settings, therefore, produce cycles of stress variation in the wing.

During conversion, the aircraft experiences a combination of loads peculiar to the two configurations. It is worthy of note that the rotor torque produces changes in state of stress in that it produces chordwise bending in helicopter mode and beam bending in fixed-wing mode, with a combination of both during conversion.

2. DESIGN CRITERIA

a. Rotating System Components

(1) General

A fatigue life of 2500 flight hours is the design objective for all rotating system components and for all components of the control system subject to rotor feedback loads.

Bell Helicopter Company's experience, both analytical and practical, has shown that, in the design of components in the rotating system, if the oscillatory stresses associated with high-speed level flight are approximately the same magnitude as the endurance limit for an aluminum structure, a satisfactory fatigue life will be obtained. If the flight loads for this condition are higher than the endurance limit, the fatigue life will be too low; conversely, if these flight loads are below the endurance, the result will be an unnecessary penalty. In the case of steel or titanium structures, a similar criterion exists, except that the endurance limit must be about 1.4 times the oscillatory loads corresponding to the high-speed level-flight condition in order to obtain a satisfactory fatigue life. This factor is due to the difference in characteristic shape of the S-N curve for these materials.

Based on experience from helicopter rotor life determination, the approach of using the level-flight maximum-speed condition as a criterion for satisfactory dynamic component life is used

for the D266. The highest oscillatory loads associated with maximum level-flight conditions, whether in helicopter or fixed-wing configuration, are therefore utilized as fatigue design loads for the preliminary design of the rotating system components.

(2) Design Fatigue Allowable Stresses for Rotating Components

Once the design fatigue loading condition is established, the component parts are analyzed and the oscillatory stresses are compared with the estimated endurance limits of the parts. The estimated endurance limits or design fatigue allowable stresses are obtained in most cases from previous fatigue tests of geometrically similar structures. Allowable stresses are based on a compilation of fatigue test data on many actual full-scale structures. Most of these data have been accumulated in Bell Helicopter Company's testing laboratories during fatigue test programs on helicopters and VTOL aircraft.

An allowable oscillatory stress for the rotor blade was derived from the test data which is representative of the fatigue strength of the inboard high mean stress regions of rotor blades. For the outboard blade skin region, the allowable oscillatory stress was increased in accordance with the decrease in centrifugal force. A modified Goodman diagram is used to express the mean-oscillatory relationship.

b. Basic Airframe

(1) General

The design of the basic airframe is in general accordance with the strength requirements of MIL-A-8866(ASG) for a utility-type aircraft. Therefore, in accordance with that document, a fatigue life of 7500 flying hours and 10,000 landings is the design objective for the airframe. Analysis has determined that the wing is the most critically loaded component of the airframe. In order to satisfy the life requirement, the wing is designed so that the fatigue life calculated by the Cumulative Damage Method, employed in conjunction with an S-N curve which is representative of the minimum strength of the structure, and a stress frequency of occurrence spectrum representative of the lifetime of the airframe, is 7500 hours or greater.

(2) Design Fatigue Allowable Stress for Wing

Since design considerations required that the wing have splice joints, the repeated stresses associated with the riveted skin joints are of primary concern in evaluating its fatigue strength. Fatigue data come from test results accumulated by Alcoa Research Laboratories from tests of similar riveted joints of the same material (7178-T6 aluminum alloy). Since

the Alcoa test specimens were dimensionally similar to the D266 wing joint, the test results are considered applicable, and the S-N curve developed from the tests was used in the fatigue analysis.

D. VERIFICATION OF MAJOR STRUCTURE

1. WING

a. Static Analysis

Bending stresses in the wing are computed by means of a normal beam type of stress distribution with the sandwich skin and rear spar caps carrying all of the bending moment. Wing section properties were derived as a function of total upper surface skin thickness. Using the critical spanwise bending moments and an allowable stress of 60,000 psi, skin thicknesses were calculated at several points on the wing between B.L. 42 and 239. The resulting plot of skin thickness versus B.L. is shown in Figure 52. The skin thickness was held constant from B.L. 239 to the outboard rib due to the high shear stresses in this area. It is felt that combined stresses can be significant; therefore, larger-than-normal axial margins of safety are held in this region. Peak compression stresses at the outer fiber are shown in Figure 53 for the critical conditions of Figure 43. Allowable compression stresses are shown in the same figure.

The outboard area of B.L. 239 to the end rib is a redistribution area for the conversion actuator loads. Bending stresses in this area are of necessity kept lower due to the interaction with the high shear stresses in this redistribution area.

The method employed in deriving the allowable stresses for the sandwich panels is a generalized solution of the methods outlined in MIL-HDBK-23.

The front and rear spar shear flows for the critical conditions and allowable shear flows are shown in Figures 54 and 55. Spar shears are calculated using the vertical shear and torsion shown in Figures 43 and 44. The shear flows are based on a conventional two-spar single-cell analysis.

b. Fatigue Analysis

The wing is designed for a maximum takeoff load factor of 3.0g. It is estimated that during its operation, the aircraft would not exceed a load factor of 1.3g on normal takeoff or 1.58g during a maximum-performance takeoff; it is also estimated that during a jump takeoff, the load factor would not exceed 2.04g.

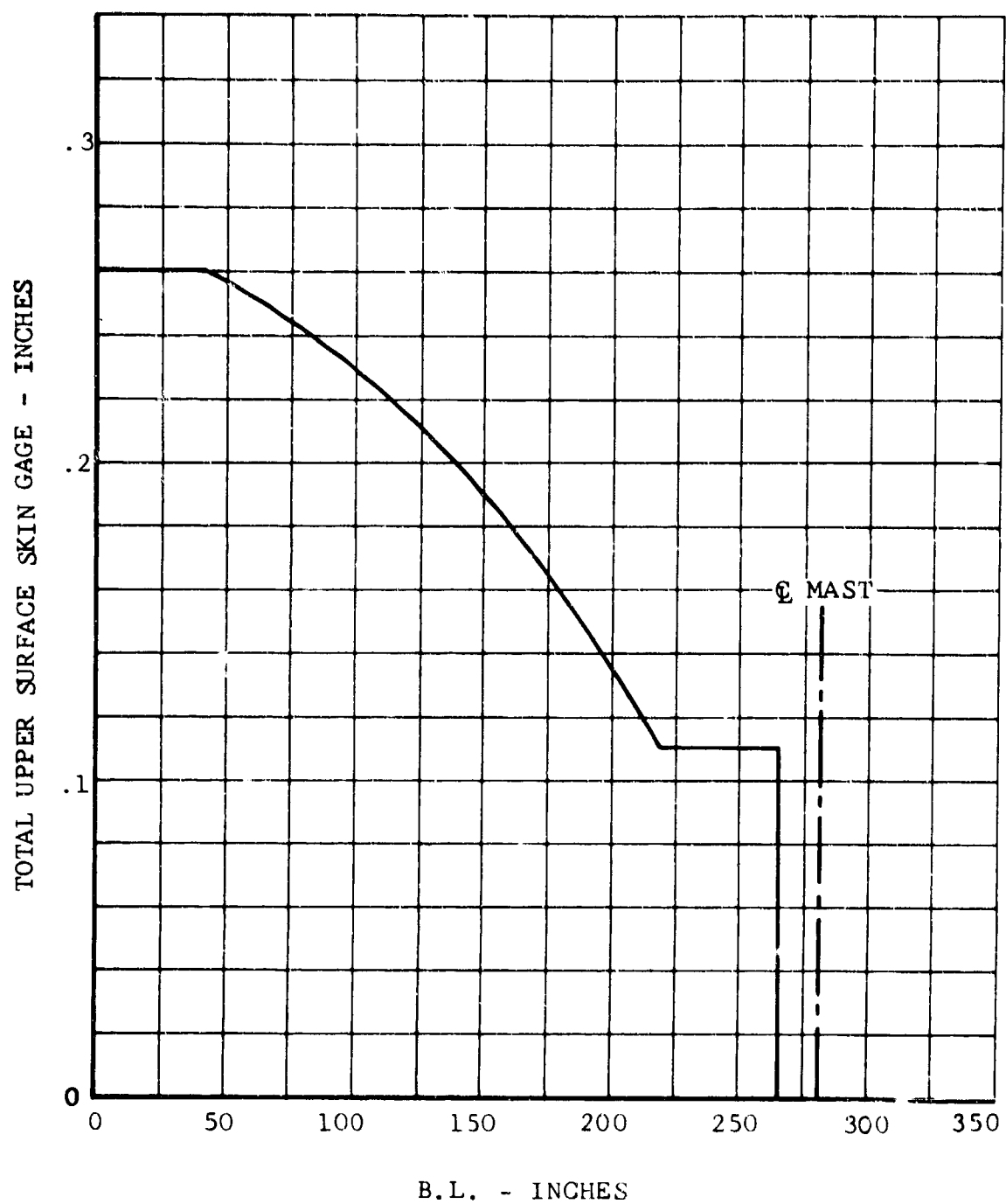


Figure 52. Wing Total Upper Surface Skin Gage.

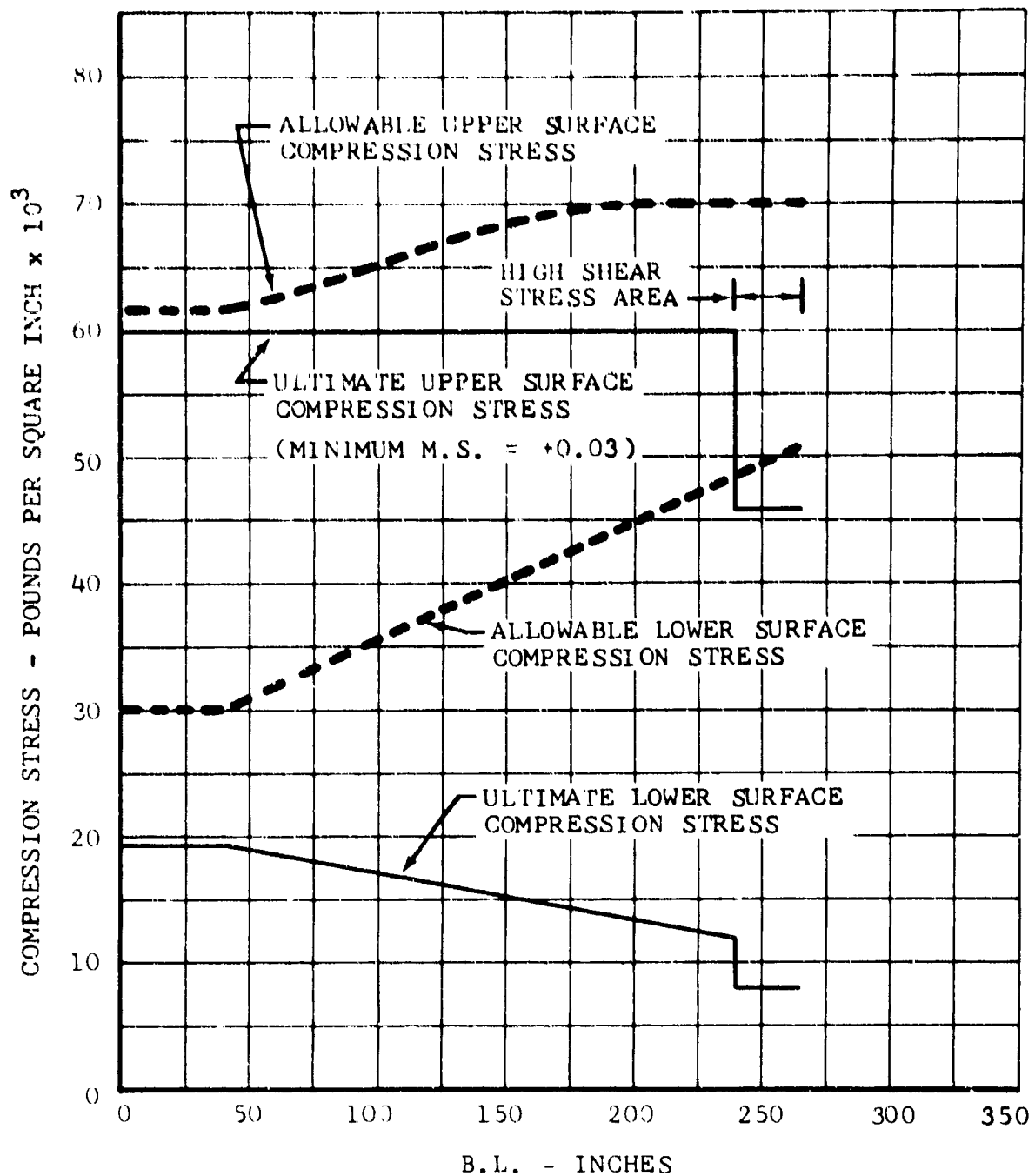


Figure 53. Wing Ultimate Compression Stress and Allowable Compression Stress.

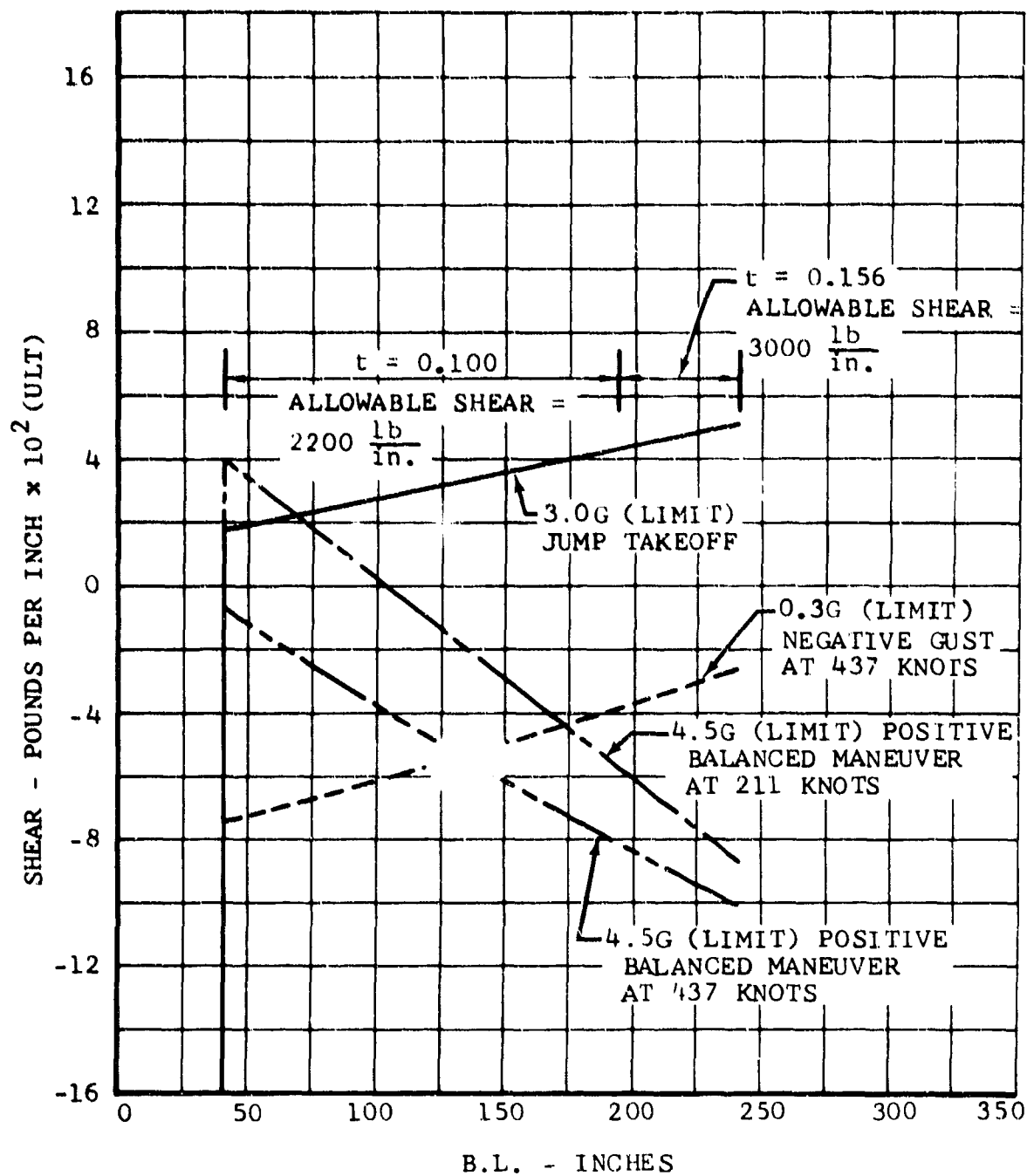


Figure 54. Wing Ultimate Front Spar Shear Flows and Allowable.

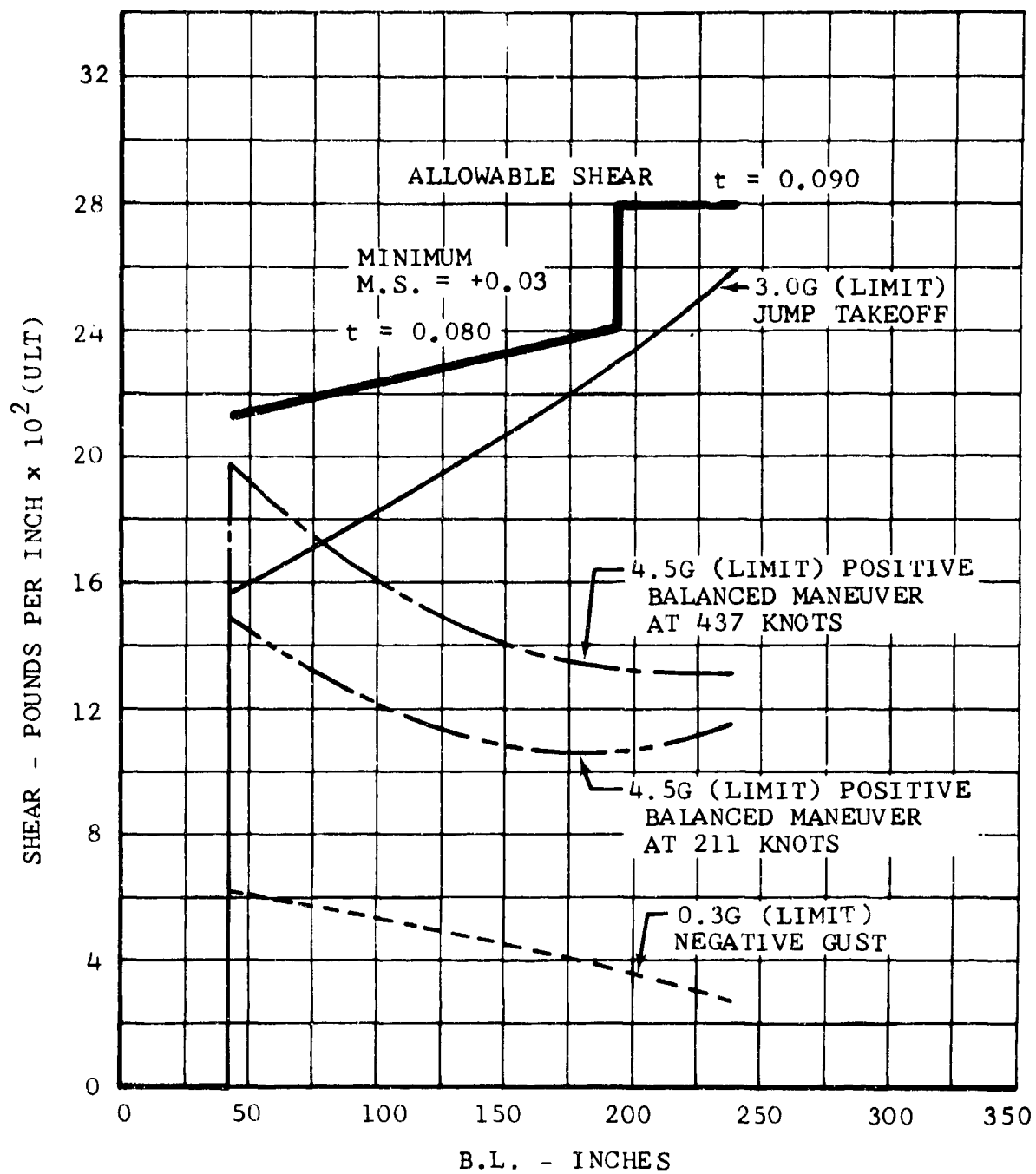


Figure 55. Wing Ultimate Rear Spar Shear Flows and Allowable.

Three major splices are made in the wing axial load carrying structure. These splices are located at Wing Stations 42, 65.5, and 195. Stresses were calculated for three maneuver conditions, as shown in Table XXV, for the critical splice at Wing Station 42.

2. ROTOR BLADE

The spanwise distributions of EI about both the beam and the chord axes are shown in Figure 57.

The blade is subjected to both static and fatigue loadings. Static loads occur relatively few times during the life of the aircraft and are the highest loads the blade is expected to receive. These loads include beam bending, chord bending, and centrifugal force. Fatigue loads occur continuously during normal operation of the aircraft. A fatigue load consists of a steady or mean component plus an oscillatory component. The mean stress has little effect on the life of the blade compared to the oscillatory stress, but it cannot be neglected. It is used to determine the allowable oscillatory stress by means of a modified Goodman diagram as shown in Figure 58.

For static analysis, two conditions are investigated. These conditions are:

- Maximum torque, with all torque applied to 2 of the 3 blades in conformance with paragraph 3.3.1 of Reference 4. This condition produces maximum chordwise stresses.
- 3g helicopter maneuver at 372 rpm. This condition produces the highest beamwise stresses.

The condition that gives the critical stresses for the blade is the 3g maneuver condition. Detailed analysis shows that the minimum margin of safety occurs at 50-percent span. The analysis of this section of the blade is typical of that used to design the entire blade. The cross section at 50-percent span is shown in Figure 56.

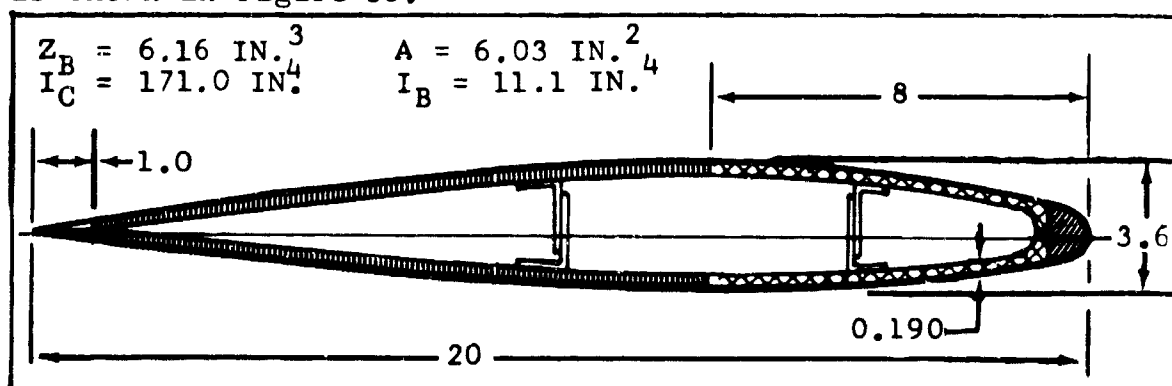


Figure 56. Cross Section of Rotor Blade at 50-Percent Span.

TABLE XXV FATIGUE LIFE DETERMINATION OF WING JOINT AT B.L. 42.0				
FLIGHT CONDITION	Cycles Per 1000 Hours of Flight (n)	Max Repeated Bending Stress (psi)	Number of Cycles to Failure (N)	Damage Fraction (n/N)
I. Helicopter Configuration				
A. Rotor Start & Stop		*	∞	
B. Takeoff - Landing				
1. Normal	1000	11,471	27,000	0.037037
2. Max Performance	263	14,182	10,300	0.025534
3. Jump	70	16,680	5,200	0.013462
C. Hover & IGE Flight		*	∞	
D. Full Power Climb		*		
E. Forward Flight		*		
1. 0.2 V_H - 0.7 V_H		*		
2. 0.8 V_H		*		
3. 0.9 V_H		*		
4. V_H		*		
F. Maneuvering Flight **				
1. 2.3g	800	5,571	420,000	0.001905
2. 2.8g	1330	5,179	560,000	0.002375
3. 3.0g	530	4,350	1,200,000	0.000442
II. Transitions				
A. Helicopter-Autorotation		*	∞	
B. Helicopter-High-Speed	1333	3,251	7,200,000	0.000185

TABLE XXV - Continued

FLIGHT CONDITION	Cycles Per 1000 Hours of Flight (n)	Max Repeated Bending Stress (psi)	Number of Cycles to Failure (N)	Damage Fraction (n/N)
III. Fixed-Wing Configuration				
A. Forward Flight				
Airspeed V_{de}				
1. $0.3V_H - 0.7V_H$	35	*	∞	
2. $0.8V_H$	30	1,640	1	
	25	1,409	4	
	20	1,178	28	
	15	936	209	
	10	705	1647	
		474	13376	
3. $0.9V_H$	35	1,847	2	
	30	1,579	6	
	25	1,324	47	
	20	1,147	350	
	15	790	2755	
	10	522	22376	
4. V_H	35	2,053	1	
	30	1,762	5	
	25	1,470	35	
	20	1,178	262	
	15	875	2061	
	10	533	16741	

TABLE XXV - Continued

FLIGHT CONDITION	Cycles Per 1000 Hours of Flight (n)	Max Repeated Bending Stress (psi)	Number of Cycles to Failure (N)	Damage Fraction (n/N)
A. Forward Flight (Cont'd)				
Airspeed				
5. V_L Dive				--
	1	2,563	90,000,000	
	2	2,199	∞	
	8	1,834		
	63	1,470		
	498	1,093		
	4044	729		
B. Maneuver Flight				
		*		
1. -1.00g	10000	1,251	∞	
2. 2.03g	3000	1,798		
3. 2.48g	1000	2,333	80,000,000	0.000012
4. 2.92g	300	2,892	10,200,000	0.000029
5. 3.38g	100	3,426	3,900,000	0.000026
6. 3.82g	30	3,973	1,900,000	0.000016
7. 4.27g				
TOTAL DAMAGE (D) IN 1000 HOURS =				0.081023
FATIGUE LIFE = 1000/D = 12,342 Hours				
* No significant oscillatory loading				
** See text for explanation of decrease in stress with increased load factor.				

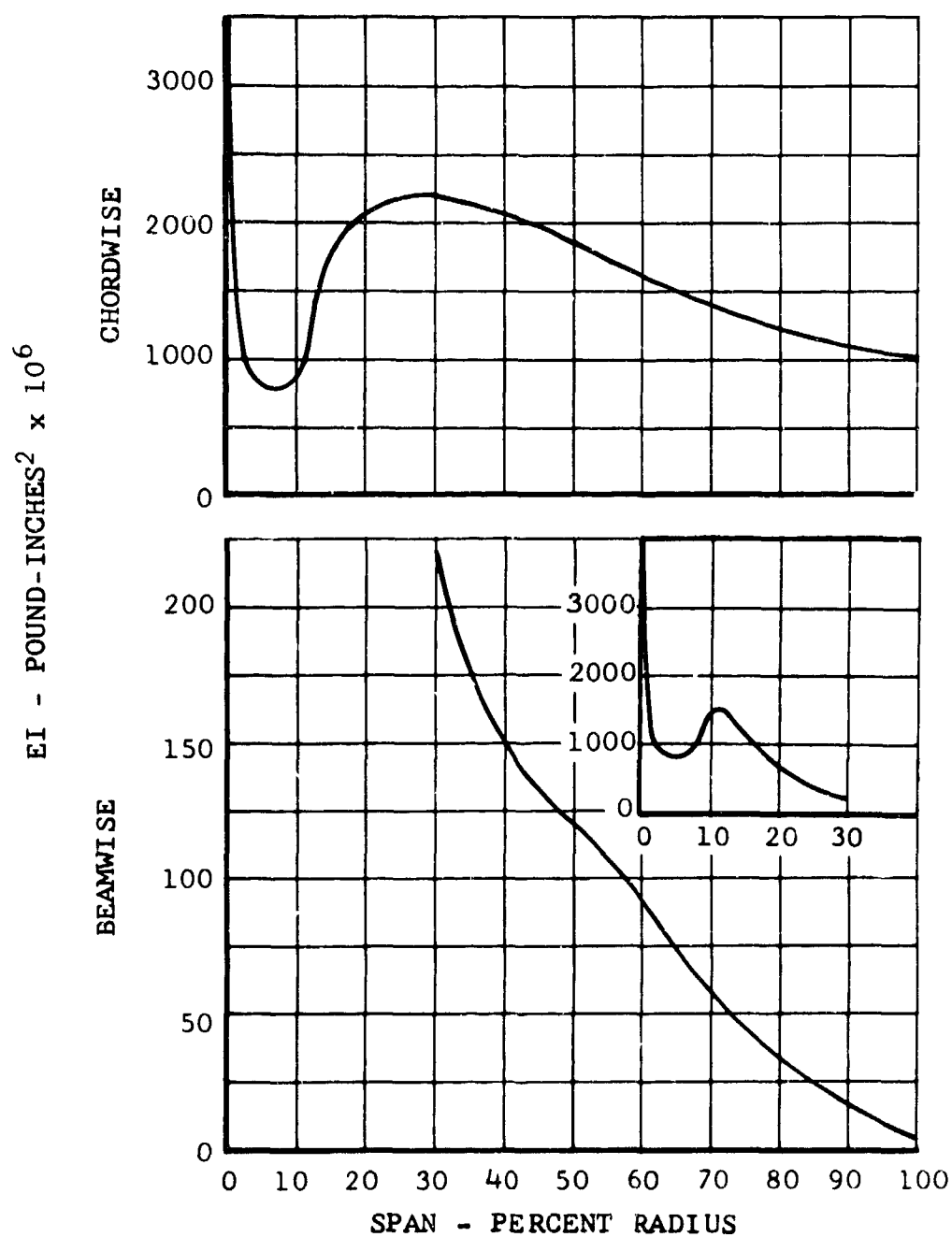


Figure 57. Beamwise and Chordwise EI Distribution.

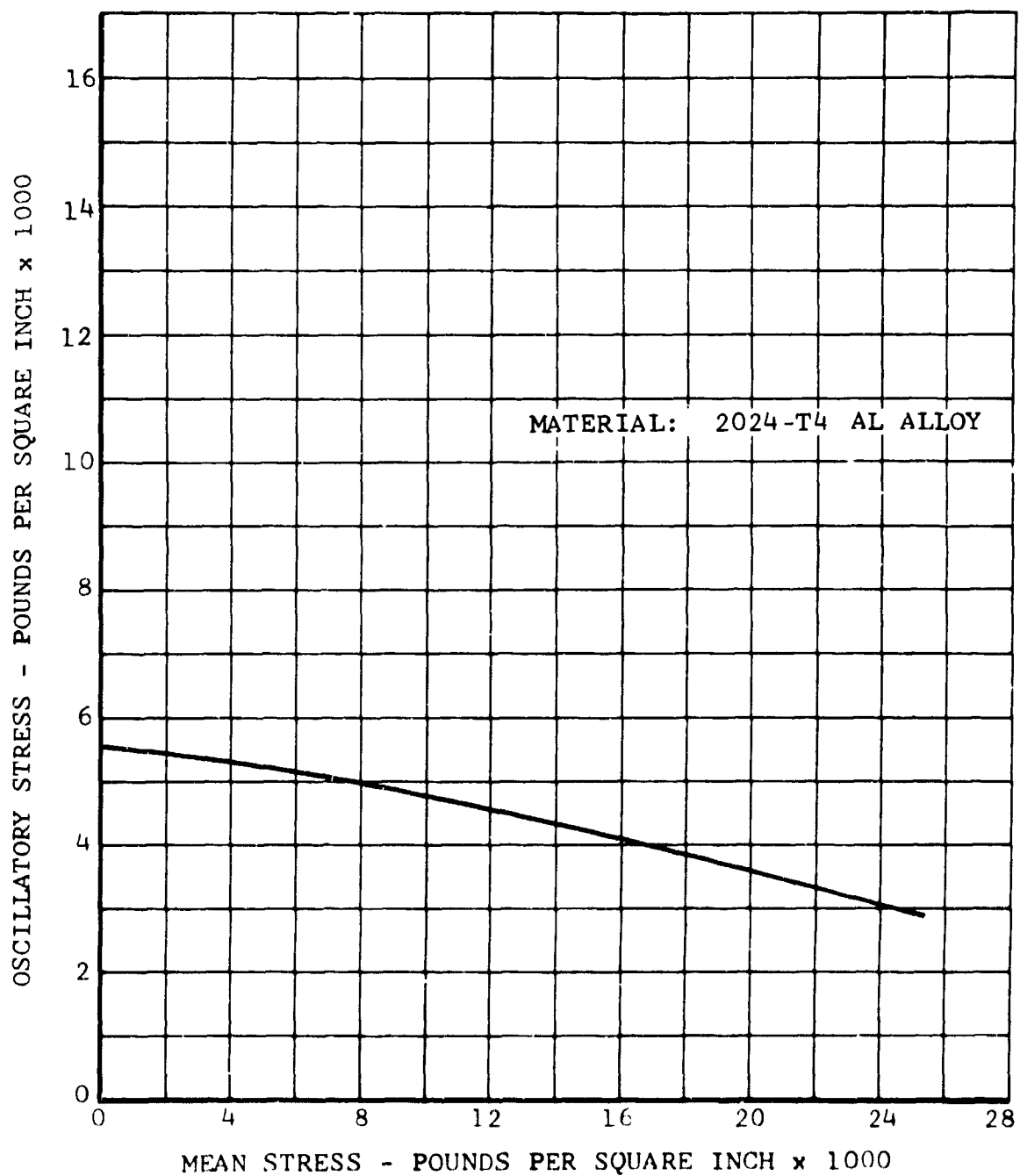


Figure 58. Modified Goodman Diagram of Allowable Stress in an Aluminum Main Rotor Blade Basic Section Outboard of Doublers.

$$M_B = 1.5 \times 120,000 = 180,000 \text{ inch-pounds ultimate} \\ (\text{Reference Figure 47})$$

$$C.F. = 1.5 \times 50,000 = 75,000 \text{ pounds ultimate} \\ (\text{Reference Figure 48})$$

$$f_B = 29,400 \text{ psi ultimate}$$

$$f_t = 12,400 \text{ psi ultimate}$$

$$f_{\text{total}} = 41,800 \text{ psi}$$

The material is 2024-T4 aluminum alloy.

$$F_{tu} = 60,000 \text{ psi}$$

$$M.S. = +0.44$$

Figure 36 shows the flight corridor for the aircraft during conversion. The blade's applied and allowable oscillatory beam-bending moment distributions, for a typical point on the boundary of the corridor, are shown in Figure 59. This point is at 150-knot airspeed and 30-degree mast angle. A typical calculation for the allowable oscillatory beam-bending moment at 50-percent radius is shown below. The mean load distributions associated with the oscillatory load distribution at 150 knots, 408 rpm, and 30-degree mast angle are shown in Figure 60 at 50-percent radius:

$$M_{BS} = 20,000 \text{ inch-pounds}$$

$$C.F. = 60,000 \text{ pounds}$$

$$f_{BS} = 3200 \text{ psi}$$

$$f_t = 9700 \text{ psi}$$

$$f_{\text{total}} = 12,900 \text{ psi}$$

The endurance limit at 50-percent radius for a steady stress of 12,900 psi is found from Figure 58 to be $F_{zB} = 4700 \text{ psi}$.

The allowable moment is $F_{zB} = 29,000 \text{ inch-pounds}$.

The applied moment is $M = 28,000 \text{ inch-pounds}$.

It might be noted that there is a very small effect due to chordwise oscillatory moments. These are sufficiently small to be neglected, as the order of magnitude of chord moment is slightly above the beam moment, but the I is an order of magnitude higher.

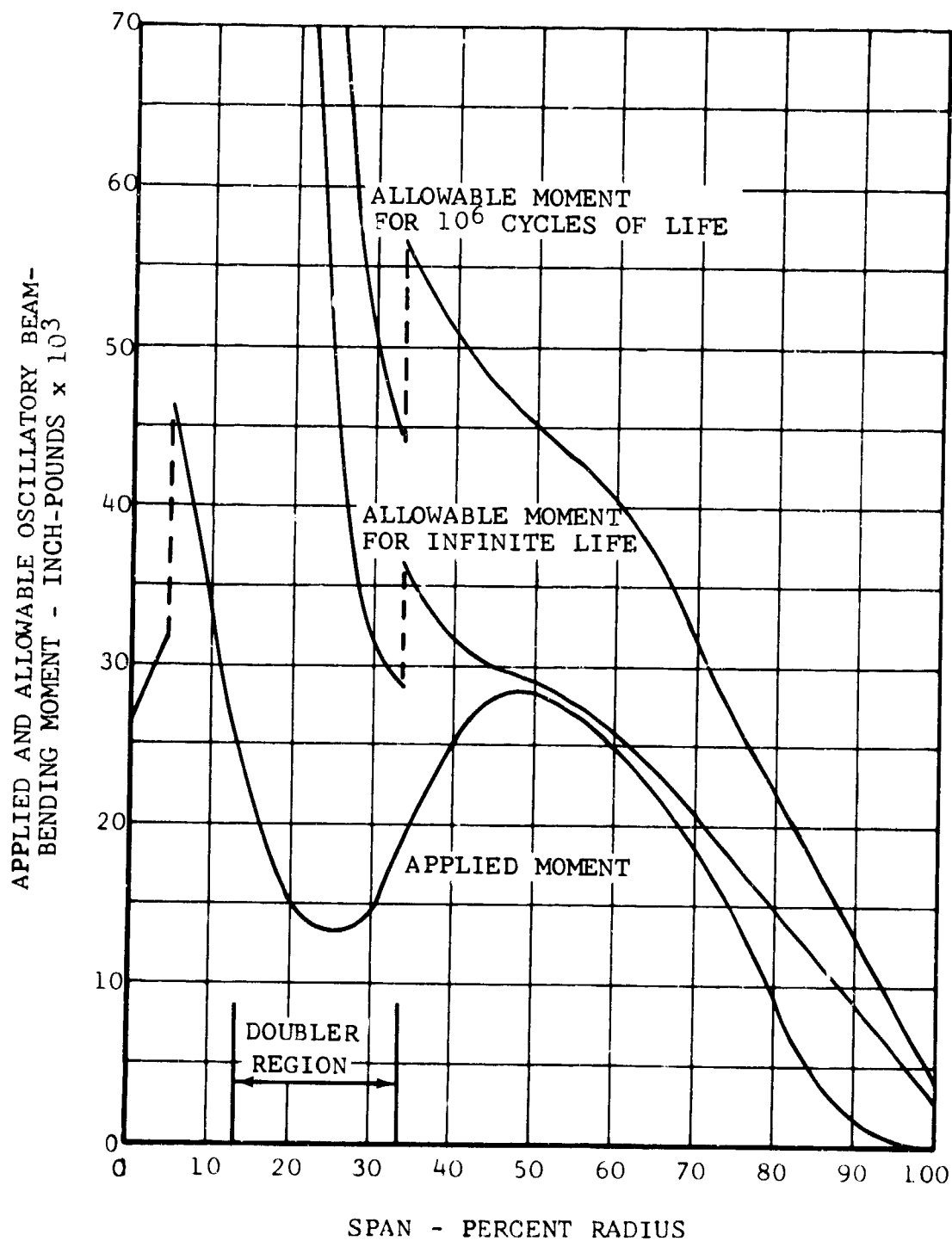


Figure 59. Blade Applied and Allowable Oscillatory Beam-Bending Moment Distributions for 150 Knots and 30° Mast Angle.

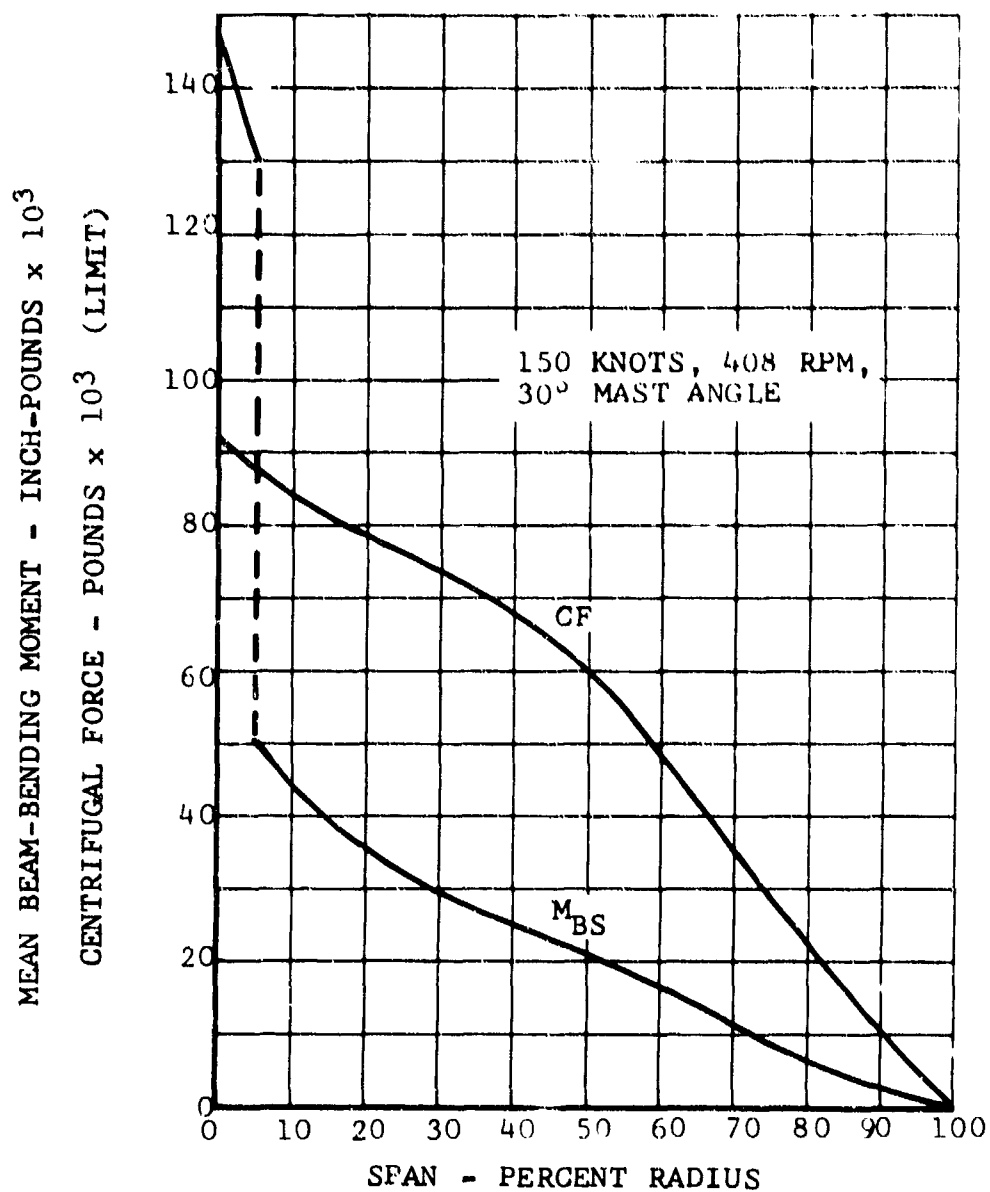


Figure 60. Rotor Mean Beam-Bending Moment and Centrifugal Force Distributions.

Figure 59 shows that the allowable bending moment for the blade drops abruptly at the outboard end of the blade reinforcing doublers. This is because the discontinuity caused by ending the doubler creates a stress concentration. For most of the blade length, the endurance limit (Figure 57) is of the order of 4500 psi; however, Reference 6 shows that for the area adjacent to the outboard end of the reinforcing doublers, the allowable stress is reduced to 3500 psi. Therefore, the allowable bending moment in this region is locally reduced until the doublers become sufficiently effective to overcome the reduced allowable oscillatory stresses.

The blade grip is critical at Station 31.75 (13.75-percent radius). The section modulus of the grip for chord bending is 18.7 cubic inches and for beam bending is 31.8 cubic inches. Therefore, the critical condition occurs when the collective pitch is such that all bending at this station is in the chord-wise direction. Detailed stress analysis of the blade grip showed adequate static and fatigue strength.

E. DYNAMIC ANALYSIS

1. AIRFRAME STRUCTURAL DYNAMICS

During the D266 design study, the airframe dynamic response has received considerable attention because of the necessity to avoid resonance with rotor-generated harmonic forces and because of the influence of wing-pylon dynamics on rotor stability (Reference 7). The airframe transient response has also been investigated.

In helicopter mode and during conversion to fixed-wing mode, normal helicopter rotor-generated oscillatory forces caused by the asymmetric airflow through the rotor will be experienced. One of the primary reasons for the choice of a three-bladed, rather than a two-bladed, rotor was the lower vibration level of the three-bladed rotor. Three per rev will be the principal harmonic vibratory force in the fixed system. One-per-rev and six-per-rev forces will be small. In fixed-wing mode, the airflow through the rotor will be axial, and rotor-generated vibratory forces reaching the airframe will be very small. Consequently, cabin vibration levels will be quite low.

a. Airframe Natural Frequencies

The airframe dynamic response and the natural frequencies were calculated using BHC computer Program A75D, which is a state vector, transfer-matrix approach to calculating the coupled, damped, forced response of the airframe. Shear deformation and rotary inertia are included in the vibration analysis. Program

A75D has been used extensively and correlated with shake test and flight test data for the UH-1-series helicopters, the Bell JetRanger (Model 206A), and the XV-3 Convertiplane.

The analytical model, used for the vibration analysis, consists of 24 fuselage-mass stations, 13 wing-mass stations per side, and a rotor pylon including the pylon-pitch isolation mount.

The wide range of rotor operating speeds and fuel and cargo loading conditions of the D266 made it difficult to avoid resonance with rotor harmonics over the entire operating range of helicopter and fixed-wing flight. For the final configuration, however, the primary wing-ylon-fuselage modes are clear of one-per-rev and three-per-rev rotor harmonics, both in steady helicopter flight and in fixed-wing flight. During the change from the helicopter-mode rotor-speed range to the fixed-wing-mode rotor-speed range, several resonances will be passed through; however, the amplitudes built up will be small because of the speed of transit. The airframe natural frequencies for helicopter and fixed-wing modes are plotted in Figures 61 and 62.

The natural frequencies of the fixed-wing configuration are calculated with the pylons in the fully converted (90-degree) position, and the helicopter natural frequencies are calculated with the pylons vertical (0 degree). During conversion, the wing-ylon coupled natural frequencies will change slightly because of the change in coupling between wing-beam and wing-chord bending. Also, the pylon pitch isolation mount spring rate increases and then decreases during conversion.

b. Crew Compartment Vibration Levels

The cabin vibration levels caused by rotor-generated harmonic forces will be very low throughout the D266 flight regime. In helicopter mode, the principal vibratory force reaching the airframe will be three per rev (20.5 cps at 409 rpm). The normalized response at the crew station to vertical oscillatory forces at the rotor hub is plotted in Figure 63. The cockpit-obtained three-per-rev vibration level, shown in Figure 64, was from calculated three-per-rev rotor vertical hub shears. The shaded area in Figure 64 indicates the range of mast angles available in helicopter mode (see Figure 36).

c. Airframe Transient Response

(1) Dynamic Landing Loads

Dynamic landing loads were analyzed to determine the wing bending moments during a hard landing. The results showed that the loads during a design-sink-speed landing (8.0 fps) are not critical.

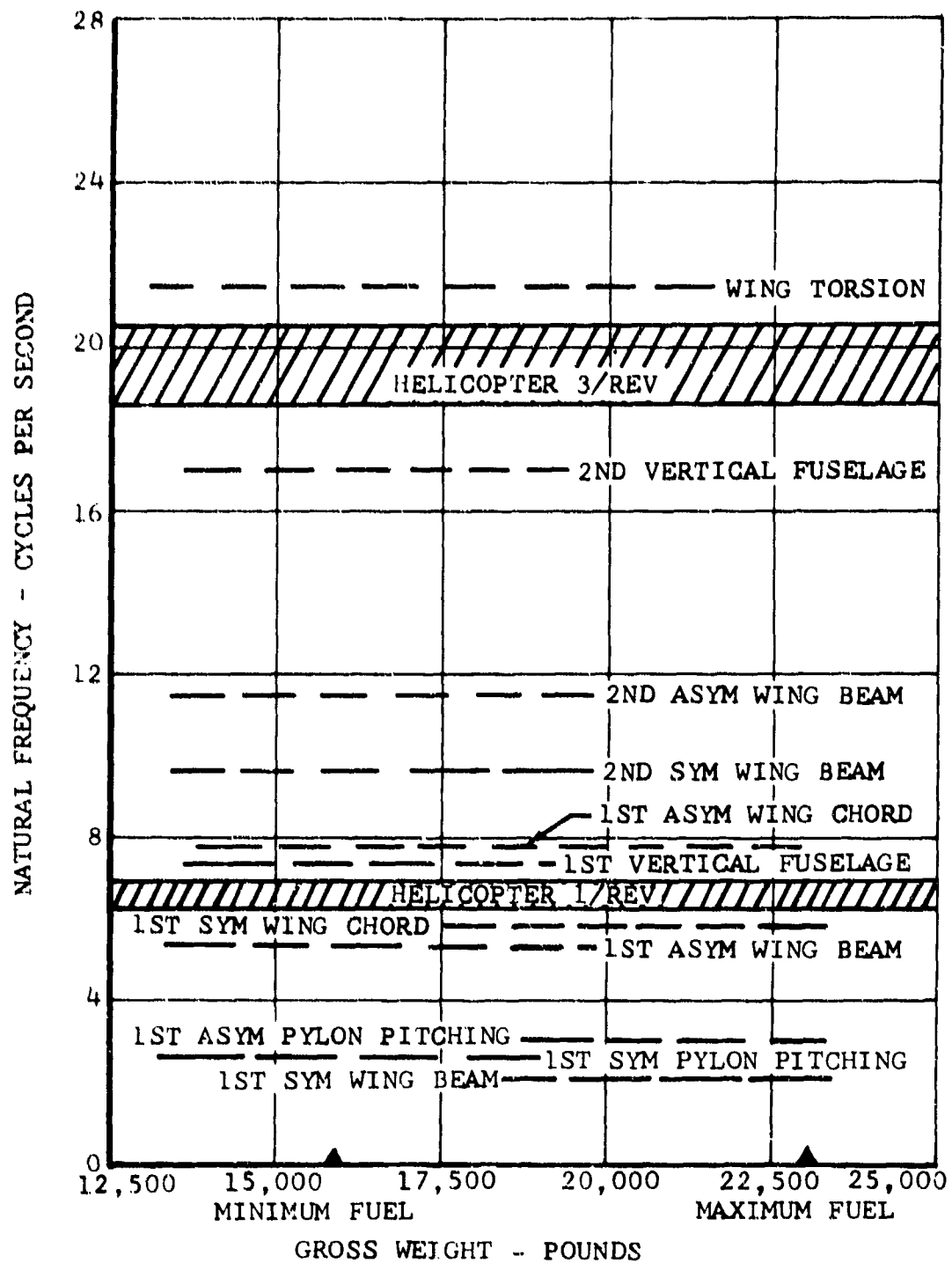


Figure 61. Airframe Natural Frequencies, Helicopter Mode.

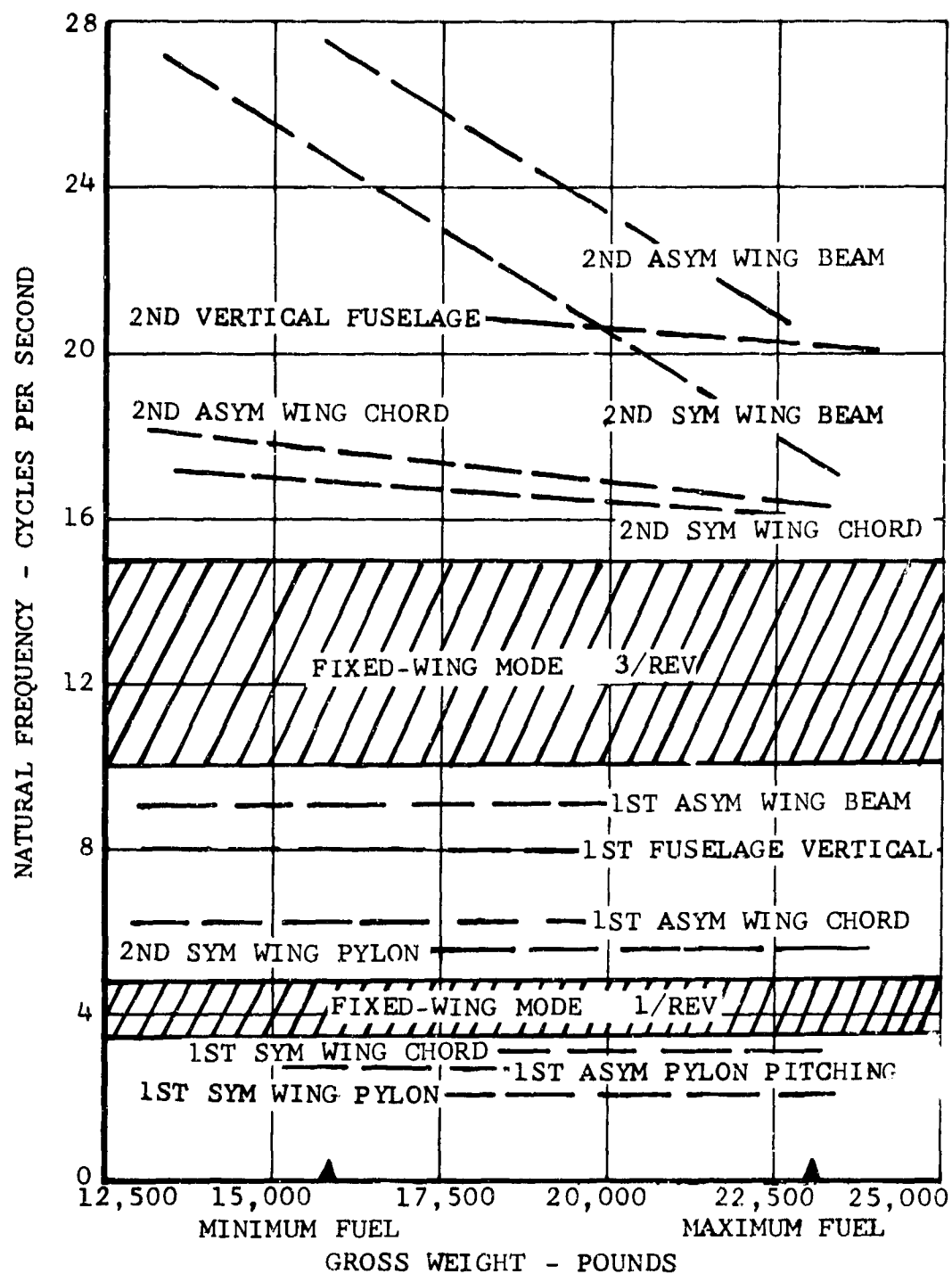


Figure 62. Airframe Natural Frequencies, Fixed-Wing Mode.

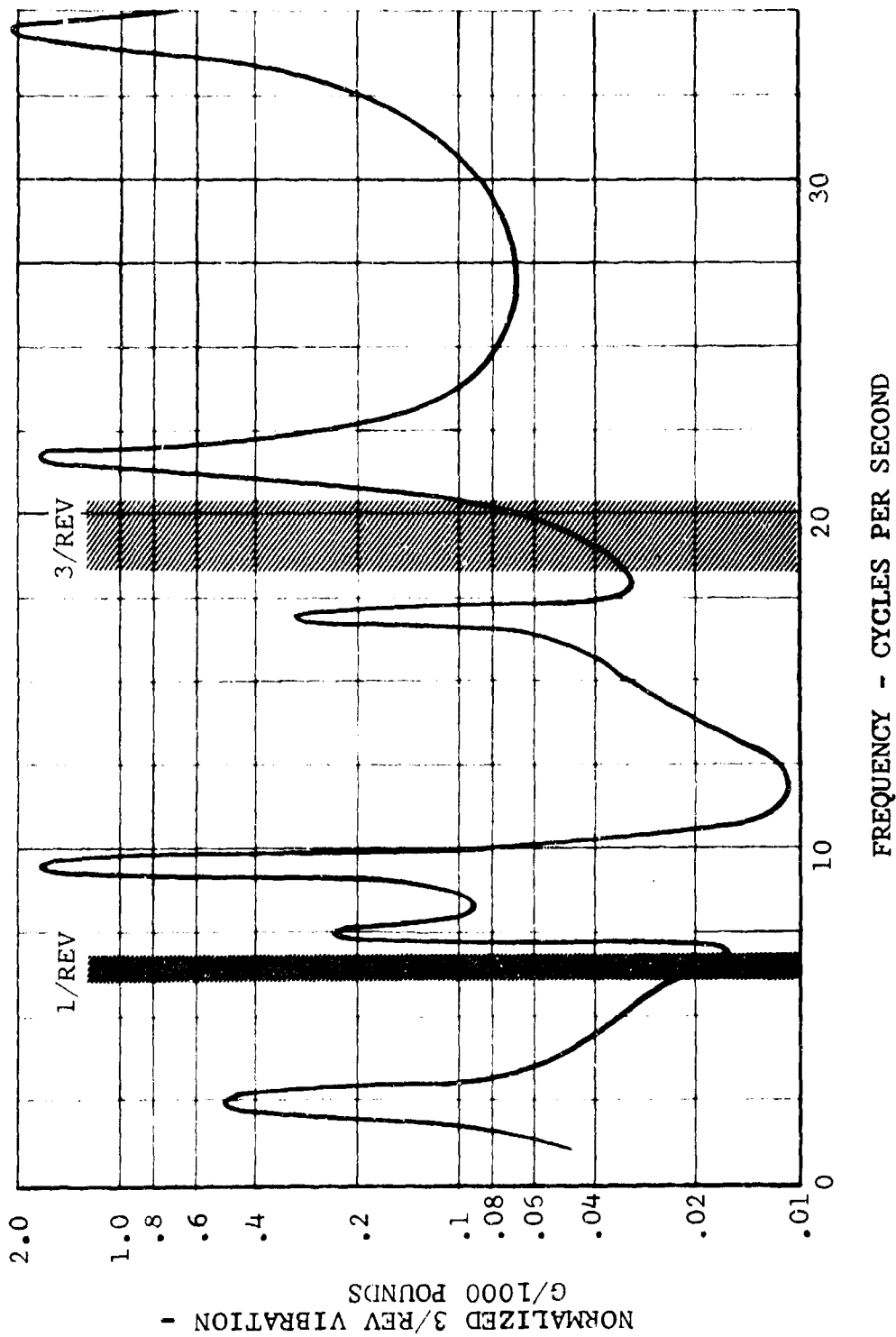


Figure 63. Helicopter-Mode Crew-Compartment Response to 1000-Pound Vertical Shear at Hub.

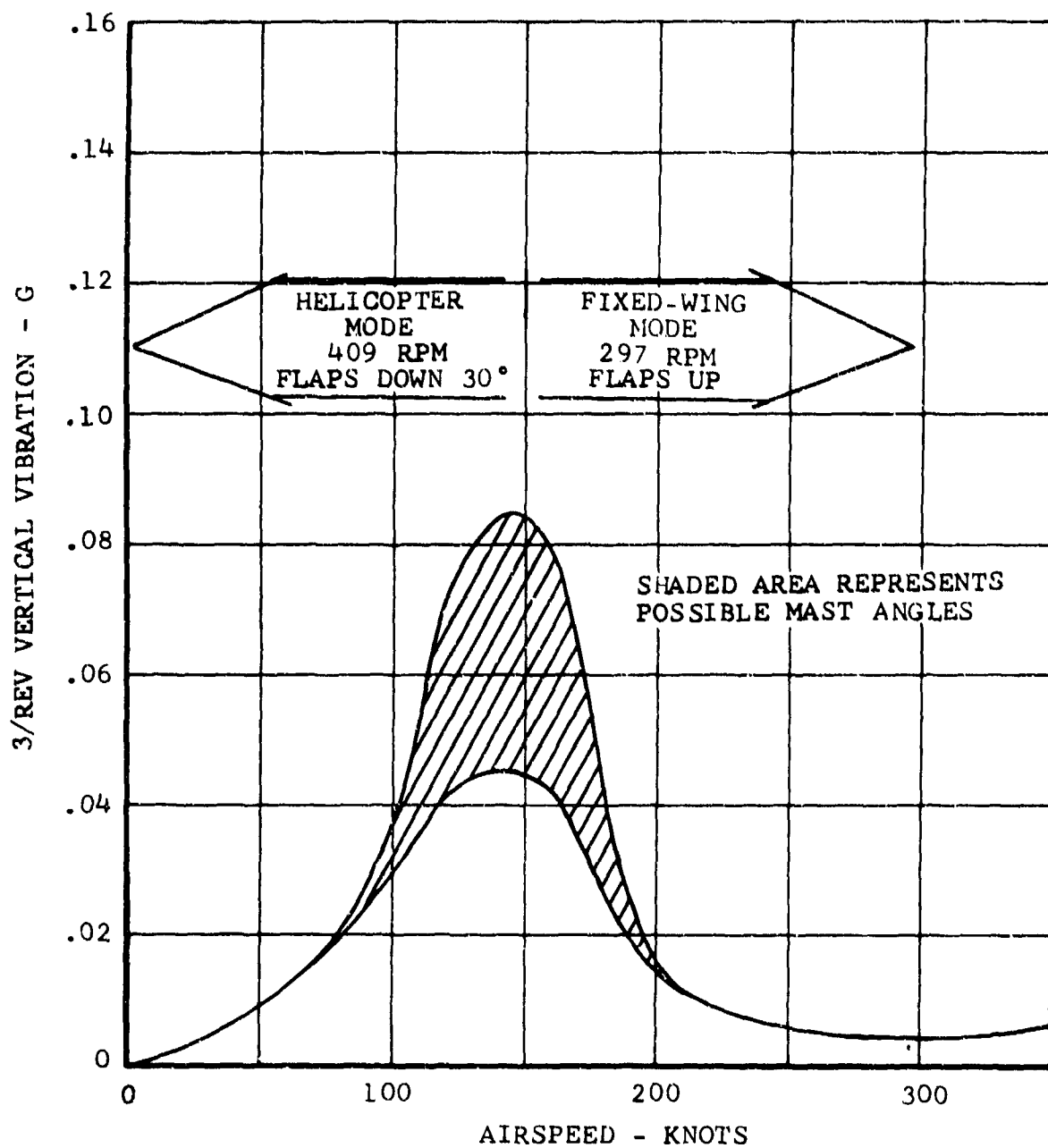


Figure 64. 3/Rev Crew-Compartment Vertical Vibration level.

(2) Gust Response

An analysis was made to determine the effect of the wing flexibility on the loads developed during flight in turbulent air. This analysis indicates that the loads with wing flexibility are 15 to 20 percent greater than those calculated for a rigid body. The response of the D266 to a 66-fps sharp-edged gust is shown in Figure 65. The 196-knot point was chosen because the maximum design gust velocity occurs at that speed (see V-n diagram, Figure 37). Note that the 2.9g load factor calculated in Program C81 agrees well with the V-n load factor. The maximum wing bending moment at butt line 42.0 is about 20 percent of the design bending moment.

The response of the D266 for an encounter with a 50-fps sine-square-shaped horizontal gust was also determined using Program C81. In order to show the effectiveness of the rotor pitch governor under severe conditions, the gust response was determined with the governor both "on" and "off". Time histories of rotor thrust and rpm and the longitudinal and pitching accelerations at the cg are shown in Figure 66. The rotor collective governor is effective in minimizing the effect of the gust. The change in longitudinal acceleration is reduced by 50 percent, from 0.4g to 0.2g, and the pitching acceleration is reduced by 70 percent.

(3) Jump Takeoff

An analysis of the jump takeoff condition was made to determine the effect of the dynamic amplification on wing loads. At maximum helicopter rpm (409 rpm), each rotor has a dynamic lift capability of 23,500 pounds. This load was applied as a ramp input with a time-to-peak of 0.3 second in conformance with MIL-S-8698(ASG). BHC Program A80 was used to calculate the loads that result from the rotor lift input. The analytical model includes the first symmetrical wing bending mode. A time history of the wing bending moments during a jump takeoff is shown in Figure 67. The resulting wing bending moments are equivalent to a 2.92g rigid-body load factor. The wing is designed for a 3.0g load factor.

2. ROTOR ANALYSIS

a. Rotor Flapping Analysis

In the helicopter mode, flapping will be the same as for any helicopter with a semirigid rotor. Well-known analytical methods were used to determine the maximum flapping amplitudes. The D266 rotor is clear of the 8-degree flapping stops throughout the helicopter-mode flight regime.

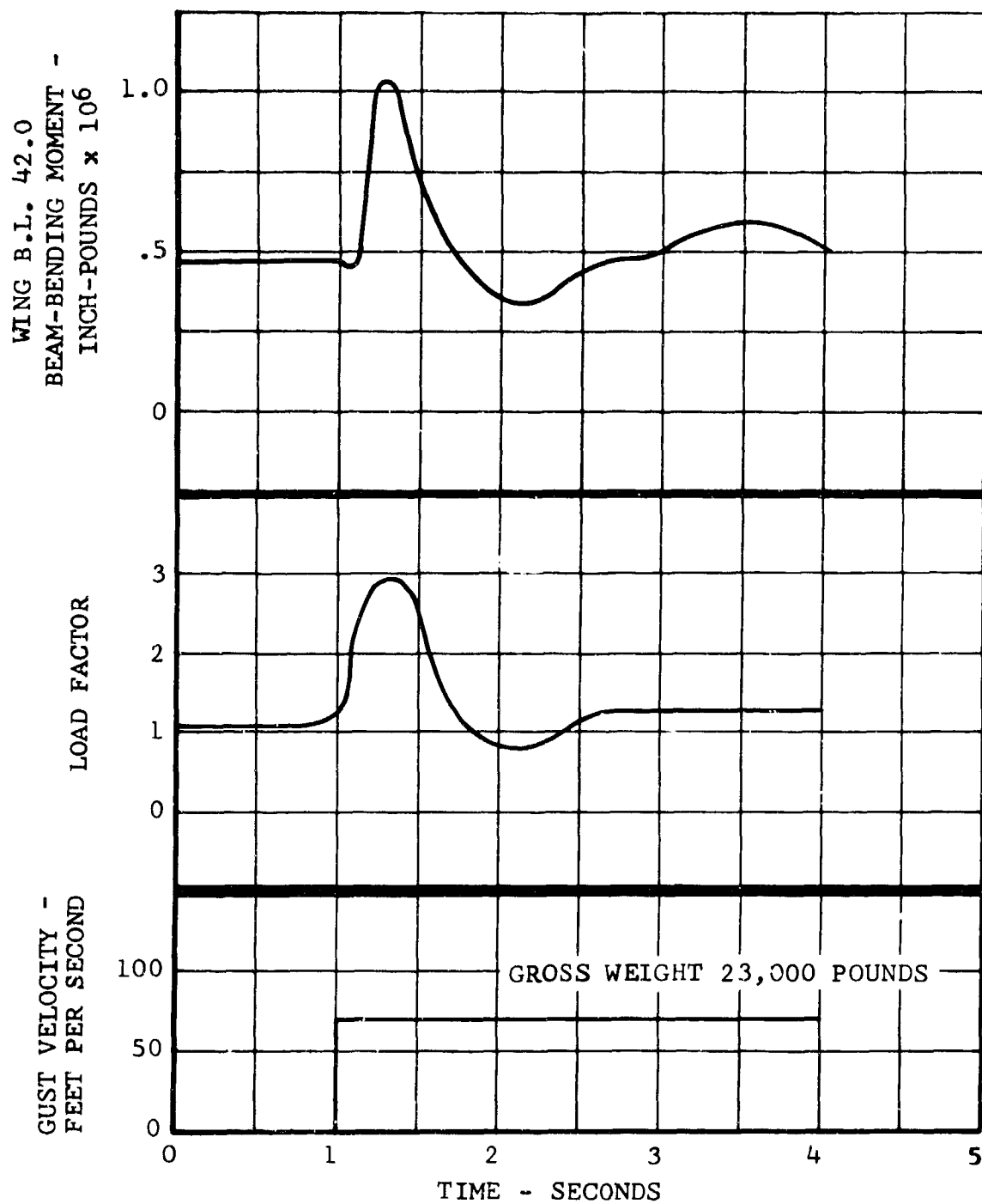


Figure 65. Gust Response Time History 196-Knot
Airspeed - 66-FPS Sharp-Edged Gust.

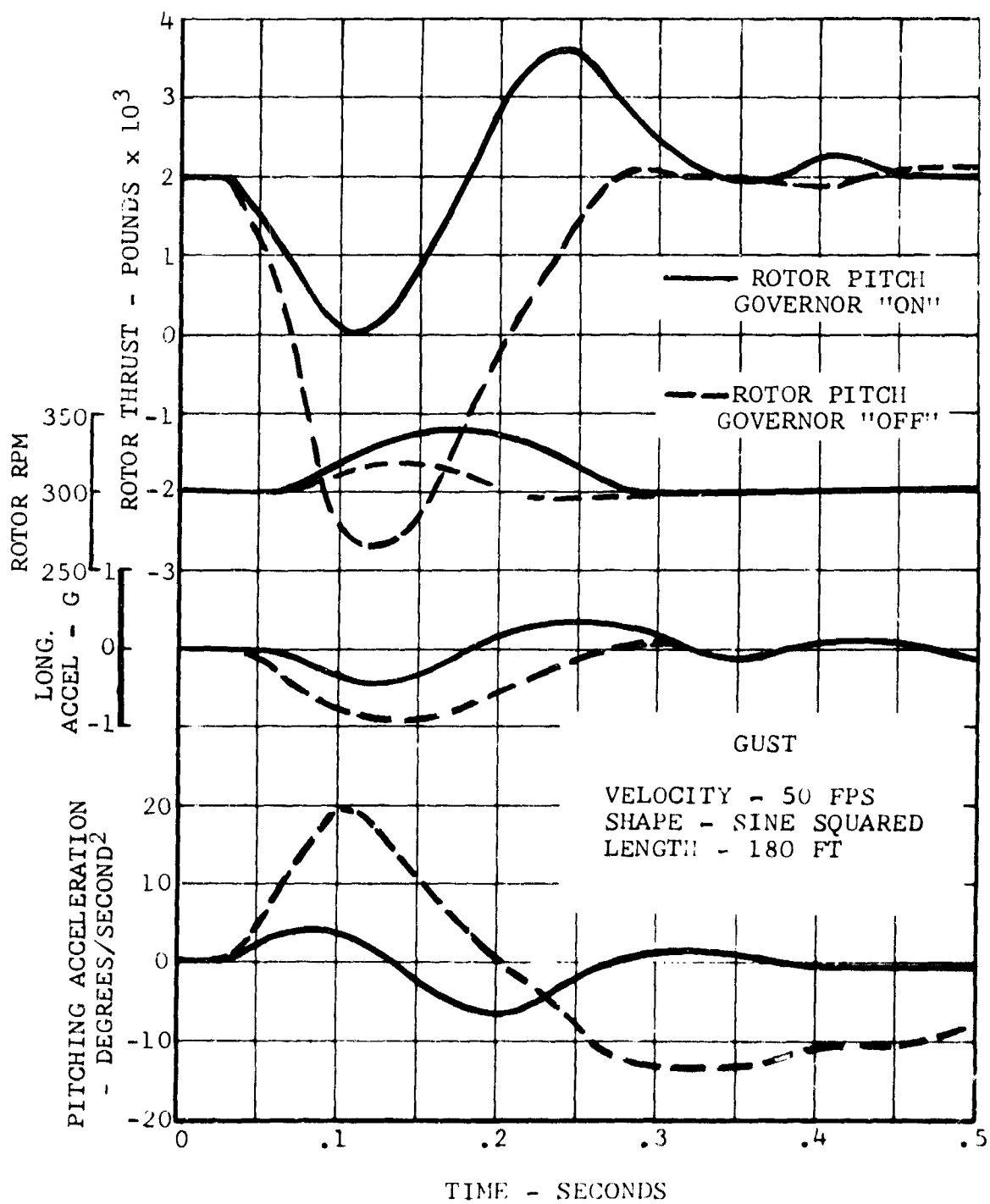


Figure 66. Time History of Encounter With Horizontal Gust at 350 Knots.

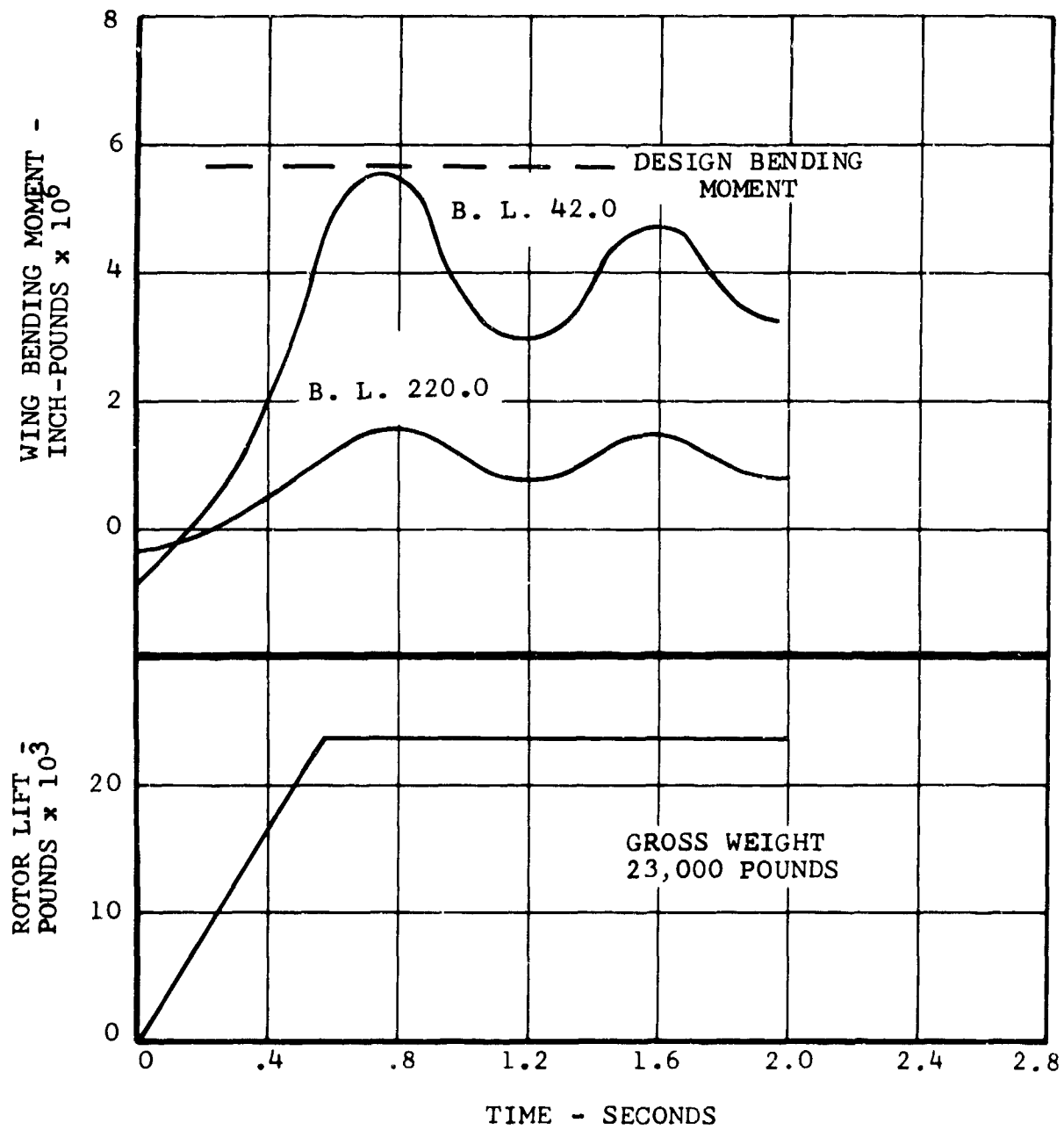


Figure 67. Jump-Takeoff Time History.

Flapping in the fixed-wing mode was calculated using several methods. One of these was the use of the equation derived in the rotor-pylon stability analysis (Reference 7). The equations are based on tip-path-plane aerodynamics. The flapping amplitude calculations are for motion in the pitch direction. Similar equations are used for motion in the lateral direction.

Values of total flapping for the D266 in level flight and in stabilized maneuvers are plotted in Figure 68. In maneuvering flight and in turbulent air, rotor operating speed will be 297 rpm, so the 8-degree flapping limit will not be exceeded within the flight envelope.

A time history of flapping in a pullup is shown in Figure 69. The in-plane steady hub force or H-force developed in the maneuver tends to cancel the g-force due to the overhung rotor weight, so the resulting pylon deflection is small during maneuvers.

b. Rotor Blade Natural Frequencies

The D266 rotor natural frequencies were calculated using Bell Helicopter Company Program C02. Program C02 calculates the coupled in-plane and out-of-plane blade natural frequencies over selected ranges of operating speed and collective pitch setting.

The natural frequencies and mode shapes for the D266 rotor are presented in Figures 70 and 71 for collective and cyclic modes, respectively. Collective modes are modes in which all the blades cone up or down and simultaneously wind up the mast. Cyclic modes are modes in which the blades deflect in opposite directions, both in and out of the plane of rotation. No mast windup occurs.

The lowest collective mode is the first symmetric blade out-of-plane bending mode. The corresponding uncoupled mode is the symmetric blade beam-bending mode. As collective pitch is increased, the frequency of this mode also increases due to rotation of the blade chord stiffness into the out-of-plane direction. This mode has only a small amount of in-plane bending associated with it.

The second collective mode is an in-plane S-ing mode. The associated uncoupled mode is in-plane chord bending. This mode decreases in frequency as collective pitch is increased because the blade beam section is rotated into the plane of rotation. Although a six-per-rev resonance is indicated at low rpm in fixed-wing flight, this mode will not present a problem, since six-per-rev airloads will be extremely small due to the symmetry of airflow in this flight condition.

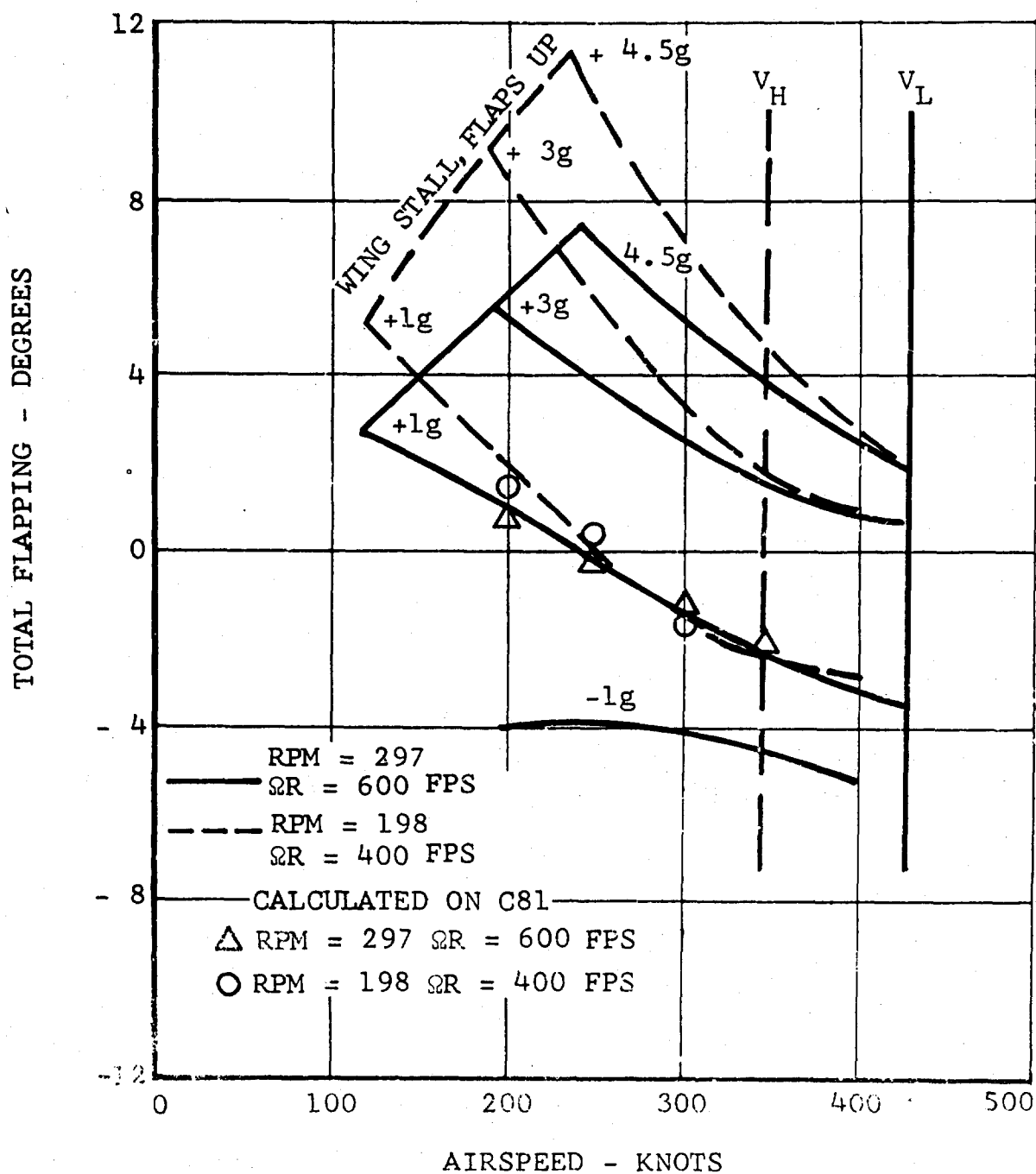


Figure 68. Steady-State Flapping, Fixed-Wing Flight.

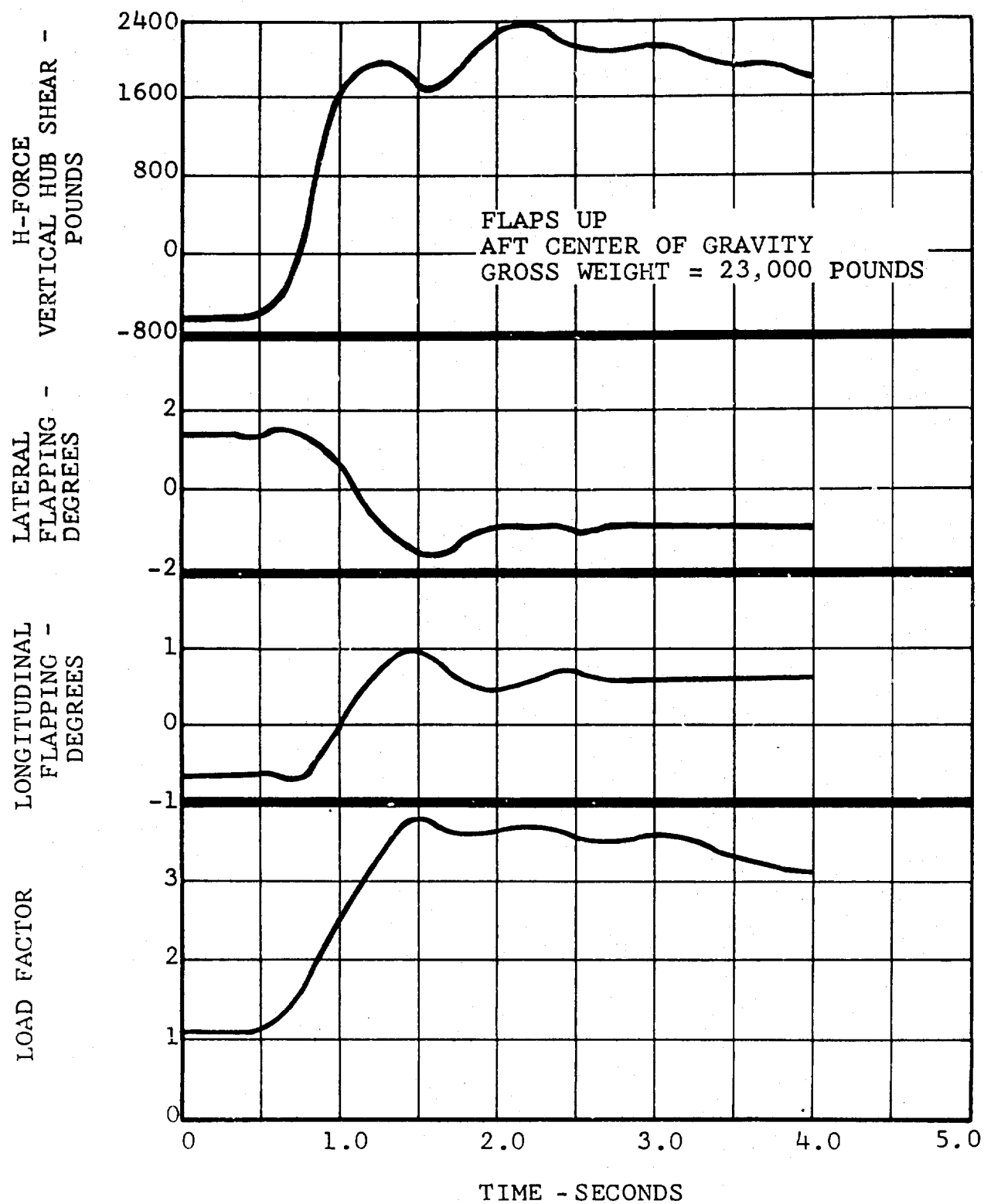


Figure 69. 350-Knot Pullup Time History.

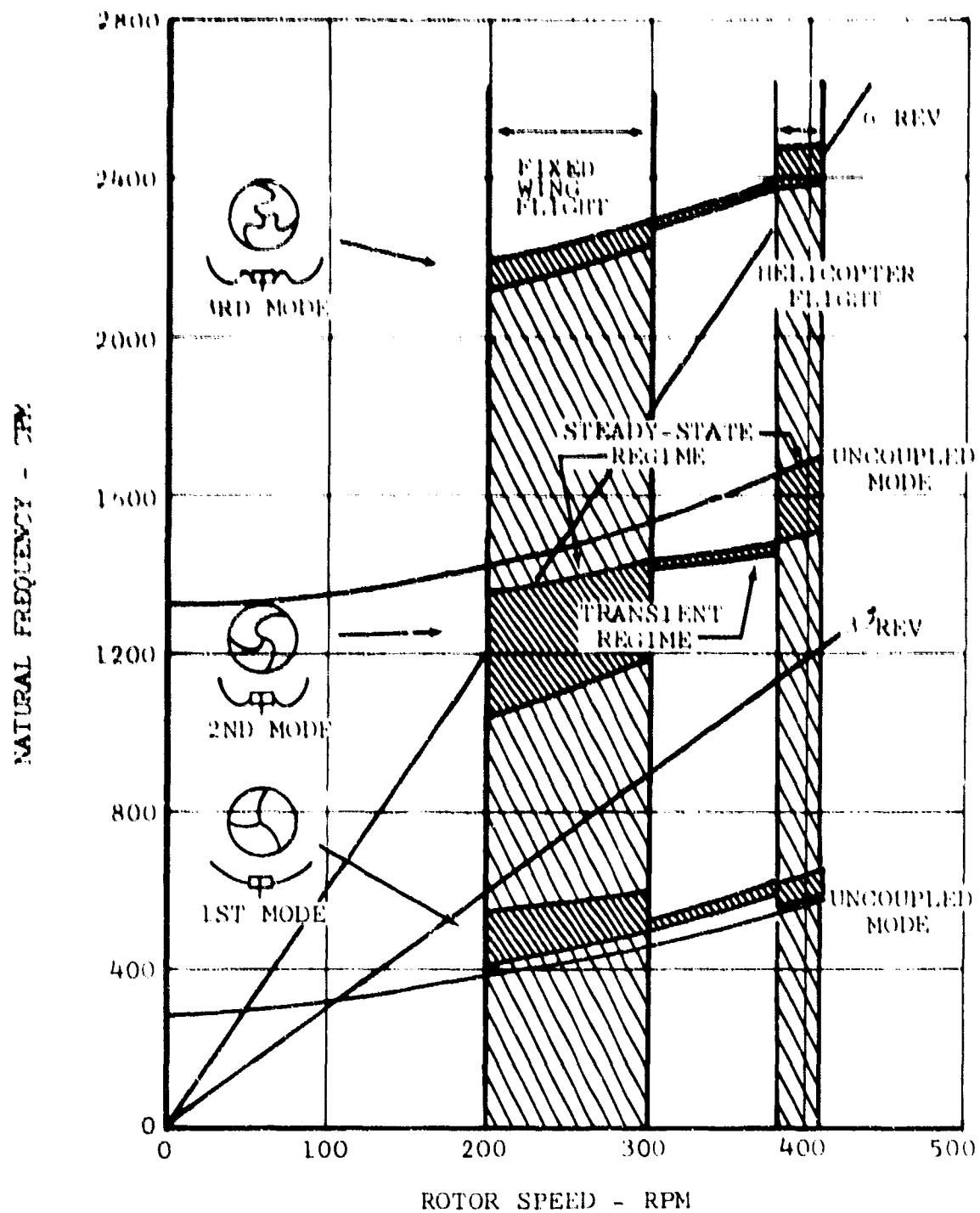


Figure 70. Rotor Natural Frequencies - Collective Mode.

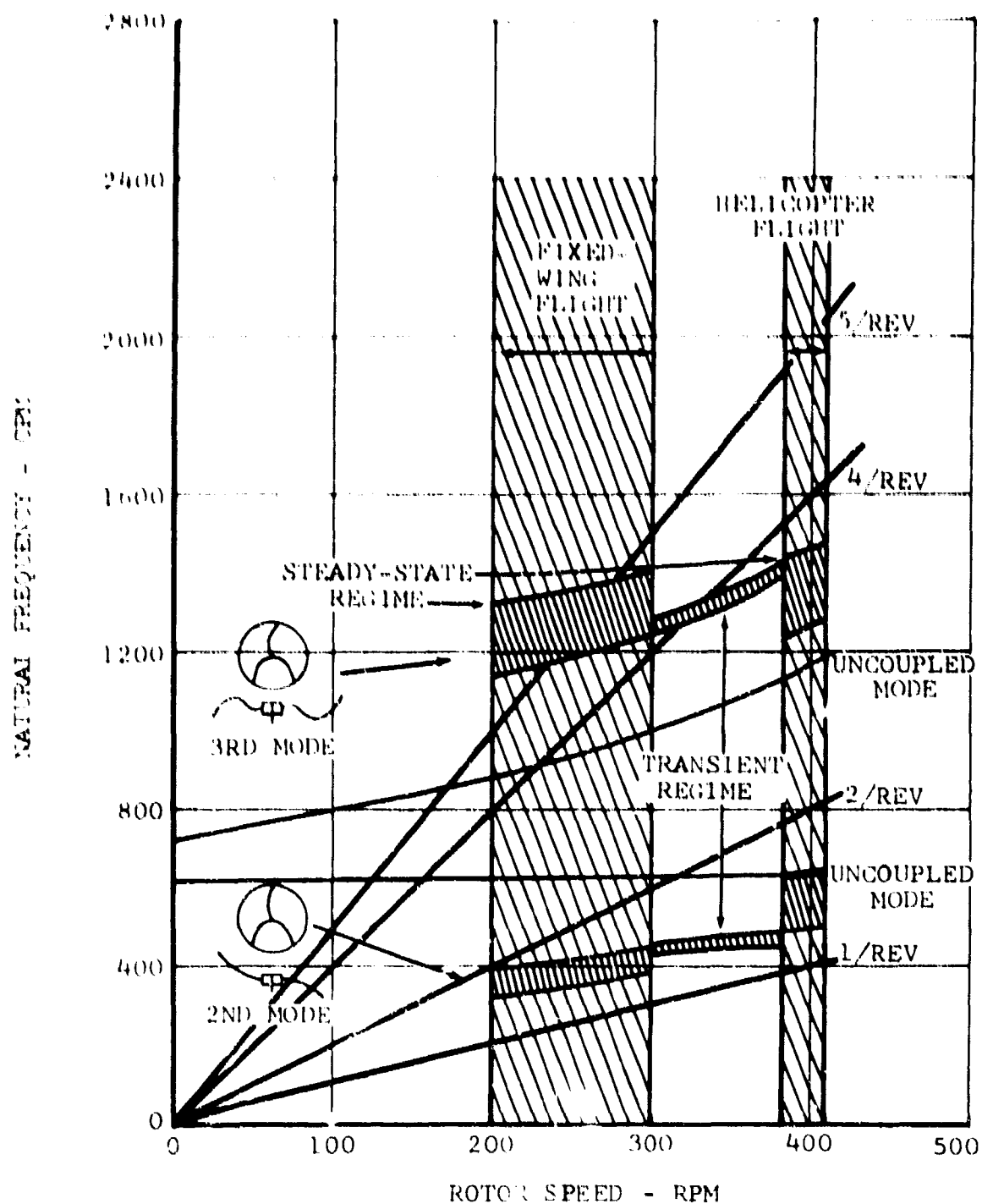


Figure 71. Rotor Natural Frequencies - Cyclic Mode.

The third collective mode is related to second symmetric blade beam bending. In the high rotor rpm range (helicopter flight), the motion of the mode is primarily out-of-plane. In fixed-wing flight (low rpm and high collective pitch), the motion is primarily in-plane. A six-per-rev resonance is indicated in helicopter flight at high collective settings. Flight test experience has shown that such high-frequency resonances are easily controlled by small weights at the antinodes.

The lowest cyclic mode is the rigid-body flapping mode. This mode is not shown in Figure 71 because it increases with airspeed due to the effect of δ_3 . The rigid-body flapping mode is normally at one per rev, but on the D266 the fixed-system hub spring and the δ_3 raise the frequency to 1.25 per rev at normal operating speeds.

The second cyclic mode is an in-plane mode that is primarily chord bending at high rpm (and low collective pitch settings) and beam bending at low rpm (and high collective pitch settings). Experience has shown that the location of the frequency of this mode is very important from a blade load standpoint. The final blade configuration was selected so as to keep the frequency of this mode above 1.3 per rev throughout the operating range. At low rotor speed, 198 rpm, this mode is close to a two-per-rev resonance, but the two-per-rev excitation will be very low in the high-speed mode.

c. Rotor Loads

During the design study, the rotor loads have been thoroughly investigated. Blade loads in both steady flight and in maneuvers, including conversion from helicopter to fixed-wing mode, were calculated. Over one hundred computer cases were run to determine blade loads of the final rotor configuration for a variety of flight conditions.

Rotor loads were calculated using the following procedure: First BHC Program C81, "Helicopter Rigid Body Dynamic Analysis," was used to calculate a trimmed condition for a given airspeed, gross weight, conversion angle, and center of gravity. This trim point defines the rotor-tip-path-plane orientation and the blade flapping. Next BHC Program F40, "Blade Bending Moment," was used to calculate the steady and oscillatory blade bending moments using the tip-path-plane orientation from Program C81. The oscillatory bending moments for one-per-rev through four-per-rev airloads are calculated. The blade loads in and perpendicular to the plane of rotation for each harmonic are first calculated; then the harmonics are summed and resolved into blade beamwise and chordwise components.

Figures 72 through 76 show blade bending moment distributions for helicopter flight, conversion, and fixed-wing flight. The oscillatory loads given in these figures are the vector sums of all of the integral rotor harmonics through four per rev. Loads are given in terms of the beamwise and chordwise directions. This procedure results in a large discontinuity at 10-percent radius, where the feathering portion of the blade begins. The discontinuity is most apparent in fixed-wing mode (high collective settings), where the blade beam section is in the plane of rotation; whereas the hub beam sections (inboard 10 percent of radius) are always perpendicular to the plane of rotation.

Figure 72 shows the blade loads in helicopter flight at 90 knots. The high blade twist required for optimum performance causes higher than normal (for a helicopter) blade beamwise loads. This is because the blade tip operates at negative angles of attack in high-speed helicopter flight, causing a large download on the tip of the advancing blade. The primary component of these higher loads is one per rev. Normal helicopter two-per-rev and three-per-rev components are also present.

Figures 73 and 74 show the effect of mast angle on the blade loads. At 150-knot airspeed, increasing the angle of the mast reduces the blade loads. Converting the pylon results in a better angle-of-attack distribution on the blade and, consequently, lower oscillatory loads. Blade load calculations indicate that the D266 can operate continuously with zero-degree mast angle (pylon vertical) at speeds up to 120 knots and even up to 150 knots for short periods of time. The conversion corridor is shown in Figure 36. The boundaries of the corridor are established by the wing stall speed and by blade oscillatory bending moments.

In fixed-wing mode level flight (Figures 75 and 76), the oscillatory blade loads are low because the airflow is essentially axial. The only significant oscillatory loads are at one per rev. Blade beamwise steady bending moments are higher than for a helicopter, because the high collective setting results in the rotor torque's being reacted in blade beam direction. Note that most flight time will be in the fixed-wing configuration where oscillatory moments are low. The effect of the fixed-system longitudinal hub spring is to increase blade-root bending moments while decreasing the bending moments in the outboard 50 percent of the blade.

The blade loads were also calculated for different maneuvers in fixed-wing flight mode. Figures 77 and 78 show typical blade loads during a pullup and an encounter with a 66-foot-per-second gust. In these maneuvers, high oscillatory loads of very short duration were encountered.

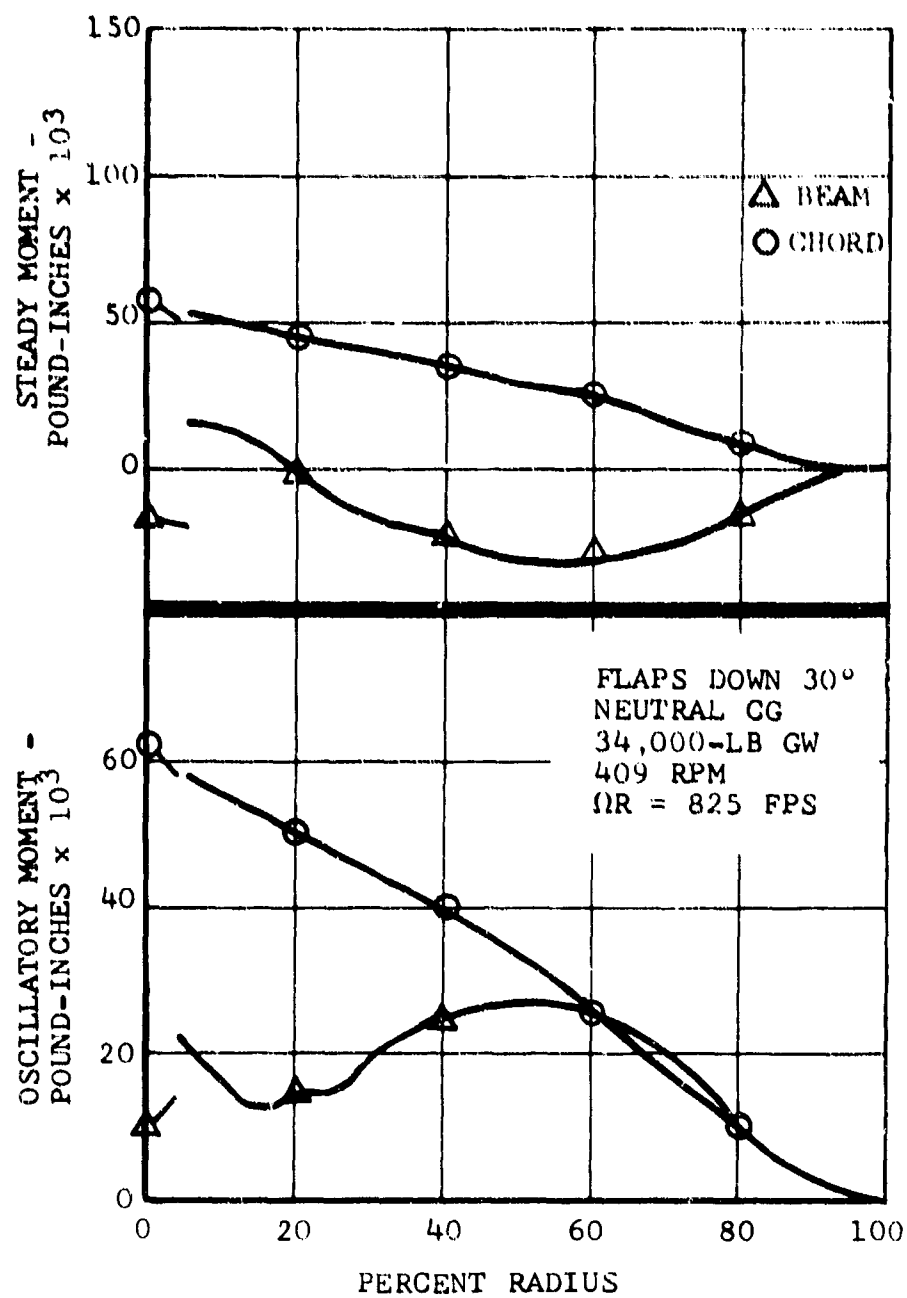


Figure 72. Blade Bending Moments -
Helicopter Mode, 90 Knots.

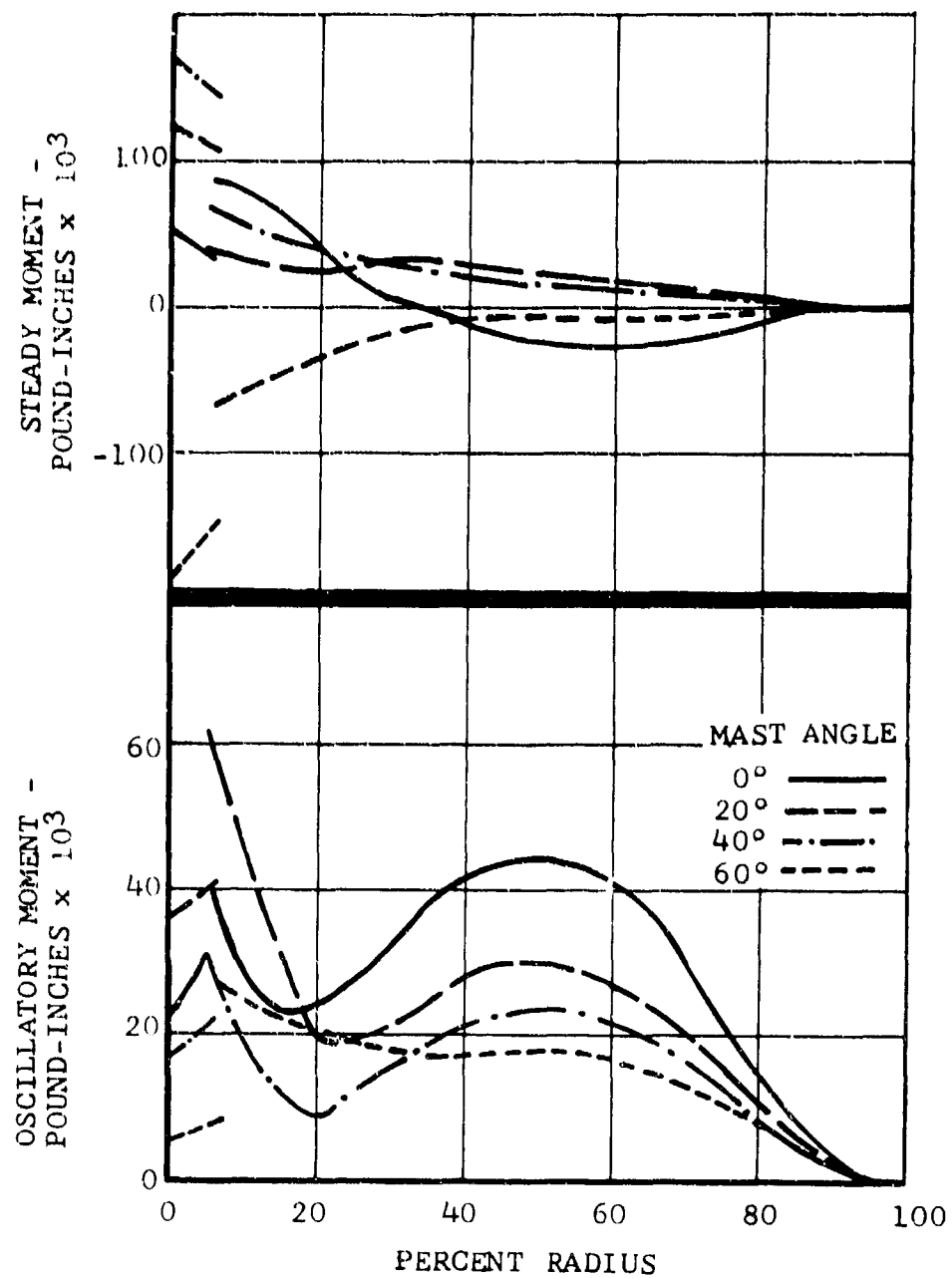


Figure 73. Blade Beam-Bending Moments - Helicopter Mode, 150 Knots.

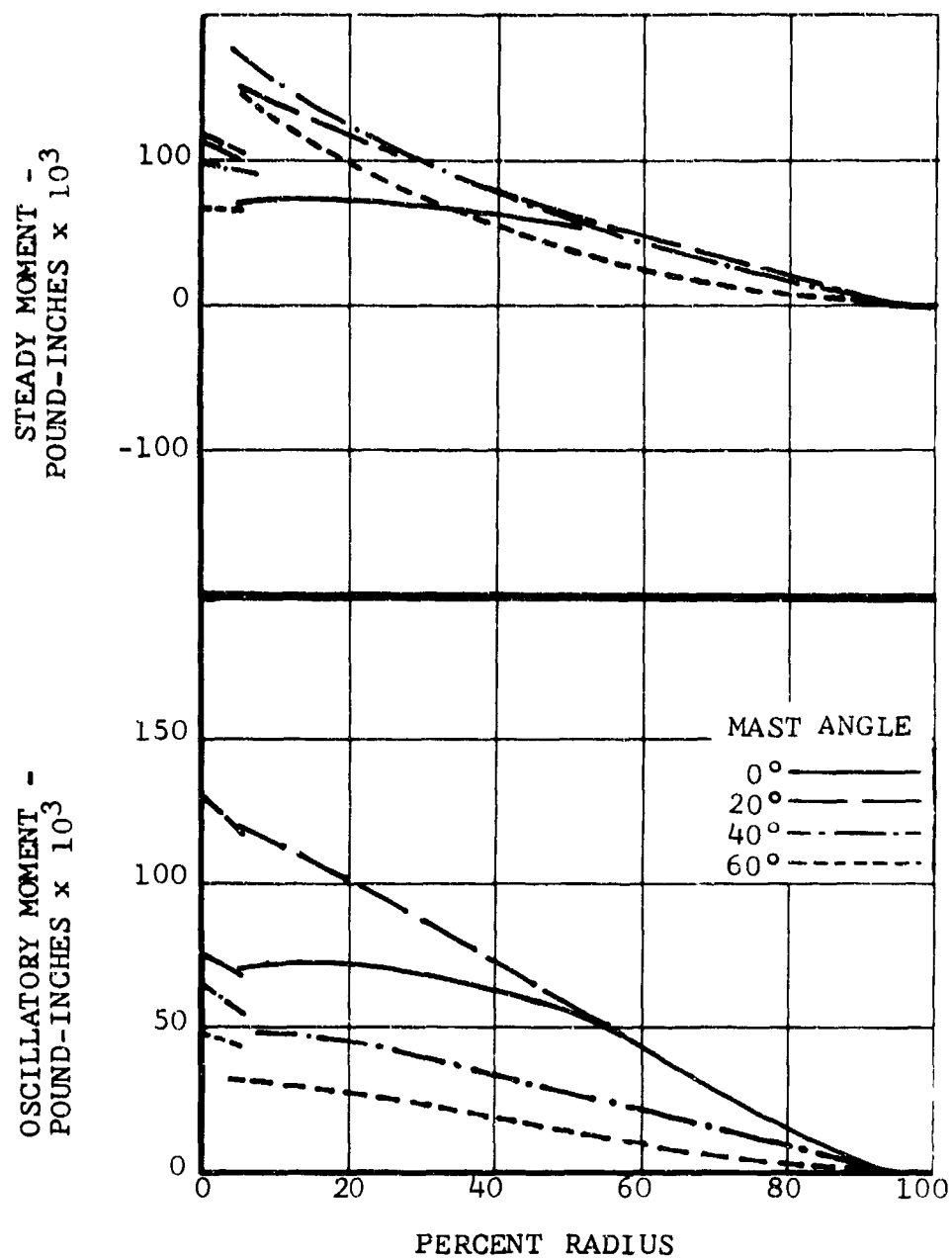


Figure 74. Blade Chord-Bending Moments - Helicopter Mode, 150 Knots.

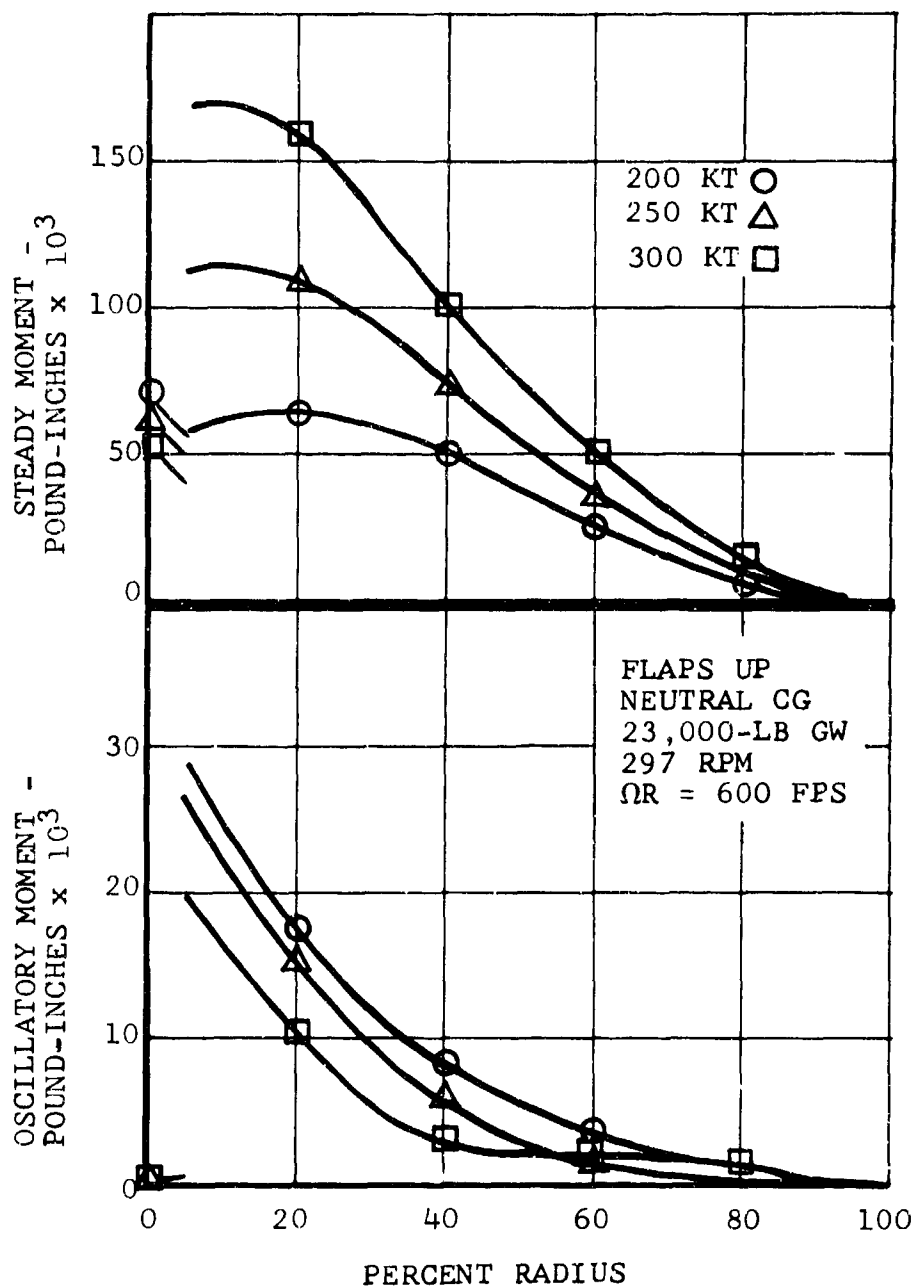


Figure 75. Blade Beam-Bending Moments - Fixed-Wing Mode.

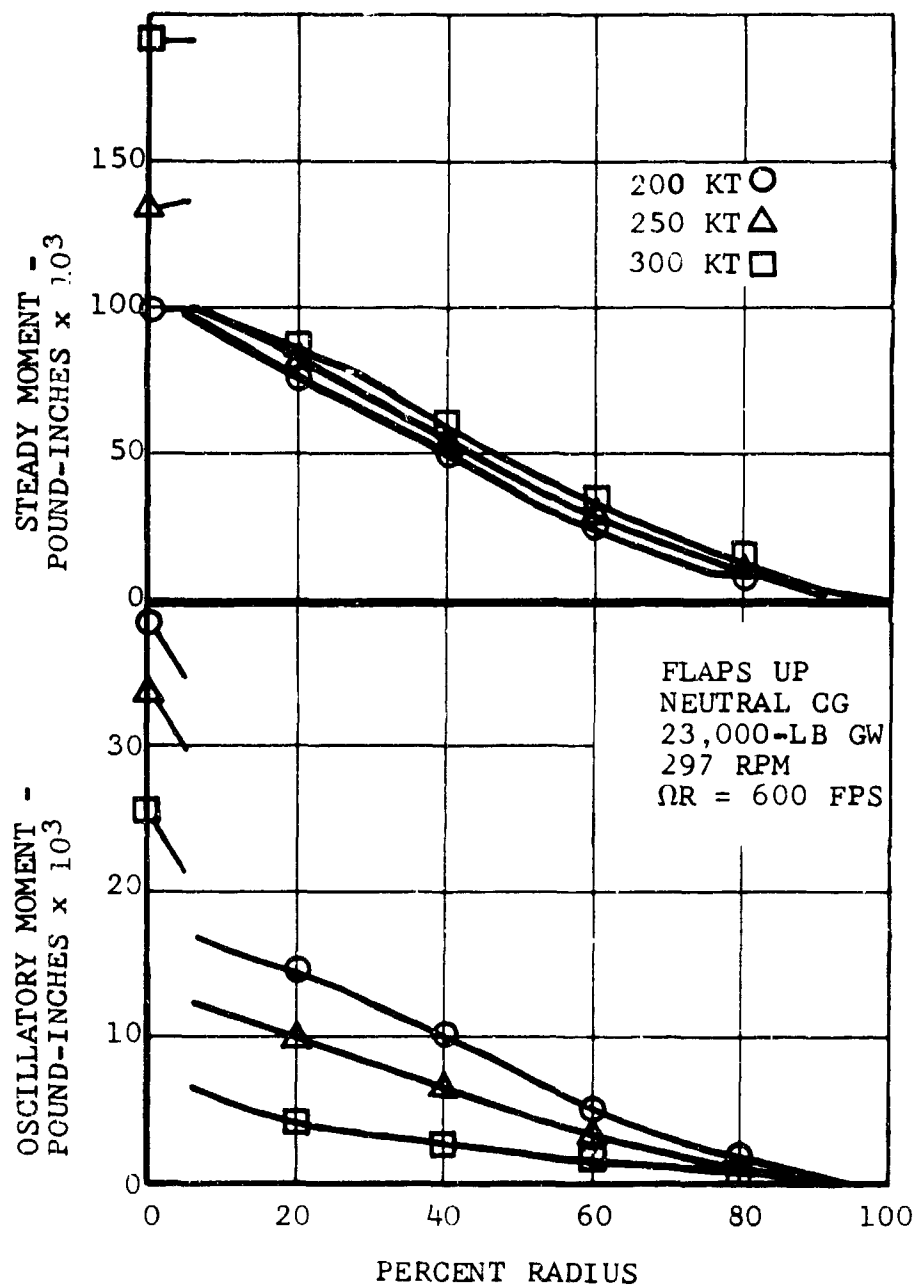


Figure 76. Blade Chord-Bending Moments - Fixed-Wing Mode.

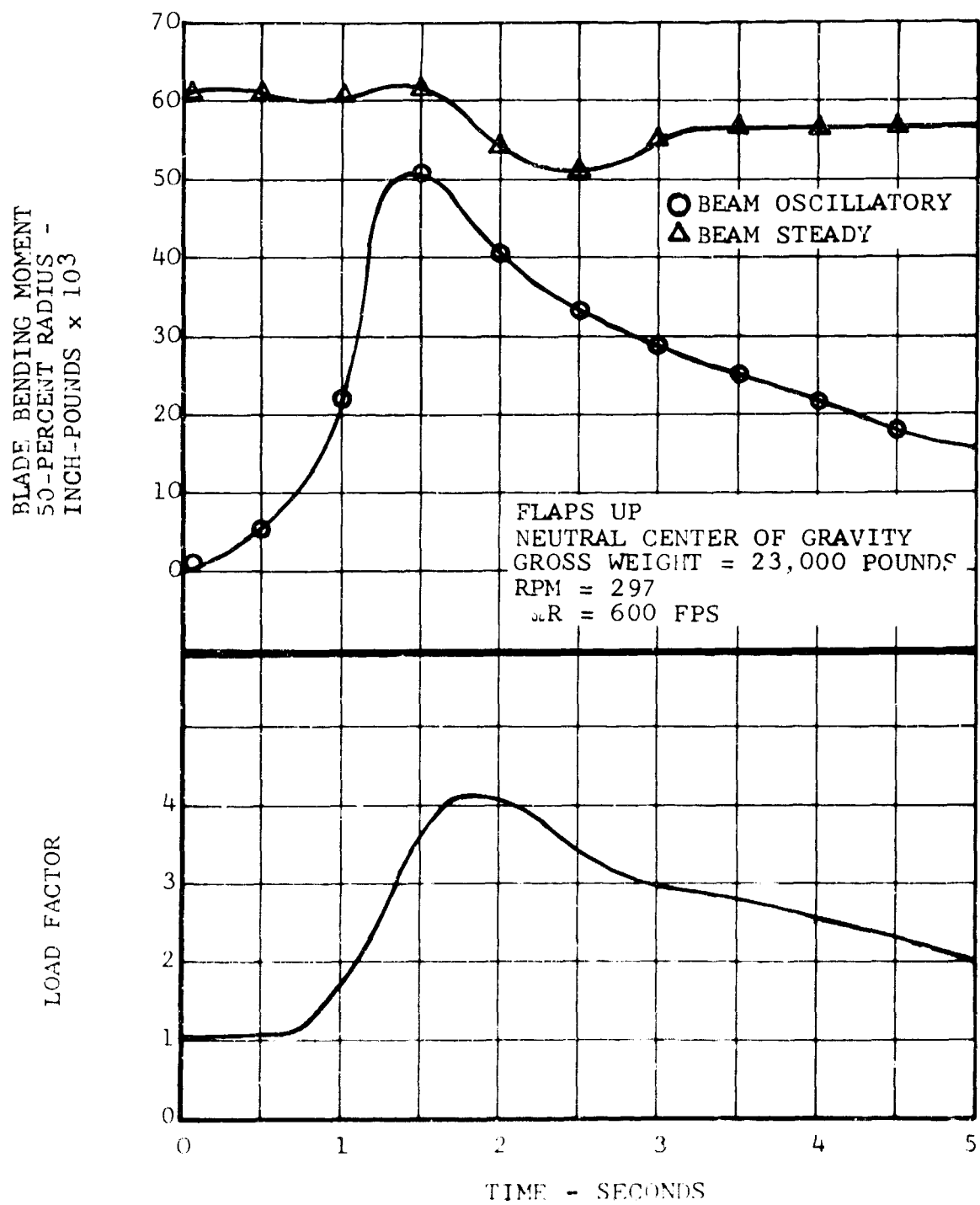


Figure 77. Blade Bending Moments, 250-Knot Pullup.

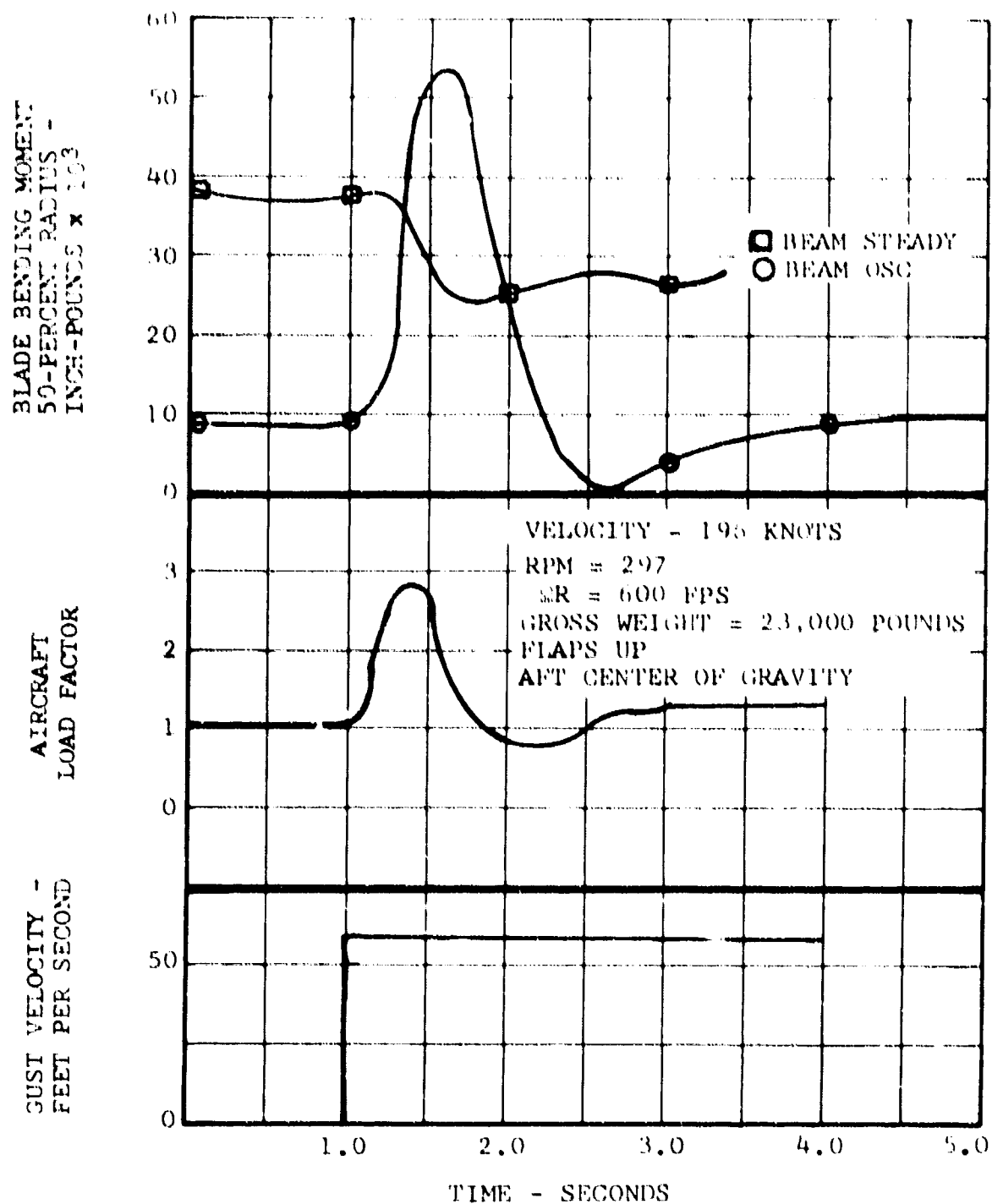


Figure 78. Blade Bending Moment Time History, 66-FPS Gust.

3. LIFTING SURFACE AEROELASTIC STABILITY

The aeroelastic stability of the D266 airframe and rotors has been thoroughly analyzed. The analysis shows that the D266 airframe and rotor are free of aeroelastic instabilities from hover to speeds in excess of $1.15 V_{\text{limit}}$ (503 knots).

The very thick wing, its forward sweep, and the extremely stiff torque box formed by the two spars and the upper and lower honeycomb wing skins combine to provide a wing configuration that is not susceptible to aeroelastic instabilities. The honeycomb wing panels which constitute most of the wing bending material are also fully effective in torsion. This efficient use of the bending material, together with the relatively thick wing section, gives the wing very high torsional stiffness. The flexibly mounted rotor on the wingtip introduces additional effects which are included in the determination of the wing flutter and divergence speeds.

The possibility of control surface flutter is eliminated by the irreversible controls of the D266. Hydraulic cylinders are located at or near the ailerons to insure a maximum free play that is less than the permissible free play specified in Reference 8. Each aileron is controlled by a dual hydraulic cylinder which is attached directly to the aileron horn. The elevator and rudder are actuated by single hydraulic cylinders in the vertical fin. Irreversible (lock-and-load) hydraulic valves maintain irreversibility in the event of a loss of hydraulic power.

a. Wing Flutter and Divergence

The wing, including the aerodynamic and inertial properties of the rotor, was analyzed using incompressible aerodynamics. A symmetric free-free flutter analysis was made using the collocation method. Bell Helicopter Company Digital Computer Program F71, which utilizes structural influence coefficients, was used for the symmetric analysis. An asymmetric free-free flutter analysis using the modal method was made using Bell Program F68. Both of these programs use a two-dimensional, incompressible, unsteady, aerodynamic influence coefficient matrix calculated with Bell Program F67, and a mass matrix calculated with Bell Program F69. The mass matrix represents the mass, inertia, and mass unbalance of each wing section. The methods and calculation procedures used in these programs are developed in References 9, 10, and 11.

The analytical model used for the wing is shown in Figure 79. Seven sections were used, with the seventh section representing the rotor pylon. The rotor pylon was represented by using the pylon-pitch-isolation mount spring rate (6×10^6 in.-lb/radian) as the torsional spring rate of the last wing section, and by using the rotor-pylon mass and inertial characteristics as the mass properties of the seventh section.

The rotor in-plane aerodynamic force (H-force) was represented by modifying the lift coefficient and pitching moment coefficient of the seventh section. Figures 80 and 81 show $dH/d\alpha$ and $dH/d\dot{\alpha}$, respectively. Values for $dH/d\alpha$ and $dH/d\dot{\alpha}$ were obtained from Program C81.

Required structural damping for sea level, 15,000 feet, and 30,000 feet, and for minimum, half, and full fuel was calculated as a function of airspeed. One-half fuel was found to be critical. Required structural damping versus airspeed is shown in Figures 82 and 83 for symmetric and asymmetric modes, respectively. The wing flutter boundary is well beyond the flight envelope.

The very high torsional stiffness of the D266 wing virtually precludes divergence from wing aerodynamic forces alone. The rotor aerodynamic forces tend to lower the wing divergence speed, however, so a divergence analysis that includes the rotor aerodynamic forces was made. The wing divergence speed was found to be 670 knots.

b. Aileron Reversal

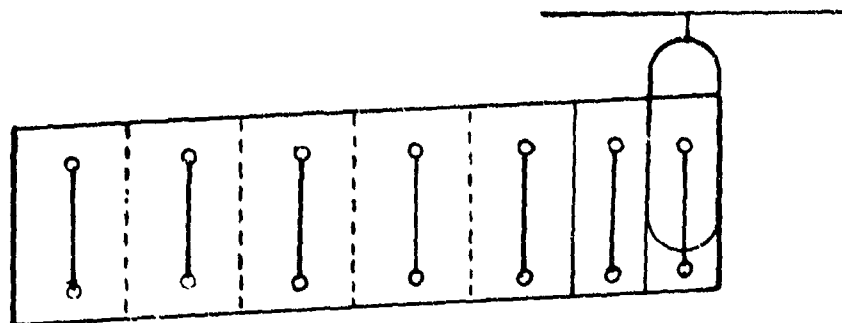
The very high torsional stiffness of the D266 wing precludes aileron reversal due to the wing and aileron aerodynamic forces alone. The reversal speed was calculated, though, because the rotor aerodynamic forces tend to lower the aileron reversal speed. Reversal speed was calculated to be well above 600 knots.

c. Empennage Flutter

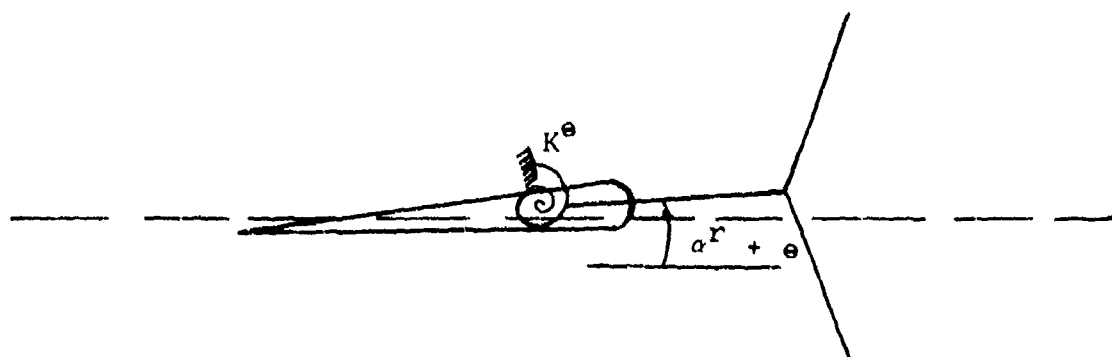
The flutter analysis of D266 empennage shows that the horizontal tail and vertical tail are free of flutter to speeds over 600 knots.

4. ROTOR AEROELASTIC STABILITY

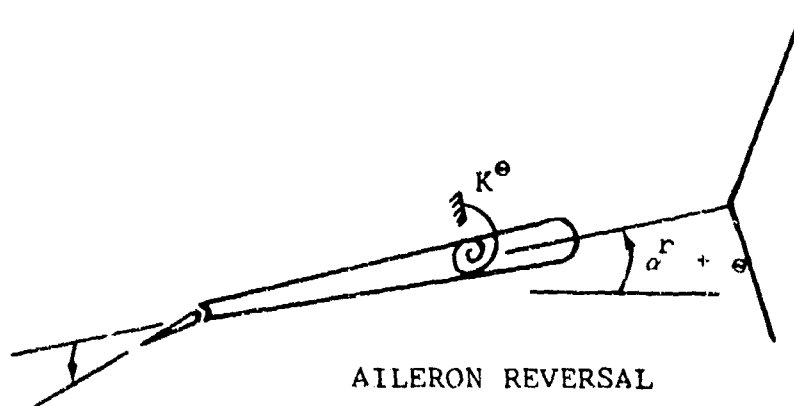
A complete aeroelastic investigation of the D266 rotor showed that the rotor is stable throughout the flight envelope. The investigation included the following areas:



WING FLUTTER



WING DIVERGENCE



AILERON REVERSAL

Figure 79. Aeroelastic Analytical Models.

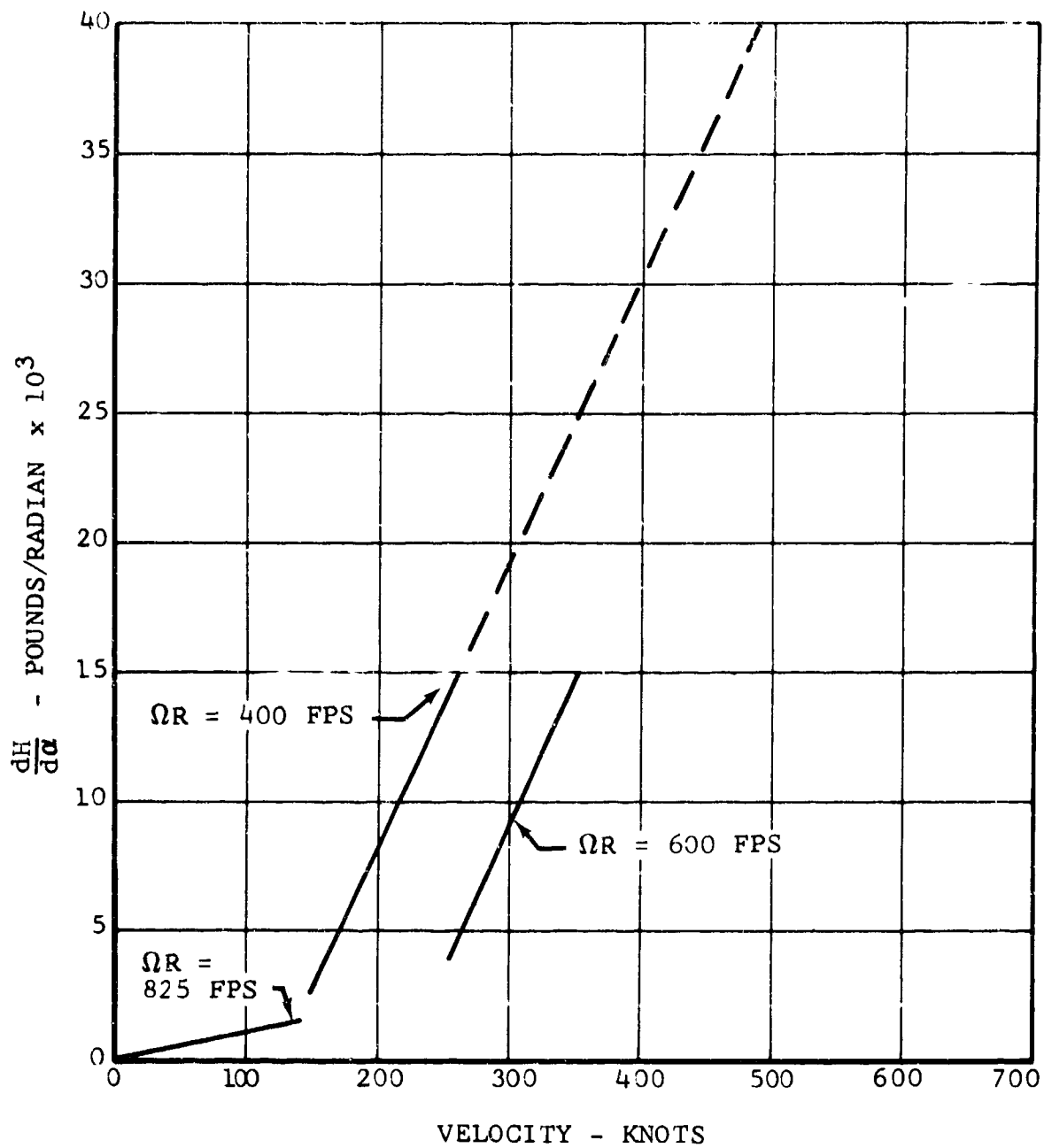


Figure 80. $\frac{dH}{d\alpha}$ Versus Airspeed.

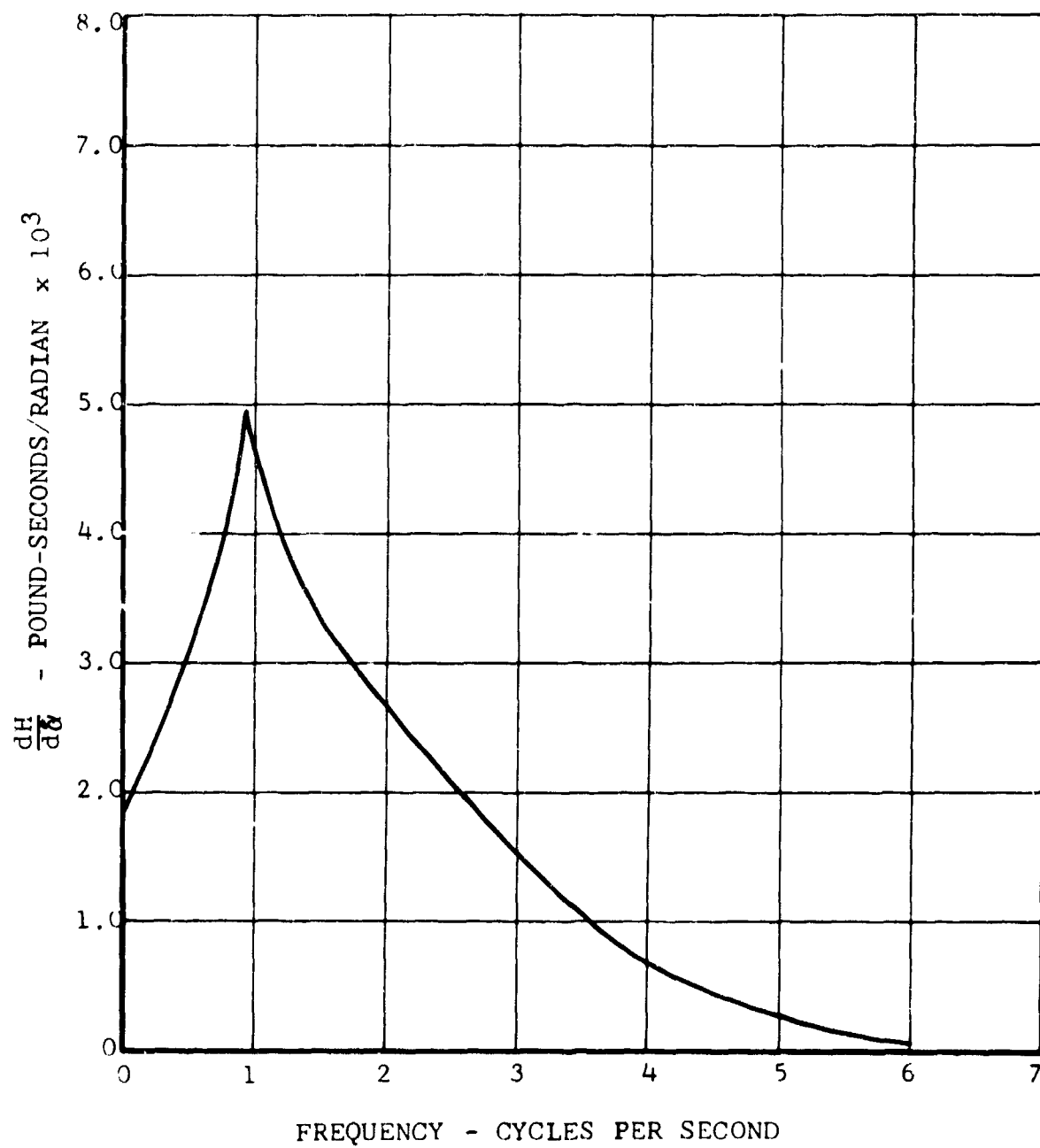


Figure 81. $\frac{dH}{d\alpha}$ Versus Frequency.

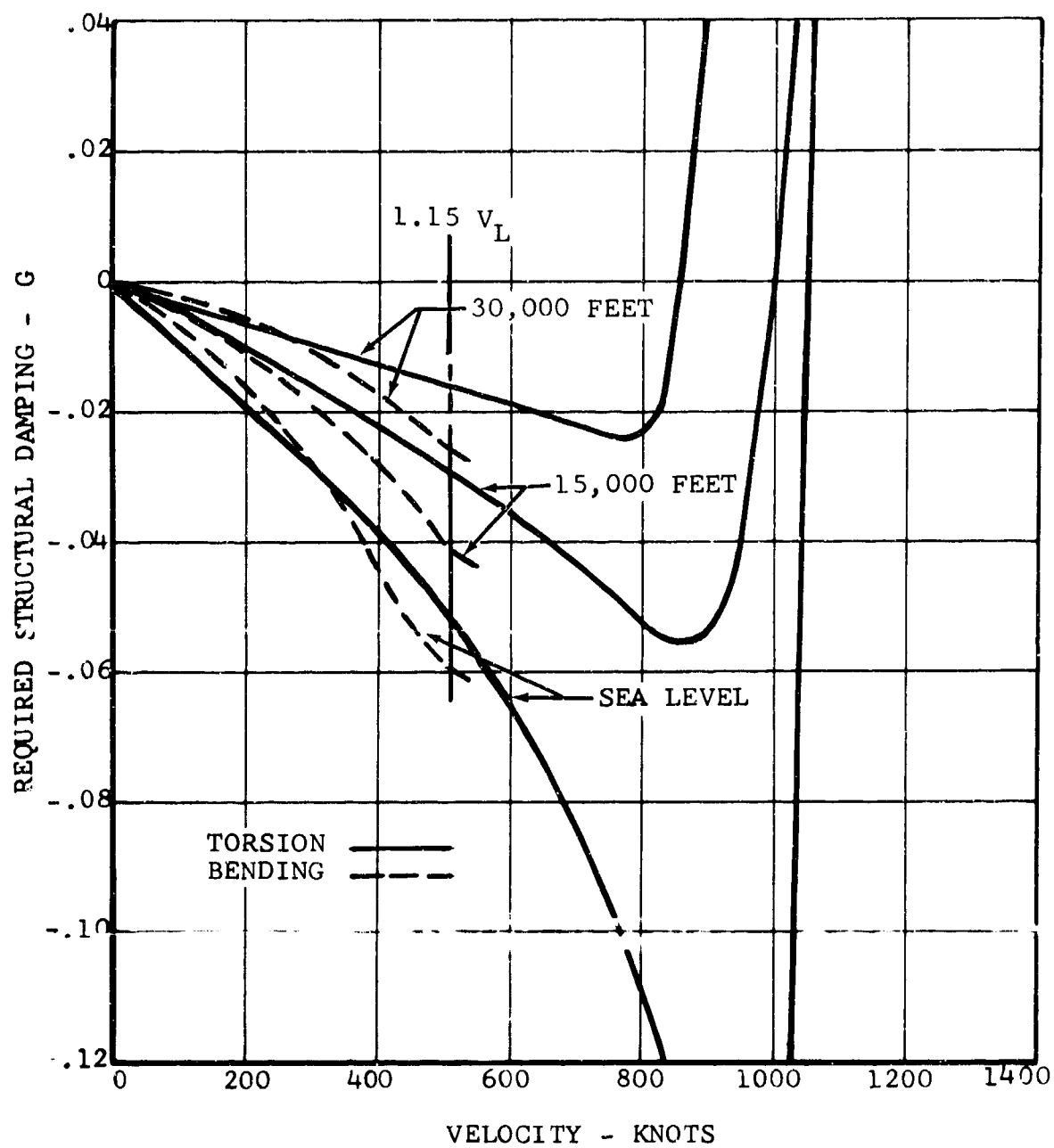


Figure 82. Symmetric Free-Free Wing Flutter, One-Half Fuel.

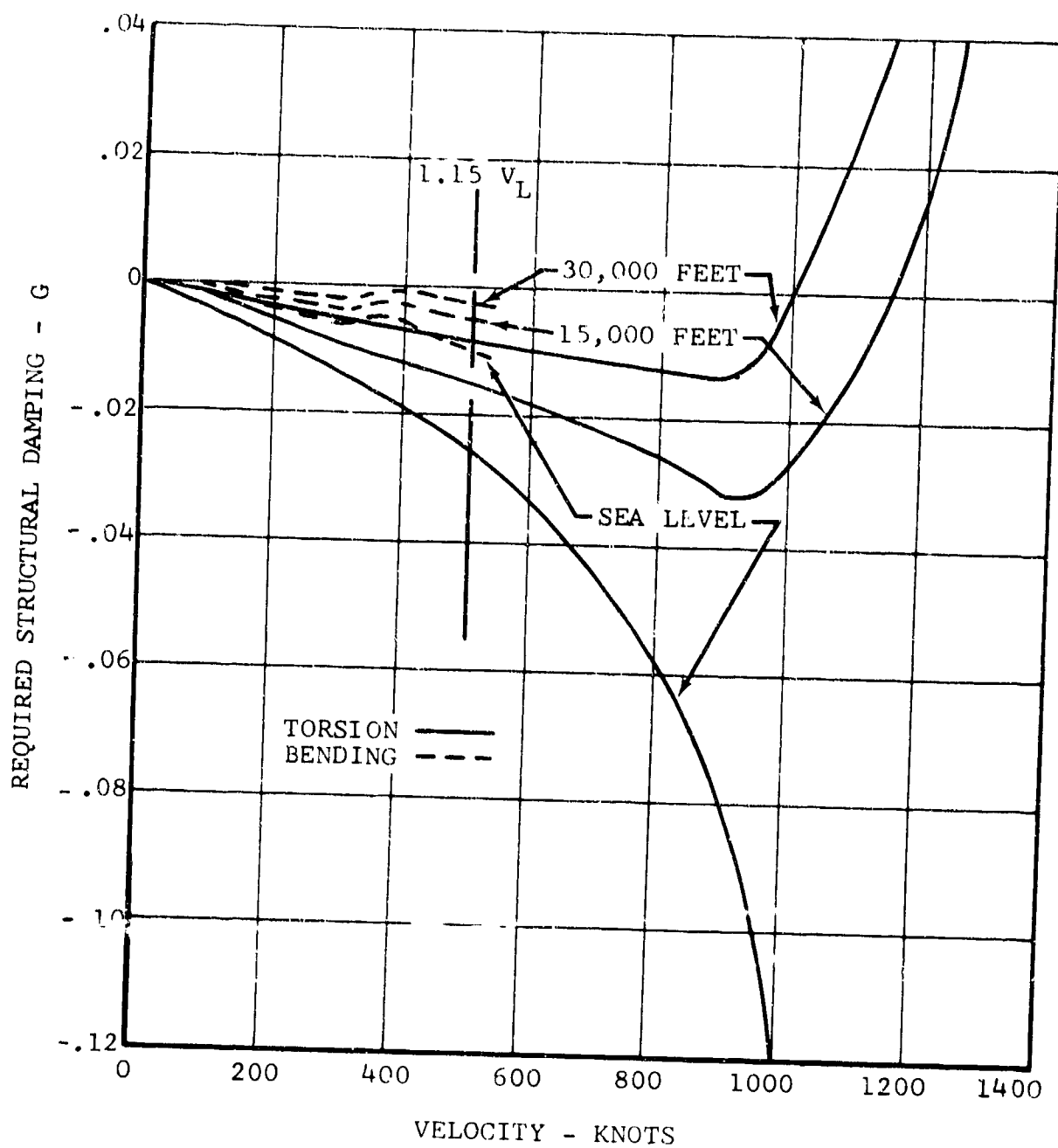


Figure 83. Wing Asymmetric Flutter,
One-Half Fuel.

- Rotor-Pylon Stability - This subject is covered in detail in References 7 and 12. The stability of the D266 final rotor-pylon configuration is discussed herein.
- Rotor Blade Motion Stability - This includes blade pitch-flap flutter and a special type of in-plane elastic motion instability. Pitch-flap flutter is precluded in the D266 by the very high blade torsional stiffness and by mass balancing (at 25-percent chord) and is not discussed further. The special type of in-plane elastic motion instability is discussed in this section.

a. Rotor-Pylon Stability

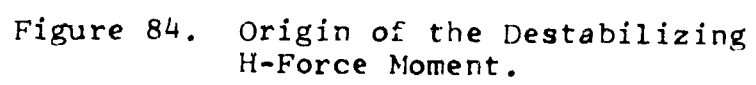
The D266 is free of rotor-pylon instabilities of the propeller-nacelle whirl flutter type throughout the operating regime. This fact has been confirmed both by an extensive analytical investigation and by scale-model wind-tunnel tests. A high level of damping is provided throughout the flight envelope by the rotor-pylon control features incorporated into the D266 design.

A comprehensive analytical study of rotor-pylon stability characteristics, published recently by Hall (Reference 13), shows that the principal destabilizing factor is the in-plane aerodynamic rotor force generated by blade flapping at high advance ratios. The basic mechanism can be understood from Figure 84, which shows that a rotor plane rotation ($\phi_x + a_1$) through the aerodynamic flapping forces ΔT_1 and ΔT_2 produces the in-plane forces ΔH_1 and ΔH_2 . Both H-forces create a moment about the pylon pivot point (P) in the same direction as the rotor plane rotational velocity ($\dot{\phi}_x + \dot{a}_1$). A simple expression for this destabilizing moment^x is given in Reference 13. The time-averaged H-force moment is

$$M_H = \frac{I_b V \cdot h}{\bar{R}^2} (\dot{a}_1 + \dot{\phi}_x) \text{ per blade.} \quad (1)$$

It can be seen that for a given blade inertia I_b and mean rotor radius \bar{R} , the destabilizing moment increases with speed V and mast length h . (The D266 rotor mast has been kept short by sweeping the wing slightly forward.)

A solution to this stability problem is found basically by making the term $(\dot{a}_1 + \dot{\phi}_x)$ negative. This is accomplished by controlling the rotor flapping (a_1) as a function of the pylon deflection (ϕ_x).



(1) Design Features

Based on these principles, the rotor control system was designed to incorporate a swashplate-pylon coupling linkage, such that rotor cyclic pitch inputs are introduced by pylon motion.

The swashplate-pylon coupling is used in conjunction with a soft pylon-pitch-isolation mount, so that the pitching moment about the conversion axis caused by the in-plane rotor force results in pylon-pitch motion relative to the wing. Figure 85 shows the principle of this swashplate coupling, which is phased in automatically with the mast angle. The swashplate-pylon coupling creates a swashplate-pitch input that is opposite in direction to the pylon motion and 1.8 times its angular magnitude. Because the pitching moment about the conversion axis caused by the rotor in-plane force also twists the wing, the actual swashplate motion, relative to the fuselage reference plane, is only 1.4 times the pylon motion. The cyclic pitch input to the rotor from the swashplate motion creates aerodynamic flapping moments and in-plane rotor forces that stabilize the rotor-pylon system.

Stability in yaw for pylon motions is achieved by mounting the pylon rigidly to the wingtip in the lateral direction. The wing provides a very high level of stiffness in this direction. The lateral system frequency is calculated to be 9.5 cps. This frequency is too high for the rotor to follow, with the result that $(\ddot{a}_1 + \phi_x)$ will be very small. Hence, no lateral instability will result.

The 1500-foot-pounds-per-degree hub spring is active only in pitch. It has been established that some damping is introduced into the rotor-pylon system by this hub spring.

The combination of soft pylon mounting in pitch, swashplate-pylon coupling about that axis, and stiff pylon mounting in yaw is optimized by the selection of the rotor plane angle to which the cyclic pitch inputs (from pylon coupling) are introduced. This is done mechanically by swashplate retardation. The swashplate retardation angle is shown in Figure 86. In selecting a value of retardation which will provide maximum damping to rotor and pylon modes, the effects of pitch-flap coupling, δ_3 , and the hub spring are included. The δ_3 angle used in the D266 rotor system is 30 degrees. The retardation angle is set at 25 degrees.

The mechanical simplicity of the swashplate-pylon coupling affords highly reliable rotor-pylon stability in the D266.

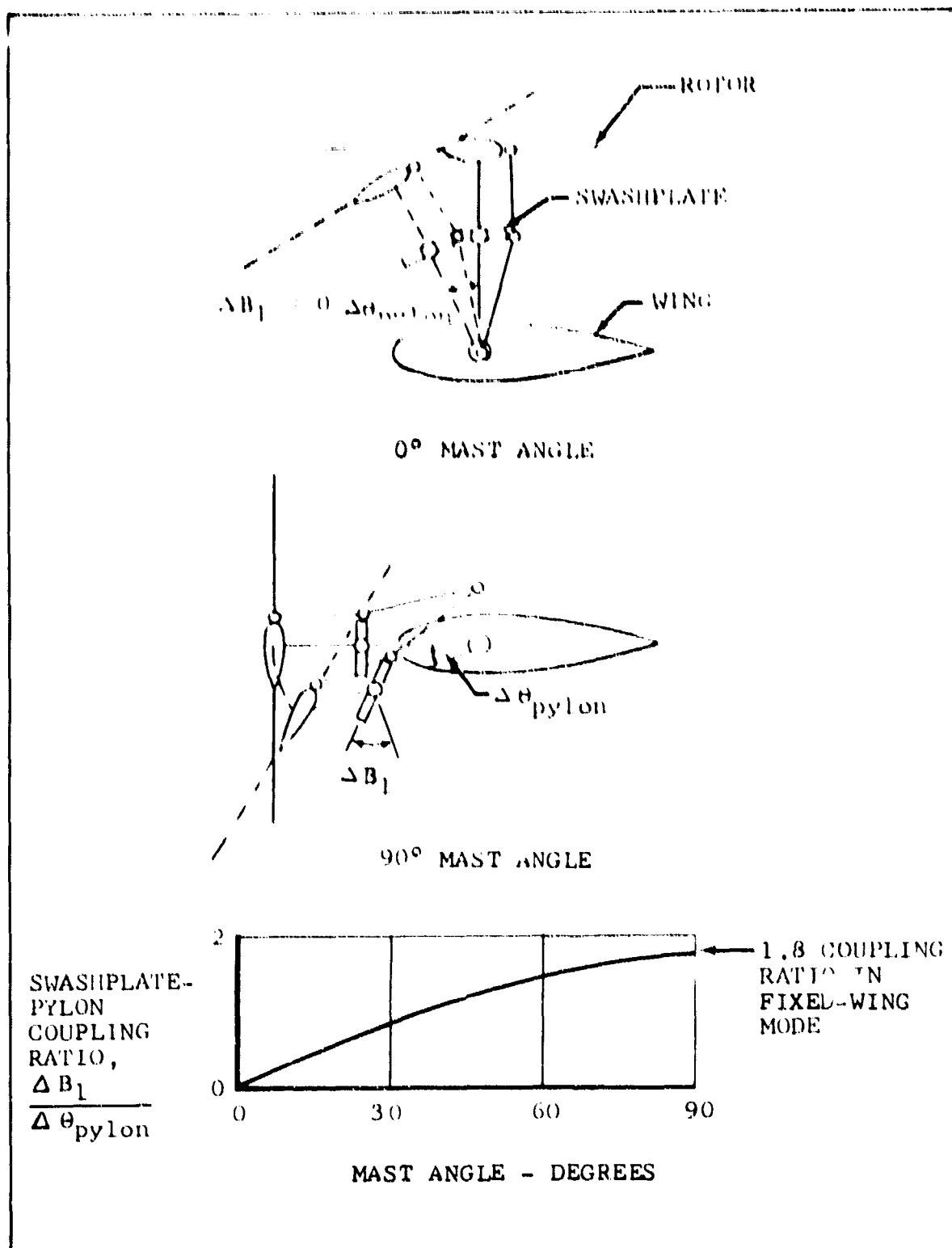


Figure 85. Swashplate-Pylon Coupling.

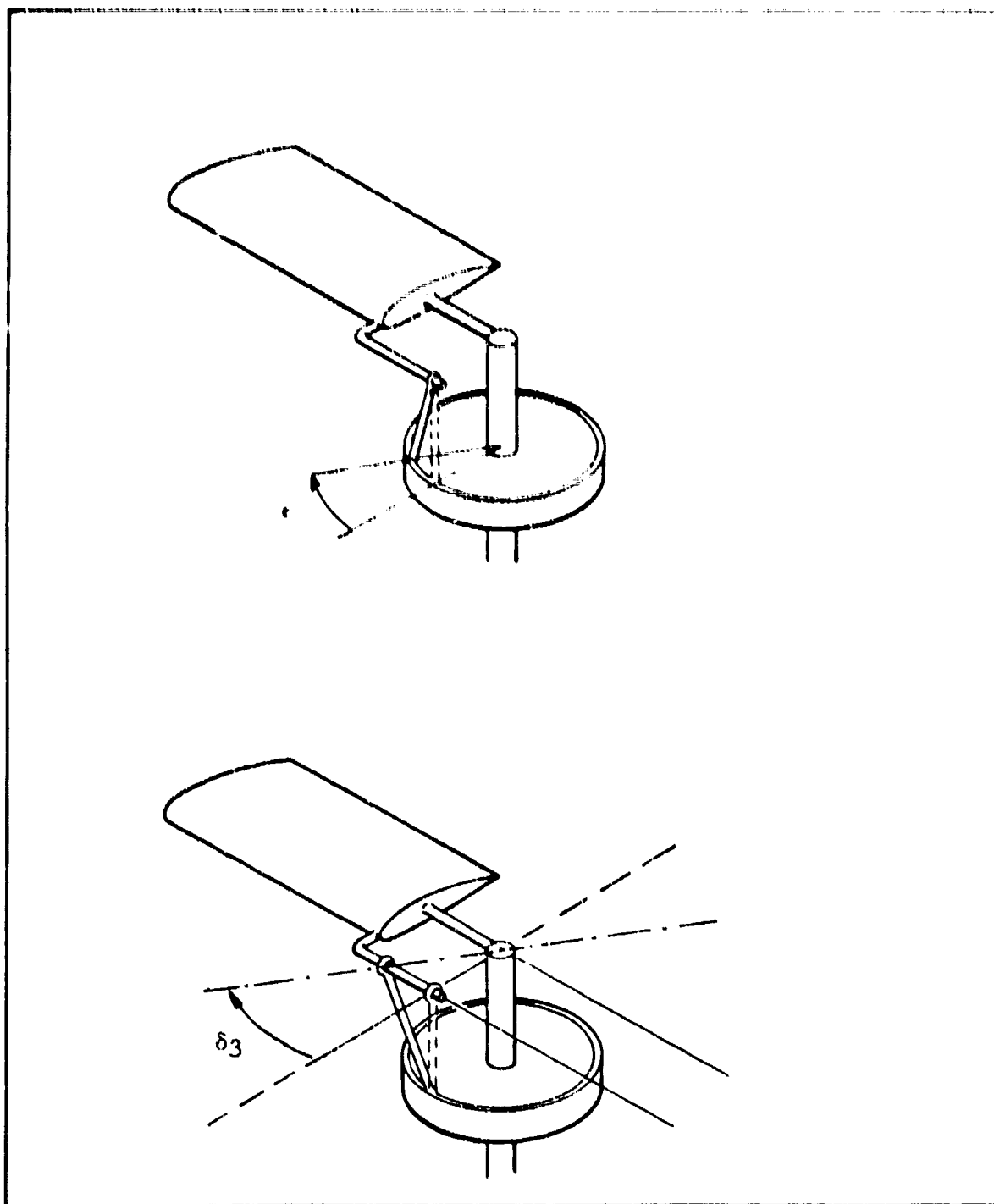


Figure 86. Illustration Of Swashplate Retardation And δ_3 .

(2) Methods of Analysis and Correlation with Test

Two methods of rotor stability analysis have been formulated to prescribe the cause and behavior of rotor-pylon instabilities:

- A step-by-step method (BHC Program S05) gives a digital solution to the blade-flapping and pylon motion equations.
- A closed-form method (BHC Program S03) uses a more simple linear analysis to indicate trends and to isolate the instability behavior.

Both methods use lumped parameter systems and include pylon-pitch, yaw, and wingbeam degrees of freedom. Program S05 is the more accurate method because of its nonlinear aerodynamic representation. It was used in the analysis of the final D266 rotor-pylon configuration. Both Programs S03 and S05 are developed in Reference 7.

Extensive wind-tunnel tests have been conducted to investigate rotor-pylon stability. These tests were conducted to isolate the important parameters, to evaluate several methods for providing stability, and to provide a basis for analytical correlation. They are summarized briefly below.

- A model of the XV-3 rotor-pylon system was tested and compared with the full-scale results from the Ames 40-by-80-foot tunnel. Good correlation was established.
- A scale model of the D266 rotor system was used to confirm the analytical results. Basic parameters such as swashplate-pylon coupling, swashplate retardation, pylon-pitch and yaw spring rate, rotor rpm, wing beam stiffness, flapping spring rate, and δ_3 were varied to determine their effect on rotor-pylon stability.

The model parameters and operating conditions were used as inputs to Program S05, and the rotor-pylon-mode natural frequency and damping were calculated. A comparison of the rotor-pylon-mode frequency and damping for a model run with that calculated with Program S05 is shown in Figures 87 and 88. The excellent correlation shows that Program S05 can predict the stability of the D266 rotor pylon. A description of the rotor-pylon model is given in Reference 1. Additional model computer program correlation plots are given in References 7 and 14. These reports show that the computer programs predict correctly all of the trends established in the model test program and that correlation with specific runs is quite accurate.

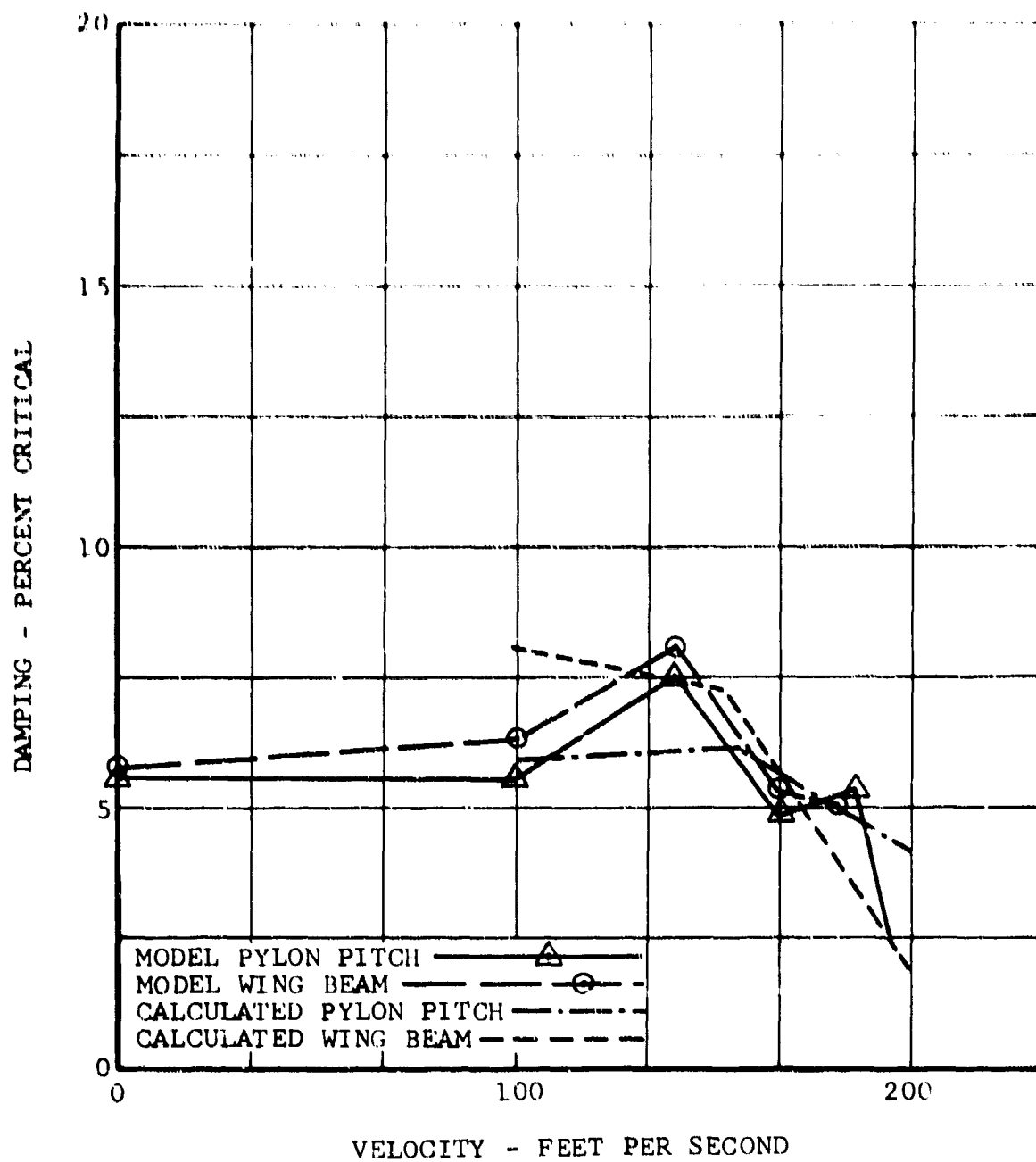


Figure 87. Model Correlation With Calculated Damping.

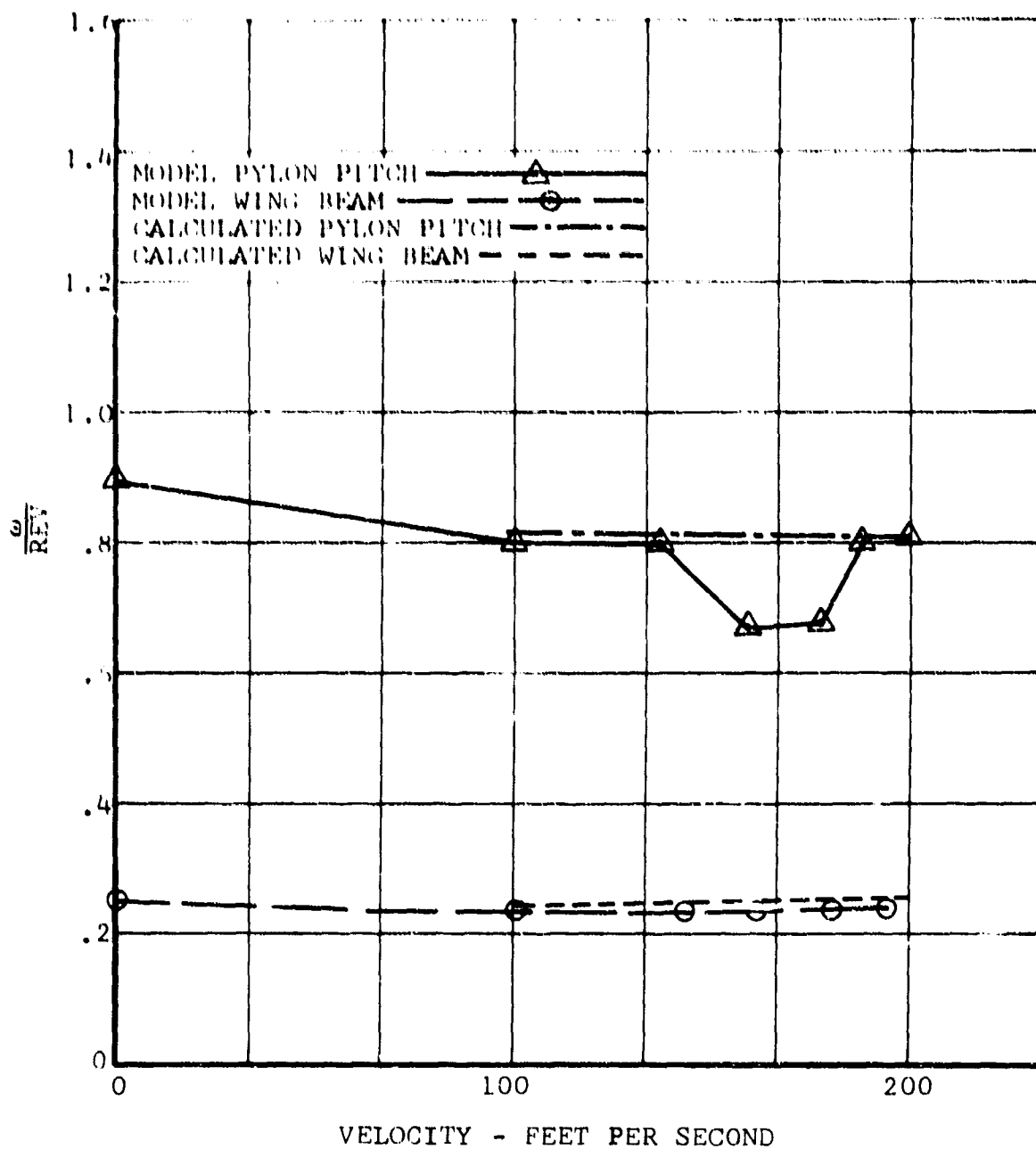


Figure 88. Model Correlation With Calculated Frequency.

(3) Stability Characteristics of the D266

The D266 rotor-pylon configuration's stability was calculated throughout the fixed-wing-mode operating range by computer Program S05. Plots of damping versus airspeed are shown in Figures 89 through 91 for altitudes of sea level, 15,000 feet, and 30,000 feet. (Note that the observed damping is shown and not the damping required, as is often presented in stability studies.)

The principal parameters used for the D266 in this study are:

Blade inertia	580 slug-ft ²
Blade lock number	5.8
Number of blades	3
Hub spring in pitch	1500 ft-lb/deg
Lateral hub spring	0
Pitch-flap coupling	30°
Swashplate retardation	25°
Swashplate coupling in pitch	1.8
Swashplate coupling in yaw	0
Pylon inertia	1921 slug-ft ²
Rotor weight	1150 lb
Pylon cg - conversion axis	4.61 ft
Rotor center - conversion axis	6.177 ft
Pylon spring rate in pitch	5×10^5 ft-lb/rad
Pylon spring rate in yaw	3.425×10^6 ft-lb/rad
Pylon damping	1.5% critical

The results for the D266 indicate that the rotor, controlled by the coupled swashplate, becomes increasingly stable with forward speed.

b. Rotor Blade Motion Stability

A specific type of rotor blade instability first suggested by Hohenemser in Reference 15 was investigated for the D266 rotor configuration. The instability involves the coupling between in-plane blade elastic bending and rigid blade flapping produced by out-of-plane static elastic deflections of the blade, together with control system flexibility. In Reference 15, it was suggested that this type of instability might be a characteristic of rotors without drag hinges. An analytical study was made and a model test program was conducted to investigate this instability. The results of both show that the D266 is stable.

Bell has test flown more than a dozen different multibladed, semirigid rotors. The first of these rotors was built and tested on the Model 47 helicopter in 1956-57. More recently,

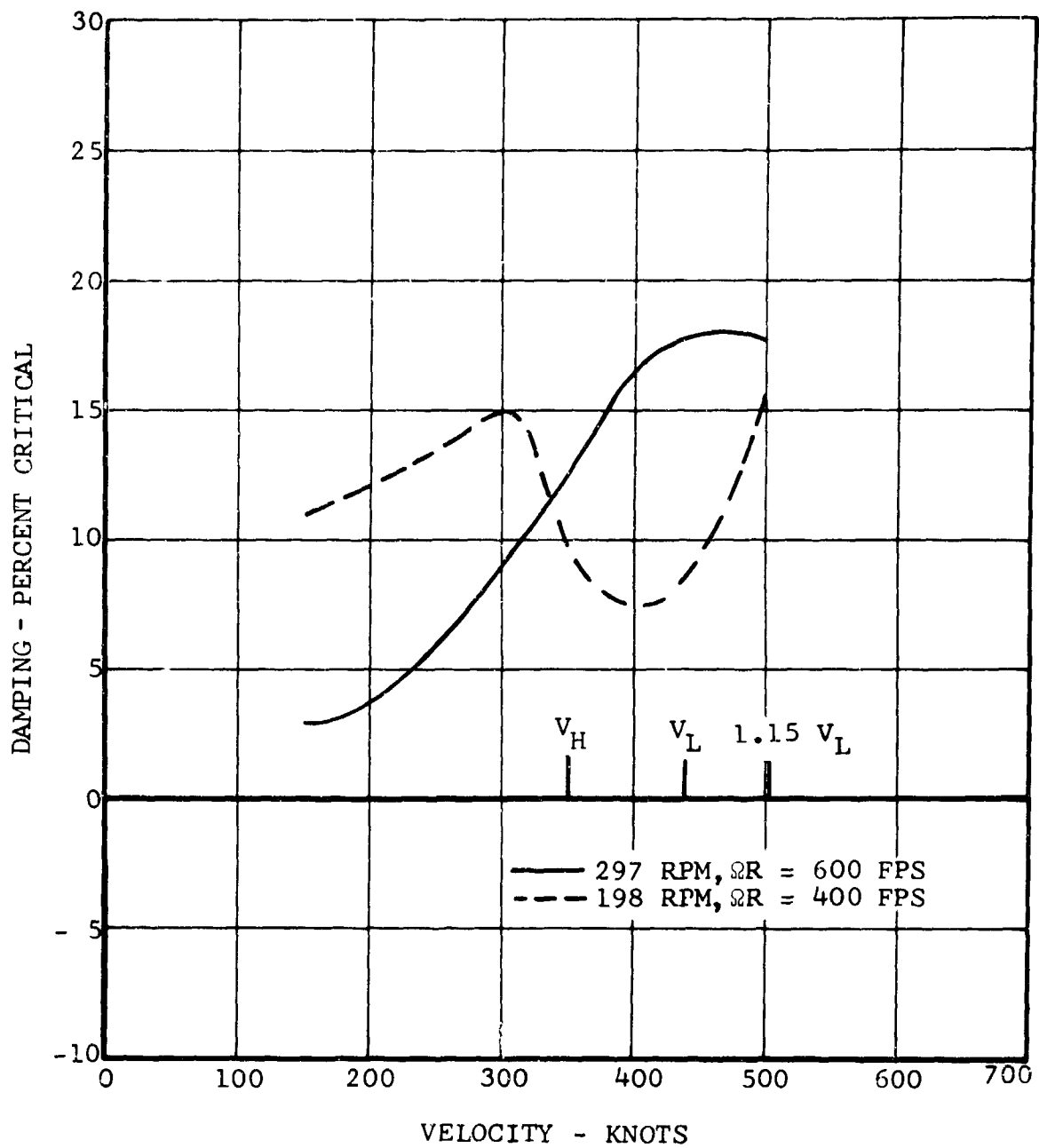


Figure 89. Rotor-Pylon Stability, Sea Level.

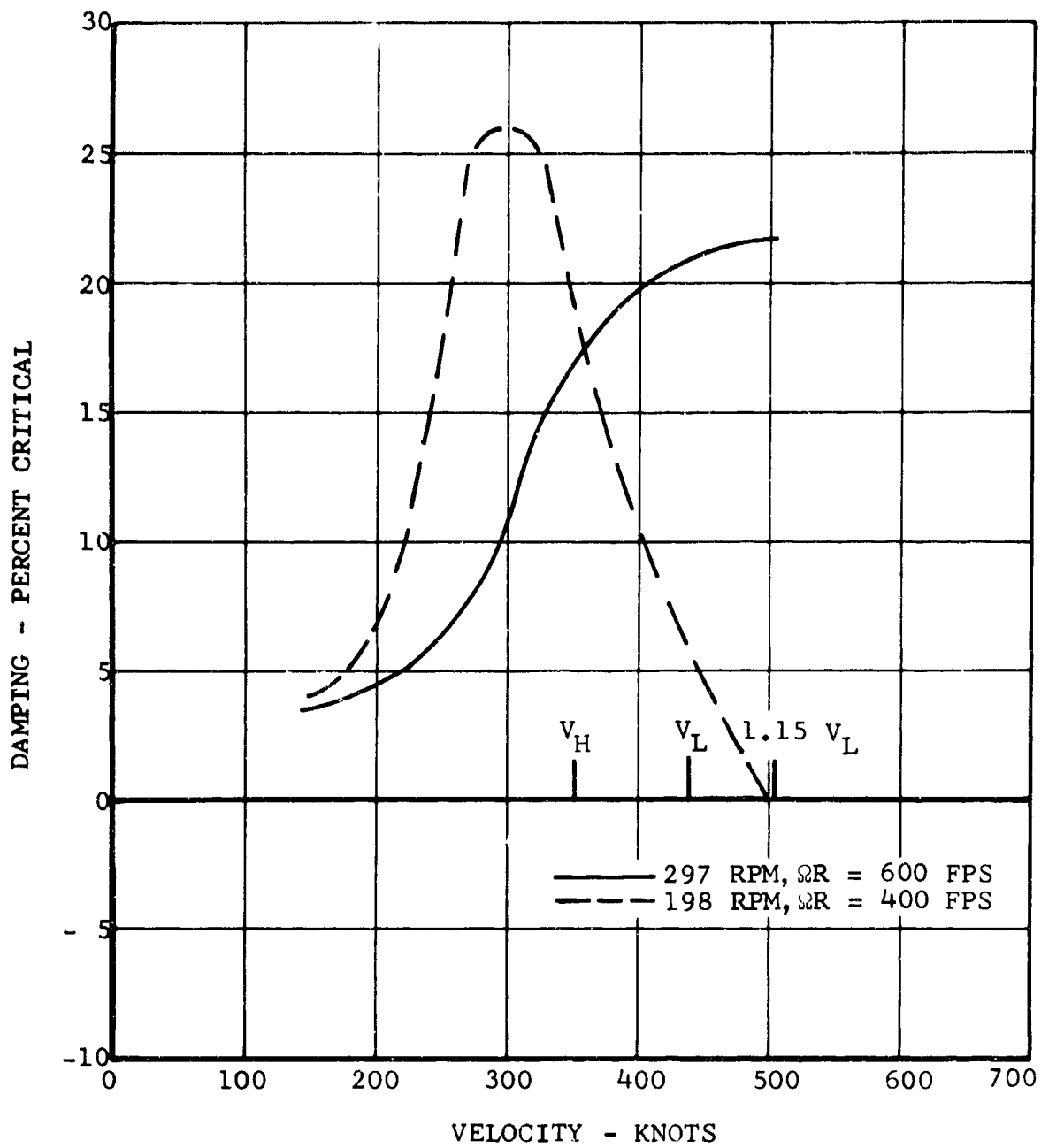


Figure 90. Rotor-Pylon Stability,
15,000 Feet.

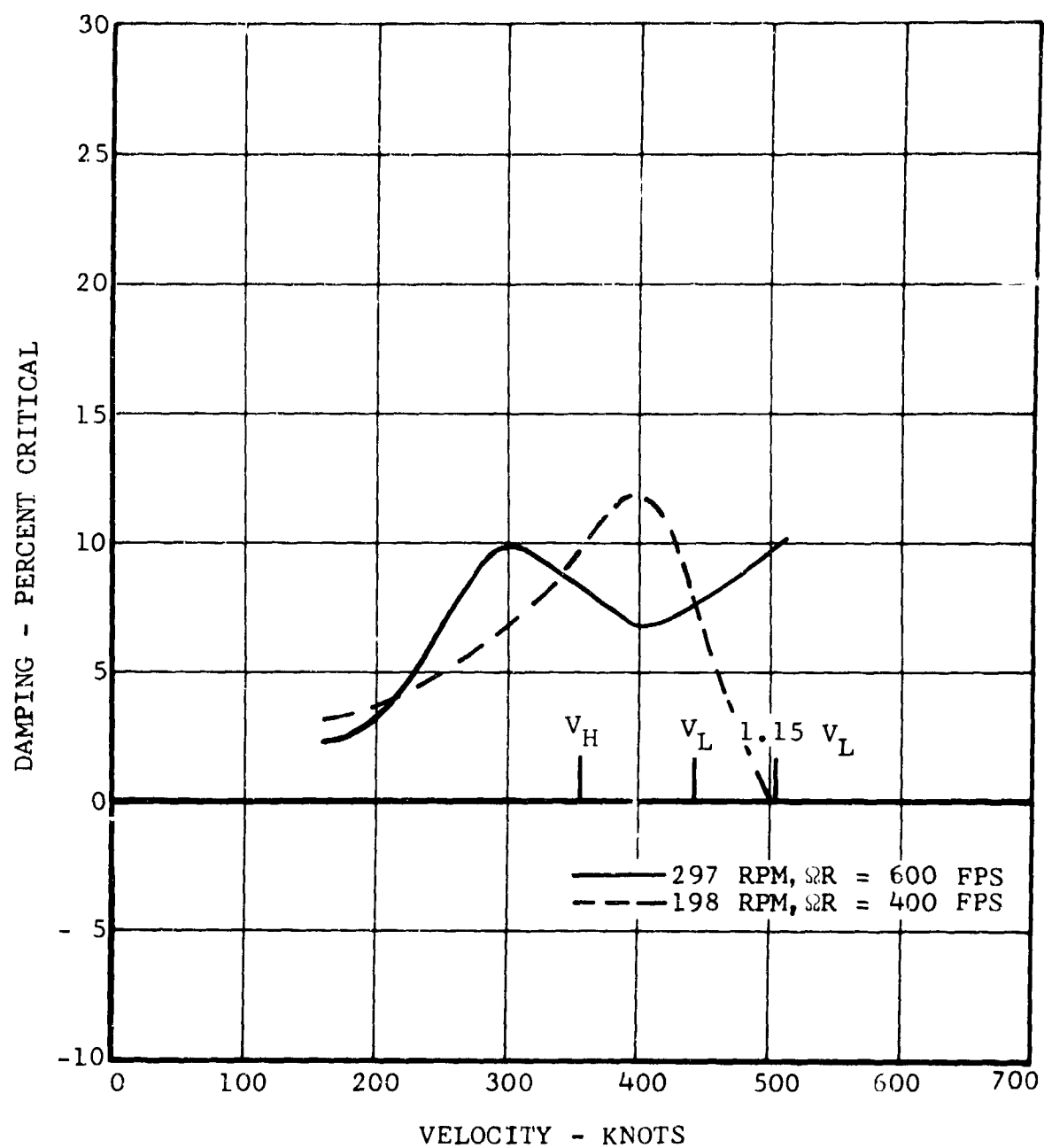


Figure 91. Rotor-Pylon Stability, 30,000 Feet.

in February 1965, a four-bladed system was flown on the Bell UH-1 high-performance test vehicle to a power-limit speed of 196 knots ($M_{ADV} = 0.935$).

In the development of these rotors, there are two prominent dynamic problems. The first is the difficulty of providing sufficient in-plane stiffness to place the first in-plane frequency higher than one per rev. A frequency of 1.25 per rev is satisfactory. The other problem is concerned with a three-per-rev resonance at the second beam bending mode of the blade.

The original three-bladed rotor tested on the XH-40 was the only multibladed rotor system to be troubled with instability problems. This rotor had very long, thin, heavy blades and was inadequately mass-balanced in an attempt to keep the first in-plane frequency above one per rev. Also, large trailing-edge doublers on the root of the blade produced a pitch-cone-coupling effect. Analytical work with the passive analog computer at Computer Engineering Associates was conducted simultaneously with the ground run program and is reported in Reference 16. When the original blades were replaced with stiffer, mass-balanced blades, the rotor proved to be quite satisfactory. This rotor had performance and vibration characteristics superior to the standard rotor of the XH-40 test vehicle, and it was flown to speeds above 120 knots and to altitudes above 18,000 feet. During maneuvers, more than 2g were obtained without difficulty.

The D266 rotor blades are very stiff, lightweight blades. The first in-plane frequency is well above one per rev (see Figure 71) and the second beam bending mode is clear of three-per-rev resonance (see Figure 70). Also, the blades are extremely stiff torsionally, and a stiff control system is provided with dual boost hydraulic cylinders mounted close to the swashplate.

(1) Analytical Work

The analysis of the D266 rotor blade motion stability is based on the two-degree-of-freedom analysis of Reference 17. This analysis has been shown to yield conservative results. The equations of motion presented in Reference 17 are based on small inflow angles; for the D266 analysis they were modified to include high inflow angles, pitch-flap coupling, a hub spring, and steady in-plane blade deflection.

Precone for a given elastic cone-up angle is destabilizing because the effect of the gyroscopic terms is increased. Figure 92 shows the relative effect of precone on the stability boundary calculated for a rotor slightly different from the D266. However, the net effect is stabilizing, since lower, and even down, elastic coning occurs as precone is increased.

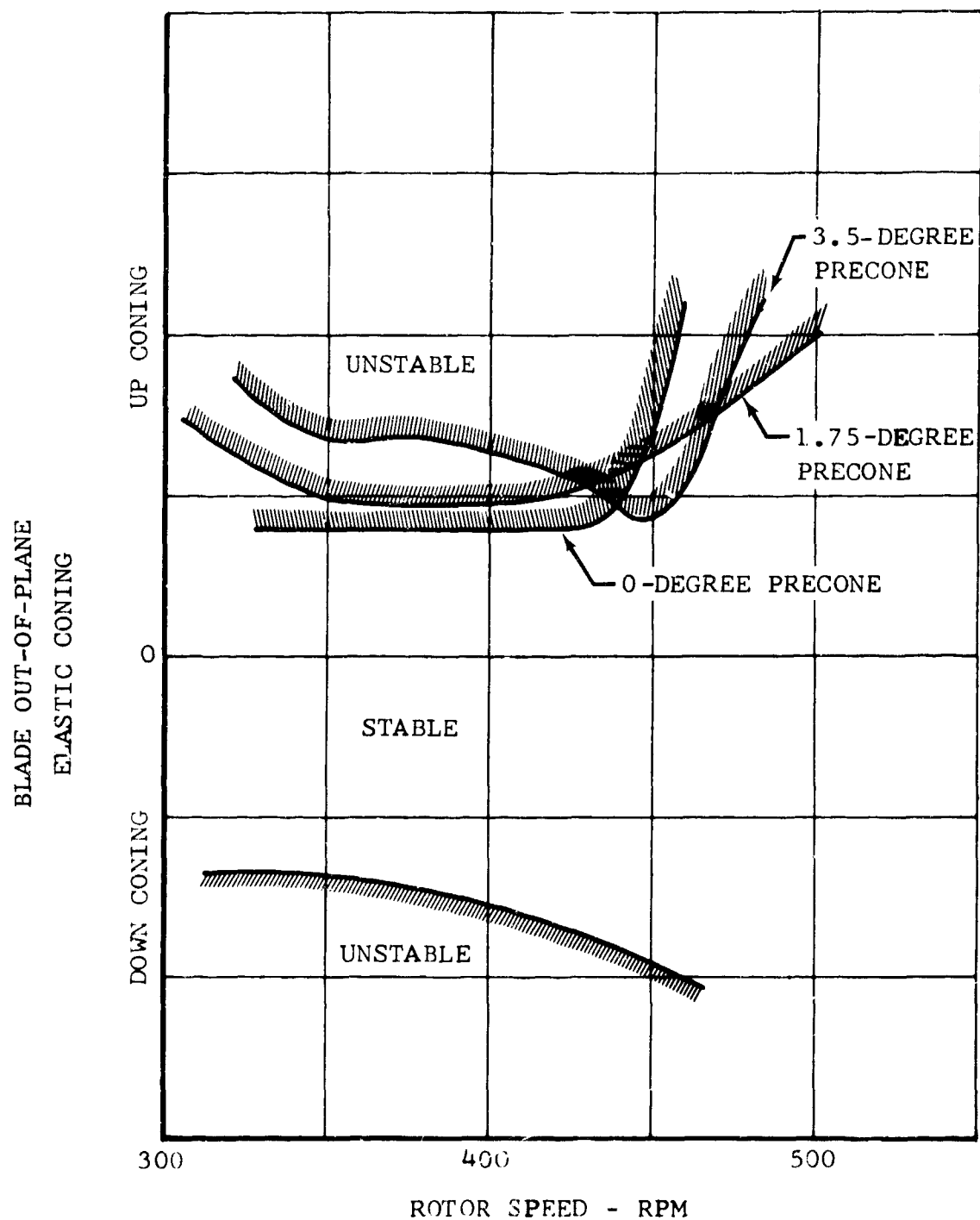


Figure 92. Relative Effect of Precone on Blade Motion Stability.

Pitch-cone coupling, δ_3 , has a slightly destabilizing effect. Thrust by itself is stabilizing, but the up-coning associated with thrust makes high thrust condition destabilizing.

(2) Model Work

The scale D266 rotor-pylon model that was used to study rotor-pylon instabilities was modified for these tests. A beamwise flexure was installed between the grip and the blade so that the scaled frequency of the first in-plane blade mode was obtained. The model was tested in hovering operation and the collective pitch was varied from minimum to maximum (blade stall), thus sweeping the minimum and maximum elastic coning. A zero-degree precone and a 2-1/2-degree hub were tested, and no instability was noted. At each collective pitch setting the mode was "plucked" by yawing it slightly, and the resulting blade motion was highly damped. The model was also tested with the pylon free in pitch. No unstable behavior was noted.

(3) D266 Blade Motion Stability

An adequate stability margin is assured since instability can occur only if the elastic cone-up is over 4 degrees. The maximum value of elastic coning calculated for the D266 is 1.8 degrees.

Even when the control system stiffness of the D266 is arbitrarily lowered to one-sixth of the calculated stiffness, the instability boundary is above the operating range. Figure 93 is a plot of the fixed-wing-mode elastic coning required for instability versus airspeed. Note that the actual coning is well below that required for instability.

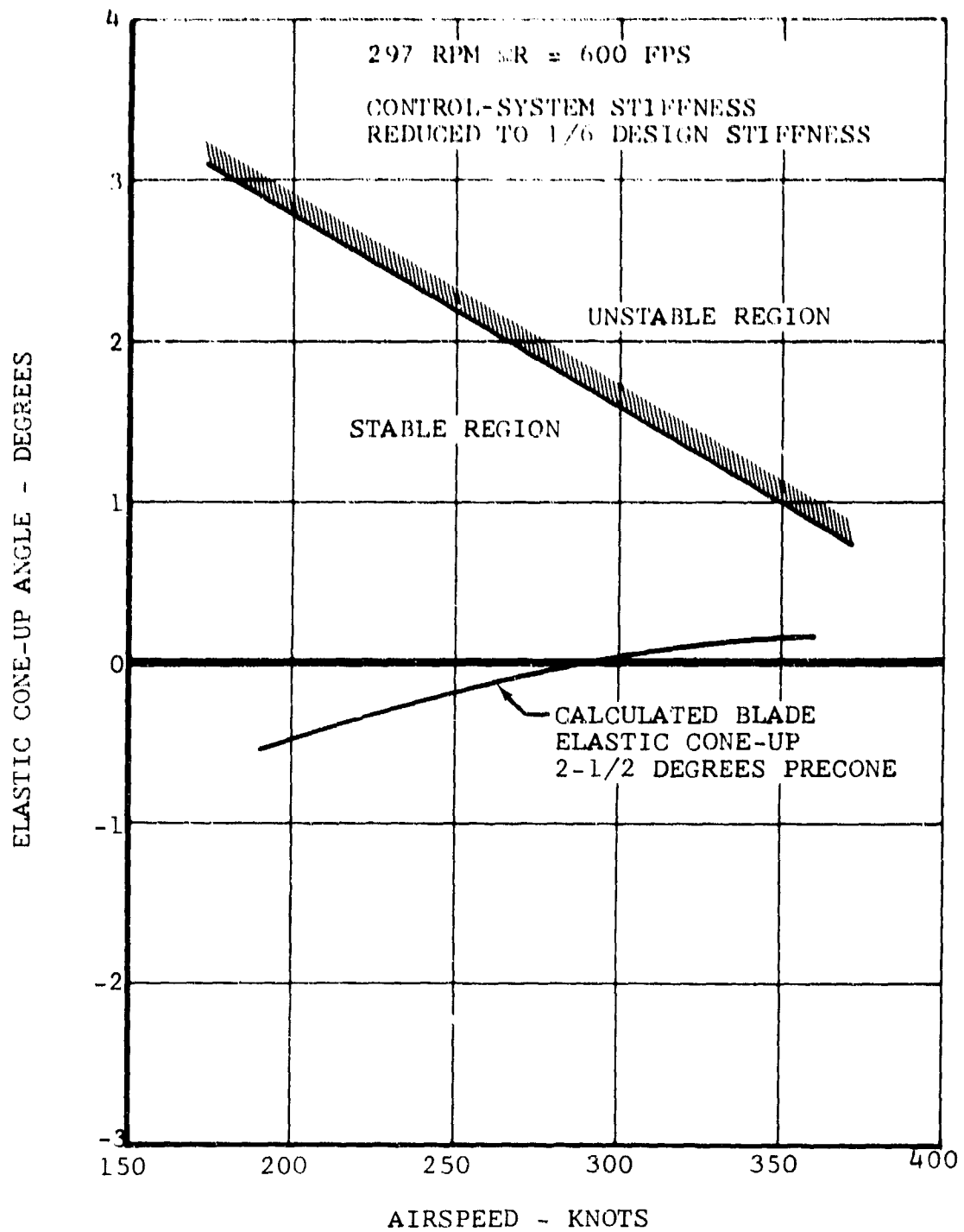


Figure 93. Blade Motion Stability,
Fixed-Wing Level Flight.

SECTION IV. WEIGHT AND BALANCE

A number of preliminary studies were conducted to determine minimum-weight configurations of the various components of the D266. The weight empty is 15,994 pounds. At the design gross weight of 23,000 pounds, the available useful load is 440 pounds greater than the 3000 pounds of fuel plus 3000 pounds of cargo specified.

Extensive studies to optimize the location of the wing with respect to the pylon conversion axis have resulted in full utilization of the maximum helicopter cg limits throughout the gross weight range up to design gross weight. Due to the decreasing cg shift, during transition at increasing gross weight, the helicopter's aft cg limits are varied above 23,000 pounds gross weight. The aircraft may be loaded, less fuel, to either the most forward or the most aft cg limit in the helicopter mode, and not exceed the fixed-wing-mode cg limits after conversion from helicopter to fixed-wing configuration. These limits are shown in Figure 94. The relatively large allowable cg range, in the helicopter configuration, is a direct result of the high-wing, tilting-pylon configuration, which places the rotor plane a maximum distance from the cargo area and the gross-weight vertical cg. Hub-restraint springs are incorporated in the rotor assemblies to provide maximum control power and cg range at high gross weights.

Specified weights for auxiliary powerplant (150 pounds), armor (300 pounds), avionics (900 pounds), and fixed equipment (1200 pounds) are included in the weight empty; however, preliminary estimates were made of the components and systems assumed to be included in the 1200-pound fixed-equipment weight, to verify that it would be adequate and to assist in balance calculations. Weights for these items were based on available, off-the-shelf equipment used in similar applications and comparable systems in existing aircraft. The results of this analysis show that, even though a weight penalty of approximately 120 pounds is included for the heavier weight of the ejection-type crew seats, as compared to standard crew seats, these items totaled only 1034 pounds. Thus, there are 166 pounds not allocated, which can be assumed to cover anti-icing and/or other unspecified equipment.

Weights of all major structural components (rotor, wing, fuselage, and tail surfaces) were estimated from layout drawings, utilizing materials and gages determined by a relatively detailed structural analysis. Allowances were added to the

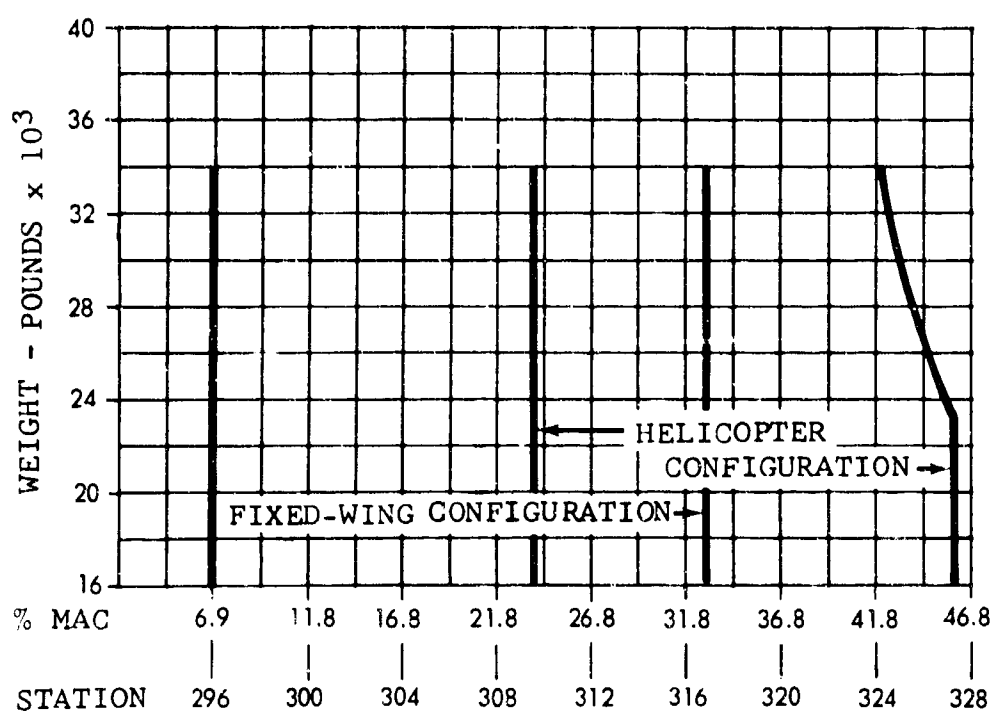


Figure 94. Center-of-Gravity Limits.

detailed estimates to account for miscellaneous joints, splices, and fasteners which are not shown on the drawings. The total weight thus derived was then verified by the use of generally accepted empirical estimating methods and by comparison of unit weights of existing proven designs.

The total calculated rotor assembly weight for the D266 is 2302 pounds, which correlates with the current average value of 10 percent of gross weight. Many features are incorporated into the D266 rotor design to achieve low optimum weight.

The total wing weight was checked by use of the wing estimating method given in Reference 18. This method considers the total wing weight to be a sum of wing basic weight, W_b , and wing secondary weight, W_s , with W_b being the wing weight caused by basic bending and shear effects due to airloads and inertia loads, both distributed and concentrated, and with W_s being the wing weight due to size and loadings of structure other than the main structural box, such as leading-edge and control surfaces, and the weight due to miscellaneous joints, hardware, access, etc.

Fuselage weights were estimated in the same manner as the other major structural components; skin, bulkhead, frame and stiffener gages, and axial member areas were based on the results of a relatively complete stress analysis, and dimensions were taken from detailed layout drawings. The estimating method of Reference 19 was used to verify the resultant total, with excellent correlation.

System weights, such as controls, engine sections, powerplant installation, etc., were estimated by detailed analysis of layout drawings, to determine component sizes, number of pivot points, cowling areas, and similar parameters. Typical unit weights were used to compute the total weight. Detailed layouts of the transmission components were the result of a rather complete design study and stress analysis of the transmission system; therefore, weights of these components were calculated from the drawings and were verified by the methods of Reference 20.

MIL-STD-491, PART 1 SUMMARY WEIGHT STATEMENT

01					
02					
03					
04					
05					
06					
07					
08					
09					
10					
11					
12					
13					
14					
15					
16	CONTRACT				
17					
18	ROTORCRAFT - GOVERNMENT NUMBER				
19					
20	ROTORCRAFT - CONTRACTOR NUMBER		0266		
21					
22	MANUFACTURED BY		BELL HELICOPTER COMPANY		
23					
24					
25					
26					
27					
28					
29	ENGINE				
30					
31	MANUFACTURED BY		GENERAL ELECTRIC		
32					
33	MODEL				
34					
35	NUMBER		T64-GE-12		
36					
37					
38					
39					
40					
41					
42					
43					
44					
45					
46					
47					
48					
49					
50					
51					
52					
53					
54					
55					
56					
57					

MIL-STD-491, PART 1

ROTORCRAFT
SUMMARY WEIGHT STATEMENT
WEIGHT EMPTY

01						
02	ROTOR GROUP					2439.0
03	BLADE ASSY				1272.0	
04	HUB				1090.0	
05	SPINNER				77.0	
06						
07						
08						
09						
10	WING GROUP					1886.0
11	BASIC STRUCTURE				1659.0	
12						
13						
14						
15	SECONDARY STRUCTURE				90.0	
16	AILERONS				68.0	
17	FLAPS				69.0	
18	-TRAILING EDGE			69.0		
19						
20						
21						
22						
23	TAIL GROUP					444.0
24						
25						
26						
27	STABILIZER - BASIC STRUCTURE				188.0	
28	FINS - BASIC STRUCTURE - INCL. DORSAL	0	LBS		173.0	
29	SECONDARY STRUCTURE - STABILIZER AND FINS					
30	ELEVATOR - INCL. BALANCE WEIGHT	0	LBS		47.0	
31	RUDDER				36.0	
32						
33	BODY GROUP					2048.0
34	FUSELAGE OR HULL - BASIC STRUCTURE				1602.0	
35						
36	SECONDARY STRUCTURE - FUSELAGE OR HULL				218.0	
37						
38	- DOORS, PANELS + MISC FUSELAGE				228.0	
39						
40						
41	LANDING GEAR - LAND TYPE					776.0
42	MAIN				609.0	
43	AUXILIARY				98.0	
44	CONTROLS				69.0	
45						
46						
47						
48						
49						
50						
51						
52						
53						
54						
55						
56						
57						

MIL-STD-451, PART 1

ROTORCRAFT
SUMMARY WEIGHT STATEMENT
WEIGHT EMPTY

01						
02	FLIGHT CONTROLS GROUP					865.0
03	COCKPIT CONTROLS				43.0	
04						
05	SYSTEM CONTROLS - ROTOR	NON-ROTATING			330.0	
06		ROTATING			302.0	
07		- FIXED WING			107.0	
08		- ELEVATOR			25.0	
09		- RUDDER			58.0	
10	ENGINE SECTION OR NACELLE GROUP					353.0
11	ENGINE MOUNT				28.0	
12	FIREWALL				35.0	
13	COWLING				290.0	
14						
15						
16	PROPULSION GROUP					4633.0
17						
18	ENGINE INSTALLATION				1412.0	
19	ENGINE (DRY WEIGHT)			1392.0		
20	RESIDUAL FLUIDS			10.0		
21	INSTALLATION HARDWARE			10.0		
22						
23						
24	CONVERSION SYSTEM				144.0	
25	AIR INDUCTION SYSTEM				24.0	
26	EXHAUST SYSTEM				41.0	
27	COOLING SYSTEM				28.0	
28	LUBRICATING SYSTEM				106.0	
29						
30						
31						
32						
33	FUEL SYSTEM				152.0	
34						
35						
36						
37						
38						
39	ENGINE CONTROLS				49.0	
40	STARTING SYSTEM				105.0	
41	ROTOR GOVERNOR CONT.				12.0	
42	DRIVE SYSTEM				2560.0	
43	GEAR BOXES			1897.0		
44	LUBE SYSTEM			97.0		
45	CLUTCH AND MISC					
46	TRANSMISSION DRIVE			294.0		
47	ROTOR MAST			272.0		
48						
49						
50						
51						
52	AUXILIARY POWER PLANT GROUP					190.0
53						
54						
55						
56						
57						

ROTORCRAFT SUMMARY WEIGHT STATEMENT WEIGHT EMPTY

01						
02						
03						
04	INSTRUMENT AND NAVIGATIONAL EQUIPMENT GROUP*					116.0
05	INSTRUMENTS				84.0	
06	NAVIGATIONAL EQUIPMENT				32.0	
07						
08						
09	HYDRAULIC AND PNEUMATIC GROUP*					144.0
10	HYDRAULIC				144.0	
11	PNEUMATIC					
12						
13						
14	ELECTRICAL GROUP*					307.0
15	A C SYSTEM					
16	D C SYSTEM				307.0	
17						
18						
19	ELECTRONICS GROUP					900.0
20	EQUIPMENT					
21	INSTALLATION				900.0	
22						
23						
24	ARMAMENT GROUP					
25	PASSIVE DEFENSE					300.0
26	FURNISHINGS AND EQUIPMENT GROUP*					533.0
27	ACCOMMODATIONS FOR PERSONNEL				189.0	
28	MISCELLANEOUS EQUIPMENT (INCL 0 LBS BALLAST)				86.0	
29	FURNISHINGS				30.0	
30	EMERGENCY EQUIPMENT				62.0	
31	WEIGHT ALLOWANCE FOR ANTI-ICING OR OTHER EQUIPMENT				166.0	
32						
33						
34	AIR CONDITIONING*					100.0
35	AIR CONDITIONING				100.0	
36						
37						
38						
39						
40						
41						
42						
43	AUXILIARY GEAR GROUP					
44	AIRCRAFT HANDLING GEAR					
45	LOAD HANDLING GEAR					
46	ATO GEAR					
47						
48						
49						
50						
51						
52						
53						
54						
55						
56						
57	TOTAL - WEIGHT EMPTY - PAGES 2, 3, AND 4					15994.0

* INCLUDED IN 1200 POUND FIXED EQUIPMENT WEIGHT

MIL-STD-451, PART 1

ROTORCRAFT
SUMMARY WEIGHT STATEMENT
USEFUL LOAD GROSS WEIGHT

01		BASIC	ALTER-	FERRY			
02		DESIGN	NATE	MISSION			
03		MISSION	MISSION				
04							
05							
06	CREW (2)	400.0	400.0	400.0			
07							
08							
09							
10							
11							
12	CARGO	3000.0	10800.0				
13							
14							
15	FUEL (462 GAL)	3000.0	3000.0	3000.0			
16	FUEL-TRAPPED	20.0	20.0	20.0			
17	FUEL-AUXILIARY (3072 GAL)			19965.0			
18	OIL-ENGINE	45.0	45.0	45.0			
19	OIL-ENG.-TRAPPED	10.0	10.0	10.0			
20							
21	OIL-XMSN.	68.0	68.0	68.0			
22	OIL-ENG. GEAR BOX	23.0	23.0	23.0			
23							
24							
25							
26							
27							
28							
29							
30							
31							
32							
33							
34	AUX FUEL TANK KIT			1535.0			
35							
36							
37							
38							
39	GROWTH POTENTIAL	440.0	440.0	440.0			
40							
41							
42							
43							
44							
45							
46							
47							
48							
49							
50							
51							
52							
53	USEFUL LOAD	7006.0	14806.0	25506.0			
54							
55	WEIGHT EMPTY (PAGE 4)	15994.0	15994.0	15994.0			
56							
57	GROSS WEIGHT	23000.0	30800.0	41500.0			

ROTORCRAFT
SUMMARY WEIGHT STATEMENT
DIMENSIONAL STRUCTURAL DATA

01 LENGTH-OVERALL		HELI 95.8 FT			
02 GENERAL DATA			FUS.		
03 LENGTH - MAXIMUM FEET			52.5		
04 DEPTH - MAXIMUM FEET			8.3		
05 WIDTH - MAXIMUM FEET			7.0		
06 WETTED AREA TOTAL - SQ. FT.			1040.0		
07 WETTED AREA GLASS - SQ. FT.			32.3		
08 WING, TAIL + FLOOR DATA		WING	H. TAIL	V. TAIL	FLOOR
09 GROSS AREA - SQ. FT.		330.5	90.0	100.0	118.1
10 WEIGHT/GROSS AREA - LBS./SQ. FT.		5.7	2.6	2.1	1.4
11 SPAN - FEET		49.6	20.1	13.15	
12					
13 THEORETICAL ROOT CHORD - INCHES		87.5	66.1	121.4	
14 MAXIMUM THICKNESS - INCHES		20.1	7.9	18.2	
15					
16					
17 THEORETICAL TIP CHORD - INCHES		72.5	41.4	60.7	
18 MAXIMUM THICKNESS - INCHES		13.7	5.0	5.5	
19					
20 TAIL LENGTH 25 PERCENT MAC WING TO 25 PERCENT MAC H TAIL				27.0 FEET	
21 AREA - SQ. FT.		FLAPS 27.5	AILERONS 27.6		
22					
23 ROTOR DATA - TYPE	SEMI-RIGID				
24	MAIN ROTOR				
25 FROM CL ROTATION - INCHES	ROOT 12.7	TIP 231			
26 CHORD - INCHES	20.0	20.0			
27 THICKNESS - INCHES	6.0	1.2			
28					
29 BLADE RADIUS - FEET			19.25		
30 NUMBER BLADES			6		
31 BLADE AREA - TOTAL - OUTBOARD - SQ. FT.			192.0		
32 DISC AREA - TOTAL SWEEP - SQ. FT.			2328.0		
33 TIP SPEED AT DESIGN LIMIT - HELI - FT/SEC			825.0		
34 TIP SPEED AT DESIGN LIMIT - HIGH SPEED - FT/SEC			600.0		
35 LOCATION FROM HORIZONTAL REF DATUM - INCHES			320.0		
36 DISC LOADING - DESIGN GROSS WEIGHT - LBS/SQ. FT.			9.88		
37					
38 POWER TRANSMISSION DATA			HP	RPM	GEAR**
39 MAX POWER - TAKE-OFF			3435	16,600	40.613/1
40 ALIGHT GEAR TYPE TRICYCLE			MAIN-AFT	AUX-FWD	
41 GEAR LENGTH-OLEO EXTND CL AXLE TO CL TRUNNION-INCHES			18.2	27.8	
42 OLEO TRAVEL-FULL EXTND TO COMPRESSED-INCHES			9.0	9.0	
43 WHEEL SIZE AND NUMBER REQUIRED			4-8.50X10	2-7.00X6	
44 FUEL AND OIL SYSTEM	LOCATION	NO.	***GALS	NO.	***GALS
45	TANKS	UNPRCTD	TANKS	PROTECTD	
46 FUEL - BUILT IN	WING	6	3000		
47 FUEL - EXTERNAL					
48 LUBRICATING SYSTEM		2	6		
49					
50 STRUCTURAL DATA - CONDITION		FUEL IN	DESIGN	STRESS	
51		WINGS-LBS	GROSS WT	GROSS WT	ULT LP
52 FLIGHT		3,000	23,000	23,000	6.75
53 LANDING		3,000	23,000	23,000	2.07
54 PERCENT DESIGN LOAD	WING(HIGH SPEED) 100	ROTOR (HELI) 100			
55					
56 TYPE OF POWER TRANSMISSION - GEARED					
57					

* PARALLEL TO CL AT CL ROTORCRAFT ** GEAR RATIO-ENG TO ROTOR
*** TOTAL USEABLE CAPACITY

SECTION V. PERFORMANCE DATA

A. SUMMARY

D266 performance in helicopter and fixed-wing modes is summarized in Tables XXVI and XXVII.

The performance requirements of Contract DA 44-177-AMC-373(T) and the applicable D266 performance are listed below:

<u>REQUIREMENT</u>	<u>D266 PERFORMANCE</u>
1. Hover OGE at 6000 feet (95°F day, 3000 pounds of fuel, 2450 pounds of additional required items)	1. Hovers OGE at 11,050 feet (95°F day at design gross weight of 23,000 pounds. All payload, fuel, and other weight requirements included.) Or: hovers at 6000 feet with 8100 pounds of payload.
2. Disc loading 10 lb/ft ²	2. Disc loading = 9.88 lb/ft ² (Design gross weight = 23,000 pounds)
3. Constant-altitude transition	3. Constant-altitude transition, over a broad speed range, or during high-power climb, or power-off descent.
4. Maximum speed = 300 knots at military rated power sea level, standard day	4. Maximum speed is 345 knots at 23,000 pounds gross weight, sea level; at 12,000 feet, 385 knots
5. Overall L/D 10	5. In fixed-wing mode, L/D is 10.1 (at sea level, 155 knots); at 25,000 feet, 240 knots, L/D = 11.1.

B. LIFT AND DRAG

1. ROTORS

Plots of rotor-blade-section lift and drag are shown in Figures 95 through 100. Figures 95 and 96 show the data for a 26-percent-thick section that are used for outboard blade from 7 percent to 20 percent of blade radius.

TABLE XXVI PERFORMANCE SUMMARY - HELICOPTER MODE				
	Units	Design	Alternate Gross Weight	STOL/Ferry
Takeoff Gross Weight	lb	23,000	30,800	41,500
Fuel Weight	lb	3,000	3,000	22,965
Payload	lb	3,000	10,800	-
Hovering Ceiling, OGE				
Standard Day	ft	17,200	8,200	-
95°F Day	ft	11,050	3,600	-
Maximum Speed*				
Two Engines, Standard Day				
Sea Level	kt	180**	180**	170**
10,000 Feet	kt	180**	175**	142
One Engine, Standard Day				
Sea Level	kt	150	147	133
10,000 Feet	kt	143	142	83
Rate of Climb, Maximum Power				
Two Engines, Standard Day				
Sea Level	ft/min	6,160	4,250	2,630
One Engine, Standard Day				
Sea Level	ft/min	2,240	1,320	420
Range, Standard Day***				
Sea Level	nm	193	190	-
Average Cruise Speed, Standard Day				
Sea Level	kt	135	135	-

* Maximum speed is determined by military rated power, transmission design torque, or structural design limits.

** Mast angle = 20 degrees.

*** Range-free allowance is 2 minutes at normal rated power for warmup and takeoff. Fuel flow is 5-percent conservative.

TABLE XXVII PERFORMANCE SUMMARY - FIXED-WING MODE				
	Units	Design	Alternate Gross Weight	STOL/Ferry
Takeoff Gross Weight	lb	23,000	30,800	41,500
Fuel Weight	lb	3,000	3,000	22,965
Payload	lb	3,000	10,800	-
Maximum Speed*				
Two Engines, Standard Day				
Sea Level	kt	345	341	334
10,000 Feet	kt	383	378	369
One Engine, Standard Day				
Sea Level	kt	259	250	228
10,000 Feet	kt	288	270	231
Rate of Climb, Maximum Power				
Two Engines, Standard Day				
Sea Level	ft/min	6,800	4,600	2,900
One Engine, Standard Day				
Sea Level	ft/min	2,600	1,430	490
Range, Standard Day				
Sea Level**	nm	431	394	-
10,000 Feet**	nm	535	463	-
25,000 Feet**,***	nm	-	-	4,275
Average Cruise Speed, Standard Day				
Sea Level	kt	202	216	-
10,000 Feet	kt	235	253	-
25,000 Feet	kt	-	-	292

*Maximum speed is determined by military rated power, transmission design torque, or structural design limits.

**Range-free allowances include 5 minutes at normal rated power for warmup, takeoff, and conversion. Fuel flow is 5-percent conservative.

***10 percent of actual fuel as reserve.

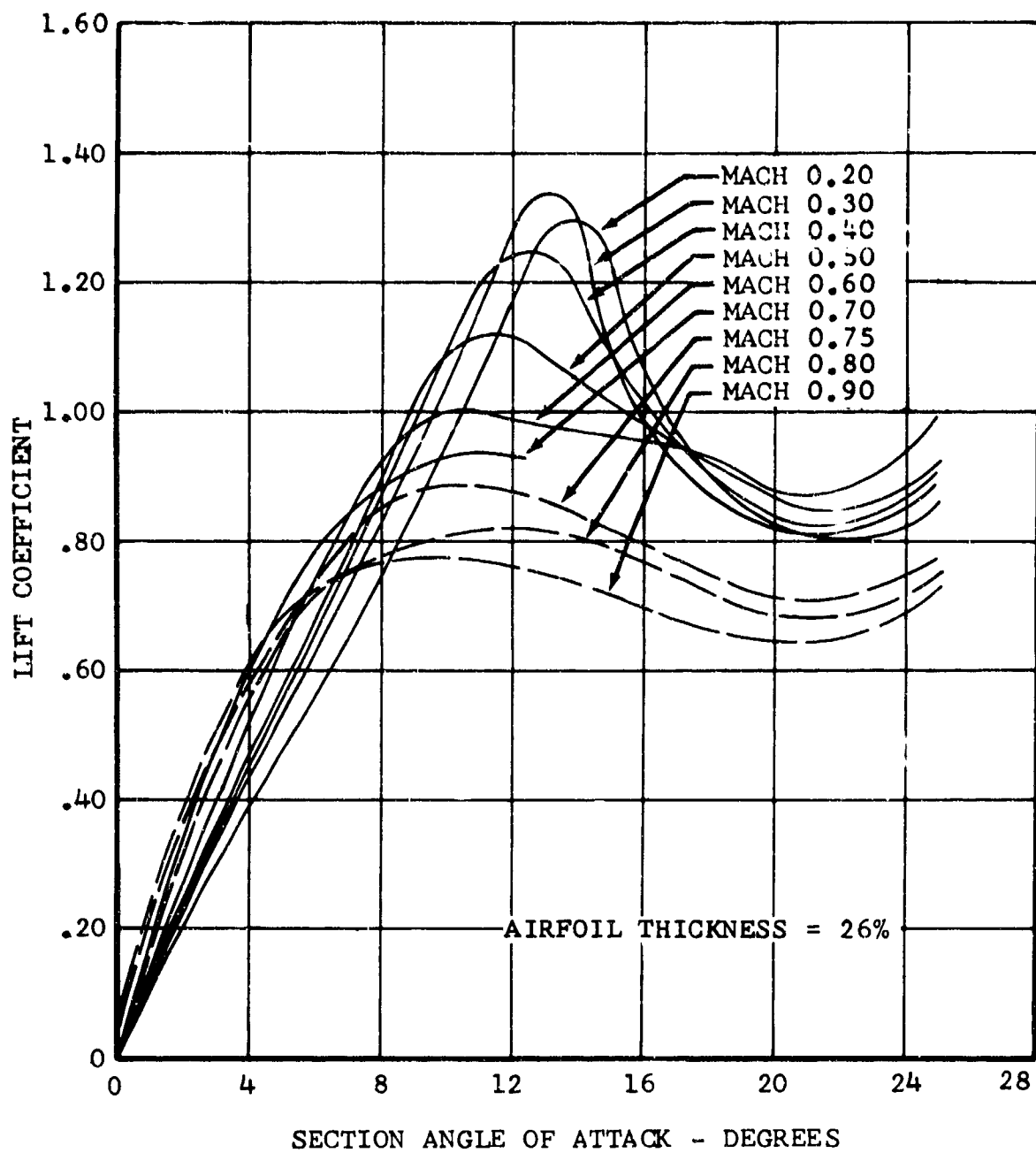


Figure 95. Synthesized Rotor Airfoil Lift Data, 7% to 20% Radius.

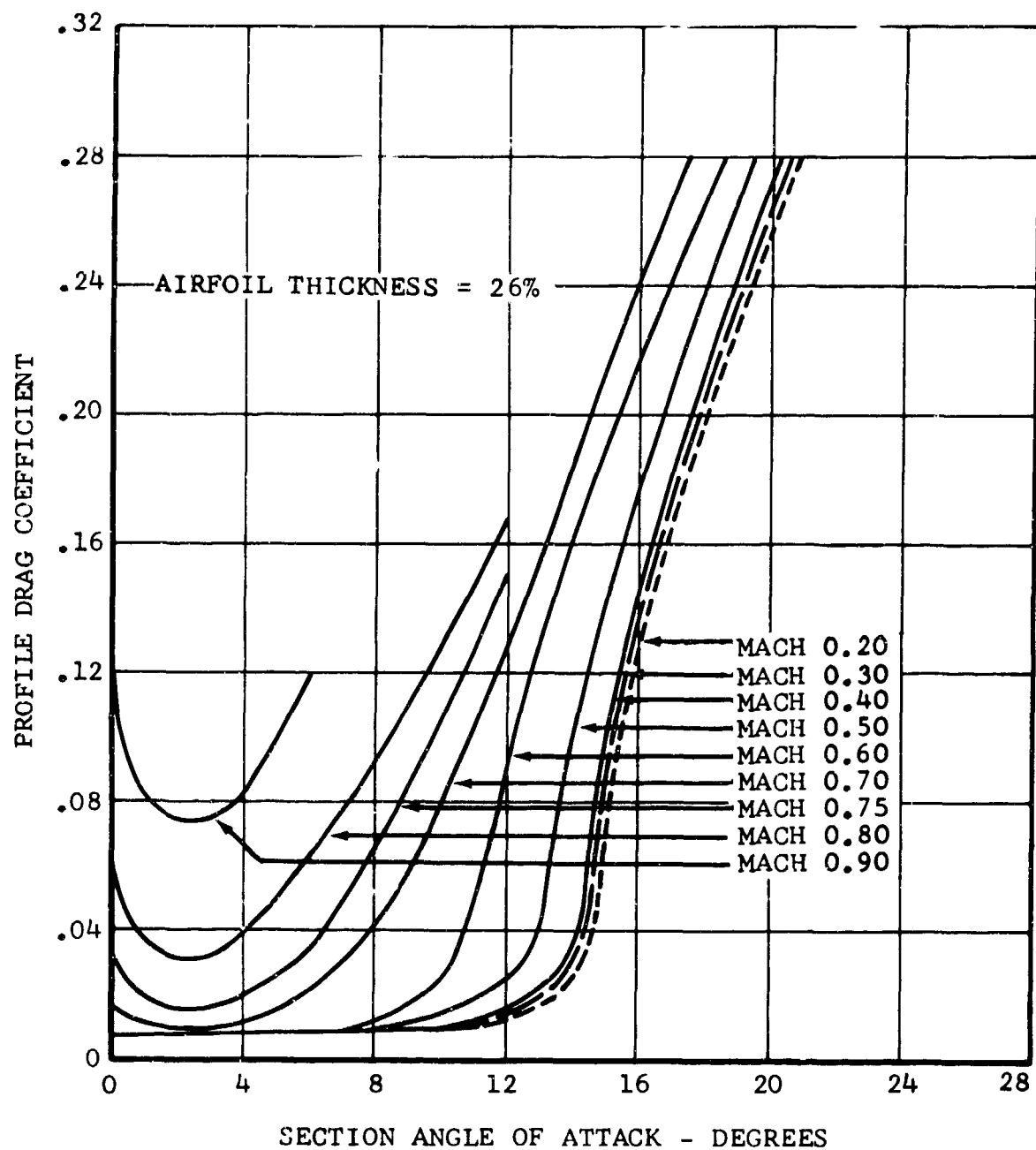


Figure 96. Synthesized Rotor Airfoil Drag Data, 7% to 20% Radius.

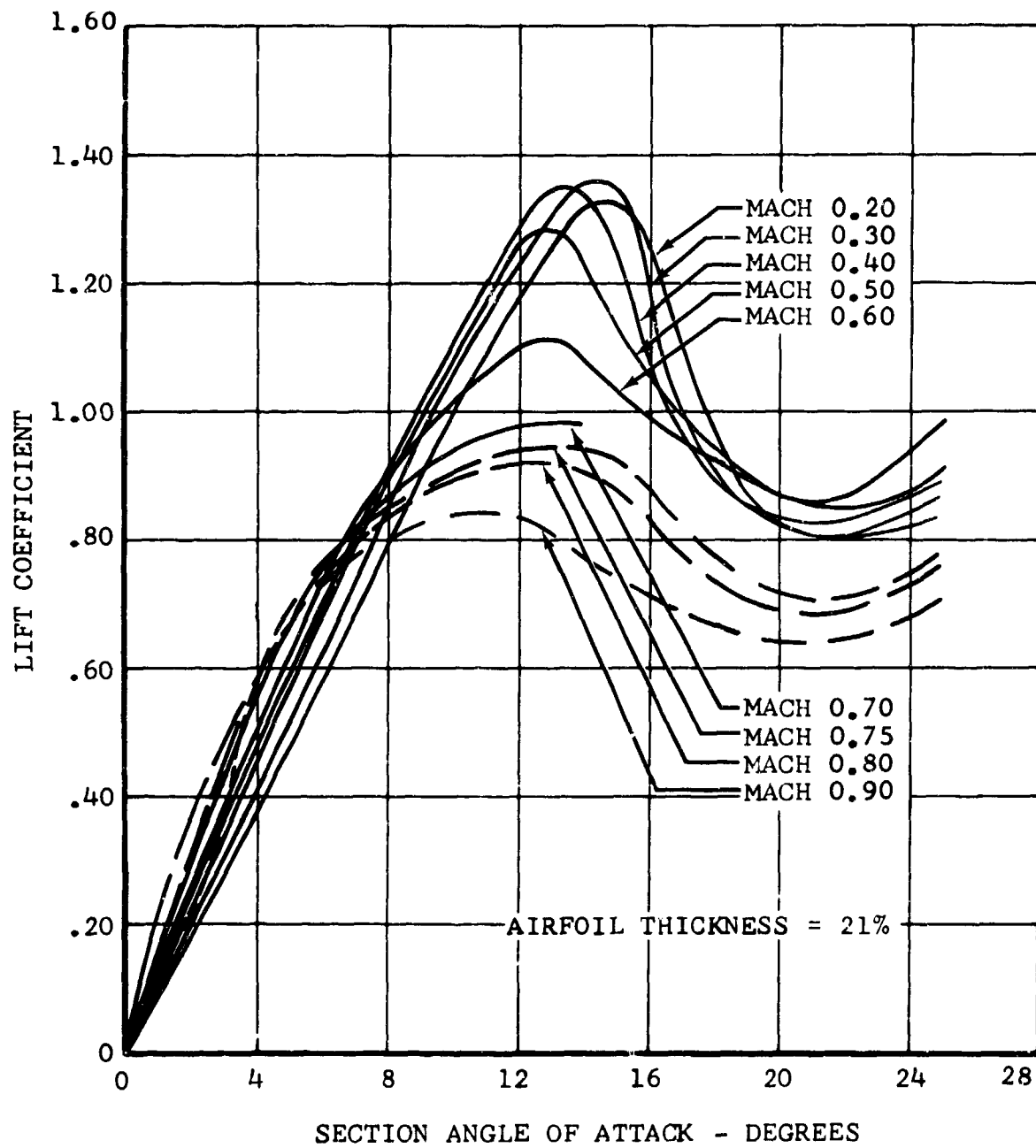


Figure 97. Synthesized Rotor Airfoil Lift Data, 20% to 50% Radius.

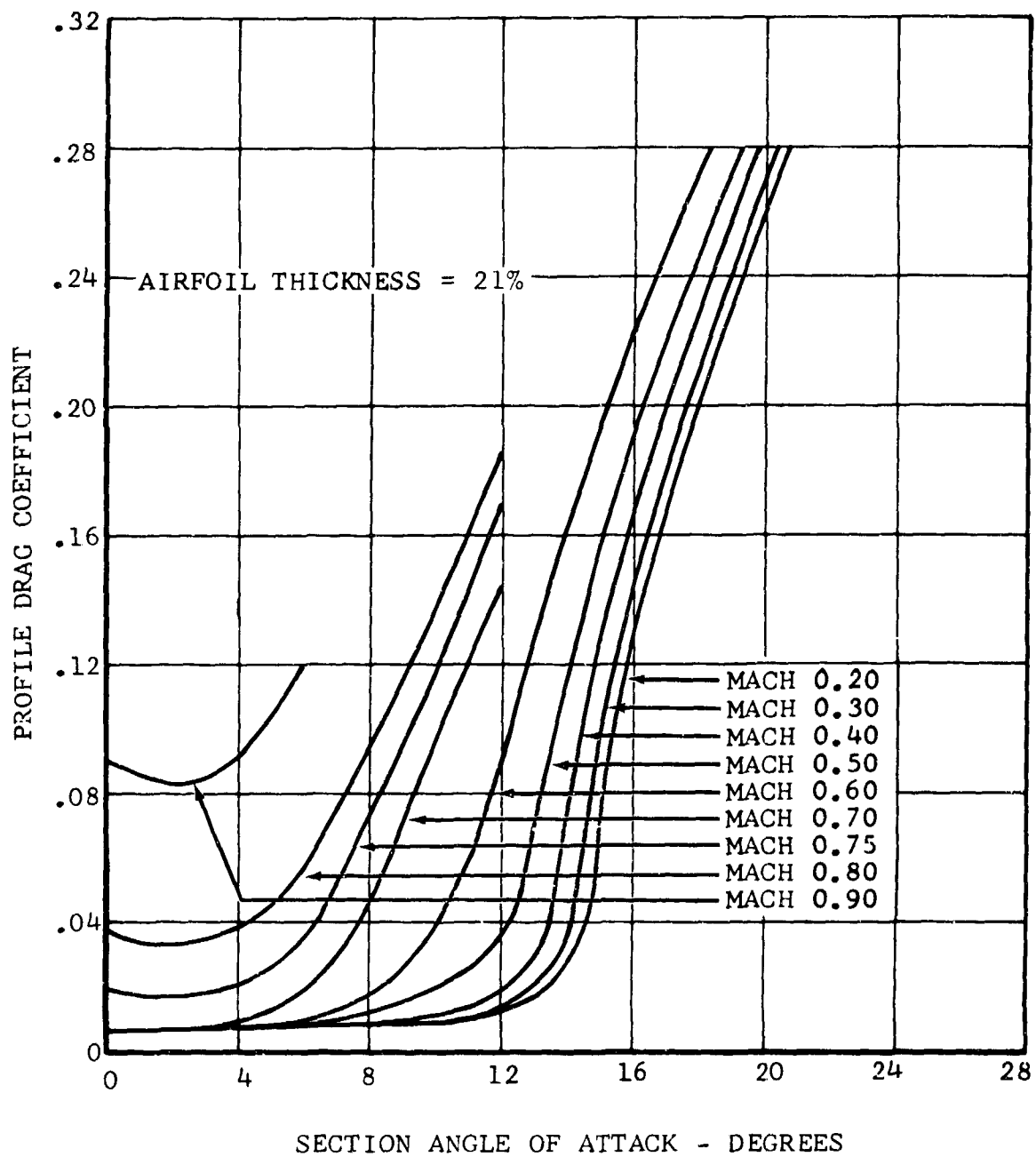


Figure 98. Synthesized Rotor Airfoil Drag Data, 20% to 50% Radius.

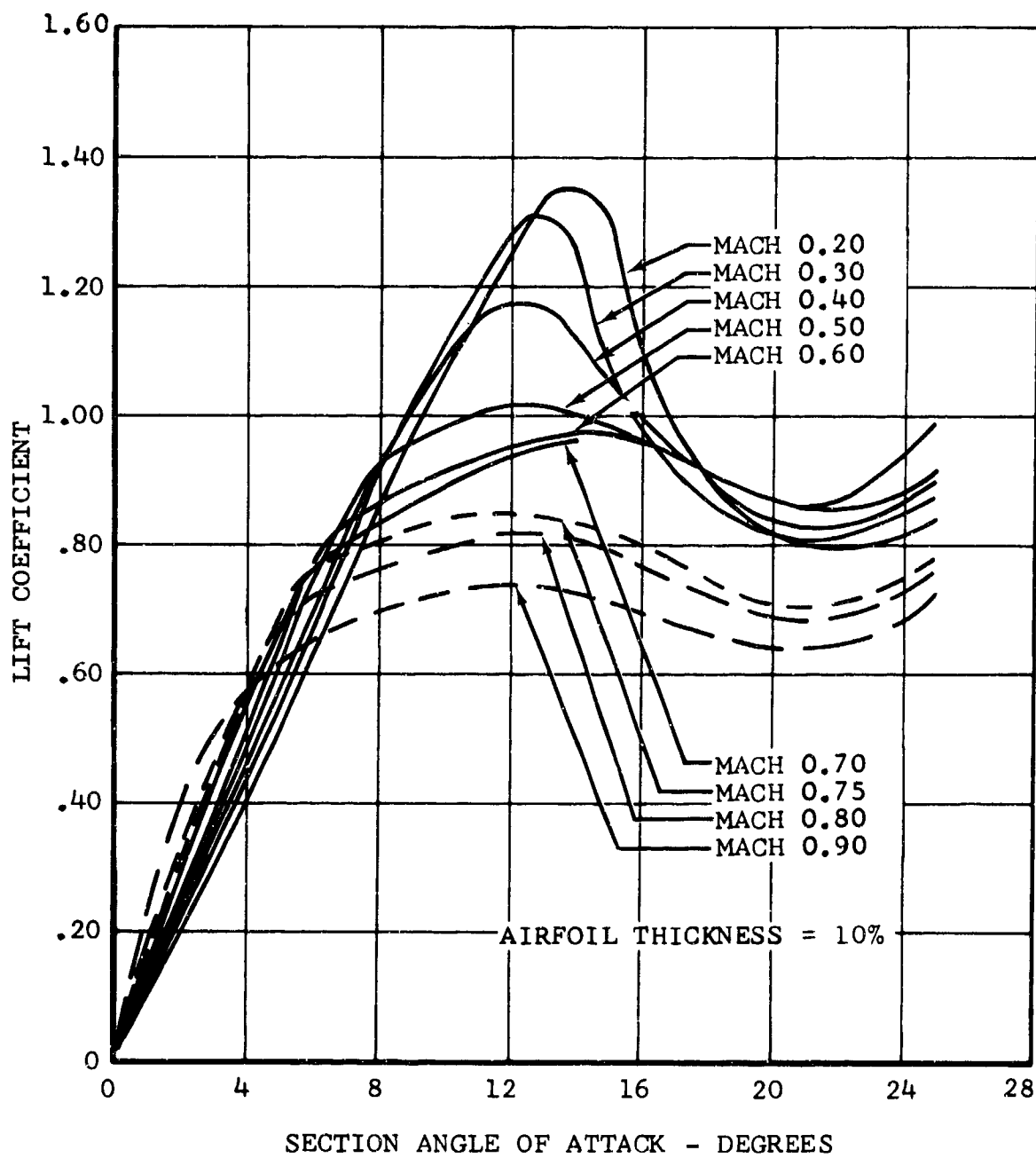


Figure 99. Synthesized Rotor Airfoil Lift Data, 50% to 100% Radius.

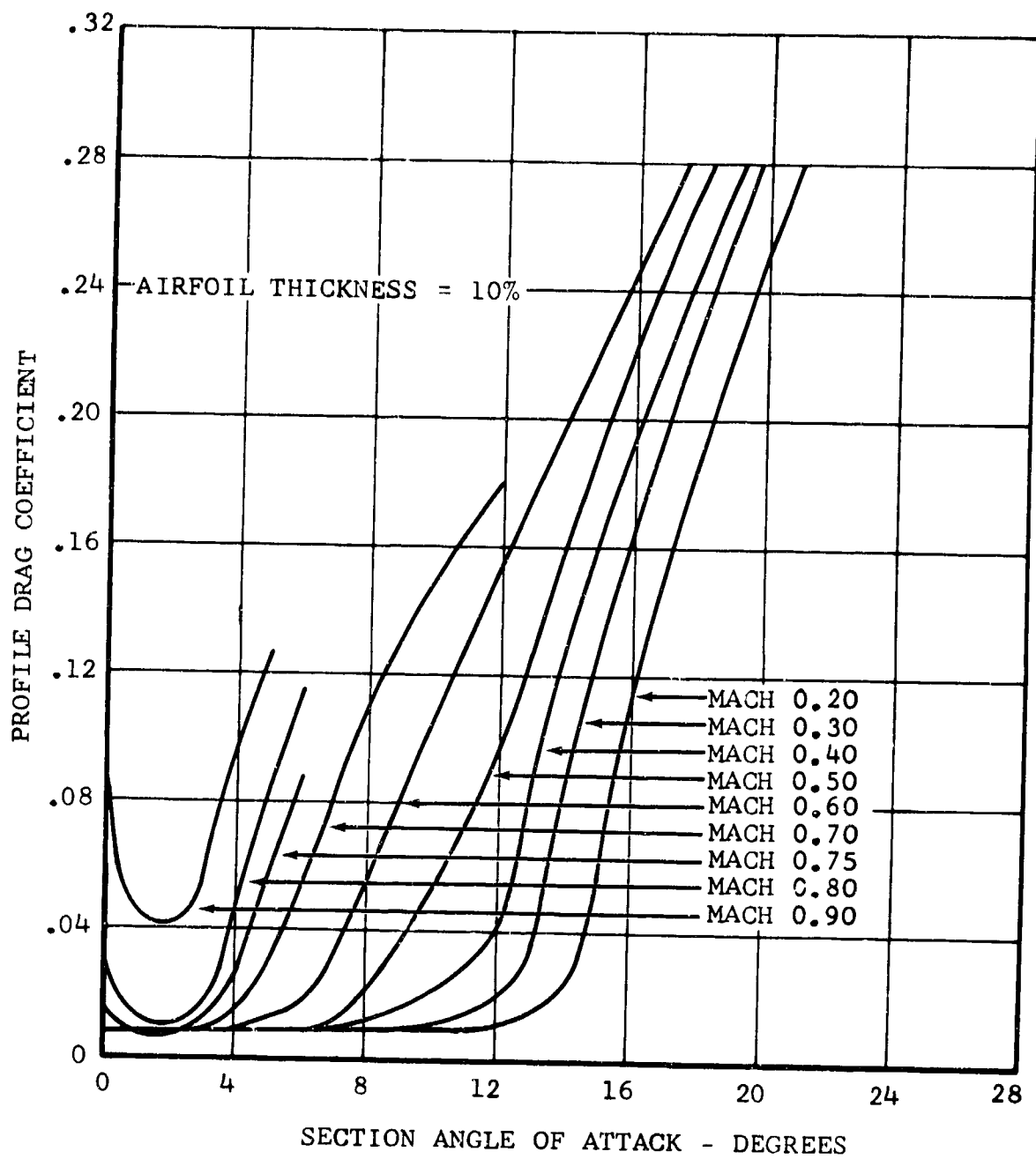


Figure 100. Synthesized Rotor Airfoil Drag Data, 50% to 100% Radius.

Figures 97 and 98 show data for a 21-percent-thick section that are used from 20-percent to 50-percent blade radius, and Figures 99 and 100 show the data for a 10-percent-thick section that are used from 50-percent blade radius to the tip.

Since it is not certain that the drag bucket values shown in Reference 21 could be realized on the D266 rotor, it was conservatively decided to set minimum drag coefficients of all the D266 sections to a value of 0.008. Figure 101 shows a comparison of low-Mach-number D266 data with Reference 21. Recent Bell experiments with boundary-layer visualization techniques on rotor blades in the hovering condition have shown that laminar flow can be obtained to nearly the same chordwise extent as in two-dimensional tests; hence, drag bucket drag values are possible. It is possible that the low minimum drag characteristics of the 64A-series airfoils will be realized in the D266 and that performance will be greater than that calculated.

2. WING

The section lift characteristics for the full-scale wing are shown in Figure 102 for both the flaps-up and the flaps-down conditions. For comparison, the wind-tunnel lift data are shown in the same figure. The wind-tunnel data include the incremental lift of the fuselage as well as wing lift, but the fuselage contribution is small compared to that of the wing. The D266 lift curve slope compares well with the mean slope of the model test results. The lift curve slope for the full-scale wing was computed using span measured to the outboard edge of the rotor nacelles and effective wing area including all that covered by the fuselage. The Figure 102 comparison validates these assumptions. This same figure illustrates that there are no sharp breaks in the lift curve at stall. The shape of the lift curve in the stall area is similar to the NASA Class D characteristics.

Maximum lift coefficient for the full scale wing is estimated to be 0.15 higher than the wind-tunnel data. This is determined from the Reynolds number increase from 1.23×10^6 for the model to 14.3×10^6 for the D266 at 200 knots. Reference 21 shows a $C_{L_{max}}$ increase due to this RN change from 0.25 to 0.30 for smooth 6-series airfoils and about 0.15 for rough 6-series airfoils. The lesser increment is conservatively used.

3. LIFT ANALYSIS

a. Helicopter

In helicopter configuration, most of the aircraft weight is supported by the rotors. With no mast tilt, wing lift is zero to 120 knots. Before approaching full conversion speed, it is desirable, therefore, to effect a partial conversion. This

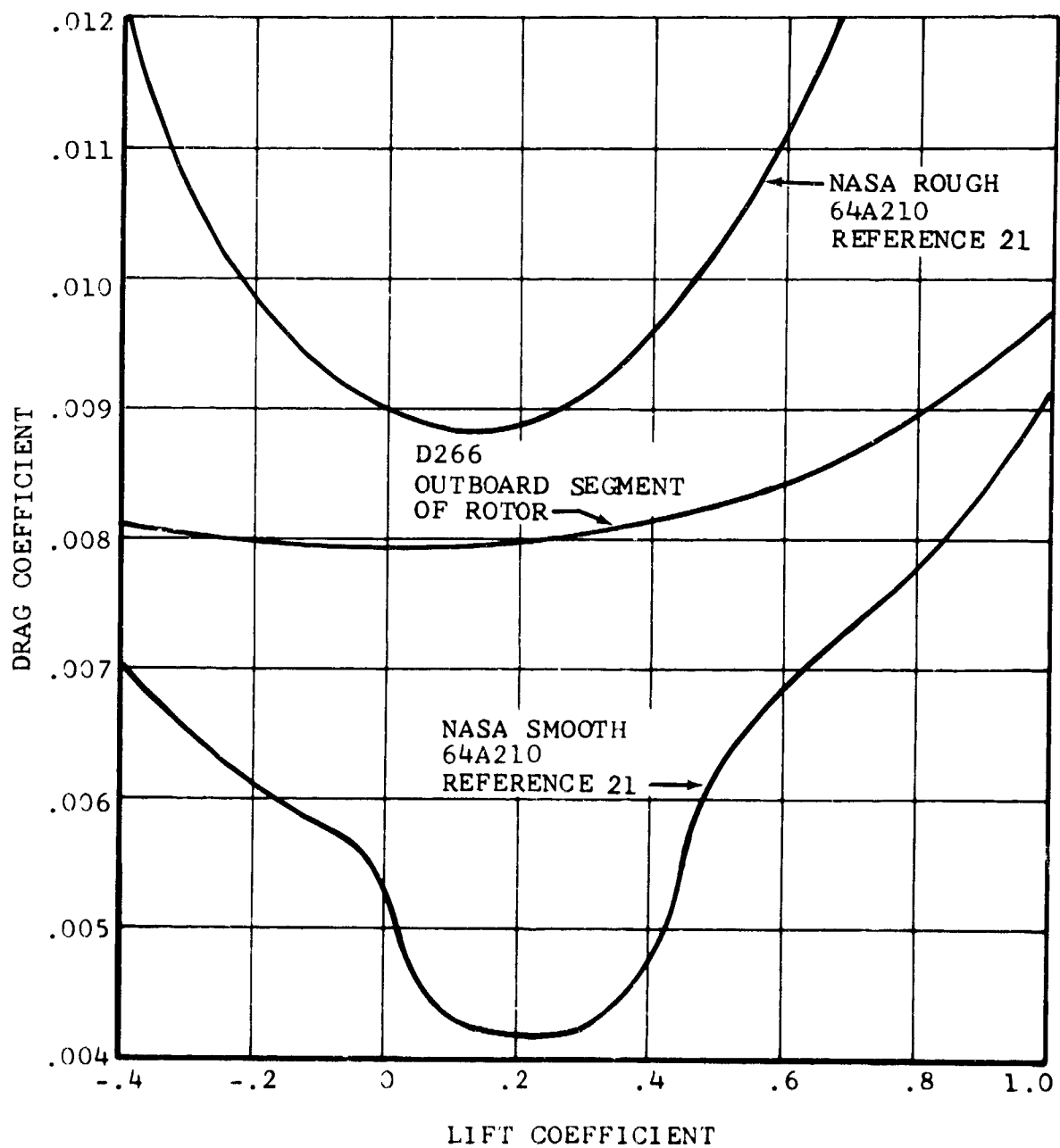


Figure 101. Rotor Airfoil Data Comparison.

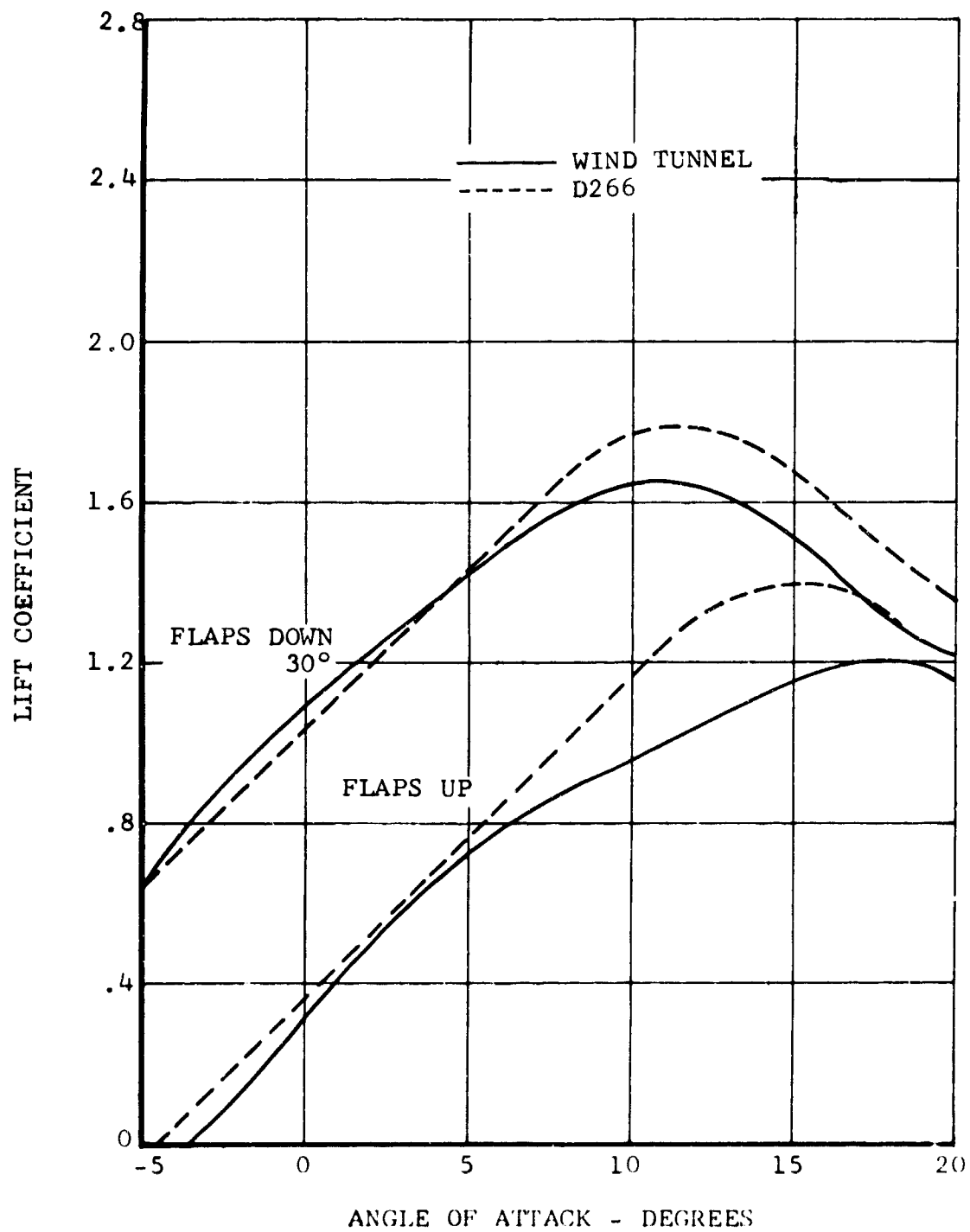


Figure 102. Lift Coefficient Versus Angle Of Attack.

results in carrying positive lift on the wing up to maximum conversion speed. The partial unloading of the rotor improves performance and reduces rotor loads. Figure 103 shows lift distribution between the wing and the rotor for level flight.

Figure 104 shows wing-rotor vertical force distribution in full autorotation (both engines inoperative). This figure shows that no excessive rotor unloading occurs up to speeds of 100 knots. At a descent speed of 75 knots, the rotor supports 60 percent of the weight of the aircraft.

The lift distribution between wing and rotors at the peak of a 2.0g symmetrical pullup is shown in Figure 105. In the speed range between 90 and 150 knots covered in this figure, the rotors produce between 60 and 70 percent of the total normal force.

b. Conversion

The lift distribution between wing and rotors during conversion is shown in Figure 106. The distribution is shown for a speed of 120 knots. Data at other speeds in the conversion envelope are not shown since the difference in distribution is small and occurs at the beginning of the maneuver. The figure shows a smooth changeover of lift during the conversion.

c. Fixed-Wing Mode

In fixed-wing configuration, the rotor supplies a very small amount of the required lift force. Throughout the fixed-wing level-flight spectrum, the rotor's contribution is negligible. A pullup maneuver results in an increase of rotor H-force which contributes somewhat to the generation of normal g. However, this contribution is relatively small compared to that of the wing.

4. DRAG ANALYSIS

a. Forward Flight

Total flat-plate drag area is 9.51 square feet in fixed-wing mode with zero wing lift. The wetted-area drag coefficient is 0.00405 referred to the total wetted area of 2340 square feet.

In helicopter configuration, with gear up, flat-plate area is 28.16 square feet. This value includes an increment of 18.65 square feet of drag area for the rotor pods at a 90-degree angle of attack. The pod drag varies as the cosine cubed of the rotor mast angle of attack.

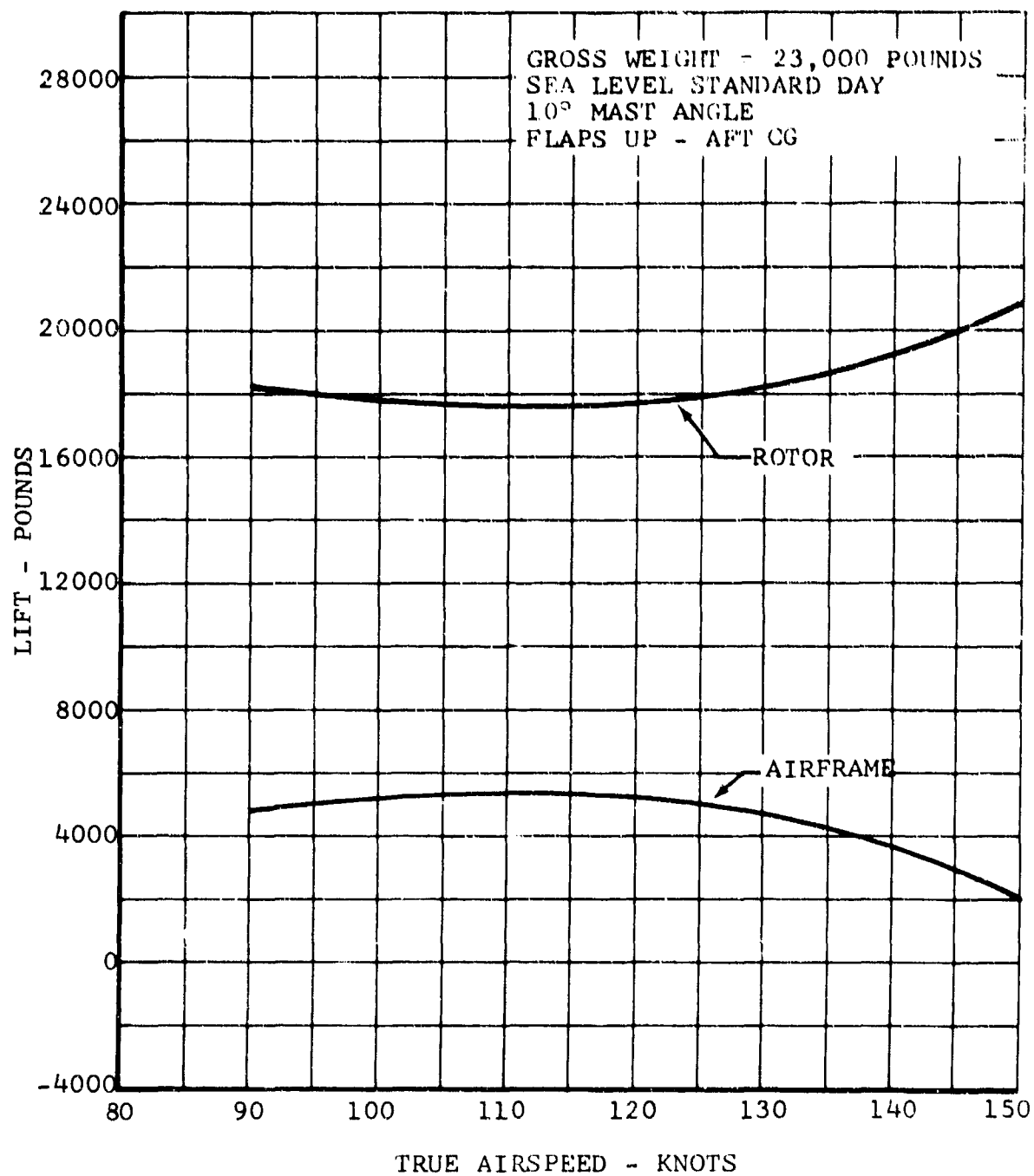


Figure 103. Lift Distribution Between Rotor and Airframe in Level Flight, Helicopter Configuration.

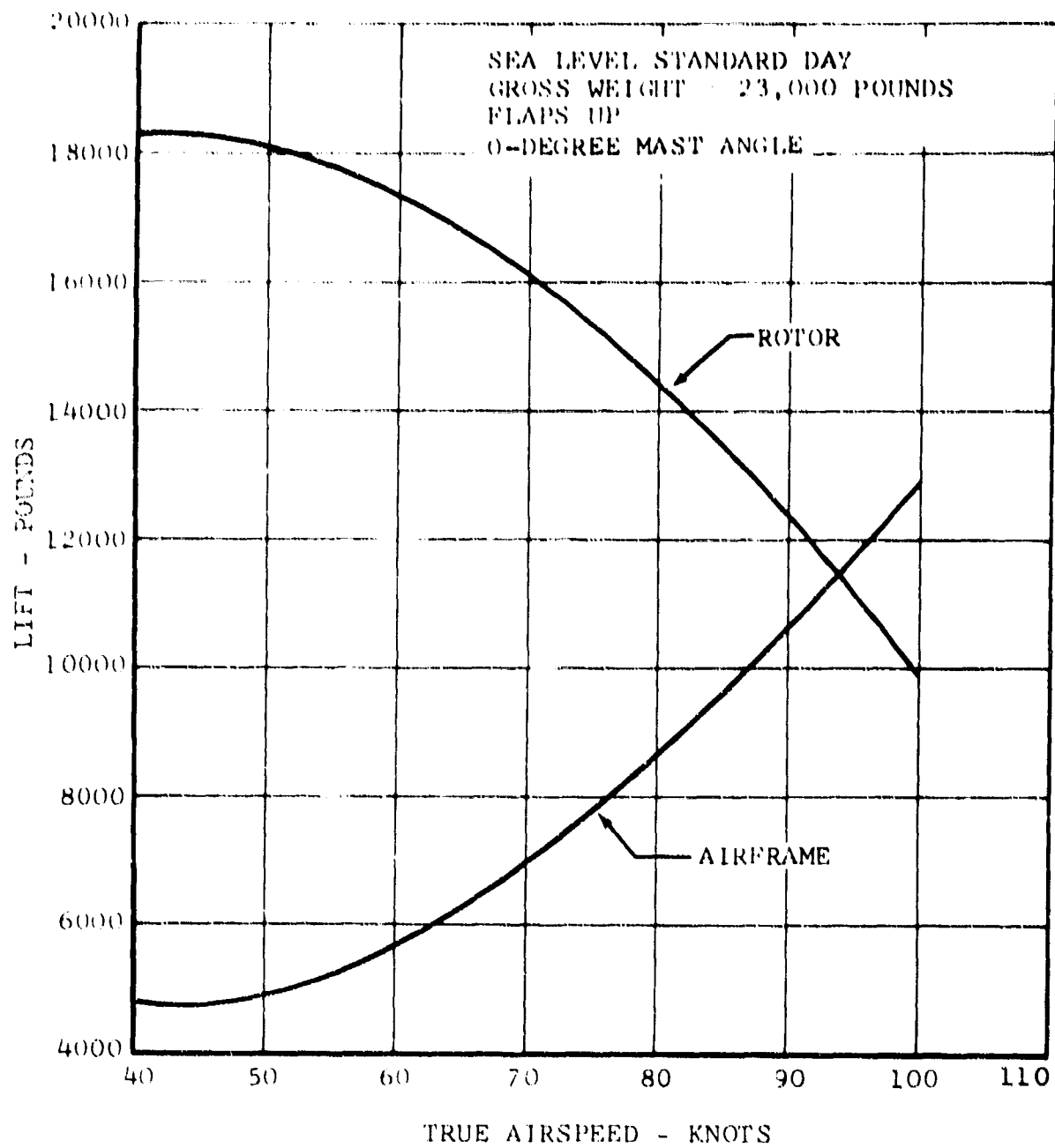


Figure 104. Lift Distribution Between Rotor and Airframe in Autorotation.

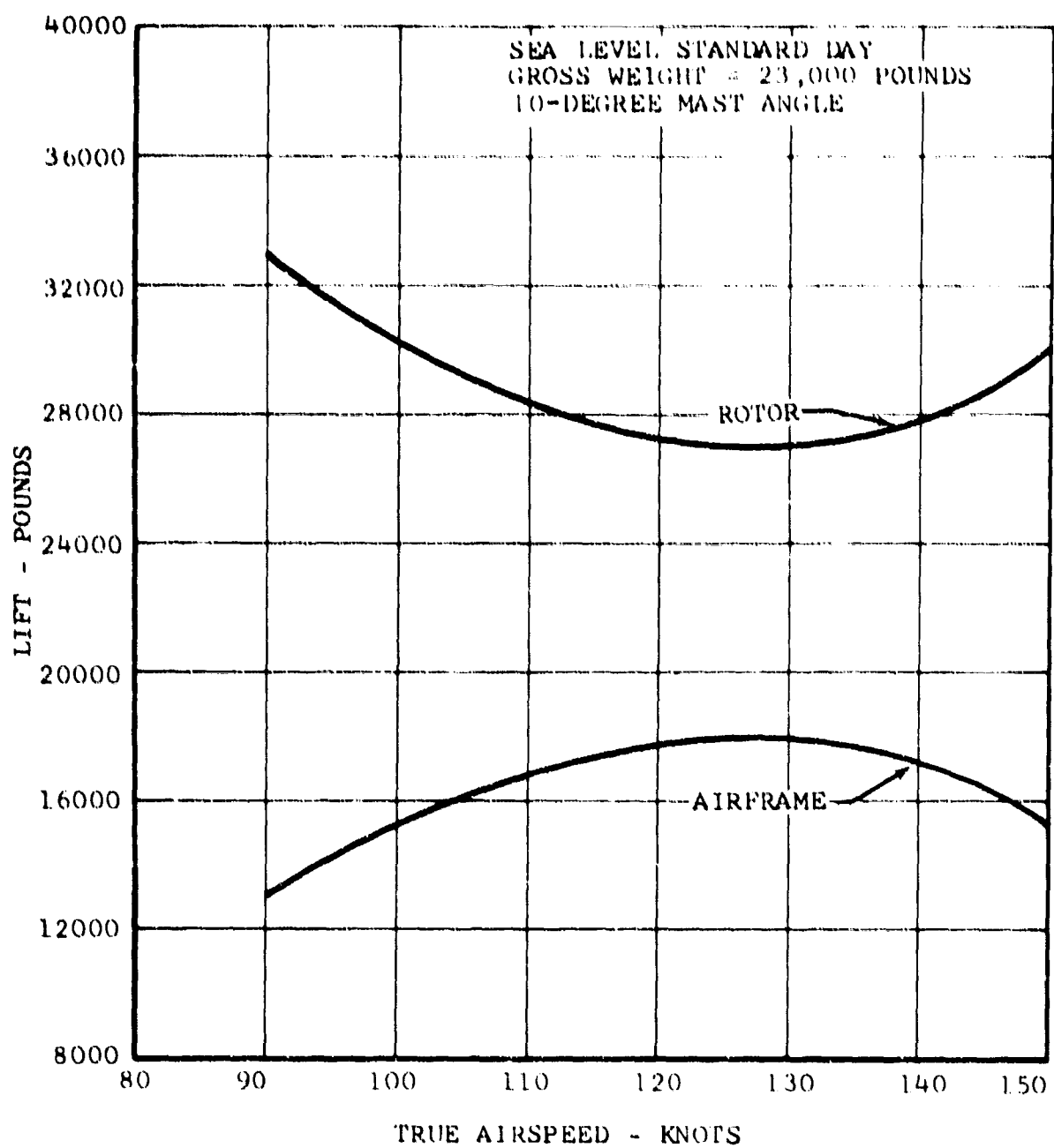


Figure 105. Lift Distribution Between Rotor and Airframe in a 2g Pullup, Helicopter Configuration.

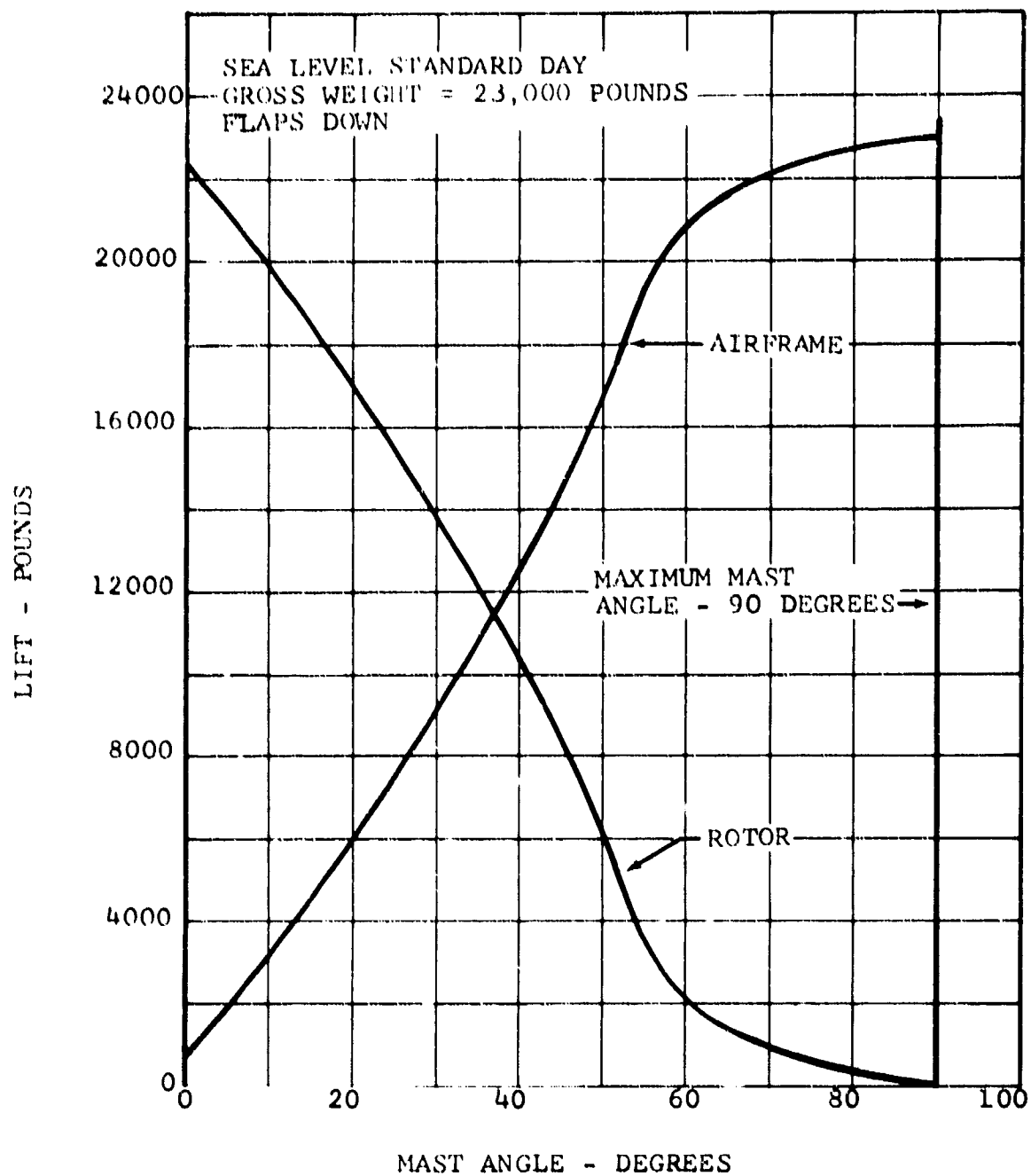


Figure 106. Lift Distribution Between Rotor and Airframe During Conversion.

A summary of the D266 drag breakdown is given in Table XXVIII. Data are given in terms of drag coefficients based on wing area and in terms of equivalent drag area for both helicopter and fixed-wing modes. Table XXIX gives a detailed breakdown of the drag estimate, including reference areas and data sources.

Another estimate of the D266 drag was made, using skin-friction drag coefficients, for comparison with Table XXIX. This estimate is shown in Table XXX. The coefficient range employed is for the surface conditions of a well-constructed aircraft. The positions for transition from laminar to turbulent boundary layers are included in the table. For the fuselage, transition is at a point 10 percent aft of the nose because of the canopy. The lifting surface transition is taken to be at 40-percent chord under zero lift conditions. The rotor nacelle transition is at the nose because of rotor-blade root wake effects. The total drag area using this method is 7.9 square feet. By adding an increment of 0.7 square foot for the effect of surface conditions and control surface gaps on the wing and empennage and the interference and miscellaneous components increment of 0.9 (Reference Table XXIX), total drag area increases to 9.5 square feet. This compares favorably with the Table XXIX estimate. The one-tenth scale-model drag was calculated and compared to the measured drag. Coefficients for aerodynamically smooth surfaces from Reference 22 are used to obtain the model drag. Table XXXI summarizes the calculations. The total drag area from Table XXXI is 5.3 square feet (referred to full-scale dimensions), and the measured drag area is 6.1 square feet (Reference 1). The difference is attributed to interference effects.

Wing-induced drag area is determined from the expression,

$$f_{i_w} = \frac{C_L^2 A_w}{\pi AR_w e} \quad (2)$$

where

$$A_w = 330.5 \text{ square feet}$$

$$AR_w = 7.44$$

$$e = 0.9$$

The drag coefficient for the total aircraft, including wing-induced drag, is shown in Figures 107 and 108.

TABLE XXVIII		
D266 DRAG SUMMARY		
	Helicopter Mode	Fixed-Wing Mode
<u>Parasite Drag</u>		
Flaps Up		
C_{D_o}	$0.0288 + 0.0565 \cos^3 \alpha_M$	0.0288
f_o	$9.51 + 18.65 \cos^3 \alpha_M$	9.51
Flaps and Ailerons Down 30 Degrees		
C_{D_o}	$0.0808 + 0.0565 \cos^3 \alpha_M$	0.0808
f_o	$26.71 + 18.65 \cos^3 \alpha_M$	26.71
<u>Induced Drag</u>		
C_{D_i}	$0.0476 C_L^2$	$0.0476 C_L^2$
f_i	$15.7 C_L^2$	$15.7 C_L^2$
<p>Notes: f = equivalent flat plate drag area. Reference area = wing area = 330.5 square feet. α_M = mast angle of attack. 0 degrees when relative wind is perpendicular to the mast axis.</p> <p>$C_{D_{total}} = C_{D_o} + C_{D_i}$</p> <p>$f_{total} = f_o + f_i$</p>		

TABLE XXIX

D266 DRAG BREAKDOWN

Item	Reference Area (ft ²)	Reference	C _D	Equivalent Flat- Plate Drag Area, f (ft ²)
Fuselage	Frontal = 55.9	Hoerner, p. 6-19	0.070	3.91
Landing-Gear Housings	Frontal = 5.0	Hoerner, pp. 8-4, 5	0.030	0.15
Engine Pods	Frontal = 12.5	Hoerner, p. 13-6	0.040	0.50
Horizontal Tail	Plan = 90.0	TR 824*	0.0070	0.63
Vertical Tail	Plan = 100.0	TR 824*	0.0070	0.70
Tail Interference	-	Hoerner, p. 8-12	-	0.10
Wing Profile Flaps Up	Plan (exposed) = 247.0	TR 824*	0.0080	1.98
Wing Interference	-	Hoerner, p. 8-15	-	0.50
Rotor Pods	Frontal = 14.0	Hoerner, p. 6-19	0.050	0.70
Miscellaneous - Lights, Antennas, etc.	-	-	-	0.34
Total (Fixed-Wing Mode) = 9.51				
Rotor Pods	Frontal = 55.3		0.35	19.35
(Helicopter, $\alpha_M = 90$ degrees)	Δf due to pods at $\alpha_M = 90$ degrees = 19.35-.70 = 18.65			
Total (Helicopter) = 28.16				
*Modified to include effects of surface condition, gaps, and slots.				

TABLE XXX
D266 DRAG ANALYSIS USING
SKIN-FRICTION COEFFICIENTS

Component	Length or Chord (ft)	$RN^* \times 10^6$	S_{WET} (sq ft)	Transition, X/l or X/c	$C_{f_{WET}}$	f^{**} (sq ft)
Fuselage and Landing-Gear Pods	50	10.8	1072	0.1	0.0039	4.2
Wing (exposed)	6.65	14.4	520	0.4	0.0027	1.4
Horizontal Stabilizer	4.56	9.9	173	0.4	0.0028	0.5
Vertical Stabilizer	7.8	16.9	223	0.4	0.0027	0.6
Rotor Nacelles	4.6	10	169	0.0	0.0042	0.7
Engine Cowling	6.56	14	183	0.4	0.0027	0.5
Total					$f =$	7.9
<p>* At 200 knots ** $f = C_{f_{WET}} \times S_{WET}$</p>						

TABLE XXXI

1/10-SCALE MODEL DRAG ANALYSIS
USING SKIN-FRICTION COEFFICIENTS

Component	Length or Chord (ft)	$RN^* \times 10^6$	S_{WET} (sq ft)	Transition, X/l or X/c	$C_{f_{WET}}$	f^{**} (sq ft)
Fuselage and Landing-Gear Pods	4.91	9.05	10.5	0.5	0.00172	1.80
Wing (exposed)	0.68	1.26	4.8	0.4	0.0030	1.45
Horizontal Stabilizer	0.45	0.83	1.65	0.4	0.00335	0.55
Vertical Stabilizer	0.92	1.70	1.37	0.4	0.00282	0.40
Rotor Pods	2.12	3.92	2.8	0.5	0.00210	0.6
Engine Cowling	1.75	3.26	1.8	0.3	0.00270	0.50
Total					$f =$	5.3
$^* \text{ At 200 knots}$ $^{**} f \text{ (full-scale equivalent)} = C_{f_{WET}} \times S_{WET} \times 100$						

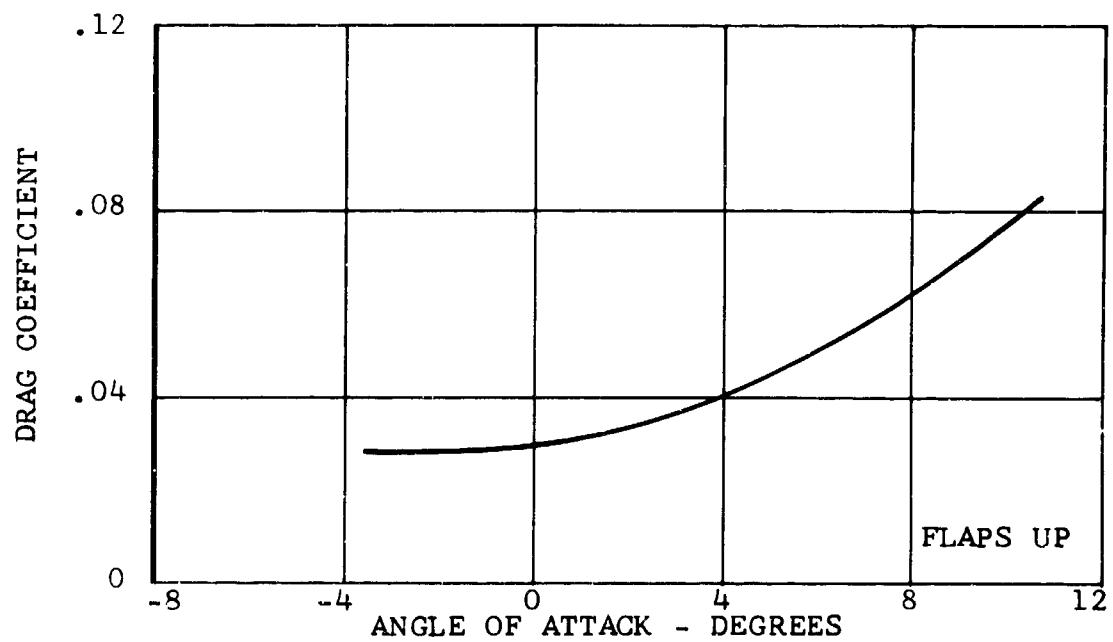


Figure 107. Drag Coefficient Versus Angle of Attack.

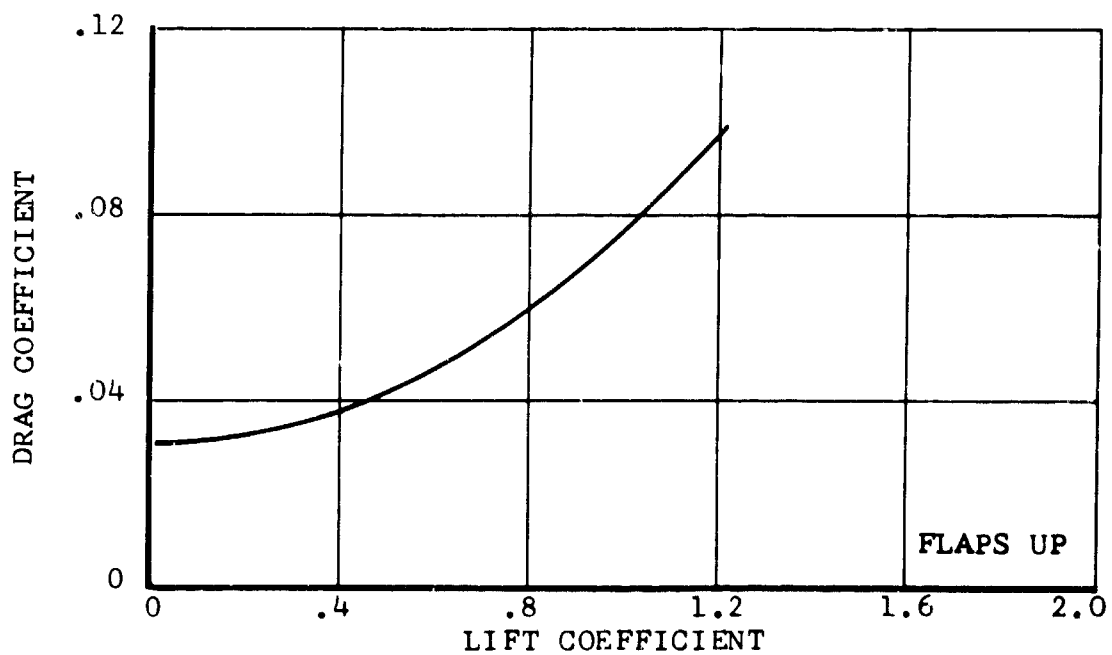


Figure 108. Lift Coefficient Versus Drag Coefficient.

b. Hovering Download

The download on the wing in hovering is 6 percent of rotor thrust. This value is obtained from the expression:

$$\frac{\text{Download}}{\text{Thrust}} = C_D \times \frac{\text{Wing Area in Downwash}}{\text{Rotor Area}} \quad (3)$$

Wing area in the downwash is based on a rotor slipstream diameter of 0.75 times rotor diameter. For the D266, the projected wing area in the slipstream is 160 square feet with the flaps and ailerons deflected 60 degrees. The rotor disc area is $2 \times 1164 = 2328$ square feet. Then,

$$\frac{\text{Wing Area in Downwash}}{\text{Rotor Area}} = \frac{160}{2328} = 0.0688$$

A C_D value of 0.817 is obtained from test results reported in Reference 23 and includes the effect of the D266 rotor twist rate. Thus,

$$\frac{\text{Download}}{\text{Thrust}} = 0.817 (0.0688) = 0.06$$

The same download factor is used for hovering in ground effect as well as out of ground effect. Reference 23 indicates that this is conservative. The increase in rotor hover efficiency due to the presence of the wing is conservatively neglected.

c. ENGINE PERFORMANCE

Rotor shaft horsepower available versus altitude for hover and vertical climb is shown in Figure 109. Power available for hover and vertical flight is shown only to 20,000 feet, since engine operation at zero airspeed is prohibited beyond that altitude.

Forward-flight normal power and military rated power available are shown versus airspeed and altitude in Figures 110 through 117 for 16,600, 12,100, 10,075, and 8050 engine rpm.

All engine limits and the transmission torque limit (1350 ft-lb) are noted on the power-available curves where encountered.

Fuel-flow data are shown in Figures 118 through 120. They cover twin-engine operation for sea level, 10,000 feet, and 25,000 feet on a standard day.

The D266 is designed to cruise at an engine rpm of 8050, so all the fuel-flow data shown are at this rpm. In mission performance calculations, warmup and takeoff allowances are for 16,600 engine rpm, and the climb fuel allowance is at 12,100 rpm. These data have been calculated but are not shown in this report.

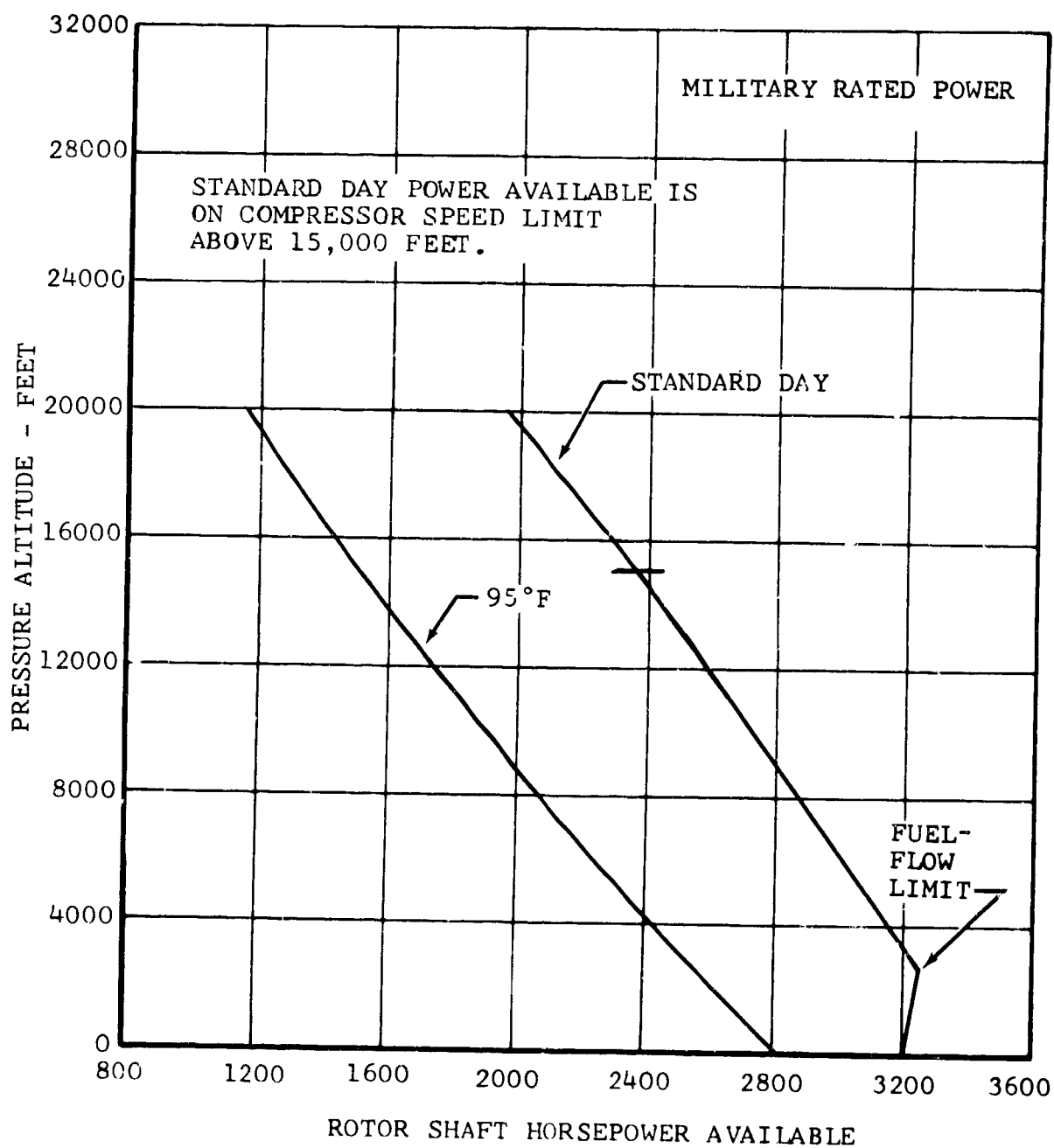


Figure 109. Vertical-Flight Power Available Per Engine, 16,600 Engine RPM, Twin-Engine Operation.

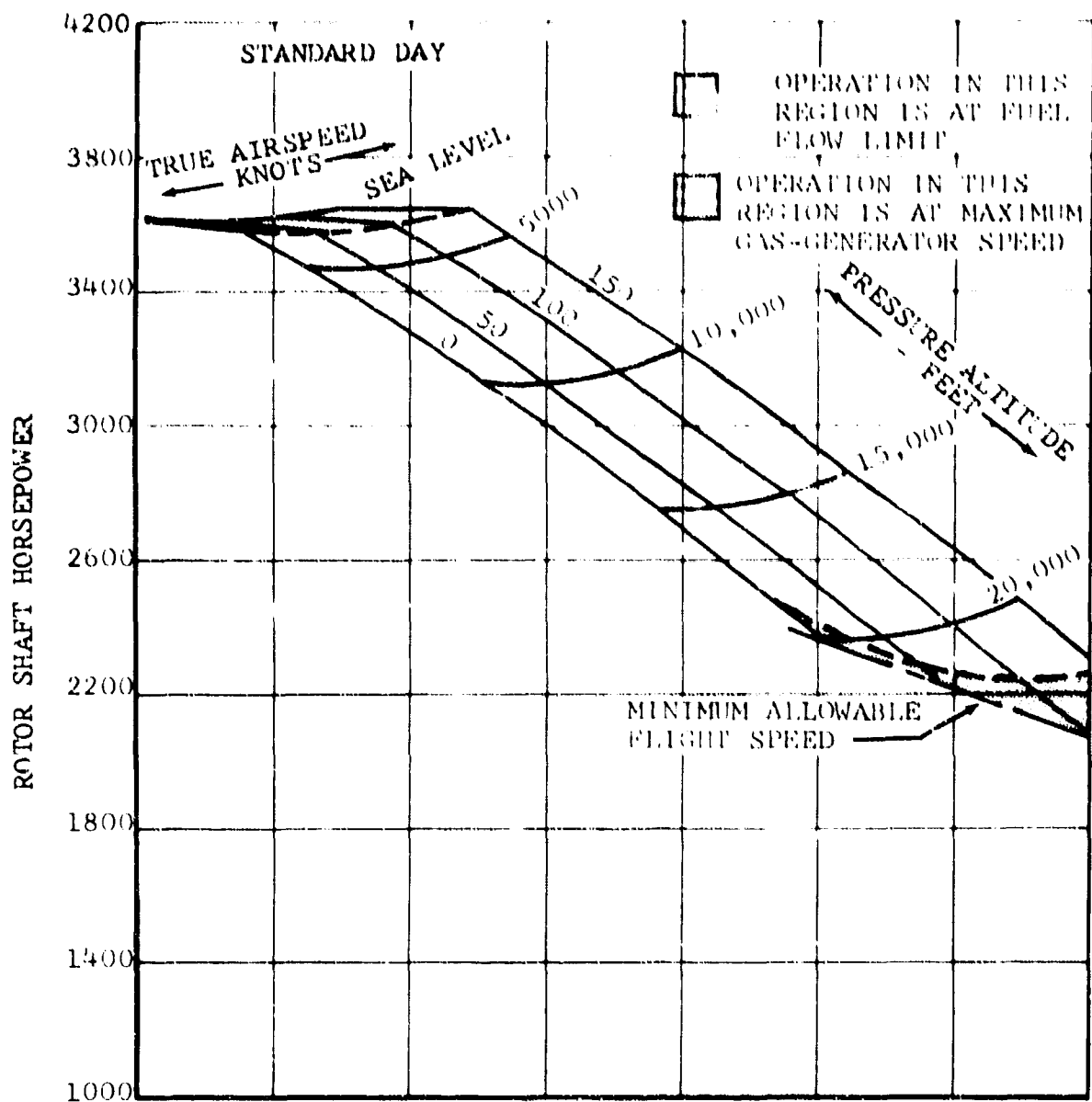


Figure 110. Rotor Shaft Horsepower Available Per Engine, Military Rated Power, 16,600 Engine RPM, Twin-Engine Operation.

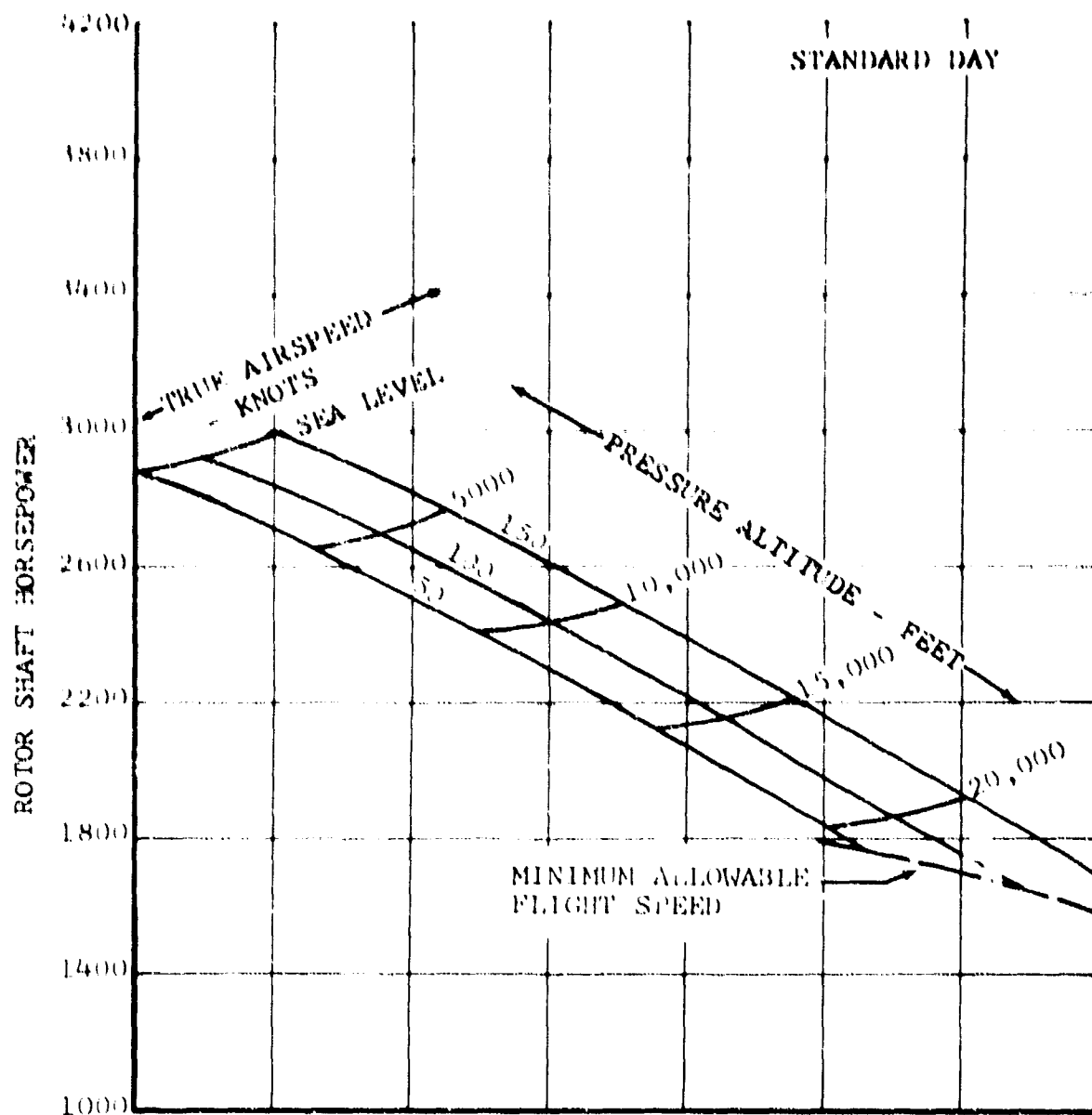


Figure 111. Rotor Shaft Horsepower Available Per Engine, Normal Rated Power, 16,600 Engine RPM, Twin-Engine Operation.

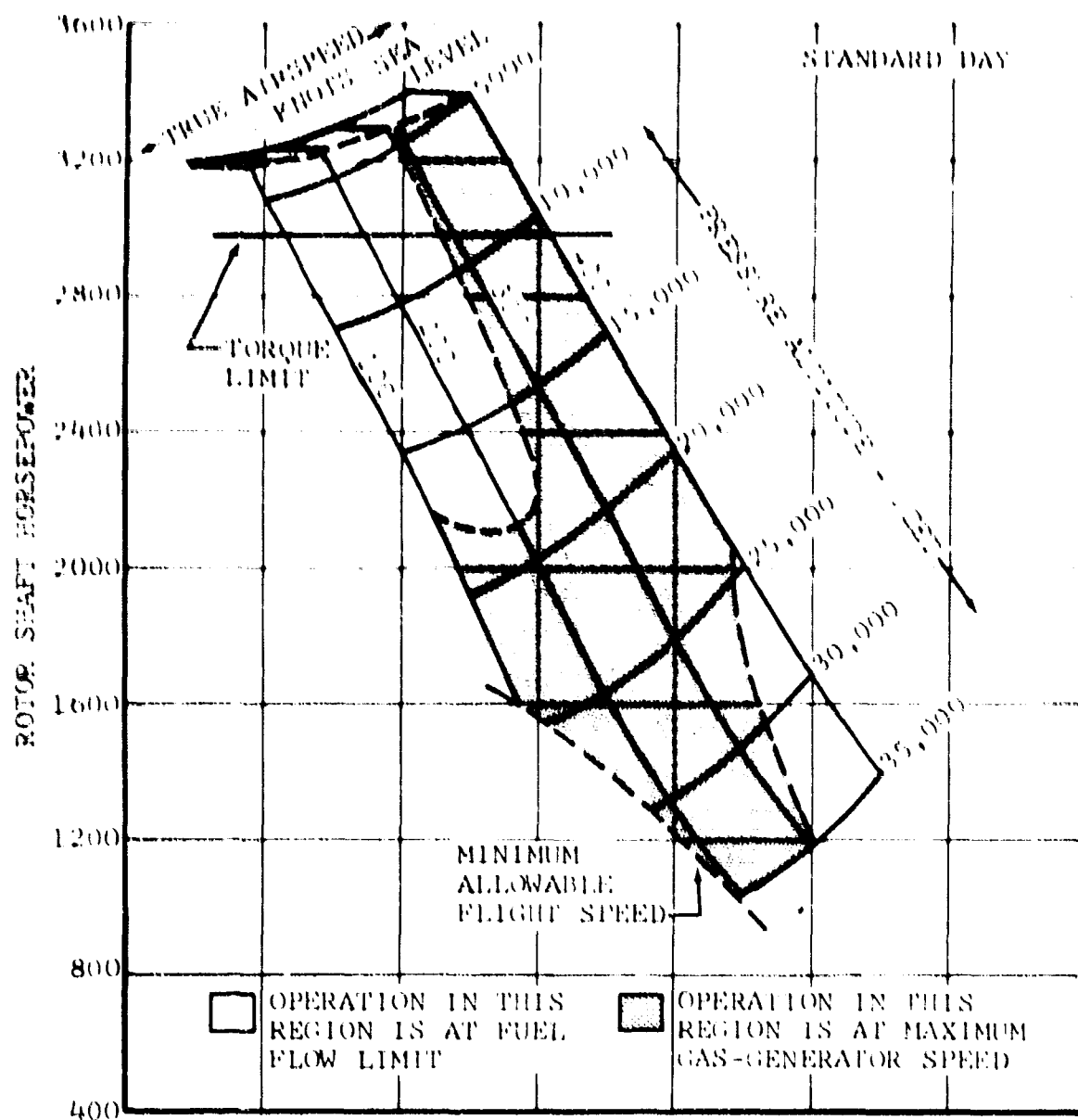


Figure 112. Rotor Shaft Horsepower Available Per Engine, Military Rated Power, 12,100 Engine RPM, Twin-Engine Operation.

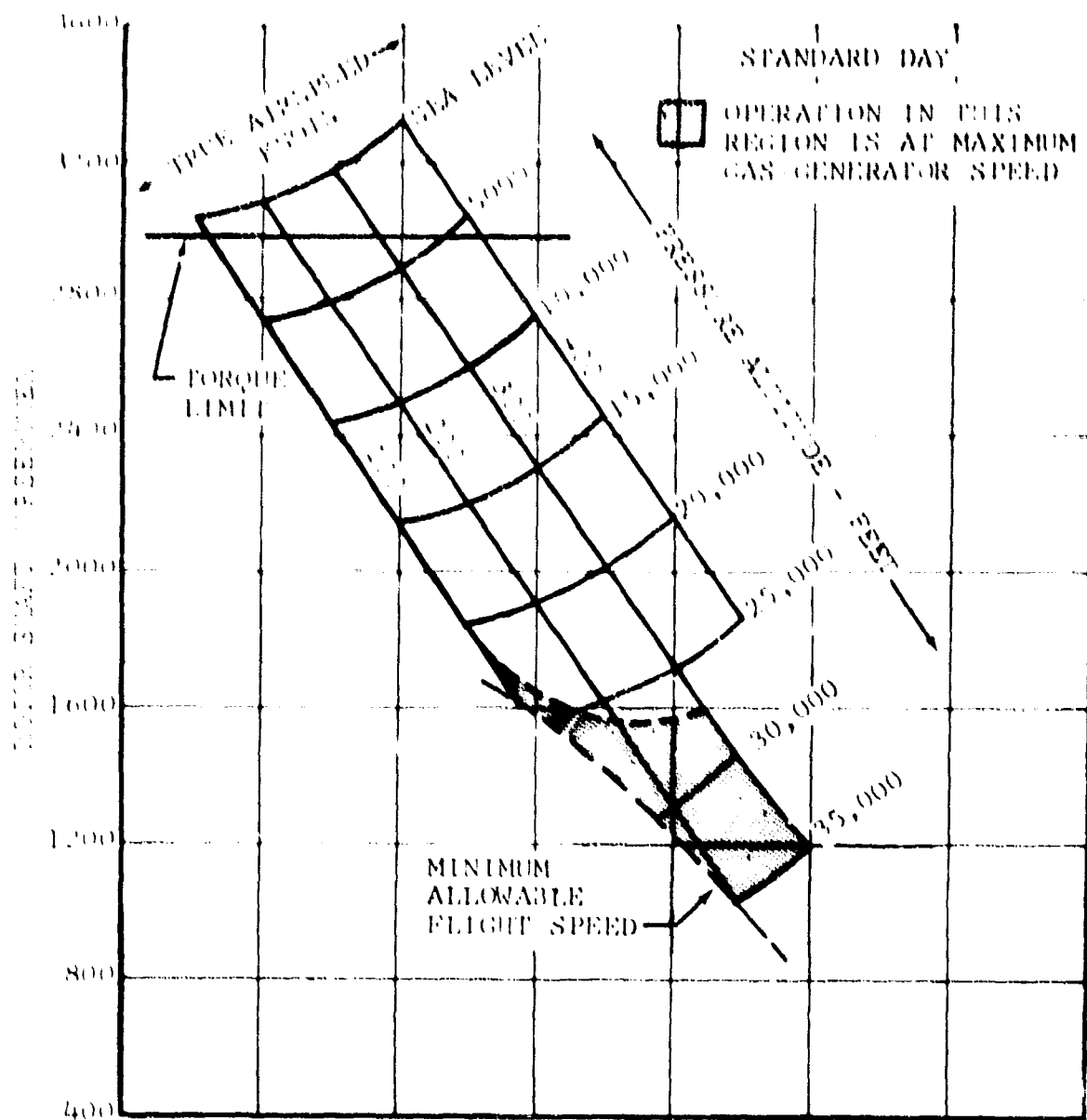


Figure 113. Rotor Shaft Horsepower Available Per Engine, Normal Rated Power, 12,100 Engine RPM, Twin-Engine Operation.

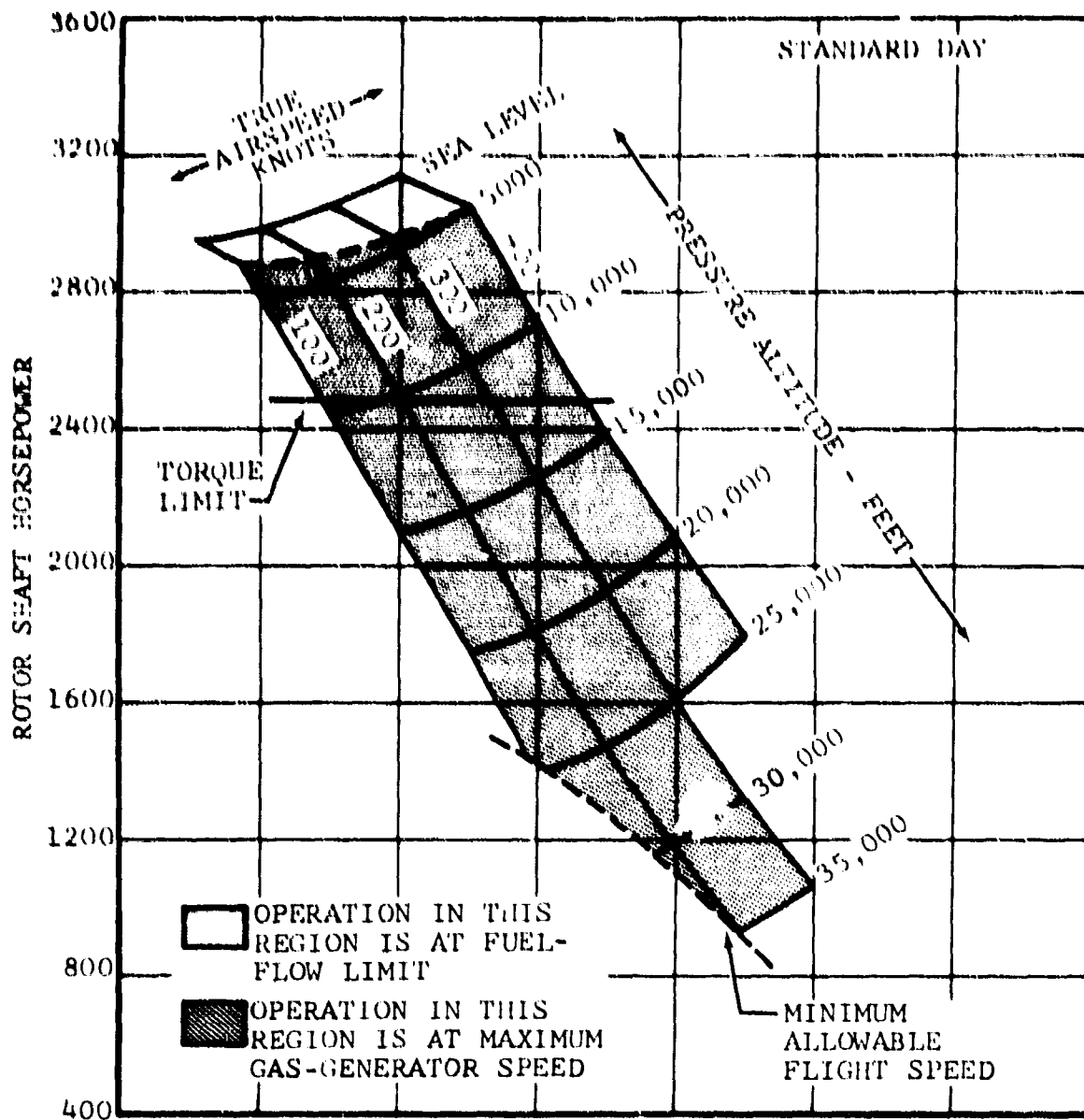


Figure 114. Rotor Shaft Horsepower Available Per Engine, Military Rated Power, 10,075 Engine RPM, Twin-Engine Operation.

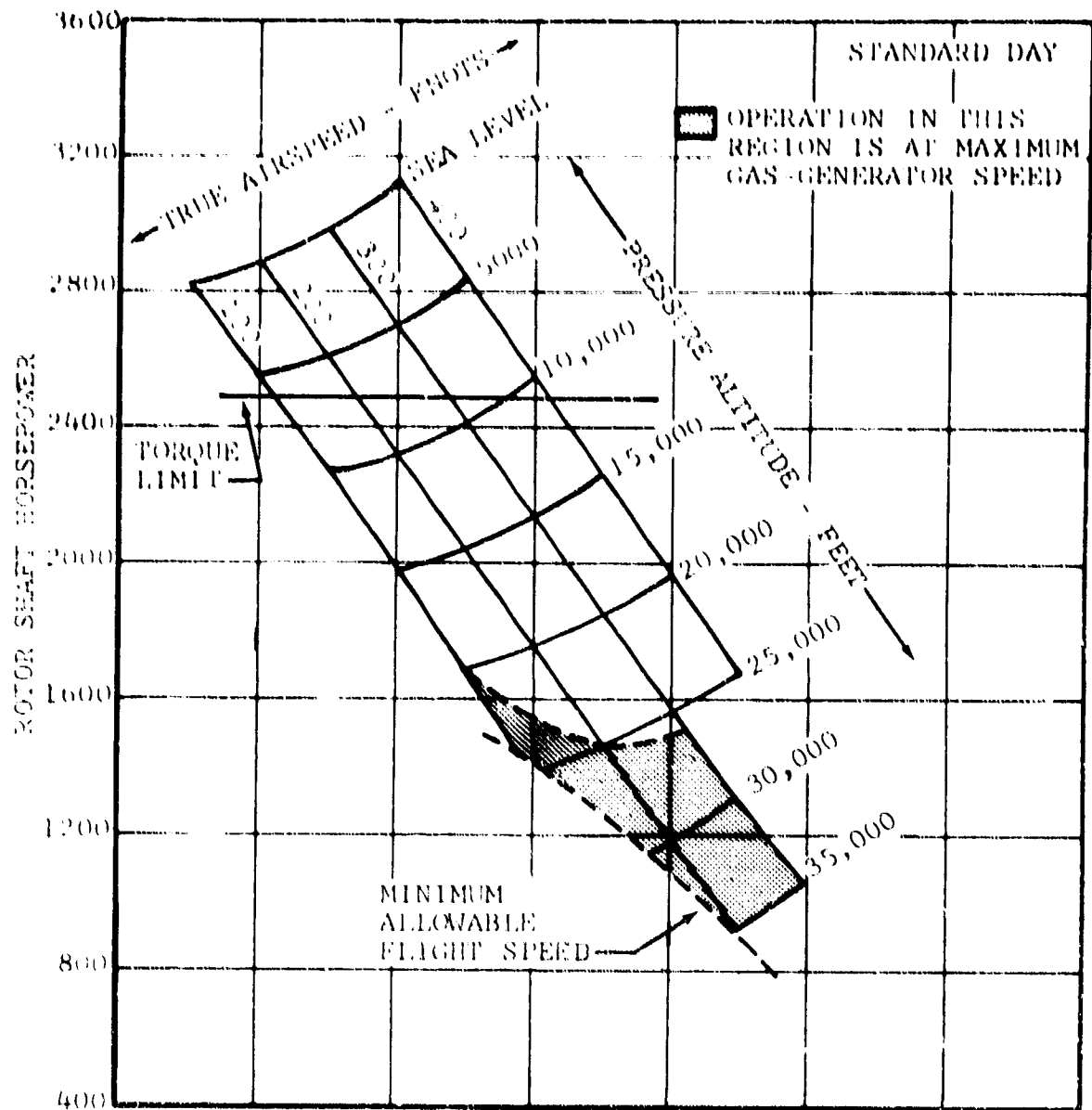


Figure 115. Rotor Shaft Horsepower Available
Per Engine, Normal Rated Power, 10,075
Engine RPM, Twin-Engine Operation.

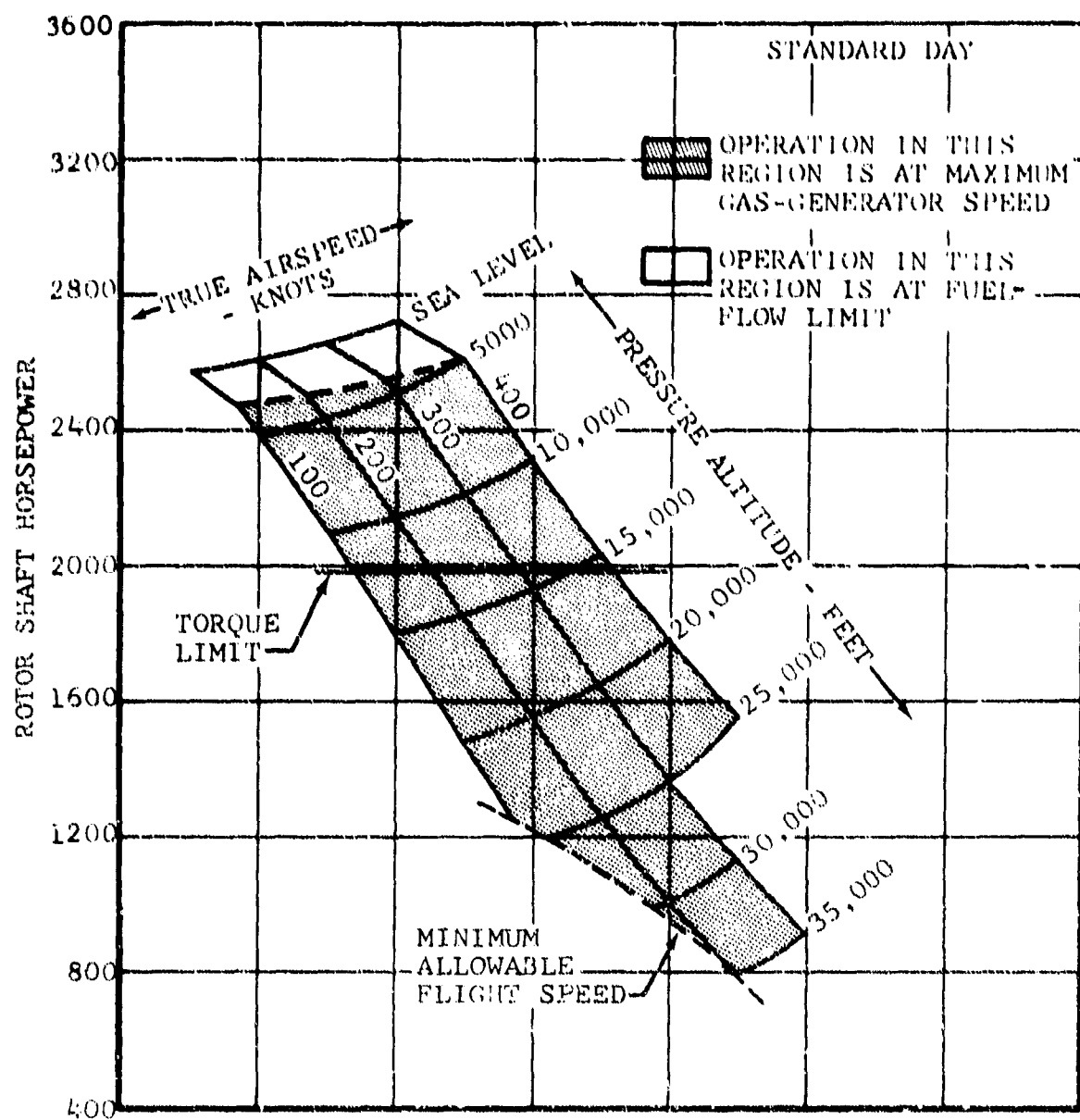


Figure 116. Rotor Shaft Horsepower Available Per Engine, Military Rated Power, 8050 Engine RPM, Twin-Engine Operation.

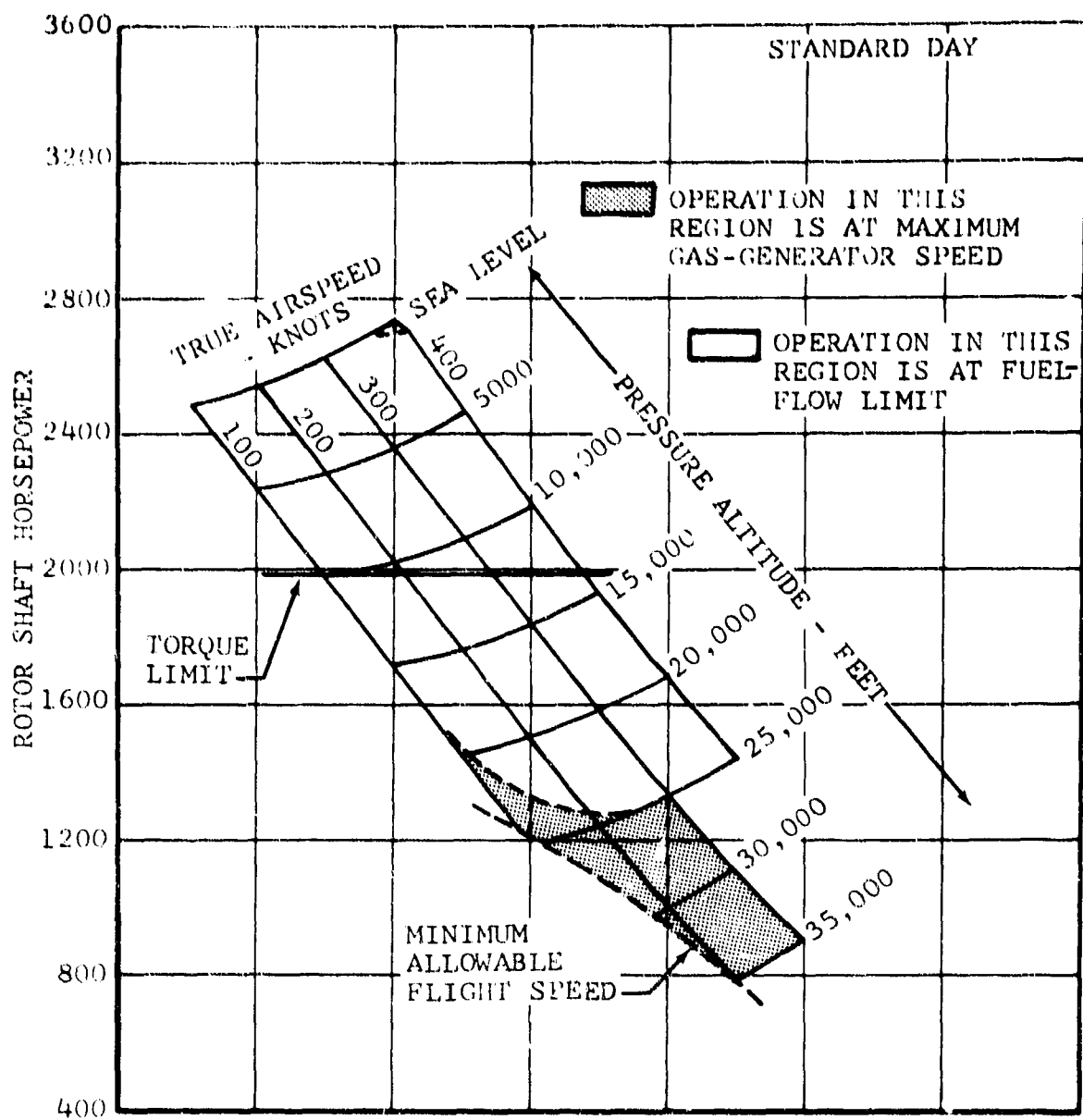


Figure 117. Rotor Shaft Horsepower Available
Per Engine, Normal Rated Power, 8050
Engine RPM, Twin-Engine Operation.

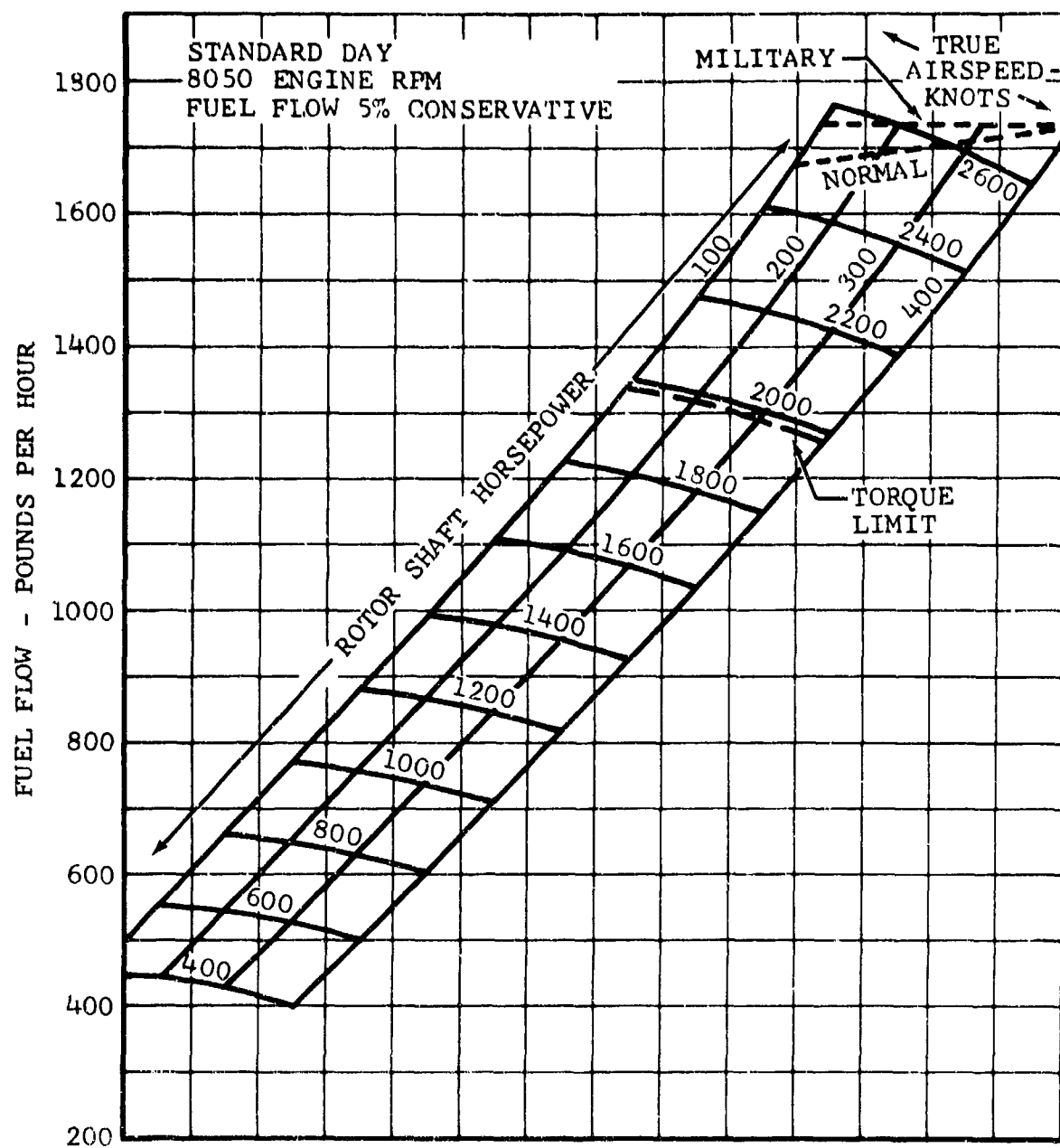


Figure 118. Fuel Flow Per Engine, Sea Level, Twin-Engine Operation.

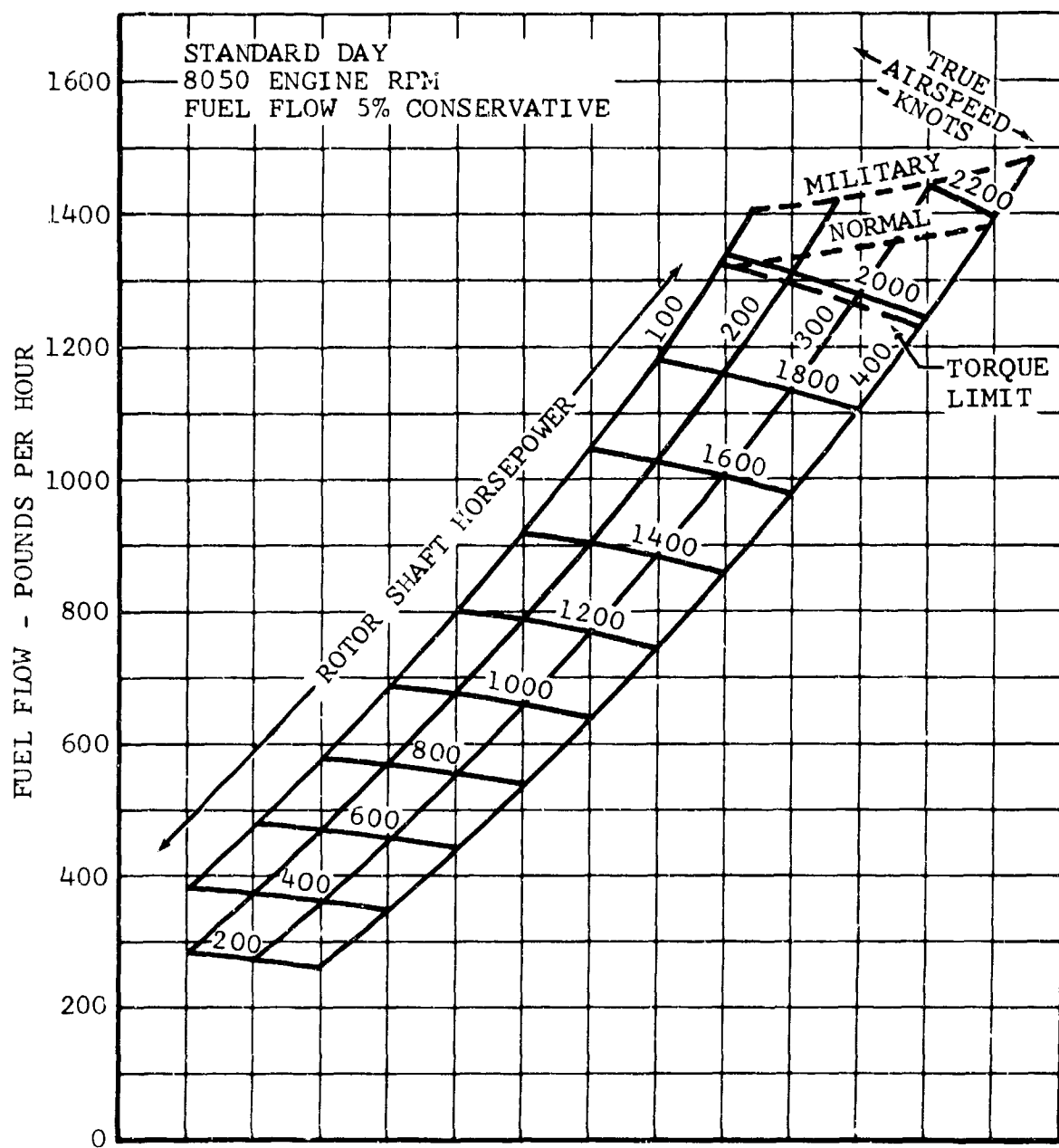


Figure 119. Fuel Flow Per Engine, 10,000 Feet, Twin-Engine Operation.

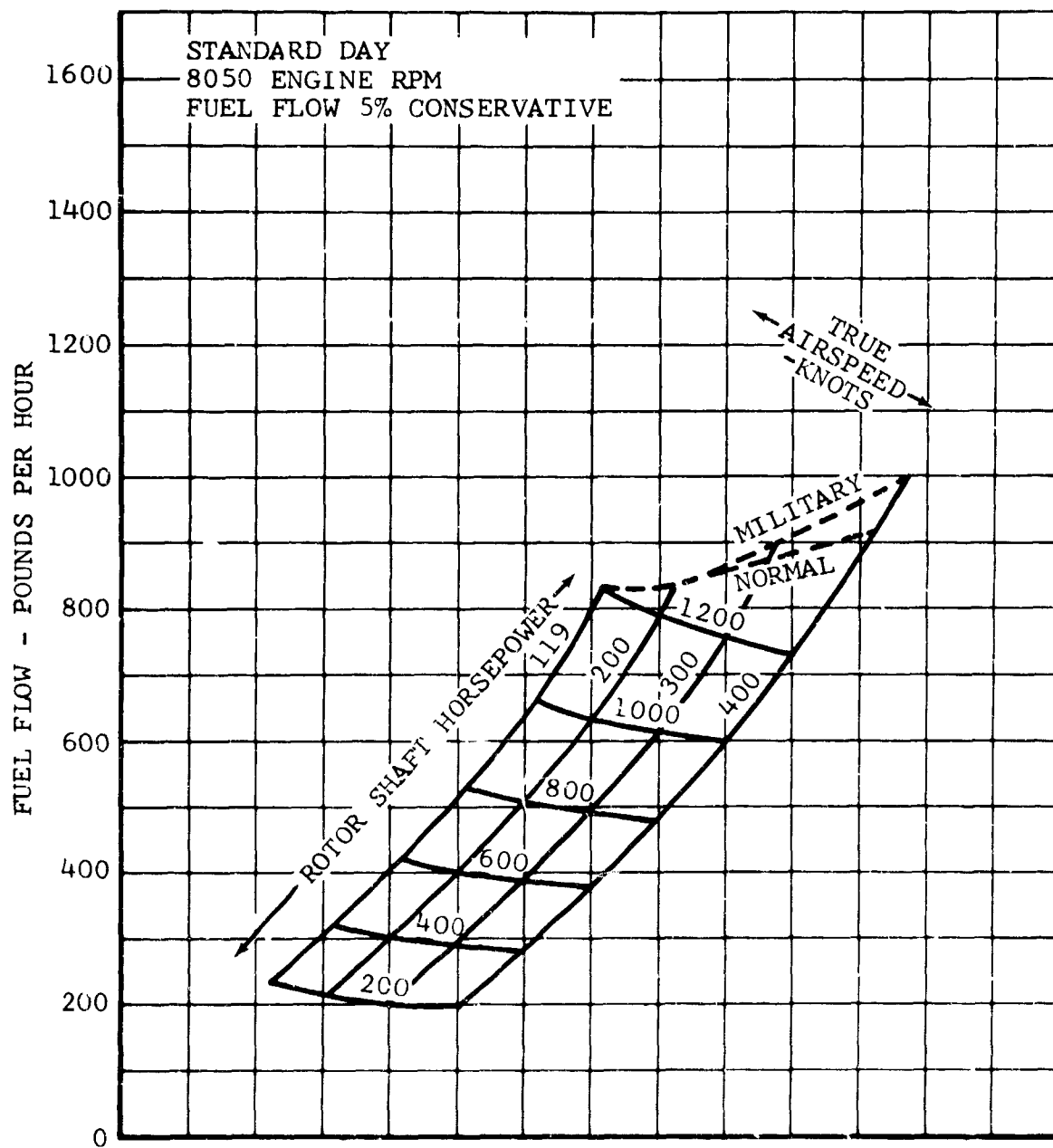


Figure 120. Fuel Flow Per Engine, 25,000 Feet,
Twin-Engine Operation.

Note that all fuel flow has been increased by 5 percent over the manufacturer's data.

Net jet thrust for the 300-square-inch tailpipe area is plotted in Figures 121 through 123 versus rotor shaft horsepower. In Figures 148 through 150, which are thrust-horsepower-required curves, are shown lines of thrust horsepower available (THP avail) at normal and military ratings. These lines are calculated using the rotor shaft power available (SHP) curves (Figures 110 through 117), the propeller efficiency (η) curves (Figures 138 through 146), and net jet thrust power (THP_{FN}) curves (Figures 121 through 123).

$$\text{THP}_{\text{avail}} = (\text{Rotor SHP}_{\text{avail}} \times \eta @ V, \text{rpm, altitude}) - \text{THP}_{\text{FN}} \quad (4)$$

where

$$\text{THP}_{\text{FN}} = \frac{\text{FN} \times V}{326}$$

V = True airspeed in knots

D. HOVERING

1. POWER REQUIRED

Power required versus thrust for hovering IGE and OGE is presented nondimensionally in Figure 124. The data are given in nondimensional form for two tip-speed values. The spread of the data for the high tip speed is attributed to compressibility effects. The OGE power required is also presented in the form of figure of merit in Figure 125. Dimensional power required versus gross weight is shown in Figure 126. These data include the effects of download and derive from the $C_p - C_T$ curves in Figure 124. It is expected that the download factor used (6 percent) will be conservative for IGE operation. IGE data were determined by modifying OGE results as a function of the ratio of rotor height above the ground to rotor diameter. The factors used to correct for ground effect were obtained from analysis of hovering data for the UH-1B helicopter.

2. CEILINGS

Hovering ceilings, in and out of ground effect, for a standard and a 95°F day, for single- and twin-engine operation, are shown in Figure 127. These ceilings were obtained as follows: Power available for the appropriate condition is obtained from Figure 109. Figure 126 is entered with the power-available value to obtain a gross weight for the desired condition.

For the single-engine hover condition, there is a performance advantage in using the lower end of the hovering tip-speed range.

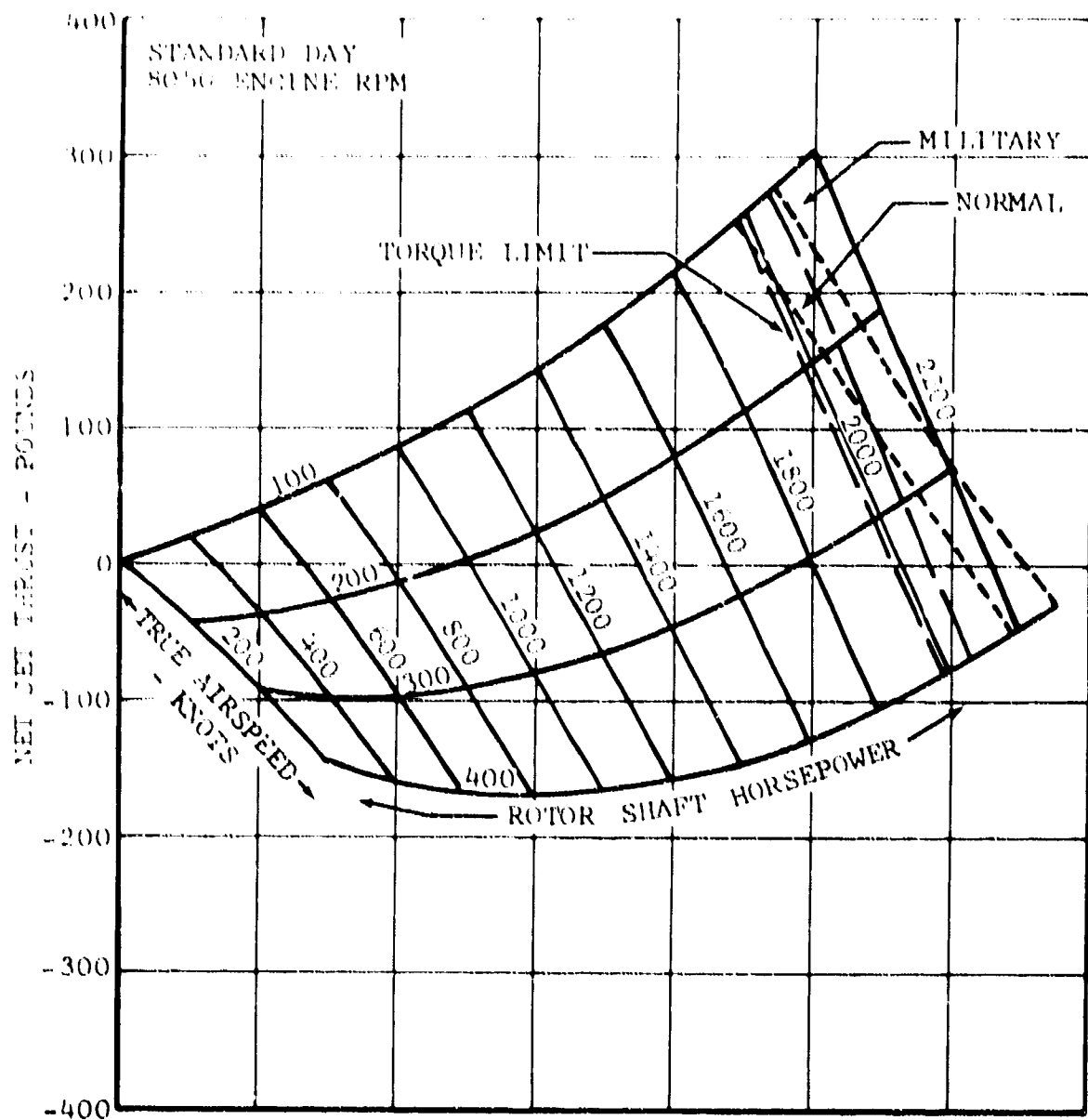


Figure 122. Net Jet Thrust Per Engine,
10,000 Feet, Twin-Engine
Operation.

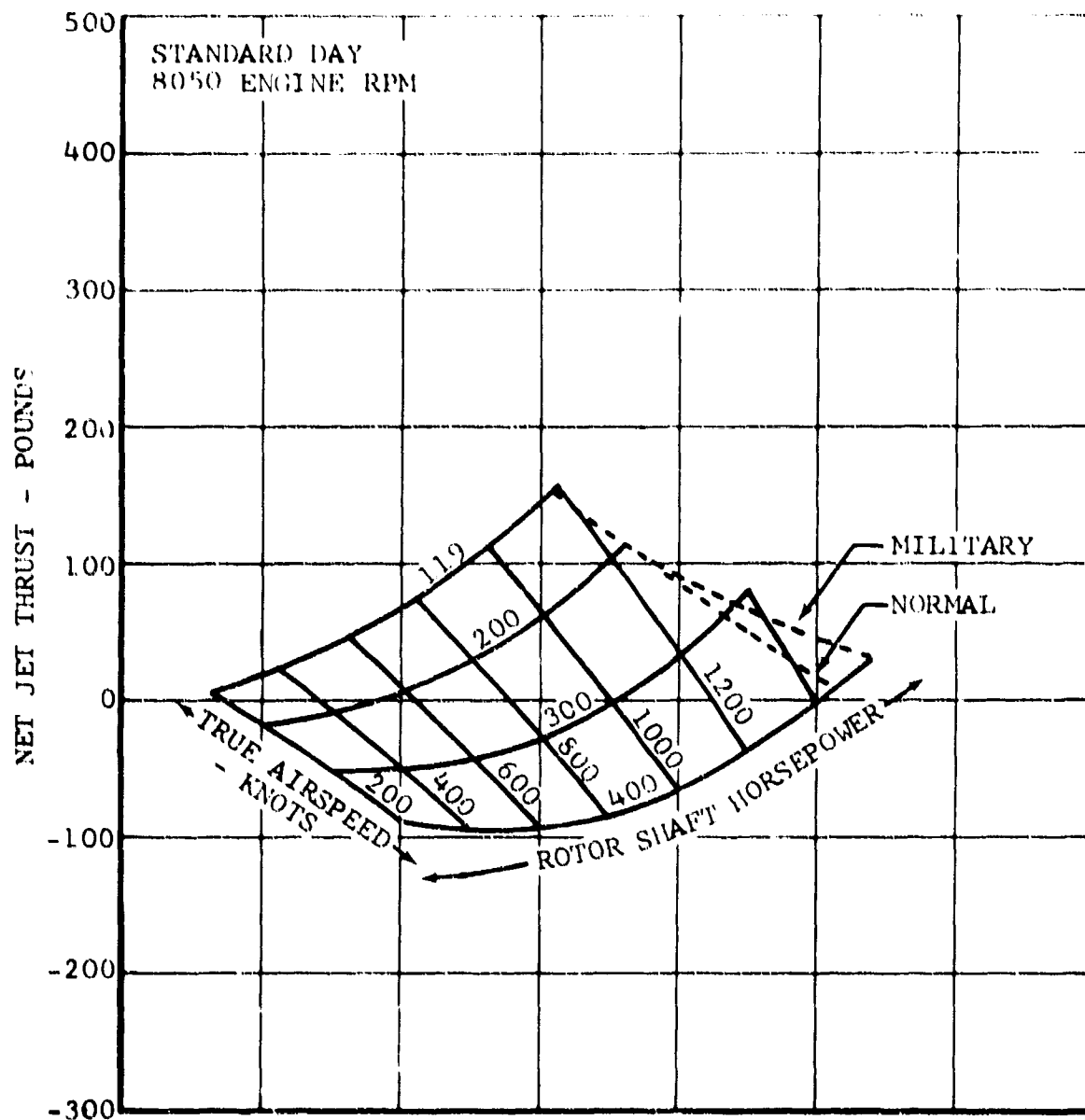


Figure 123. Net Jet Thrust Per Engine, 25,000 Feet, Twin-Engine Operation.

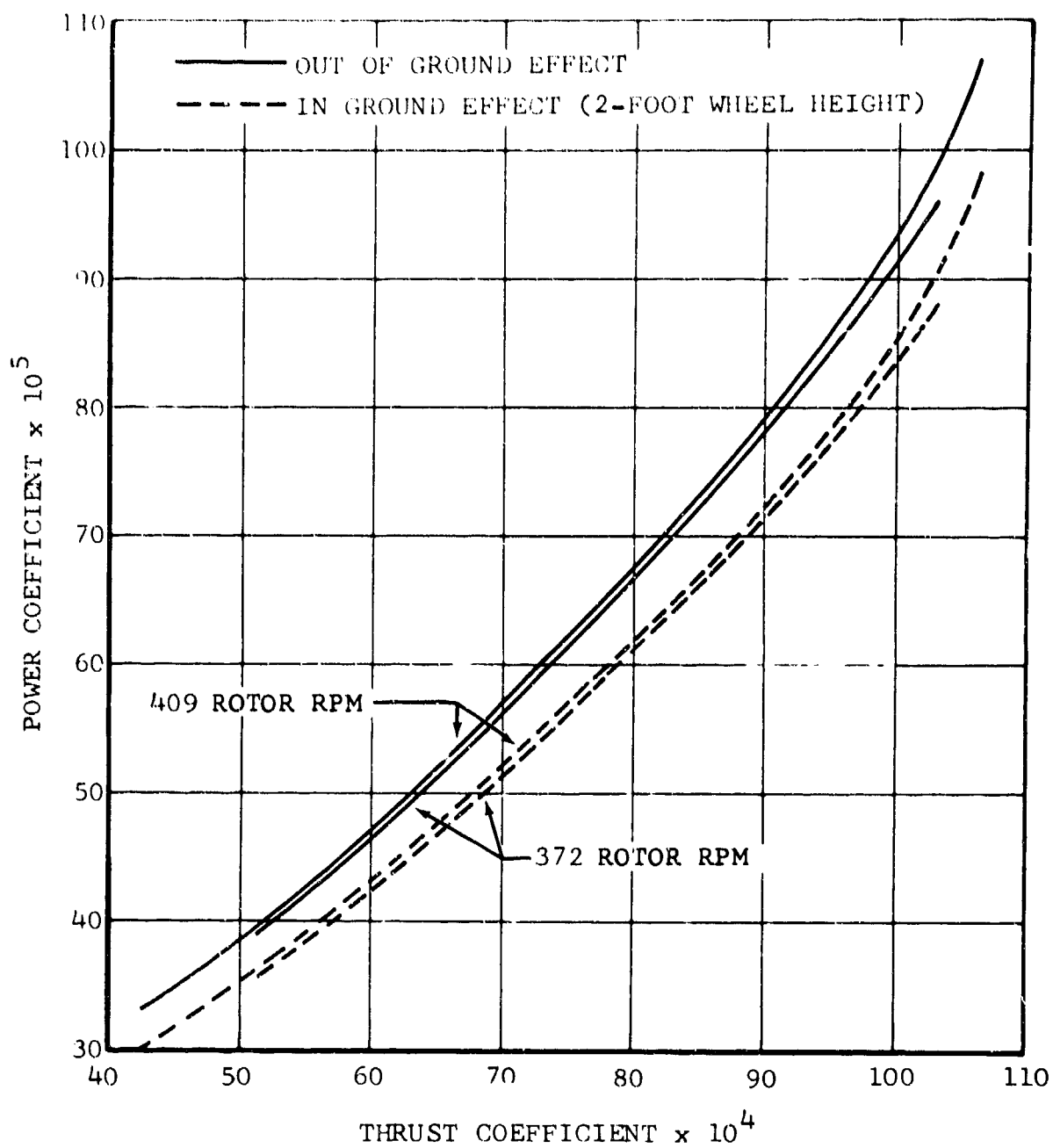


Figure 124. Nondimensional Hovering Power Required.

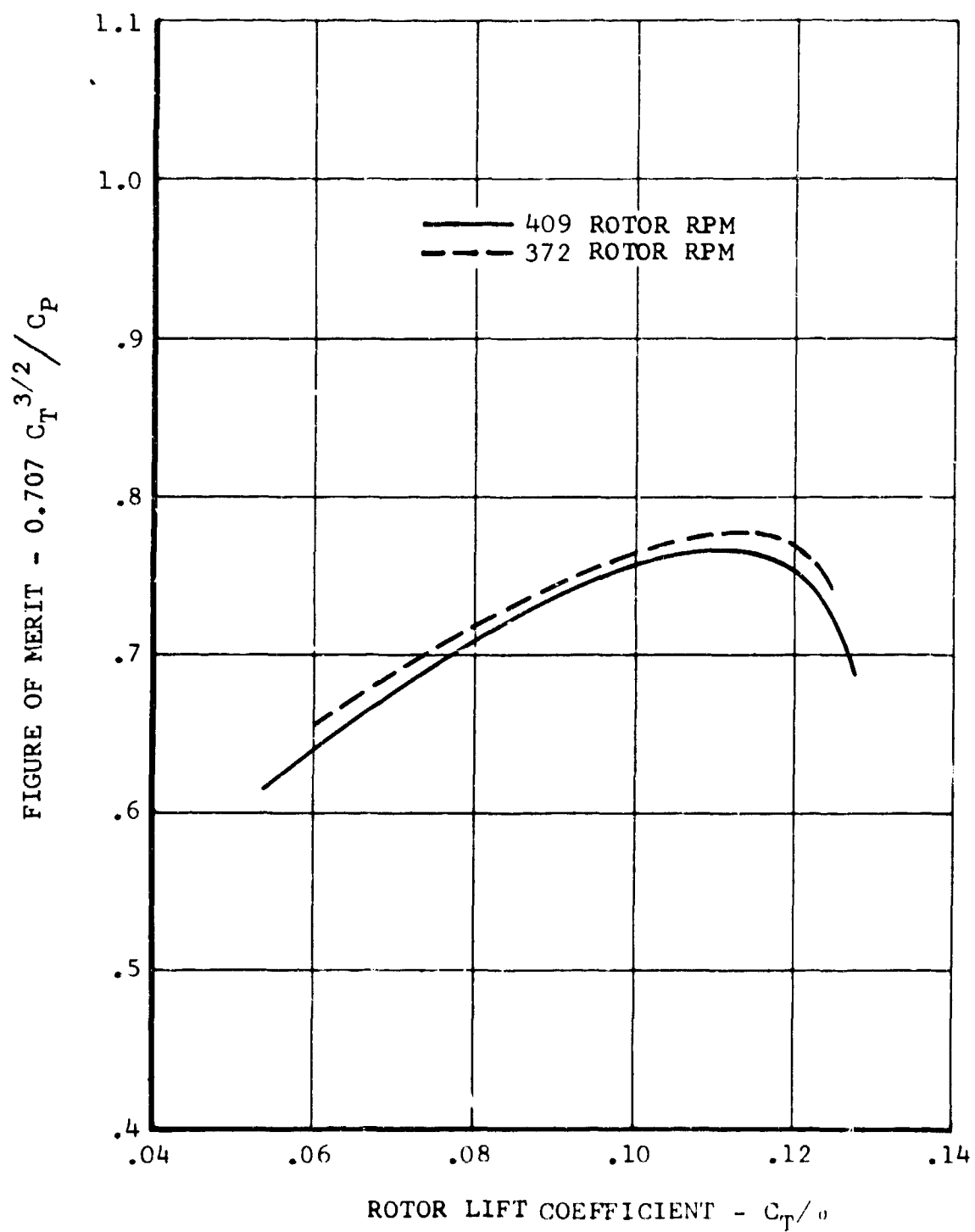


Figure 125. Rotor Figure of Merit.

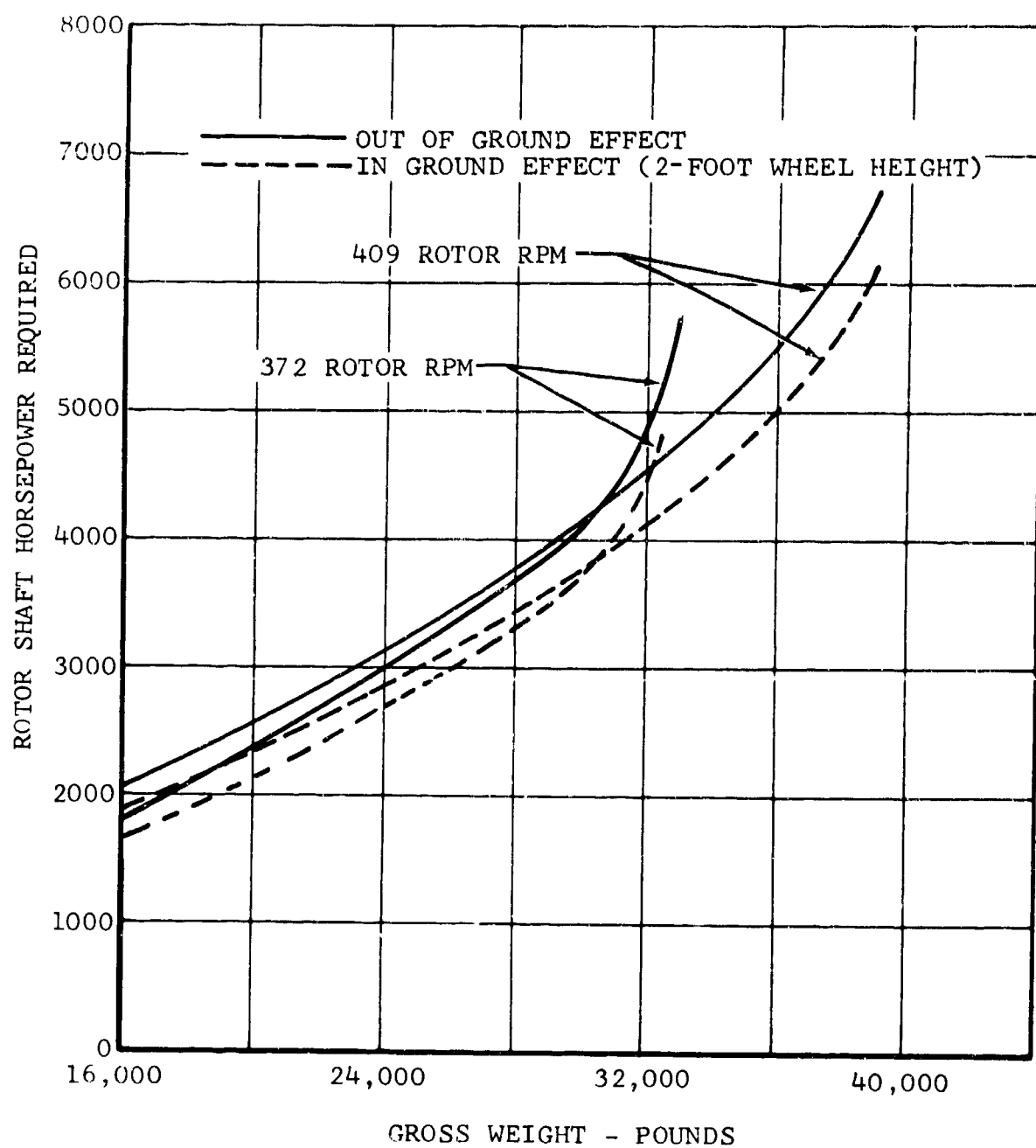


Figure 126. Dimensional Power Required to Hover.

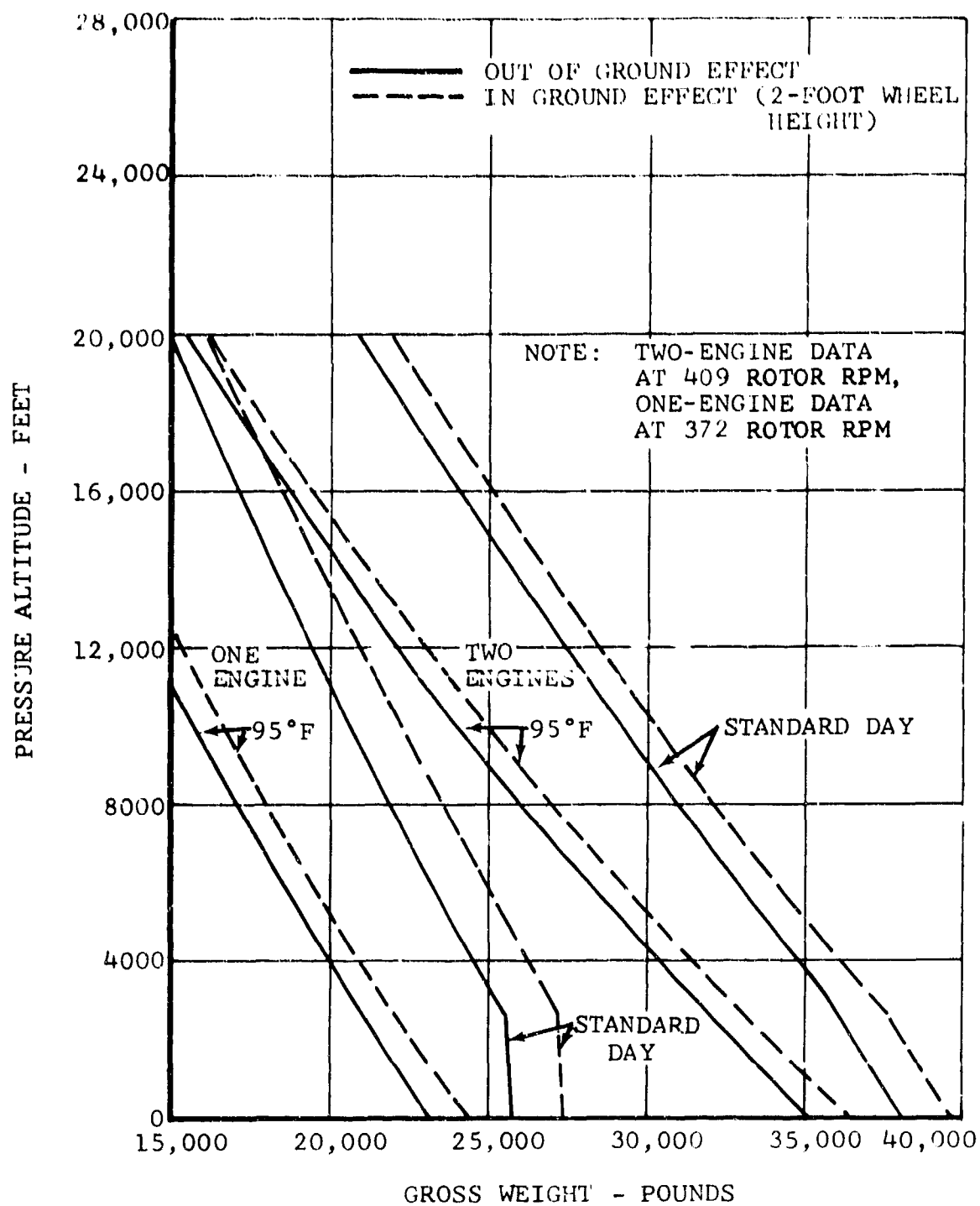


Figure 127. Hovering Ceiling.

For twin-engine hover, the upper end of the range yields better performance. Therefore, single-engine hovering ceilings are shown at a tip speed of 750 feet per second, and the twin-engine ceilings are at 825 feet per second.

3. VERTICAL CLIMB

The excess power available for vertical climb is the difference between power available and power required to hover out of ground effect. This is shown in Figure 128.

E. HELICOPTER FORWARD FLIGHT

1. POWER REQUIRED

Forward-flight curves are shown in Figures 129 and 130 for the high tip speed of 825 feet per second. For normal operation, where conversion takes place shortly after takeoff, there is no particular need to optimize power required in helicopter flight. However, if long-duration helicopter flight is desired, then use of the lower range of tip speeds may result in lower power required. The power-required figures shown are developed for the optimum rotor-mast-angle setting in the range from 0 to 20 degrees.

2. CLIMB

Climb data are shown in Figures 131 through 134 for both single- and twin-engine operation at military and normal power. The curves reflect the wing lift and drag effects for the climb condition. An overall efficiency factor of 0.85 is used. This is determined from computer analysis of several climb conditions. The equation employed is

$$R/C = \frac{\text{excess power} \times 33000 \times 0.85}{\text{gross weight}} \text{ ft/min} \quad (5)$$

Excess power is the difference between power available and power required for level flight at best-rate-of-climb speed. Best-rate-of-climb speed does not necessarily correspond to minimum-power level-flight speed, since the changes of wing lift and drag in climb affect the power required.

Substantiation of the efficiency-factor value of 0.85 is given in Table XXXII. The data are based on F35 calculations using the lift and drag associated with the airframe angle of attack in climb. Rotor downwash effects on the wing are also included. The maximum rate for design gross weight at sea level on a standard day is 6,160 feet per minute for twin-engine operation and 2,240 feet per minute for single-engine operation.

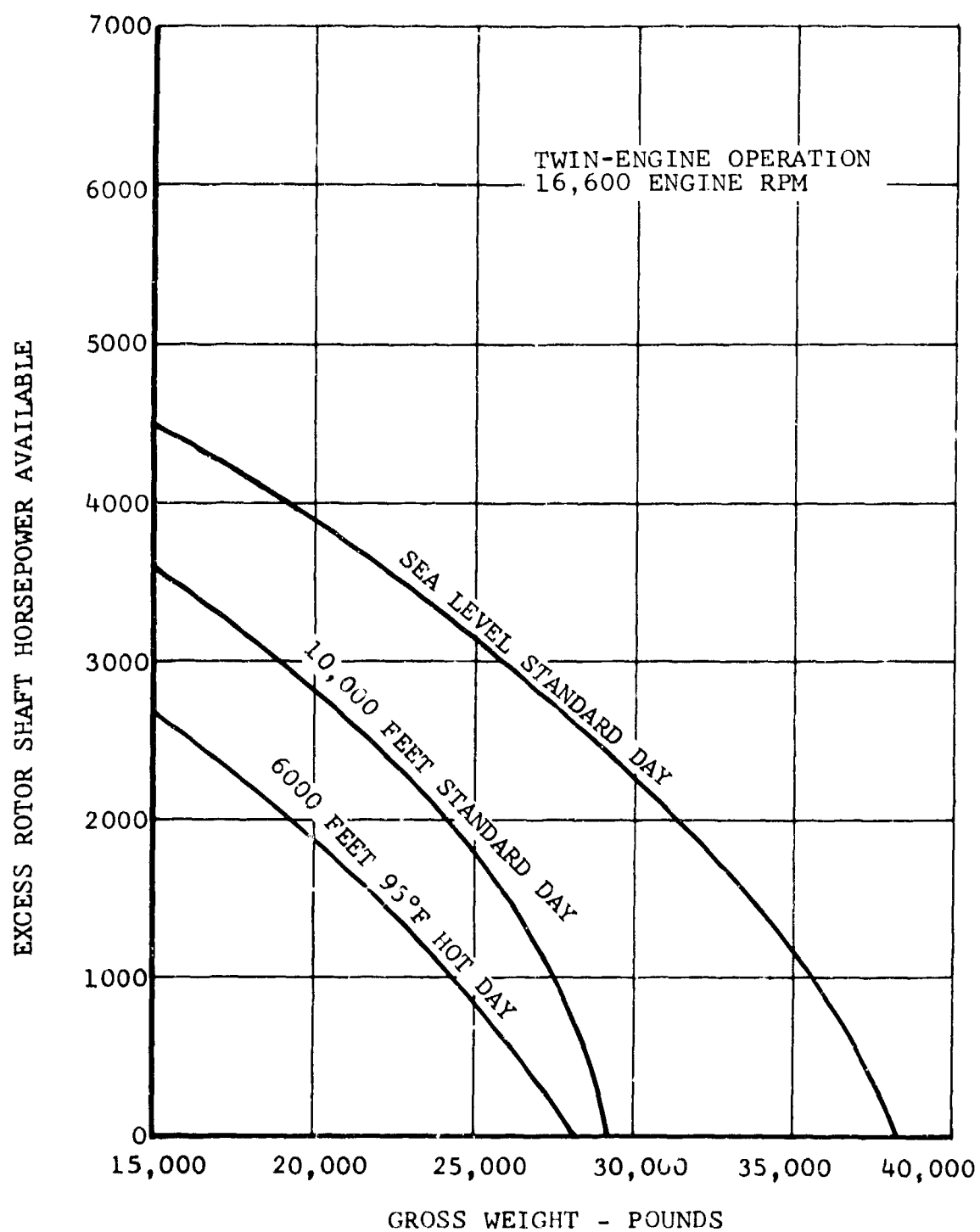


Figure 128. Excess Rotor Shaft Horsepower Available for Vertical Climb.

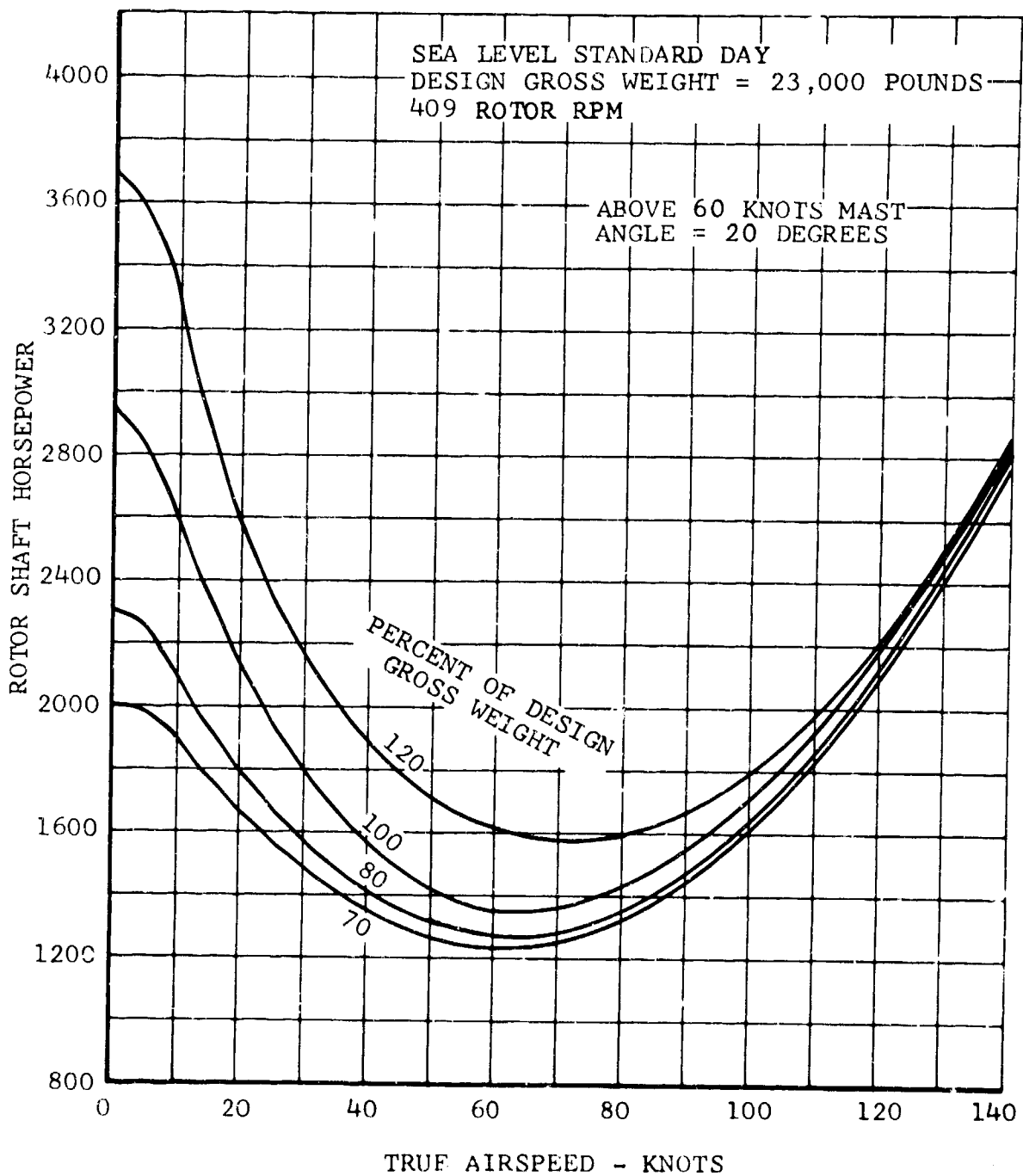


Figure 129. Helicopter Power Required, Flaps Up.

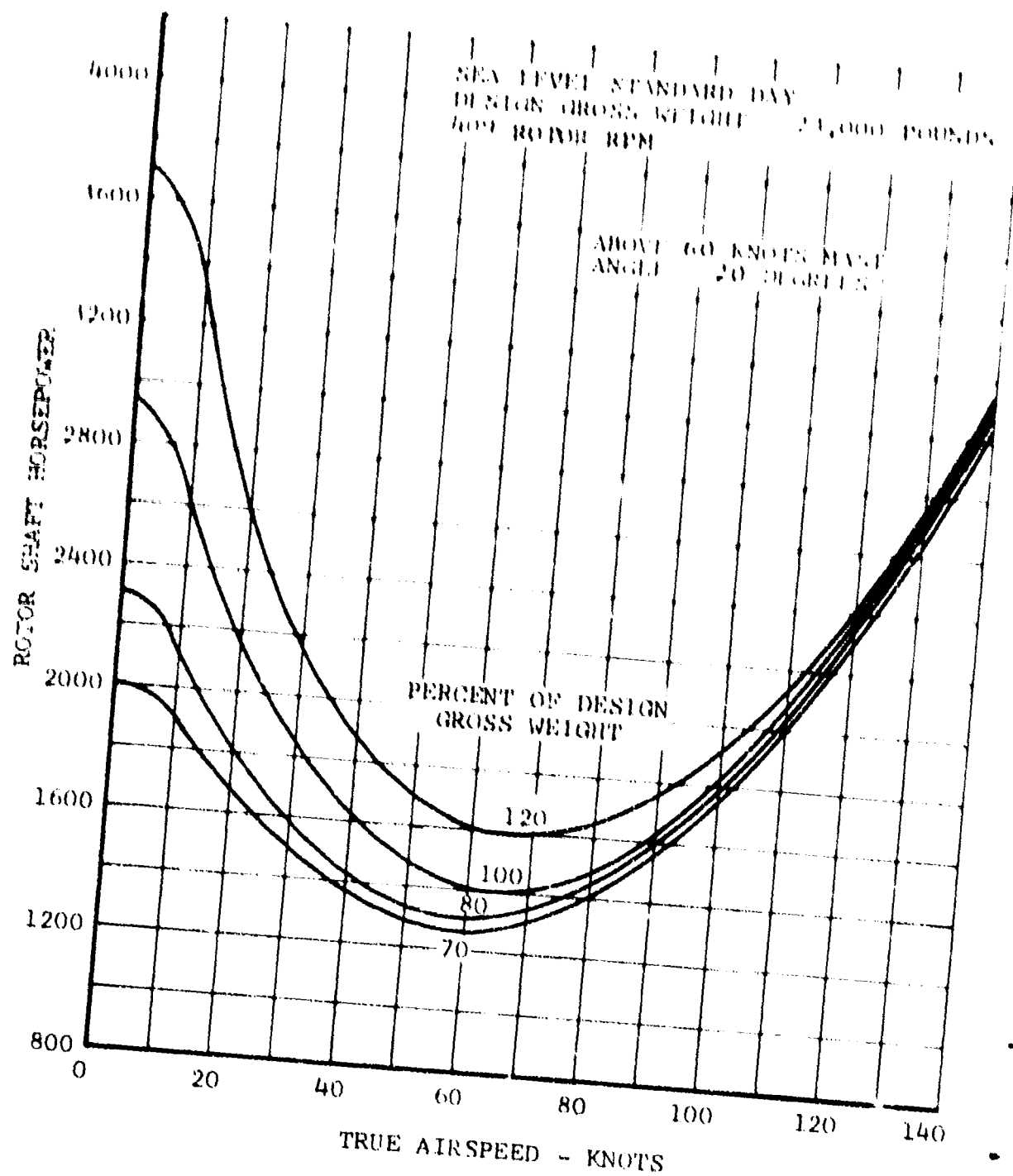


Figure 130. Helicopter Power Required, Flaps Down.

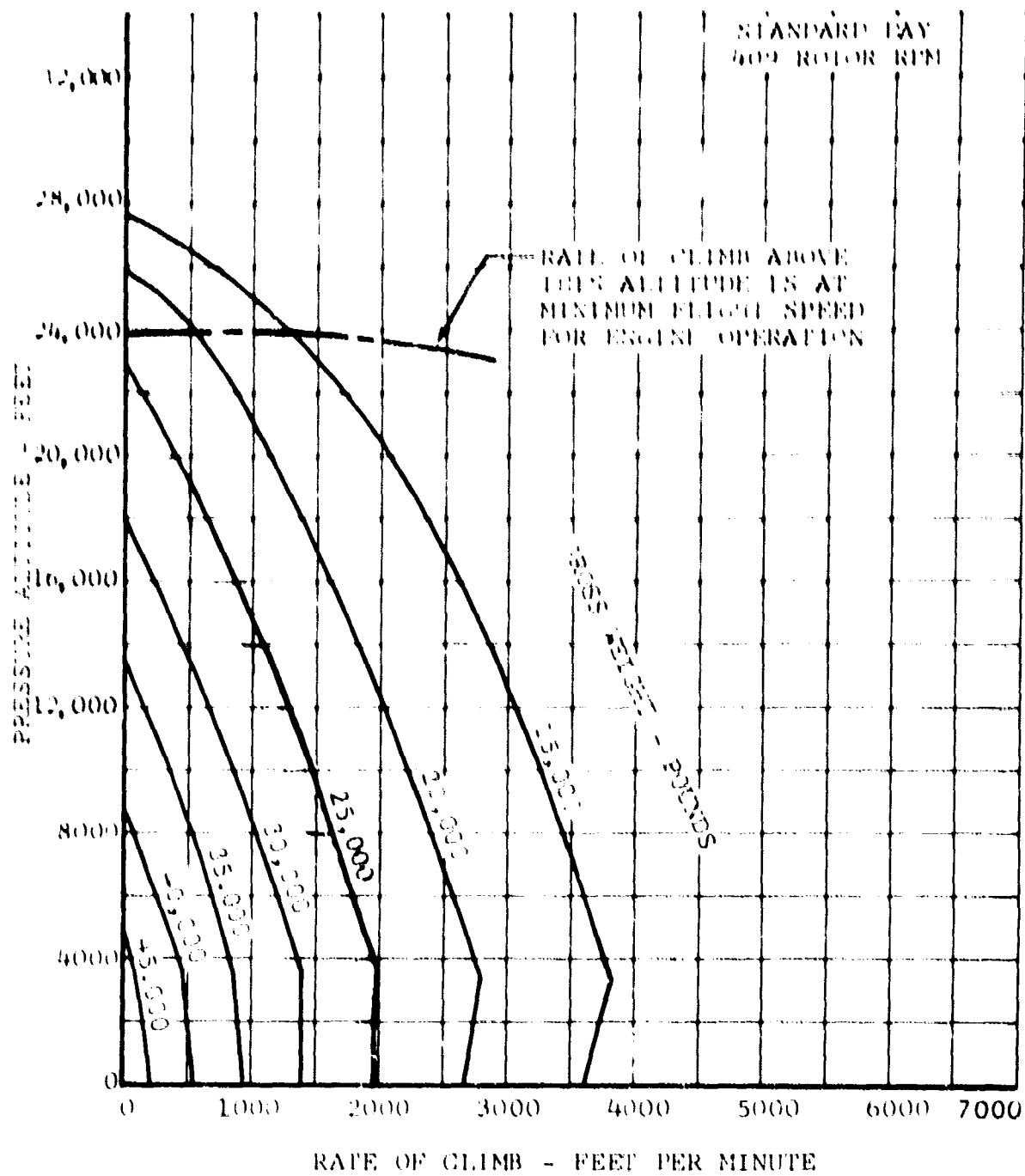


Figure 131. Maximum Rate of Climb, Military Rated Power, Single-Engine Operation, Helicopter Configuration.

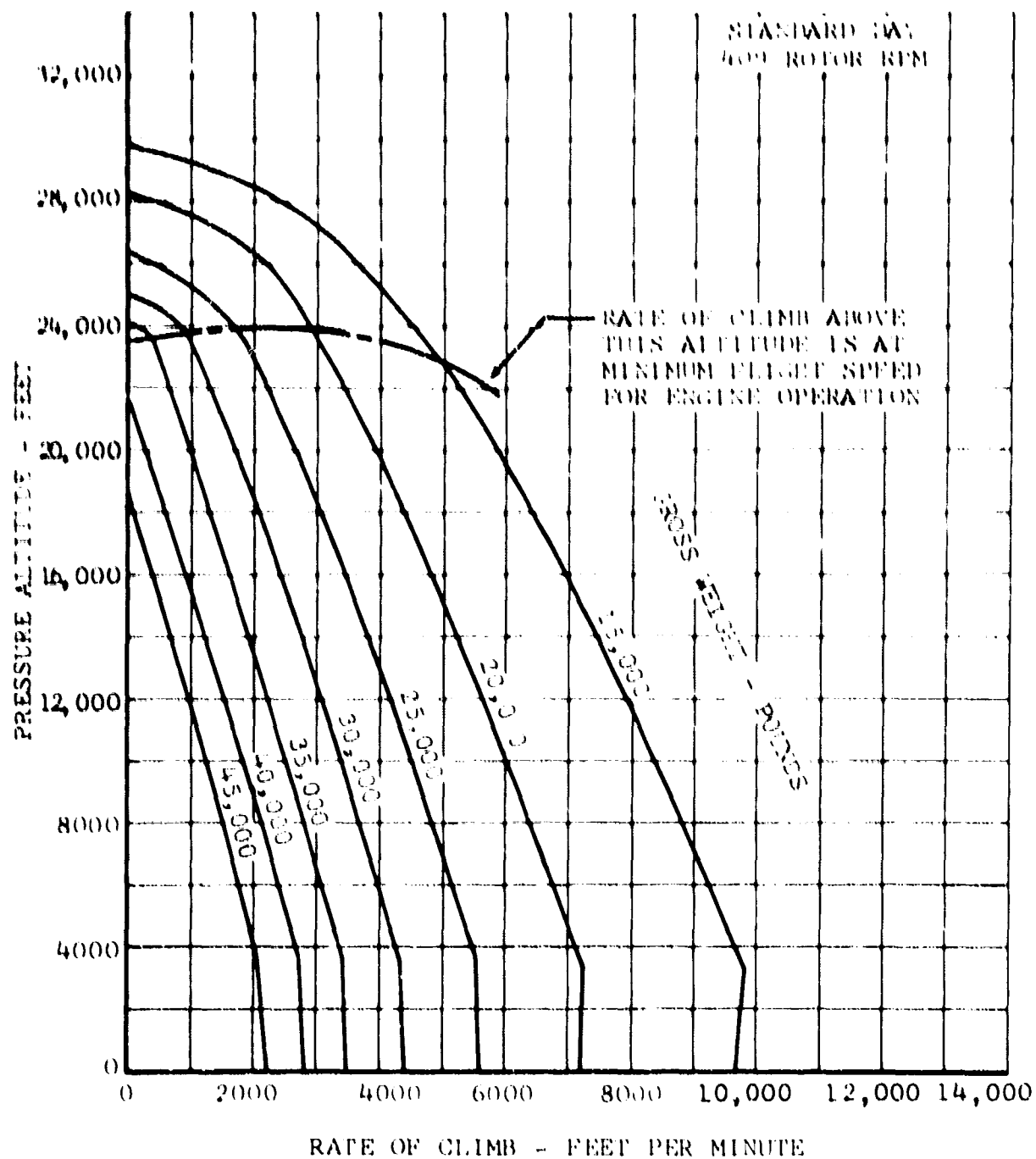


Figure 132. Maximum Rate of Climb, Military Rated Power, Twin-Engine Operation, Helicopter Configuration.

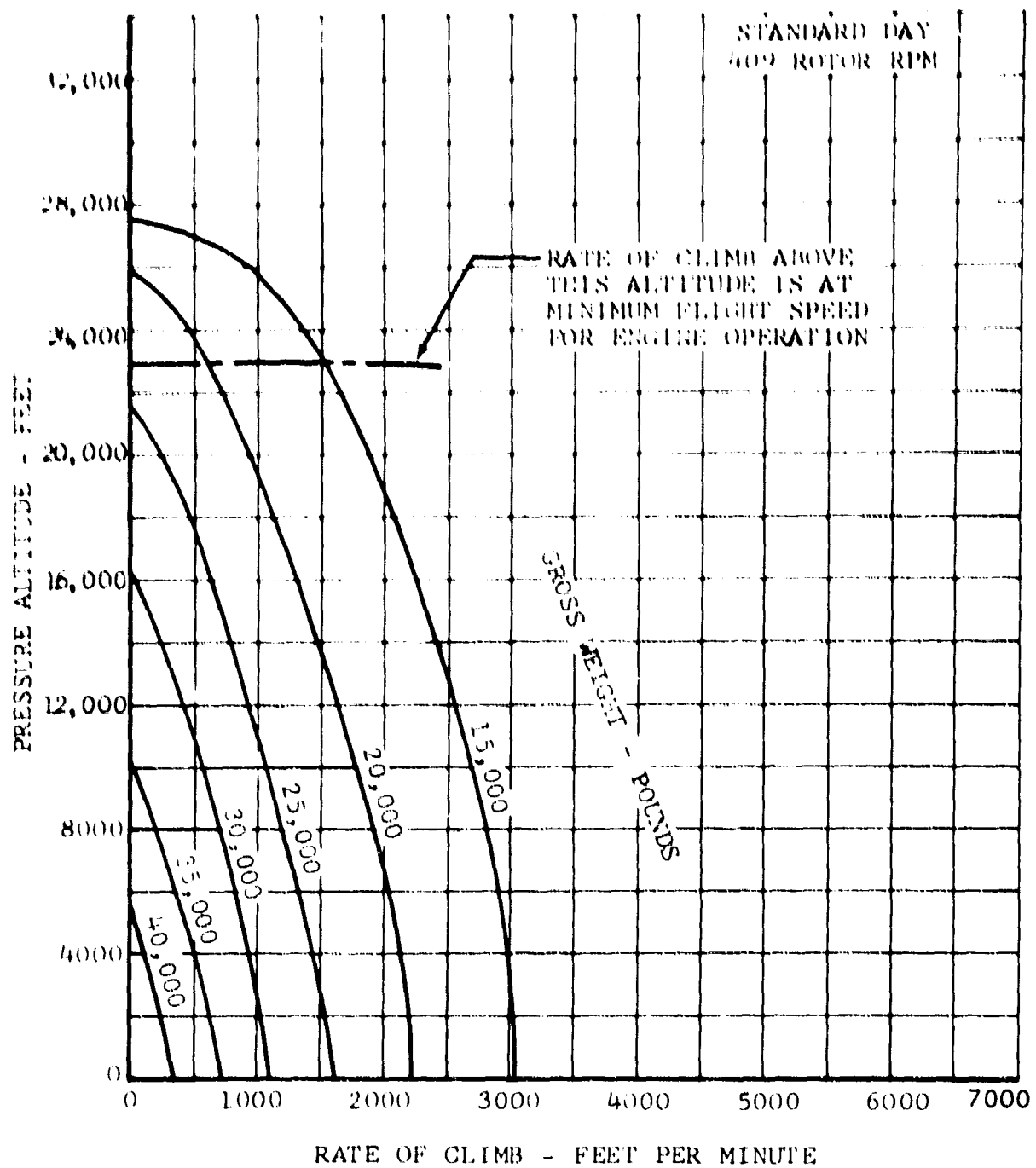


Figure 133. Maximum Rate of Climb, Normal Rated Power, Single-Engine Operation, Helicopter Configuration.

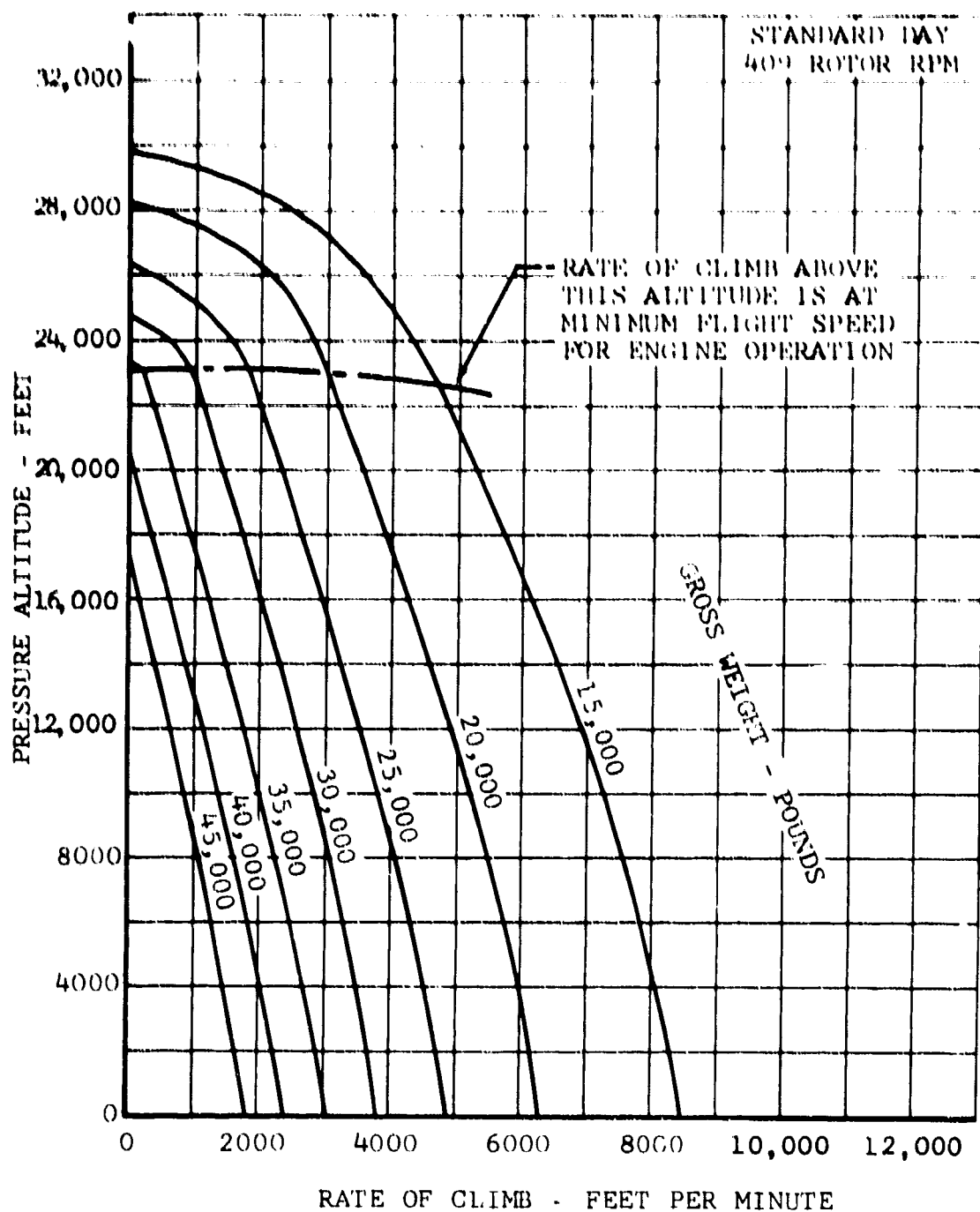


Figure 134. Maximum Rate of Climb, Normal Rated Power, Twin-Engine Operation, Helicopter Configuration.

TABLE XXXII				
SUBSTANTIATION OF CLIMB EFFICIENCY FACTOR				
①	True Airspeed (kt)	80	84	91
②	Gross Weight (lb)	23,000	23,000	23,000
③	Power Required (hp)			
③a	Level Flight	1,674	1,710	1,792
③b	Climb	6,262	6,700	2,528
④	Power to Climb (hp)			
	(= ③b - ③a)	4,588	4,990	736
⑤	Calculated Rate of Climb, (ft/min) Simple Energy, $\eta = 0.85$ $\left(= \frac{④ \times 33,000 \times 0.85}{②} \right)$	5,590	6,080	895
⑥	Calculated Rate of Climb, F35 (ft/min)	5,650	5,970	1,000

3. MAXIMUM SPEED

Maximum speed at 20 degrees conversion angle has been calculated for single-engine and full-power operation. These are plotted versus altitude at design gross weight and are shown in Figure 135. Maximum speed is 180 knots for twin-engine operation (oscillatory blade load limit) and 150 knots at sea level for single-engine operation. Both of these speeds are above the maximum allowable continuous speed for unlimited blade life shown in Figure 137. The maximum allowable continuous speed for 20 degrees mast conversion angle is found to be 135 knots from Figure 137. This airspeed is shown in Figure 135 to indicate continuous operation. Airspeeds above this value should be used only for limited operation.

F. CONVERSION

1. POWER REQUIRED

Power required versus mast angle is plotted in Figure 136 for one gross weight and airspeed. The variation shown is representative for other gross weights and conversion speeds. It is seen from the figure that there are no abrupt variations in power during the conversion.

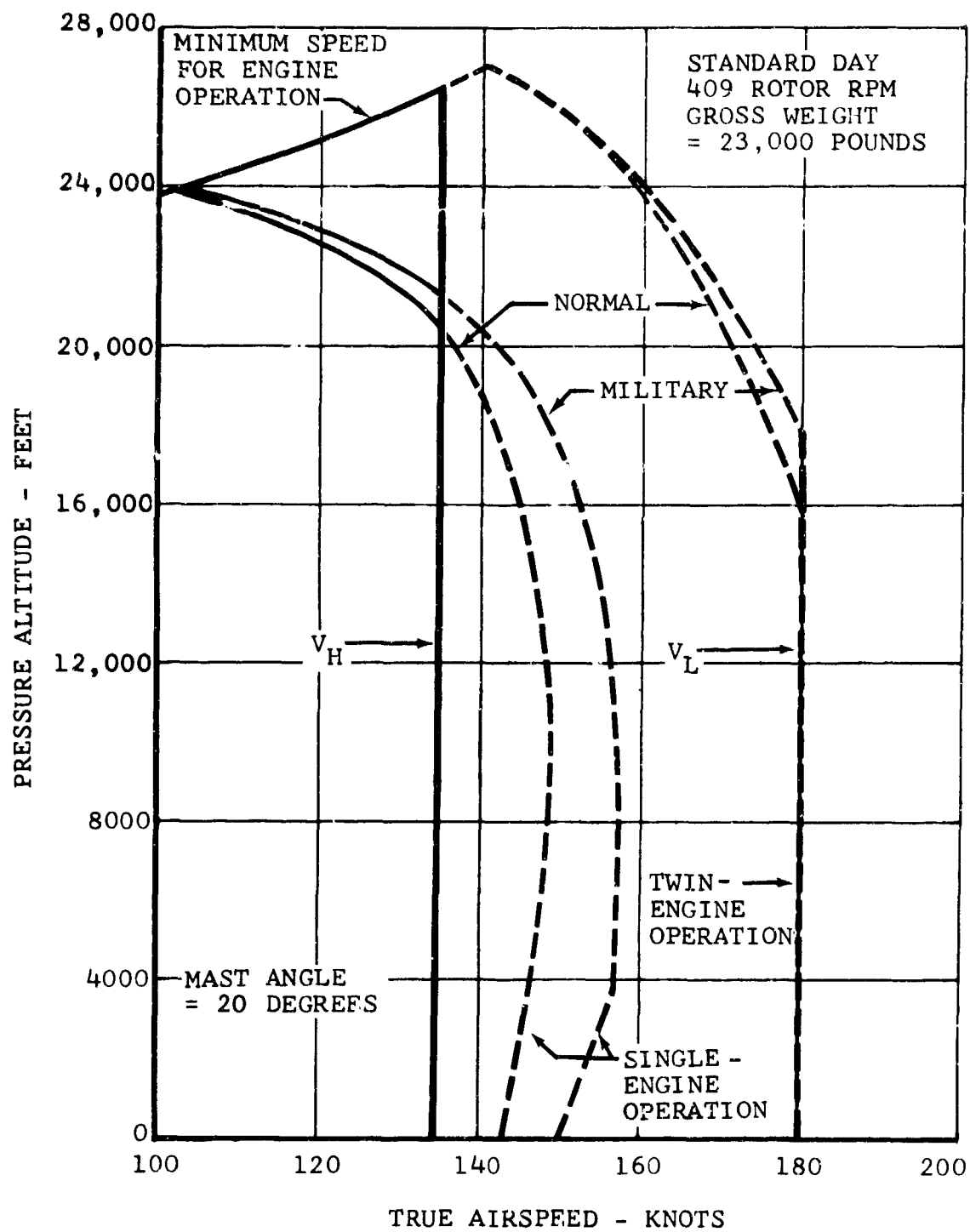


Figure 135. Maximum Speed, Helicopter Configuration.

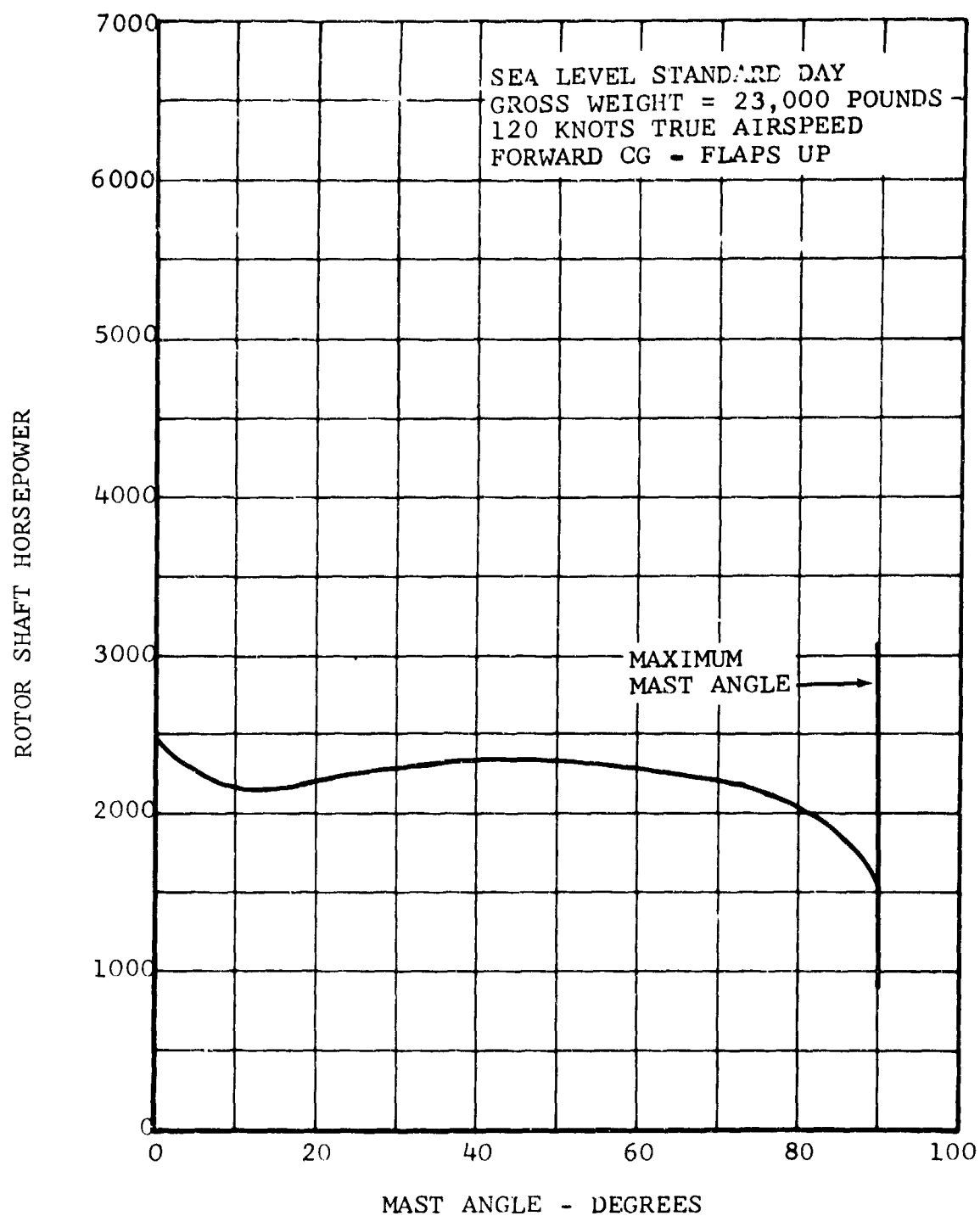


Figure 136. Conversion Power Required.

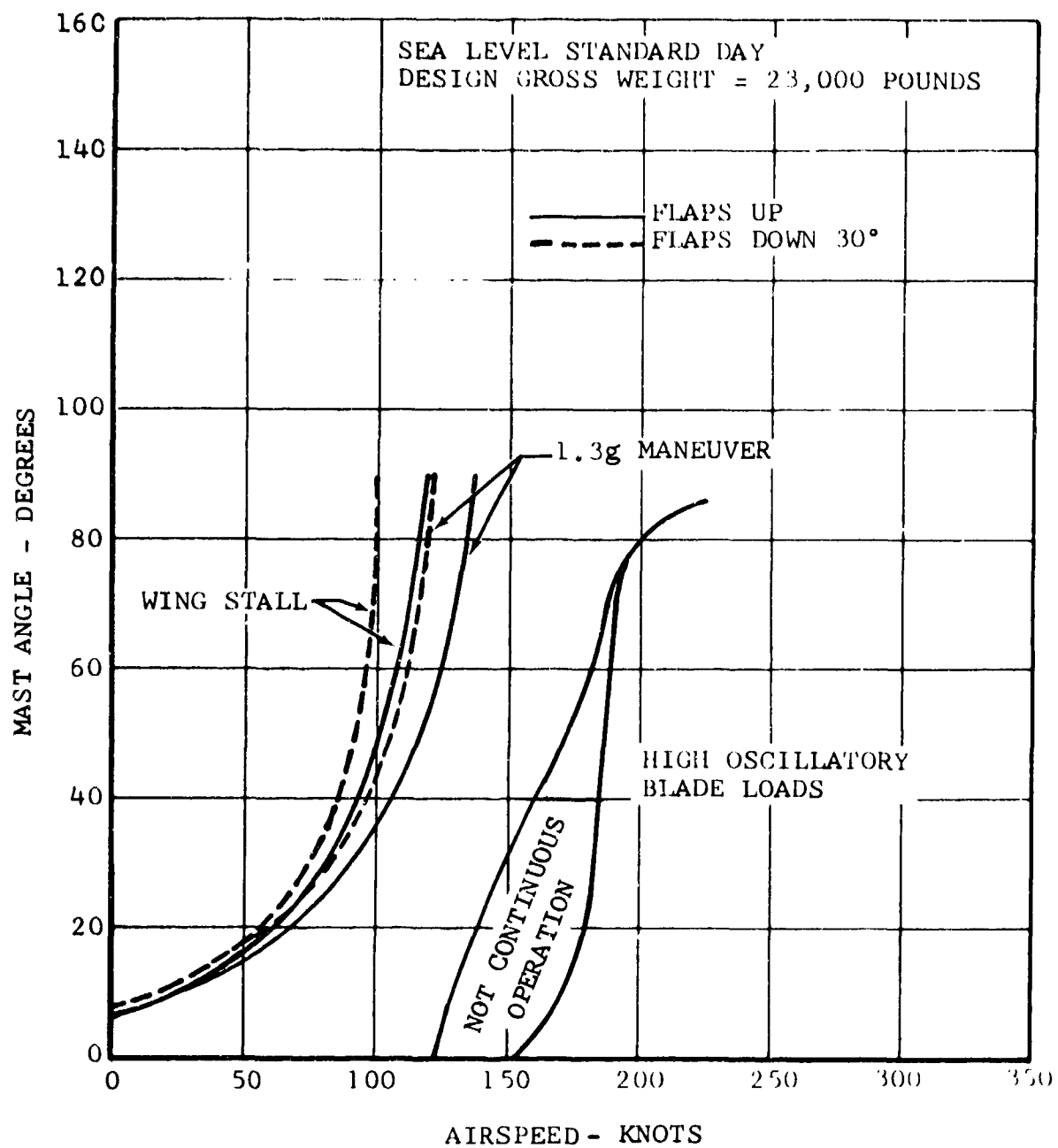


Figure 137. Conversion Corridor.

2. SPEED RANGE

The D266 conversion corridor for design gross weight at sea level is shown in Figure 137. This figure shows that conversion can be performed through a wide range of speeds. Factors involved in determining this envelope are rotor mast angle setting, rotor rpm, power available, and rotor blade oscillatory loads. The lower limit depends on wing $C_{L_{max}}$ and is shown for both the flaps-up and the flaps-down conditions. There are two upper limits presented which are based on oscillatory loads. One curve, V_H , is the speed for infinite life; the other curve, V_L , is for limited-life operation or a maximum-speed condition.

G. FIXED-WING FLIGHT

1. PROPELLER EFFICIENCY

For helicopter hovering computations, the in-plane component of induced velocity has traditionally been neglected. For the fixed-wing axial-flight condition encountered by the D266, neglect of this in-plane velocity component leads to optimistic computations of performance. Therefore, the induced angle equations are modified to account for this velocity component. The use of these more exact equations results in about a 3-percent increase in cruise power requirements. Rotor performance is presented in the form of propeller efficiency versus rotor shaft horsepower per rotor for a range of speeds, rpm, and standard-day altitudes in Figures 138 through 146.

To check the validity of the analytical techniques employed in determining performance in the D266 fixed-wing mode, a correlation study was made using NASA model propeller data. The comparison of measured and calculated efficiency is shown in Figure 147.

2. POWER REQUIRED

a. Airframe Thrust Horsepower Required (THP)

The airframe thrust horsepower required is the product of the forward-flight velocity and the propulsive thrust required to balance the drag of the airframe in steady-state level flight.

Figures 148, 149, and 150 contain results of the calculations for 70, 80, 100, and 120 percent of design gross weight, and for flight altitudes of sea level, 10,000 feet, and 25,000 feet on a standard day.

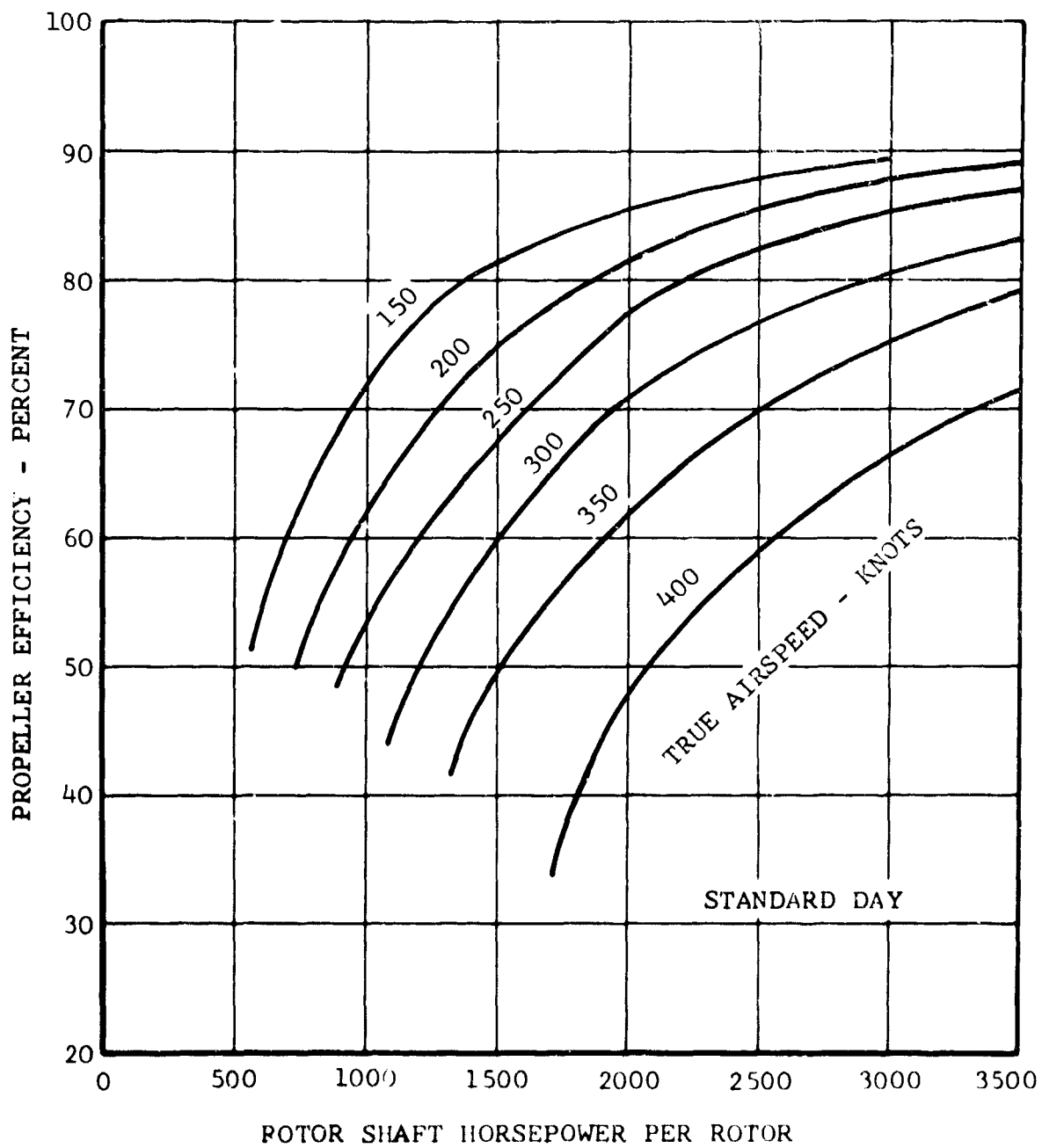


Figure 138. Propeller Efficiency,
297 RPM, Sea Level.

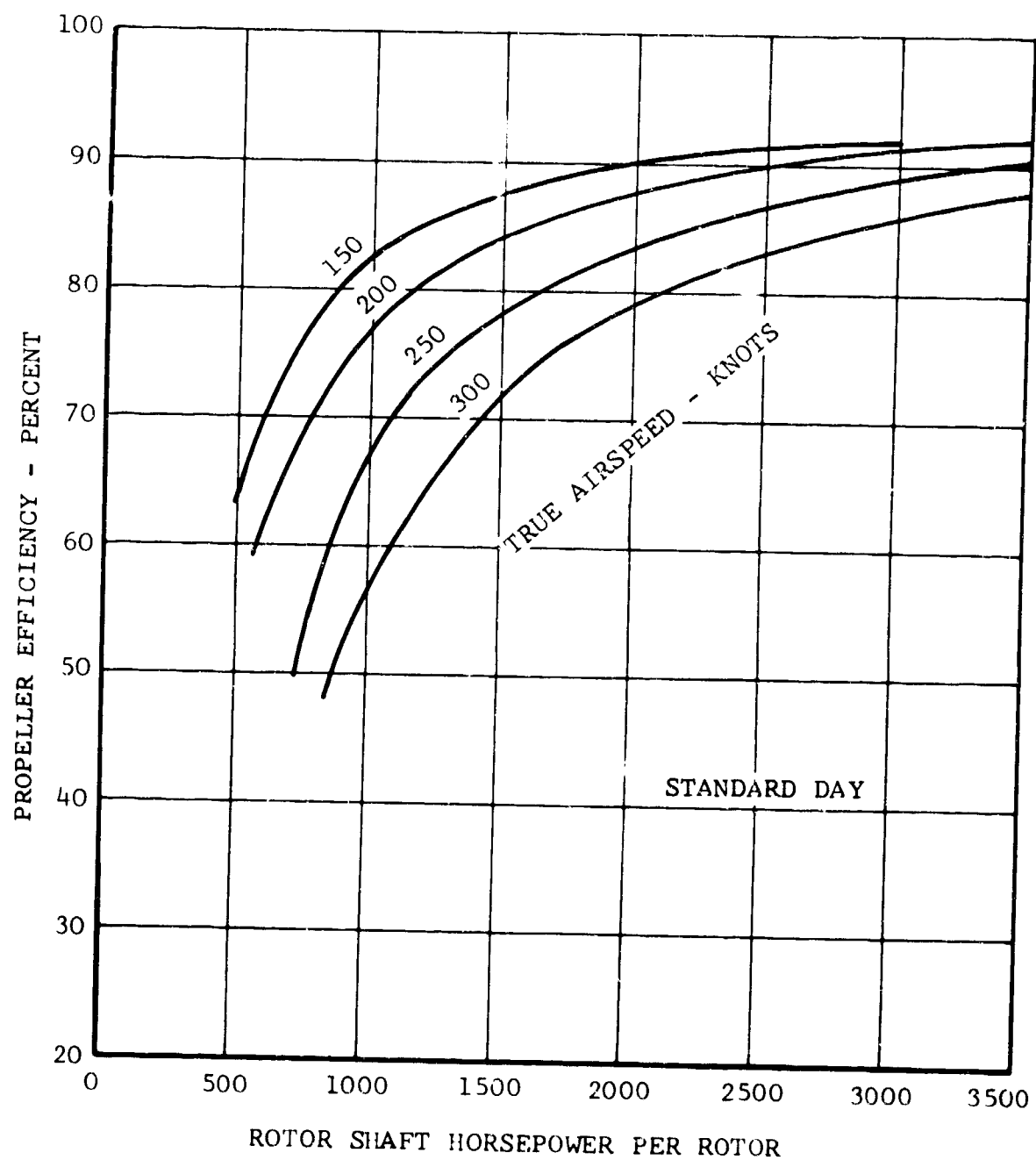


Figure 139. Propeller Efficiency,
248 RPM, Sea Level.

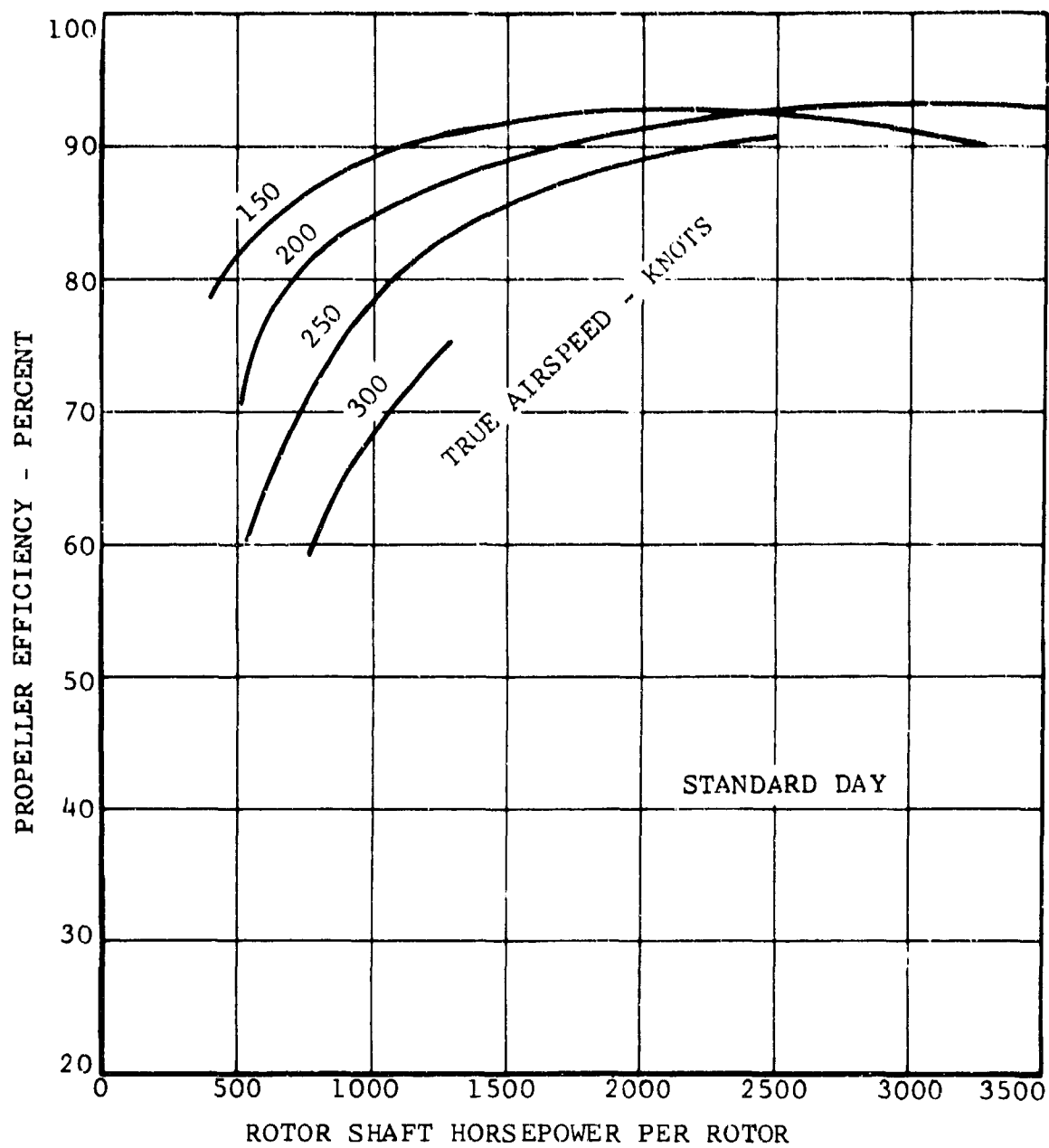


Figure 140. Propeller Efficiency,
198 RPM, Sea Level.

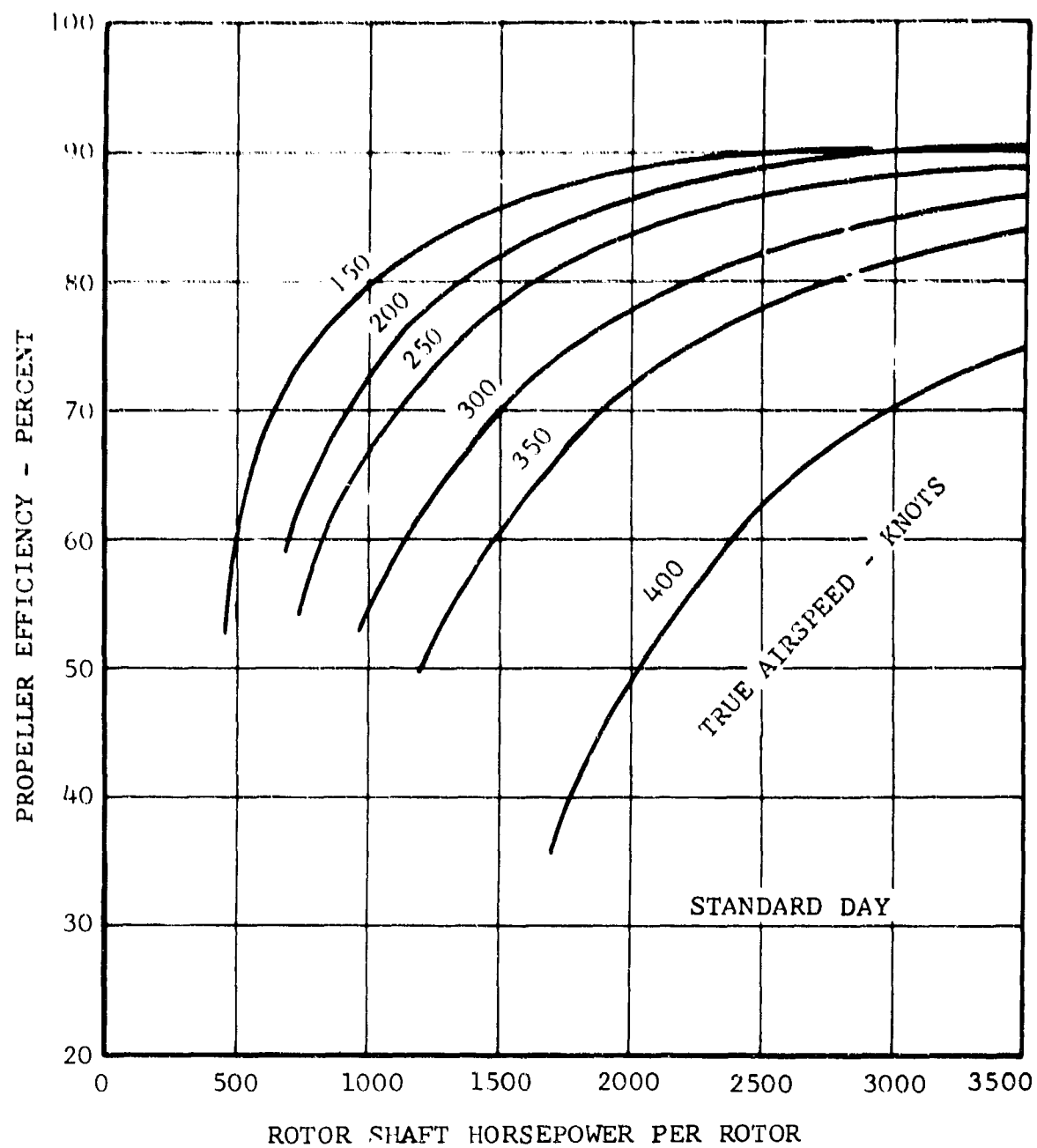


Figure 141. Propeller Efficiency,
297 RPM, 10,000 Feet.

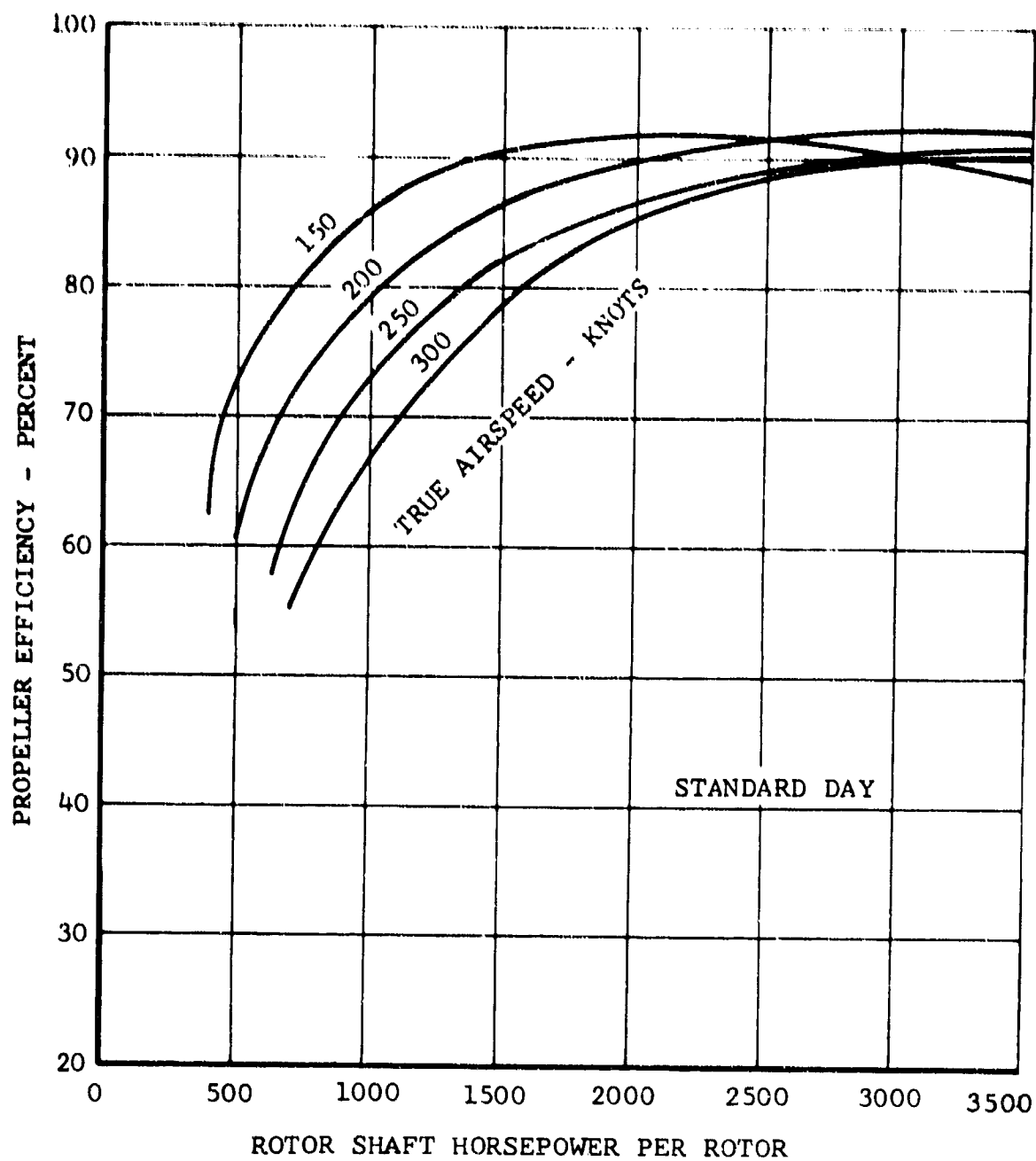


Figure 142. Propeller Efficiency,
248 RPM 10,000 Feet.

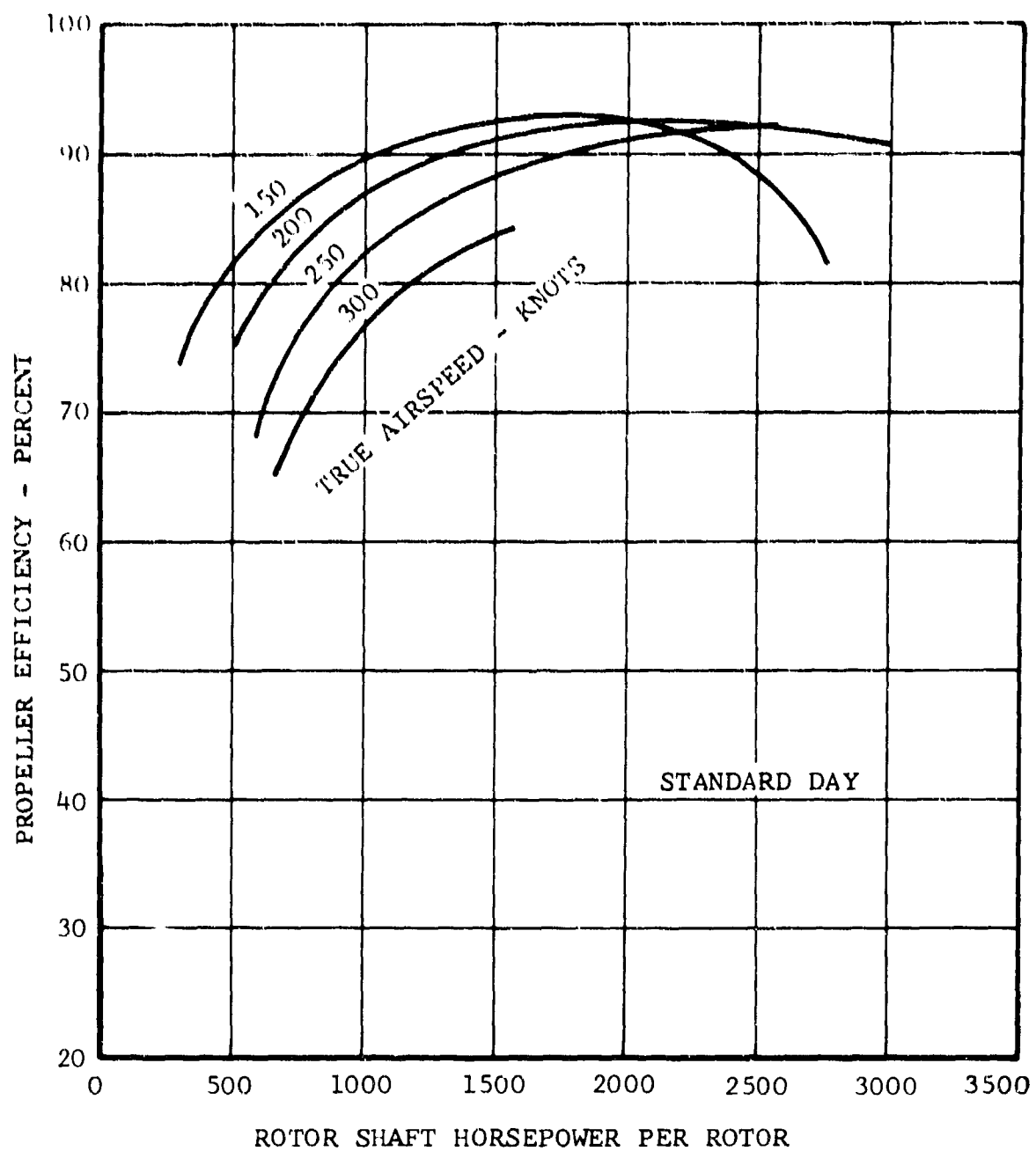


Figure 143. Propeller Efficiency,
198 RPM, 10,000 Feet.

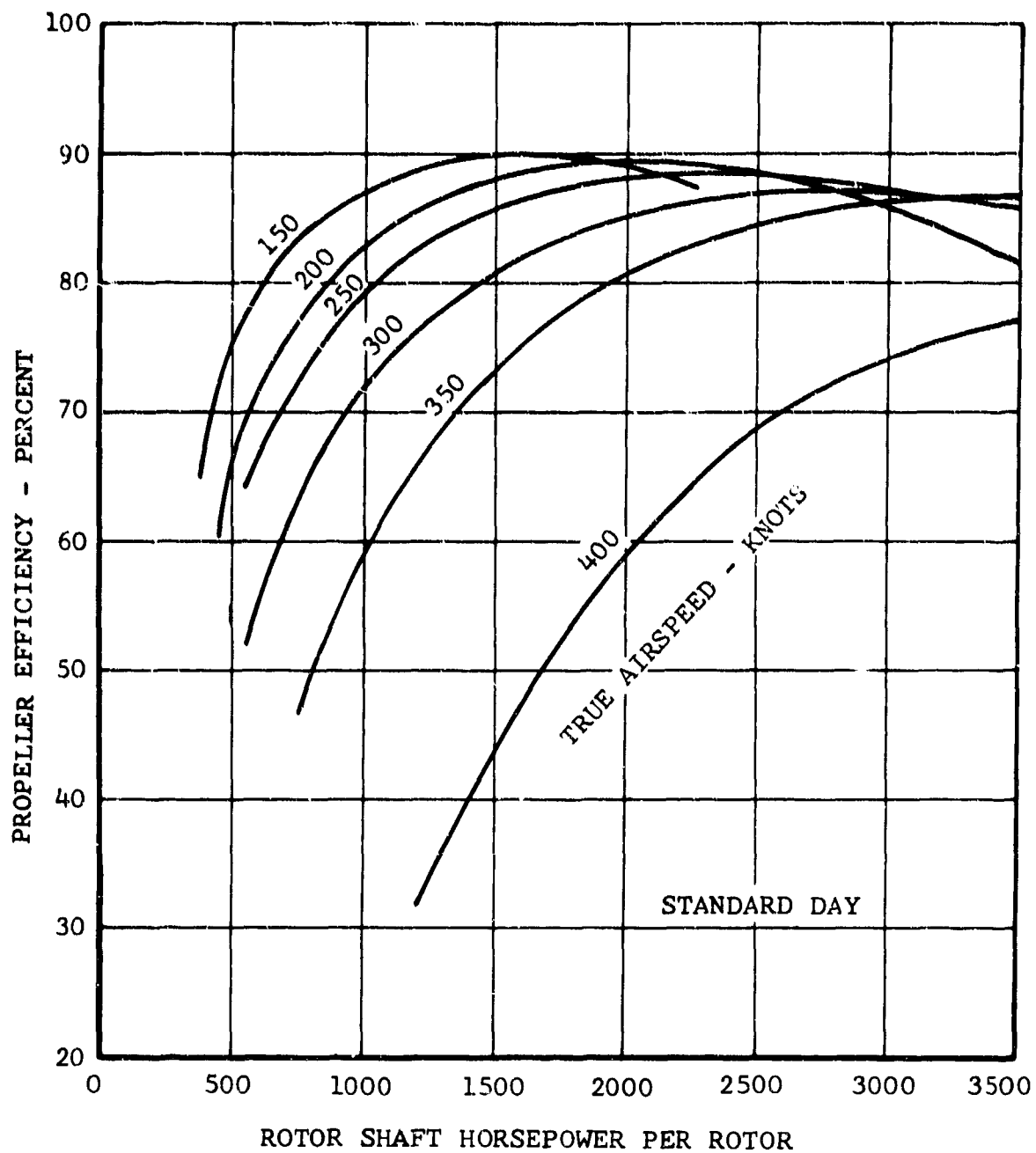


Figure 144. Propeller Efficiency,
297 RPM, 25,000 Feet.

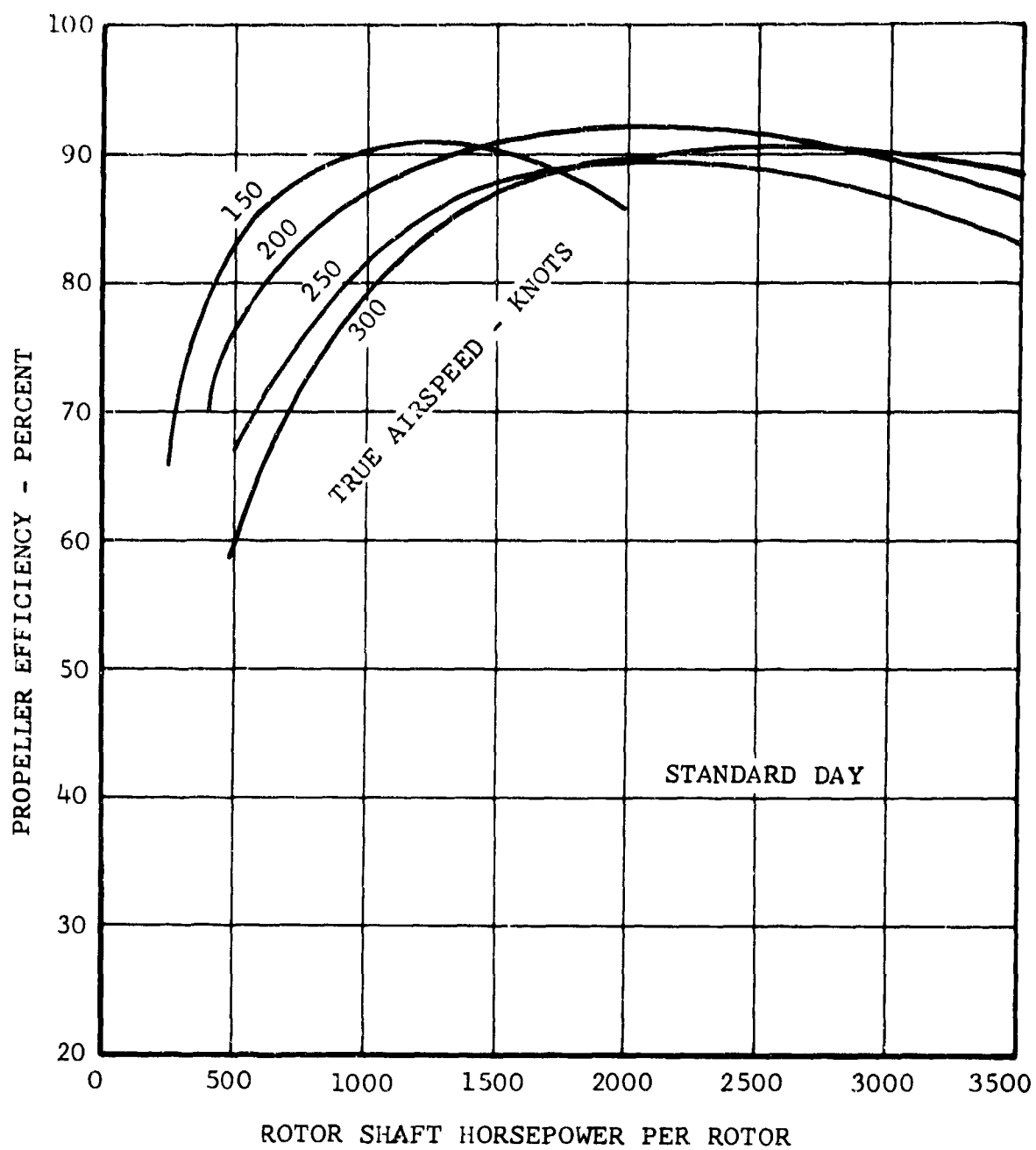


Figure 145. Propeller Efficiency,
248 RPM, 25,000 Feet.

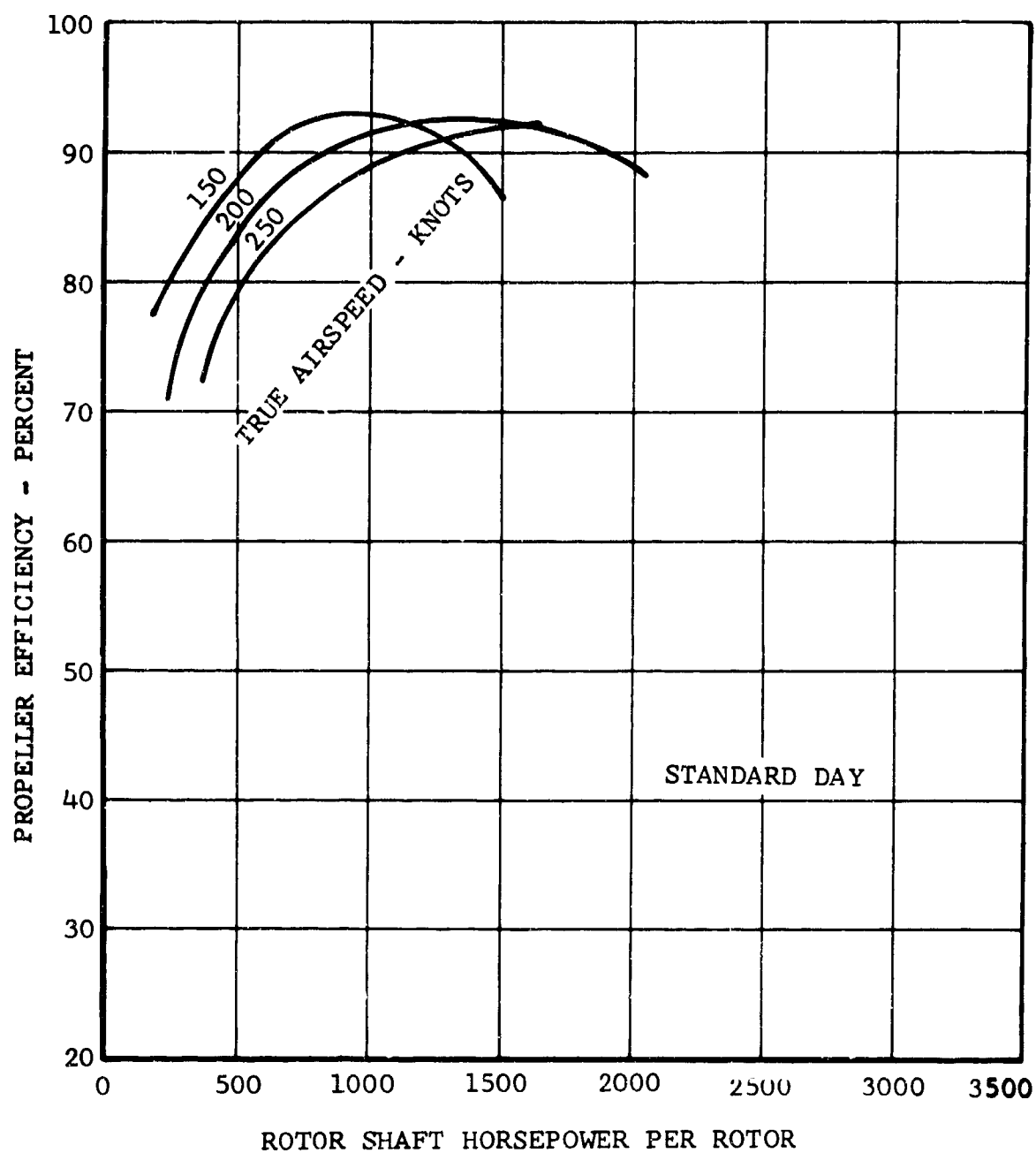


Figure 146. Propeller Efficiency,
198 RPM, 25,000 Feet.

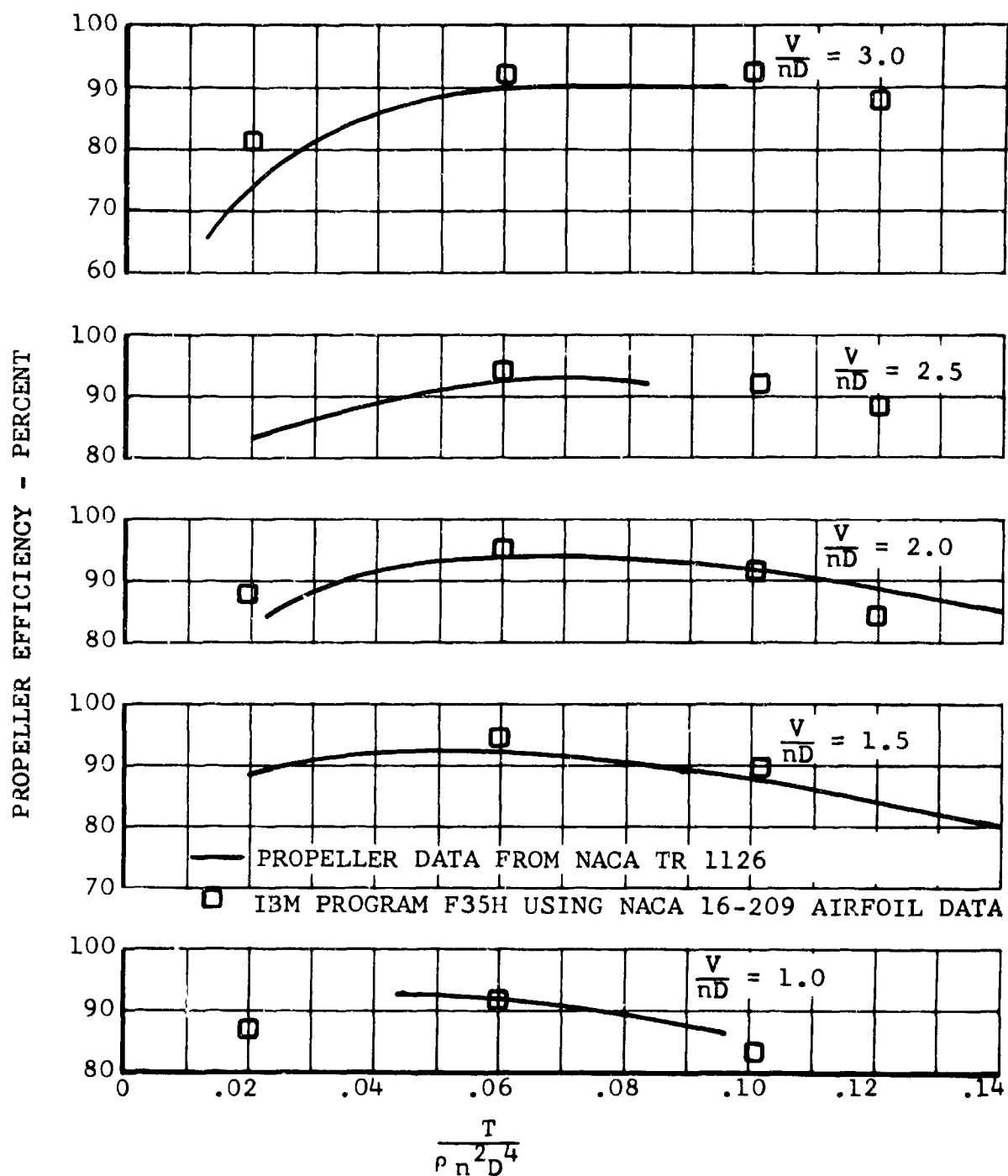


Figure 147. Propeller Efficiency Correlation.

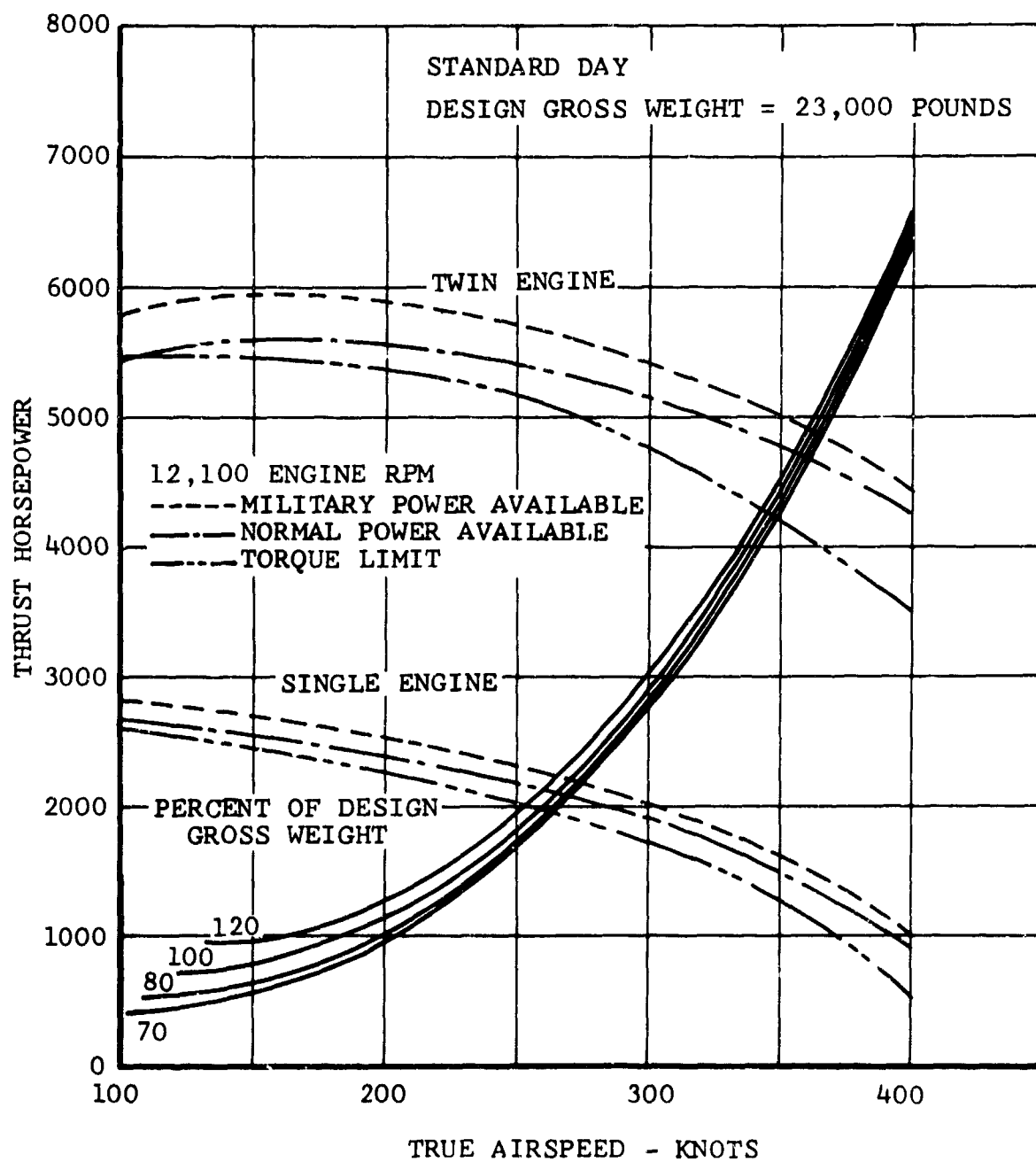


Figure 148. Thrust Horsepower Required, Sea Level.

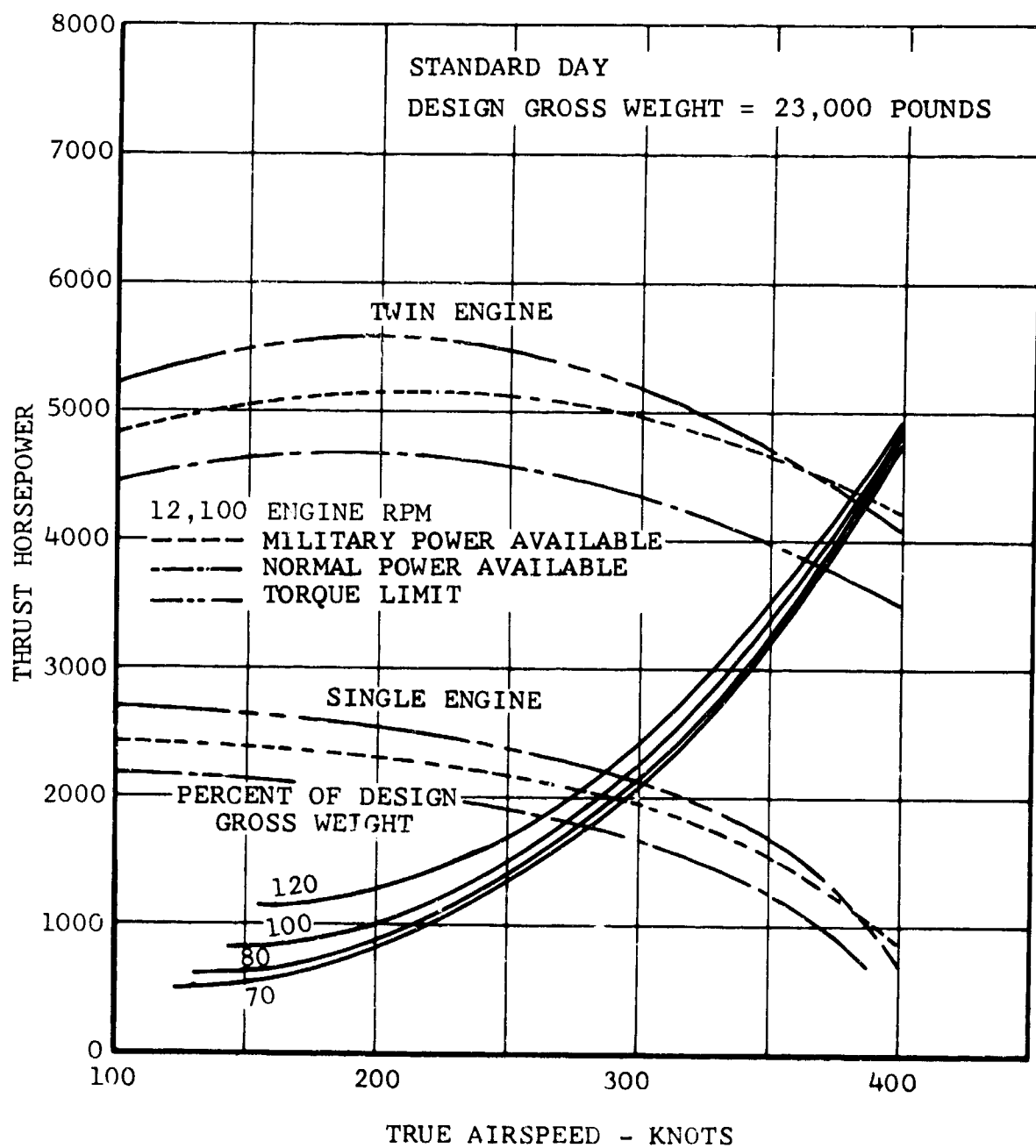


Figure 149. Thrust Horsepower Required, 10,000 Feet.

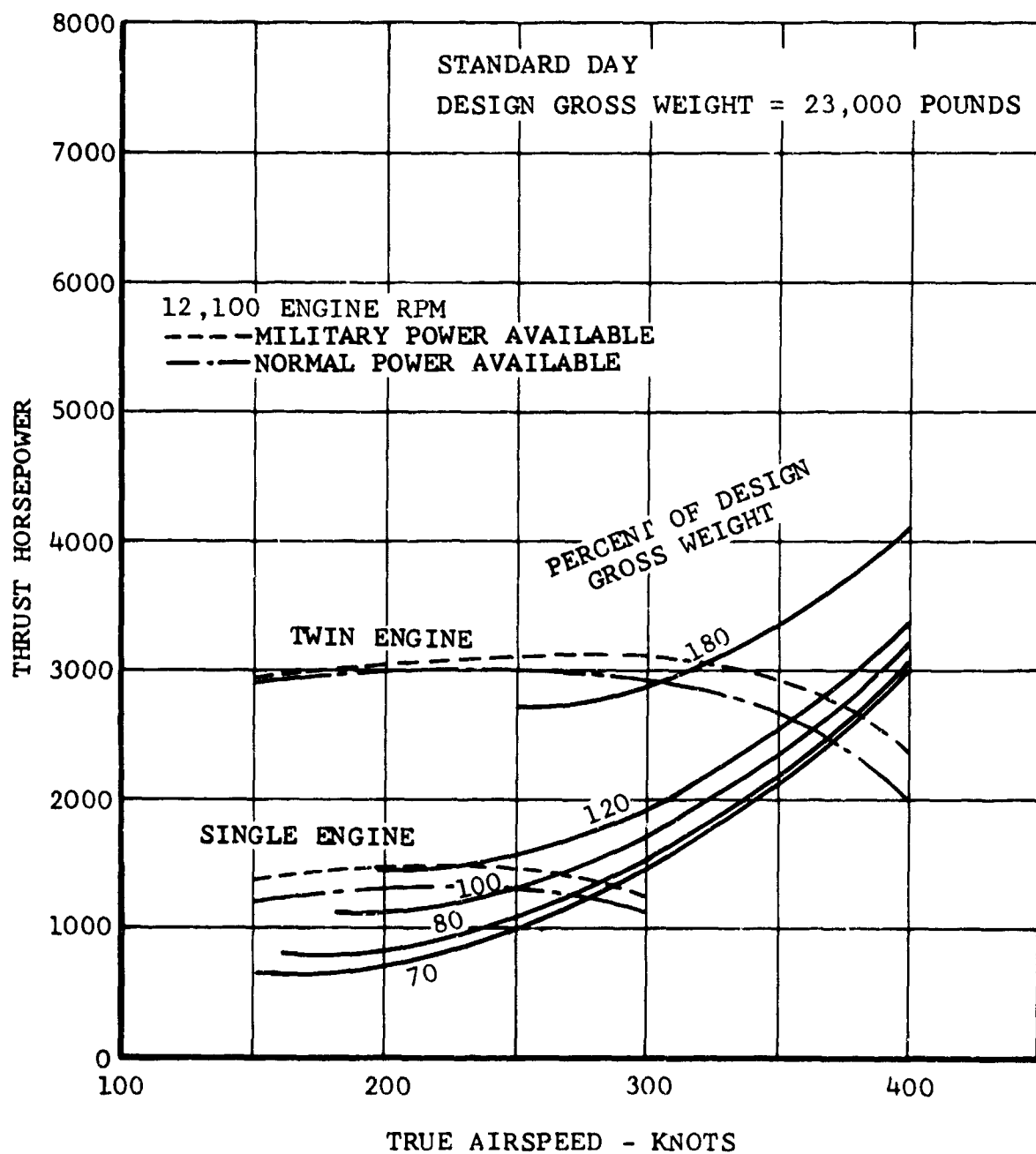


Figure 150. Thrust Horsepower Required, 25,000 Feet.

b. Net Engine Jet Thrust Horsepower per Engine (THP_{FN})

To determine the actual thrust and the thrust horsepower which the rotors are required to produce, it is necessary to include the contribution of the engine jet exhaust thrust. This thrust may be positive or negative and may add or subtract from the airframe drag.

Results are plotted in Figures 151 through 153 in a form convenient for use in determination of total airframe and engine jet thrust horsepower required. Data are shown for ranges of airspeed and thrust horsepower, for three altitudes (sea level, 10,000, and 25,000 feet), and for a single engine.

The curves are entered at the airframe thrust horsepower required per engine ($1/2$ THP for normal flight with both engines) at the true airspeed, and the net jet thrust horsepower per engine is read.

c. Total Airframe and Engine Jet Thrust Horsepower per Rotor (THP_{TOT})

This is the sum of the airframe thrust horsepower required and the engine jet thrust horsepower.

d. Rotor Shaft Horsepower Required per Rotor (SHP)

Including the propeller efficiencies of the rotors in the fixed-wing mode, the rotor shaft horsepower required to produce the total airframe and engine jet thrust horsepower is calculated and presented in Figures 154, 155, and 156.

Plots are made as a function of true airspeed and for the three flight altitudes. These data are used together with fuel flow data in Figures 118 through 120 to calculate specific range.

e. Total Engine Shaft Horsepower Required (SHP_{ENG})

With the mechanical transmission efficiency and the accessory power required included, the total engine shaft horsepower required, for both rotors, is shown in Figure 157 for 70, 80, 100, and 120 percent of design gross weight. These data are used in determining the overall aircraft lift-to-drag ratios in the fixed-wing flight mode.

3. LIFT/DRAG RATIO

Overall lift-to-drag ratio versus airspeed is shown in Figure 158. Curves are shown for sea-level conditions and for 10,000- and 25,000-foot altitudes at design gross weight.

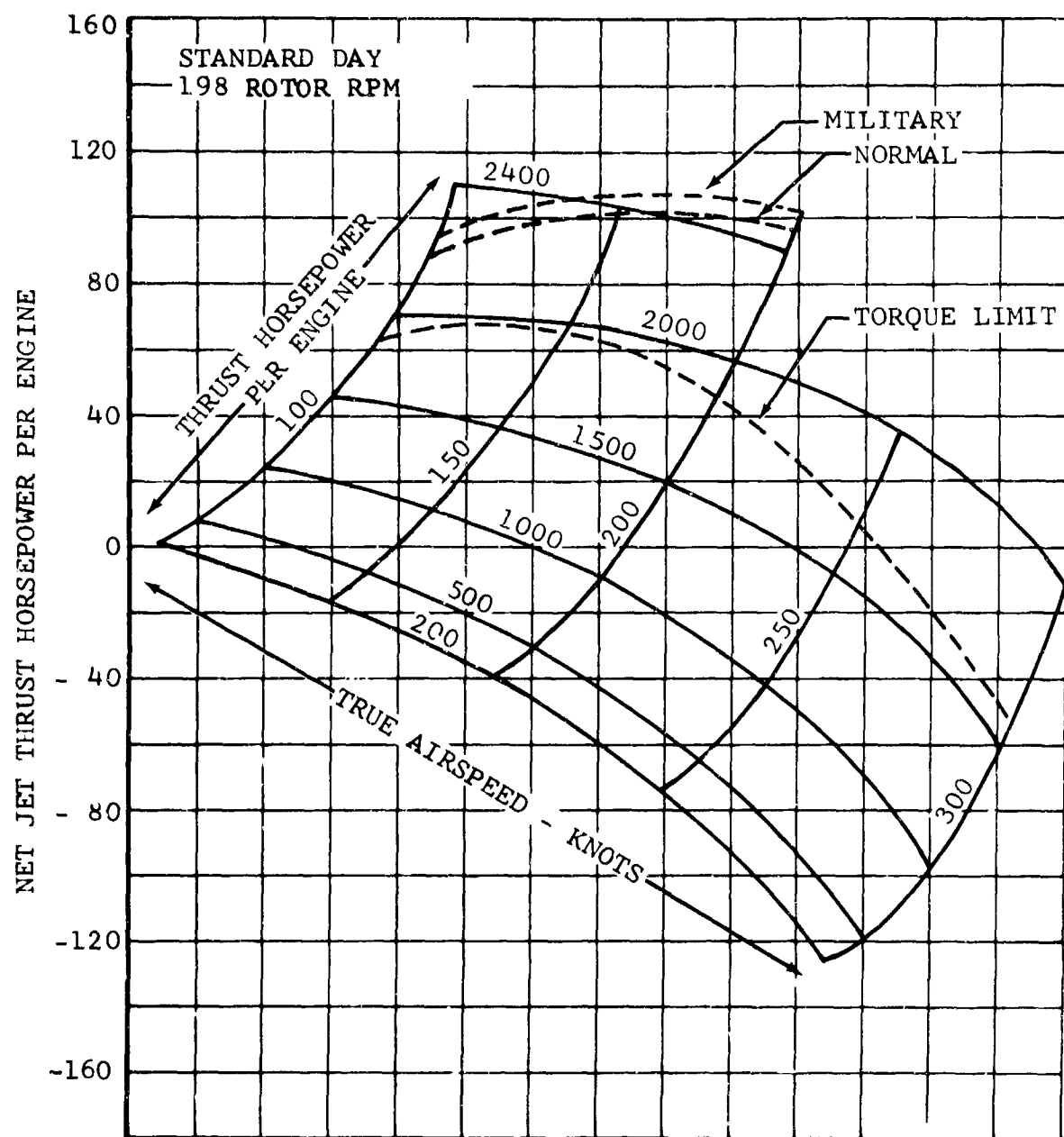


Figure 151. Net Jet Thrust Horsepower Versus Thrust Horsepower, Sea Level, Twin-Engine Operation.

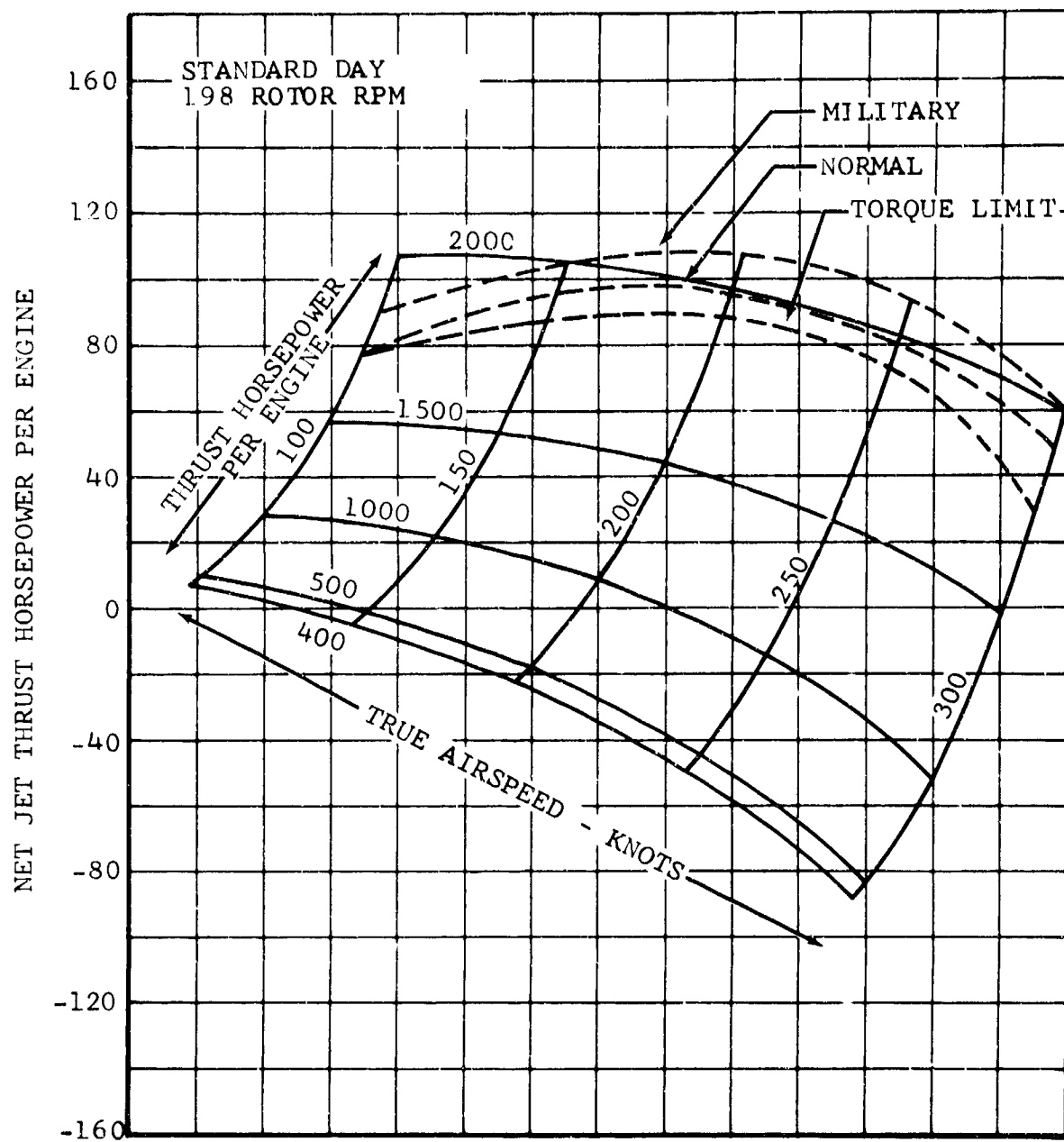


Figure 152. Net Jet Thrust Horsepower Versus Thrust Horsepower, 10,000 Feet, Twin-Engine Operation.

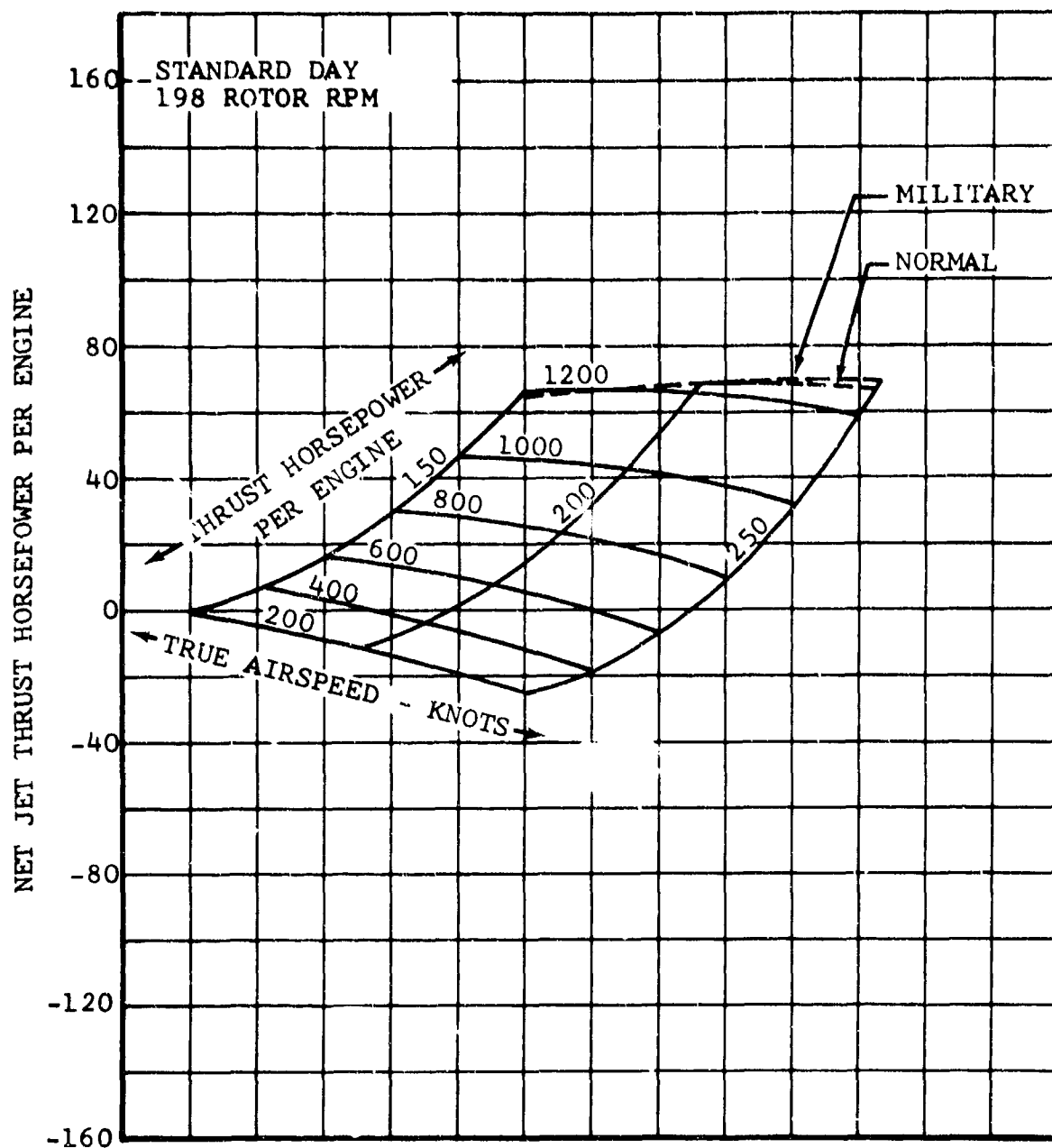


Figure 153. Net Jet Thrust Horsepower Versus Thrust Horsepower, 25,000 Feet, Twin-Engine Operation.

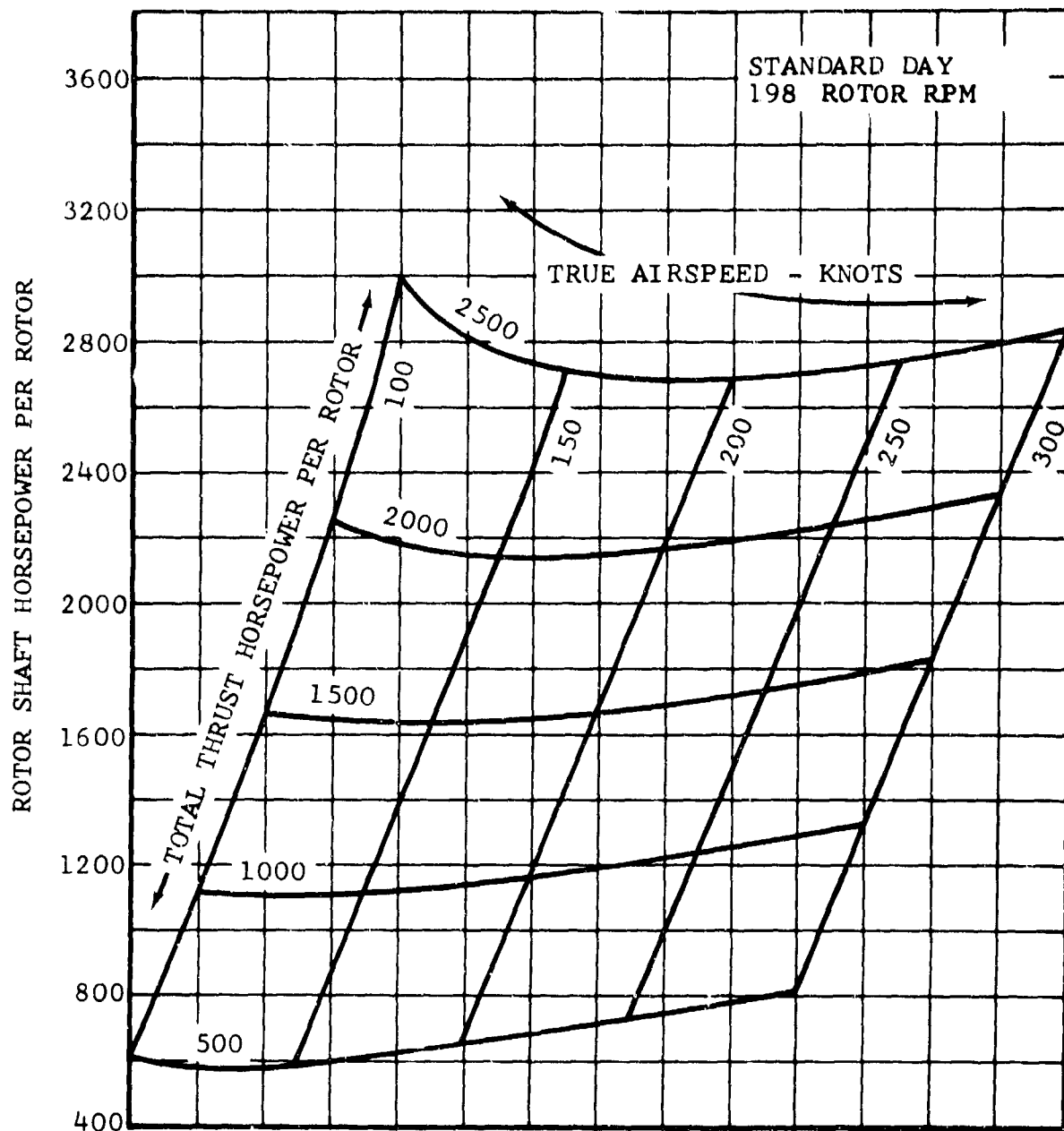


Figure 154. Rotor Shaft Horsepower Versus Total Thrust Horsepower, Sea Level.

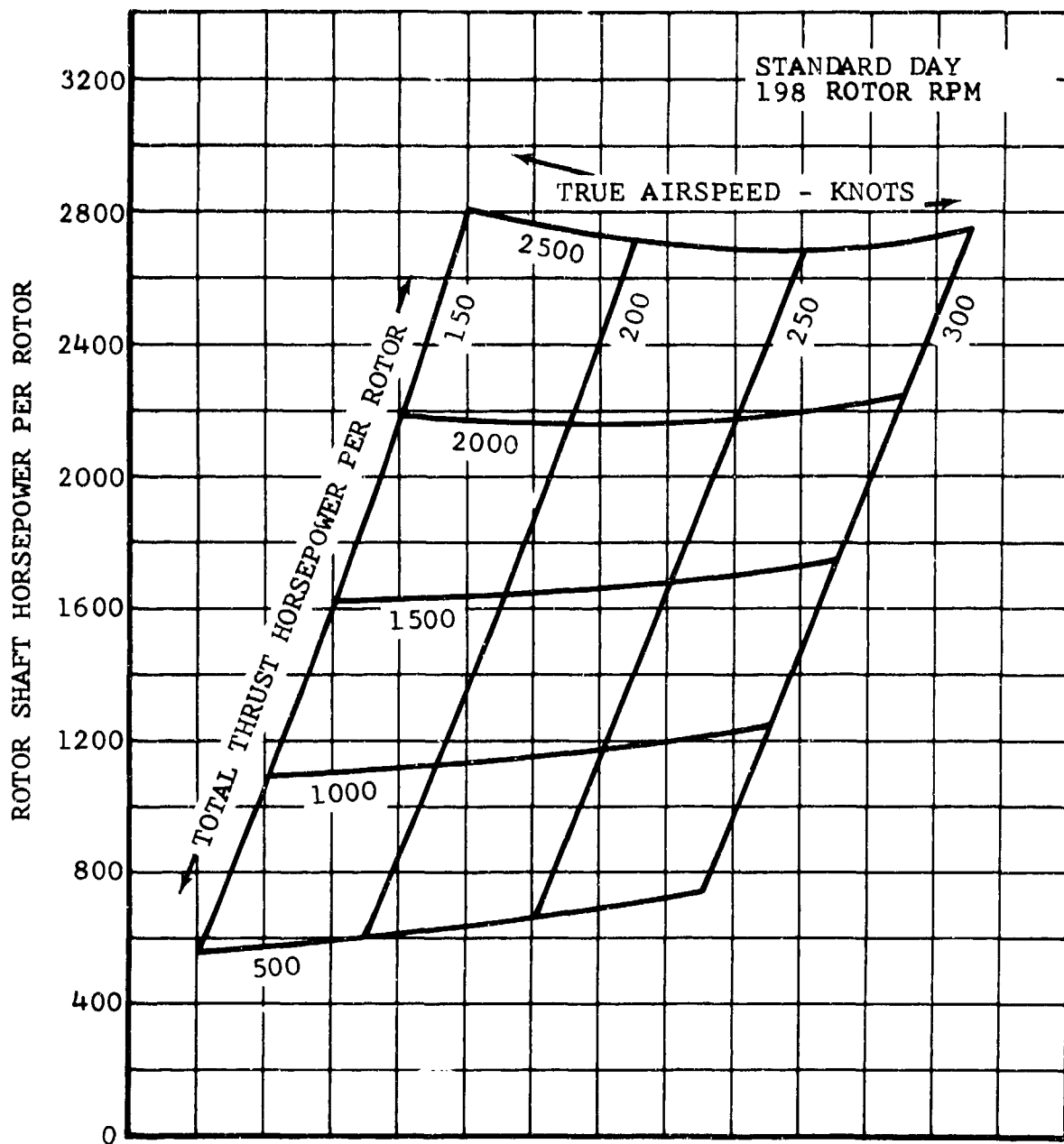


Figure 155. Rotor Shaft Horsepower Versus
Total Thrust Horsepower, 10,000 Feet.

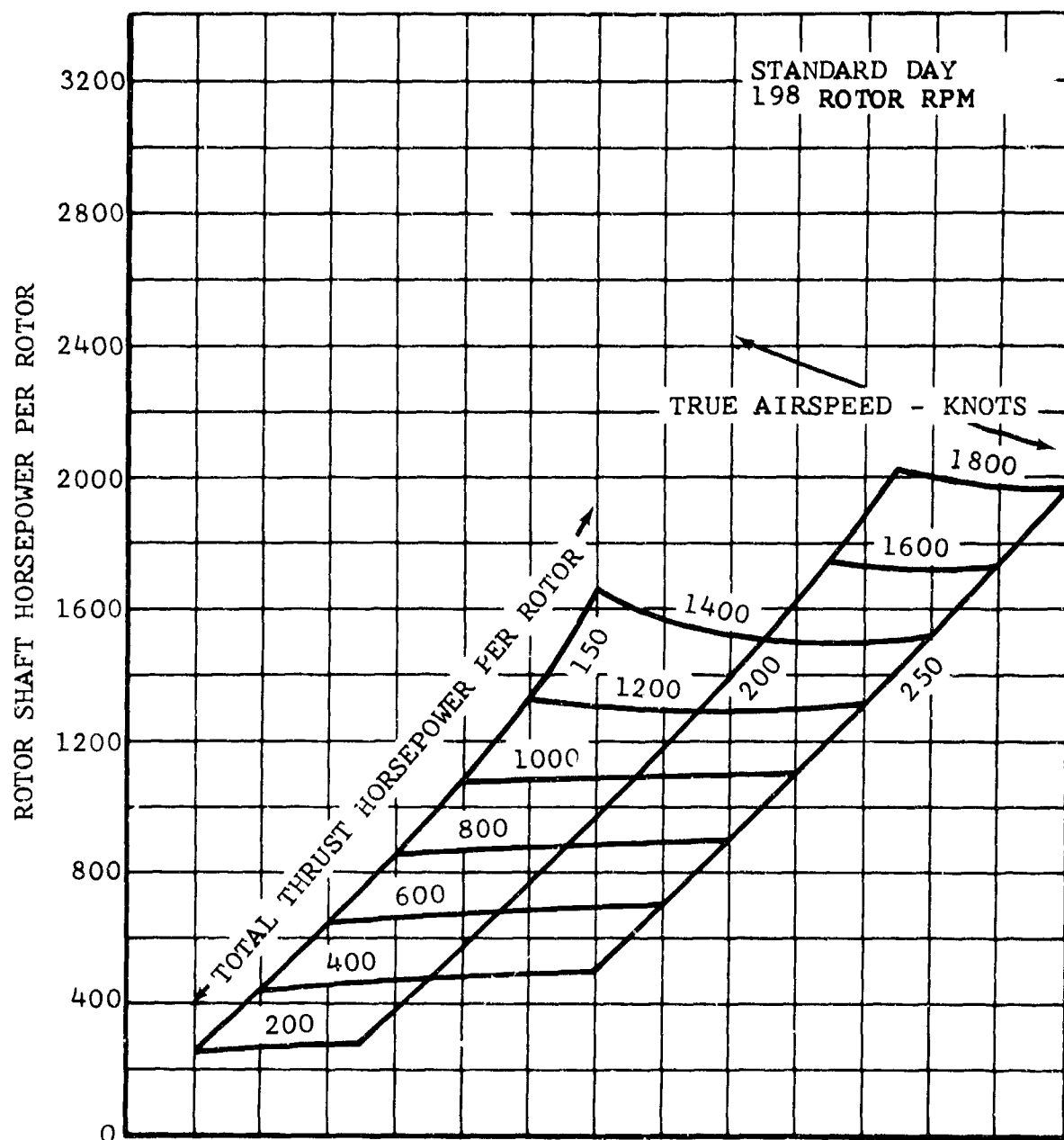


Figure 156. Rotor Shaft Horsepower Versus
Total Thrust Horsepower, 25,000 Feet.

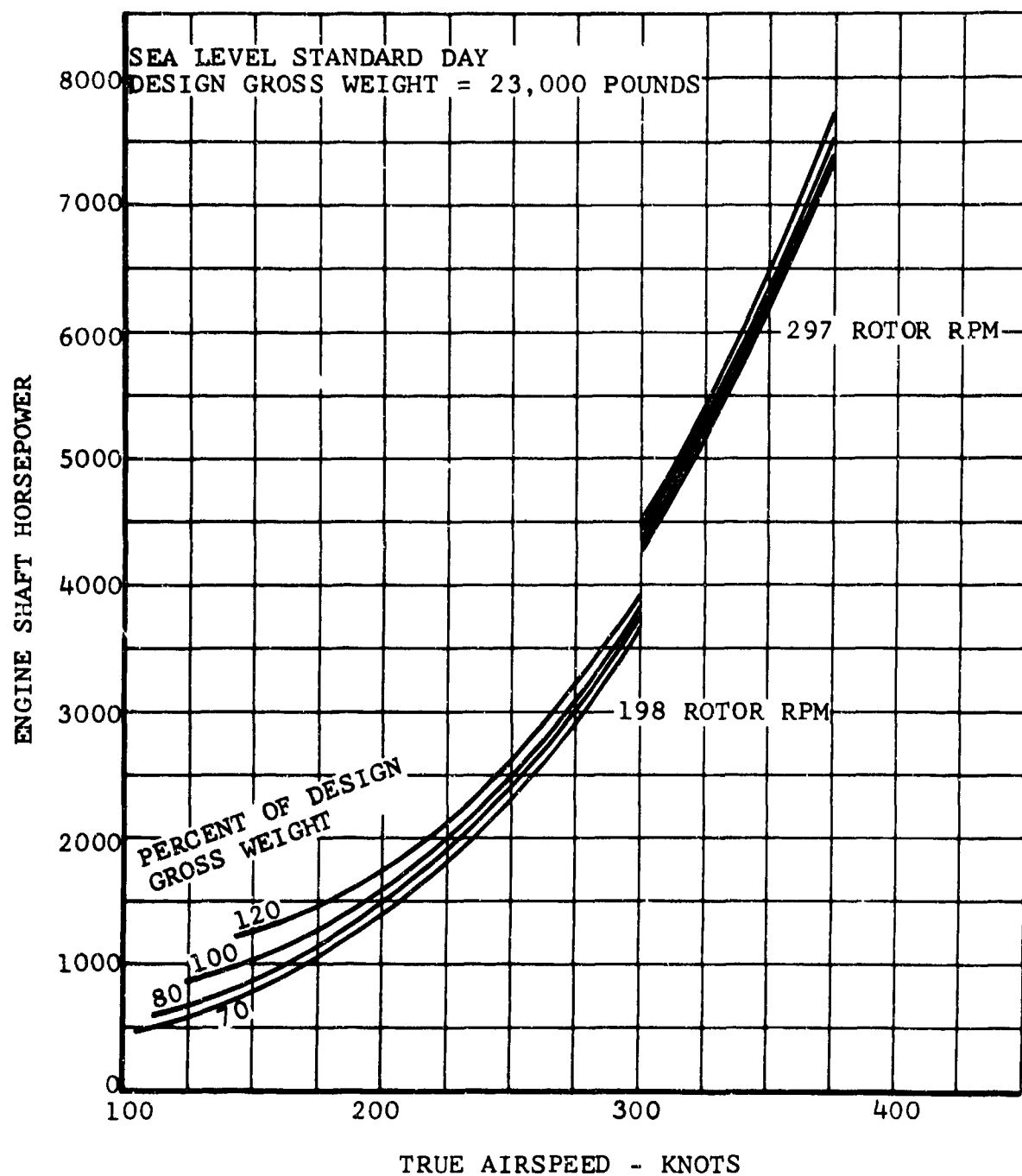


Figure 157. Engine Shaft Horsepower Required.

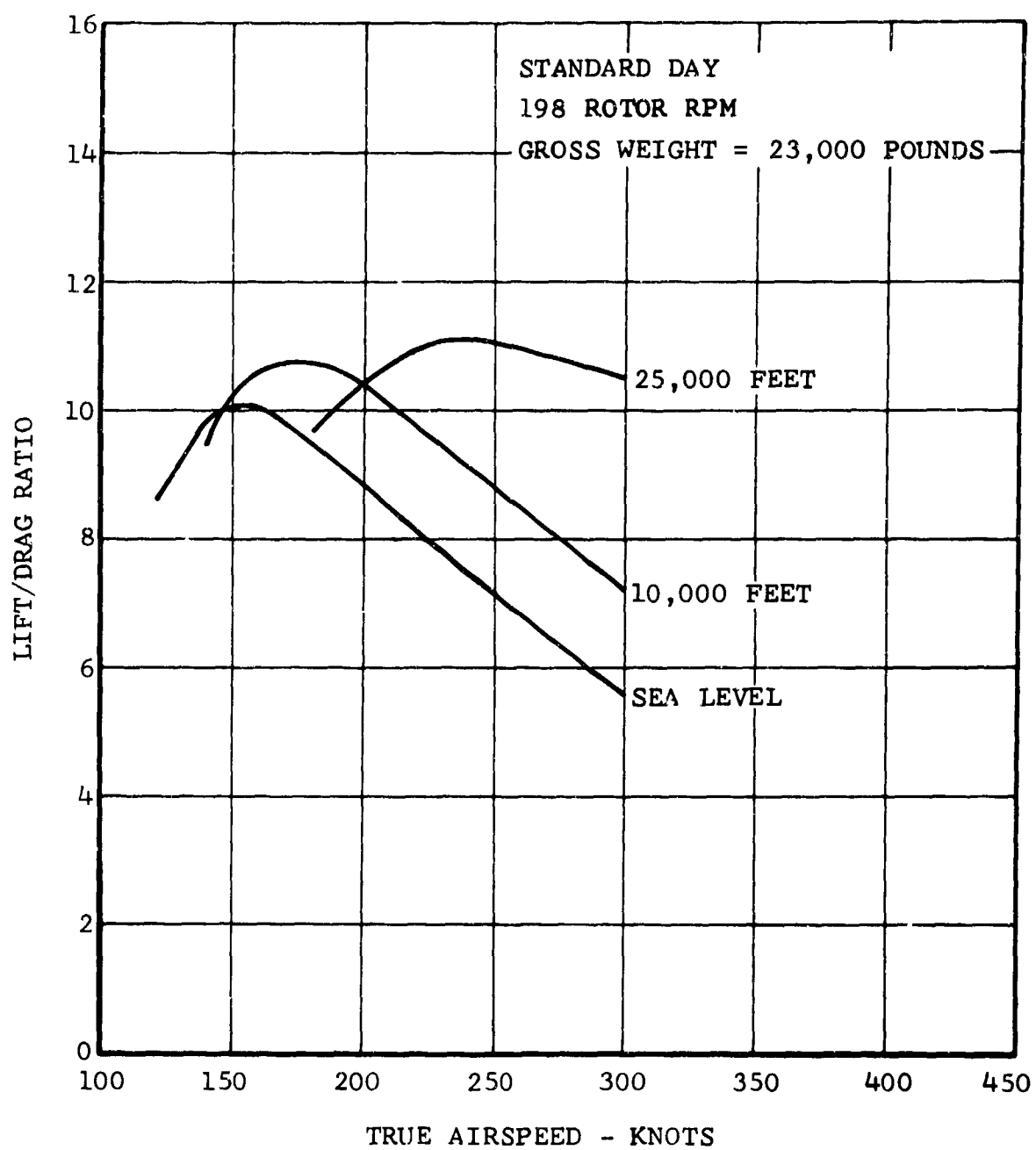


Figure 158. Overall Lift/Drag Ratio.

L/D is obtained from engine shaft horsepower required as follows:

$$L = \text{gross weight}$$
$$D = \frac{\text{SHP}_{\text{eng}} \times 326}{V}$$

The maximum values are 10.1 at sea level, 10.7 at 10,000 feet, and 11.1 at 25,000 feet. The sea-level requirement of 10 is met.

4. MAXIMUM SPEED

Maximum speed at design gross weight versus altitude for single-engine and full-power operation is shown in Figure 159. The limits considered are military rated power or maximum torque (1350 ft-lb), whichever comes first. Maximum speed is 345 knots at sea level and 385 knots at 12,000 feet for twin-engine operation. With one engine inoperative, maximum speed is 259 knots at sea level and 288 knots at 12,000 feet.

The maximum allowable continuous speed (V_H) is 350 knots. This speed is also shown in Figure 159 and indicates areas where full-power operation is not allowed for continuous operation. Limit dive speed is 437 knots.

5. RANGE

Specific range, in nautical miles per pound of fuel, is shown versus airspeed in Figures 160 through 165 for sea level, 10,000-, and 25,000-foot altitudes for single- and twin-engine operation. Payload-range curves are shown in Figure 166 for three gross weights and altitudes of sea level and 10,000 feet on a standard day. At a takeoff gross weight of 30,800 pounds, more than 11,000 pounds of payload can be transported 540 nautical miles with a normal fuel load.

At design gross weight of 23,000 pounds, the D266 has a range of 431 nautical miles at sea level with 3000 pounds of fuel and a 3000-pound payload. If the payload is increased to 10,800 pounds, the range is 394 nautical miles with a takeoff gross weight of 30,800 pounds. These ranges are based on a fuel allowance of 5 minutes of normal power at helicopter rpm for warmup, takeoff, and conversion. This amounts to 270 pounds of fuel.

Ferry range at 25,000 feet is calculated to be 4275 nautical miles for a takeoff gross weight of 41,500 pounds with 22,965 pounds of fuel. This range permits unescorted flight capability across both the Atlantic and Pacific Oceans. Because of the high gross weight, a rolling takeoff is selected instead of the

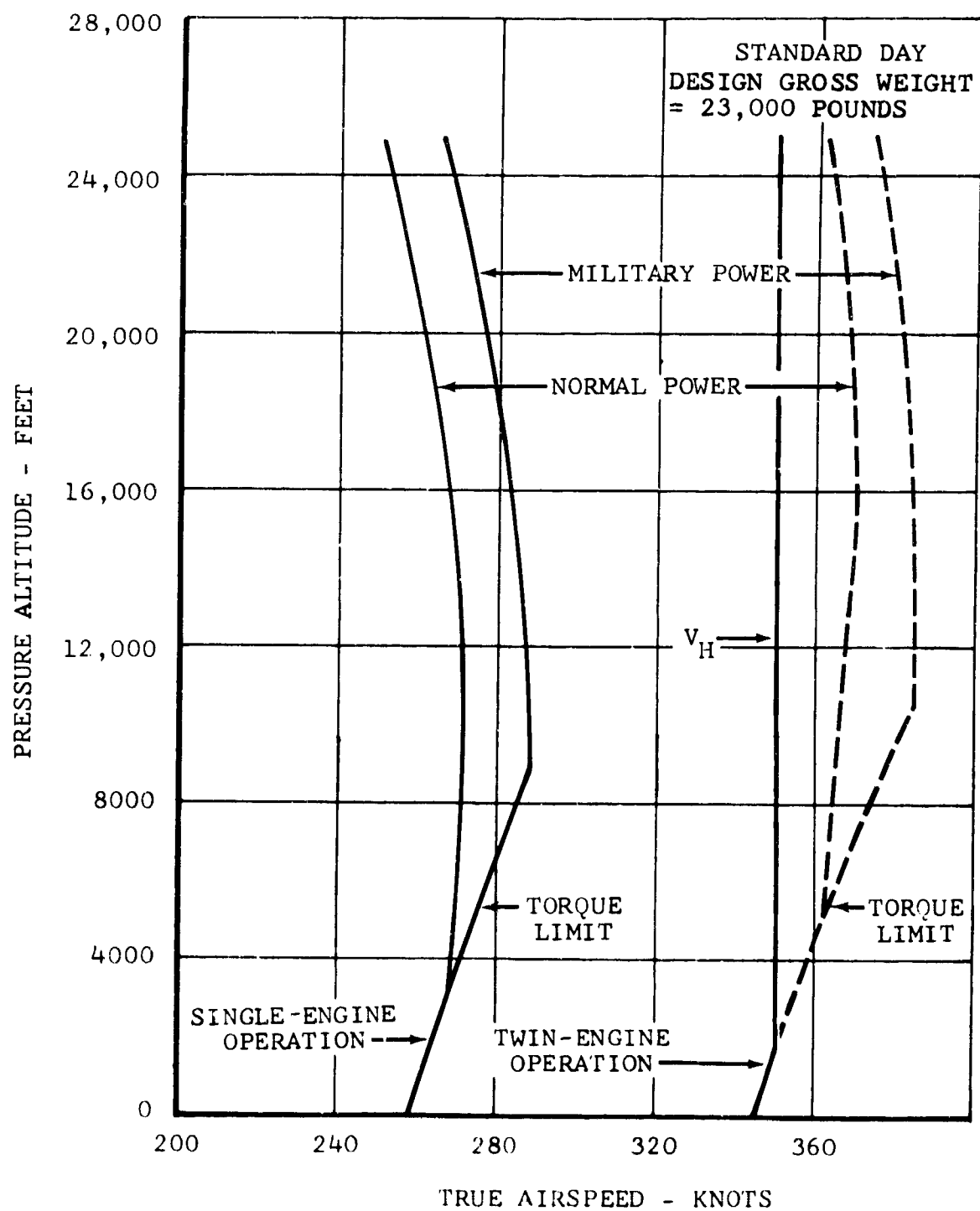


Figure 159. Maximum True Airspeed,
Fixed-Wing Configuration.

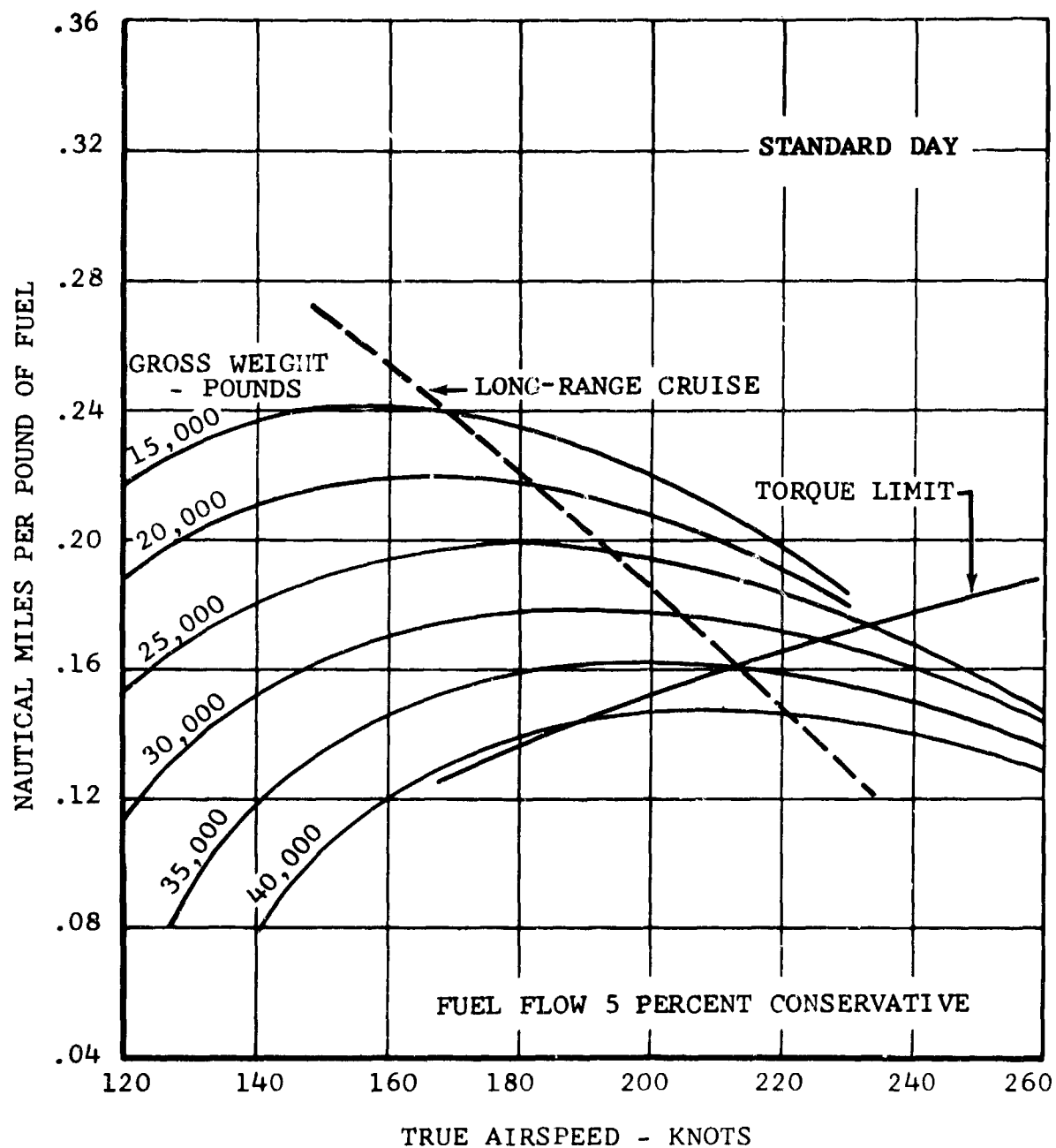


Figure 160. Specific Range, Sea Level, Single-Engine Operation.

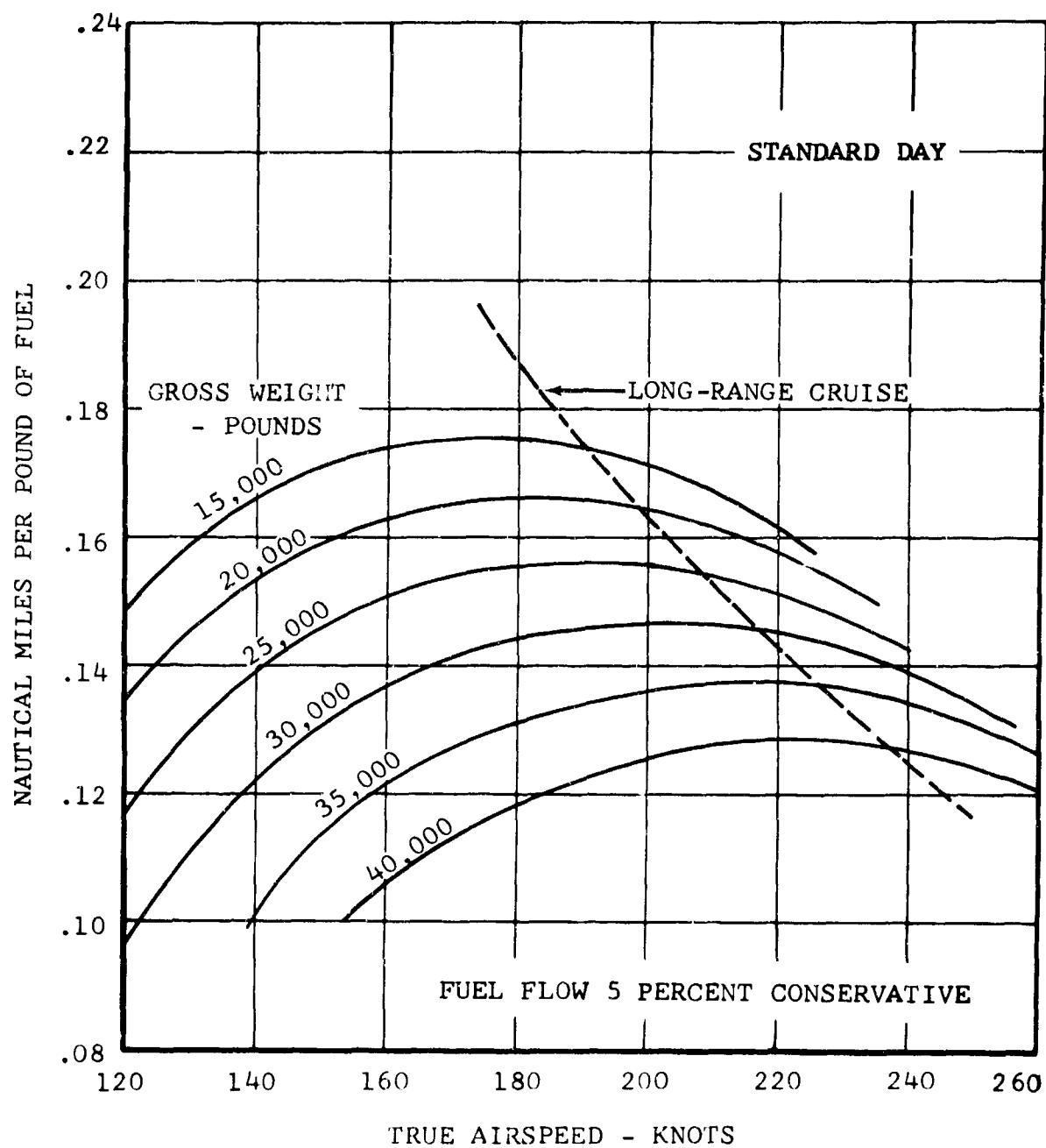


Figure 161. Specific Range, Sea Level, Twin-Engine Operation.

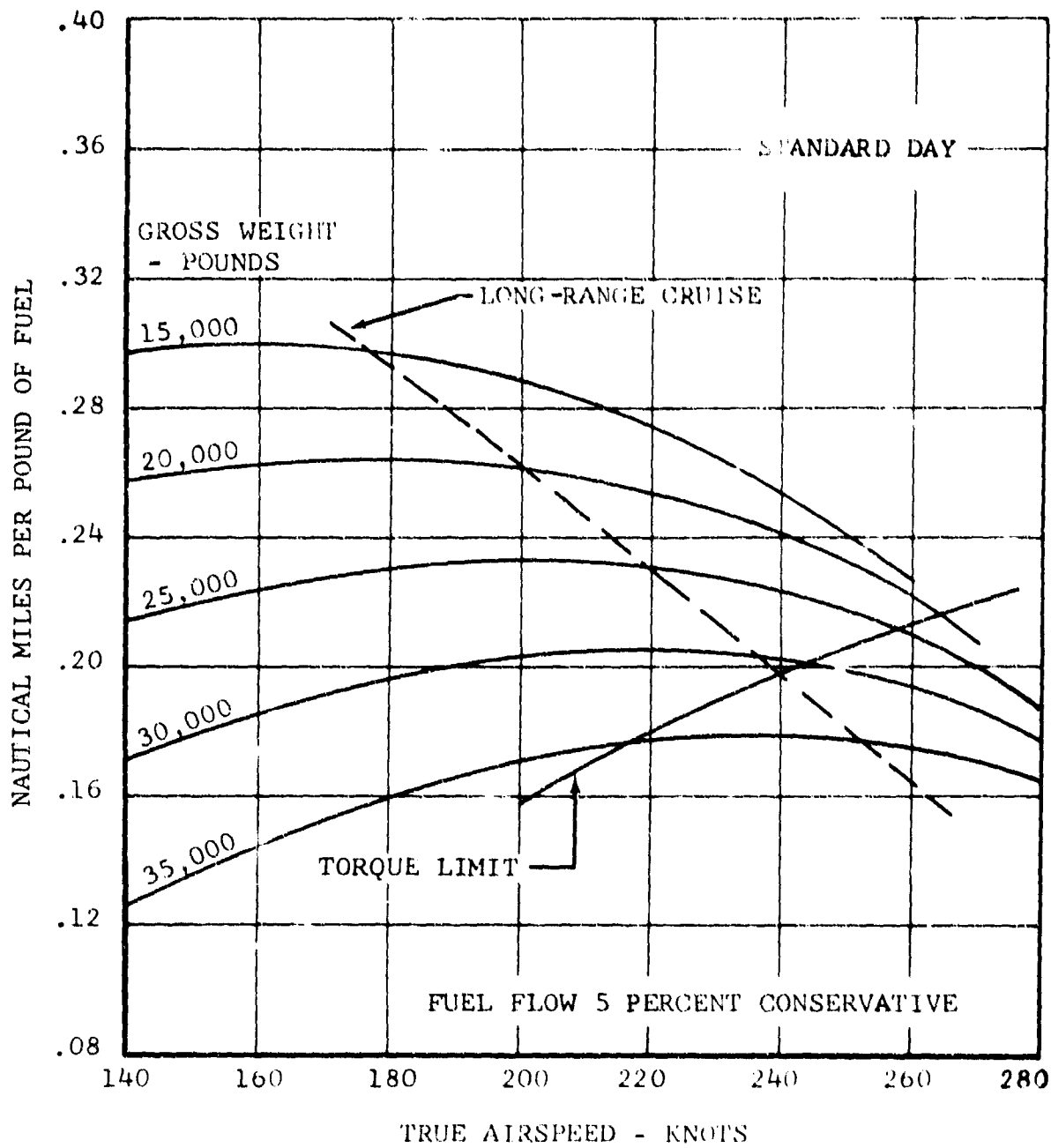


Figure 162. Specific Range, 10,000 Feet, Single-Engine Operation.

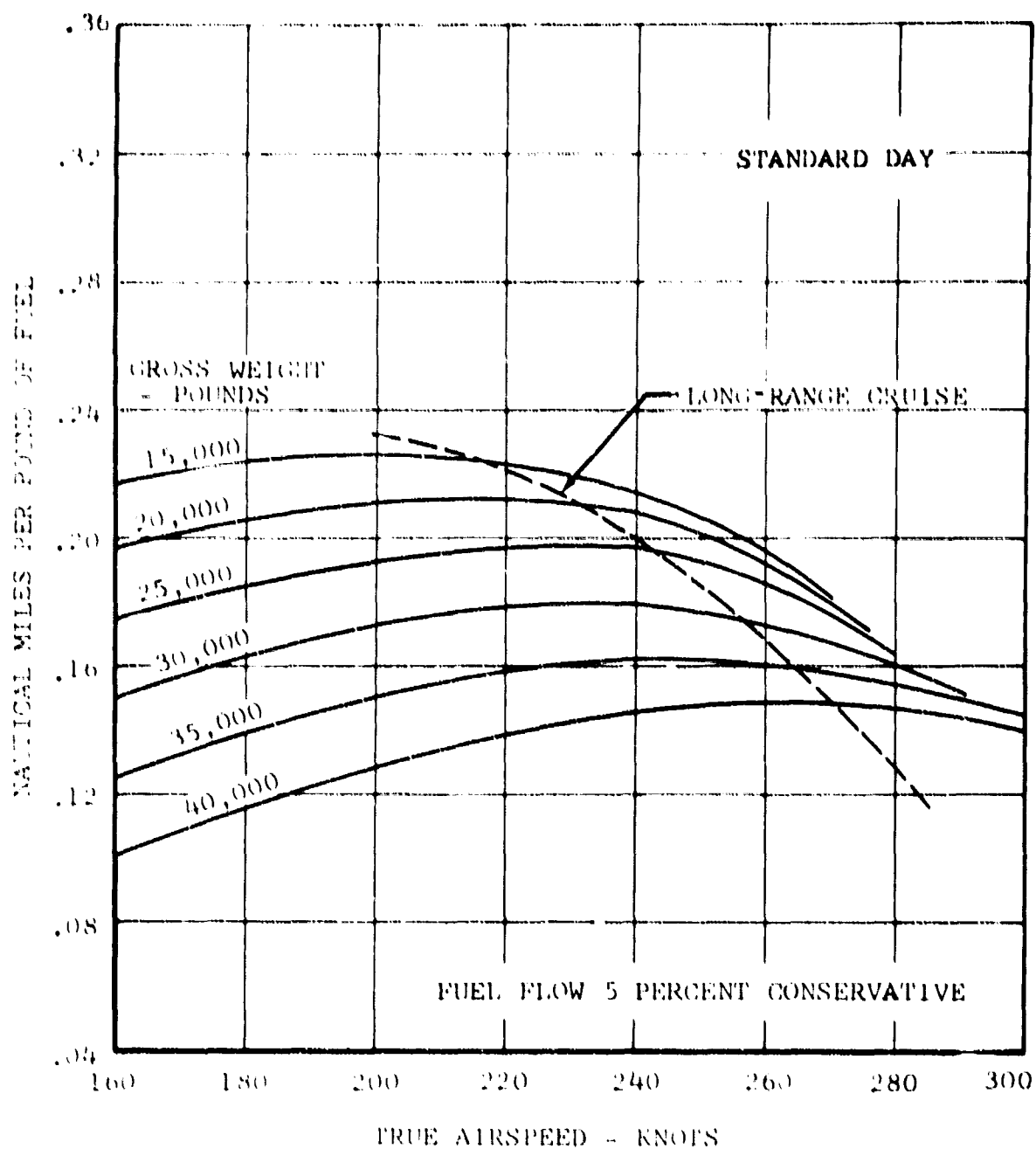


Figure 163. Specific Range, 10,000 Feet, Twin-Engine Operation.

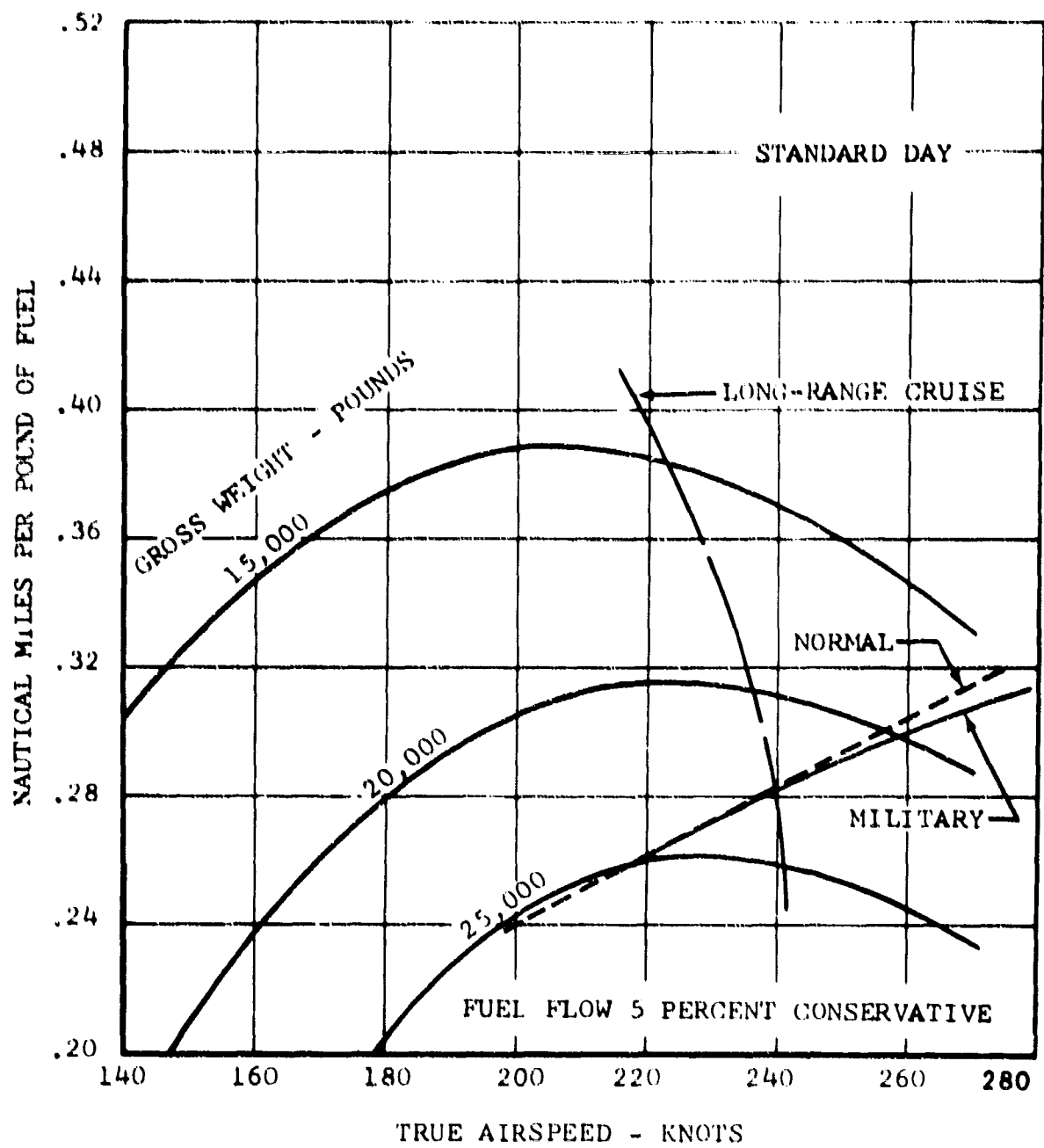


Figure 164. Specific Range, 25,000 Feet, Single-Engine Operation.

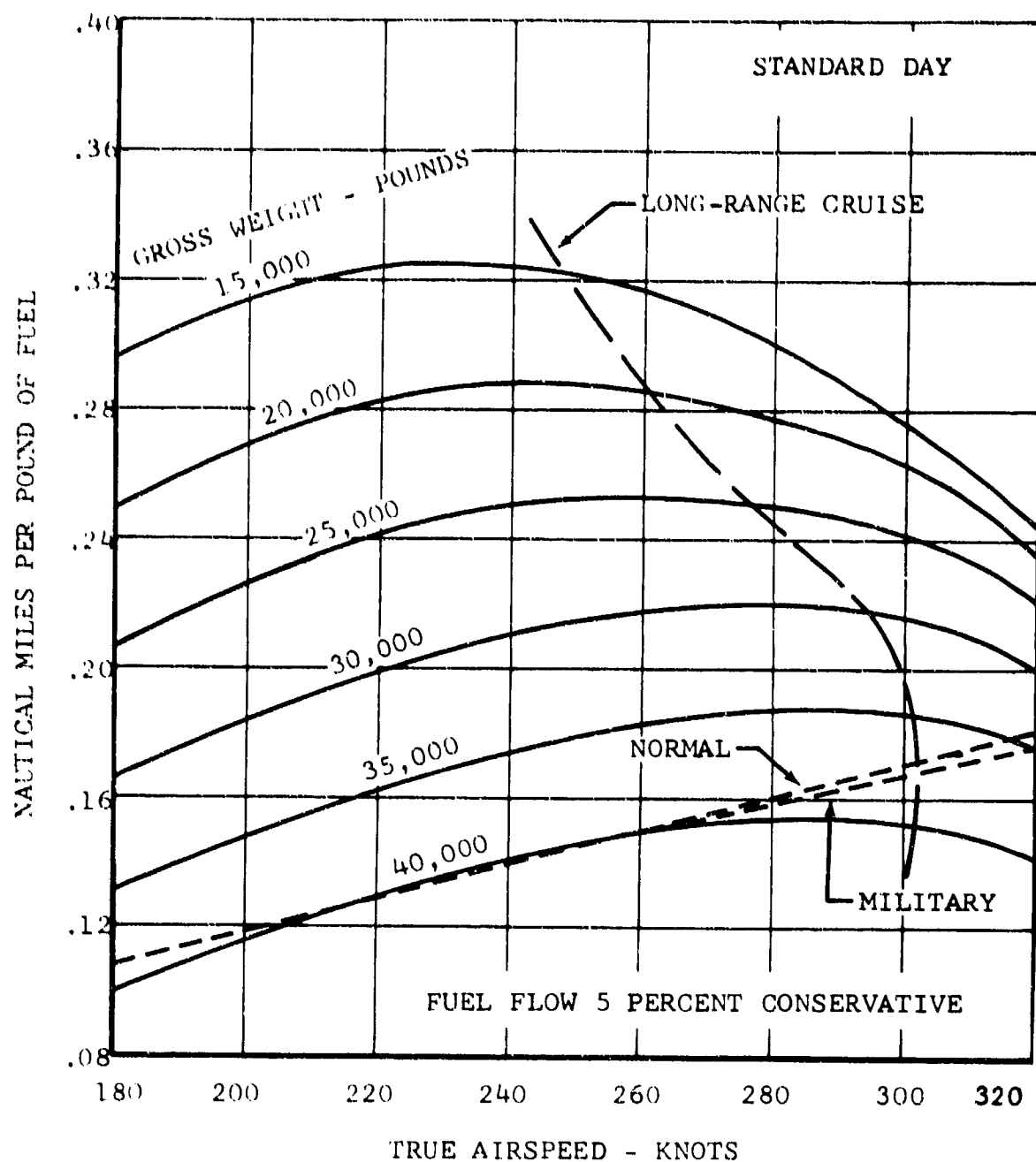


Figure 165. Specific Range, 25,000 Feet, Twin-Engine Operation.

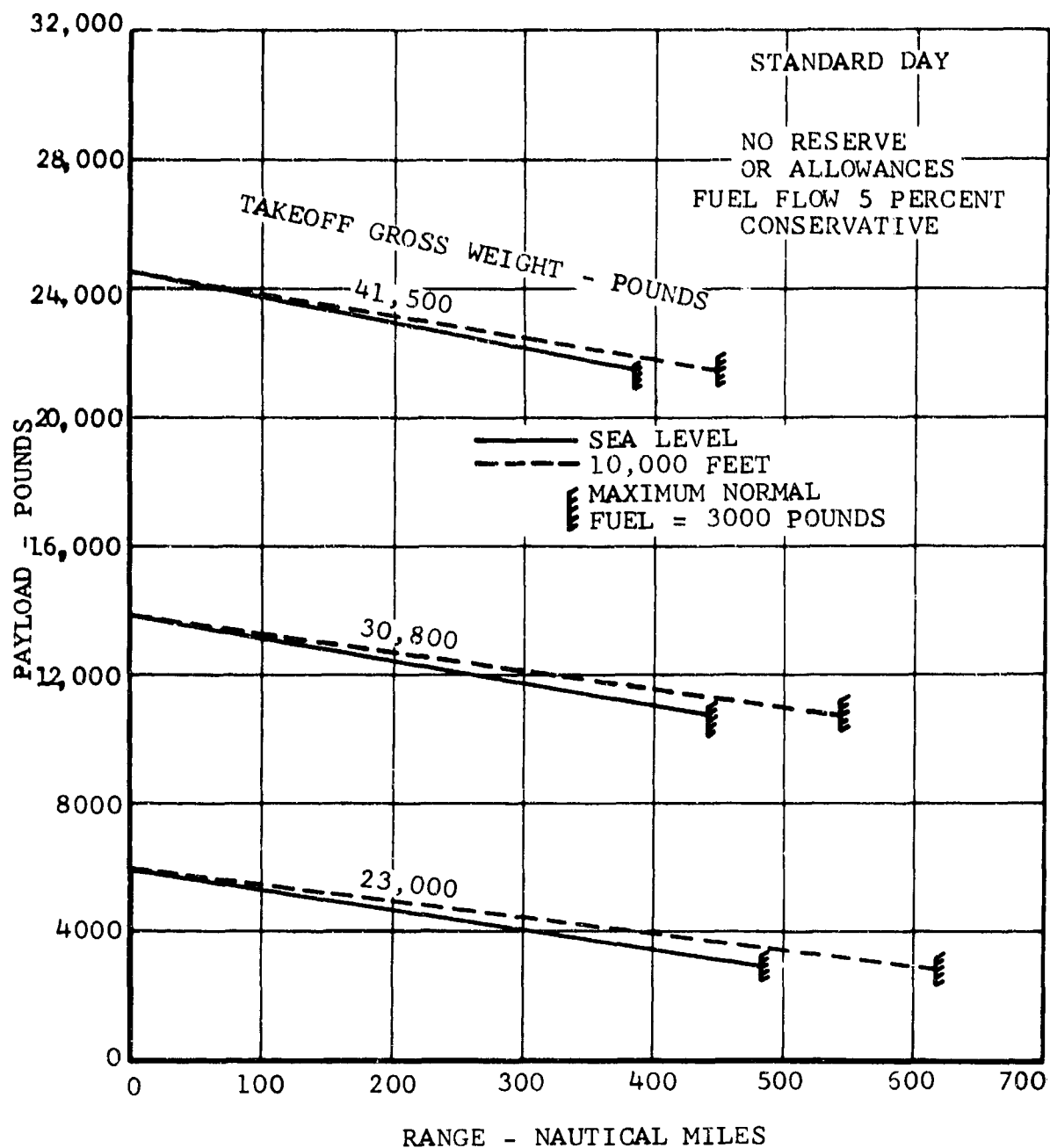


Figure 166. Payload Range.

normal helicopter procedure. The ground run is made with the rotor mast tilted forward 30 degrees and flaps down 30 degrees. The ground run is calculated to be 2400 feet to a climbout speed of 120 knots. In addition to the warmup, takeoff, and conversion fuel allowance, the ferry range was calculated using 10 percent of initial fuel load for reserve. Fuel used to climb to 25,000 feet was also taken into account.

All fuel-flow data used for the range calculations are 5 percent conservative.

6. RATE OF CLIMB

Rate of climb versus altitude is shown in Figures 167 through 170 for several gross weights for single- and twin-engine operation, and for military and normal power.

H. SINGLE-ENGINE AND POWER-OFF FLIGHT

1. POWER-OFF DESCENT

Power-off rate of descent versus airspeed is shown in Figure 171 for two rotor rpm. The minimum rate of descent is 2100 feet per minute at 80 knots and 297 rotor rpm. The minimum rate of descent at 347 rotor rpm is 2950 feet per minute at 65 knots. Lines of constant collective pitch setting are also given in Figure 171. These data show that if constant collective is held, the rate of descent decreases and the airspeed for minimum rate of descent increases as rpm is decreased.

2. SINGLE-ENGINE FAILURE

There is a wide range of speed within which single-engine level flight is possible in helicopter configuration. This is illustrated in Figure 172. If a single-engine failure should occur in this region, a very small height loss will occur during the time it takes the working engine to build up the power required for single-engine operation. If failure occurs below or above the single-engine level-flight envelope, then an acceleration or a deceleration must be made to get into the single-engine flight envelope where level flight can be maintained. Landings can be made with no difficulty, since rate of descent can easily be checked by use of the engine power available and the stored energy in the rotors.

The fixed-wing mode single-engine failure situation is similar to that for the helicopter, in that there is a wide range of speed in which single-engine level flight is feasible. This is shown in Figure 173. Before a landing is made, the procedure is to decelerate to conversion speed, to make the conversion, and to enter the helicopter flight regime.

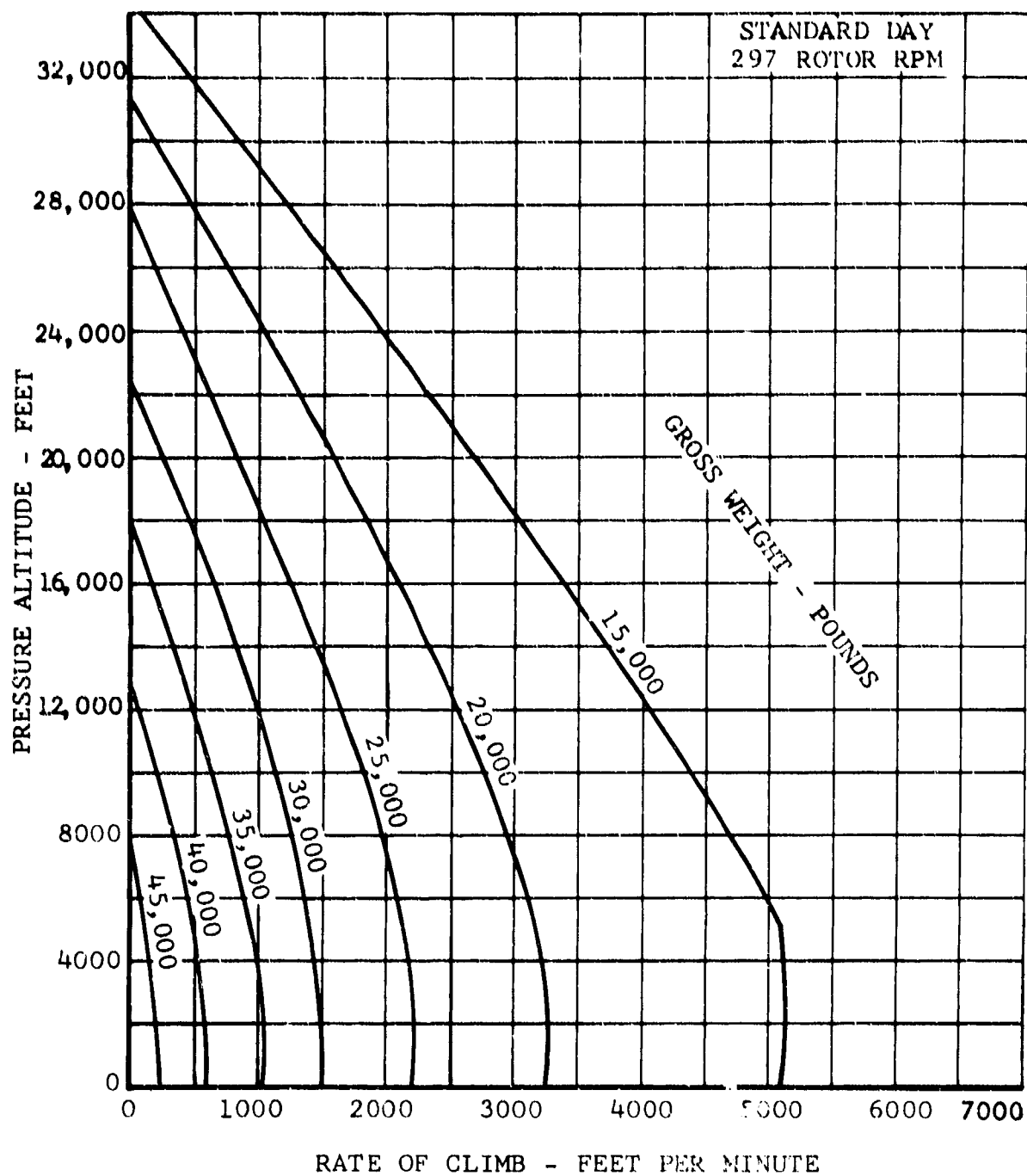


Figure 167. Maximum Rate of Climb, Military Rated Power, Single-Engine Operation, Fixed-Wing Configuration.

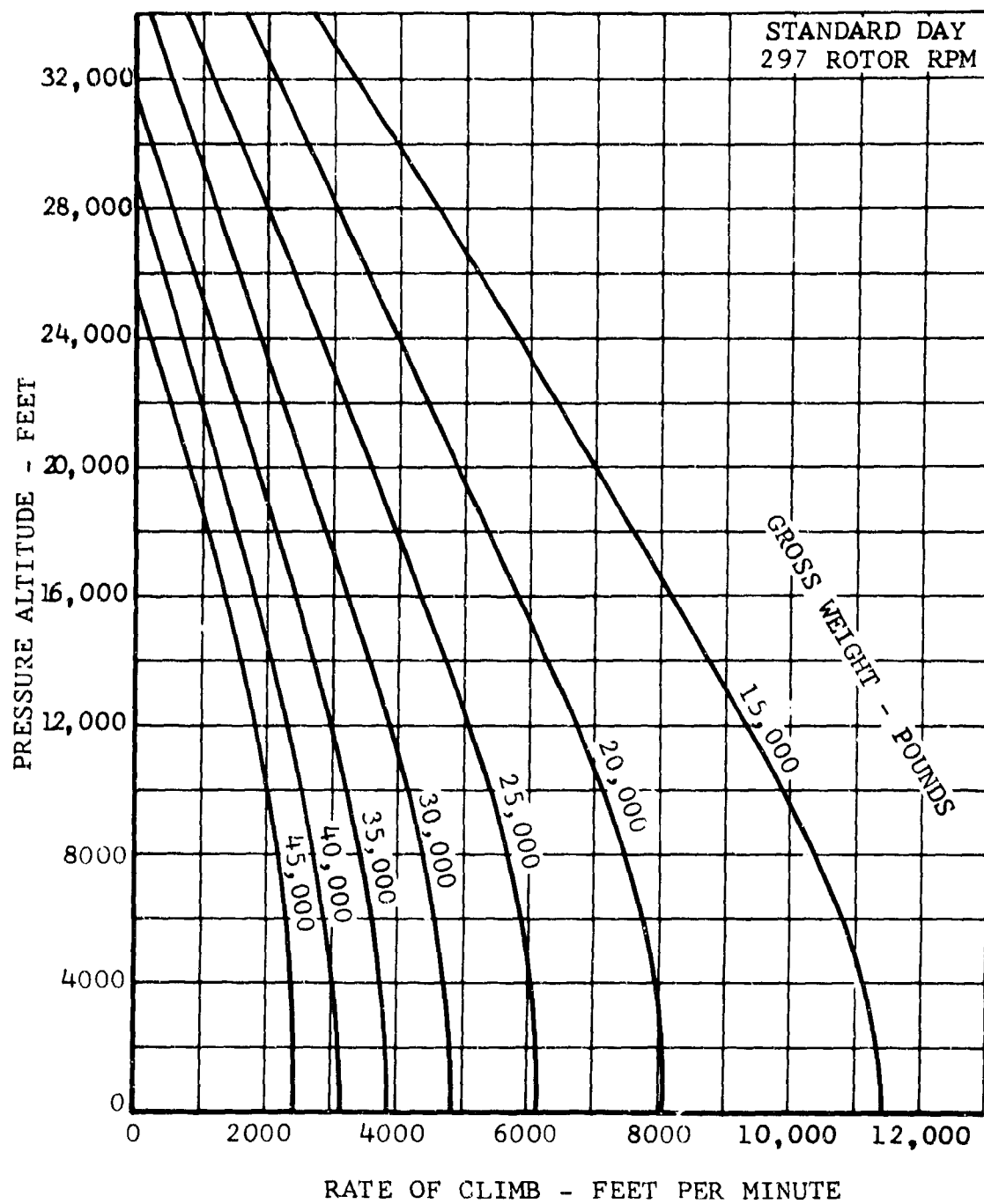


Figure 168. Maximum Rate of Climb, Military Rated Power, Twin-Engine Operation, Fixed-Wing Configuration.

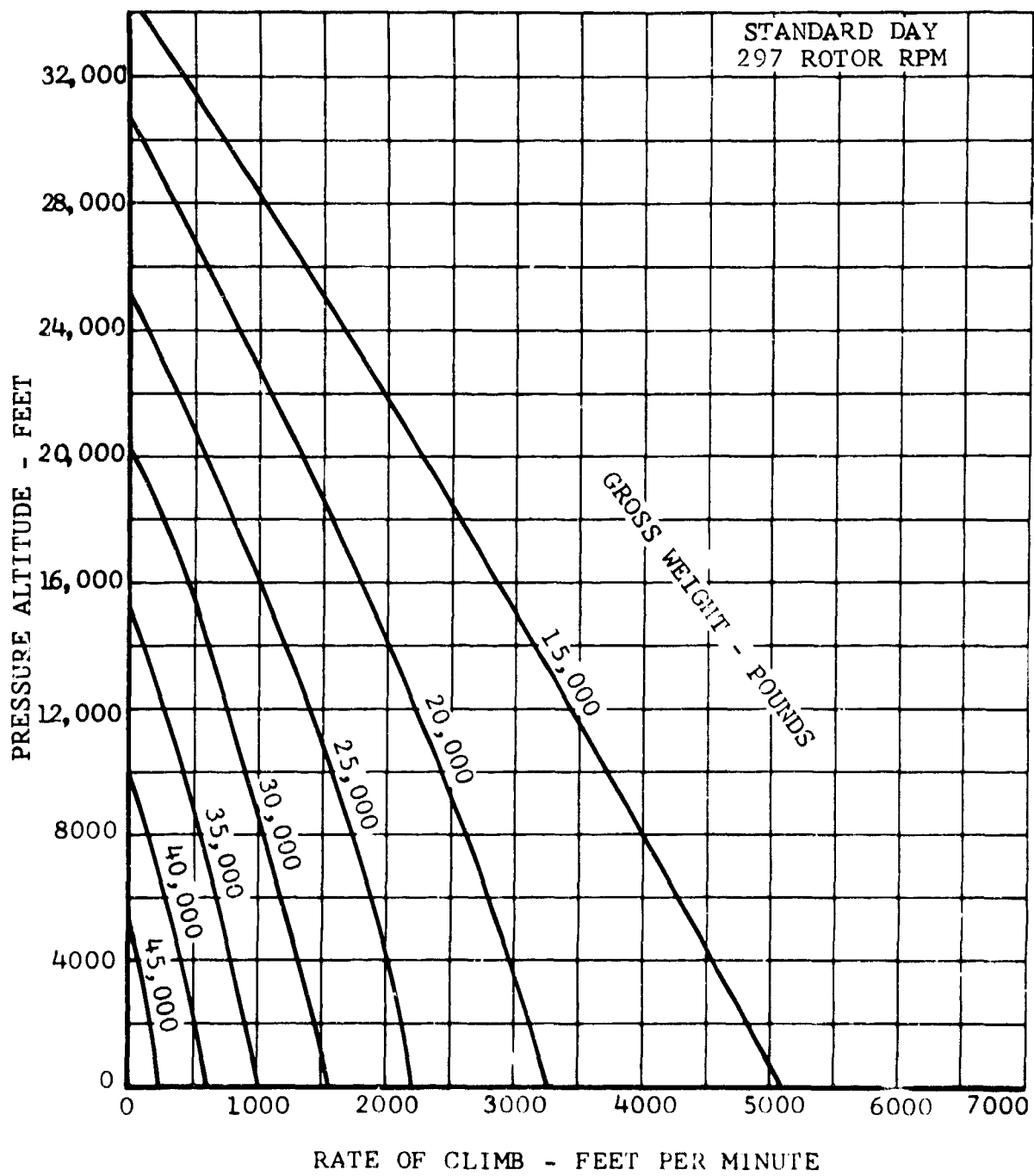


Figure 169. Maximum Rate of Climb, Normal Rated Power, Single-Engine Operation, Fixed-Wing Configuration.

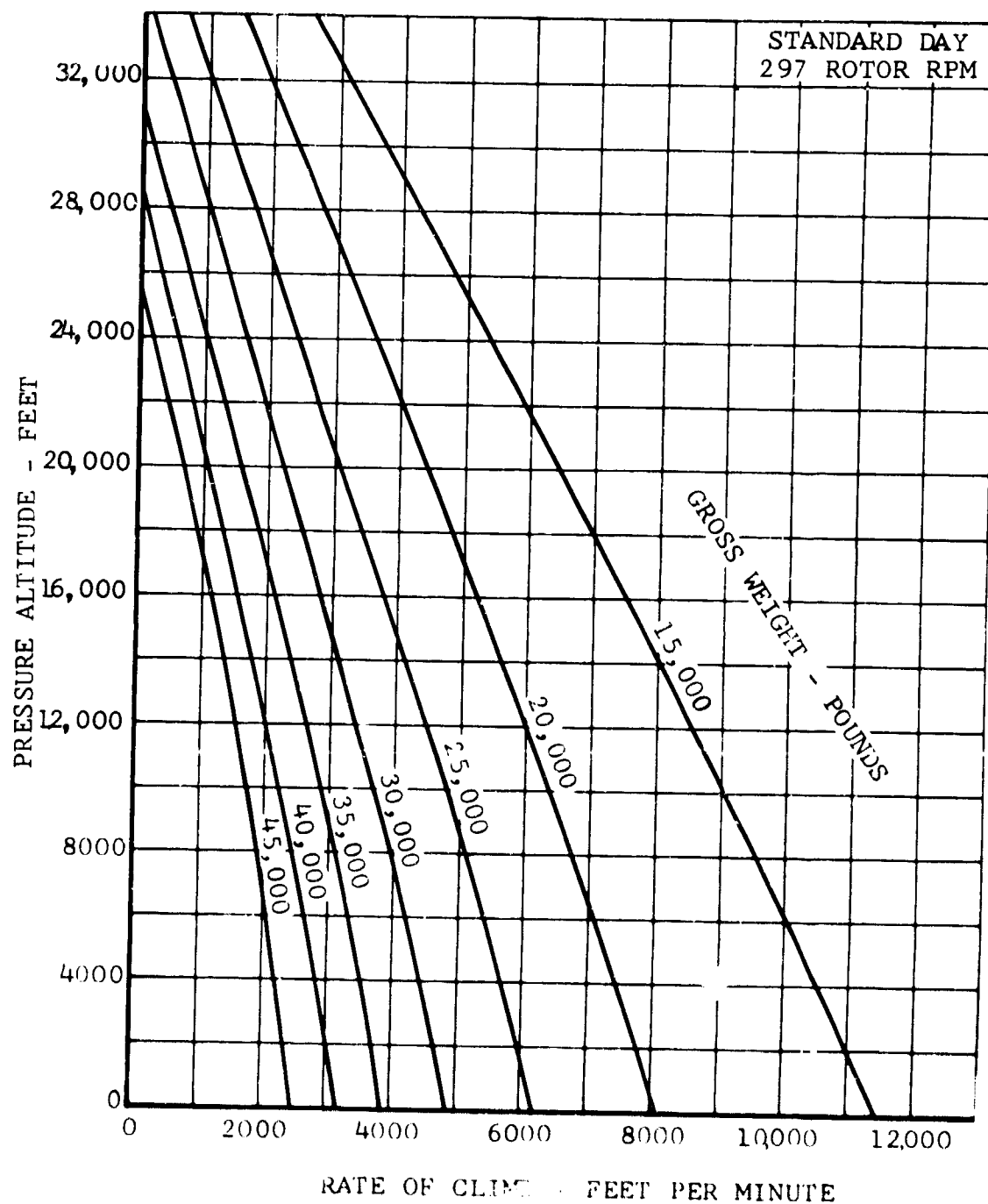


Figure 170. Maximum Rate of Climb, Normal Rated Power, Twin-Engine Operation, Fixed-Wing Configuration.

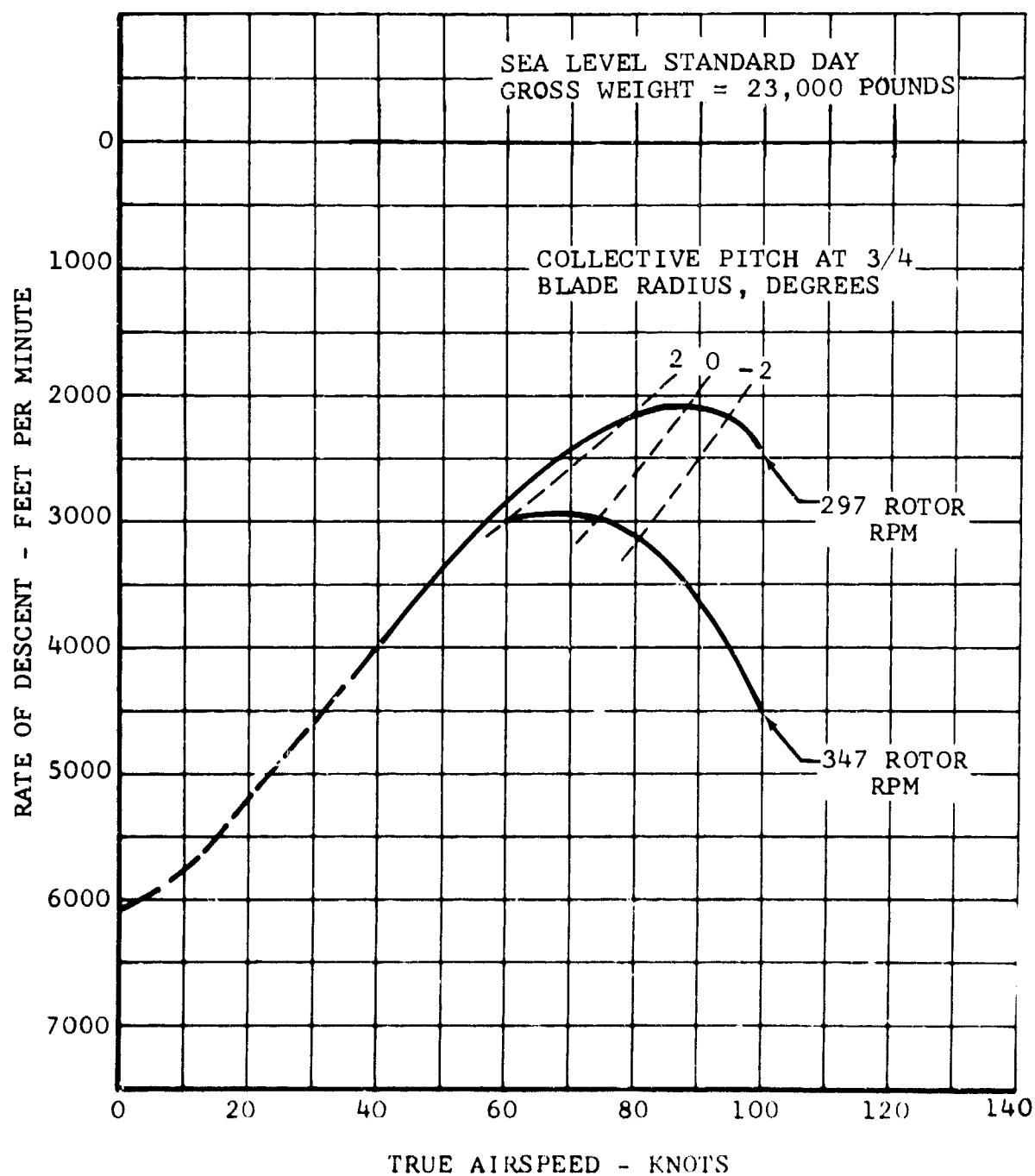


Figure 171. Rate of Descent in Autorotation.

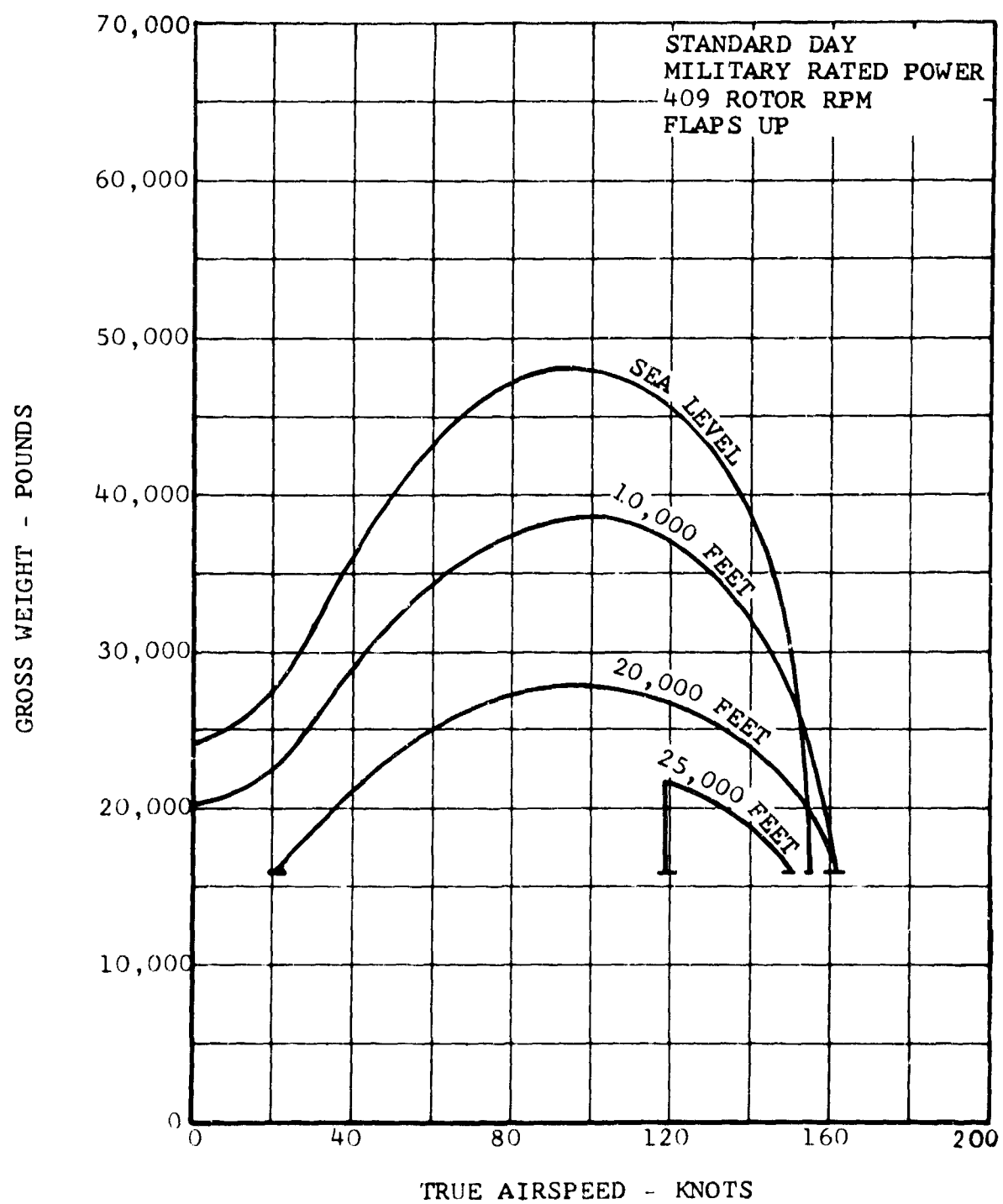


Figure 172. Single-Engine Flight Capability, Helicopter Configuration.

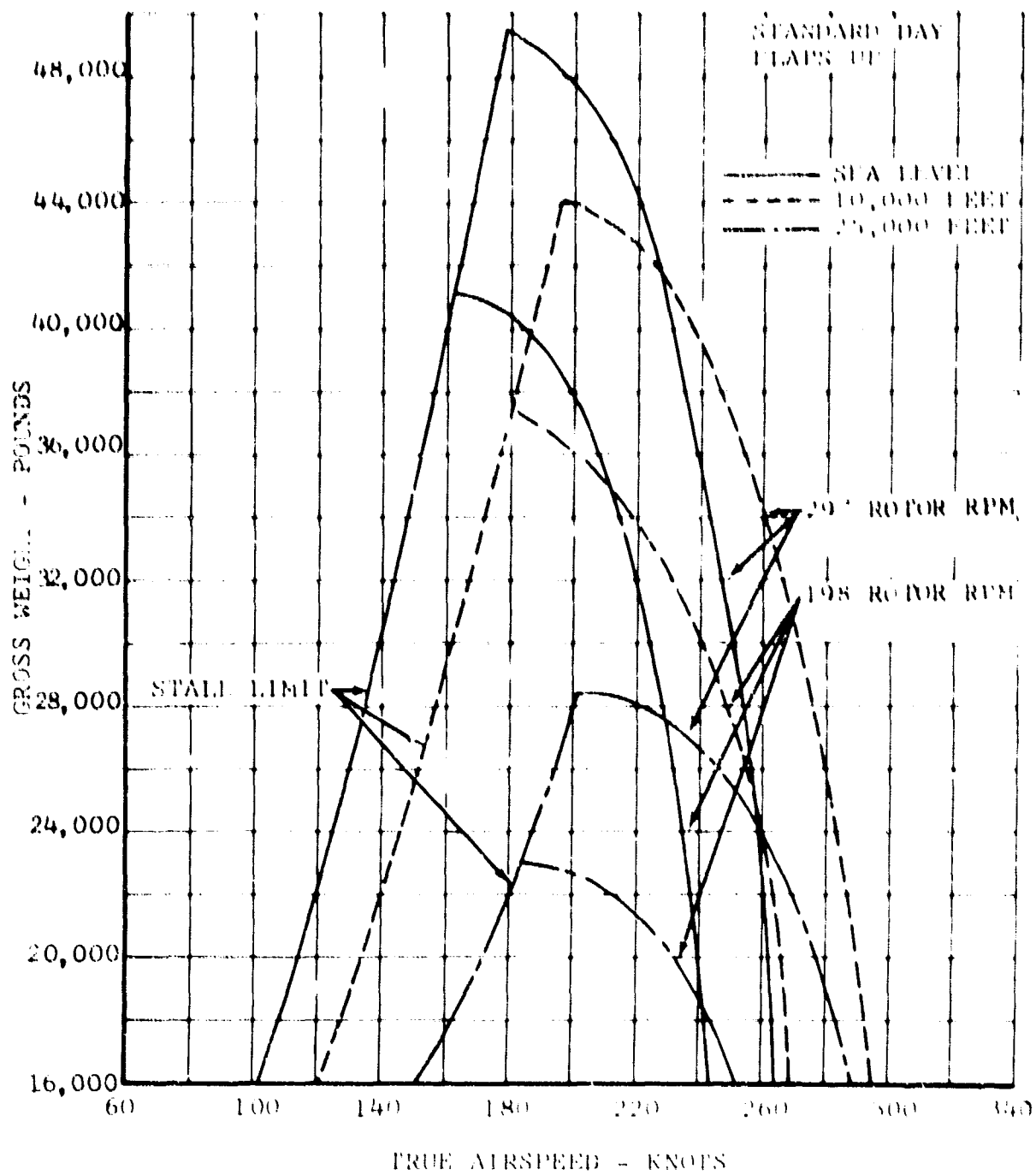


Figure 173. Single-Engine Flight Capability, Fixed-Wing Configuration.

If a single-engine failure should occur during conversion from helicopter to fixed-wing configuration, the process can immediately be reversed in order to return to helicopter flight. If conversion is being made to helicopter configuration and a single-engine failure occurs, then the reconversion can be continued to enable single-engine flight in helicopter mode. If circumstances so warrant, conversion to the fixed-wing mode can be completed for single-engine flight in this condition.

3. TOTAL POWER FAILURE

a. Helicopter Mode

Three conditions are investigated for complete power failure in helicopter mode. The first one is in ground effect hover, the second is landing from a steady-state autorotation with forward speed, and the third is out of ground effect hover.

The height from which a touchdown can be made with an 8-foot-per-second sink rate (landing-gear design limit) is calculated to be 8 feet. A delay of one second is made between failure and collective control input. Figure 174 shows the time history of the maneuver. Touchdown occurs 1.9 seconds after failure of both engines.

The height from which landing can be achieved for the OGE hover point is determined in two steps. The first step is to calculate the height lost during flare and landing and to determine the minimum forward speed at which a flare can be made for a safe roll-on landing. Figure 175 shows two cases, one flare initiated at a 75-knot steady autorotation and a second flare starting from a 90-knot autorotation. The flare from 75 knots results in a 9-foot-per-second vertical touchdown speed, and zero-rate-of-descent landing results from the 90-knot condition. For a safe autorotational landing with both engines out and for the rpm investigated, a minimum forward speed in autorotation of about 80 knots is indicated by these results. An altitude of 120 feet is required to perform this landing.

The second step in computing the OGE hover point is to compute the height lost from the time of power failure to an 80-knot steady descent. The time history for this case is presented in Figure 176. A 2-second waiting period after failure of both engines is used before the pilot's actions are taken. The collective is then lowered and the cyclic stick is moved forward to initiate the horizontal acceleration. A considerable drop in rpm occurs while the rate of descent builds up. The rpm drop and the increase in rate of descent are arrested and reversed, and the required forward speed is attained within about 12 seconds. Some time is subsequently required to stabilize the situation prior to the moment that the flare can be

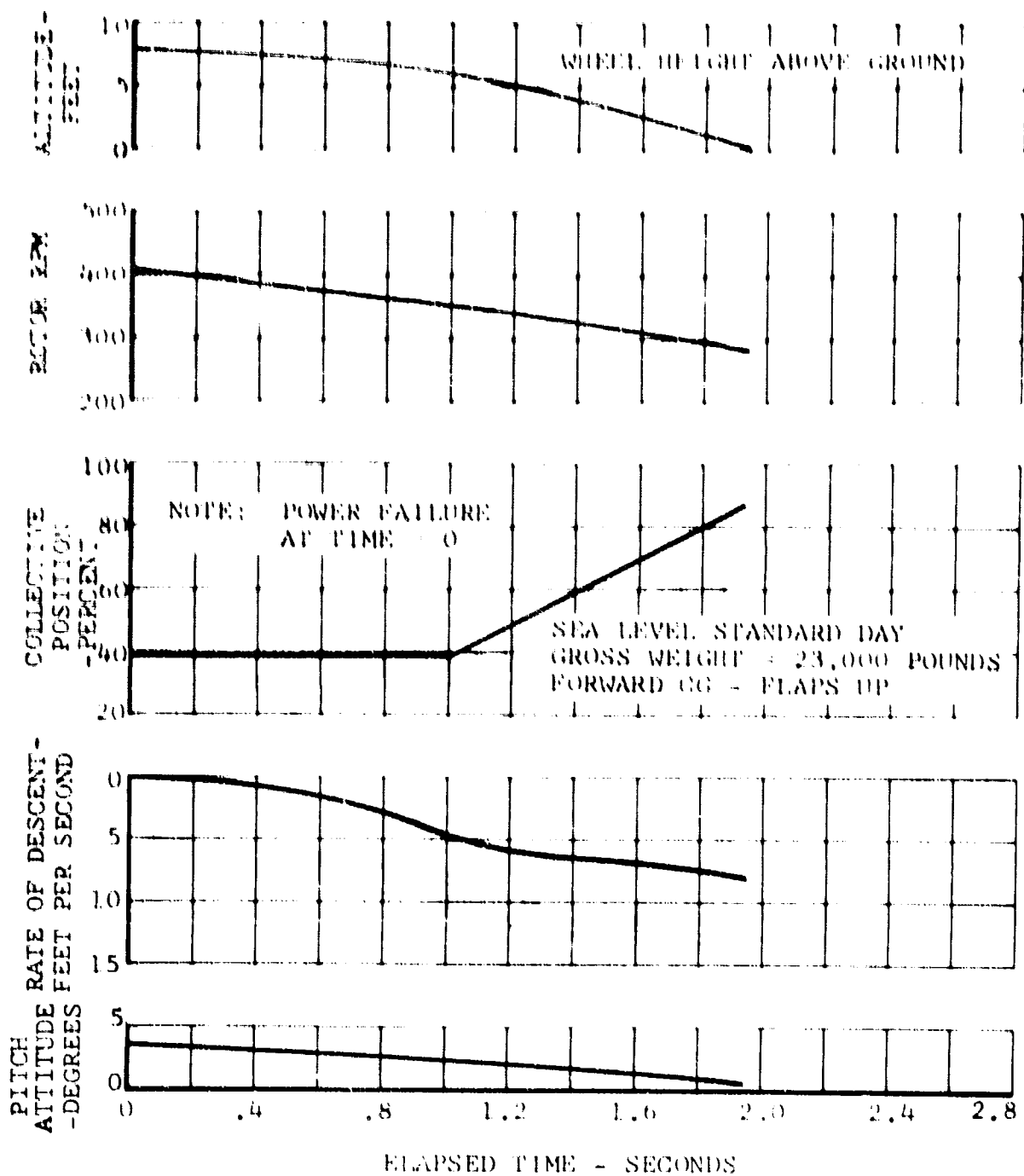


Figure 174. Time History of Power Failure in Hover, 8-Foot Wheel Height.

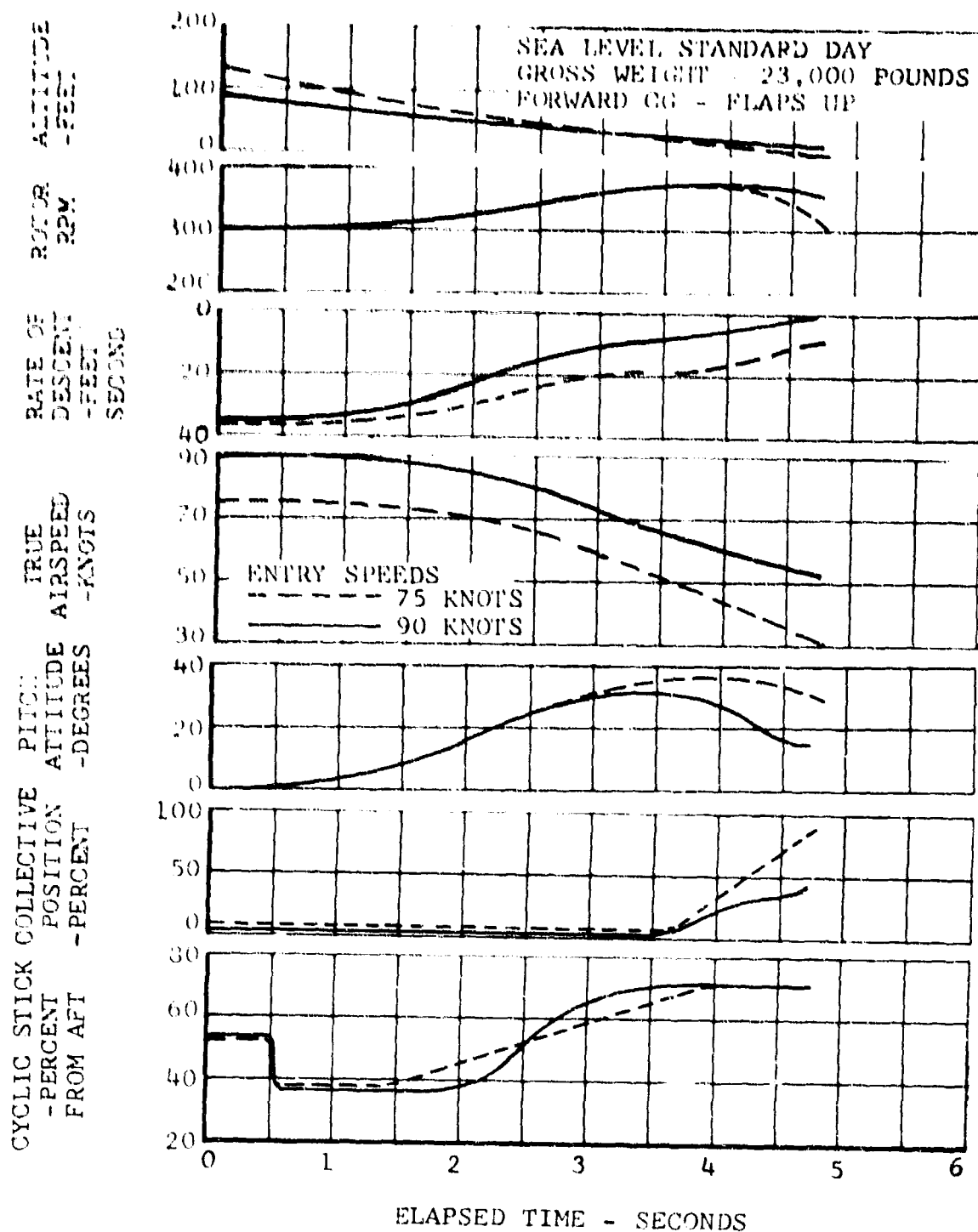


Figure 175. Time Histories of Power-Off Flare and Landing.

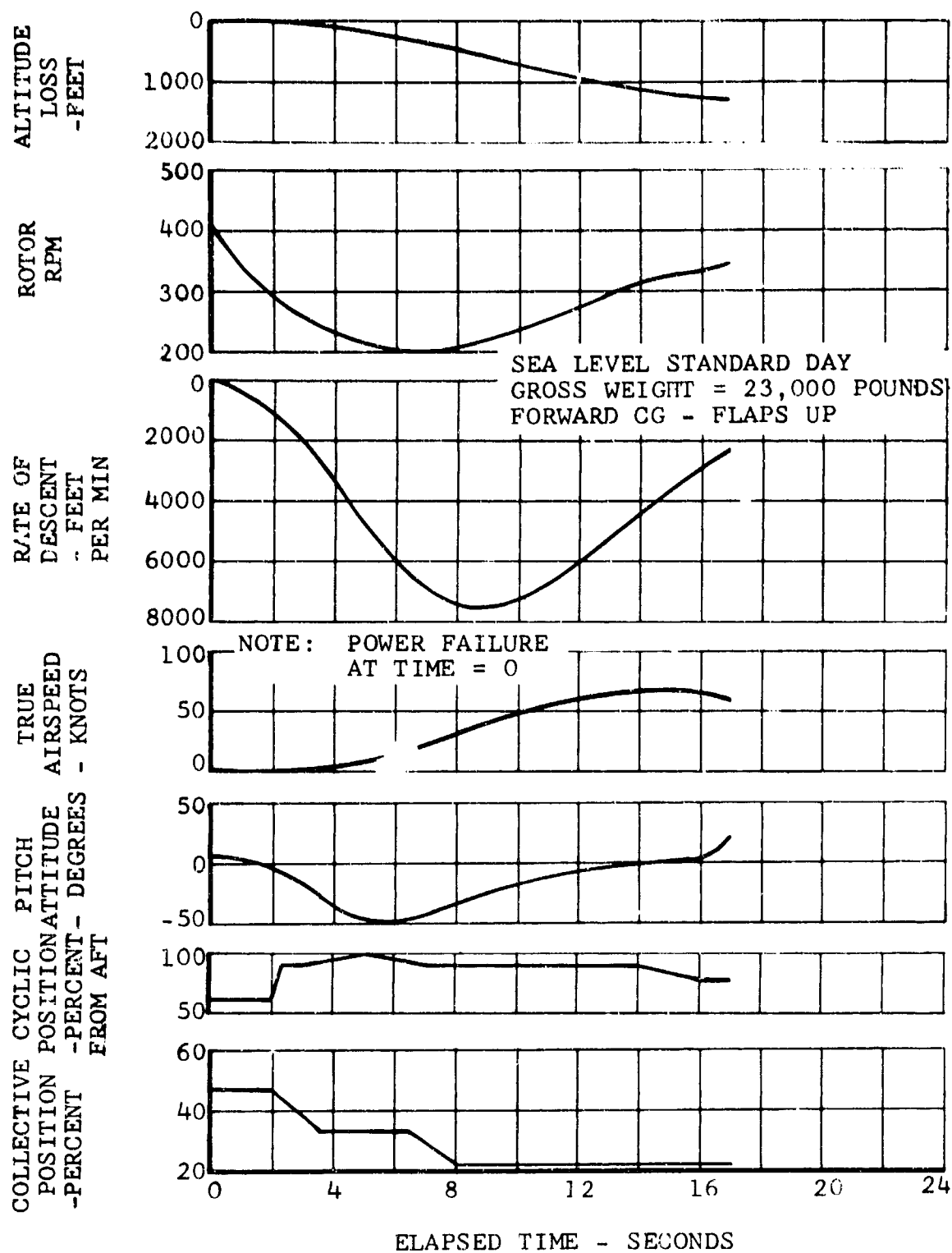


Figure 176. Time History of Power Failure in Out of Ground Effect Hover.

initiated. This point is reached after 16 seconds and an altitude loss of 1250 feet. The total height lost is the sum of the height lost for each of the two steps, which is about 1400 feet.

In general, when a helicopter-mode power failure occurs at speeds less than 80 knots, then acceleration to 80 to 100 knots should be made and a steady descent established, followed by a conventional helicopter-type flare and landing. When failure occurs at speeds above 100 knots, then a deceleration should be made to 80 to 100 knots and a steady descent should be set up, followed by flare and landing.

b. Fixed-Wing Mode

The general response following a total power failure in the fixed-wing mode is to flare and thereby exchange airspeed for altitude until conversion speed is reached. Reconversion can be performed as the deceleration continues. Once helicopter configuration is attained, the rotor-pitch governor is switched off so that rpm can be built up prior to flare and landing.

Power failure at two speeds has been investigated in detail. Figure 177 is a time history of the 150-knot case in which the power failure is followed by a continuous reconversion at 15 degrees per second and a deceleration to 80 knots in helicopter autorotation. About 300 feet of altitude is gained during the reconversion. During the flare, 120 feet (see Figure 175) of altitude will be lost, so that the complete maneuver can be performed with no altitude loss. Figure 178 is a time history of the 350-knot case in which the failure is followed by a flare, during which 2000 feet of altitude are gained and speed is reduced to 150 knots. From here, reconversion can be made as shown in the previous figure.

c. Height-Velocity Diagram

The height-velocity diagram for the case of a failure of both engines, Figure 179, is made from the calculations described above. A 2-second delay is used for the high-speed and OGE points. For the IGE hovering point, a 1-second delay is used, since it is assumed that pilot concentration will be such that a longer delay is not required. At high speed, an unsafe altitude is shown only to indicate the danger of flying close to the ground at these speeds. Near wing-stall speed, the curve is slightly raised to allow forward speed to be built up before initiation of reconversion. The fairing between the computed points follows the normal relationship between altitude and forward speed as determined by flight tests of helicopters. For a single-engine failure, no unsafe altitudes are indicated.

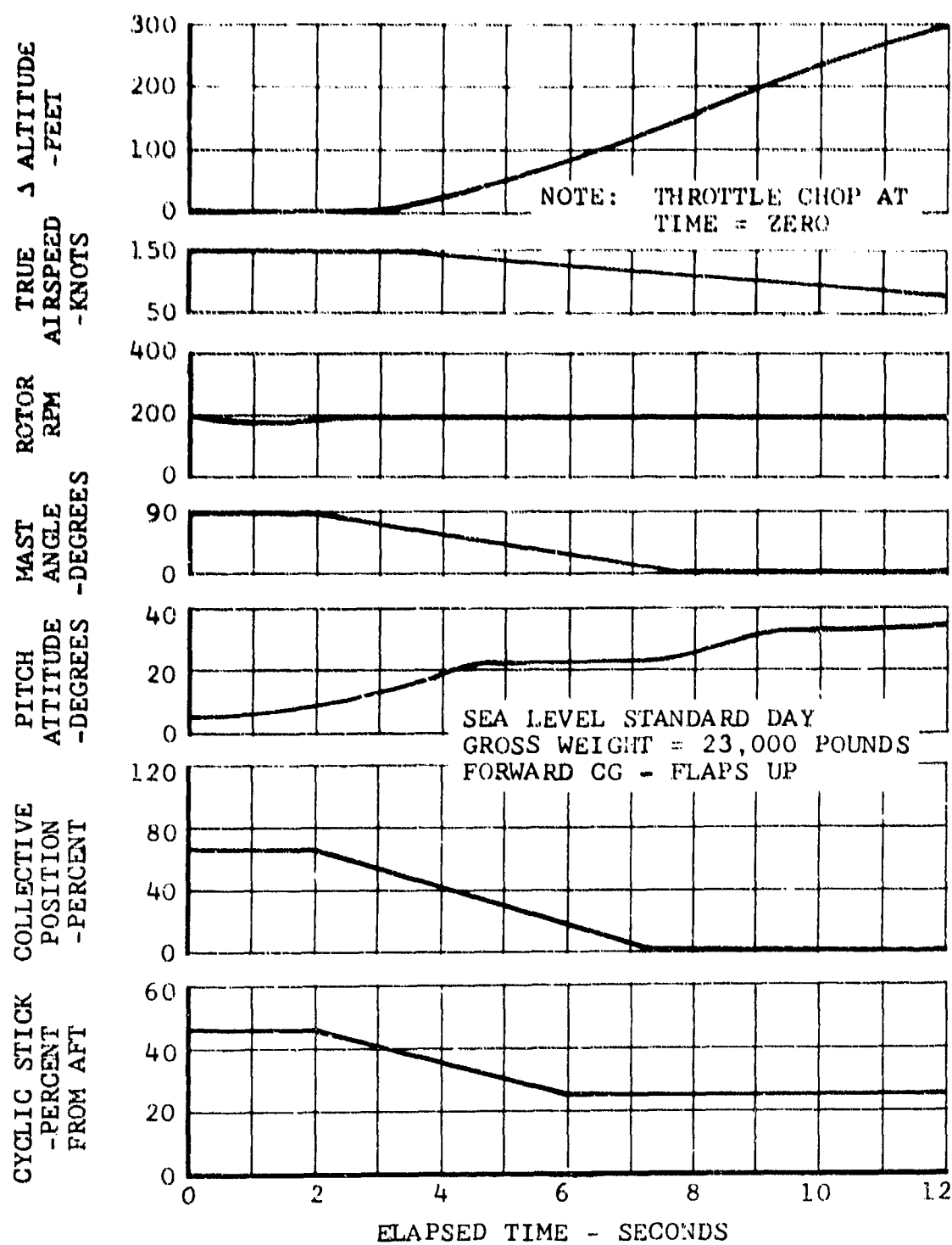


Figure 177. 150-Knot Power-Off Reconversion Time History, Rotor Governor On.

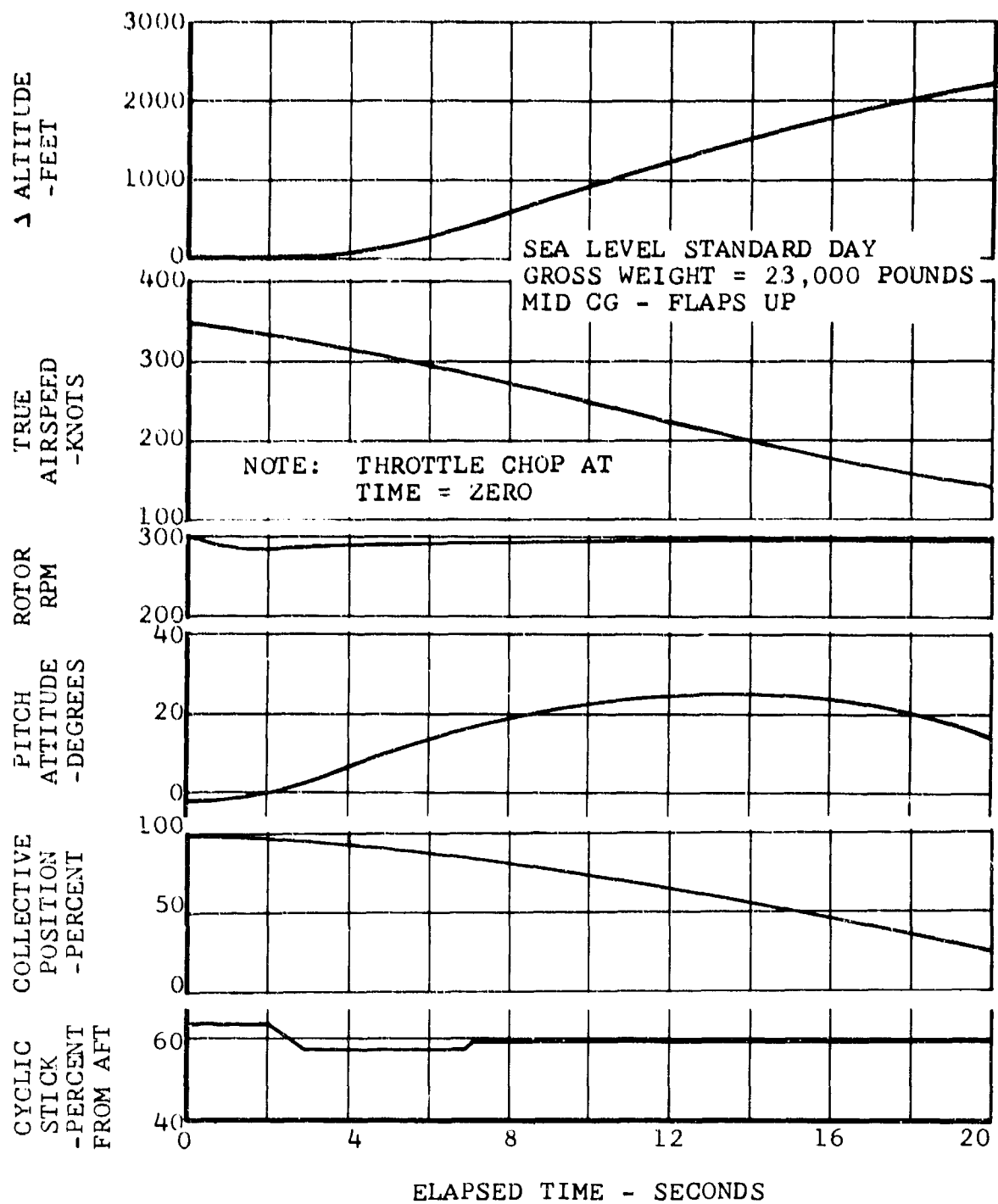


Figure 178. 350-Knot Throttle-Chop Time History, Rotor Governor On.

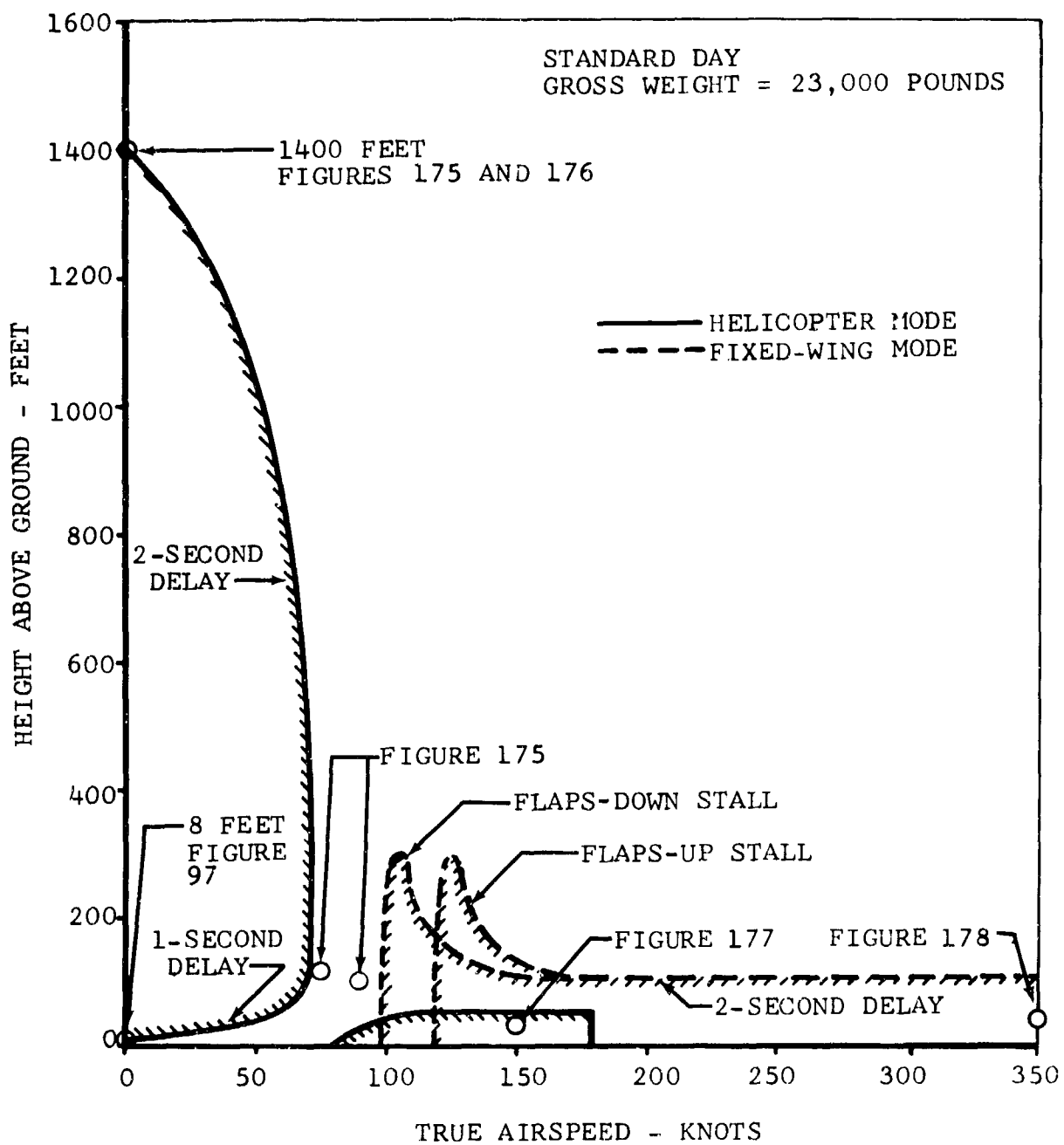


Figure 179. Height-Velocity Diagram.

SECTION VI. ELECTRICAL, HYDRAULIC, AND MECHANICAL SYSTEMS

A. FLIGHT CONTROLS

1. GENERAL DESCRIPTION

The flight controls of the D266 Composite Research Aircraft combine the basic elements of conventional helicopter and fixed-wing aircraft control systems. The control system is so arranged that a single pilot can maintain full control throughout the flight envelope, including conversion. It is shown schematically in Figure 262. The cockpit controls are connected to the respective rotor or surface controls by mechanical push-pull linkages and mixing levers, which provide the relationships among the cockpit, rotor, and control-surface travels given in Table XXXIII.

The control phasing during conversion is accomplished mechanically by means of mixing levers and the geometric arrangement of the control components. It varies only as a function of the rotor-pylon position. The rotor provides the primary control in the helicopter flight mode. Conventional aircraft control surfaces are used in the fixed-wing flight mode. Aircraft control during conversion is provided by both the rotor and the control surfaces.

a. Helicopter Flight Configuration

In helicopter configuration, control is provided by the following pilot inputs to the rotor:

- Pitch - forward or aft cyclic blade pitch on both rotors
- Yaw - differential cyclic blade pitch on the rotors
- Roll - differential collective blade pitch on the rotors
- Thrust - collective blade pitch increase or decrease on both rotors

A momentary up-down switch with a position indicator controls the position of the flaps and the neutral position of the ailerons. The flaps and the ailerons may be deflected 60 degrees to provide an effective full-span flap for reducing the rotor download on the airframe.

b. Conversion Configuration

To provide proper authority of the controls during conversion between the helicopter and the fixed-wing flight modes, some

TABLE XXXIII FLIGHT-CONTROL-SYSTEM TRAVELS						
Control (Effect)	Cockpit		Travel			Fixed-Wing Mode
	Control	Travel	Surface	Helicopter	Conversion	
Pitch	Control Stick Fore and Aft	±6.0"	Cyclic Pitch Elevator	±9° 24° up 16° down	varies 24° up 16° down	0 24° up 16° down
Roll	Control Stick Lateral	±6.0"	Differential Collective Ailerons	±2° ±15°	varies ±15°	±0.2° ±15°
(Roll/Yaw Trim)	Rotor Trim		Differential Collective	±.5°	±.5°	±.5°
Yaw	Rudder Pedals	±3.25"	Differential Cyclic Pitch Rudder	±4.25° ±10°	varies ±10°	0 ±10°
(Favorable Roll)			Differential Collective	±.25°	varies	0°
Flaps (Decrease Download)	Flap Setting	-	Flaps Ailerons	0-60° 0-60°	0-30° 0-30°	0° 0°
Thrust	Collective Stick Lever	13.25"		0-18°	varies	20°-55°

controls are phased out, changed in authority, or phased in. The change in control authority during conversion is shown in Figures 180 and 181.

The sequence of control authority changes mechanically as the pylon is converted from helicopter (vertical) to fixed-wing (horizontal) mode and is as follows:

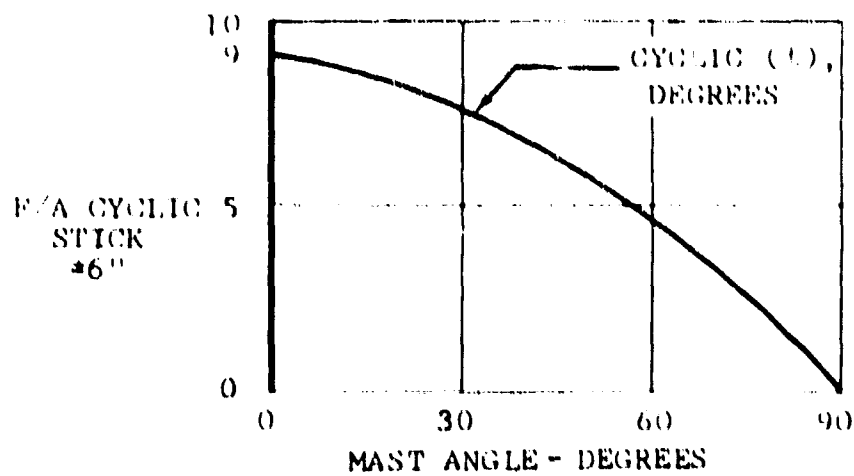
- The authority of the control stick on the longitudinal cyclic blade pitch, as shown by Figure 180a, is reduced approximately as the cosine of the mast angle.
- The authority of the control stick on differential collective blade pitch, as shown by Figure 180b, is reduced approximately as the cosine of the mast angle.
- The authority of the rudder pedals on the differential collective and cyclic blade pitch is shown by Figure 181a. Differential cyclic pitch is reduced in authority approximately as the cosine of the mast angle. Differential collective pitch is increased to ± 1 degree at a 40-degree mast angle and then is phased out when the rotor mast reaches the vertical position. This change in differential collective pitch is included as a secondary feature to provide a more favorable roll-with-yaw characteristic during conversion.
- The authority of the collective lever on collective blade pitch is shown by Figure 181b. The collective pitch and the collective pitch range are both increased with increasing mast angles.

Thrust control during conversion is accomplished by selecting a desired engine power lever and rotor speed. The rotor pitch is controlled automatically by the rotor-pitch governor. A two-way momentary switch on the control stick actuates the conversion system. The switch is moved forward to rotate the pylon to the fixed-wing flight position and aft to return it to the helicopter position. Conversion can be continuous or incremental. The conversion can be stopped and the pylon locked in any selected position by releasing the conversion switch.

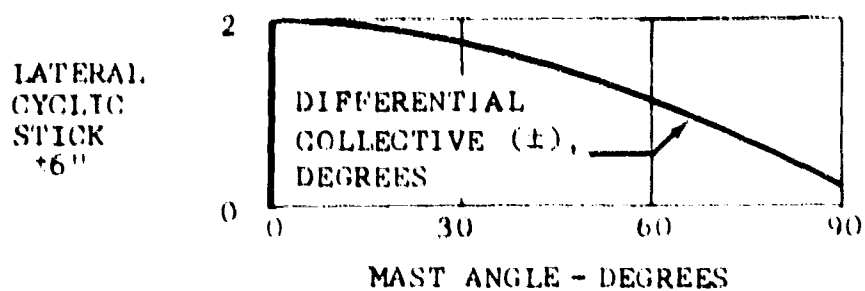
c. Fixed-Wing Configuration

In the fixed-wing flight configuration, primary control of the aircraft is identical to that of fixed-wing, propeller aircraft. The control surfaces are also active in the helicopter mode but have limited authority, owing to the low dynamic pressures and the high moment capability of the rotors.

The rotor trim provides aircraft yaw trim in fixed-wing flight by equalizing the thrust of the rotors. The rotor thrust is

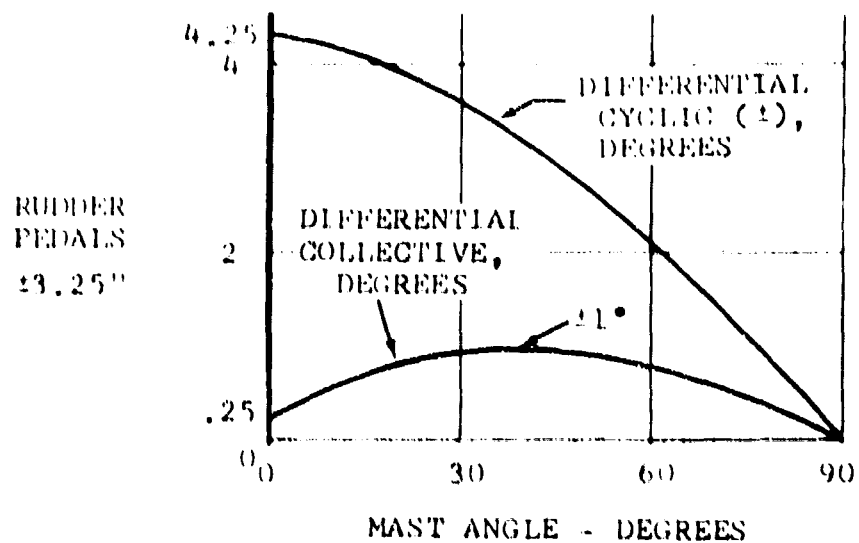


a. Pitch

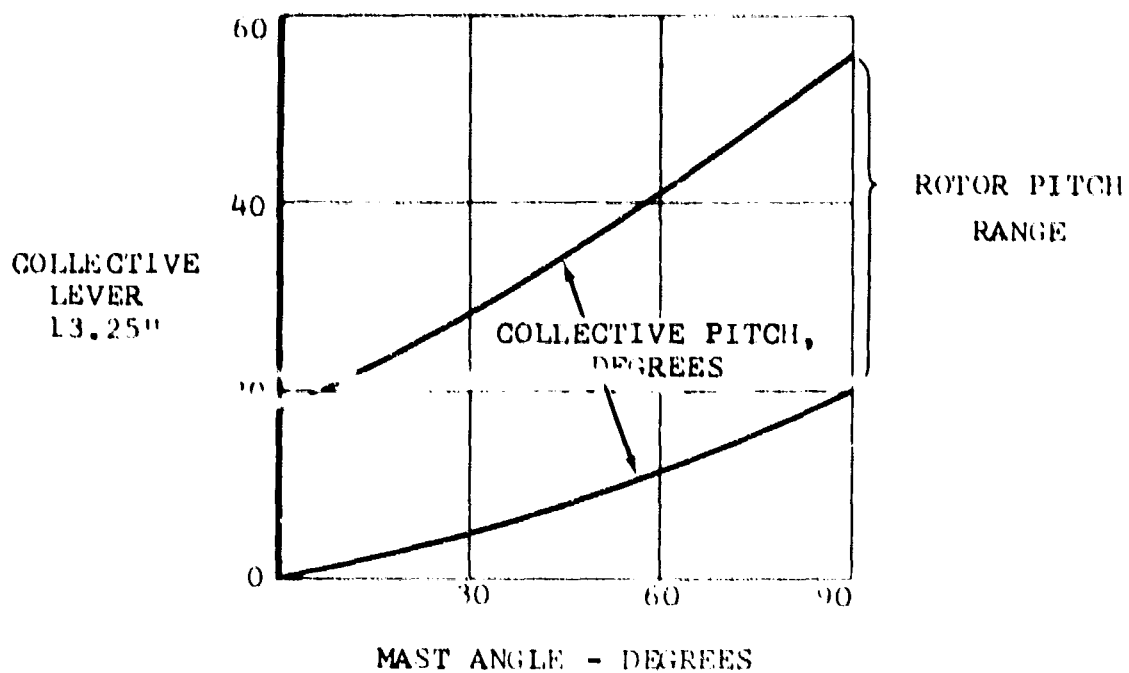


b. Roll

Figure 180. Control Relationship - Pitch and Roll.



a. Directional



b. Thrust

Figure 181. Control Relationship - Directional and Thrust.

controlled by setting the power level of the engines with the power-management levers.

2. COCKPIT CONTROLS

The control sticks are gimbal-mounted at the floor directly in front of the pilot and copilot, and they are interconnected by push-pull linkages. Longitudinal movement imparts a push-pull motion to the longitudinal control linkage to produce cyclic blade pitch changes on the rotors and to deflect the elevator surfaces. Lateral movement of the stick imparts a push-pull motion to the lateral control linkage to produce differential collective blade pitch change and differential deflection of the ailerons.

Directional control of the aircraft is provided by conventional rudder pedals. The pedal pivot attachment is mounted below the floor level. Each pedal is connected by a link to a walking-beam-type bellcrank with a single lateral output. The control pivot of the bellcranks is moved forward or aft to adjust the pedals. The lateral outputs of the bellcranks are connected to the directional-control linkages, which deflect the rudder and make differential cyclic blade pitch changes. Wheel toe brakes are provided on the pilot's rudder pedals.

Rotor thrust is controlled by interconnected collective levers, pivoted at the floor. Upward or downward motion of these levers imparts a push-pull motion to the collective blade-pitch-control linkages. Collective pitch is controlled either manually by the collective lever or automatically by the rotor-pitch-governor actuator that is connected in parallel with the lever. When engaged, the actuator automatically moves the linkage and the lever. The pilot can override the actuator input by manually operating the collective lever.

The power-management levers are interconnected with the twist-grips on the pilot's collective lever. Friction for the power levers and the collective twist-grips is controlled by a lever adjacent to the power levers. The rpm-select lever is located on the left of the engine power control levers. A detent prevents inadvertent retardation of the control below 95-percent rpm. The governor is automatically engaged when the lever is retarded past the detent position. A button on the head of the lever may be depressed to prevent governor engagement at an undesired rpm.

The flaps are controlled by a momentary switch on the pedestal and a position indicator on the instrument panel. Either pilot can operate the flaps by depressing and holding the

switch in the desired direction of flap travel. The flaps may be positioned at any setting between trail and 60 degrees down. The neutral setting of the ailerons follows the wing-flap position. A pitch-trim switch controls a tab on the elevator to permit trimming of forces in the event of a failure of the hydraulic boost system. A rotor-trim switch on the console changes collective pitch differentially for trim in both the helicopter and the fixed-wing modes.

3. ROTOR CONTROLS

The rotor controls provide all primary control of the aircraft during helicopter flight, and thrust control (power) in fixed-wing flight.

a. Fixed Controls

The fixed controls provide rigid mechanical connections between the cockpit and the rotating control system and control surfaces. All controls are hydraulically power-boasted. All mixing and phasing bellcranks (except cyclic phasing) are located above the cabin in the area of the fuselage-wing junction.

(1) Cyclic

Longitudinal control stick and rudder pedal motions are mixed to provide a single control motion to each rotor. The control mixing lever arrangement is shown in Figure 182. A longitudinal movement of the control stick, shown in the upper sketch, provides a cyclic control input to the mixing levers and identical cyclic blade-pitch changes at both rotors. Rudder pedal movement, shown in the lower sketch, provides a differential cyclic control input to the mixing levers and produces equal but opposite blade-pitch changes at the rotors.

The mixed control output is independently transferred to the rotors by means of a push-pull control routed inside the leading edge of each wing. The push-pull controls connect to a torque tube, Figure 183, that is mounted at each wingtip. The other end of the torque tube is attached to the transmission. The torque tube is offset from the conversion axis and has a preloaded ball spline that accommodates the change in length during conversion. The preloading precludes the possibility of looseness in the control.

(2) Cyclic Phase-Out

The output arm of the torque tube, in Figure 183, travels in a vertical plane and is connected to control tube "A" which

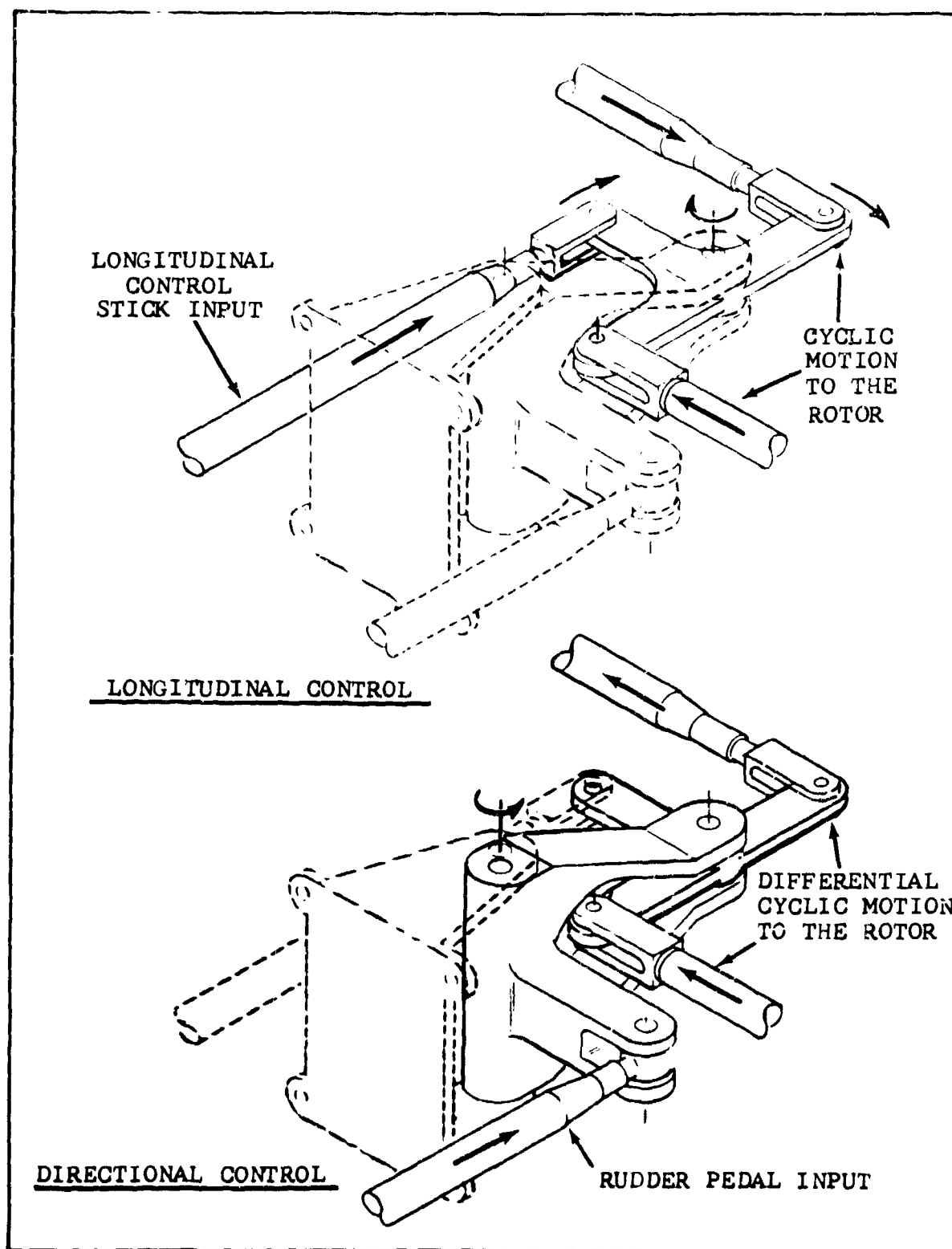


Figure 182. Cyclic-and-Differential-Cyclic Mixing.

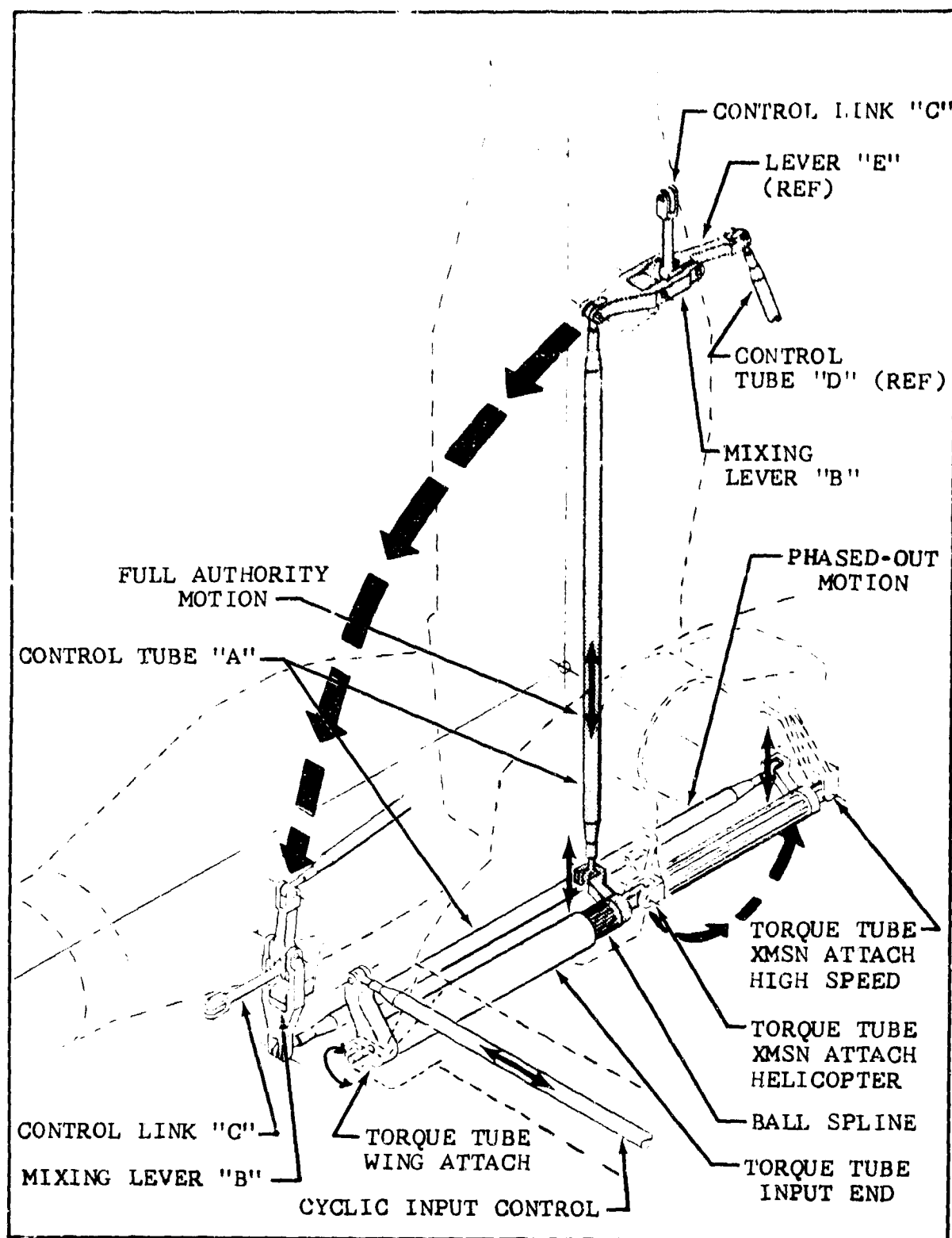


Figure 183. Longitudinal Control Phasing Levers.

moves parallel to the rotor mast. As a result of this geometry, the torque tube input to the rotor is phased out as the pylon rotates from the vertical to the horizontal position. In the helicopter configuration, rotation of the torque tube imparts a vertical push-pull motion to the attached control tube "A" which causes the rotor blade pitch to change cyclically. As the pylon rotates forward toward the fixed-wing position, the authority of the torque tube output is geometrically reduced. When the pylon reaches horizontal, the pilot (torque tube) control authority is completely phased out.

The upper end of the control tube "A" attaches to the pylon coupling mixing lever "B" located at the side of the pylon below the swashplate.

Control link "C" is the tie between mixing lever "B" and a dual hydraulic cylinder. The hydraulic cylinder is based on the transmission. The output end of the cylinder piston rod is attached directly to the swashplate. This arrangement reacts the rotor steady and oscillatory loads as close to the rotor as possible and minimizes the number of loaded linkages.

(3) Swashplate-Pylon Coupling Control

A swashplate-pylon coupling control increases rotor stability in the fixed-wing flight mode. It introduces cyclic control opposite to the pitching of the pylon. The swashplate-pylon coupling control is phased out (inactive) in helicopter flight mode and is phased in as a function of mast angle during conversion to the fixed-wing flight mode.

The pylon is spring-mounted by means of a rubber mount attached between the conversion actuator, which is wing-based, and the main transmission. Deflection of the rubber mount occurs on the axis of the conversion actuator. A control tube "D", as shown in Figure 184, is attached to the conversion actuator end of the rubber mount and a lever on the transmission. This control tube rotates with the pylon during conversion, is positioned approximately parallel to the actuator in the fixed-wing mode, and is 90 degrees to the actuator in the helicopter mode. These control tube positions relative to the conversion actuator change authority of the swashplate-pylon coupling control as a function of the pylon position. In helicopter mode, this control is phased out. During conversion, it is phased in as a cosine function of the mast angle.

As the pylon is deflected in the fixed-wing mode, in the direction shown in Figure 184, the motion of tube "D" as the result

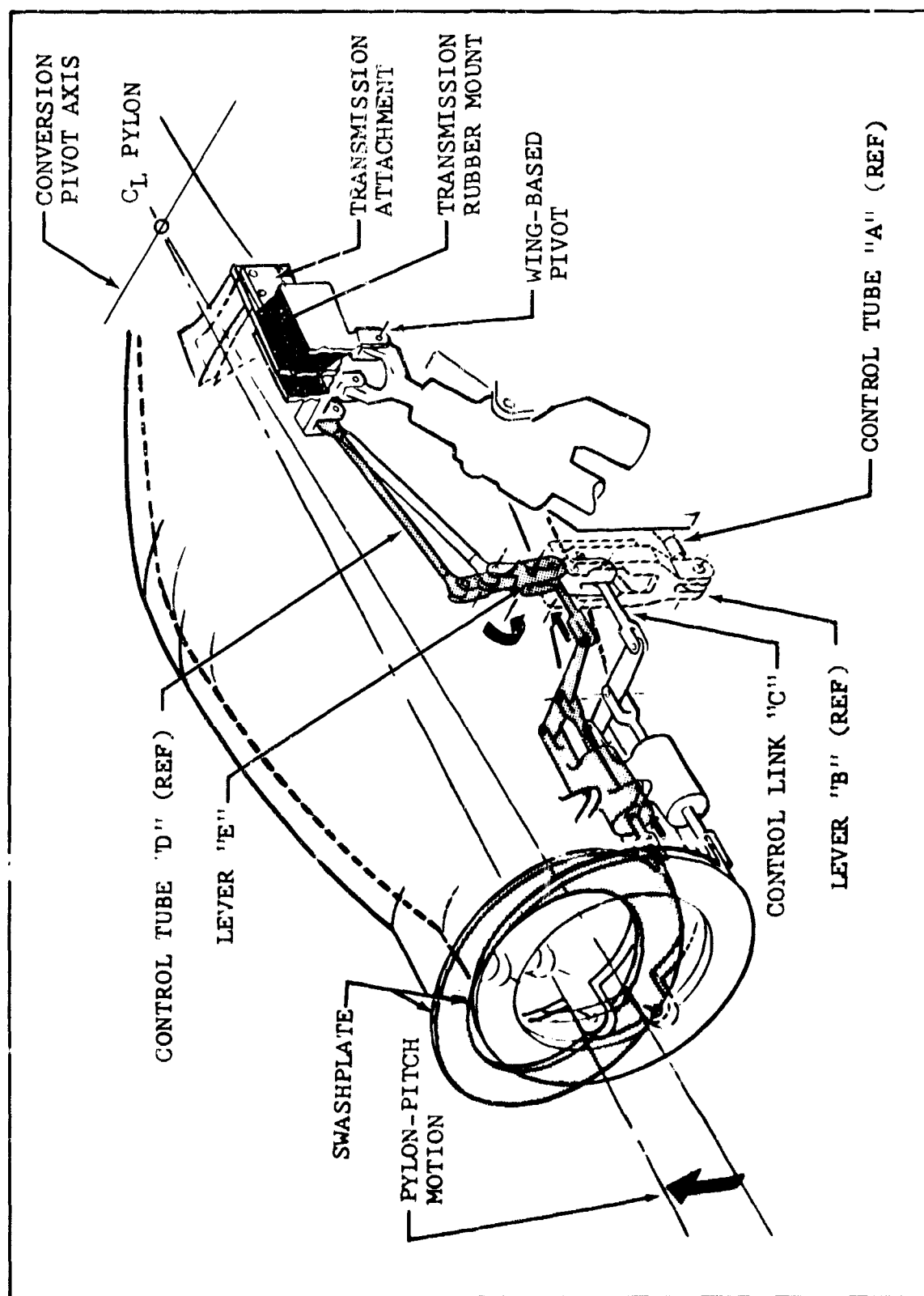


Figure 184. Swashplate-Pylon Coupling Control.

of this deflection causes motion in lever "E" in a counterclockwise direction and moves control link "C" toward the rubber mount. This actuates the swashplate in the direction which opposes the pylon-pitch motion and tends to restore the pylon to its neutral position. Lever "B", which is stationary in fixed-wing mode, provides the fulcrum for lever "E".

(4) Collective

Collective blade pitch of both rotors is changed manually by the collective lever or automatically by the rotor-pitch-governor actuator. Differential collective-pitch changes are produced primarily by lateral motion of the control stick. The rudder pedals and the rotor trim control provide secondary differential collective-pitch changes. The authorities of the collective controls are automatically changed during conversion. This change is accomplished through mechanical linkages which are driven by the conversion system.

(5) Collective Range-Shift Phasing Control

The upward and downward motion of the collective lever is routed to a collective range-shift phase-control bellcrank. During conversion, collective pitch is automatically increased with mast angle. The output from the phase-control crank results in a 0- to 18-degree pitch range in the helicopter mode and a 20- to 55-degree pitch range in the fixed-wing mode. The collective lever travel is the same (13.25 inches) for both modes. The phase control of the collective system is accomplished by a simple walking-beam-type lever with a movable fulcrum, as shown in Figure 185. The collective pitch is controlled manually, or automatically by the rotor-pitch-governor actuator. This actuator is connected in parallel with the collective system and actuates the collective lever with pitch-change demands.

(6) Differential Collective (Lateral Control-Stick Motion)

Lateral motion of the control stick is routed through a lateral phase-control bellcrank which introduces the proper differential collective blade-pitch control authority during conversion. This bellcrank is shown in Figure 186. The output decreases differential collective from ± 2 degrees in the helicopter mode to ± 0.2 degree in the fixed-wing mode. The rate of control authority changes approximately as the cosine of the conversion angle.

(7) Differential Collective (Rudder Pedal Motion)

The control motion from the rudder pedals is routed through a rudder phase-control bellcrank, as shown in Figure 187. This

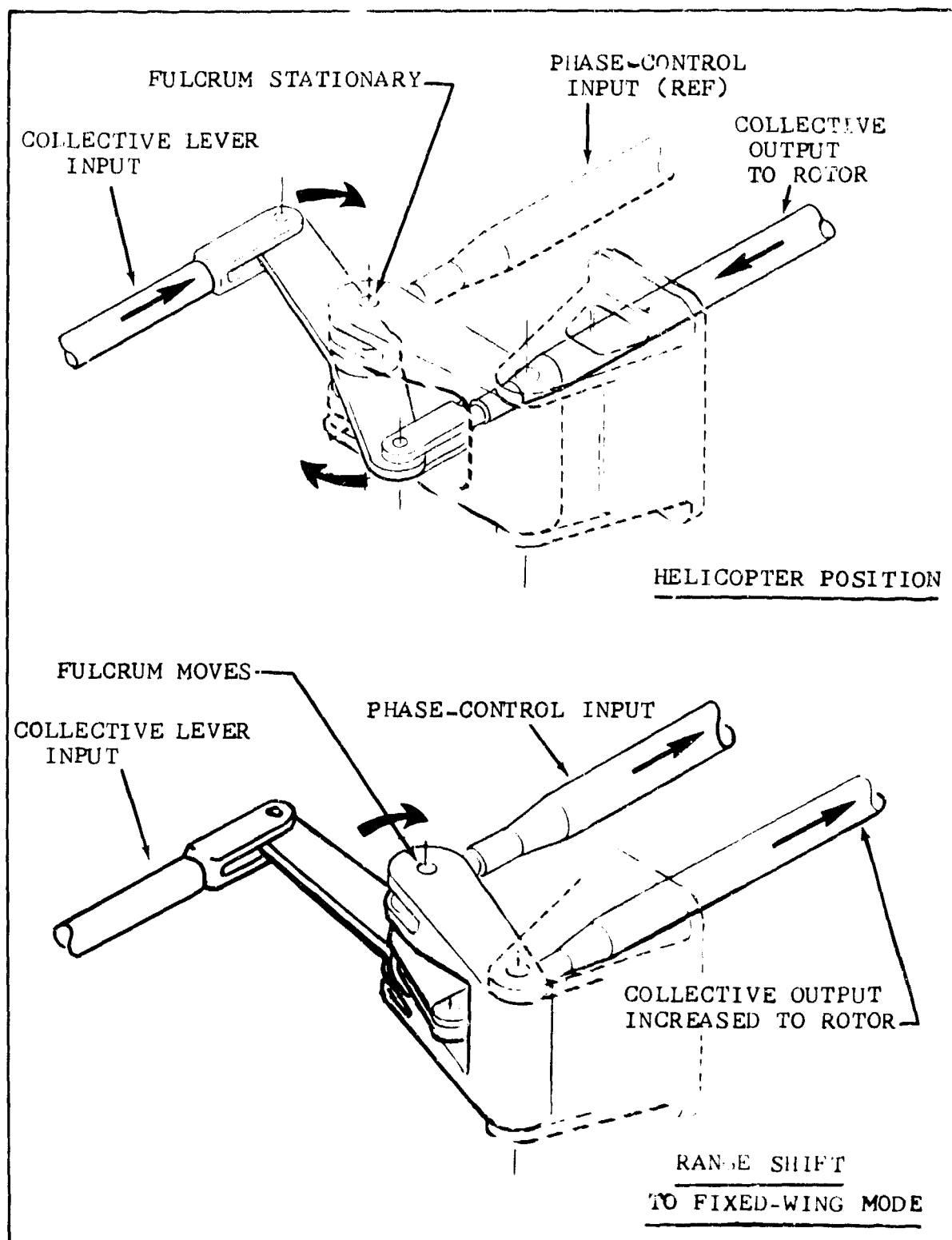


Figure 185. Collective Range-Shift Phase Control.

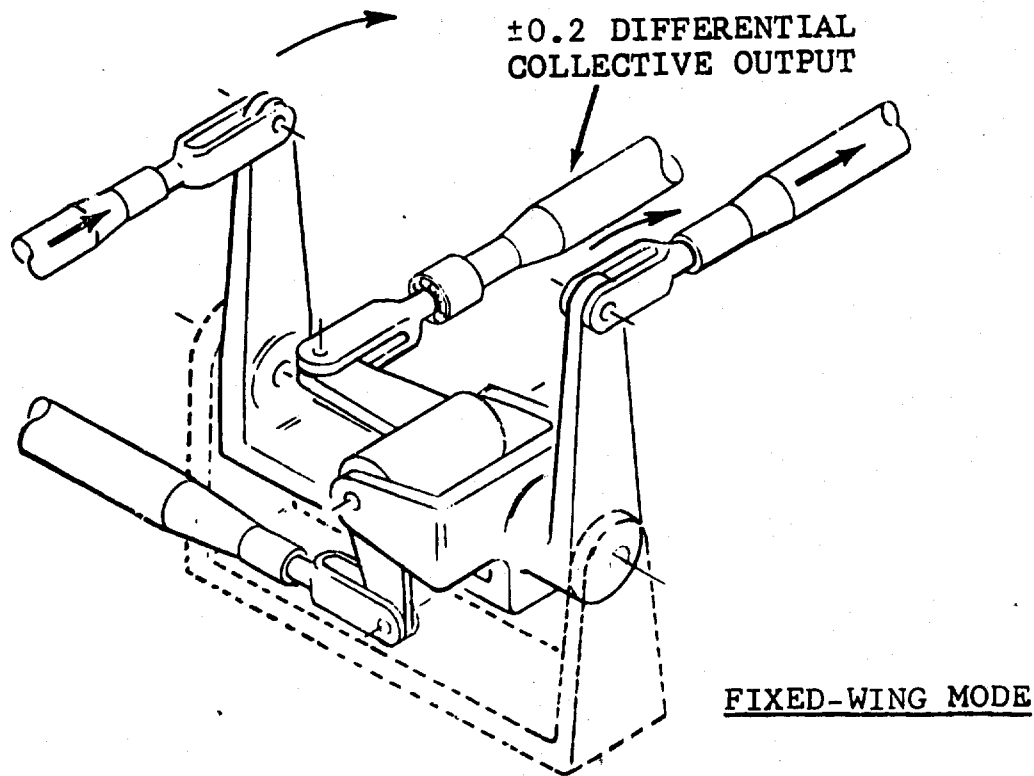
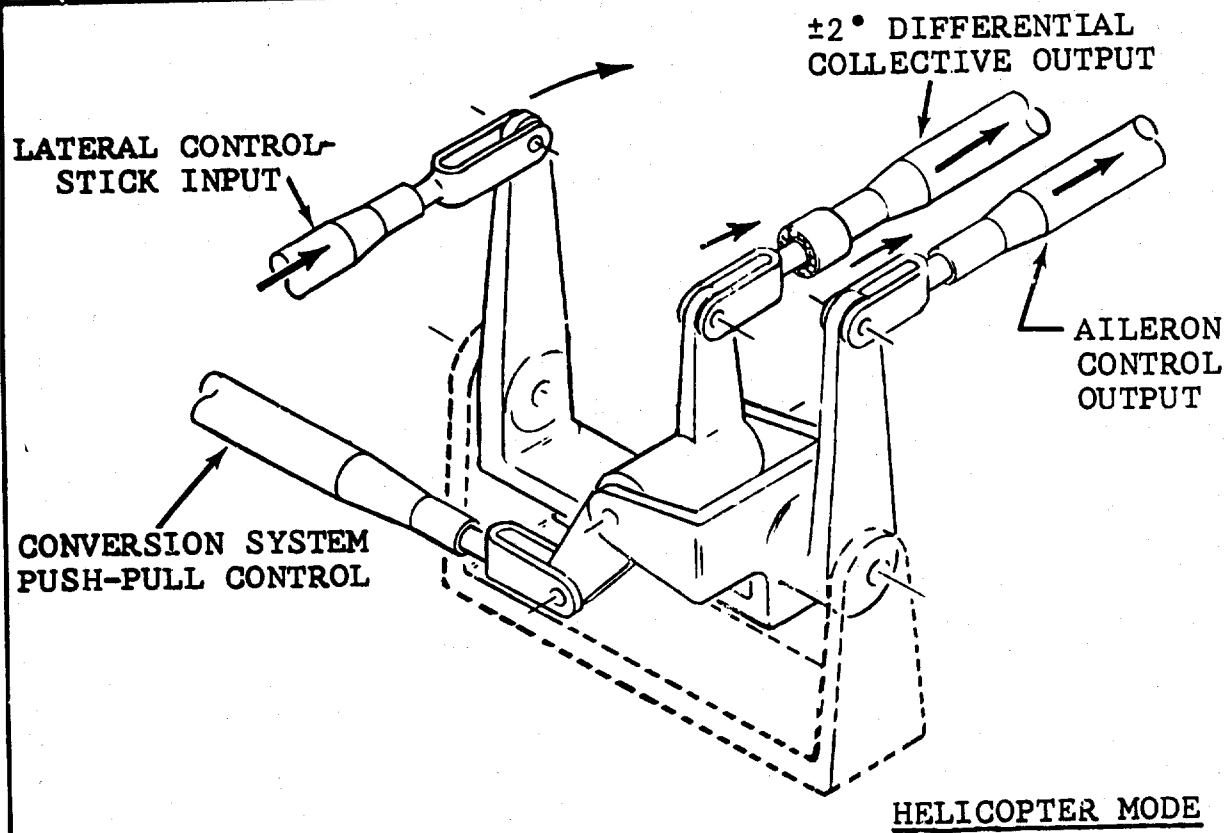
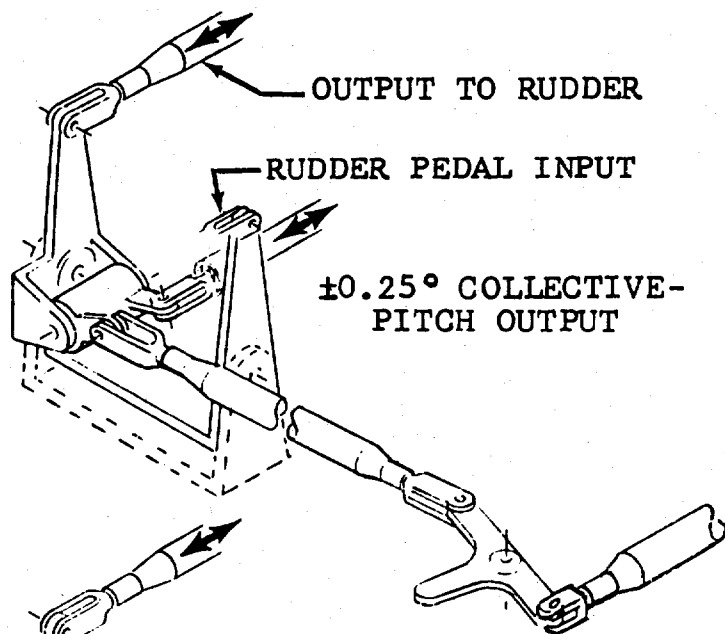
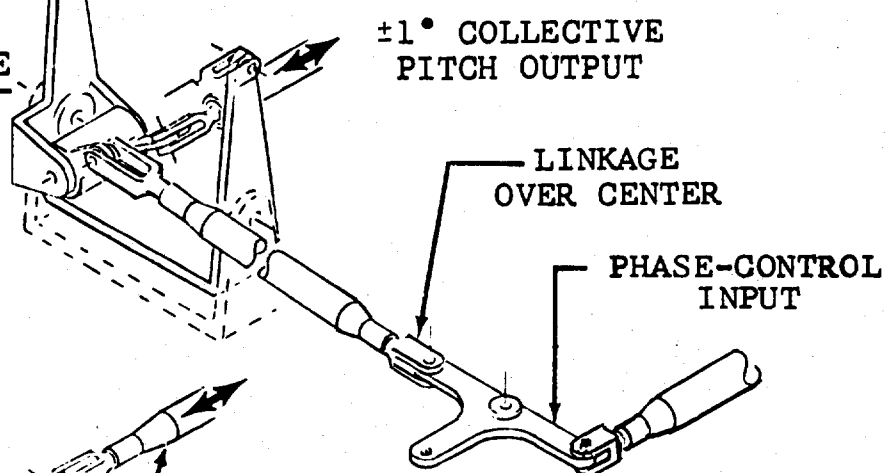


Figure 186. Lateral Control Phasing Levers.

HELICOPTER
MODE



40° MAST ANGLE



FIXED-WING
MODE

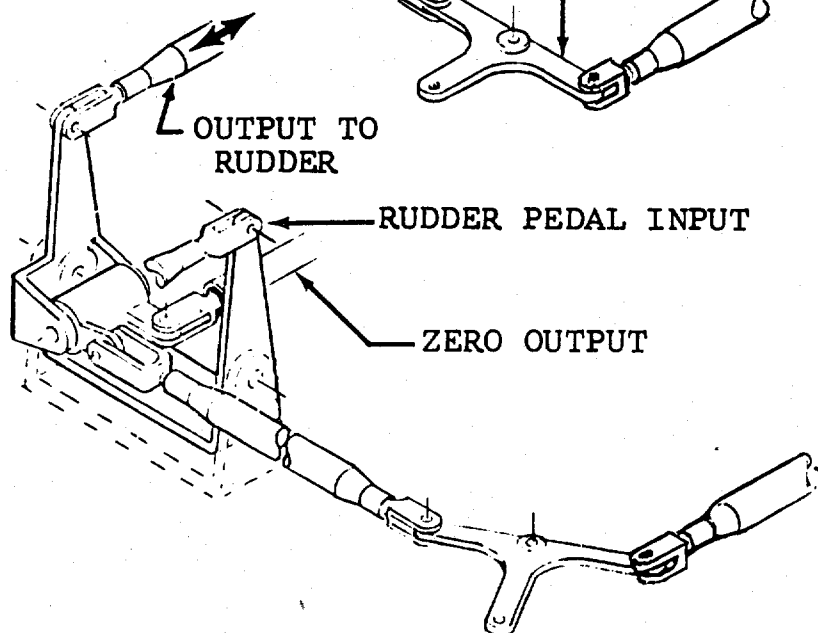


Figure 187. Rudder Pedal Phase Control.

bellcrank arrangement changes the authority of the rudder output motion as a function of the conversion position.

In the helicopter mode, full pedal motion results in ± 0.25 degree of differential collective pitch change. During conversion, the control authority is increased to ± 1 degree of pitch change at 40 degrees of conversion, and then it is reduced to zero in the fixed-wing (fully converted) mode.

(8) Differential Collective (Rotor Pitch-Trim Actuator)

The phased differential collective outputs due to lateral control-stick and rudder-pedal motions are routed through a combining crank and emerge as a single output, as shown in Figure 188 (Link "A" in lower sketch). Link "A" is the input to the collective-and-differential-collective mixing levers. The rotor-trim actuator is connected in series with control Link "A", and extension or retraction of the actuator introduces differential collective pitch change for rotor thrust trim. Collective control inputs (upper sketch) are routed directly to the output bellcrank and produce identical outputs for both rotors.

The collective pitch output is routed to each rotor by push-pull controls installed aft of the wing spars. At the wing-tip, the differential collective control is routed to the outboard side of the pylon to a walking beam with the output on the center of rotation of the conversion axis. The walking beam is linked on the conversion axis to the transmission-mounted dual hydraulic cylinder. This allows the pylon to rotate through its conversion angles without introducing collective pitch.

The dual hydraulic servo-cylinder is installed through the center of the mast and is then directly coupled to the rotating control system.

b. Rotating Controls

Collective control inputs are introduced by means of a non-rotating dual hydraulic cylinder and tube extension inside the rotor mast. The nonrotating collective control tube transmits the collective motion to a rotating collective head by means of duplex angular-contact bearings. The collective head slides inside the rotor shaft, and it is splined to the mast at its lower end to provide rotation with the mast.

Cyclic control inputs are introduced through the hydraulic cylinder, which is mounted on the side of the transmission case and is connected to the nonrotating ring of the swashplate.

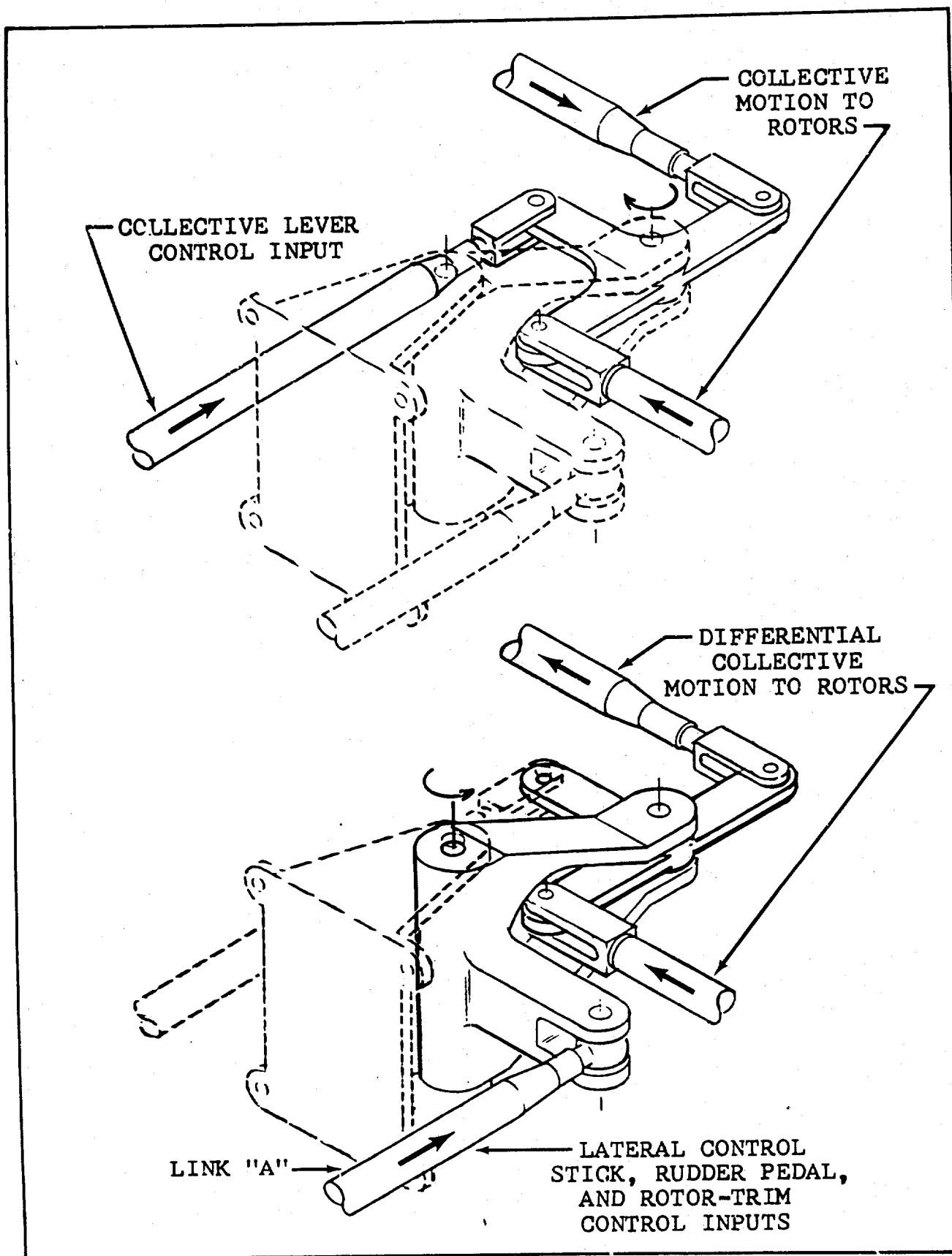


Figure 188. Collective-and-Differential-Collective Mixing Levers.

The swashplate is mounted on a support which permits ± 10 degrees of motion. Only one axis of tilt is provided, and this is oriented so that retraction of the hydraulic cylinder (down on the swashplate input) introduces a cyclic blade pitch change which tilts the rotor downward and forward. Bearings mounted around the fixed ring transmit the cyclic inputs to the rotating ring of the swashplate.

Cyclic motion is transmitted from the rotating ring to the collective cyclic mixing levers located above the hub by means of a fixed-length control tube. There are three mixing levers, one for each blade, which combine the cyclic and collective motions into one output. They are pivoted near their center on the collective head, with one end attached to the cyclic control tube and the other end attached to the pitch-change tube. The pitch-change tube is connected to the blade pitch horn and is adjustable to provide for tracking the blades.

The links, attached between the spinner support ring and the swashplate ring, drive the rotating controls without interfering with the swashplate-tilting motion.

4. SURFACE CONTROLS

Movable surface controls provide the control of the aircraft in fixed-wing mode. They also provide a degree of effectiveness in the higher-speed helicopter spectrum and during conversion. The surface controls, except flaps, are coupled with the rotor controls.

The rudder control is a direct link from the pedals to the rudder. Near the wing-fuselage juncture it is coupled with the rotor control. A single, hydraulically powered cylinder is mounted in the fin. An irreversible valve prevents control feedback in the event of hydraulic system failure. The output motion is directed through a bellcrank and links to the rudder. The full movement of the rudder pedals produces full rudder travel in all flight modes.

The elevator controls are coupled to the fore-and-aft motion of the control stick and are routed directly to a single, irreversible, hydraulically powered cylinder that is mounted in the vertical fin. The output of the hydraulic cylinder is directed by bellcranks and linkage to each elevator surface. Full control-stick travel produces full elevator travel in all flight modes. An electrically actuated trim tab, on the left elevator control surface, provides control-force trim in the event of a hydraulic power failure.

The aileron control is connected to the lateral output of the control stick and is directed aft to a bellcrank at the wing-fuselage juncture. This bellcrank provides equal-but-opposite

motions to push-pull controls, routed aft of the wing spar, and to a mixing bellcrank. This mixing bellcrank provides for normal differential aileron deflections due to control-stick inputs, and for changing the neutral position of the ailerons with extension or retraction of the flaps. The mixing of the flap and aileron control inputs is accomplished by a walking-beam-bellcrank combination that allows the aileron to deflect with the flap and that also provides a variation of aileron travel with flap deflection. With 100-percent flap extension, the total aileron travel is approximately 10-percent-down and 50-percent-up of full aileron travel. The output from the walking beam is linked with a bellcrank to a dual hydraulic cylinder which is attached directly to each aileron.

The flaps are controlled by hydraulically driven screw jacks. One hydraulic motor is powered by hydraulic System III and provides normal flap actuation. The second hydraulic motor is powered by the APU hydraulic system and provides flap actuation in the event of primary hydraulic system failure. The flap actuation screw jacks are interconnected with shafting to assure synchronization. The screw jacks are irreversible to provide positive locking of the flaps in any position.

B. HYDRAULIC SYSTEM

The D266 Composite Research Aircraft has three independent transmission-driven hydraulic systems in addition to one system driven by an auxiliary power unit. All flight controls are powered by the transmission-driven hydraulic systems so that hydraulic power is independent of the engines. The hydraulic systems use MIL-H-5606 hydraulic fluid and operate at 3000 psig. Dual servoactuators are provided in the primary rotor controls and for the ailerons.

1. SYSTEMS I AND II

Systems I and II (Figure 189) are identical and are located on the left and right pylons, respectively. Each system supplies power to one side of the rotor and aileron control actuators located on or near the pylons. Each system also powers a conversion actuator. "Bootstrap"-type pressurized reservoirs permit system operation in any conversion position.

The basic hydraulic power system components are unitized into one compact modular assembly, which simplifies installation and increases reliability, as it eliminates all of the fittings, tubes, and joints which would be used to interconnect individual components. It also saves space and weight, and it is easily replaceable.

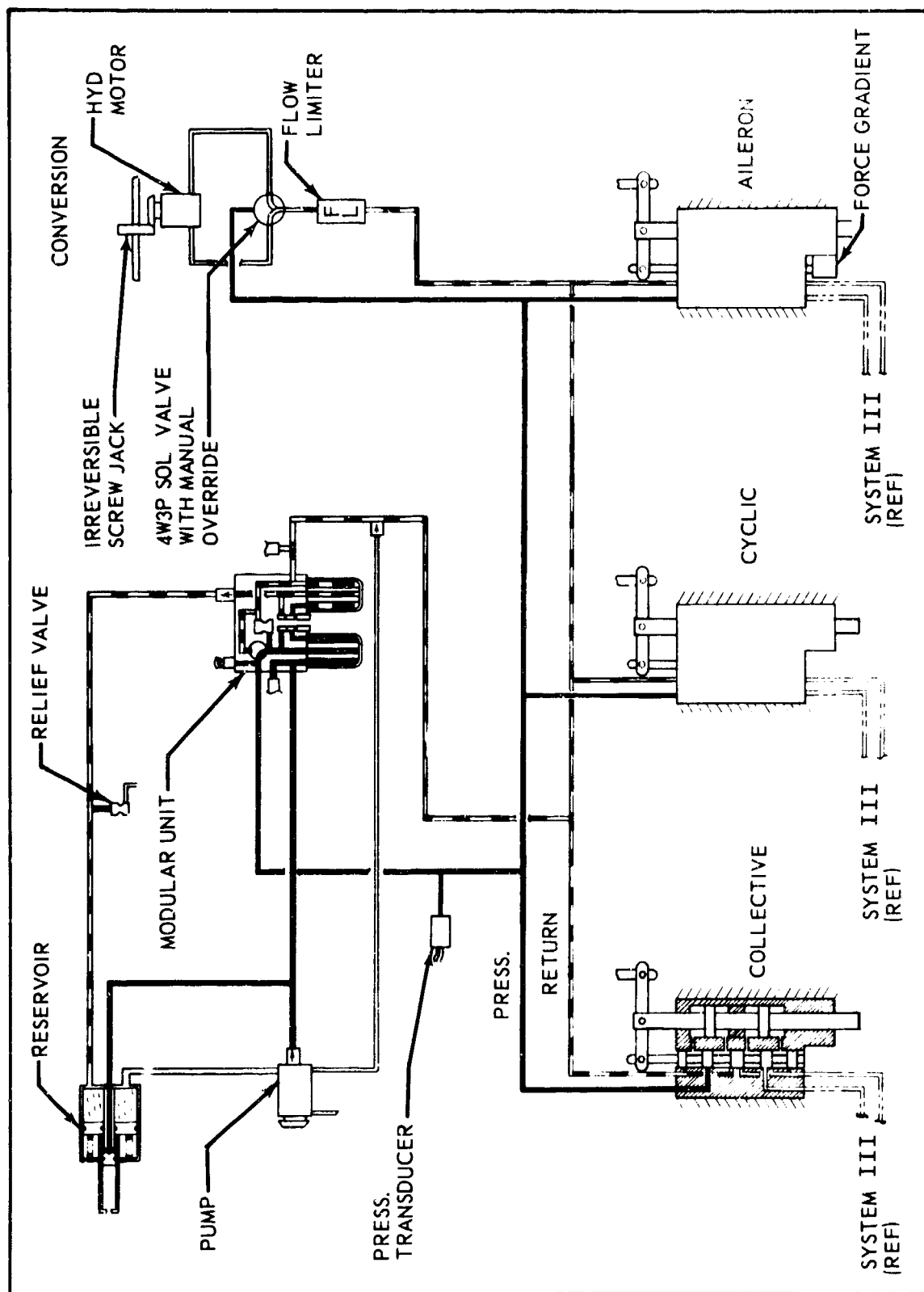


Figure 139. Hydraulic Systems I and II, Schematic.

a. Rotor Controls

Each rotor is controlled by two servoactuators; one actuator controls collective pitch and the second actuator controls fore-and-aft cyclic. The servoactuators have dual cylinders which are independently controlled by a tandem hydromechanical servovalve.

In the event of the loss of System I or II hydraulic power source, System III will still provide full service rate. The actuator will automatically bypass fluid from one side of the inactive piston to the other. Trimmable force gradient devices are built into the cyclic actuator, providing the pilot with a force proportional to control position and airspeed.

b. Surface Controls

The servoactuators which control the ailerons are similar to the rotor actuators. Systems I and II supply power to one side of the actuators for the left and right ailerons, respectively. System III supplies power to the other side of both aileron actuators. Trimmable force gradient devices are built into the actuators, providing the pilot with a force proportional to control position and airspeed.

c. Conversion

During conversion, the rotors are rotated by means of hydraulically powered irreversible screw jacks located at each pylon. A mechanical interconnection between the conversion actuators permits conversion by either system in the event of a failure of one system. Flow regulators are installed to maintain a constant rate of conversion. The conversion process can be stopped or reversed at any time.

2. SYSTEM III

System III (Figure 190) is a combination flight-control-utility system. It supplies power to one side (opposite to Systems I and II) of the rotor and the aileron control actuators. It also supplies power to the rudder, elevator, flaps, stability augmentation system, force-gradient system, ventilation fan, and retractable landing gear. This system can also be used for in-flight engine starting. A variable-delivery pump is driven from the accessory gearbox so that hydraulic power is independent of the engines. A "bootstrap" reservoir assures an adequate supply of oil to the pump suction port at sufficient inlet pressure to prevent pump cavitation. In case of a failure in this system, the APU can be started and used as an auxiliary power source, provided that the fluid reservoir is not depleted.



Figure 190. Hydraulic System III, Schematic.

a. Rotor Governor

Power is controlled primarily by the collective lever position in helicopter flight and by power lever position in fixed-wing flight. The rotor rpm is controlled by the engine power turbine governor in helicopter configuration and by the rotor governor in fixed-wing flight. The rotor-governor controls an electrohydraulic servoactuator that is connected in parallel with the rotor collective pitch controls. The actuator incorporates velocity limiting to prevent undesirable rapid pitch changes. The actuator is located on the pilot's side of the manual servovalves of the collective actuators. Relief valves in the actuator limit its output force and allow the pilot to override the actuators if desired. When hydraulic pressure is removed from the actuator, a pressure-operated bypass valve connecting both sides of the piston opens, and the actuator can be moved as required without appreciable resistance to the pilot.

b. Surface Controls

System III provides power for the elevator, rudder, and aileron control actuators, and the flap-control motor. The aileron servoactuators are dual, with one side powered by System III and the other side powered by System I or II. The servoactuators for the rudder and elevator are powered only by System III; however, in case hydraulic power is not available, the servoactuators are designed so that if the pilot makes a control motion, the input control engages position stops on the actuator, permitting the pilot to move the control surfaces through a direct mechanical coupling. For this condition, irreversible valves on the servoactuators prevent the feedback forces from moving the pilot's control against his command.

The rudder and elevator servoactuators incorporate electrohydraulic pressure control valves and force-control pistons, which supply a force at the pilot's control that is proportional to the stick position and airspeed. The flaps are mechanically interconnected and are powered by a hydraulic motor driving an irreversible mechanism.

c. Landing Gear

System III provides power for extending, retracting, and locking the landing gear. Separate actuators are provided for each gear. Internal locks are incorporated in the actuators to lock the gear in the extended position. External locks, operated by small actuators, lock the gear in the retracted position. Sequence valves assure proper sequencing of the locks and actuators. Four-way, three-position solenoid valves

provide the pressure for retraction and extension. Flow-limiting valves are provided in the return line from the landing-gear actuators to control the velocity at which the gear retracts or extends.

A limit switch attached to the air-oil shock absorber and an integral downlock on the actuating handle prevent inadvertent retraction of the landing gear when the aircraft is on the ground. For emergency conditions, operation of a manual control in the cockpit releases the uplocks on the gear, allowing the wheels to free-fall to the down-and-locked position.

d. Stability Augmentation System

Electrohydraulic servoactuators are installed as integral links in the fore-and-aft, lateral, and directional control systems. Stability augmentation system (SAS) inputs cause the control links to change length. Figure 191 is a schematic of the SAS hydraulic system. Engaging the SAS channel directs hydraulic pressure to the actuator, disengaging the main piston-rod lock. The actuator then functions as directed by the electrohydraulic servovalve, up to the limit of its control authority. Loss of hydraulic pressure causes the actuator piston to automatically center, lock, and act as a fixed control link.

e. Force-Gradient System

The electrohydraulic force-gradient system, integral with the flight-control system, provides a variable control-force gradient as a function of airspeed from any selected trim position. Force-center-trim provisions are provided at each cockpit flight station. The actuator is shown schematically by Figure 192. An electronic unit processes the various control-position and airspeed-sensor signals, and it supplies input control information to the pressure control valve. This valve controls the hydraulic pressure differential across the force piston, which is connected to the servovalve input linkage. The force from this piston is transmitted to the servo-actuator input linkage and requires the pilot to exert an equal force to prevent control motion. Relief valves across the piston limit the maximum force so that the pilot may override the system at any time. Stops limit the aircraft control rate due to the force gradient. An override velocity gap permits full servovalve spool displacement by the pilot.

3. AUXILIARY POWERPLANT SUBSYSTEM

The APU-powered hydraulic system is used primarily for engine starting. The APU system can also be used for checking out Systems I, II, and III; it also provides hydraulic and

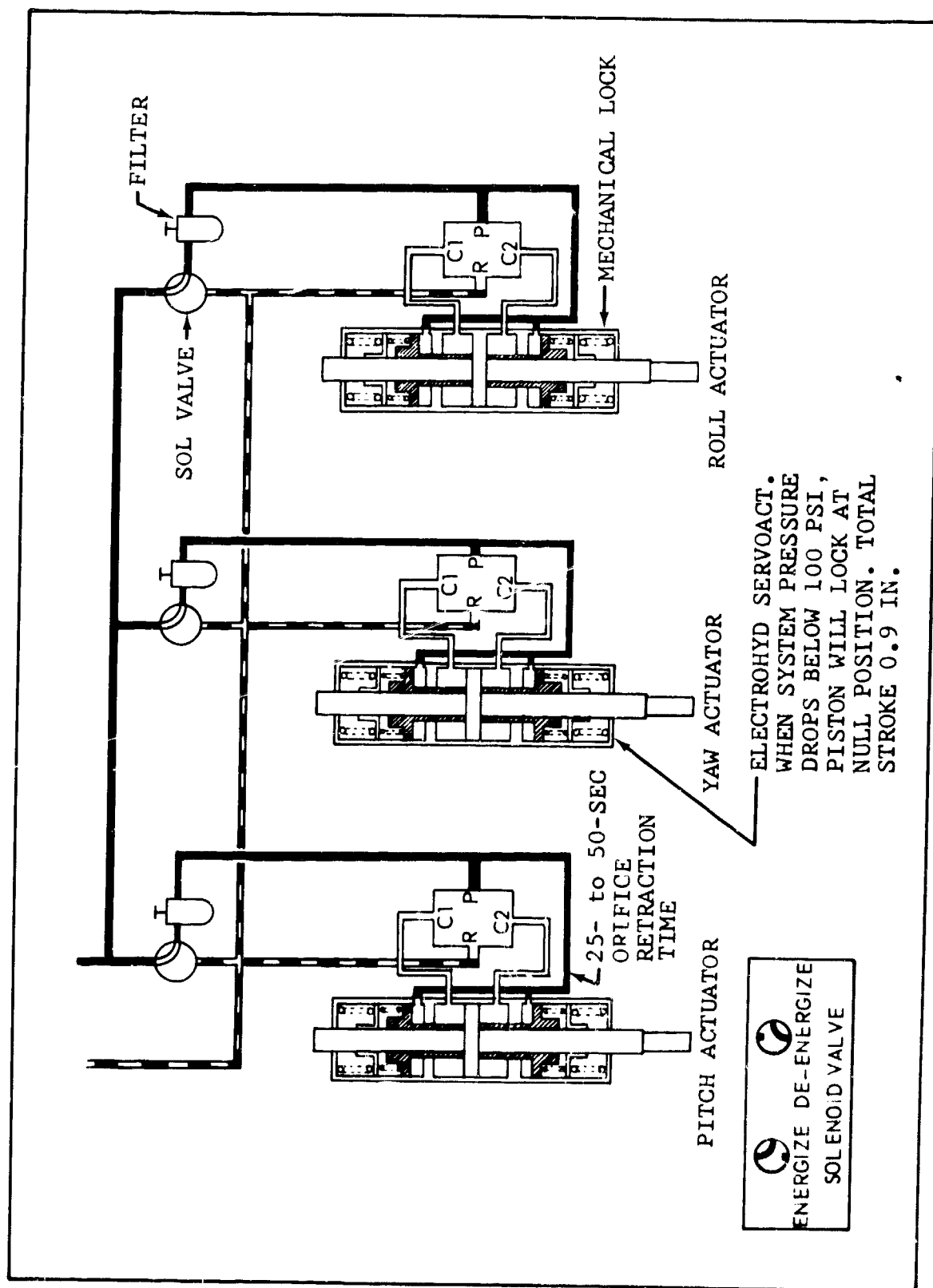


Figure 191. SAS Hydraulic System, Schematic.

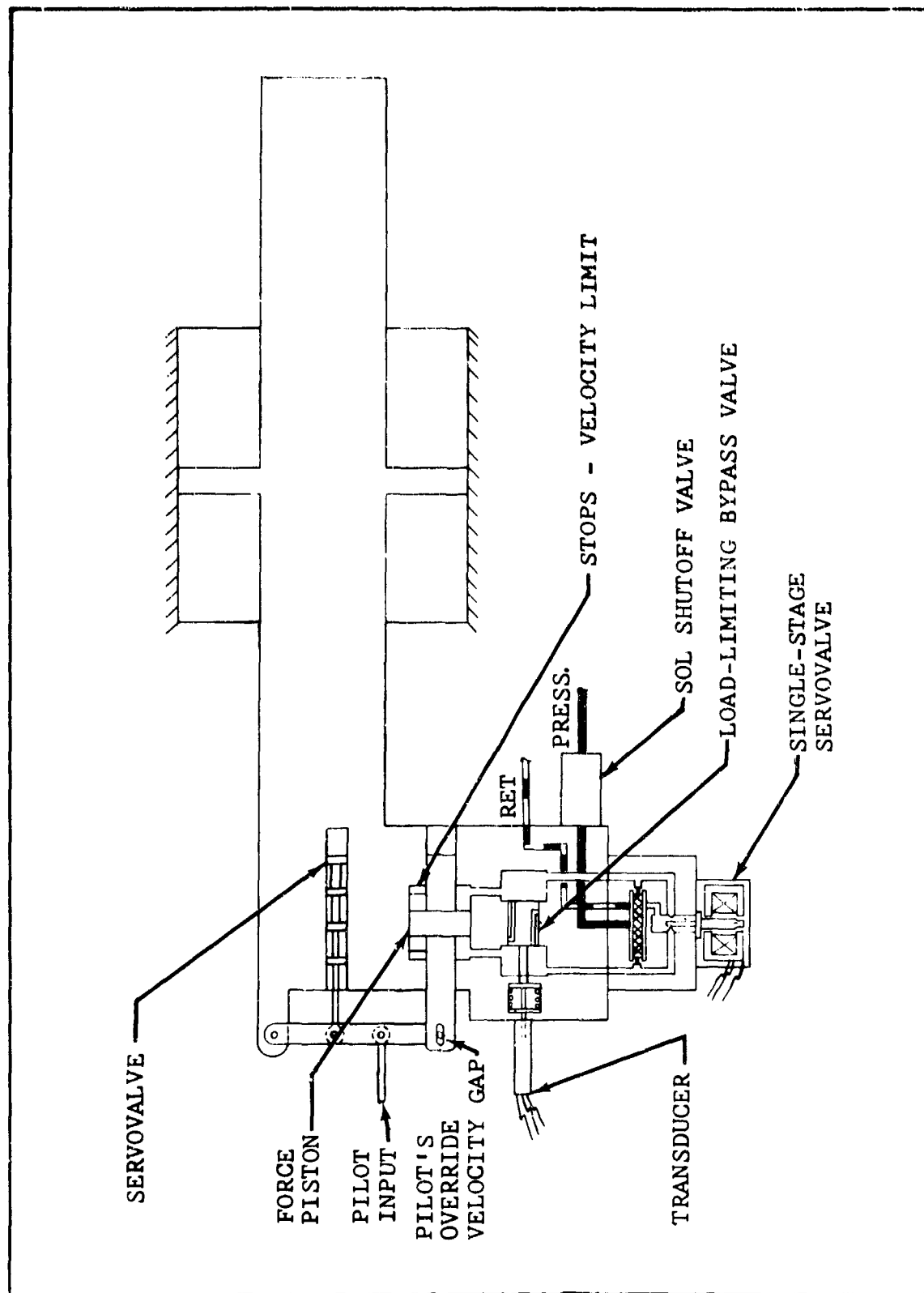


Figure 192. Force-Gradient Actuator, Schematic.

electrical power for ground operation and is the in-flight backup for System III. The Solar T62-T-16B auxiliary power unit drives a variable-displacement pump supplied from a "bootstrap" reservoir. A shutoff valve normally isolates the APU system from System III and the engine-starting motors.

Each main engine is started by a variable-displacement hydraulic motor that drives the engine through a gearbox and an overrunning clutch. The unit operates as a fixed-displacement hydraulic motor at speeds below the firing range of the engine. As engine speed increases beyond the firing range, the motor inlet pressure drops due to the limited capacity of the APU unit. The decrease in inlet pressure causes the auxiliary compensator in the motor to meter high-pressure fluid to the stroking piston, and it reduces the motor displacement; the power output of the motor remains constant until the engine reaches the self-sustaining speed. Beyond this self-sustaining speed, the overrunning clutch disengages the motor from the engine, and a speed-sensing switch closes the engine-starting valves. The engine-starting valves are normally closed and are located outside of the fire zone. As a result, there is no hydraulic fluid under pressure in the engine compartment except during the engine-starting cycle. See Figure 193.

C. FLIGHT ASSIST SYSTEMS

1. ROTOR-PITCH-GOVERNOR SYSTEM

The rotor-pitch-governor system is a closed-loop control system that maintains a selected rotor rpm by controlling blade pitch. The governor cannot be engaged at power-turbine speeds above 95-percent rpm. Sufficient deadband is provided at that setting to prevent interaction between the rotor-pitch and power-turbine governors. The system is shown schematically by Figure 194. A block diagram of the system is shown by Figure 195. The system utilizes one of the aircraft's standard rotor tachometer generators as the sensor for the controlled variable and compares this signal with the pilot-selected rotor rpm. The resultant error signal produces a prescribed displacement of the rotor-governor actuator which changes the blade pitch of the rotor to correct the rpm error.

The governor control loop is a compensated, integrating-type system which provides high-quality static and transit error-control characteristics. To promote safety, the governor actuator can be manually overpowered and is velocity-limited. A signal is provided to the master warning panel if the rpm speed error exceeds approximately 10 rpm.

The electrohydraulic governor actuator is connected in parallel with the blade-pitch control, as shown in Figure 194. It has 100-percent displacement authority; however, as a

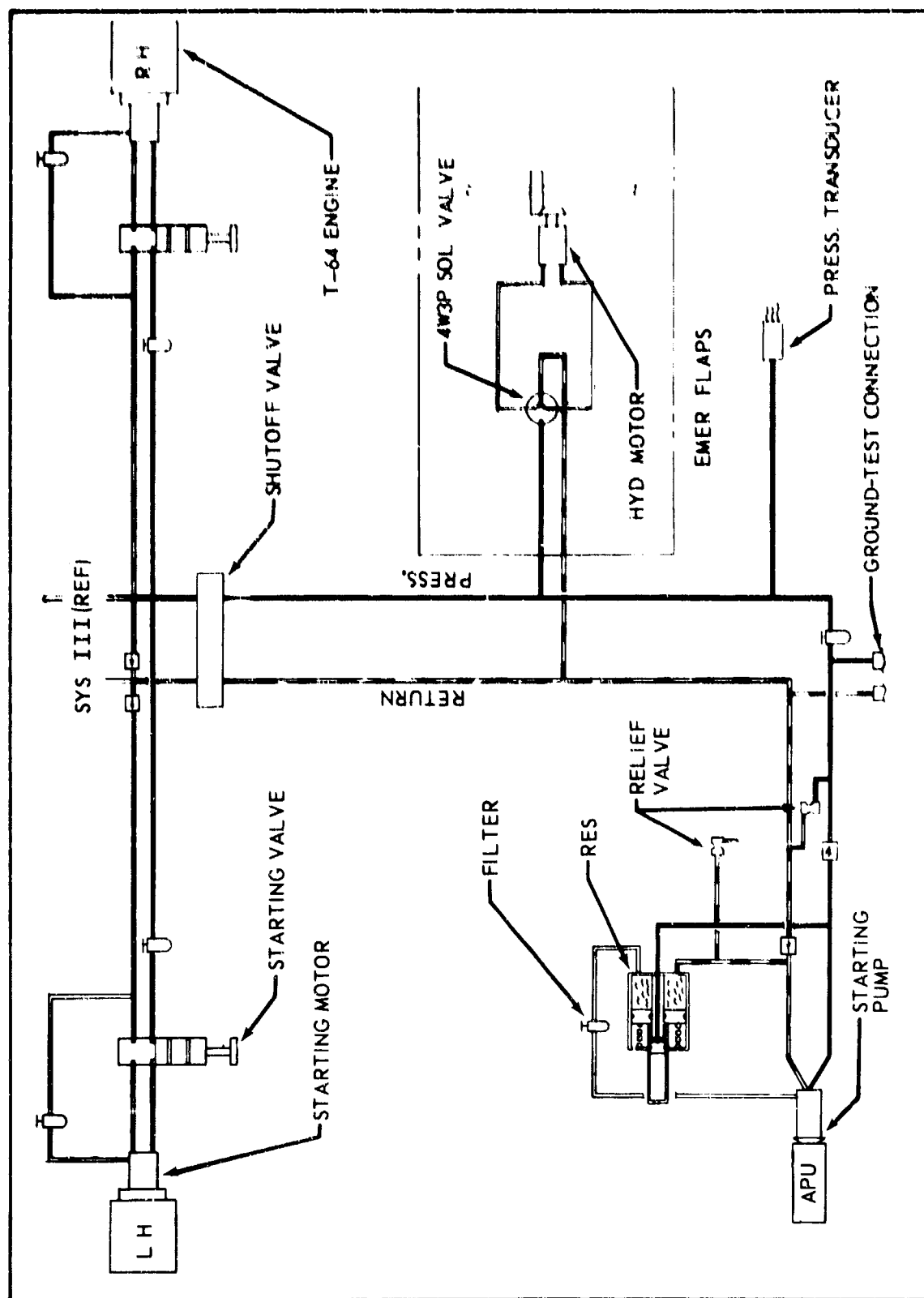


Figure 193. APU Hydraulic Subsystem, Schematic.

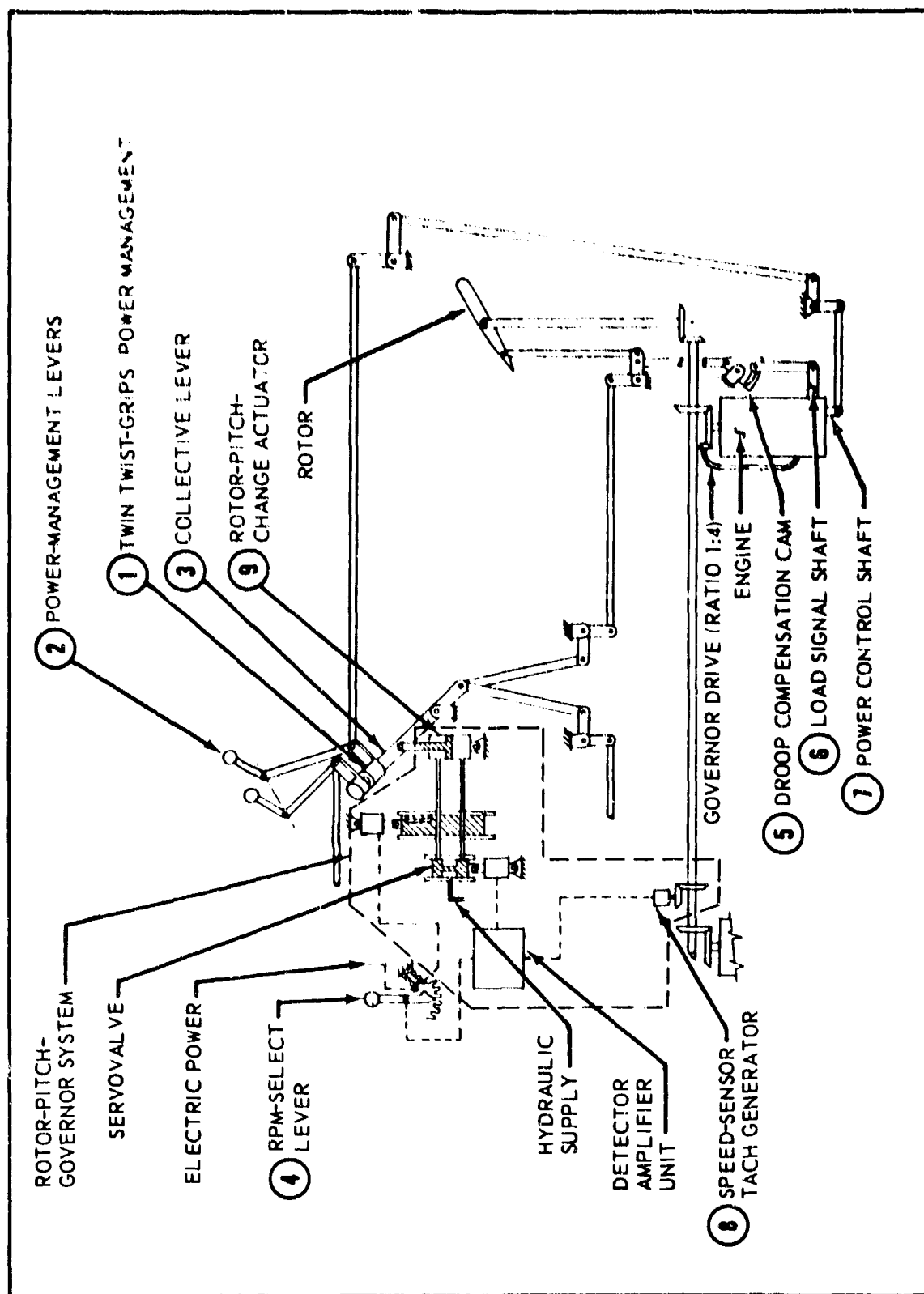


Figure 194. Rotor-Pitch Governor, Schematic.

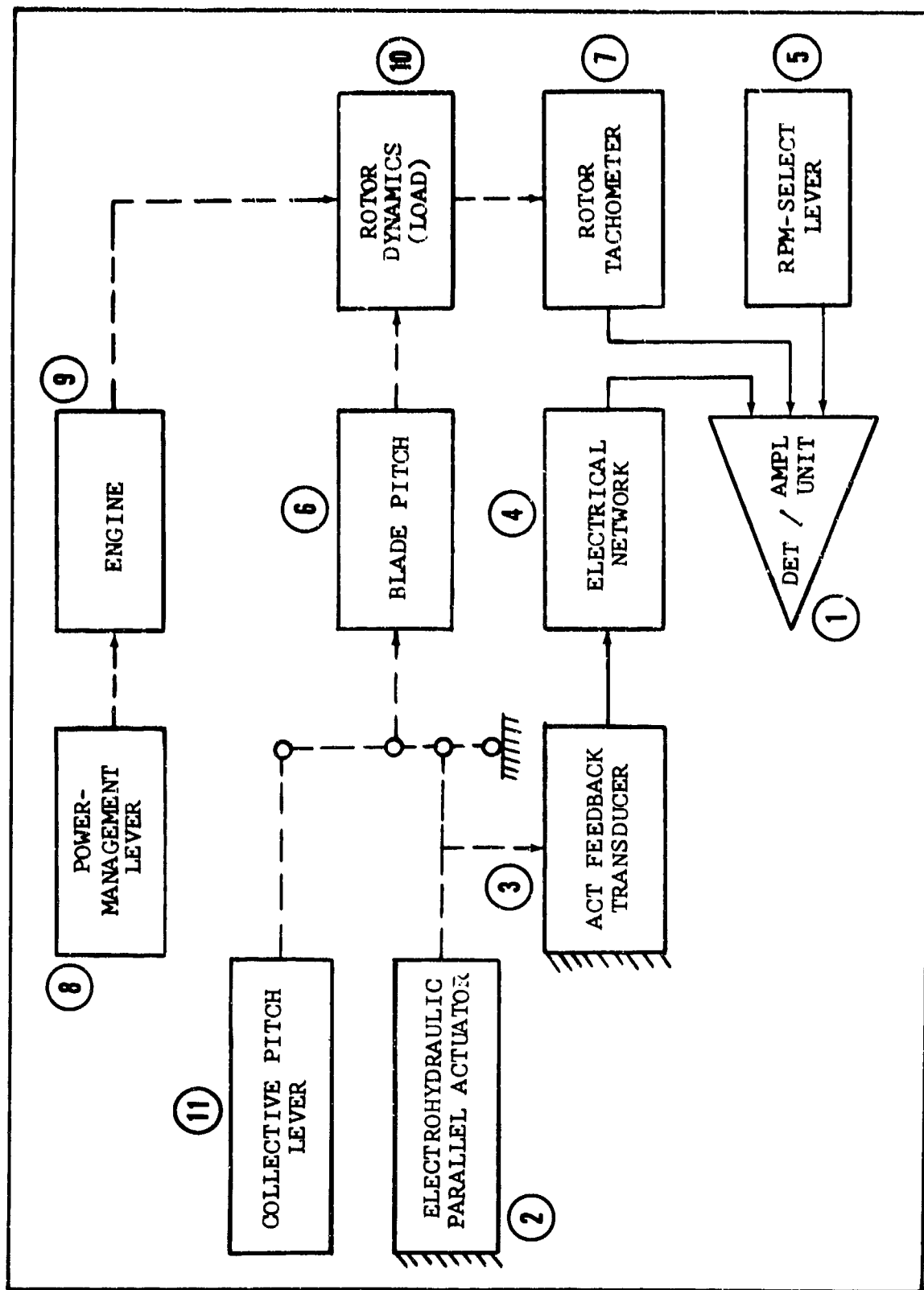


Figure 195. Rotor-Pitch Governor, Block Diagram.

safety measure, it has a velocity limit of 3 degrees per second and an override force capability of 40 pounds.

The amplifier unit will accept ac, dc, or variable-resistance-type signals. It serves as an amplifier to drive a load such as the hydraulic actuator valve. This unit also provides an indication of governor malfunctions by proportionally detecting the error between the selected and the measured rpm. The width of the sample period is utilized to provide a warning signal on the caution panel when the rpm error exceeds prescribed limits.

The rotor speed sensor is one of the standard transmission-mounted tachometer generators used to provide rotor speed indication for the pilots. The output signal from this generator is fed into the detector/amplifier.

2. FORCE-GRADIENT SYSTEM

The control-feel characteristics of the D266 are provided by the force-gradient system. The level of the forces is controlled as a function of airspeed so that the pilot is appropriately informed of the effectiveness of his controls during both helicopter and fixed-wing flight.

The system is shown schematically by Figure 196. Control position and dynamic pressure sensors are combined in the amplifier/control unit to provide the controlling signals for the hydraulic force actuators on the valve heads of the control servoactuator assemblies. These forces are applied to the pitch, roll, and yaw controls and are felt by both the pilot and the copilot. Hydromechanical feedback within the force actuator valve assures that the forces produced are linear with the electrical signal. Stick jump is eliminated by circuitry which provides zero-force signals prior to initial engagement.

Forces are developed in each channel independently from the forces in other channels. Hence, there is no interaction between the controls. Breakout forces are held to 1 ± 0.5 pound for the longitudinal and lateral channels and 5 ± 2 pounds for the yaw channel. Normal control friction due to bearings provides these forces in the longitudinal and lateral channels. Mechanical adjustable friction is also provided on the pilot's control stick. In the yaw channel, however, a simple diode and resistor combination within the electronic circuitry provides the 5-pound breakout force function.

The system is so designed that safe flight criteria are met in the event of either an electrical or a hydraulic component failure. An electrical failure-detection circuit senses the rate

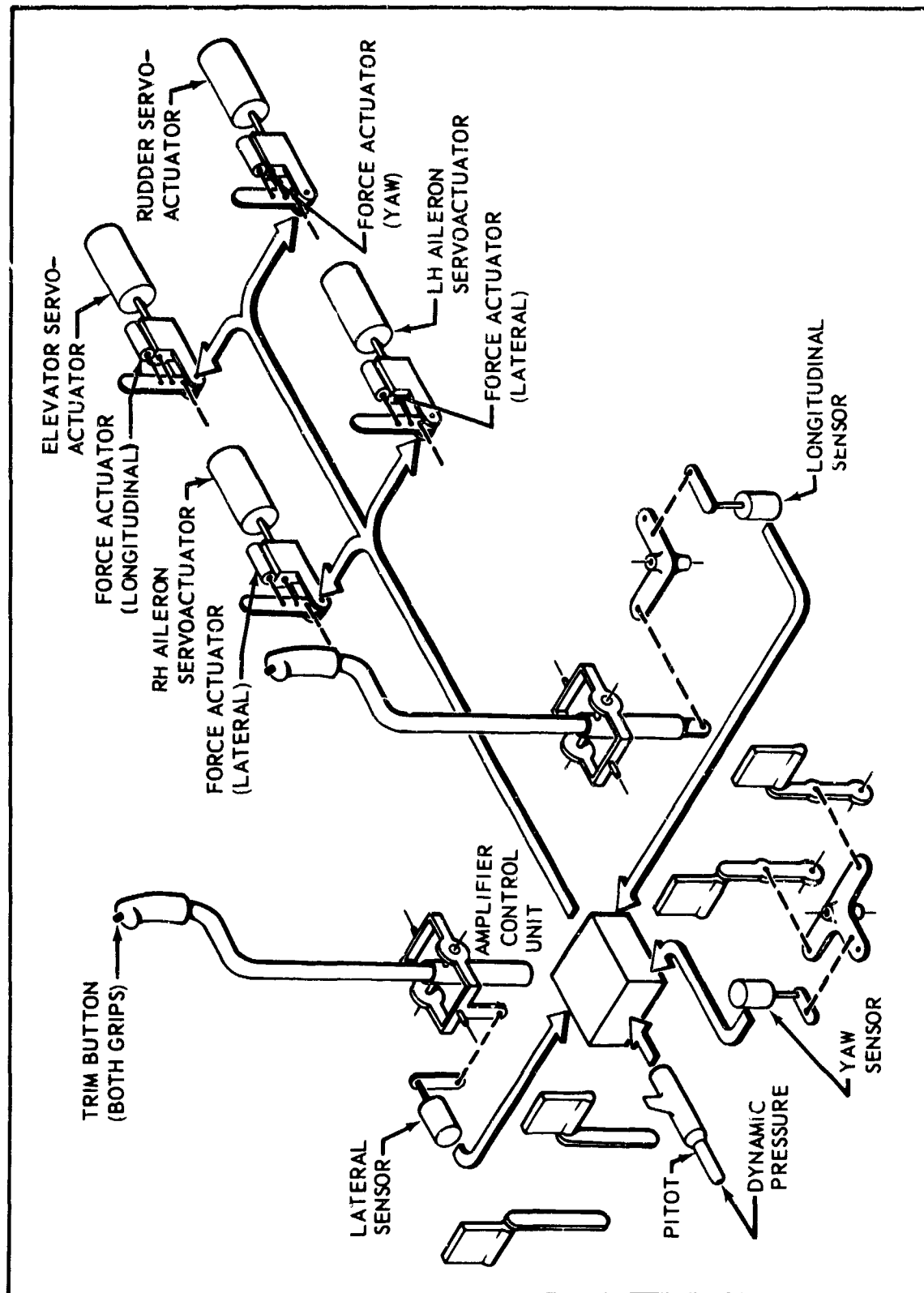


Figure 196. Force-Gradient System, Schematic.

of change of the force-producing signal at the hydraulic actuator valve. If an abrupt failure occurs, a cockpit warning light is actuated, and the force existing at the time of failure is programmed to decay slowly. If hydraulic failure occurs, the velocity authority of the force actuator is mechanically limited to assure that the controls are held to a safe velocity. Also, the maximum override forces are limited to an acceptable level.

Figure 197 is a block diagram of the complete system for the pitch channel. Roll and yaw channels are functionally similar. The multiplier is biased to produce a constant minimum-force displacement gradient.

Longitudinal	1.4 lb/inch
Lateral	1.0 lb/inch
Yaw	5.6 lb/inch

With the multiplier bias established, the force actuator produces a force proportional to the control displacement and tends to return the control to the neutral trim position. Thus, the spring-like function is obtained. This function is derived through the dynamic "loop", shown as blocks 2-3-4-5-2 of Figure 197.

A constant control force of 16 lb/g in fixed-wing flight is provided by increasing the stick force gradient as a function of dynamic pressure. Lateral and pedal force gradients are also increased as a function of dynamic pressure.

The force-gradient functions are:

Longitudinal	$1.4 + 0.12 (q - 50)$
Lateral	$1.0 + 0.15 (q - 50)$
Yaw	$5.6 + 0.29 (q - 50)$

where q represents a dynamic pressure of 50 lb/sq ft. The resulting variations in force gradients are shown in Figure 198.

Lateral and longitudinal force system trimming is accomplished by a four-way switch on top of the pilot and copilot control sticks. No yaw force trim is provided.

For servo stability, rate signals are generated from the control-position sensor. In addition to providing rate damping to the basic "spring loop", a frequency-sensitive network generates a high feedback force at the pylon natural frequency to prevent pilot-induced oscillations. The spring-loop gain for the longitudinal channel is increased as shown by Figure 199. The lateral channel has similar characteristics.

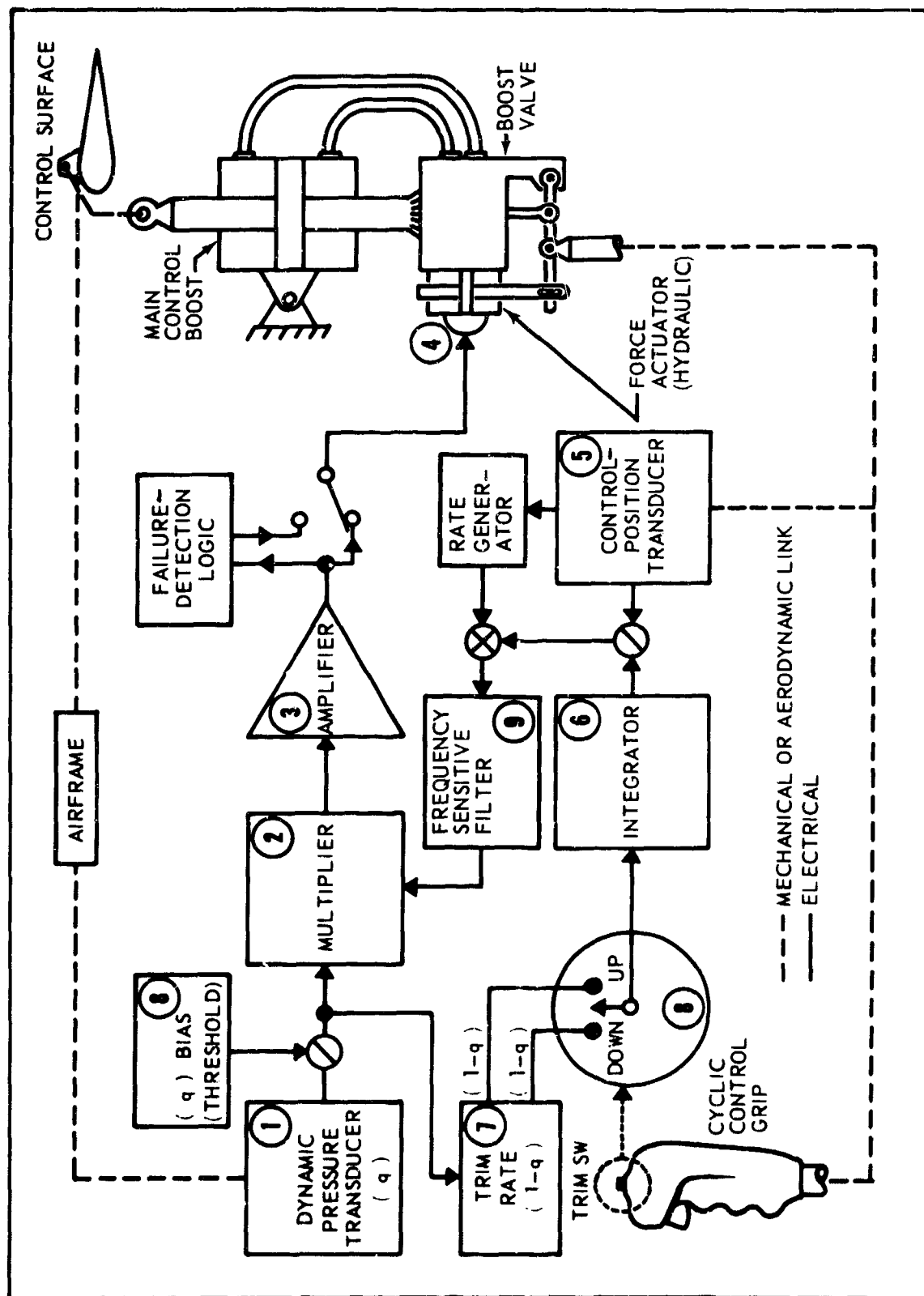


Figure 197. Force-Gradient System, Block Diagram.

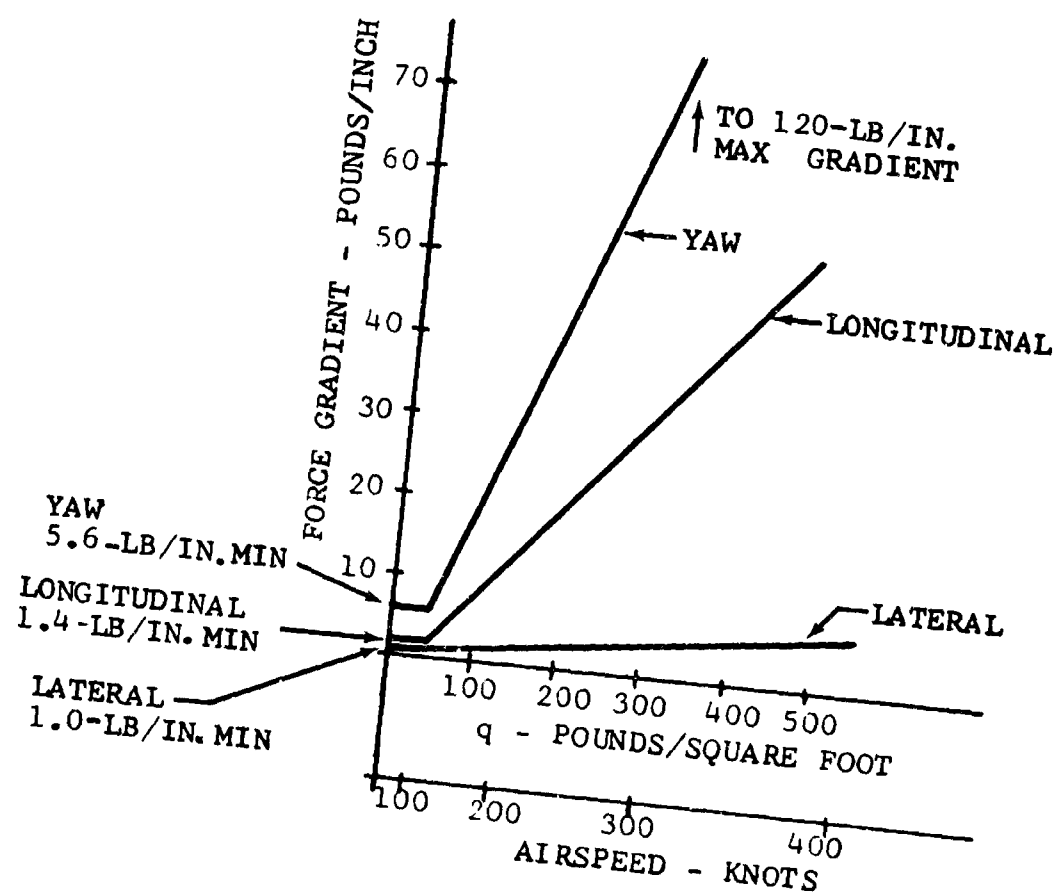


Figure 198. Variations in Force Gradient With Dynamic Pressure and Airspeed.

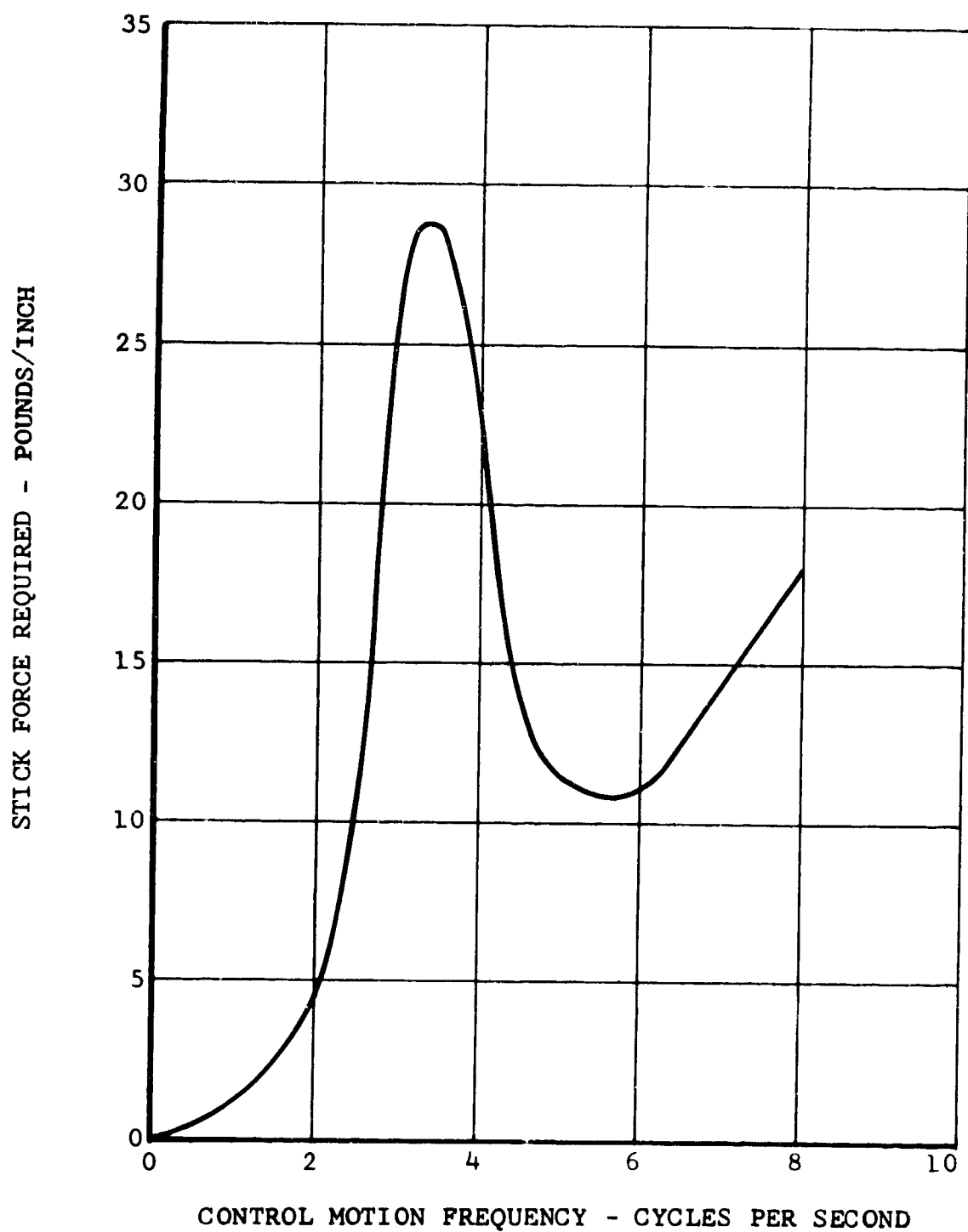


Figure 199. Stick Force Gradient Versus Frequency of Motion.

3. STABILITY AUGMENTATION SYSTEM

The stabilization system for the D266 is functionally a three-axis (pitch, roll, and yaw) stability augmentation system (SAS), with auxiliary electrical control inputs in each axis to supplement the conventional mechanical control inputs. The combination of the stability-augmented airframe and the auxiliary pilot inputs results in an airframe that is well damped for disturbing functions, yet is very responsive to pilot control inputs.

The system is shown schematically by Figure 200. A block diagram of the system is shown by Figure 201. Operationally, each axis of the system consists of a conventional control loop, a compensated attitude rate feedback loop, and a supplemental pilot control loop which is summed with the pilot's mechanical input. The control transducers sense control motion and provide the basic signals for the supplemental loops. These signals provide for differentiating between pilot inputs and disturbances, and they allow the parameters of the rate feedback loop to be considered independently (i.e., the feedback loop is designed without concern for the pilot control/response characteristics, to satisfy the stability requirements of the basic airframe throughout the flight envelope). The freedom afforded by this design enables the overall system to be tailored for specific mission requirements, pilot comfort, minimization of fatigue in the physical control system, etc.

The merits of the system are summarized below:

- SAS provides a well-damped airframe for external disturbances while providing an airframe with a desired response for pilot control inputs.
- SAS provides a short-term attitude memory for external disturbances.
- Operational requirements are simple and logical to facilitate maximum use of the SAS.
- The SAS uses limited-authority (approximately 15 percent of total) series actuators to enhance safety of flight.
- The actuators automatically center and mechanically lock when the SAS is disengaged or in the event of electrical and/or hydraulic power failure.

D. LANDING GEAR

The landing gear is a hydraulically operated, retractable, tricycle configuration with a dual-wheeled nose gear and a

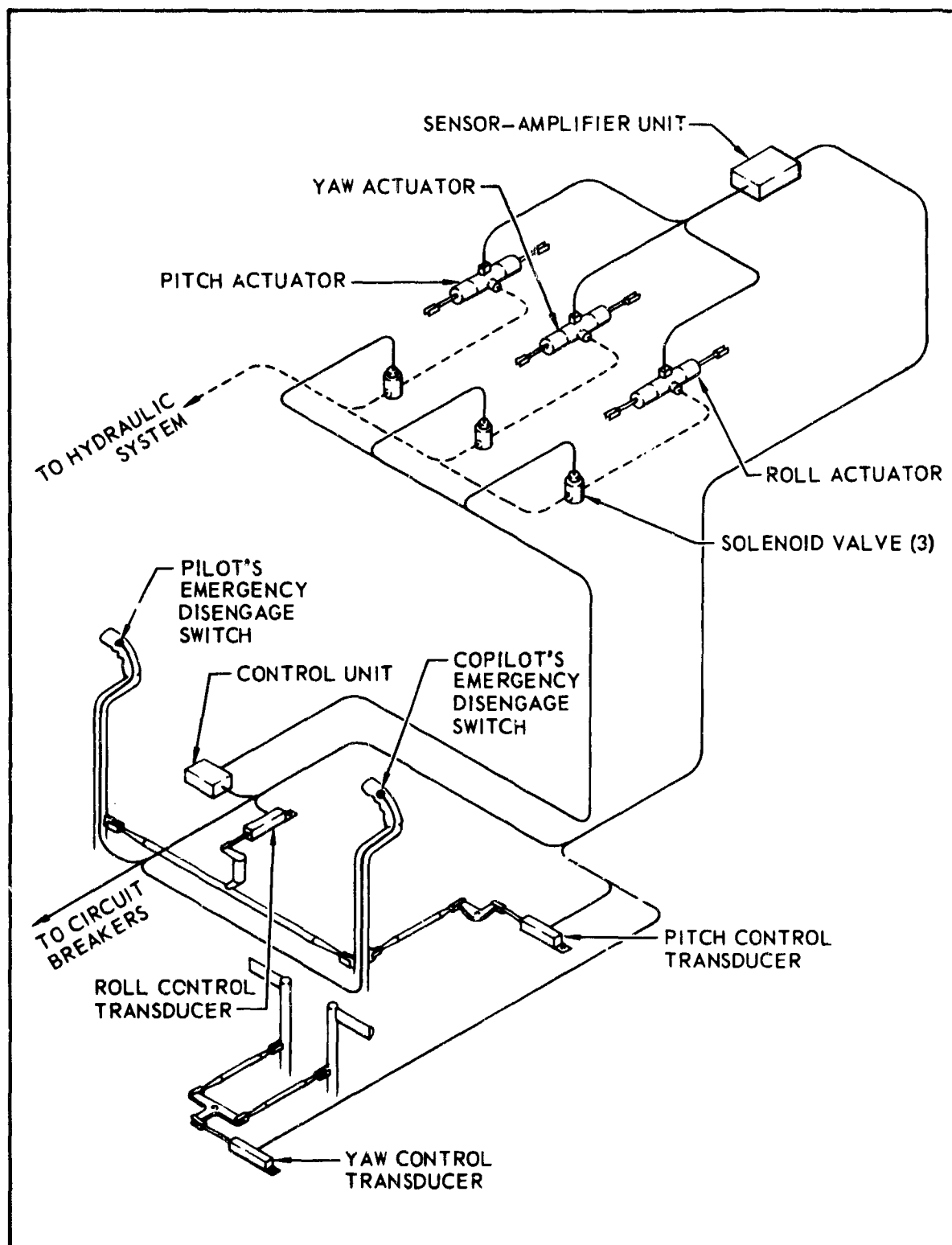


Figure 200. Stability Augmentation System, Schematic.

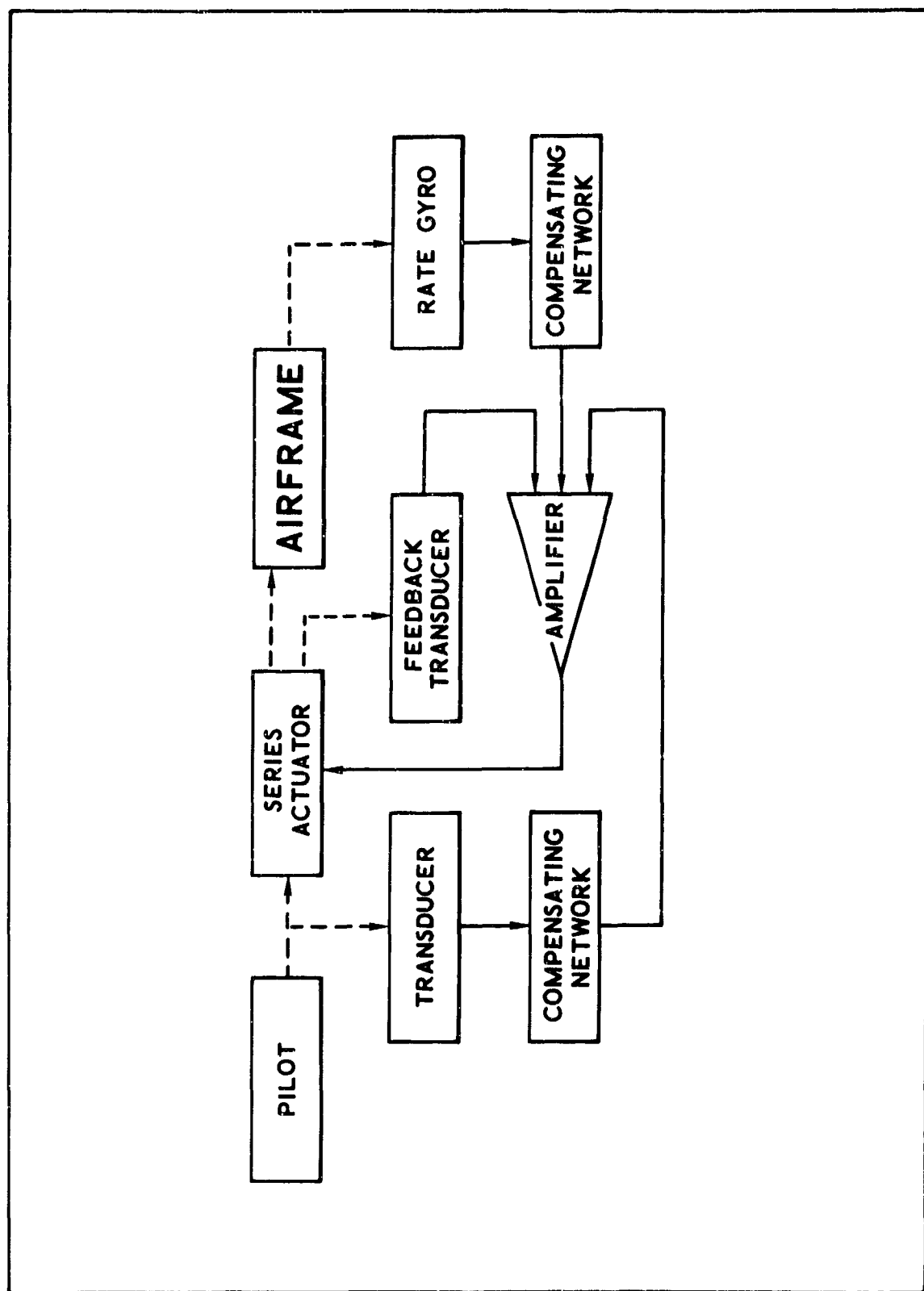


Figure 201. Stability Augmentation System, Block Diagram.

tandem-wheeled main gear. The nose gear retracts upward and inward and is partially contained within the side of the fuselage. The portion of the gear remaining outside the fuselage is enclosed by an external fairing. The tandem-wheel main gear arrangement results in a fuselage frontal area which is comparable to that of a single-wheel gear configuration.

Two low-pressure tires are used on each gear. The inflation pressures are 44 psi and 61 psi for the nose and main gear tires, respectively. The effective ground pressure at normal gross weight is 24 psi for the nose gear and 37.7 psi for the main gear.

Single disc-type brakes are provided on the aft wheel of each main gear. Aircraft steering is accomplished by differential rotor thrust and/or wheel braking. The nose wheel is castored and free-swiveling to accommodate this type of steering.

The main gear tread is 170 inches. The gear arrangement provides a fuselage ground clearance of 18 inches and results in a turnover angle of 35 degrees.

E. CONVERSION SYSTEM

The primary functions of the conversion system are (1) to rotate the rotor pylon from the vertical helicopter position to the horizontal position and return and (2) to lock the pylon safely in either extreme or intermediate positions. The system also serves as a reference for rotor control system and provides for phasing rotor control a function of flight regime.

The major components of the conversion system are the two actuators, an interconnect shaft, and a phasing gearbox. A hydraulically powered screw-jack actuator is located on each wingtip. To assure synchronization, the actuators are interconnected by a shaft which passes through the leading edge of the wing. A small gearbox, in the center of the wing over the fuselage, is driven by the interconnect shaft and provides a linear motion in proportion to the conversion angle, for use in phasing the rotor controls.

1. NORMAL OPERATION

The pilot controls the conversion operation by a three-position (momentary on) switch on the cyclic stick grip. The switch is moved forward to move the pylon from helicopter to horizontal position; it is moved rearward to move the rotor back to helicopter position. This process may be stopped or reversed at any position of the mast. The total pylon motion which is controlled in this manner is 90 degrees.

The conversion switch activates a solenoid valve located at each wingtip. The valve controls the flow of hydraulic fluid to the motor on the screw jack. The hydraulic power is supplied to the screw-jack motors by the pump mounted on each respective main transmission.

The normal conversion time is approximately six seconds, varying slightly with the load on the rotors. The conversion rate is controlled by flow limiters in the pressure line to the solenoid valve.

2. EMERGENCY OPERATION

In the event of failure of one of the hydraulic systems or of the electrical circuit to one solenoid, the screw jack is driven by the actuator motor on the opposite wingtip through the interconnect shaft. There is no hydraulic back-pressure in the system being driven by the interconnect shaft, as the solenoid valve position allows free flow, in a closed loop, through the nonoperating system. The switch movement by the pilot is the same as with normal operation, and the time to convert is also the same as in normal conversion.

The two solenoid valves are connected to separate electrical buses. If an electrical failure of one valve should occur, a normal conversion can be made in either direction. If electrical control of both solenoids is lost while in the fixed-wing configuration, the solenoids may be operated normally by pulling the emergency reconversion handle located on the center console. This handle is mechanically connected by cables to both solenoid valves, and it opens the valves to extend the actuator hydraulically to the helicopter configuration.

A safe conversion can be made in the unlikely event of an interconnect shaft failure. Under these conditions, the hydraulic-flow limiters control the conversion rate of the two pylons to within a few degrees of one another.

3. ACTUATORS

The conversion actuators are hydraulically powered, double-extension, recirculating ball-type screw jacks with a stroke of 42 inches. The hydraulic motor is a Vickers model PFM, 3909 series. The motor is well suited for this application, since it is designed for intermittent duty and has a very high power-to-weight ratio. The maximum rating of the motor is 11.0 horsepower at a pressure of 3000 psi; 5 horsepower per actuator is required for normal conversion. The flow limiter controls the motor speed at 7800 rpm. This motor is mounted to the gearbox of the actuator.

The initial speed reduction from the motor is 2:1 by spur gears. At this point, small bevel gears provide the right-angle takeoff for the interconnect shaft. A further 4.65:1 reduction drives the outer, large nut of the ball screw. An irreversible clutch is used in the gear train between the interconnect takeoff and the final reduction. This device prevents the screws from moving or creeping under load, yet unlocks when driven by the motor or the interconnect shaft.

Both the inner and outer screws have a lead of 0.5 inch. The ball nuts are preloaded to eliminate backlash and are provided with wiper seals to prevent dirt from entering the nuts. Dry lubricants are used on the screws to reduce the accumulation of dirt on the threads. The drive reduction gearbox itself is oil-lubricated and sealed at each end of the large ball nut.

Two trunnions are incorporated in the gearbox case for attachment to the outer wing rib. A clevis is provided at the end of the small screw for attachment to the pylon-isolation mount on the main transmission.

4. INTERCONNECT SHAFT

The synchronizing shaft connecting the two screw jacks runs the full span of the wing inside the leading edge. The shaft revolves 300 times during the conversion process at approximately 3000 rpm. The shaft is made from 2024 aluminum alloy tubing, 3/4 x 0.028 wall. The surface of the tube is hard anodized to resist wear and corrosion. Two small universal joints are used to allow for the motion of the conversion actuator and to allow small changes in length.

The shaft is supported by Teflon fabric bearings to eliminate the need for lubrication. A long bearing life is assured since the shaft bearing surfaces are burnished, the duty cycle is short, and the normal loadings are negligible. The shaft transmits very little torque in normal operation; and since the diameter was dictated by dynamic considerations, the shaft is considerably over-strength even for emergency loading.

The small phasing gearbox, located near the center of the interconnect shaft, has an 18-to-1 worm gear reduction that drives a 3/4-inch-diameter, 10-pitch, Acme screw. The gearbox provides a linear output of 1.66 inches that is proportional to the conversion angle. This linear motion is used in the control system as a mechanical reference to conversion angle and also provides the signal for the conversion angle indicator in the cockpit.

F. ELECTRICAL SYSTEM

Primary power for the D266 is provided by two parallel 300-ampere, 28-volt, dc generators driven by the accessory gearbox located in the aircraft fuselage. AC power is supplied by a 2.5-kva, 115/200-volt, three-phase, 400-cps static inverter. A 20-kva, 115/200-volt, three-phase, 400-cps generator, mounted with a constant-speed drive to the auxiliary power unit in the aft fuselage, provides an alternate ac source. A block diagram of the system is shown in Figure 202. The system provides power for all the basic aircraft requirements, and it has the additional capacity to supply the power needed for the test program instrumentation. All components of the system are designed, as applicable, in accordance with relevant military specifications, and the systems are in accordance with MIL-E-25499A.

The controlled generator outputs from the right- and left-hand dc generators are connected to the Number 1 and Number 2 dc essential buses, respectively. The Number 3 dc nonessential bus is connected through relays to both essential buses and is normally supplied by both generators operating in parallel. The Numbers 1 and 2 buses are also normally connected through a relay and are supplied by both generators operating in parallel.

The peak average continuous load for the dc system is in the takeoff condition. This load is 37 percent of the continuous rating of the dc generators. The peak average continuous load for the emergency condition, with only one generator operative, is 56 percent of the continuous rating of this generator.

The ac inverter is supplied by the Number 2 essential bus. Alternate ac power is obtained from the ac generator driven by the APU, which is started from the battery connected through the Number 1 bus. Either of the essential buses will supply all the equipment necessary to complete a mission safely, should a fault occur in one of the systems.

The peak average continuous ac load is in the cruise-landing condition. This load is 49 percent of the continuous rating of the ac inverter. The loads on the ac system have been split to provide good phase balance. Also, when one system has failed and the loads have transferred, good phase loading is maintained.

The aircraft is equipped with a turbine auxiliary power unit (APU) located in the aft fuselage. The APU drives the hydraulic pump for the engine-starting system and a 20-kva ac

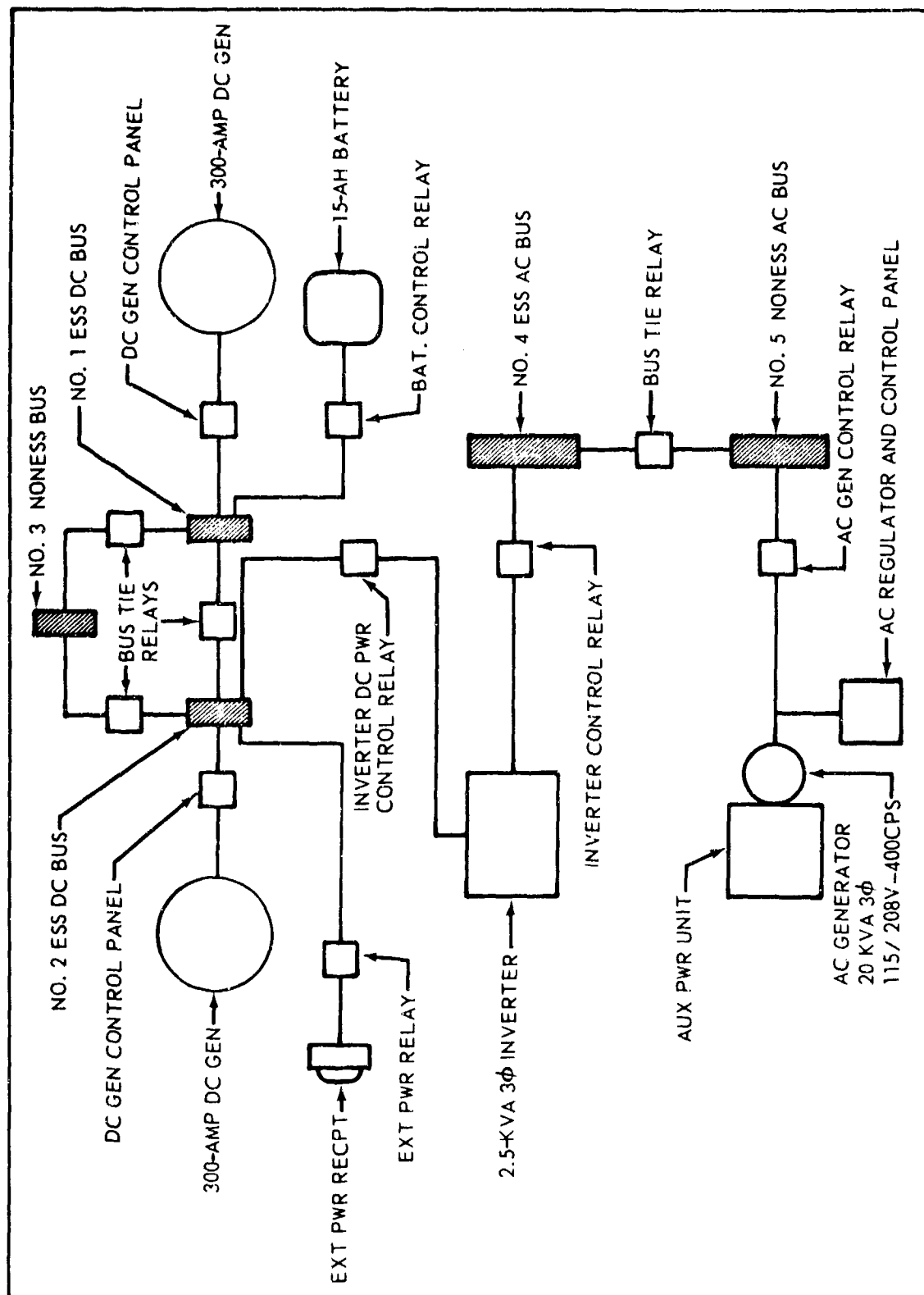


Figure 202. Electrical System, Block Diagram.

generator. The ac generator may be used for ground checkout of all ac systems.

A 13-ampere-hour battery supplies power for starting the APU and for lighting as needed in ground operation at night. The battery is a nickel-cadmium type CA-10H.

A receptacle is provided for external dc power. Reversed polarity protection is provided in the external power relay by a diode in the relay coil circuit. When an external power unit is connected to the dc receptacle, all buses may be energized.

Engine starting is accomplished hydraulically using the APU. The APU is started either by battery or by external power. On-board battery starts can be made at temperatures down to -25°F ; below -25°F , external power is required.

The systems on the composite research aircraft offer an excellent potential for growth of both ac and dc systems. It should also be noted that, should additional capacity be required, the rating of the machine can be increased by 33 percent and still maintain the same envelope size.

G. HEATING, VENTILATION, AND ICE PROTECTION SYSTEM

A heating and ventilation system is provided for the crew and cargo areas. The system also provides air for defogging the windshield and other transparencies. Ice protection systems may be required for an operational vehicle; however, they are not required or provided for the research machine.

The heating and ventilation system is shown schematically in Figure 203. Outside air is drawn in by a hydraulically driven, variable-speed, vaneaxial blower and is delivered to the cargo and crew compartment outlets through ducting. The blower is sized to provide a complete air change every 35 seconds. Engine bleed air is introduced into the airstream downstream of the blower for heating. The noise suppressor is installed in the main supply duct downstream of the bleed-air exit nozzle, to reduce noise generated by the high-velocity bleed-air jet. An overheat switch is installed in the main supply duct and is connected electrically, in series, with the bleed-air shutoff valves. The overheat switch opens at a preset temperature, and the bleed-air supply is shut off to prevent overheating of the ducting or adjacent structure.

The heating and ventilating air is ducted through the fuselage and to the heating and ventilating outlets in the crew and cargo compartments. Six outlets are provided in the cargo area. Outlets are provided near the pilot's and copilot's feet and by the windshield and lower transparencies.

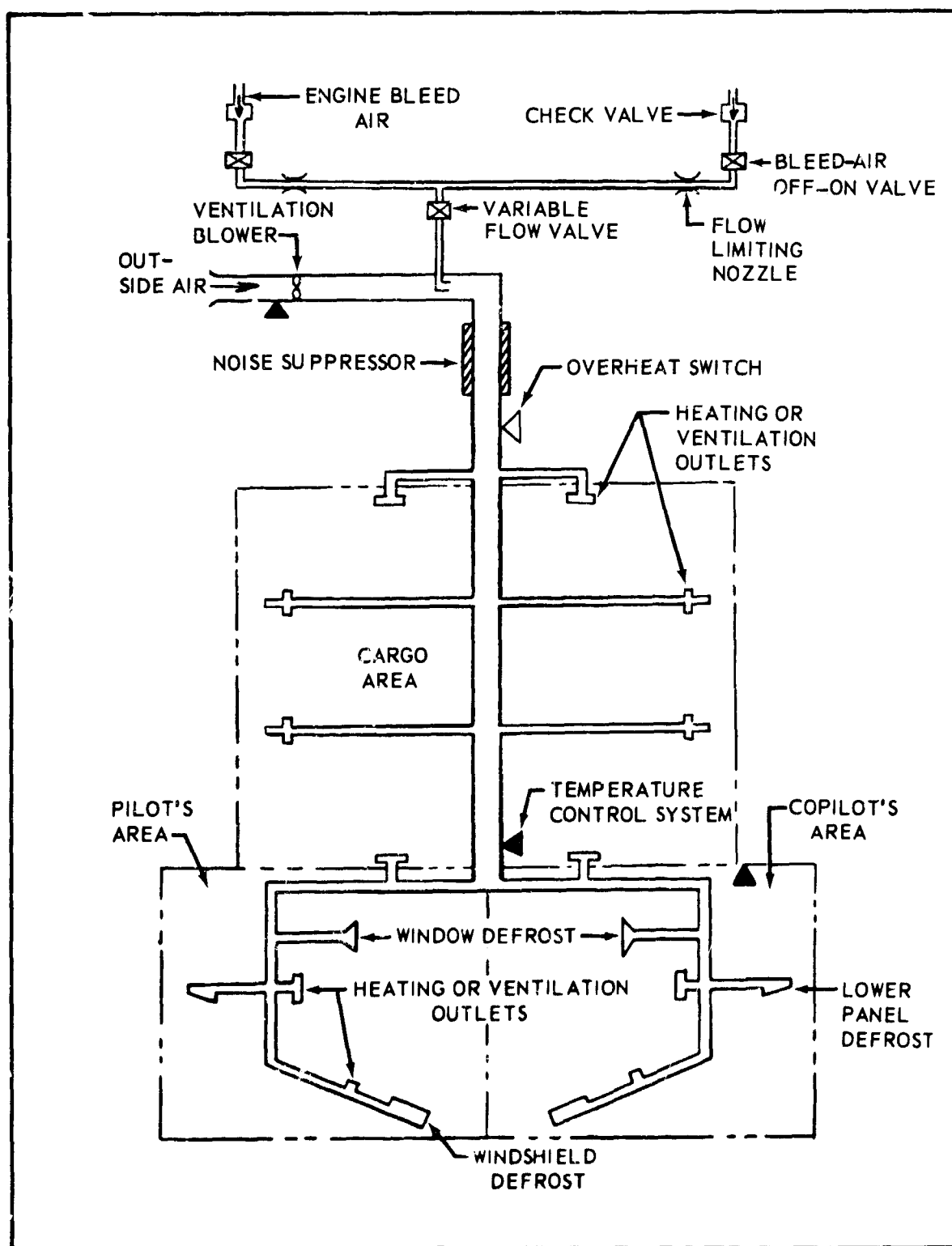


Figure 203. Heating and Ventilation System, Schematic.

The heating capacity of the system is sufficient to maintain a 40°F compartment temperature at an ambient temperature of -65°F. The heating requirements and system capability to maintain a 40°F compartment temperature are shown as a function of ambient temperature by Figure 204. The estimated time to attain a 40°F compartment temperature is ten minutes at -25°F ambient and 30 minutes at -65°F ambient. The capability of the system exceeds the specification requirements.

The D266 is a research vehicle and does not require ice protection systems. An operational vehicle will require this protection if it is to have an all-weather flight capability. For an operational machine, ice protection will be required for the windshield, engine inlets, essential instruments, aerodynamic surface, and rotors.

The thermal energy for anti-icing can be provided. About 50 percent of the engines' available bleed-air supply is used for cabin heating and other purposes. The excess available bleed air is more than adequate for inlet duct anti-icing, which is accomplished by piping bleed air through a shutoff valve to double-walled areas of the inlet duct.

Electrothermal deicing equipment can be provided for all essential instruments, antennas, etc., except radomes where performance may be degraded by electrical interference. For these applications, pneumatic-boot deicing can be provided.

The critical areas of the aerodynamic surfaces would be anti-iced by conventional pneumatic deicing boots on the wing, the horizontal stabilizer, and the vertical fin.

Electrothermal anti-ice systems will be provided for the rotor blades and spinner. The forward portion of the spinner will be continuously heated. Cyclic heating will be used for the aft portion of the spinner. The rotor blades will be cyclically heated. The blade heating elements will be laminated in the blade leading-edge abrasion strips and will have variable power density.

The electrical power provided for the research vehicle is inadequate for supplying the ice protection systems described. The electrical system for the operational vehicle will include two 20-kva alternators mounted on the drive system and one 20-kva alternator mounted on the auxiliary power unit. This installation is anticipated to be adequate for the normal aircraft electrical requirements and also for operation of the ice protection systems. These systems can be installed within the 166-pound equipment allowance included under the "furnishings and equipment" group in the weight statement.

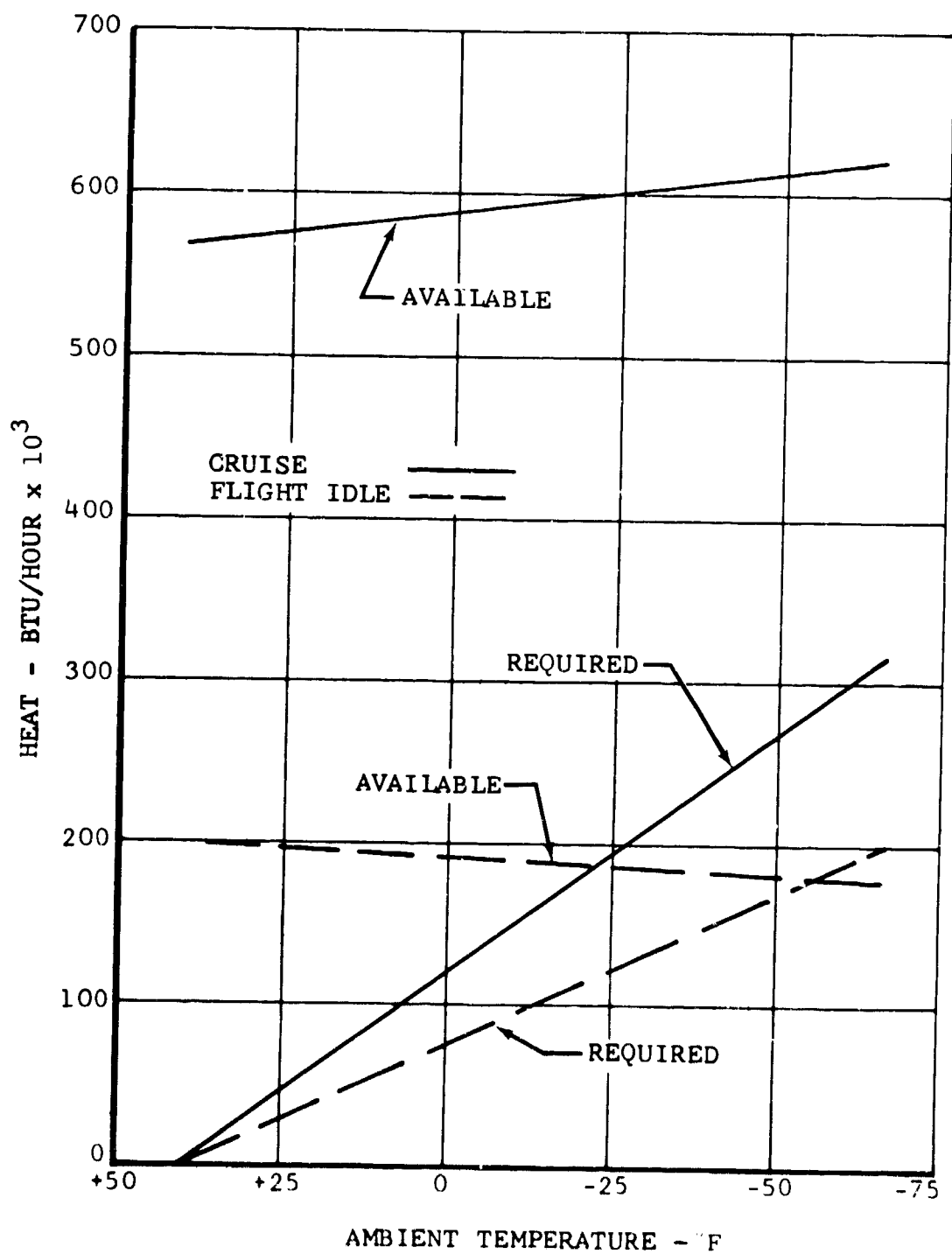


Figure 204. Heat Requirements Versus Ambient Temperature for 40°F Cabin Temperature.

SECTION VII. STABILITY AND CONTROL

A. INTRODUCTION

This section presents the flight and handling characteristics of the D266 and the results of the analysis that was conducted in areas that required special design attention. Methods used in the analysis included closed-form stability equations, analog and digital computer programs for open- and closed-form solutions for static trim and dynamic maneuvers, a moving-base flight simulator for evaluation of handling qualities, and wind-tunnel tests of a tenth-scale model.

The design study was directed toward analyzing areas requiring special design attention and assuring acceptable stability of the vehicle with the SAS inoperative. All of the stability and control requirements of MIL-H-8501A and MIL-F-8785 (ASG) can be met by the D266 with the SAS off--except for yaw damping in hover and roll acceleration and stick force per g in high-speed flight. The proposed requirements of References 24 and 25 which refer to the conversion flight regime are met. With SAS on, yaw damping in addition to that provided by the basic aircraft augments the damping and stability characteristics about the other axes. The yaw damping in hovering is about the same as that normally associated with tandem-rotor helicopters. The control power is sufficient to meet the yaw response requirement of Reference 26 with the SAS off. With the SAS active, yaw damping is increased by the "lead" network. The stability augmentation system is not required for flight because of the good stability characteristics of the basic airframe. The pilot effort required to fly the D266 with the SAS inoperative will be similar to that in present-day helicopters.

Table XXXIV is a summary of the most important requirements of Reference 26 compared with the values for the D266 found in this analysis. Table XXXV similarly shows the requirements of Reference 24.

Roll acceleration in the fixed-wing flight mode results in values of $pb/2V$ after 0.97 second that are somewhat less, at speeds below 300 knots, than the required 0.07. At design cruise speed, the value is 77 percent of the required $pb/2V$ --only slightly lower than the requirement. If flight tests show that this acceleration capability is not acceptable, aileron travel could be increased to +24 degrees to meet the requirement throughout the speed range.

The stick force is within the required values of 12.9 to 34.3 pounds per g (Reference 27), except at two "corner" conditions in the fixed-wing flight envelope: at 150 knots at the most

aft cg, the stick force gradient is 10 pounds per g (meets Reference 24 recommendation); at 350 knots at the most forward cg, the value is 39 pounds per g. These calculated values are based on the parameters of the proposed force-gradient system. If necessary, these parameters can be changed; however, the proposed system is believed to be the best compromise of conflicting requirements. Figure 205 shows the variation of control power throughout the flight regime.

B. HELICOPTER FLIGHT

Calculations of helicopter flight characteristics at sea level, NASA Standard Atmosphere, at the most forward and most aft center-of-gravity locations, were made. Although stability characteristics change somewhat with altitude and temperature, experience indicates that analysis of sea-level conditions is adequate for most design purposes. The "required" characteristics are those of Reference 26 unless stated otherwise. An analog computer program was used in calculating much of the helicopter stability data. The digital computer Programs C81, F35, and F06P were used to determine maneuver and trim characteristics, rotor performance, and helicopter stability, respectively.

Closed-form equations were used, when possible, to substantiate the digital and analog computer results.

1. HOVERING AND LOW-SPEED CHARACTERISTICS

The control power, damping, and response characteristics of the D266 have been summarized in Table XXXIV and have been compared to Reference 26 requirements. The inherent control power and damping in pitch and roll are greater than the minimums required for VFR flight. Although yaw damping without SAS is less than that required, the control power is sufficient to meet the yaw response criteria. Figure 206 compares the control power and damping characteristics of the D266 with those reported in Reference 28. With SAS, damping is increased and the initial control power is changed, so that the desired response characteristics are attained. All control power, response, and damping calculations were made at overload gross weight. Total rotor thrust is found by multiplying gross weight by 1.06, to account for wing download.

Pitch is controlled by fore-and-aft cyclic-pitch changes applied equally to both rotors. The pitching moment is generated by tilting the thrust vector, and by the hub moment caused by flapping. The resultant rotor force is assumed to be perpendicular to the tip-path plane for static control-power calculations, and the tip-path-plane deflection with cyclic pitch is all that needs to be determined. There are four

TABLE XXXIV

STATIC AND DYNAMIC STABILITY, HELICOPTER MODE

MIL SPEC H-8501A

Characteristics	Unit	Requirements	Paragraph	DMSS
-----------------	------	--------------	-----------	------

LONGITUDINAL

Fraction of Max Hover Control Moment at 120 Knots, Aft cg Climb	%	10	3.2.11	24
Change in Control Position With Power. Collective at Constant Speed	in.	3	3.2.10.2	2.7
Static Control Position Stability with Speed	-	positive	3.2.10	positive
Control Force Gradient	$\frac{\text{lb}}{\text{in.}}$	≥ 0.5 ≤ 2.0	3.2.4	1.4
Control Breakout Force	lb	≥ 0.5 ≤ 1.5	3.2.6	1:0.5
Limit Control Force	lb	≤ 8	3.2.6	5
Damping in Hover	$\frac{\text{lb-ft}}{\text{rad/sec}}$	≥ 15000	3.2.14	19700
Attitude - Second After 1-Inch Control Displacement in Hover	deg	1.4	3.2.13	5.33
Time for Normal Acceleration to Become Concave Down (Above Speed for Minimum Power Required)	sec	≤ 2	3.2.11.1a	≤ 0.9
Max Normal Acceleration Within 10 Seconds of Disturbance (At 100 knots)	g	≤ 0.25	3.2.11.2	0.3
Period of Oscillation (at 120) Time to Half Amplitude	$\frac{\text{sec}}{\text{knots}}$ periods	when P 5 TH < 2	3.2.11a	~ 4.5 ~ 0.3

LATERAL

Control Margin Hovering in 35-Knot Wind	5	10	3.3.4	20
---	---	----	-------	----

bance (At 100 knots)

Period of Oscillation (at 120) sec	when P 5	~4.5
Time to Half Amplitude (knots) periods	TH < 2	3.2.11a ~0.3
LATERAL		
Control Margin Hovering in 35-Knot Wind	%	3.3.4 20
Dihedral Effect Between 50 Knots and Max Speed	-	positive 3.3.9 positive
Control Displacement With Side-Slip Angle	-	positive 3.3.9 positive
Control Force Gradient	lb/in.	≥0.5 3.3.11 1.0
Control Breakout Force	lb	≥0.5 3.2.6 1±0.5
Limit Control Force	lb	≤7 3.2.6 5.4
Damping in Hover	lb-ft rad/sec	33500 3.3.19 252900
Attitude 1/2 Second After 1-Inch Control Displacement in Hover	deg	≥0.85 3.3.18 1.05
DIRECTIONAL		
Minimum Control Margin to Turn in a 35-Knot Wind	in.	≥0 3.3.6 2.15
Controls Fixed Stability From 50 Knots to Maximum Speed	-	positive 3.3.9 positive
Pedal Displacement Versus Side-Slip Angle	-	positive 3.3.9 positive
Pedal Displacement Versus Side-Slip Angle for ±15 Degrees	-	approx linear 3.3.9 linear
Control Breakout Force	lb	≥3.0 3.2.6 5±2
Damping in Hover	lb-ft rad/sec	≥105000 3.3.19 2790
Attitude 1 Second After 1-Inch Control Displacement in Hover	deg	≥3.47 3.3.5 3.53

B

A

TABLE XXXV

STATIC AND DYNAMIC STABILITY, FIXED-WING MODE

MIL SPEC F-8785(ASG)

D266

Characteristics

Unit

Requirements

Paragraph

LONGITUDINAL

Stick Force Gradient

$\frac{\text{lb}}{\text{in.}}$

-

-

>1.4
 ≤ 77

Stick Breakout Force

lb

≥ 0.5
 ≤ 5

3.2.1

1 : 0.5

Stick Force per g

$\frac{\text{lb}}{\text{g}}$

≥ 12.9
 ≤ 34.3

3.3.9

Within limits
at neutral cg
4C at 400 kt,
fwd cg; 8 at
120 kt, aft
cg

Stick Force During Trim
Changes

lb

<20

3.3.19

7

Primary Boost System
Failure

-

Control
forces must
be trimmable
to zero

3.7.2

Horizontal
stabilizer
trim tab with
separate motor
can zero hinge
moment

Neutral Points Position
Relative to Most Aft cg
Position

-

Aft

3.3.1

Aft

Elevator Deflection for
Increasing Normal
Acceleration

deg

Positive up

3.3.4

Positive up

Stall Characteristics

-

Preferably no
nose-up moment
Small roll
accelerations

3.6.4

Nose-down
moment. Wings
stall inboard
first

Phugoid Period Time to

Elevator Deflection for Increasing Normal Acceleration	deg	Positive up	3.3.4	Positive up
Stall Characteristics	-	Preferably no nose-up moment Small roll accelerations	3.6.4	Nose-down moment. Wings stall inboard first
Phugoid Period Time to Half-Amplitude	sec	If $P < 15$ $T_H \leq \infty$	3.3.6	37 at 150 kt 58
Short Period Time to Damp to 1/10 Amplitude	cycle	Less than one cycle	3.3.5	0.7
LATERAL - DIRECTIONAL				
Lat Stick Force Gradient	$\frac{lb}{in.}$	-	-	>1 ≤ 10.2
Pedal Force Gradient	$\frac{lb}{in.}$	-	-	>5.6 <180
Lat Stick Breakout Force	lb	>0.5 <4	3.2.11	1 = 0.5
Pedal Breakout Force	lb	1 14	3.2.11	5 = 2
Pedal Deflection for Positive Sideslip	in.	Negative	3.4.4	Negative
Variation of Pedal Position vs. Sideslip Within $\pm 15^\circ$, Wings Level	-	Essentially linear	3.4.4	Essentially linear
Effective Dihedral Position	Force	Positive	3.4.7	Positive
	Position	Positive	3.4.6	Positive
Lat Stick Force for Steady Roll of $\frac{pb}{2V} = 0.07$	lb	<25	3.4.16.3	23
Rolling Performance Parameter $\frac{pb}{2V}$		0.07 for stick forces < 25 lb	3.4.16	0.075 flaps up 0.053 flaps down
Steady Roll Rate	$\frac{deg}{sec}$	≥ 15	3.4.16.7	≥ 15
Rolling Acceleration	-	Must reach $\frac{pb}{2V} = 0.07$ in less than 0.97 sec	3.4.16.2	$\frac{pb}{2V} = 0.054$ at 250 kt after 0.97 sec

		in.		≤10.2	
Pedal Force Gradient	lb in.	-	-	>5.6 <180	
Lat Stick Breakout Force	lb	>0.5 <4	3.2.11	1 ± 0.5	
Pedal Breakout Force	lb	1 14	3.2.11	5 ± 2	
Pedal Deflection for Positive Sideslip	in.	Negative	3.4.4	Negative	
Variation of Pedal Position vs. Sideslip Within ±15°, Wings Level	-	Essentially linear	3.4.4	Essentially linear	
Effective Dihedral Force Position	-	Positive	3.4.7	Positive	
		Positive	3.4.6	Positive	
Lat Stick Force for Steady Roll of $\frac{pb}{2V} = 0.07$	lb	<25	3.4.16.3	23	
Rolling Performance Parameter $\frac{pb}{2V}$		0.07 for stick forces <25 lb	3.4.16	0.075 flaps up 0.053 flaps down	
Steady Roll Rate	$\frac{deg}{sec}$	≥15	3.4.16.7	>15	
Rolling Acceleration	-	Must reach $\frac{pb}{2V} = 0.07$ in less than 0.97 sec	3.4.16.2	$\frac{pb}{2V} = 0.054$ at 250 kt after 0.97 sec	
Asymmetric Power	-	No dangerous flt condition after engine failure	3.4.17	Interconnect shaft between both rotors maintains symmetry	
Adverse Yaw in Abrupt Roll	deg	<15	3.4.9	2.06	
Spiral Stability: Double Bank Angle	Time to sec	>4	3.4.2	Stable	
Dutch Roll Stability Cycles to Damp to Half Amplitude = $f(\phi/\beta)$	-	Specified minimum requirement	3.4.1	Well above requirements	

9

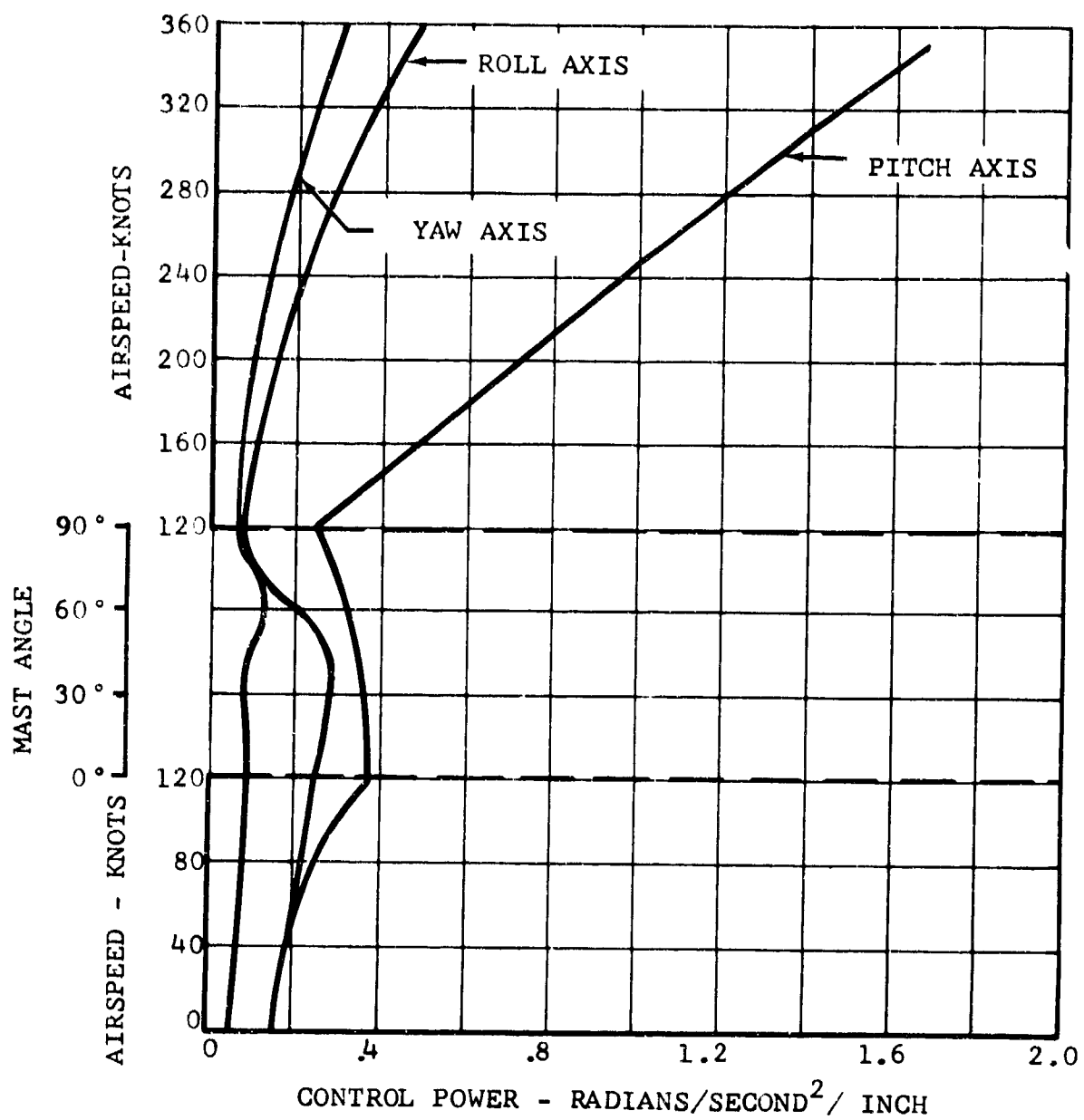


Figure 205. Control Sensitivity Throughout Flight Regime.

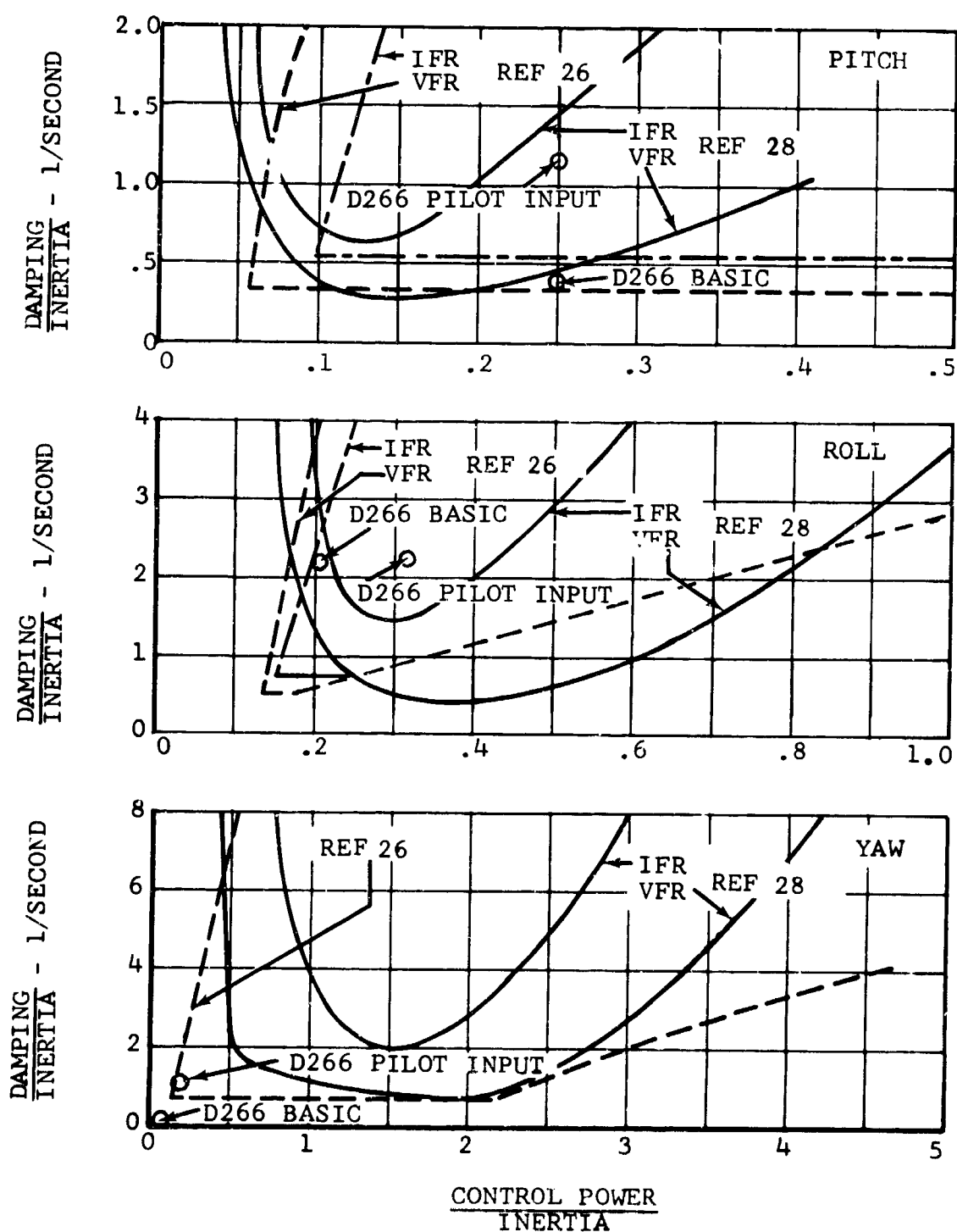


Figure 206. Control Power and Damping Characteristics.

predominant effects that must be considered: pitch-flap coupling, swashplate phasing, torsional wing deflection, and pylon-mount deflection.

Figure 207 shows the pitch response, calculated with the analog and digital computers, to a 1-inch cyclic step in hover. The analog indicates an attitude change of 5.2 degrees after 1 second, and a maximum rate of 13.7 degrees per second. The time constant is 1 second, which is similar to that of a conventional helicopter. The pitch-control power over inertia, as indicated by the maximum slope of the pitch-rate trace, is 0.27. This value correlates well with the calculated value.

Roll control in hover is obtained by differential collective pitch. Inherent roll damping is caused by the thrust change with inflow which is induced at the wingtips by a roll velocity.

Yaw control is obtained by differential fore-and-aft cyclic pitch. The thrust is assumed to be perpendicular to the tip-path plane; and the horizontal component of the thrust, acting at the wingtip, provides a yawing moment. Wing and pylon deflections were taken into account in determining the static location of the tip-path plane.

Yaw damping results from the speed stability of the rotors. This effect is small, however, and the SAS is the primary source of damping.

The change in thrust with collective pitch increases linearly with speed in helicopter flight (Reference 29). Since aileron effectiveness also increases with speed, the total roll-control power increases with speed. Yaw-control power also increases with speed, owing to the effectiveness of the rudder and the increase of $dH/d\alpha$ with speed.

Roll- and yaw-control sensitivity in low-speed forward flight is greater than in hover, as illustrated in Figure 205, and less stick motion is required to produce desired rates of roll and yaw. No lateral control is required for trimmed flight because of the contrarotating rotors; 10 percent of the hovering rolling moment is available throughout the flight regime.

Sideward flight at 35 knots requires 1.8 degrees of differential collective pitch. Approximately 40 percent of the hovering induced velocity of the "front" rotor appears at the "rear" rotor at 35 knots. Since 4 degrees is available, roll control in sideward flight is sufficient. The rudder "drag" in sideward flight creates a yawing moment, which is balanced by 1.2 degrees per rotor of differential cyclic pitch. Since 4.25 degrees is available at each rotor, there is sufficient yaw-control power to overcome fin "drag" at 35 knots.

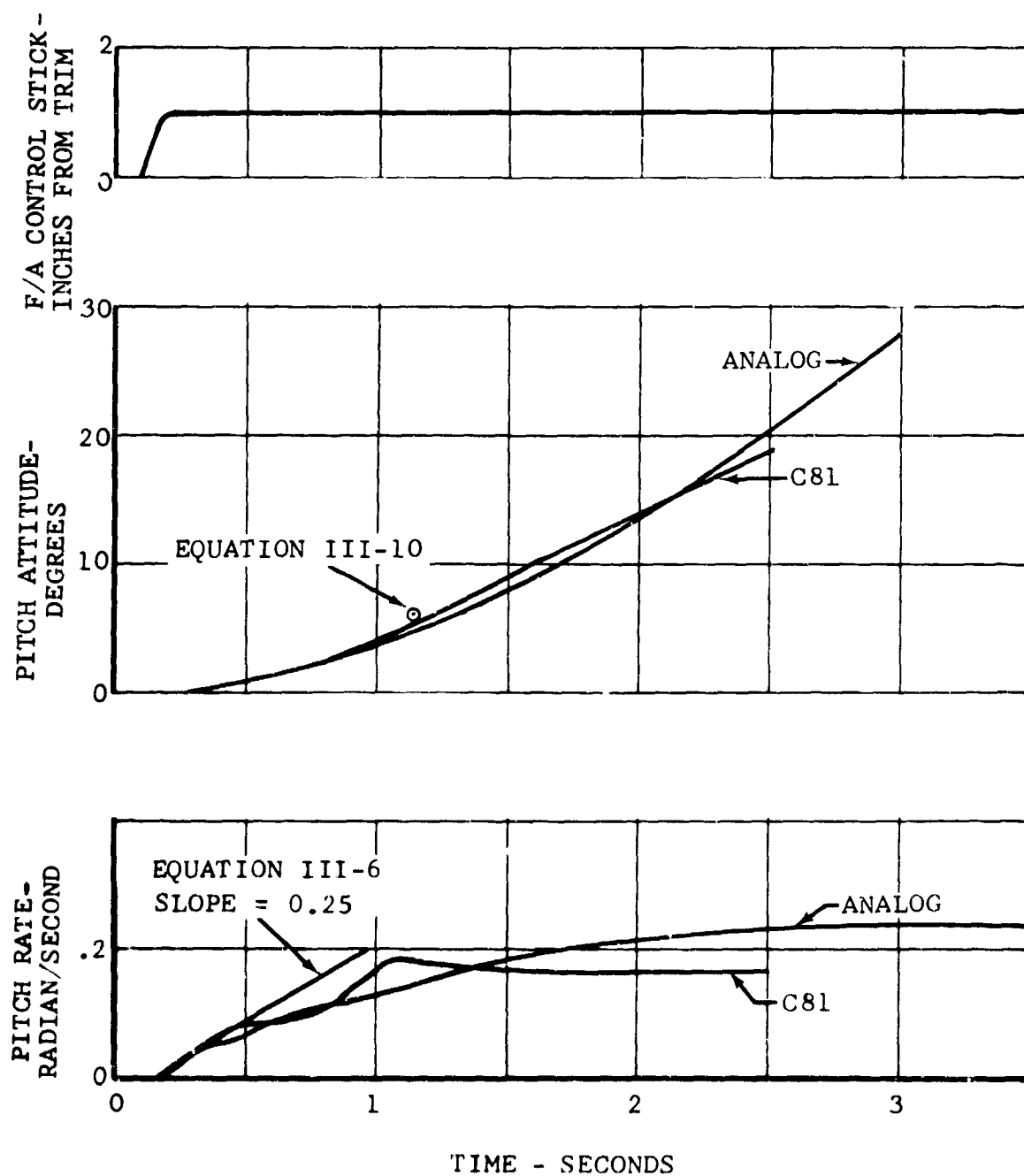


Figure 207. Pitch Response in Hovering to F/A Stick Input.

The D266 employs a power-turbine governor to control fuel flow in helicopter flight. The droop compensating cam is so designed that there is little lag in response and no vertical oscillation in hover.

The collective sensitivity is approximately the same as that of the UH-1; therefore, hovering with less than 1/2 inch of stick motion will be as easy in the D266 as in a conventional helicopter.

2. STATIC STABILITY

a. Longitudinal

The analog and digital computer programs provided the data of this subsection. Since the analog program was restricted to zero-degree mast angle, the digital program was used to determine static-stick positions required for trim at partial conversion angles. The two computer programs do not quite agree, probably because simplified rotor equations were used in the analog program. Therefore, the digital program is used for determining level-flight trimmed-stick positions, and the analog program is used to determine static stability about a trimmed condition with the collective lever fixed. All longitudinal static stability requirements of Reference 26 are met or exceeded.

The control-stick positions required for trimmed level flight are shown in Figure 208 at forward and aft cg locations, as determined on the digital computer.

A unique feature of the D266 is the ability to convert partially in helicopter flight. This technique increases the wing incidence, unloads the rotor, increases the propeller efficiency, and reduces the power required. These effects were noticed on the XV-3 and were reported in Reference 30. At 75 knots, the horsepower required was reduced from 425 to 295 as the rotors converted from 0 to 15 degrees. In addition to the power saving, the longitudinal stick position required for trimmed level flight moves aft. The stick position required for flight at 20-degree conversion is shown in Figure 208. Static-stick margins increase considerably for partial conversion angles.

The analog computer was used to determine the collective-fixed speed stability, and the results are shown in Figure 209. The slope of stick position versus speed is always positive. It becomes shallow at high speeds, as it does for conventional helicopters.

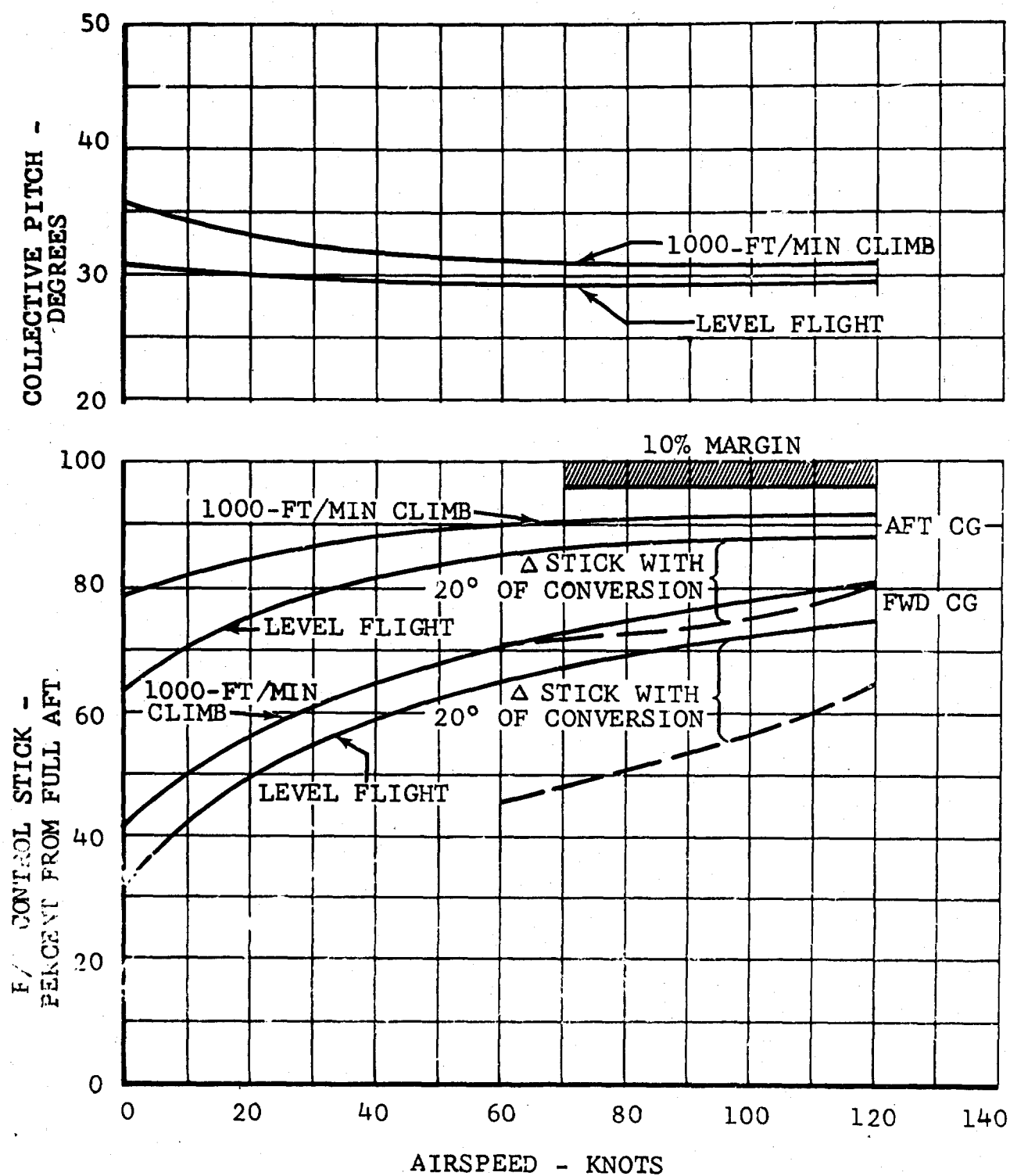


Figure 208. Control Positions for Trimmed Flight.

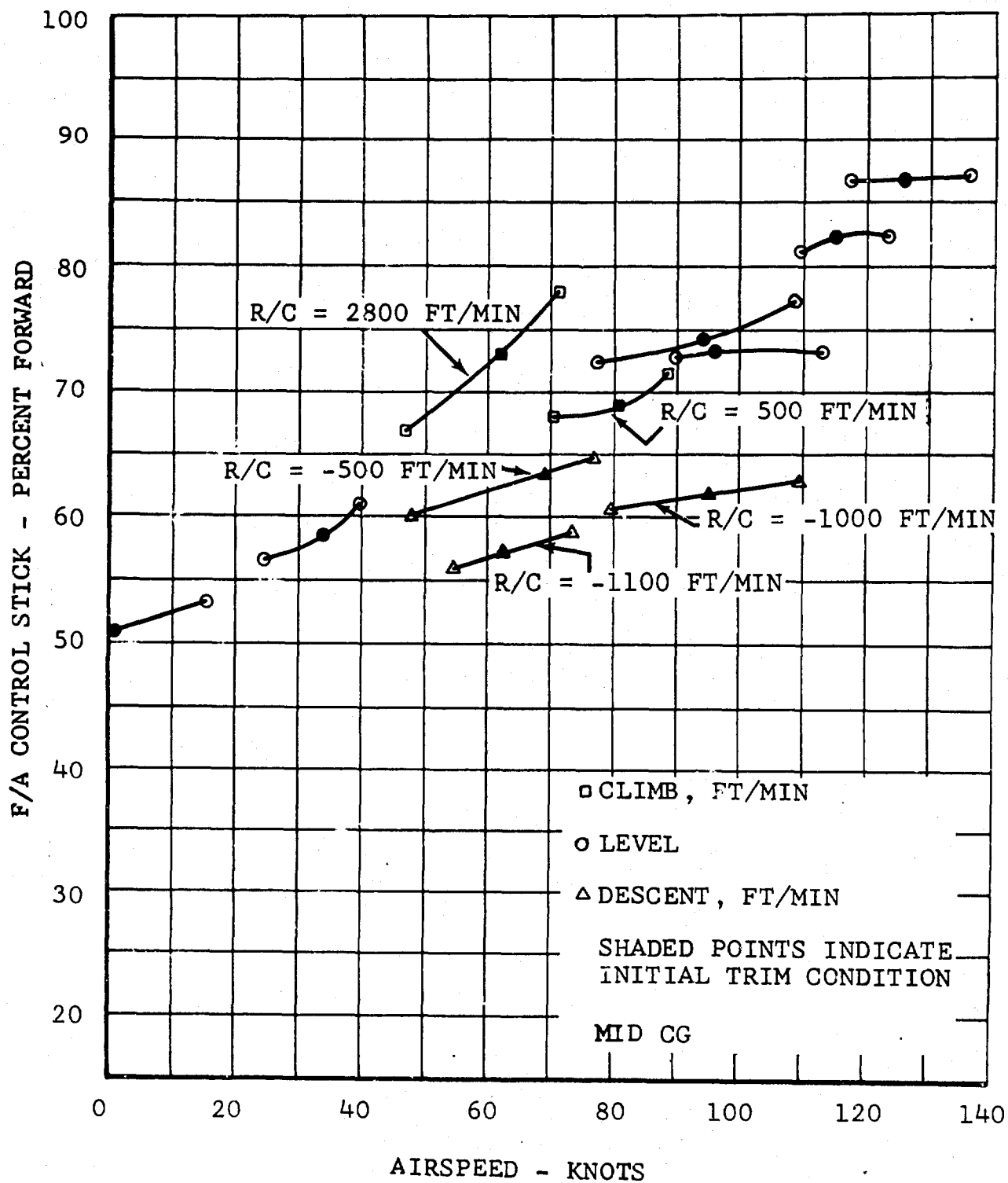


Figure 209. Collective-Stick-Fixed Speed Stability.

b. Lateral-Directional

The effect of lateral-directional control coupling was investigated (Reference 31), and handling-quality boundaries were determined for an IFR approach task. Figure 210 and Table XXXVI show these data. The shaded area indicates the D266 coupling that has been calculated for all modes of operation. The data indicate that the coupling is within the normal operation boundary for the IFR approach task. Figure 210 shows handling qualities rated better than 3.5 on the Cooper scale.

Figure 211 shows the roll response to a lateral step at 85 knots, obtained with the digital computer. No roll rate is evident, and the maximum roll rate is 14 degrees per second per inch, which is less than the allowed maximum of 20 degrees per second.

The effect of the SAS on the roll response characteristics is to increase the apparent control power. This is done with an electronic lead network that momentarily puts in more control than the pilot commands. This extra control is quickly "washed out" and the response time is improved. The initial roll acceleration is increased about 70 percent above the basic value. The improvement in roll characteristics is evident in Figure 206.

The pedal and lateral stick displacements required at the required sideslip angles (Reference 29) are indicated in Figure 212.

Figure 213 shows the response to a lateral stick displacement at 85 knots. The adverse yaw is only 1/2 degree. This would probably not be noticeable to the pilot, and it certainly would not be objectionable. The adverse yaw requirements of Reference 26 are met. Figure 213 shows the response to a pedal input at 85 knots. The beneficial effect of the differential coupling in reducing roll rate is apparent.

3. DYNAMIC STABILITY

a. Longitudinal

Three methods were used for the investigation of the longitudinal dynamic-stability characteristics of the D266 in the helicopter mode: the analog computer program, the digital computer program (C81), and the closed-form uncoupled equations of motion. The results of the different methods correlate reasonably well. They show the dynamic-stability characteristics of the D266. Over the entire helicopter-mode speed range, the requirements of Reference 26 are met without the SAS engaged,

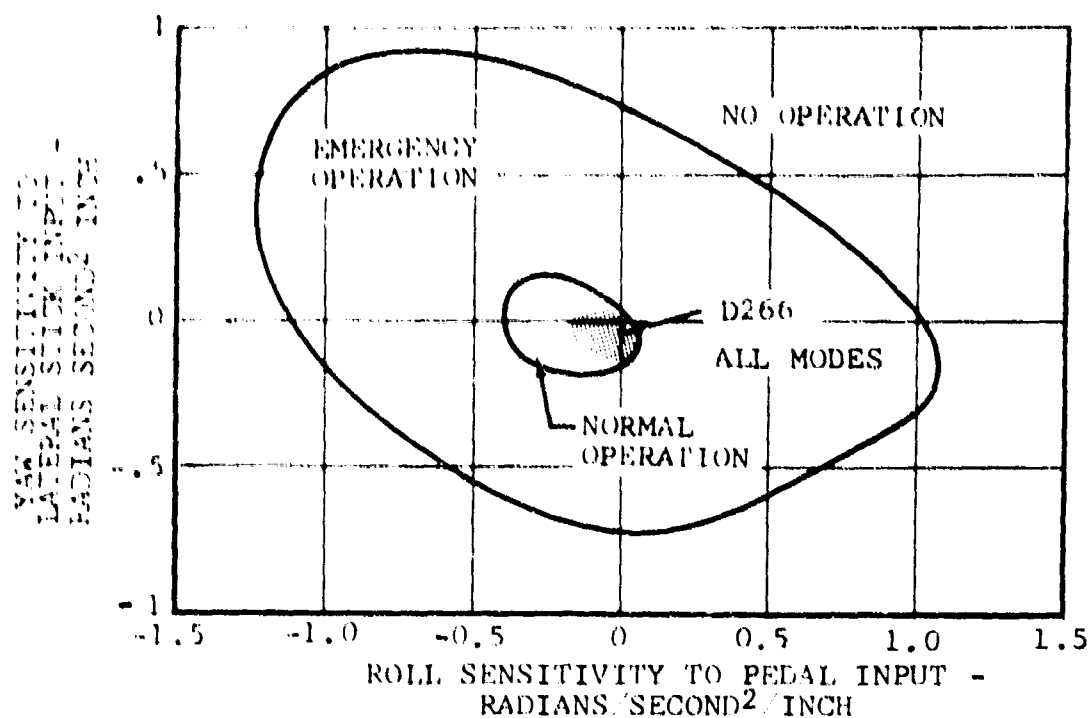


Figure 210. Handling Quality Boundaries Affected by Lateral-Directional Coupling.

TABLE XXXVI					
HANDLING QUALITIES					
Airspeed (knots)	Mast Angle (degrees)	Pedal Input (in.)	Lateral Input (in.)	$\frac{L_{Ixx}}{\text{In. Pedal}}$ (rad/sec ² /in.)	$\frac{N_{Izz}}{\text{In. Lat Stick}}$ (rad/sec ² /in.)
85	0	1		-0.097	
85	0		1		0
120	0	1		-0.185	
120	0		1		0
120	30	1		-0.024	
120	30		1		-0.095
120	60	1		+0.056	
120	60		1		-0.115
150	90	1		-0.015	
150	90		1		0
350	90	1		-0.085	
350	90		1		0

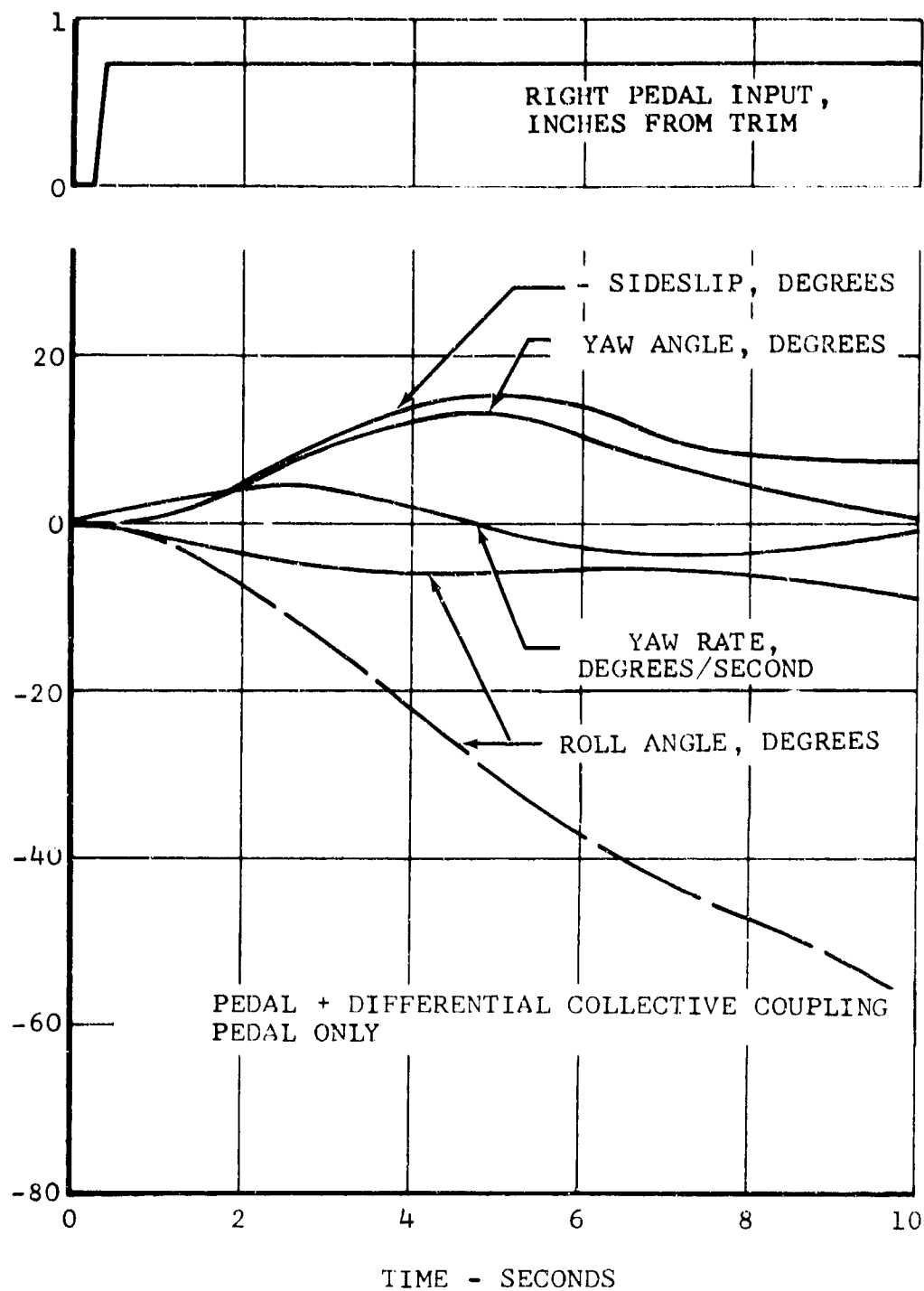


Figure 211. Roll and Yaw Response at 85 Knots to Pedal Input, Helicopter Mode.

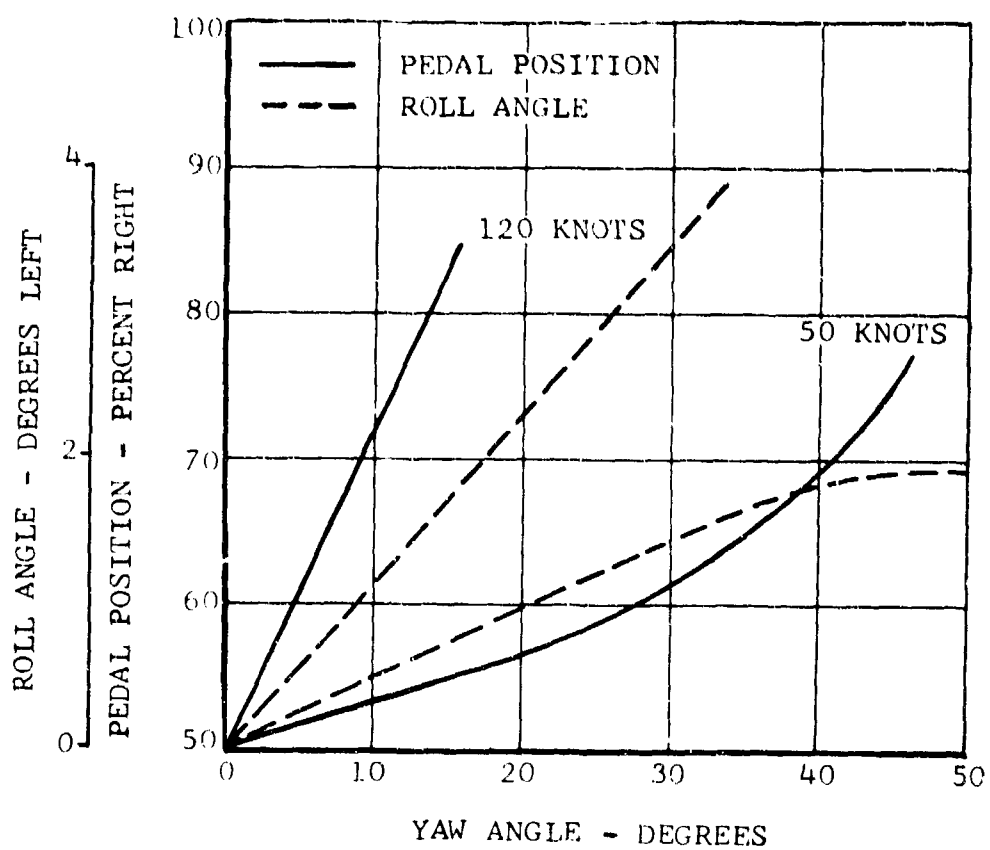
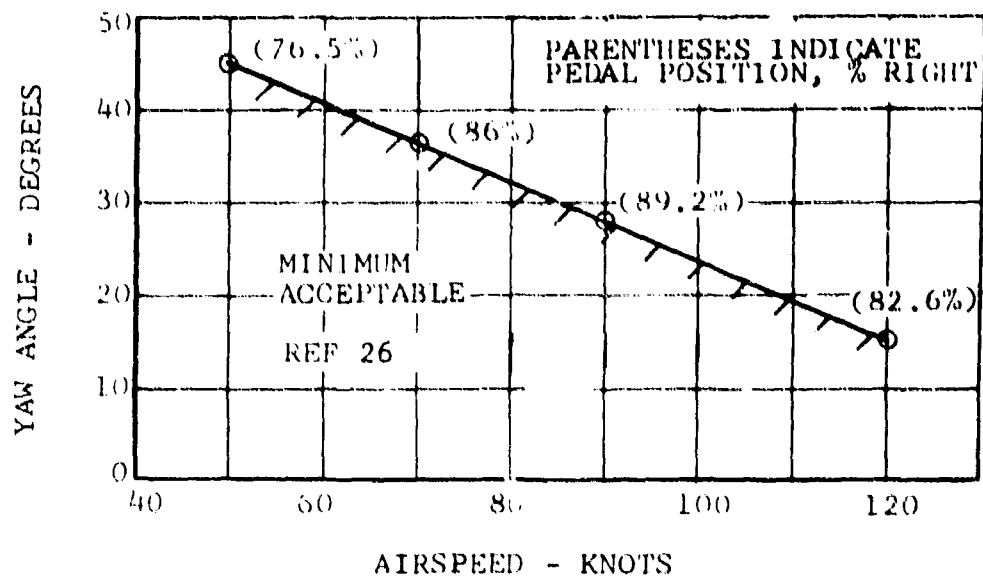


Figure 212. Sideslip Characteristics.

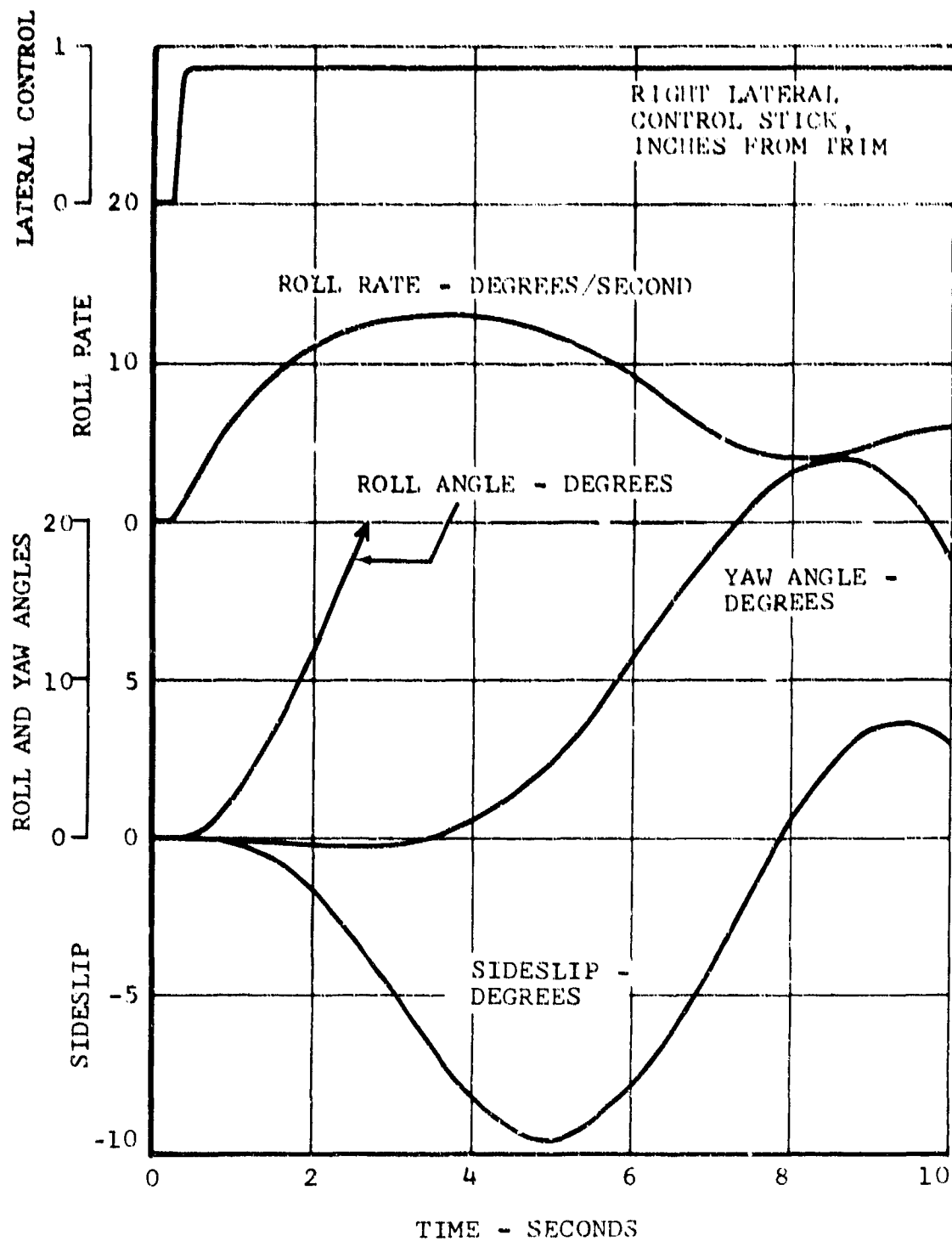


Figure 213. Roll and Yaw Response at 85 Knots to Lateral Control-Stick Input, Helicopter Mode.

as shown in Figure 214. With SAS active, pitch damping is increased, and the times to half-amplitude are further decreased.

The normal acceleration and pitch-rate characteristics obtained on the analog computer are shown in Figure 215 at 70, 98, and 120 knots.

The response to an artificial disturbance was simulated on the analog computer by introducing an aft pulse. The same pulse amplitudes as the step inputs needed to attain 1.5 g within 3 seconds were used for about 0.5 second. Figure 216 shows time histories of the resulting normal acceleration.

b. Lateral-Directional

Digital Program C81 was used to determine lateral-directional stability. Time histories of response following a right-lateral control step and a right-pedal step are shown in Figure 211. The directional oscillation is well damped, with a period of about 8 seconds. The roll-subsidence mode has a time constant of about 0.4 second, which is better than that of either single- or tandem-rotor helicopters. No reversal of rolling velocity occurs, and there is only a small amount of adverse yaw.

4. AUTOROTATION

The D266 can safely enter autorotation at any speed after holding all controls fixed for 2 seconds and reducing power as required by Reference 26. Figure 217 shows a time history of a throttle chop while hovering at 2000 feet. Rotor speed is maintained and steady autorotative flight is established. Figure 218 shows a power-off landing that was initiated from 75- and 90-knot autorotative flight. Touchdown is made at 30 and 35 knots, as required by Reference 26. These data were obtained with the C81 Computer Program. Pitch, roll, and yaw displacements do not exceed the maximum allowed, and rotor speed control is maintained by reducing collective pitch as in a conventional helicopter after delaying the required 2 seconds.

Flare capability of the D266 is better than that of conventional helicopters at the same disk loading because of the more efficient lift configuration and the laterally disposed rotors. Flares may be initiated by aft cyclic or by converting the masts from 10 degrees forward to zero as the ground is approached. Touchdown speeds below 35 knots will be attainable with the D266, because high fuselage attitudes are permissible near the ground.

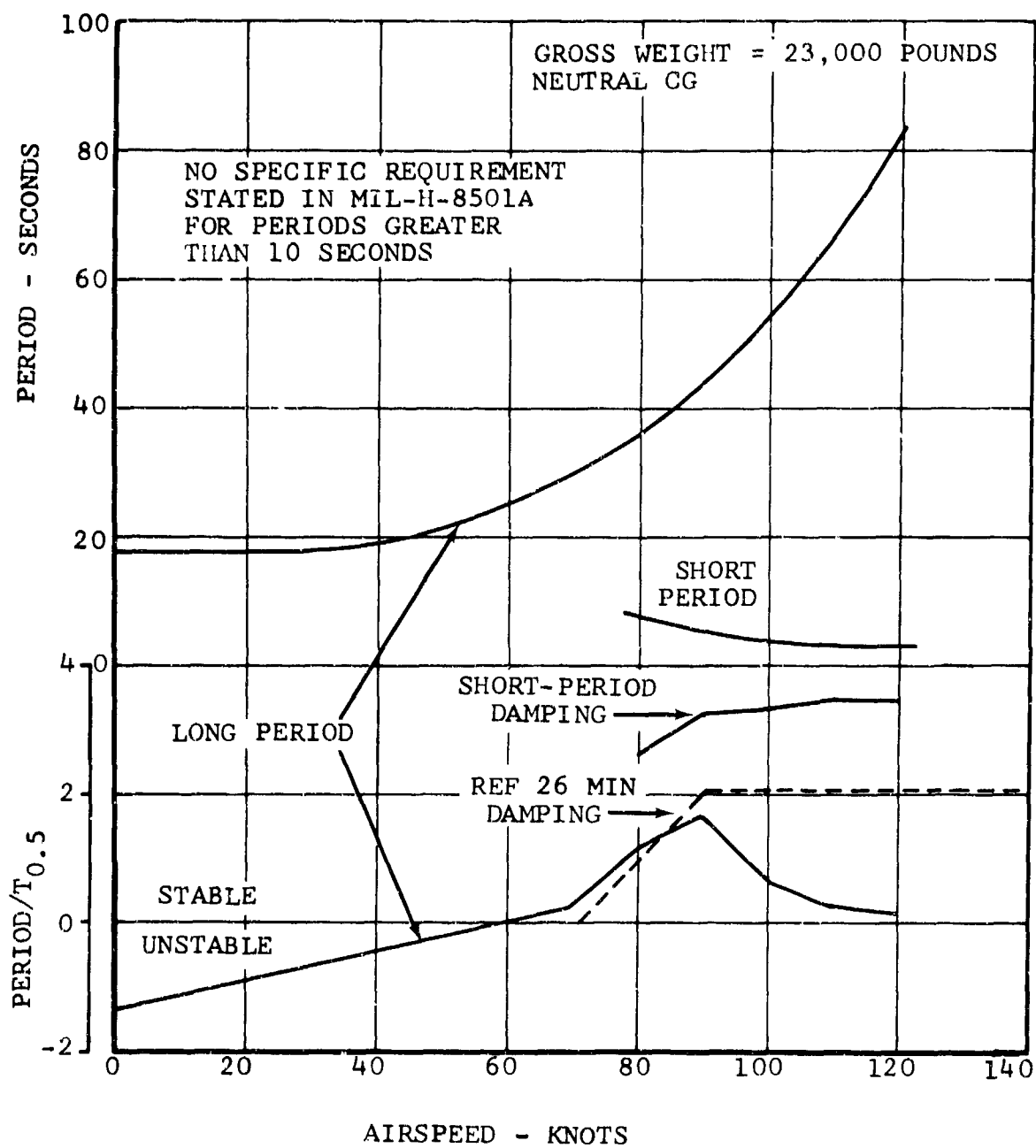


Figure 214. Longitudinal Dynamic-Stability Characteristics.

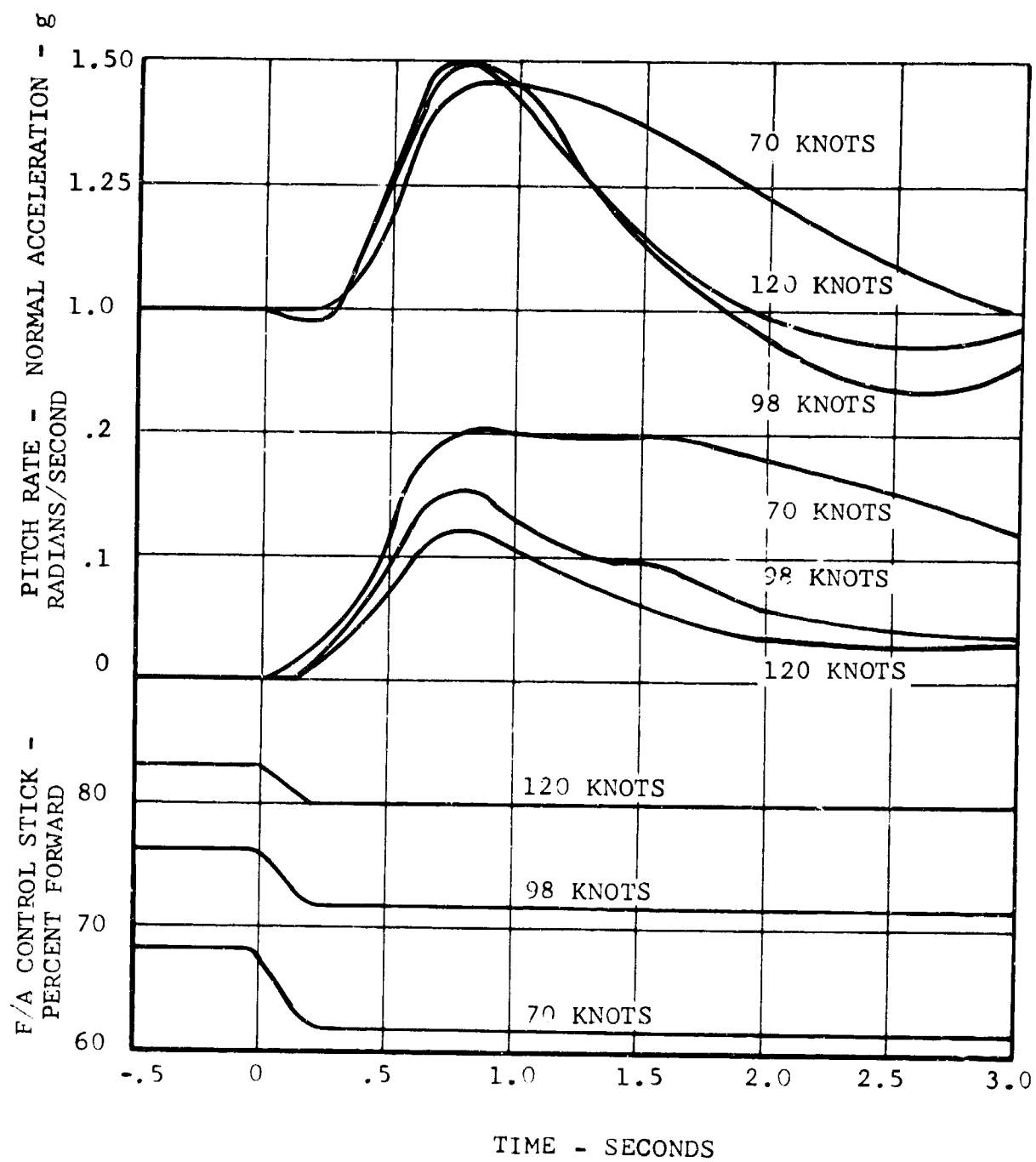


Figure 215. Normal Acceleration and Pitch-Rate Characteristics at 70, 98, and 120 Knots - Analog.

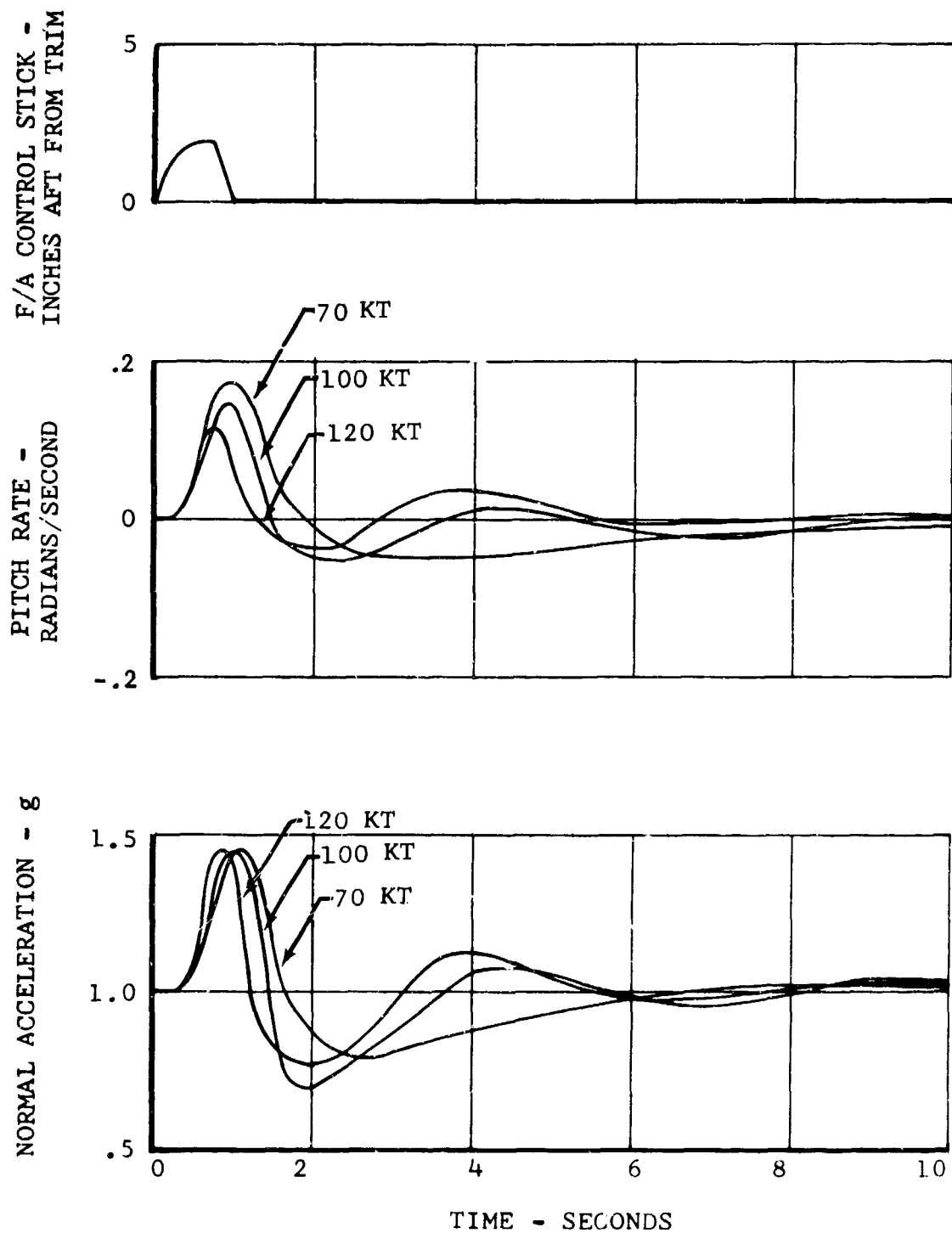


Figure 216. Normal Acceleration Response to Pulse Input at 70, 98, and 120 Knots - Analog.

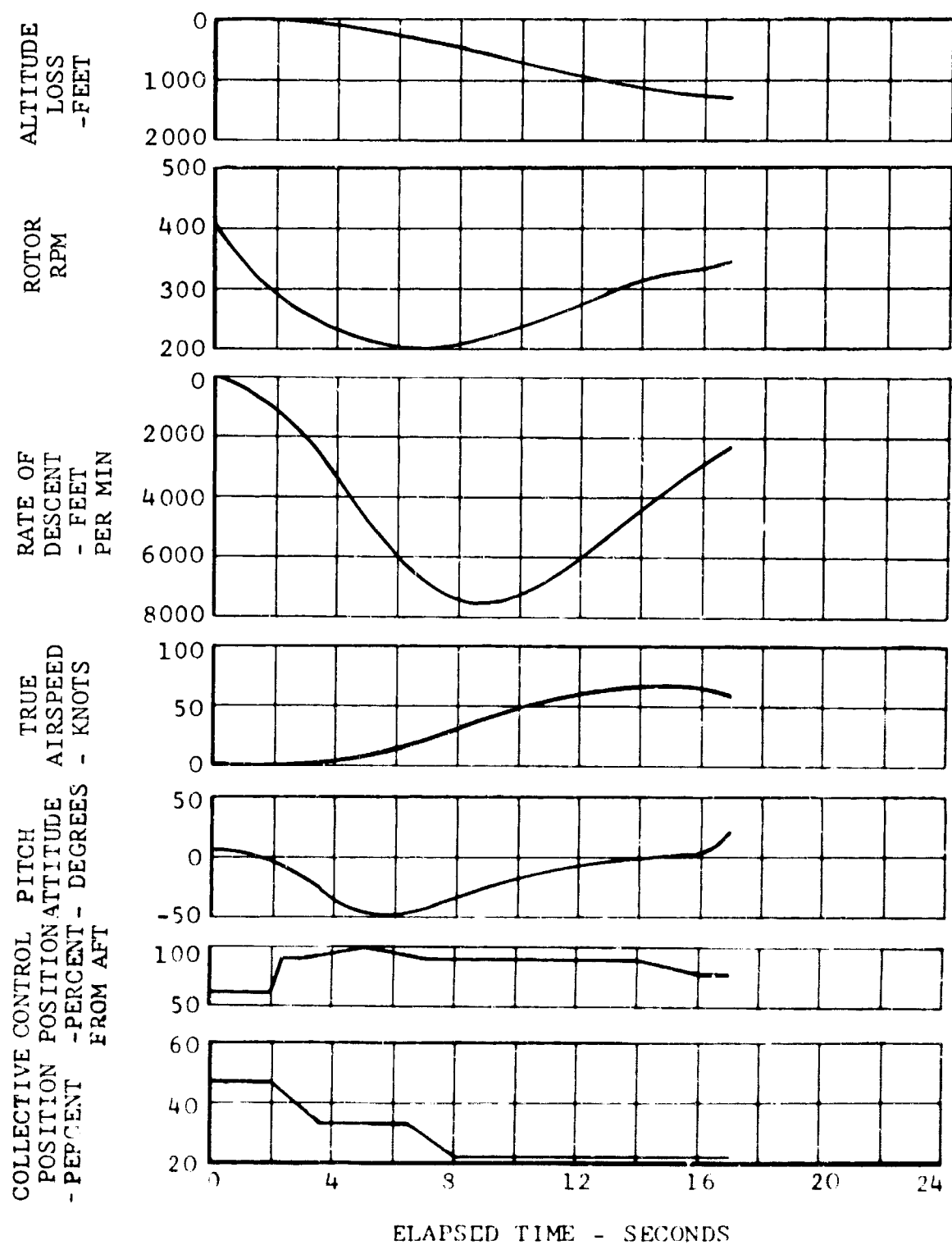


Figure 217. Time History of Power Failure in Out of Ground Effect Hover.

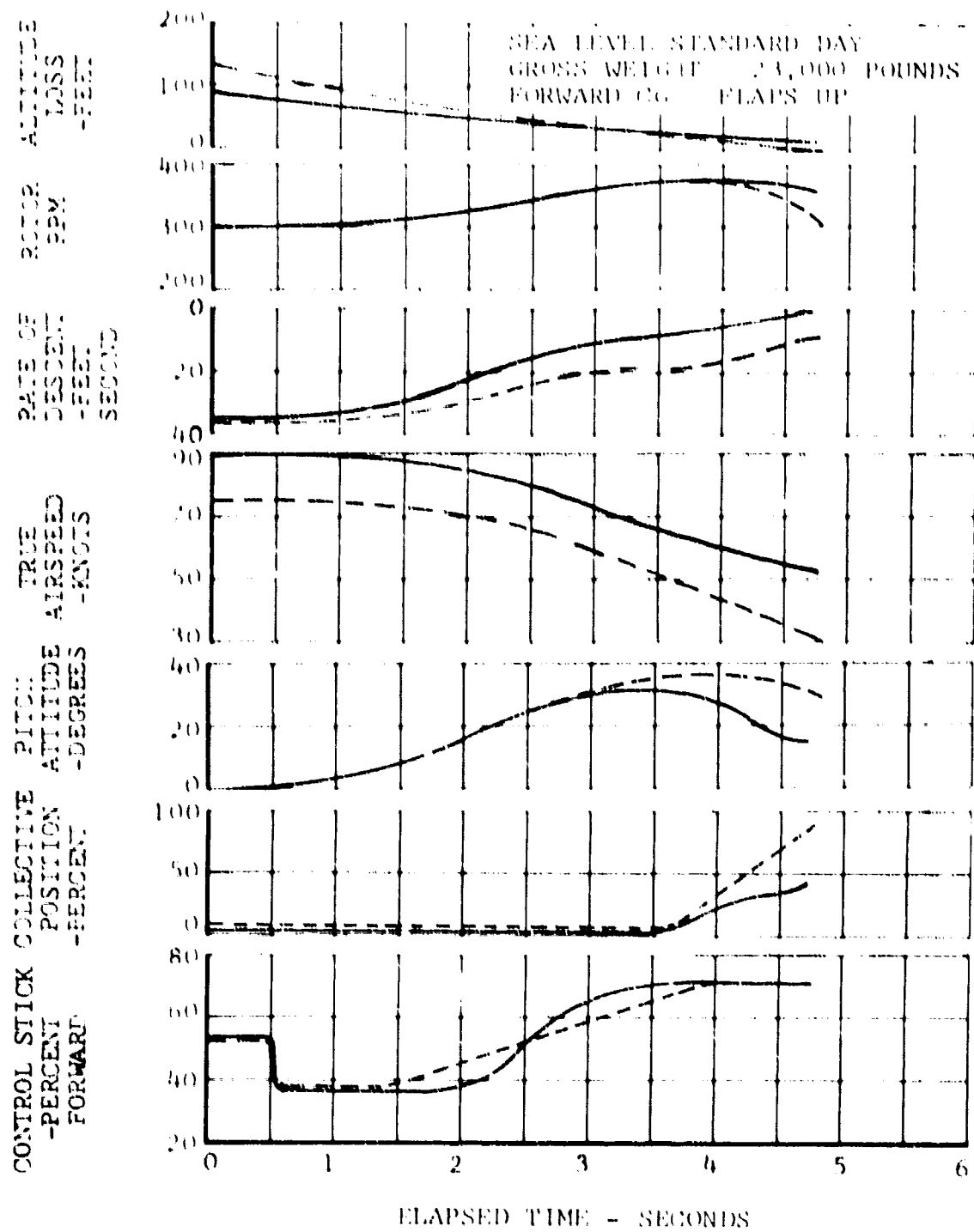


Figure 218. Time History of Power-Off Flare and Landing.

C. FIXED-WING FLIGHT

1. CONTROLLABILITY

a. Longitudinal

The trimmed stick positions in level flight were calculated and compared with the information obtained from the C81 output. Both sets of data agree well and are shown in Figure 219. The C81 maneuver program was used to determine the angles of attack necessary to develop limit load or to stall the wing at forward cg. Figure 221 shows the results of that investigation. It can be seen that for all speeds above 245 knots, the D266 can develop the limit normal acceleration of 4.5g.

The stick force per g, shown in Figure 222, was found using the longitudinal stick-force gradient and the stick displacement per g shown in Figure 220.

The lift characteristics at stall were investigated extensively in the wind tunnel for level flight, power on, flaps up and down. Figure 223 gives the results of these tests. The lift decreases gradually at stall.

The C81 maneuver program was used to investigate the difference in response between a stick pull-and-hold maneuver and a stick pull-and-return. Figure 224 is a time history of the normal acceleration resulting from two such pullups at 250 knots, using stick displacements of 0.5 inch. The pull-and-return had a duration of 0.3 second. The time history shows that the peak normal acceleration resulting from the pull-and-return is less than the final acceleration developed during the pull-and-hold maneuver.

b. Roll Controllability

(1) Steady Roll Performance

Some of the rolling performance requirements for Class II aircraft are given in Table VI of Reference 27. Using these requirements for the D266 and a V_H of less than 500 knots, the design conditions for steady roll performance are:

- $\frac{pb}{2V}$ of at least 0.07 at $0.8V_H = 280$ knots
- $\frac{pb}{2V}$ of at least 0.015 at M_H
- $\frac{pb}{2V}$ of at least 0.07 and a $\frac{pb}{2}$ of at least 10 feet/second at $1.1 V_{S_L} = 118$ knots.

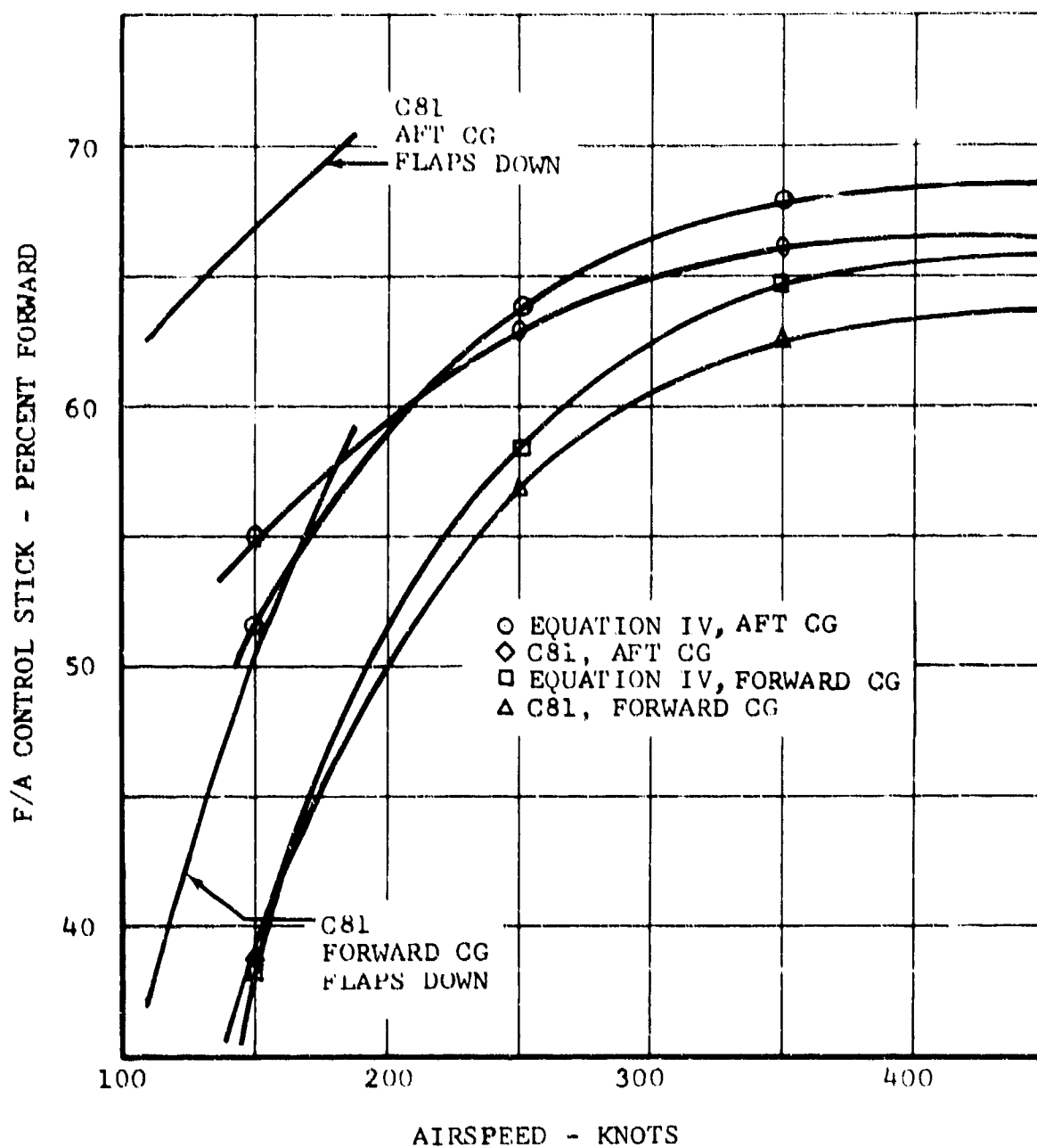


Figure 219. Longitudinal Stick Position in Trimmed Fixed-Wing Flight.

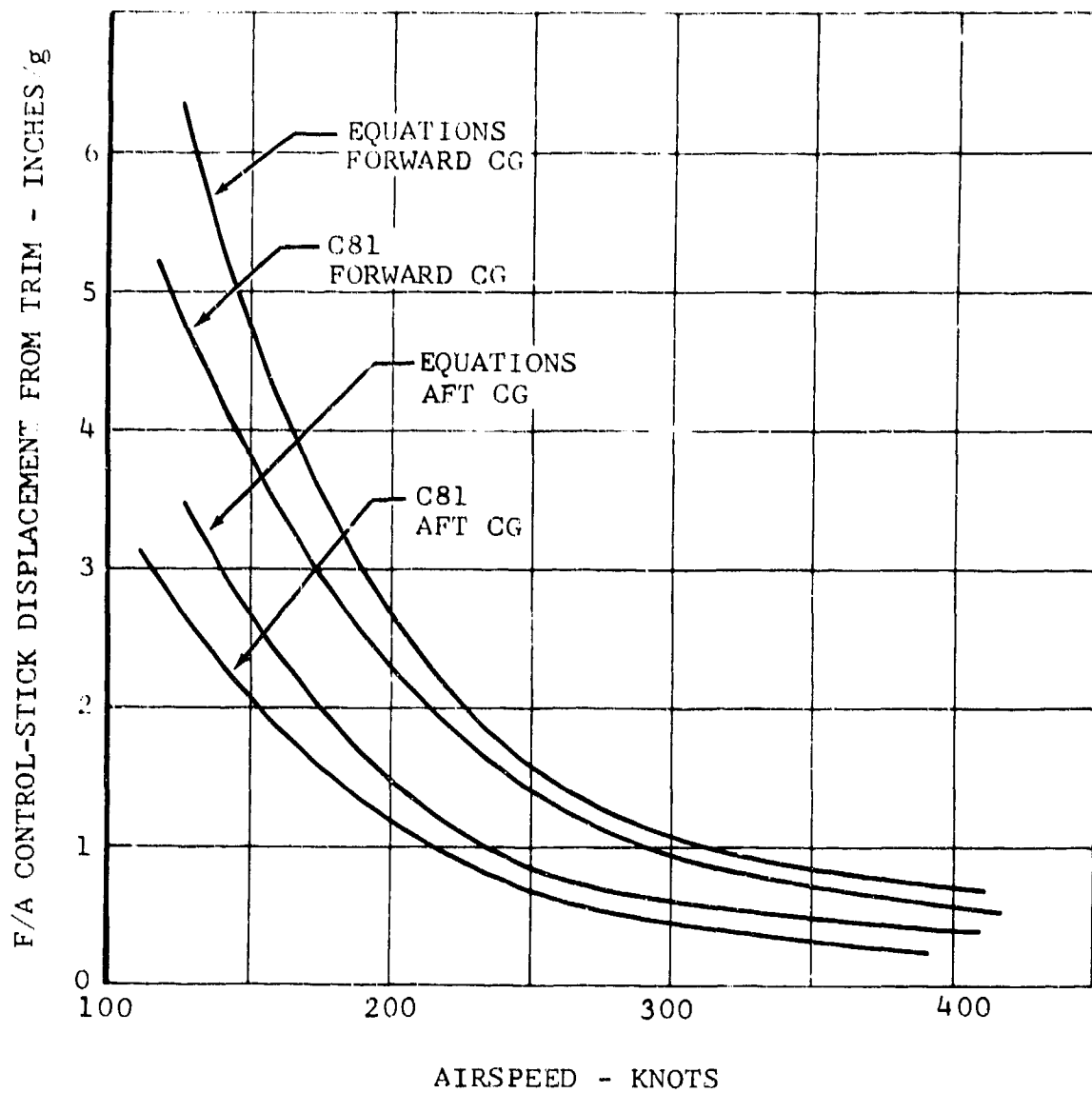


Figure 220. F/A Control-Stick Displacement Per g.

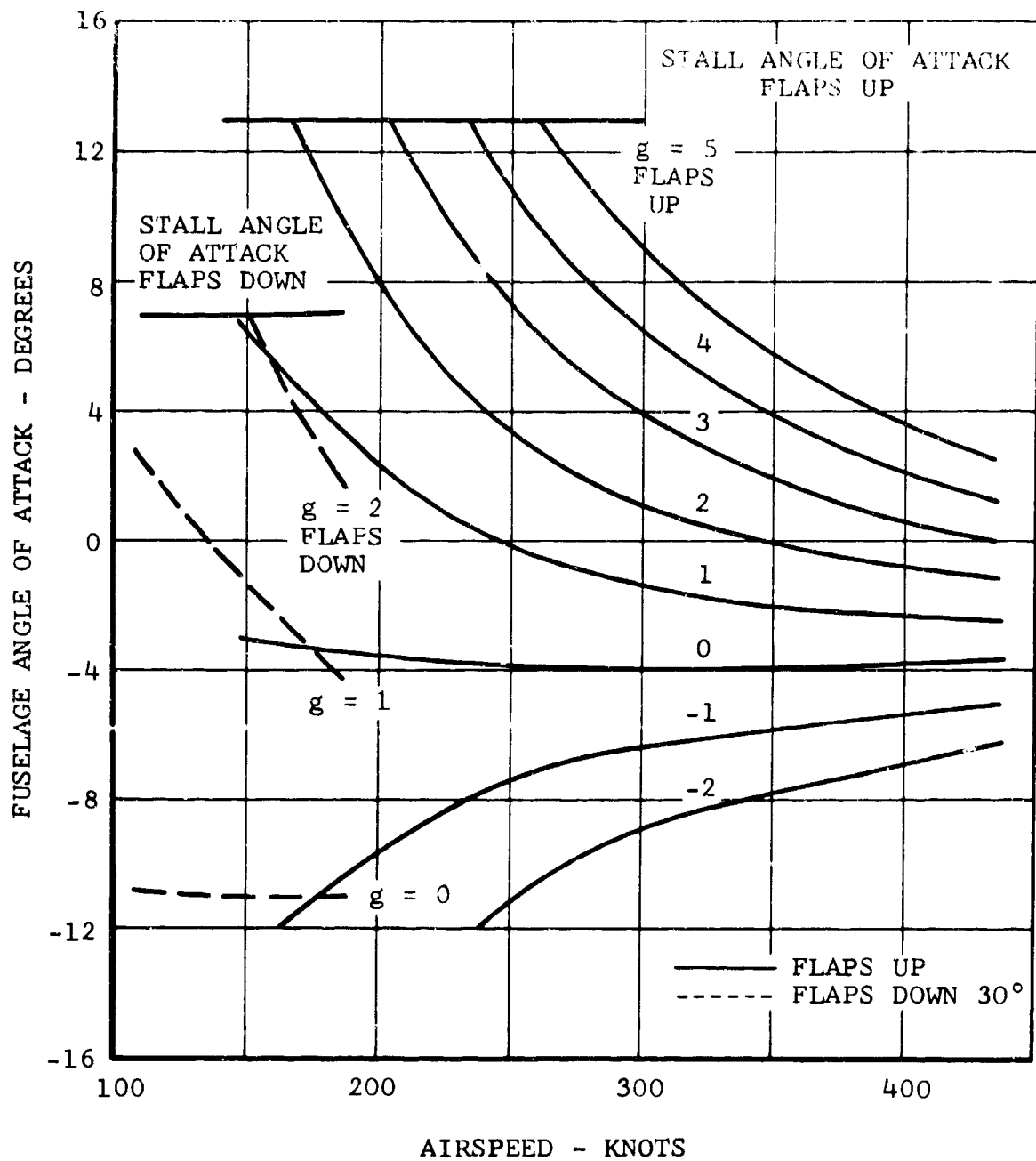


Figure 221. Fuselage Angle of Attack Versus Speed At Various Levels of Normal Acceleration.

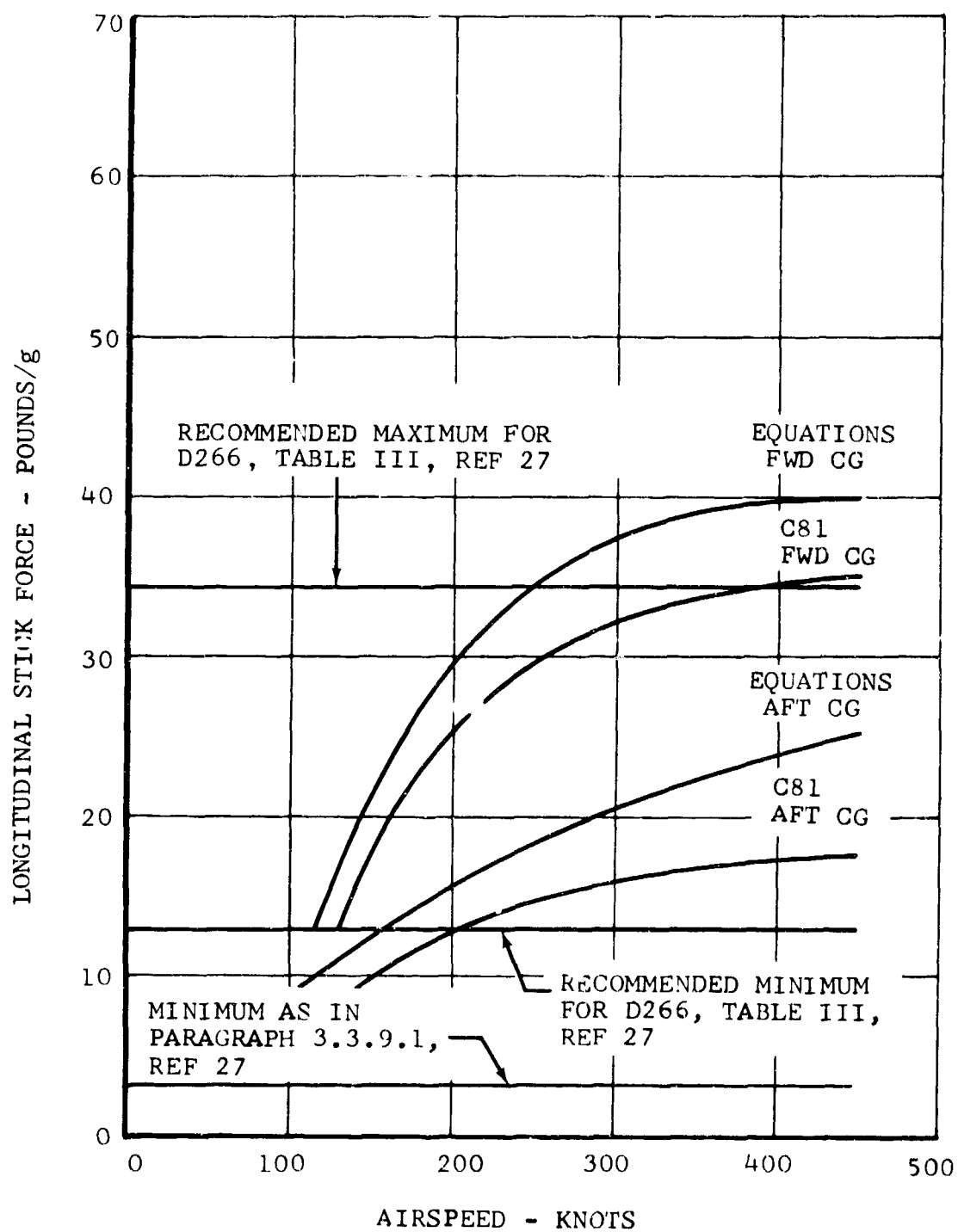


Figure 222. Longitudinal Stick Force Per g.

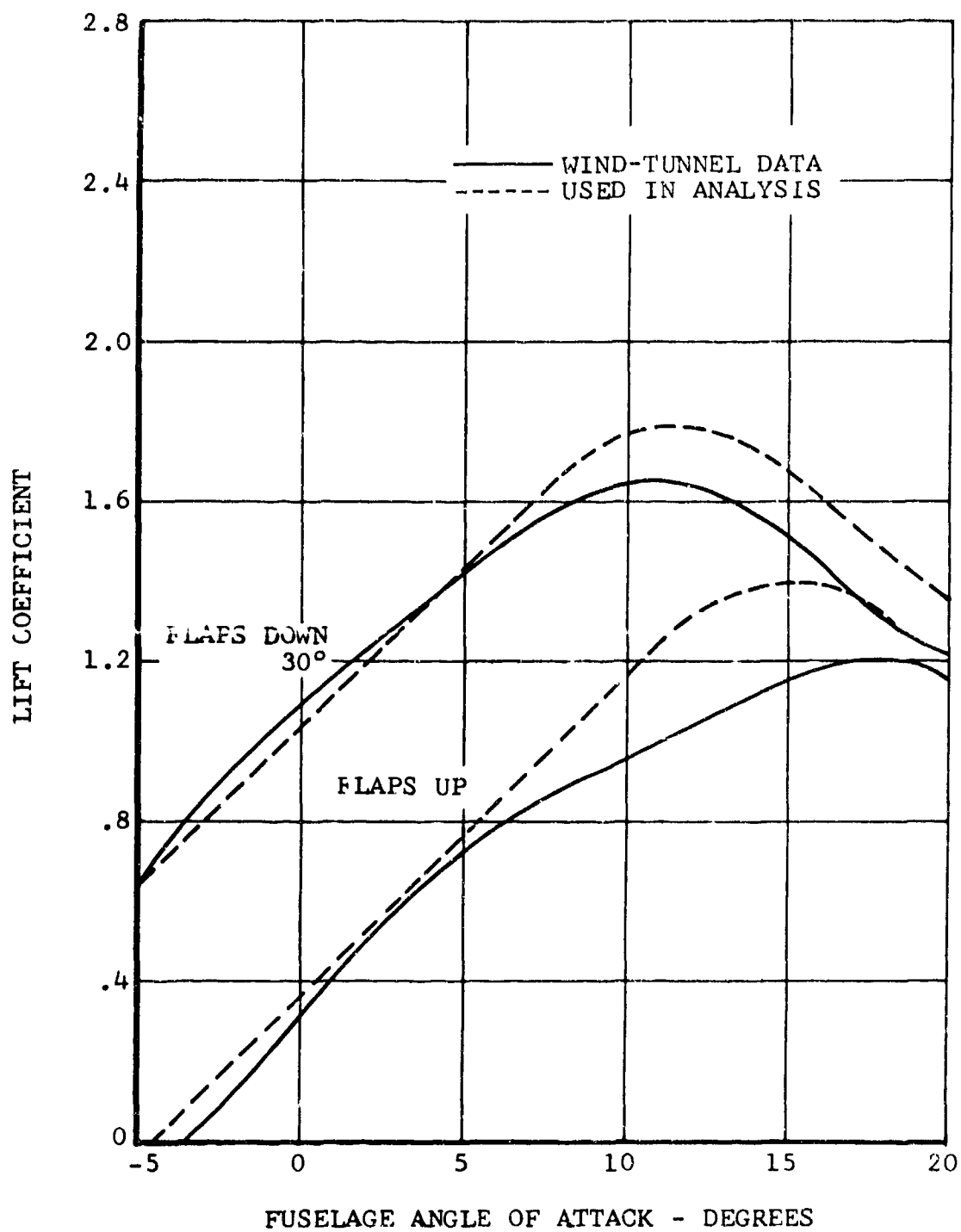


Figure 223. Fixed-Wing Lift Coefficient.

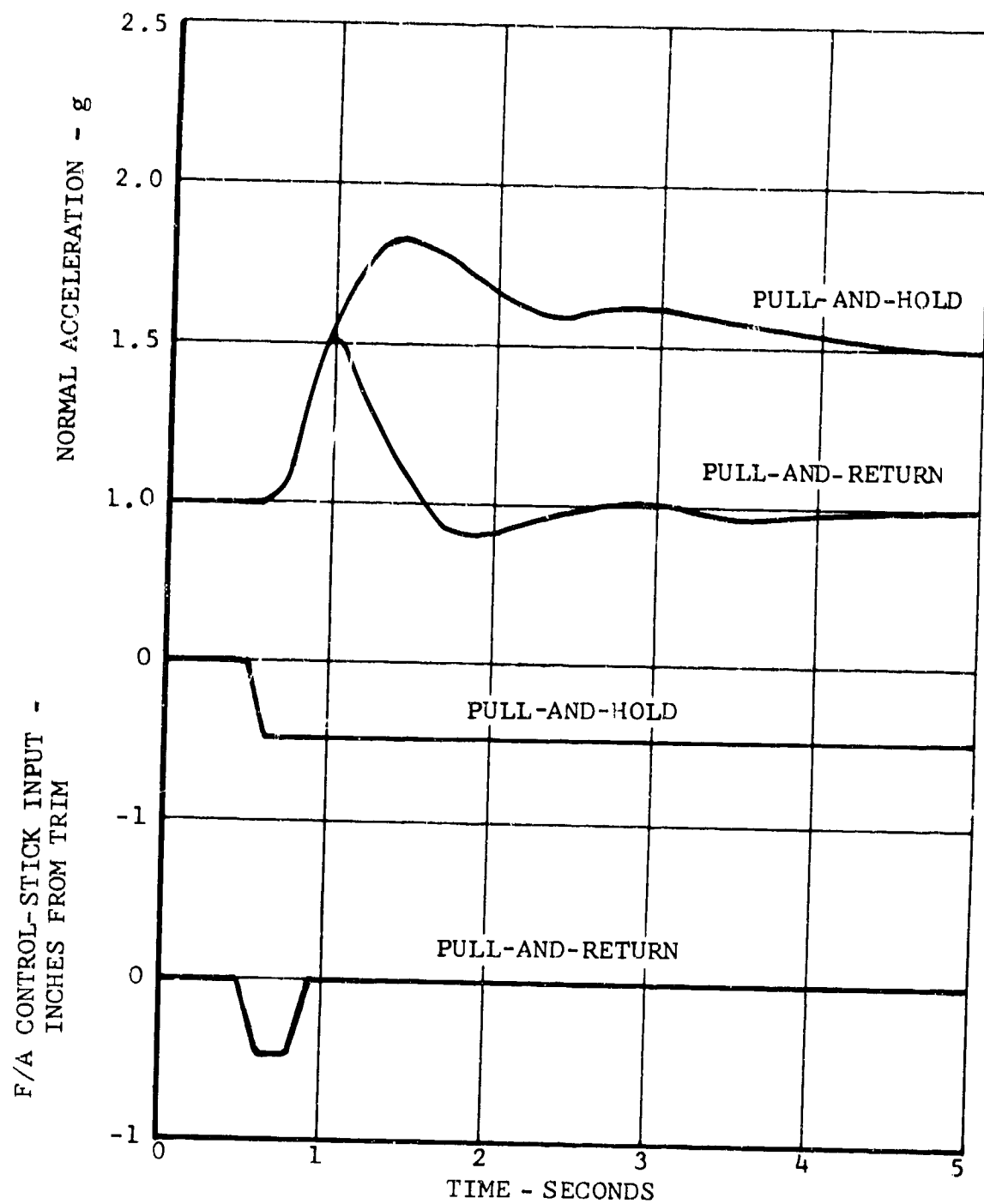


Figure 224. Time History of Normal Accelerations for a Pull-and-Hold and a Pull-and-Return at 250 Knots.

The ailerons extend from $0.55 \frac{b}{2}$ to $0.915 \frac{b}{2}$ and are 25 percent of the wing chord. The deflection range varies with flap setting. For this aileron configuration, Figure 18 of Reference 32 gives the effective change in wing-section angle of attack for a unit change in the aileron deflection to be $\frac{da}{d\delta_a} = 0.53$ for a sealed aileron. A wingtip helix-angle parameter γ' is defined in Reference 33 such that

$$C_{l_{\delta_a}} = \gamma' \frac{da}{d\delta_a} (C_{l_p})_w \quad (6)$$

This is the value of the change in rolling moment coefficient for a total aileron deflection of both the right ailerons of $\Delta\delta_a$ degrees. The equation can also be shown to give the relationship of Equation 2 of Reference 33, which is

$$\frac{pb}{2V} = \gamma' \frac{da}{d\delta_a} \Delta\delta_a \quad (7)$$

Since this equation takes into account only the wing contribution to C_{l_p} , it is necessary to correct the parameter γ' when making an analysis of the entire aircraft. The effective value is

$$\gamma'_{\text{eff}} = \gamma' \frac{(C_{l_p})_{\text{WING}}}{(C_{l_p})_{\text{TOTAL}}} \quad (8)$$

Substituting in Equation 2, we find that

$$\frac{pb}{2V} = \gamma'_{\text{eff}} \left(\frac{da}{d\delta_a} \right) \Delta\delta_a \quad (9)$$

It is necessary to make a correction for large aileron deflections to the value of $pb/2V$ by a factor K , shown in Figure 9-16 of Reference 34. The value of γ' used for the D266 is 0.0072 per degree as determined by Figure 2 of Reference 33. Using this value of γ' and calculating the ratio $(C_{l_p})_w / (C_{l_p})_{\text{total}}$, we determined the deflection per aileron that is required to develop a steady roll rate. The results are shown in Figure 225. In the case of the flaps-down configuration, the value $pb/2V$ is shown for the deflection of the up-going aileron, δ_{au} .

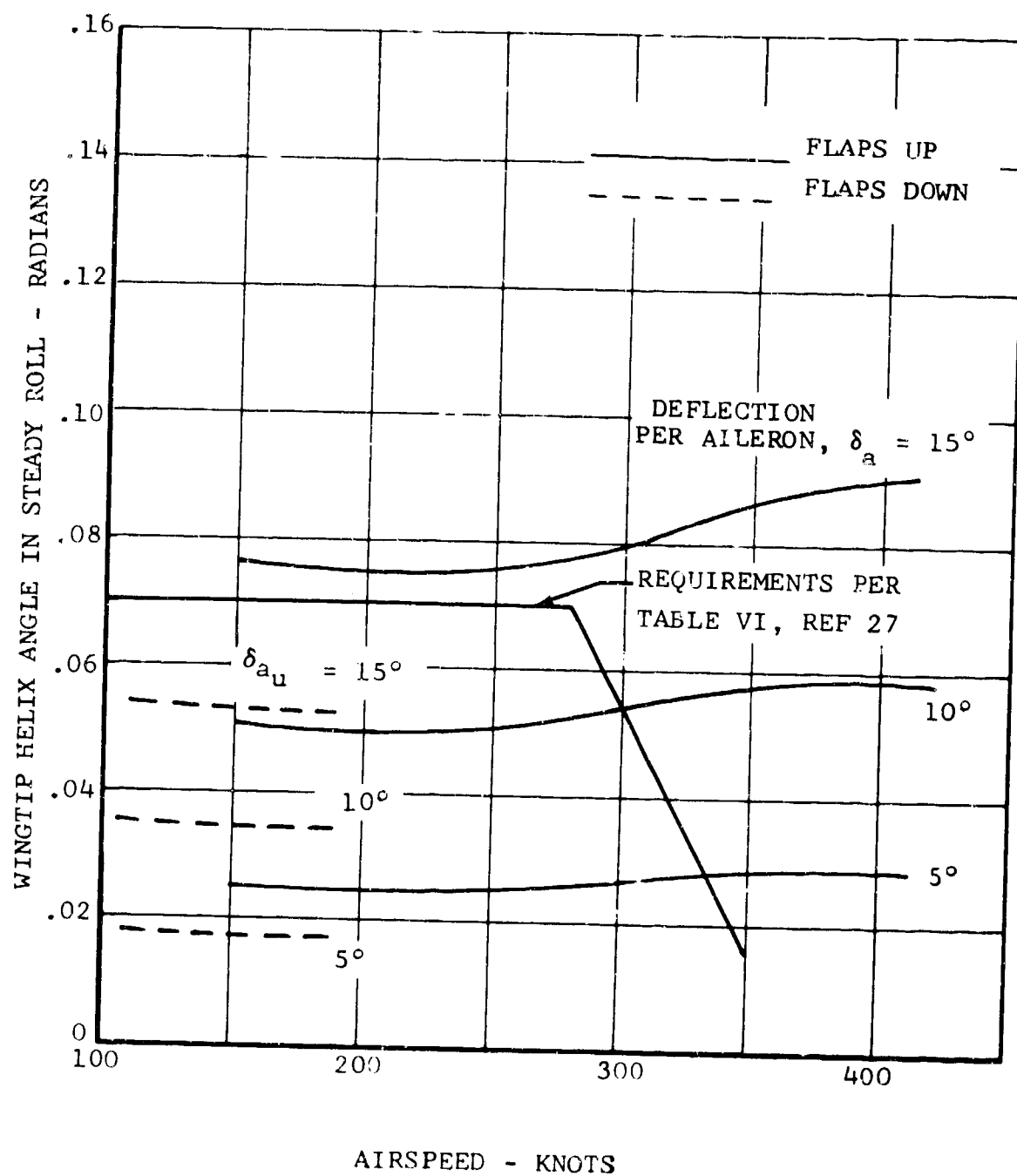


Figure 225. Steady Roll Rate Performance.

With flaps up, the D266 can meet the steady roll requirements at all speeds. With flaps lowered 30 degrees, the steady roll performance at low speeds is less than the desired levels specified in Table VI of Reference 27. It is believed that the requirements at the low speeds are intended to insure sufficient roll performance when landing conventional aircraft. The D266 lands and takes off in the helicopter mode where roll-control power is high.

(2) Roll-Acceleration Capability

Paragraph 3.4.16.2 of Reference 27 specifies that the roll-acceleration capability must be such that the roll rates, specified in Table VI of Reference 27, can be reached within $(0.5 + \frac{b}{100})$ seconds. For the D266, this time is 0.97 second.

The roll acceleration was investigated by introducing lateral stick displacements at 150, 280, and 350 knots and by computing the response with C81. Time histories of the resulting roll and sideslip responses are shown in Figures 226 to 228, respectively. The roll rate attained is 0.97 second, measured and ratioed to full-lateral control by assuming linear aerodynamics. The following pb/2V values are obtained:

- 0.0235 at 150 knots
- 0.0535 at 280 knots
- 0.0525 at 350 knots

The value at 350 knots exceeds the required value of 0.015. The accelerations at the lower speeds are below the required values. The 150-knot value is 34 percent of the required value; however, the requirement is largely based on the necessity for rapid roll response of conventional aircraft during landing and takeoff maneuvers. The D266 will be operating in helicopter mode for these maneuvers, and roll-control power will be considerably increased.

c. Lateral Control in Sideslips

The stick displacement required at different trimmed sideslip angles is shown in Figure 229 for speeds of 150, 250, and 350 knots. These stick positions and the lateral stick-force gradients were used to calculate the forces associated with these displacements.

2. STATIC STABILITY

a. Longitudinal

The stick-fixed neutral point for the D266 was calculated using Equation 5-35 of Reference 34, which was modified to include the

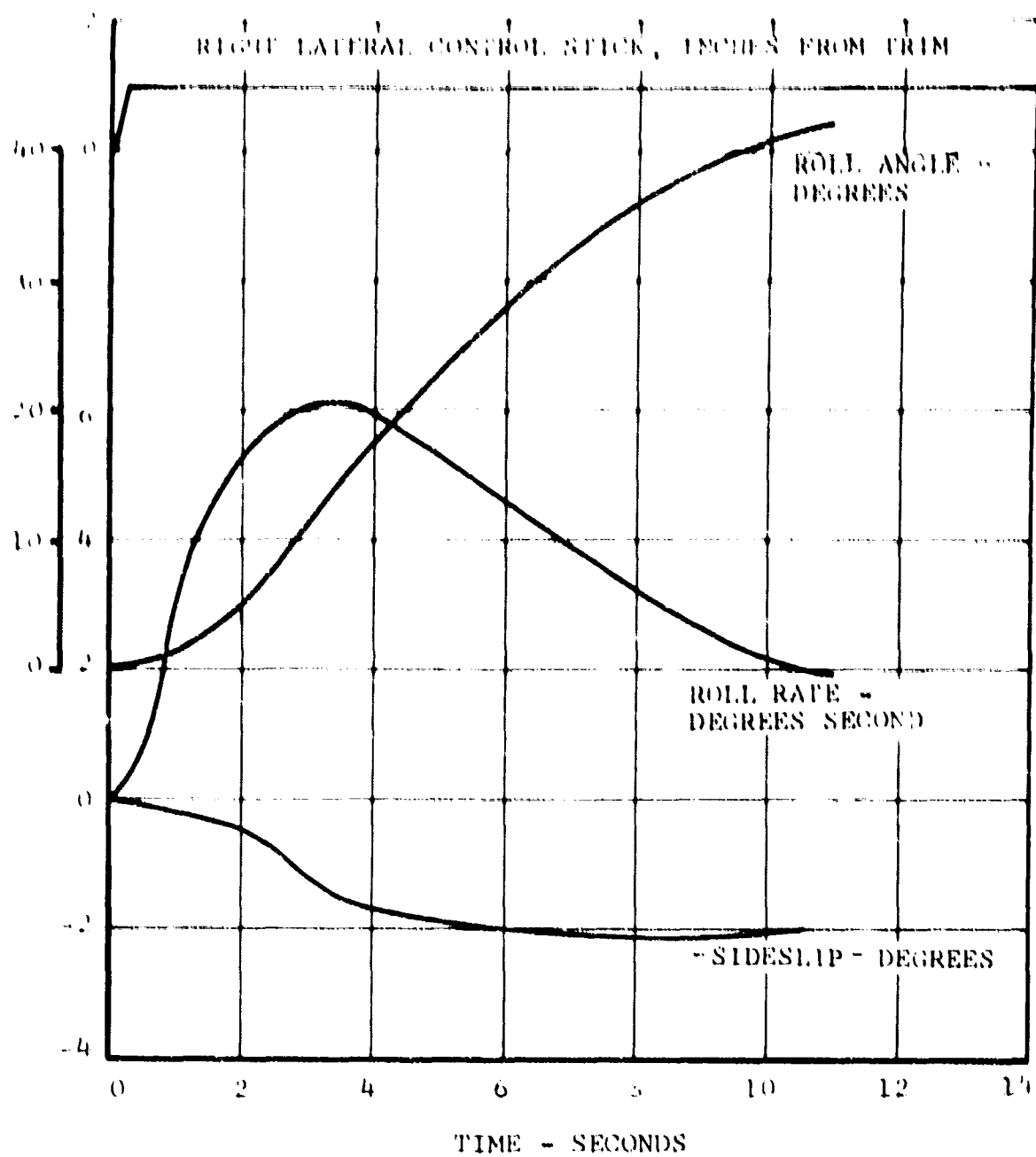


Figure 226. Roll and Yaw Response to Lateral Control Stick In, t at 150 Knots.

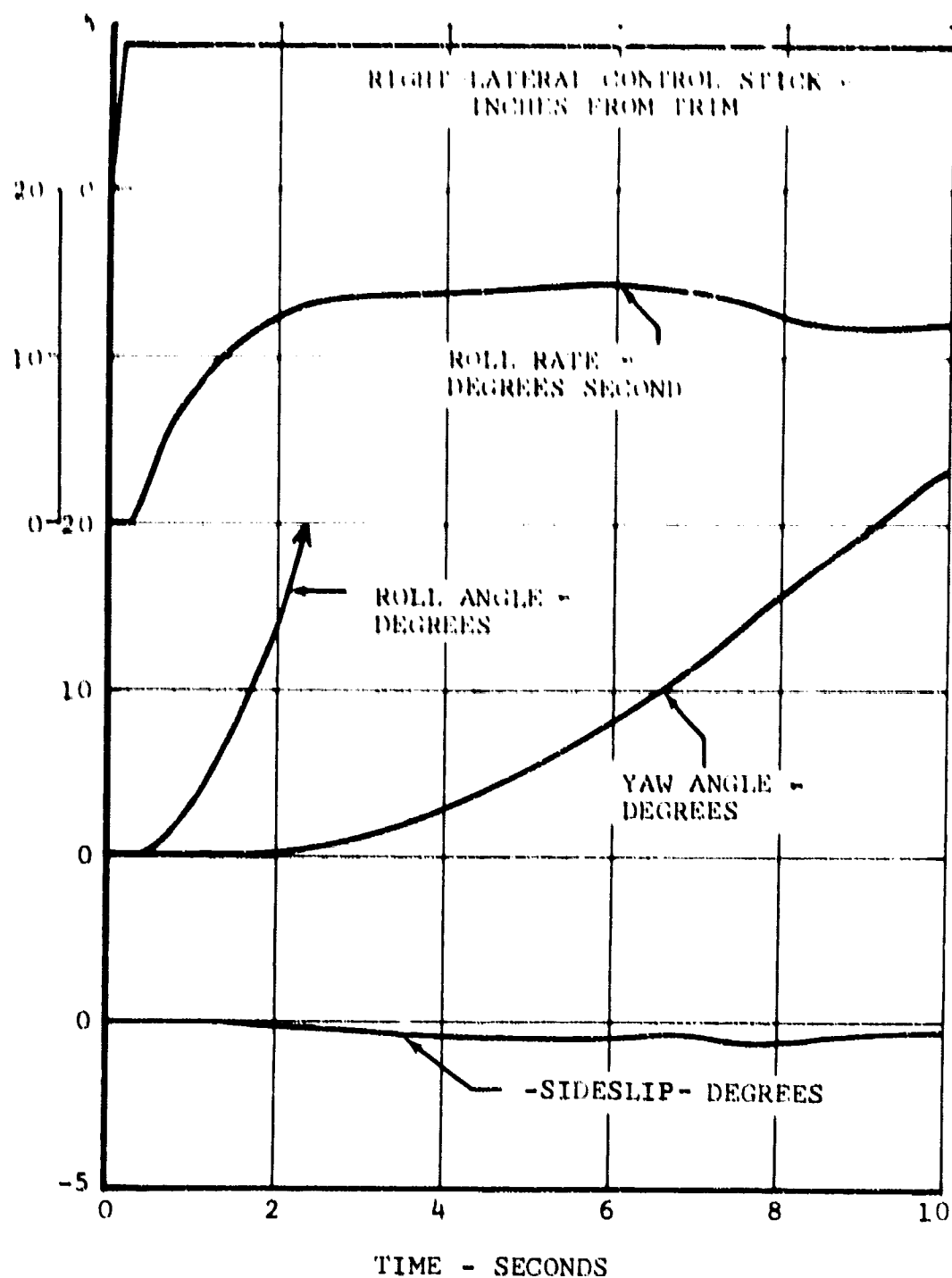


Figure 227. Roll and Yaw Response to Lateral Control Stick Input at 280 Knots ($0.8 V_H$).

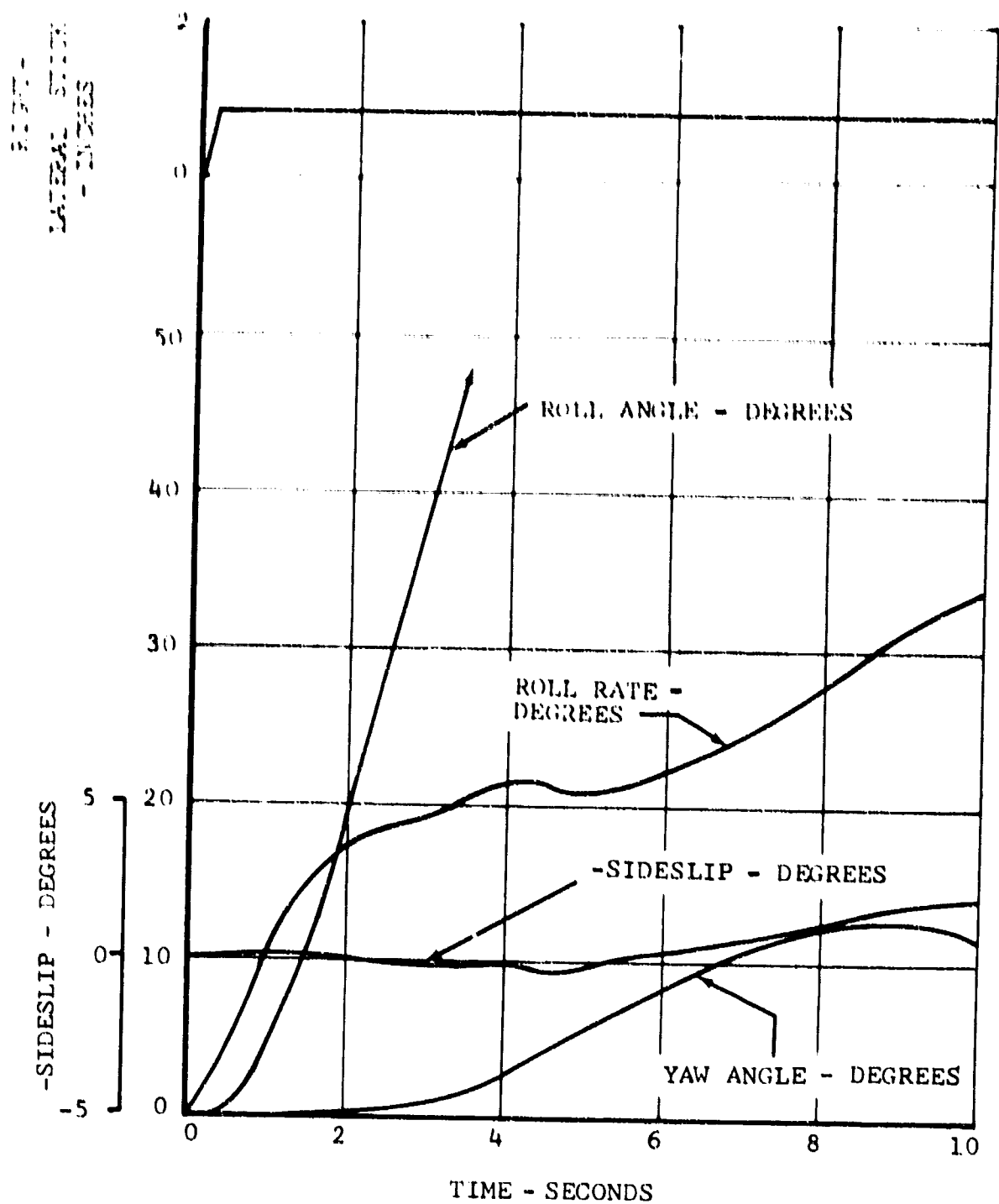


Figure 228. Roll and Yaw Response to Lateral Control Stick Input at 350 Knots.

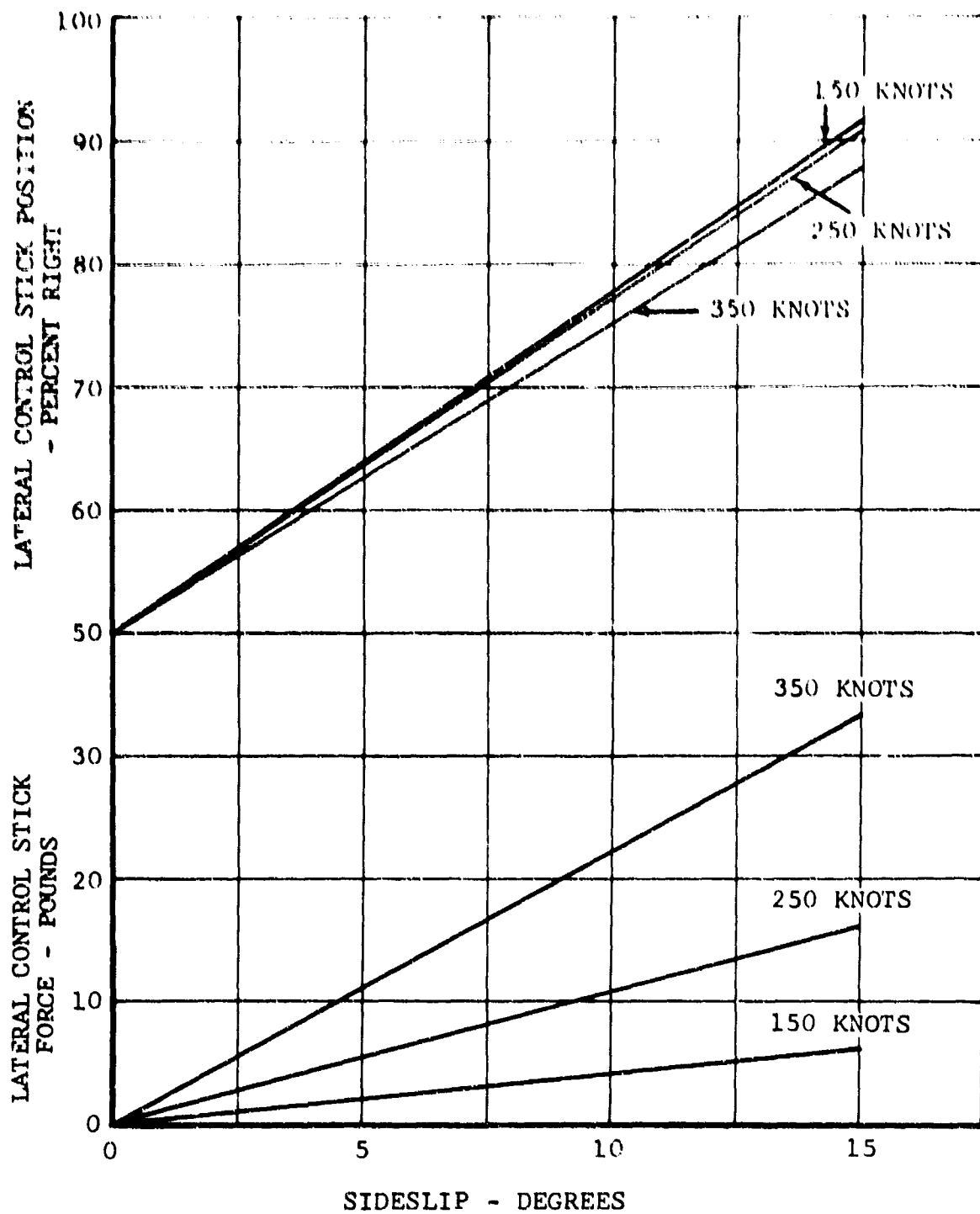


Figure 229. Lateral Control Displacement and Stick Force in Sideslips.

effects of the rotors. These data show that the neutral point is aft of the most rearward allowable cg position by a margin of 18.5 percent. Therefore, the longitudinal static stability with respect to the lift coefficient or angle of attack at constant speed is positive for all flight conditions. The elevator-free static stability will be the same as the elevator-fixed stability, because the boosted control system does not permit control surface loads to feed back to the pilot stick control.

Throughout the speed range in fixed-wing flight, a rearward stick movement will generate a nose-up pitching moment, which in turn result in the initiation of a climb and a decrease in speed. A maneuver was run on C81 to get a quantitative feeling for the change in trim speed due to a stick position change. A stick ramp input of -0.2 inch was applied over a period of 10 seconds from an initial level-flight cruise at 250 knots with the most aft cg. The speed along the flight path decreased from 250 knots to a steady 210 knots after 27 seconds. A time history of the speed during the above maneuver is shown in Figure 230. An aft-stick force of about 2 pounds is required to maintain the -0.2-inch stick displacement throughout the pullup.

b. Lateral-Directional

The D266 will possess directional static stability and desirable dihedral and side-force characteristics, as determined by wind-tunnel data which have been modified to reflect final configuration changes. The wind-tunnel tests indicated that the aircraft was neutrally stable in yaw with the smaller stabilizer, at the small angles of sideslip, but the aircraft became more stable at angles larger than about 8 degrees. This trend is shown in Figure 231, which shows the yawing moment coefficient of the wind-tunnel model as a function of the sideslip angle. The increase in directional stability at angles of sideslip larger than 8 degrees indicates that the sidewash factor and dynamic pressure reduction adversely affect the fin effectiveness at small sideslip angles. The D266 fin area is 54 percent larger than the fin used in the wind-tunnel tests in order to improve the directional stability. Most of the added area came about through an increase in the span of the fin, so that the sidewash factor and dynamic pressure reduction, near the fuselage, will affect a smaller percentage of the fin area.

The rudder deflection was calculated for steady sideslips at speeds of 150, 250, and 350 knots. The pedal positions associated with these rudder deflections are shown in Figure 232. That figure indicates that the D266 has the capability of developing a 10-degree sideslip, as required by paragraph 3.4.11.1 of Reference 27.

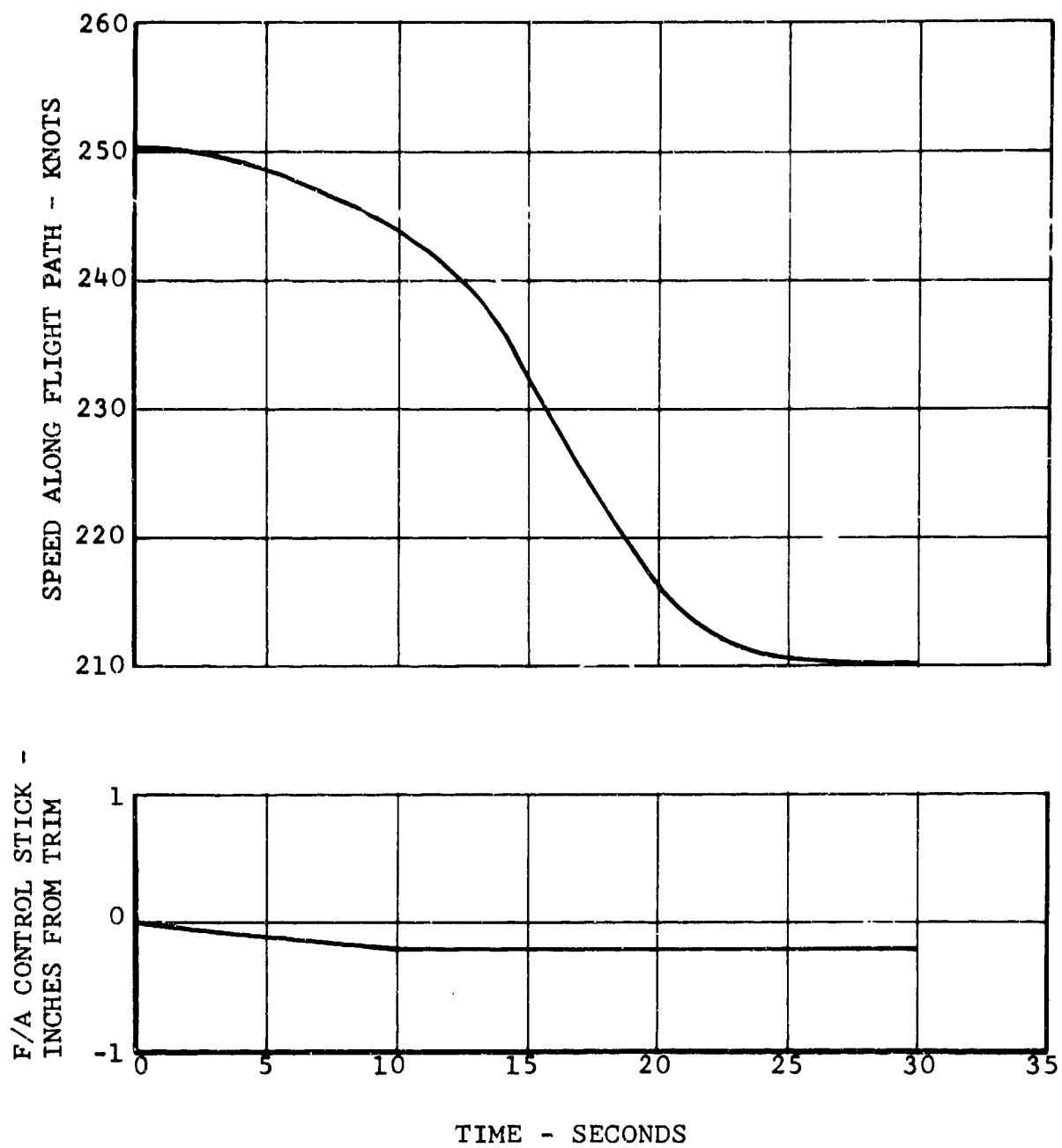


Figure 230. Time History of Speed Reduction Due to Aft Stick Displacement.

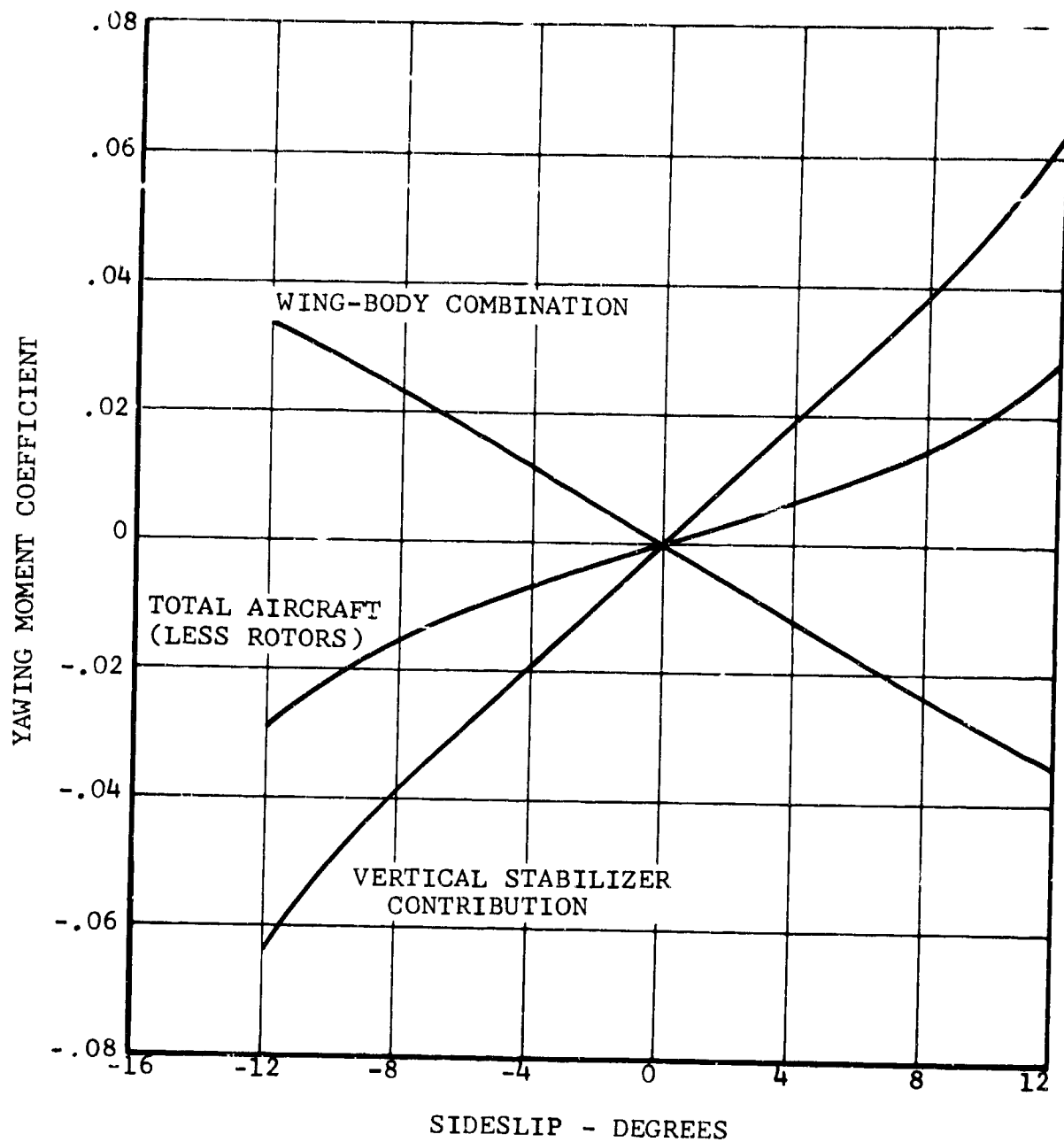


Figure 231. Yawing Moment Coefficient in Sideslips.

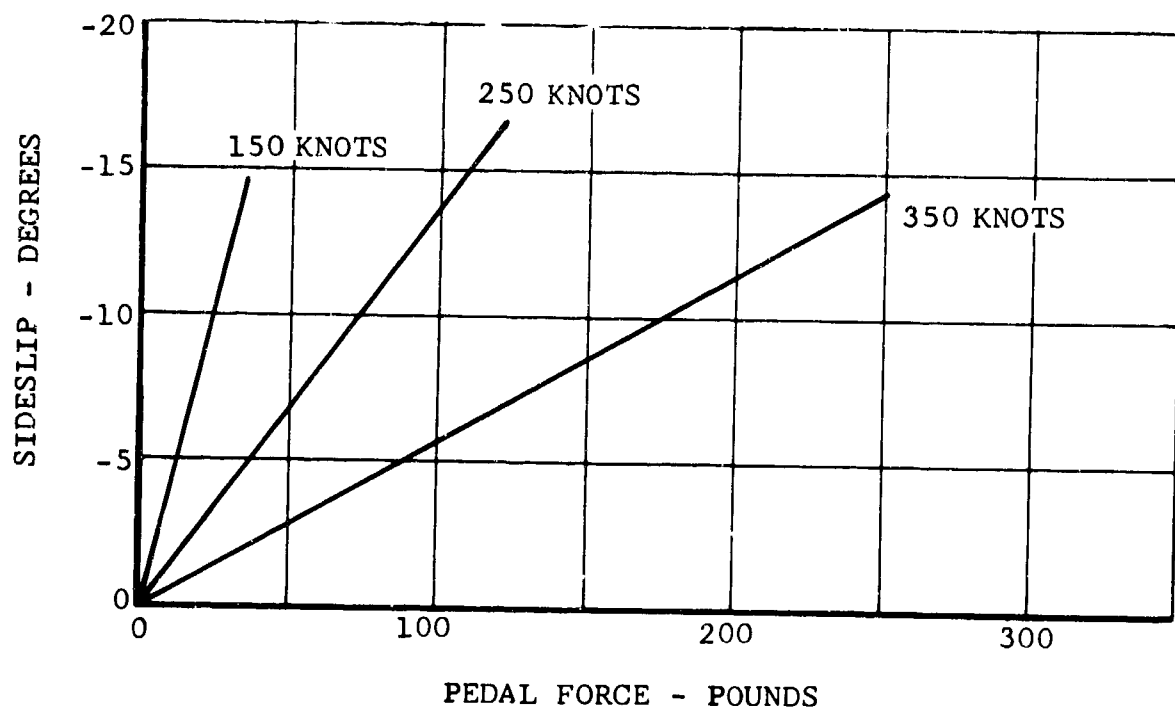
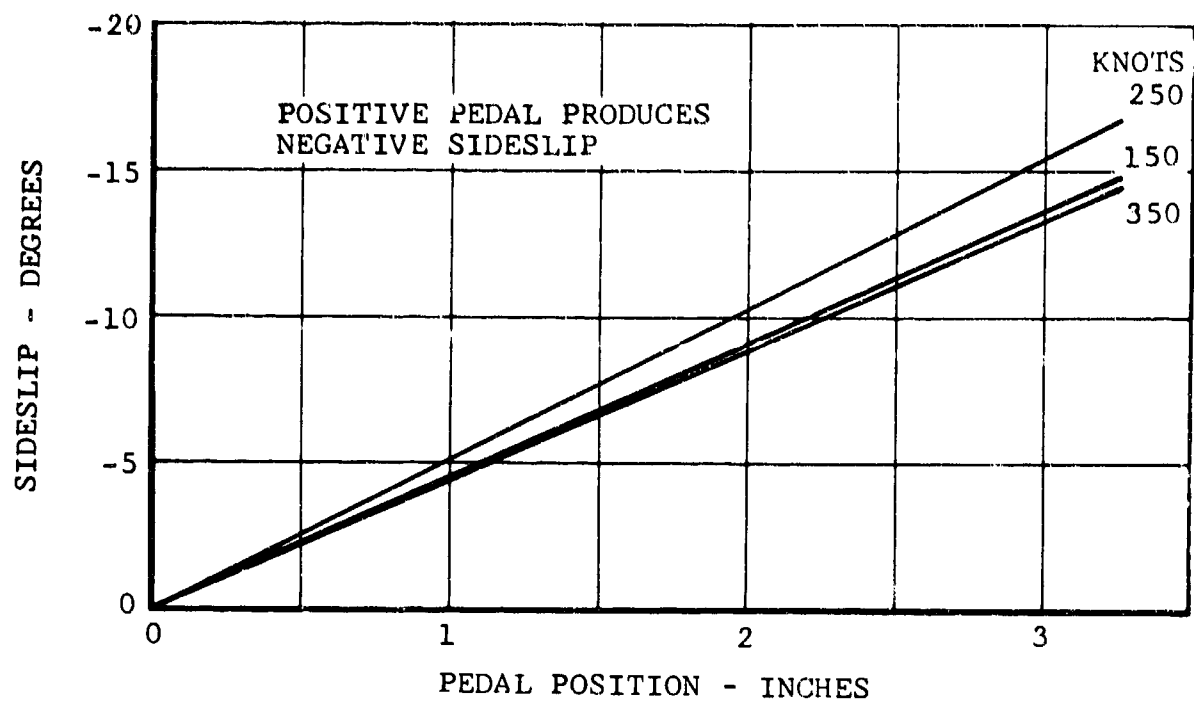


Figure 232. Pedal Displacement and Pedal Force in Sideslips.

The D266 will have a large, positive, effective dihedral. The high wing location, the tall vertical fin, the positive wing dihedral angle, and the rotor forces all contribute to this high value. Wind-tunnel data agree well with the calculations made using the appendix of Reference 35.

3. DYNAMIC STABILITY

Longitudinal and lateral-directional modes of motion are investigated separately in the conventional manner. The short-period motion was found to be heavily damped. The phugoid and lateral-directional modes are stable, well above the requirements of Reference 27. The calculations indicate the spiral mode to be damped.

a. Longitudinal

Dynamic stability was calculated by linearized theory and compared with the results from the digital computer maneuver Program C81.

The time history of short-period longitudinal oscillation is shown in Figure 233. Figure 234 compares the short-period-mode characteristics, as obtained from rigid-body analysis, with the case of flexible blades and changed rotor aerodynamic forces and the case of rigid blades and flexible pylons. Due to the swashplate-pylon coupling linkage, a higher damping is obtained in the case of the flexible pylon, whereas a destabilizing effect is indicated when only blade flexibility is considered. It is seen that the requirement of Reference 27 to damp the short-period mode to one-tenth amplitude in less than one cycle is met. There is no specific requirement for the long period when it is longer than 15 seconds. The period is considerably longer and the mode is stable.

b. Lateral-Directional

The equations used to investigate the lateral-directional dynamics were obtained from chapters 4 and 7 of Reference 35. The solution was obtained in the same manner as for the longitudinal case and yielded one pair of complex roots associated with the Dutch-roll oscillation and two real roots associated with the rolling motion and spiral mode.

Time histories as obtained from the computer program C81, for lateral and directional step inputs at 350 knots, are shown in Figures 228 and 235.

D. CONVERSION FLIGHT

There are no current military specifications that define flying qualities requirements in the conversion flight regime;

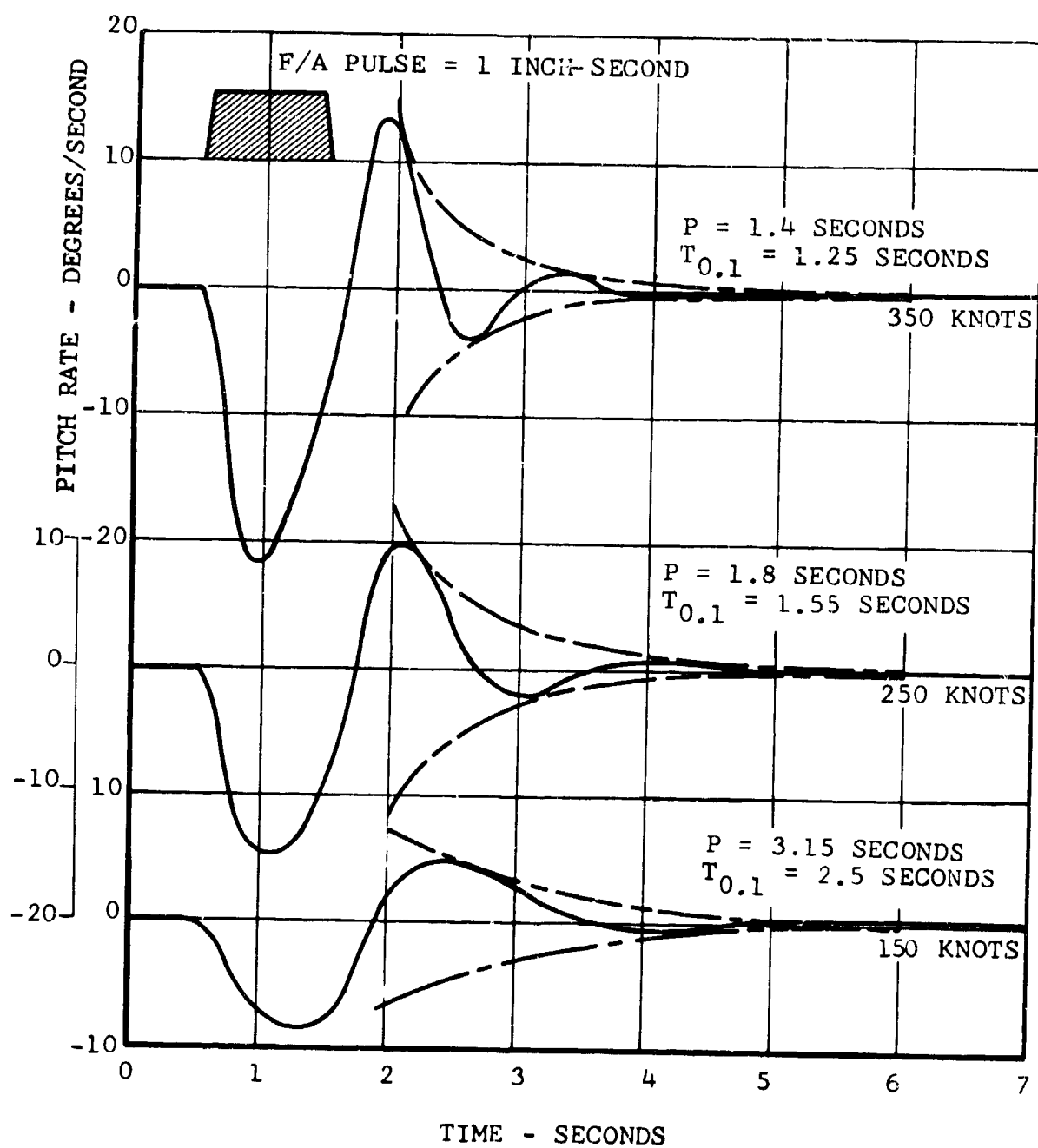


Figure 233. Time History of Short-Period Longitudinal Oscillation.

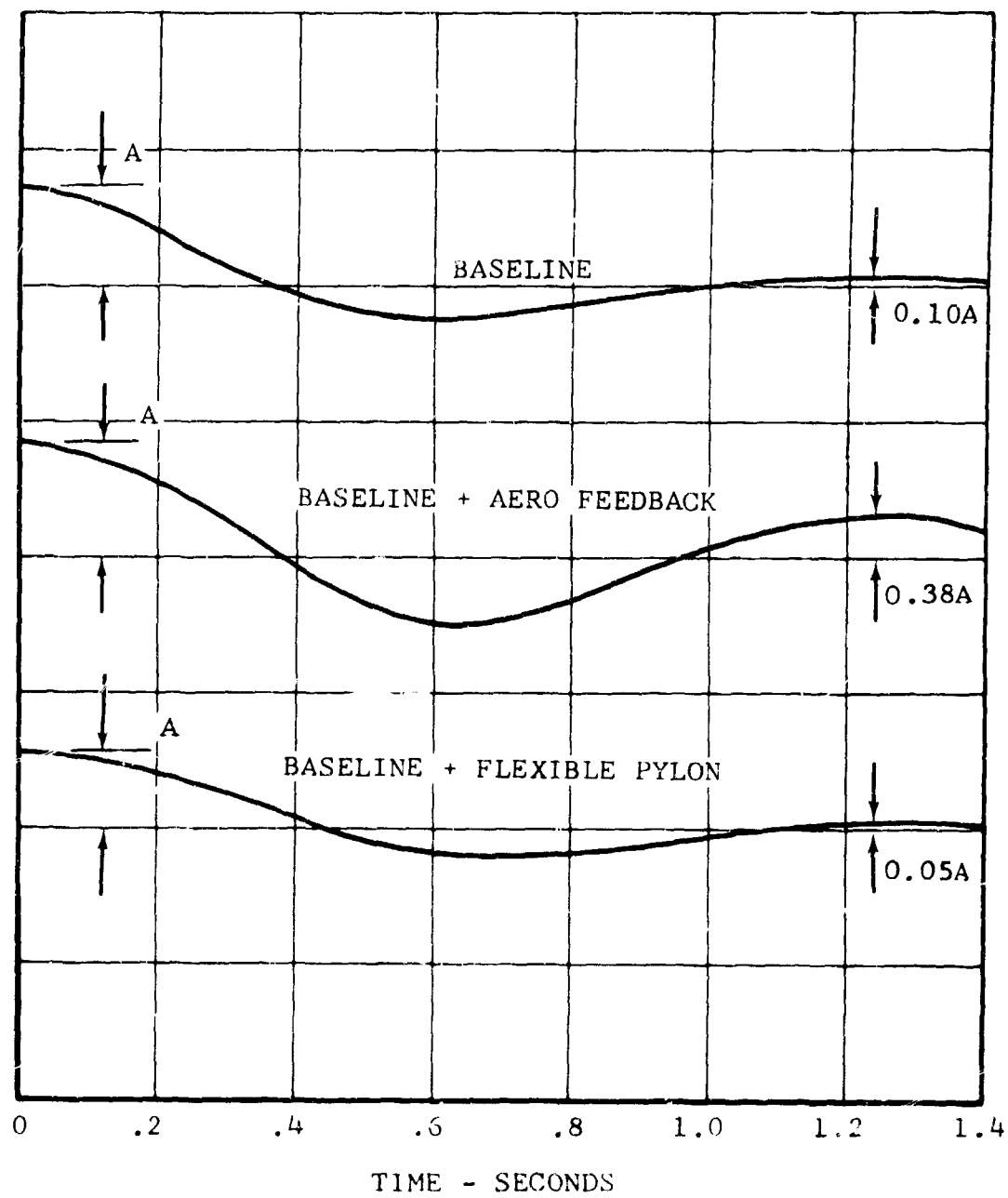


Figure 234. Longitudinal Short-Period Damping at 350 Knots.

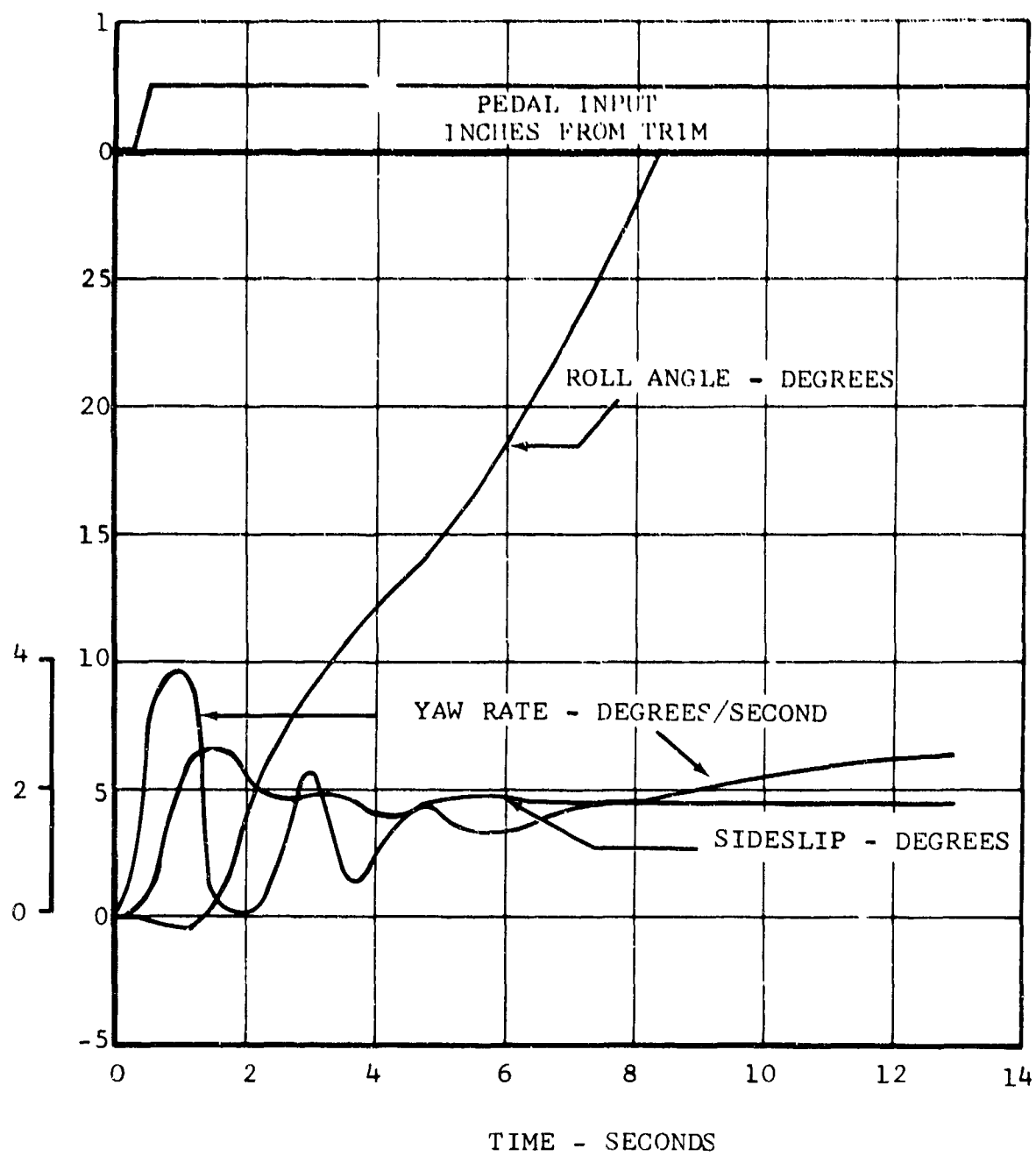


Figure 235. Roll and Yaw Response to Pedal Input at 350 Knots.

therefore, the recommendations of References 24 and 25 are used as guides. The contract schedule states that "there shall be no discontinuities in stability and control characteristics during transition from vertical lifting device to cruise lifting device and vice versa," and that the aircraft will be capable of "transition from vertical lifting device to cruise lifting device and vice versa, at constant altitude. Continued flight shall be possible with no abnormal stability and control gradients and shall be possible at any conversion configuration. Conversion shall be reversible at any point in transition." These characteristics have been achieved in the D266 design.

The difficulty in analyzing the conversion condition by conventional equations made it desirable to utilize the unique capabilities of the Bell Helicopter Company Computer Program C81 to determine the D266 characteristics. Since good agreement between C81 results and conventional analyses has been obtained for the other two modes of flight for the D266 and in numerous helicopter configuration studies conducted in the past, the conversion characteristics determined herein are believed to be valid.

1. CONVERSION FLEXIBILITY

The wide range of airspeed in which the D266 can make partial or full conversions is shown in Figure 236. Normally, conversions would be made in the area between the maneuver margin line and the line indicating reduced-life loads. The lower value of the upper speed limits is established by the endurance stress level of the rotor components and defines the speed and conversion angles where continuous flight operation is permissible. There are two sets of lower speed-limit lines shown in the figure; one shows 1.0g (stall) and 1.3g capability for the flaps-up condition; the other set shows the same information for the 30-degree flaps-down condition. Flaps are normally used for conversion and reconversion. Flight can be maintained, within the conversion corridor, with no limits of control or stability being encountered.

Several conversions have been performed with Program C81 to obtain time histories of control motions during steady level-flight conversions. Figure 237 shows a time history of a conversion from helicopter to fixed-wing mode at a speed of 120 knots. Figure 238 shows a conversion from fixed-wing to helicopter mode while holding speed and altitude. As seen from the figure, altitude and airspeed changes are negligible, rotor speed remains constant, and only small stick movements are required.

To demonstrate the simplicity of stopping and reversing the conversion procedure, Figure 239 shows a time history of a

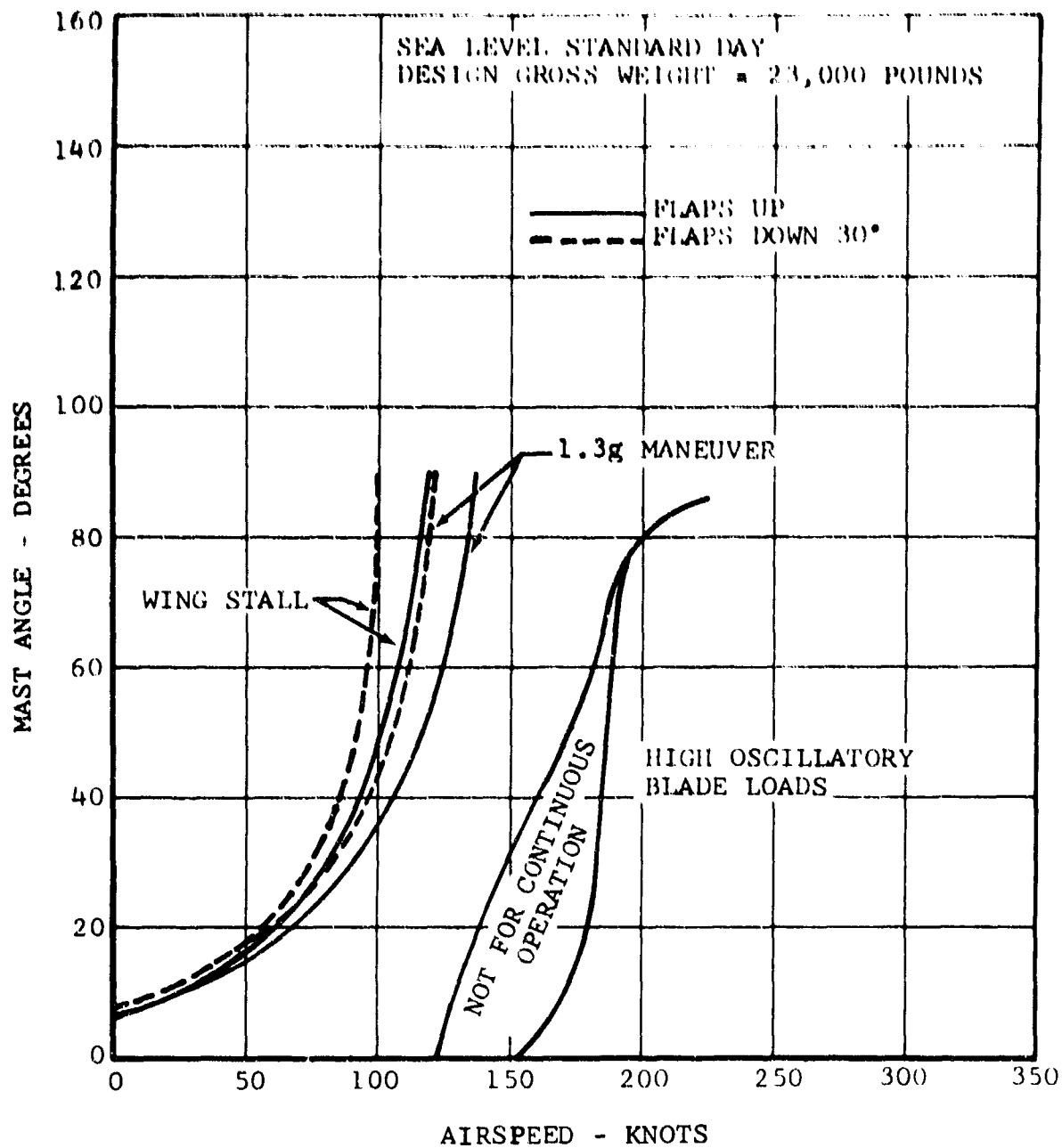


Figure 236. Conversion Corridor.

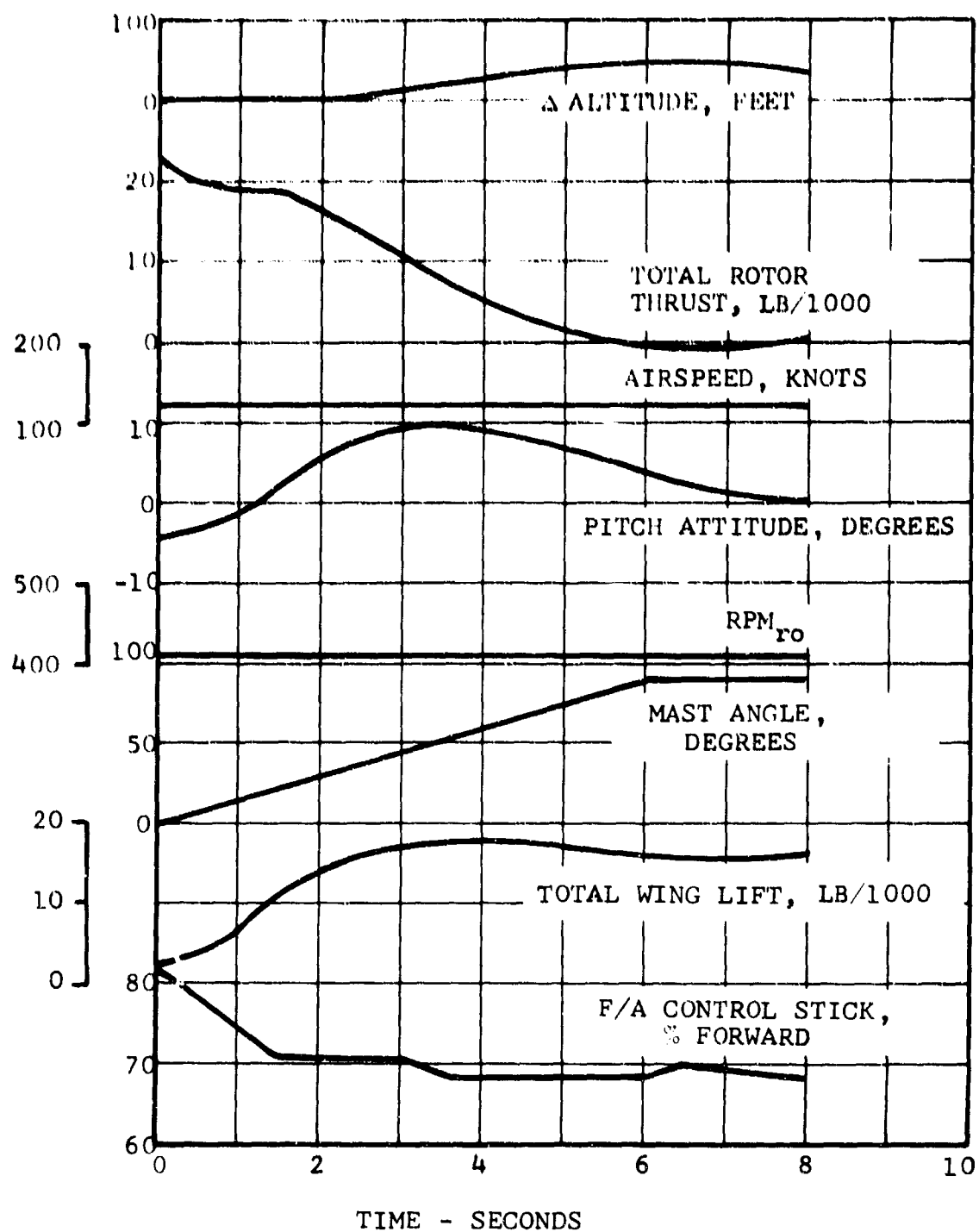


Figure 237. Conversion Time History to Fixed-Wing Mode at 120 Knots.

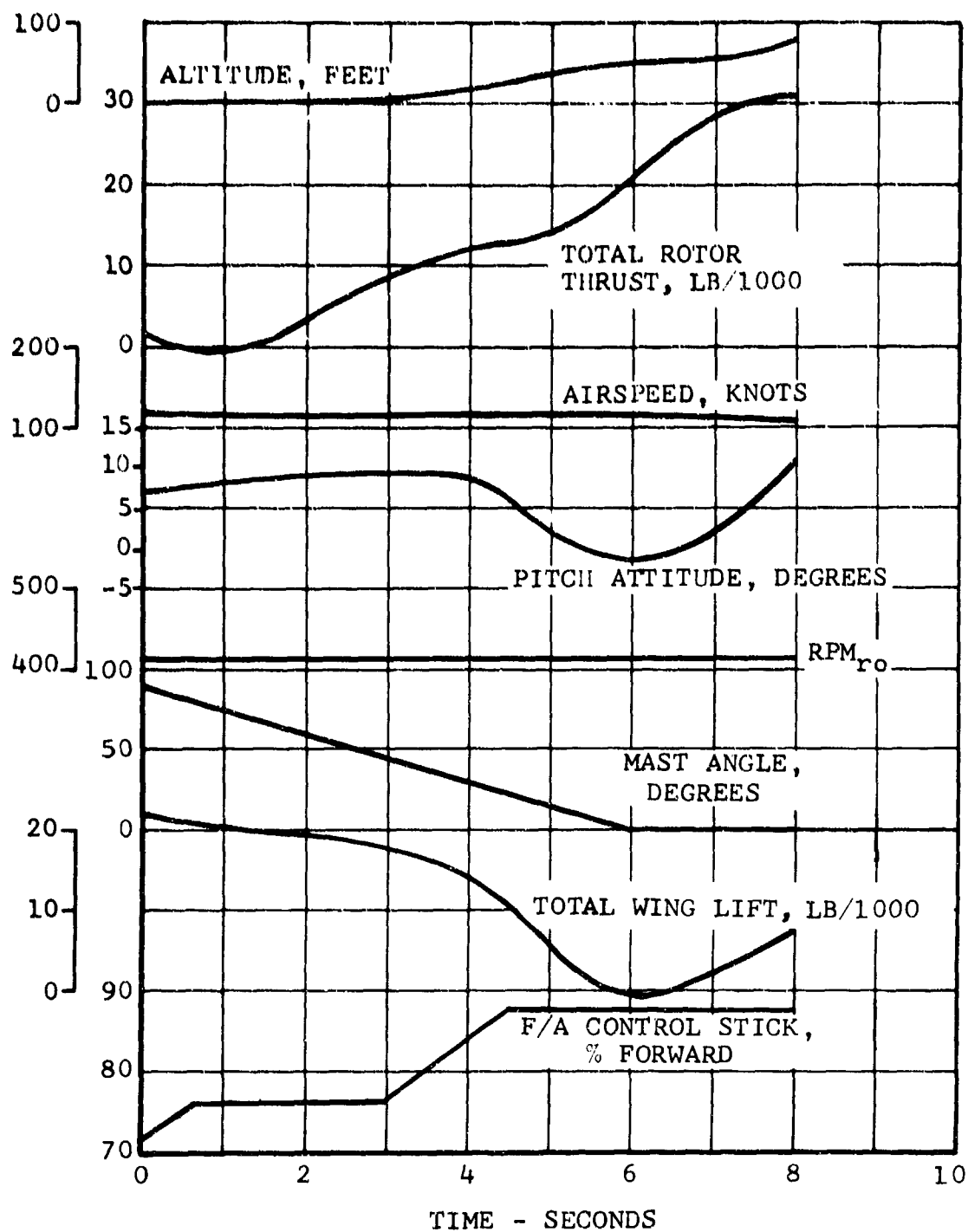


Figure 238. Conversion Time History to Helicopter Mode at 120 Knots.

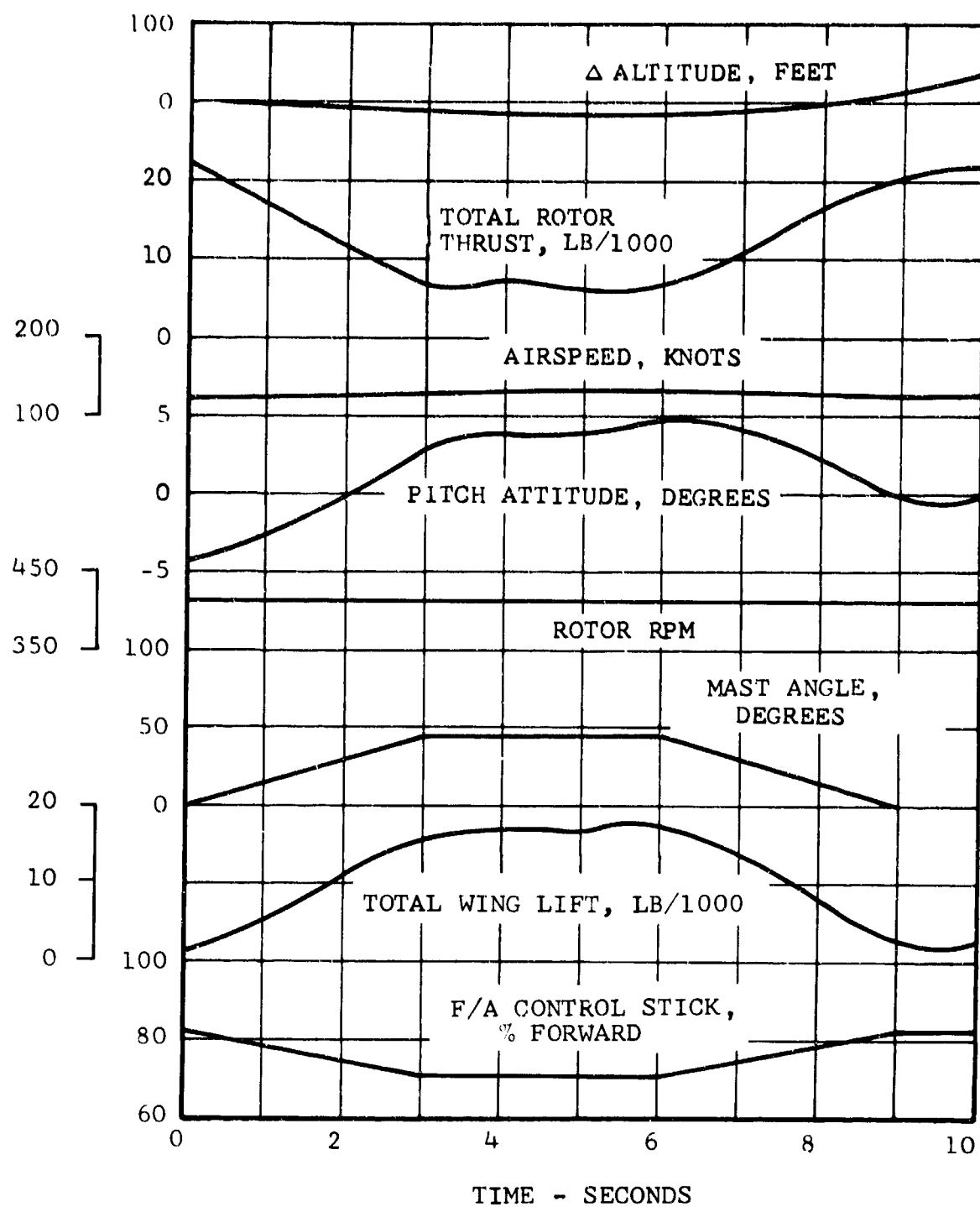


Figure 239. Time History of Conversion to 45 Degrees and Abort.

conversion that was aborted at 45 degrees. Again, there is negligible change in altitude and airspeed, and no excessive stick motion is required.

Since the D266 configuration is similar to that of the XV-3, some pilot comments concerning the XV-3 conversion characteristics are presented for information. In Reference 30 (p. 24), it is stated that: "One outstanding feature of the XV-3 was that conversions and reconversions could be made, either in 'beeped' steps or continuously from any flight condition." Also, "From a safety standpoint, a schedule of airspeed, altitude, mast angle, fuselage angle, wing stall, flap position, power setting or trim position was not required at any time during conversion or reconversion." It should be noted that the XV-3 was converted and reconverted in the following ways: holding altitude, holding airspeed, during a standard rate turn, during a climb, during autorotation, and at altitudes of 600 and 10,000 feet. The present analysis indicates that similar characteristics will be exhibited by the D266.

2. STATIC TRIM

Program C81 was used to obtain static trim data in the conversion region. Cases were run for several mast-angle settings at airspeeds of 90, 120, and 150 knots and at forward and aft center-of-gravity positions. From these data, three cases that exhibit the greatest control motion have been selected for the illustration of control stick position and other pertinent parameters. Figure 240 shows 90-knot cases at forward cg with flaps up and with 30 degrees of down flap. The breaks in the curves between 30 and 40 degrees of mast angle are due to wing stall in the flaps-up condition. Trim at mast angles beyond 40 degrees could not be maintained, due to wing stall.

Figure 241 shows a 120-knot case at aft cg with flaps up. Trimmed level flight was attainable here throughout the mast-angle range. Figure 242 shows data throughout the mast-angle range at 150 knots, with flaps up and the cg forward. The variation in trim-control position is small and gradual.

Pedal position and lateral stick position versus sideslip angle are computed at a mast angle of 30 degrees and are shown on Figure 243. Stable gradients are exhibited for both the pedal and the lateral stick.

3. DYNAMIC STABILITY

The D266 is designed to be inherently stable in all regimes of forward flight above 60 knots, including conversion. The stability augmentation system is incorporated as a pilot aid and is not required for stability. To demonstrate D266 stability,

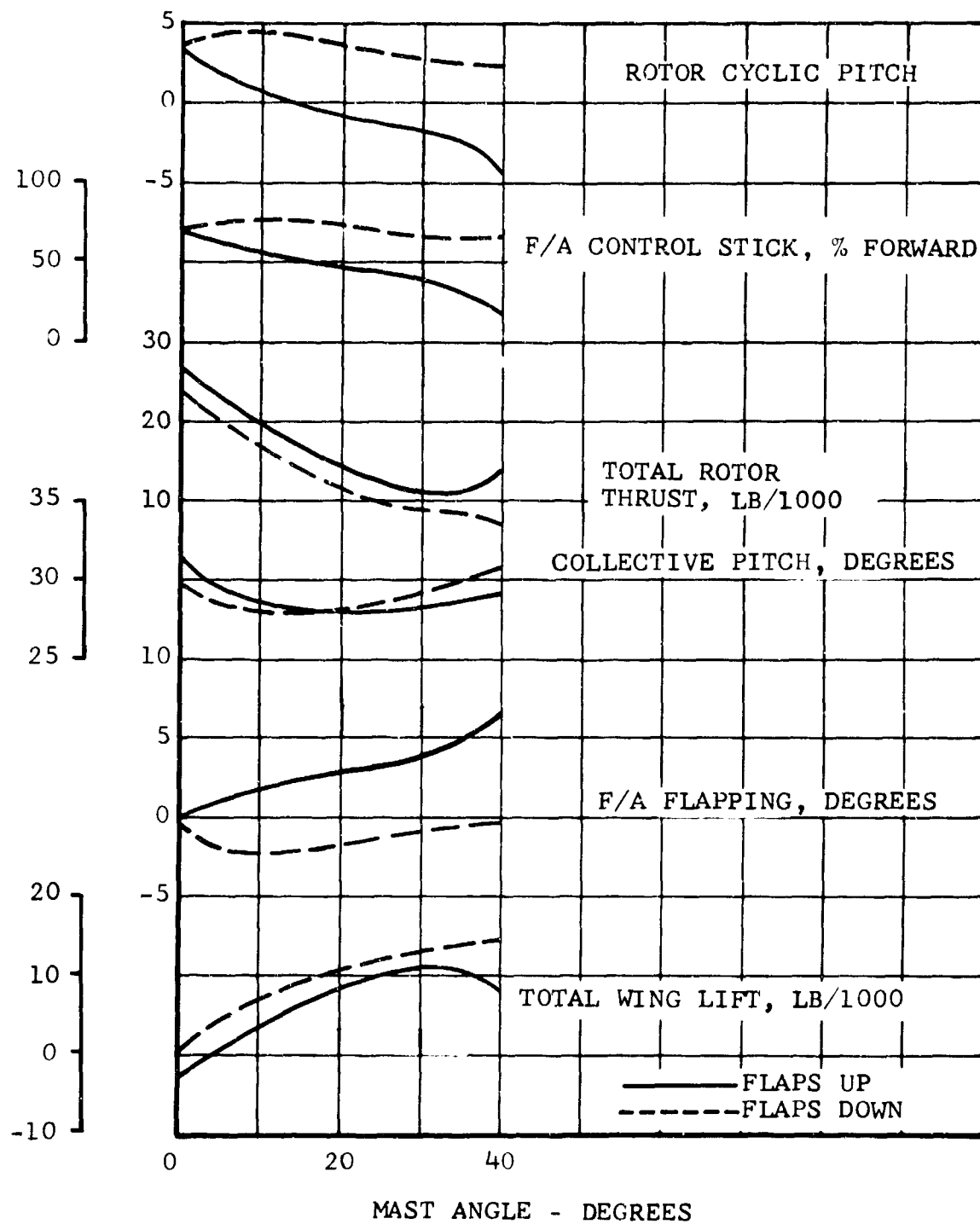


Figure 240. Static Trim at Partial Mast Angles - 90 Knots.

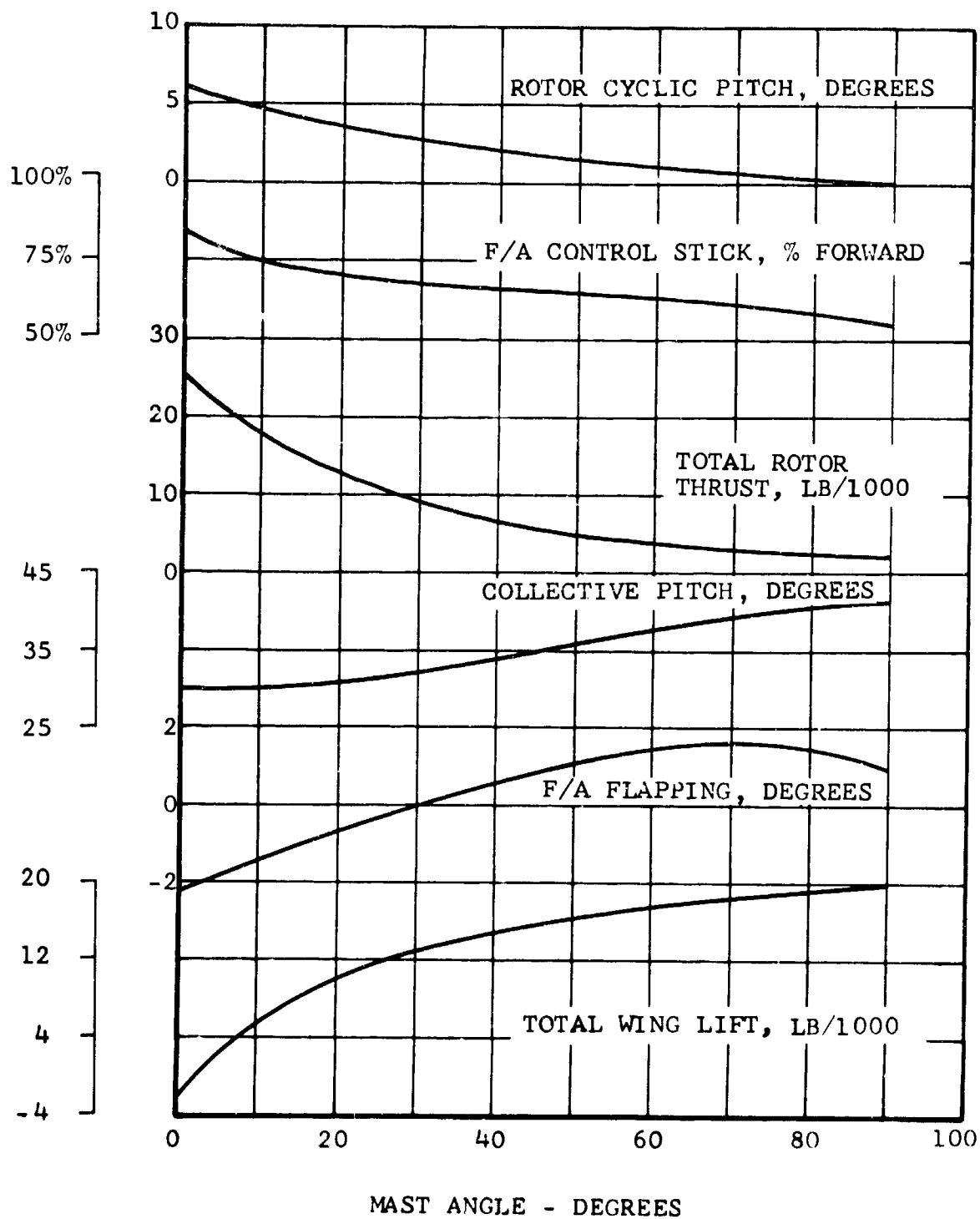


Figure 241. Static Trim at Partial Mast Angles - 120 Knots.

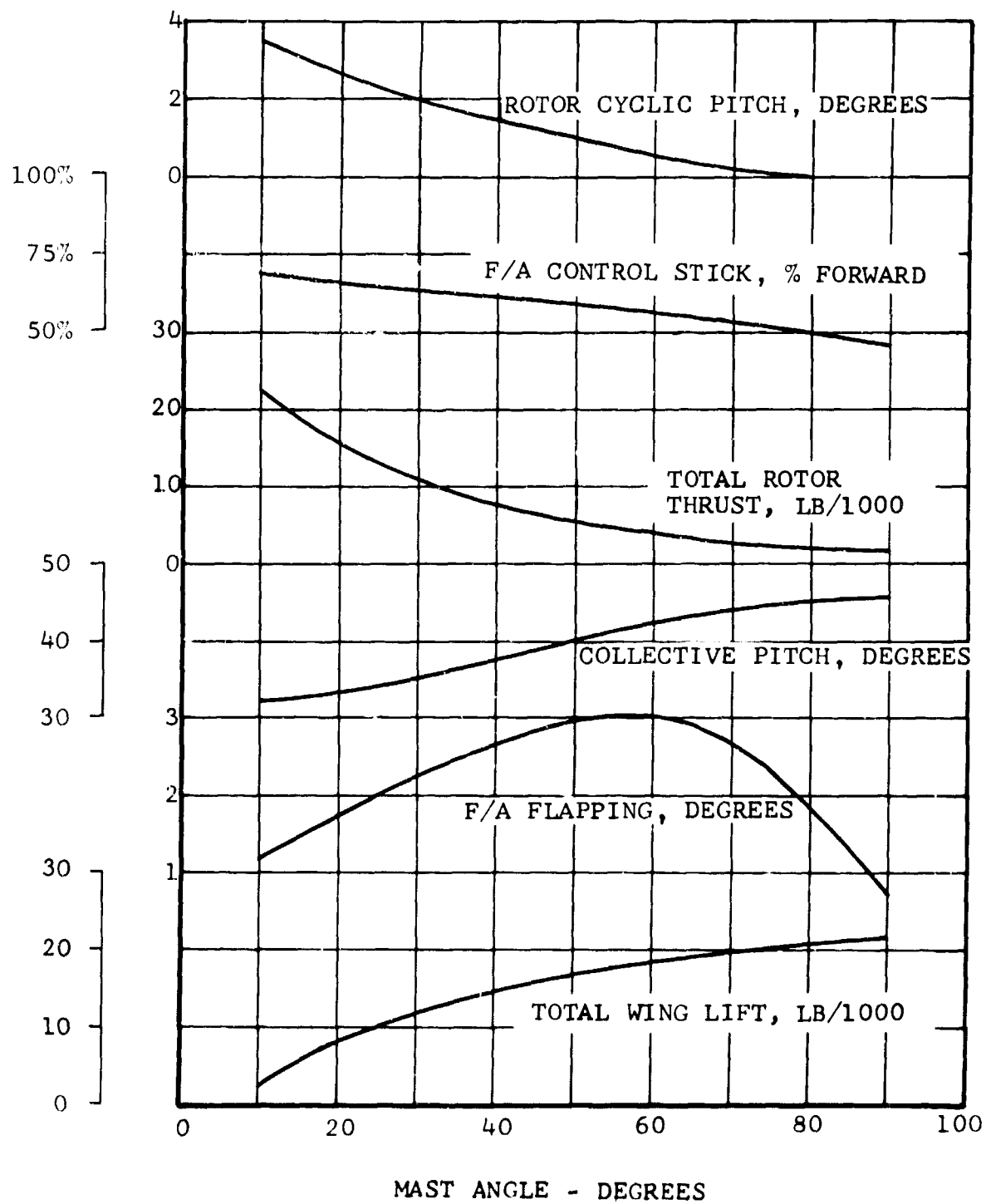


Figure 242. Static Trim at Partial Mast Angles - 150 Knots.

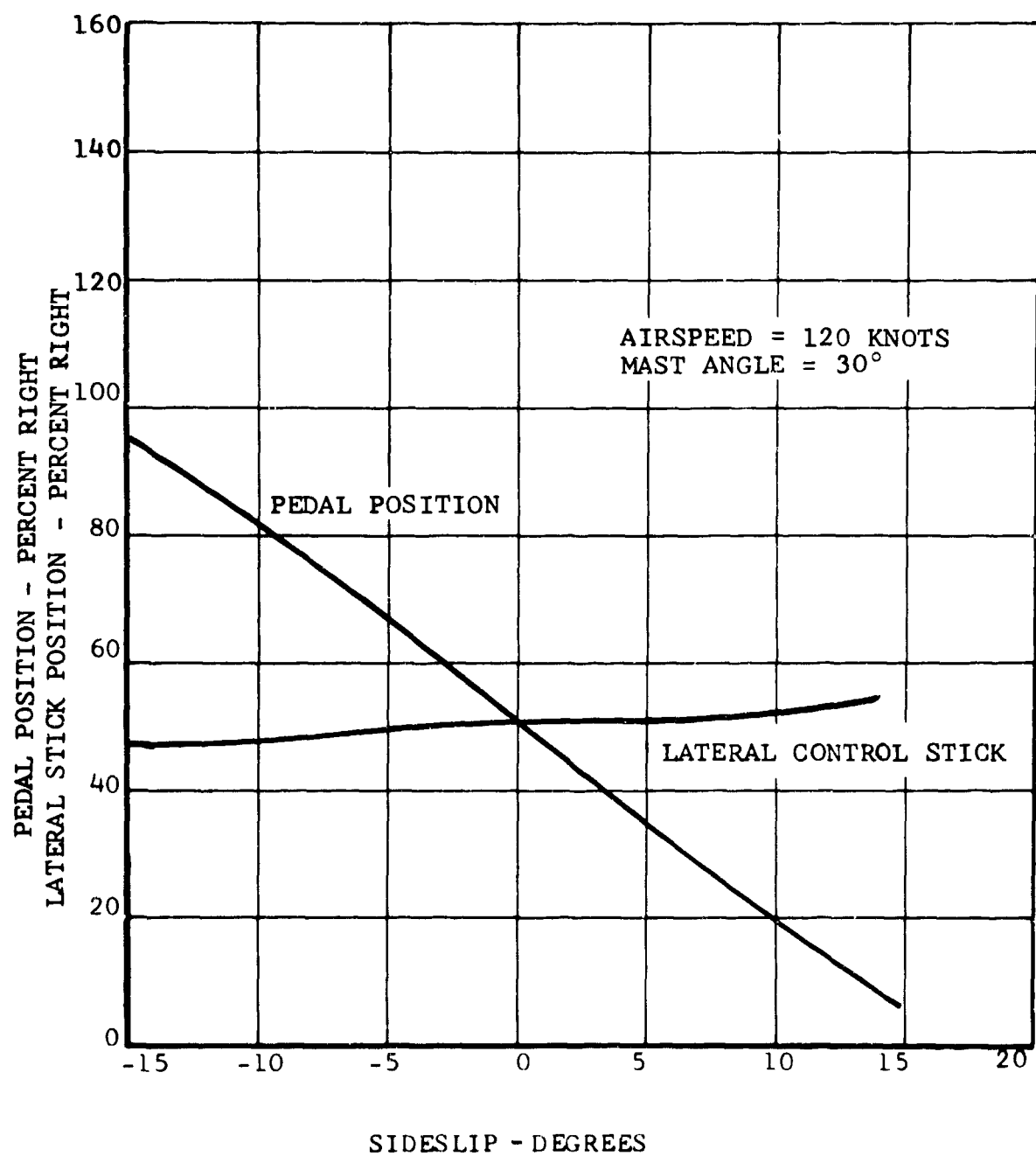


Figure 243. Sideslip Characteristics at 30-Degree Mast Angle.

calculated responses to stick pulses, in the partially converted state with SAS inoperative, are shown in Figure 244. These curves show the pitch oscillations to be rapidly convergent. Response to a step input at 30 degrees mast angle is shown in Figure 245. The pitch rate is concave downward in about 0.9 second.

Lateral-directional stability in the partially converted state is investigated by introducing pedal and lateral-stick inputs and by analyzing the C81 output.

Figure 246 shows the time histories of the effect of a pedal displacement in level flight with 30 degrees of mast angle at 120 knots. Figure 247 shows the effect of a lateral-stick input at the same condition. Figures 248 and 249 show similar time histories at a conversion angle of 60 degrees.

These figures illustrate that there is some degree of roll-to-yaw coupling. This coupling results in a small-amplitude, well-damped roll oscillation after pedal inputs. This will not adversely effect the handling qualities as indicated in Figure 210.

Yaw-to-roll coupling is not significant, as can be seen on Figures 246 and 249. The initial response to a lateral stick input is an almost pure roll.

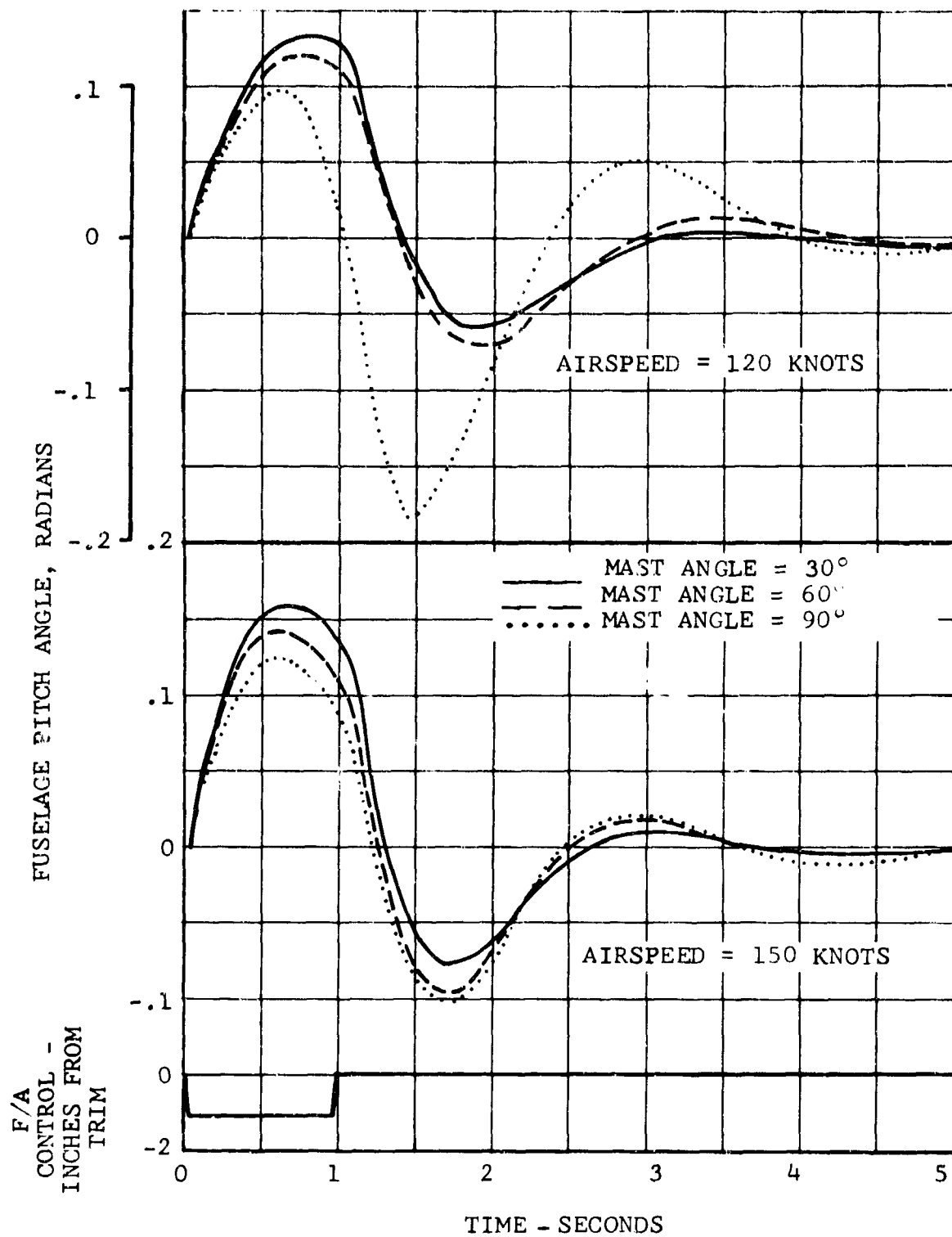


Figure 244. Pitch Response to F/A Control Input.

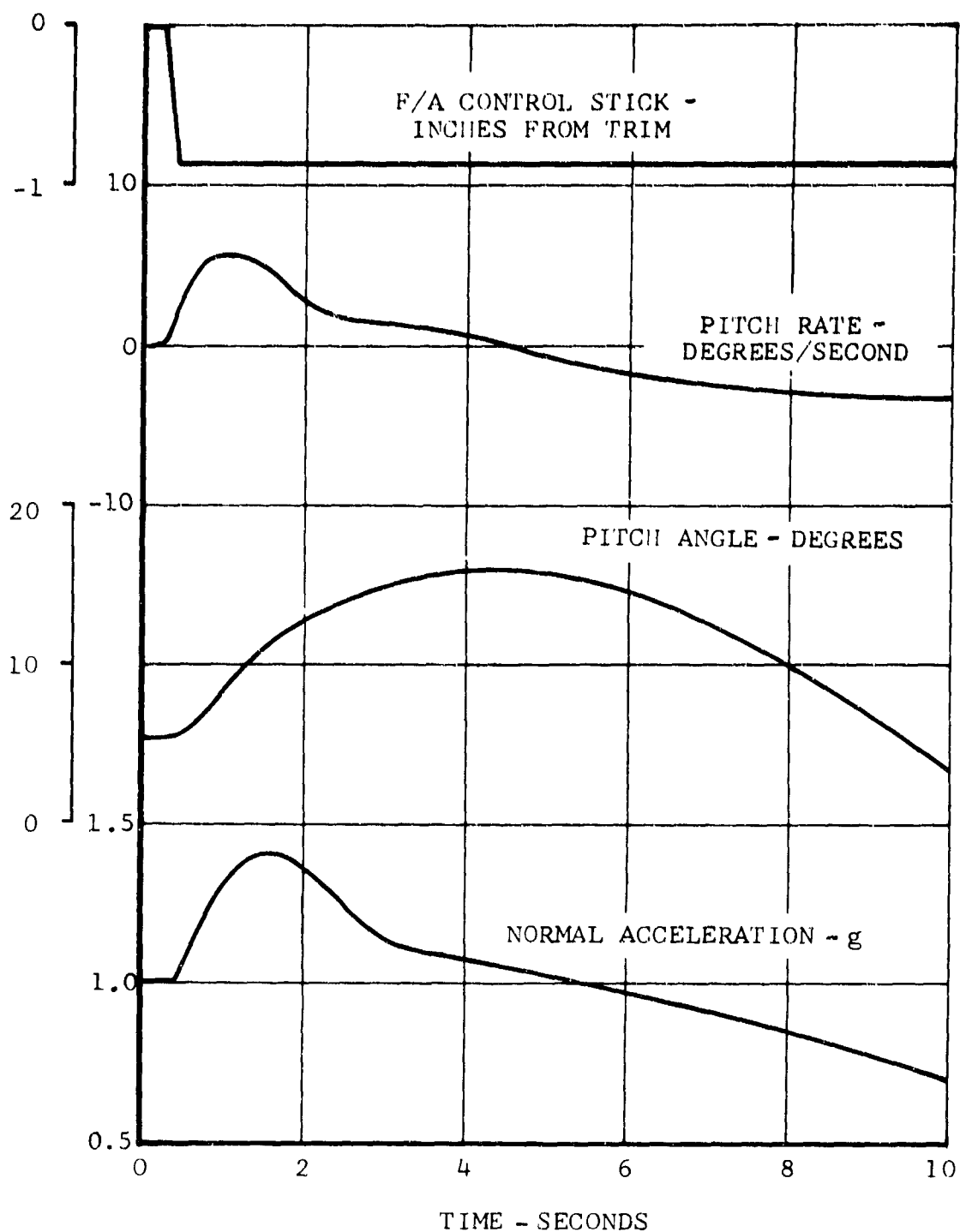


Figure 245. Normal Acceleration and Pitch Response to an Aft Control Displacement 30-Degree Mast Angle.

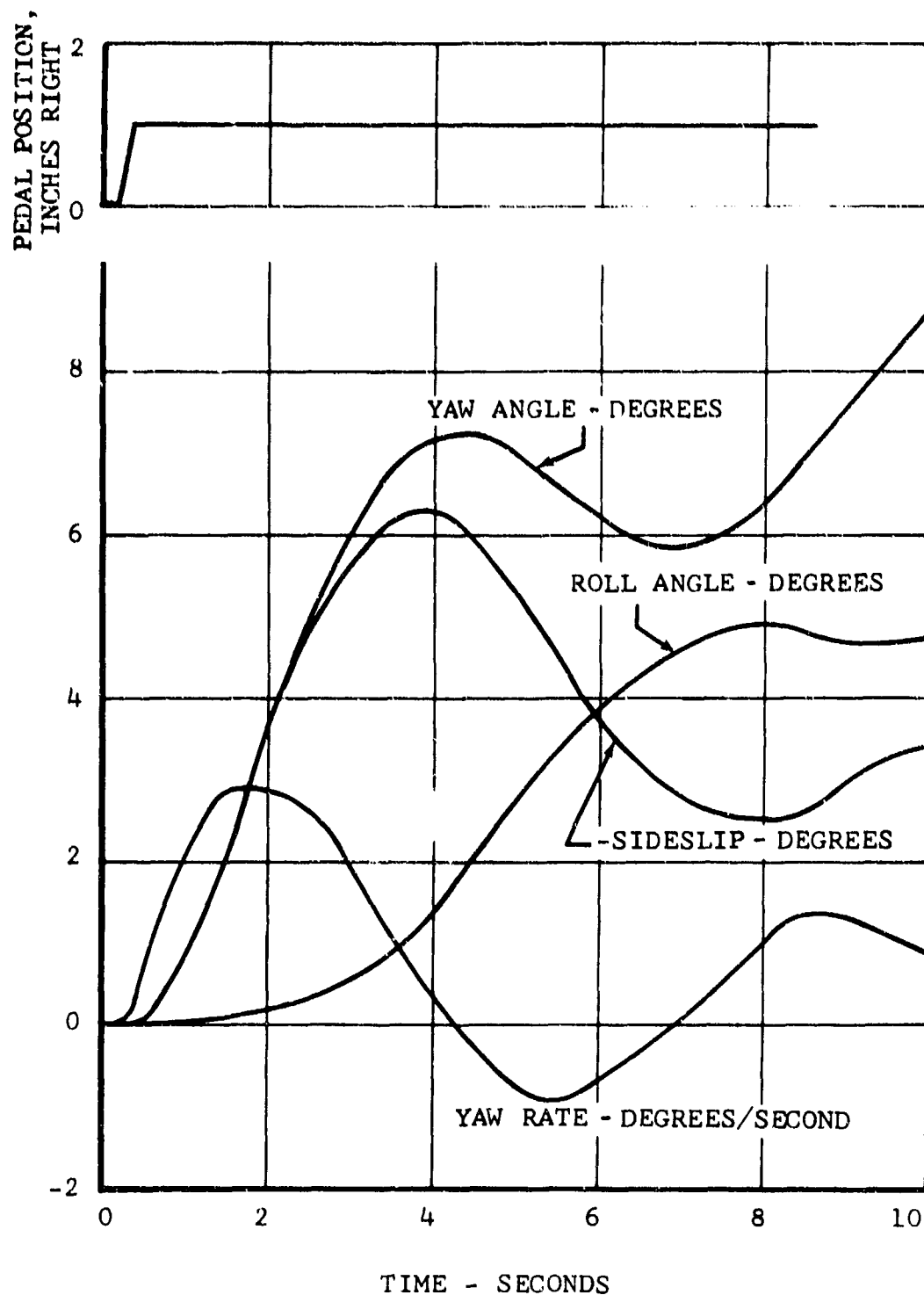


Figure 246. Lateral-Directional Response to Pedal Input at 30-Degree Mast Angle at 120 Knots.

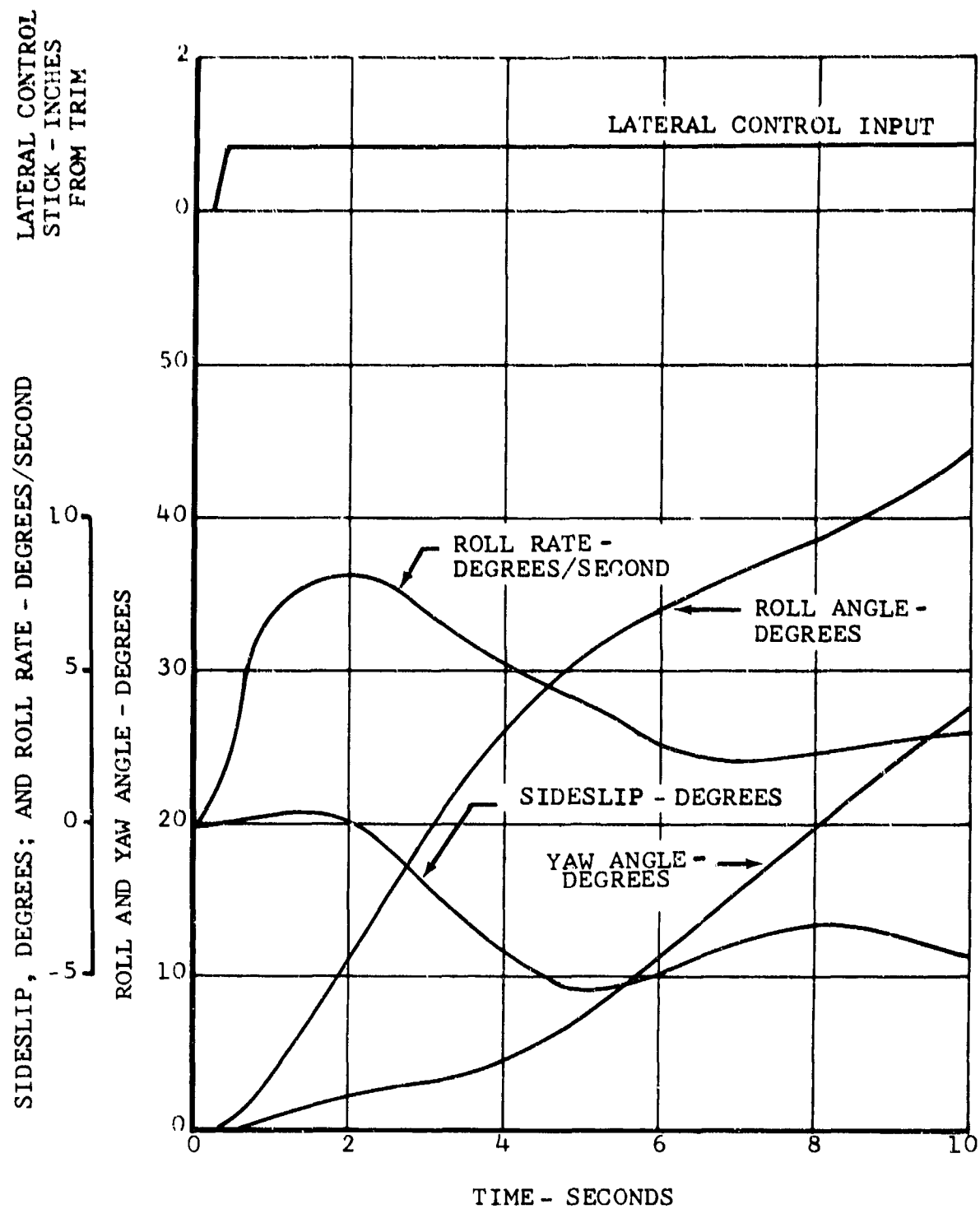


Figure 247. Lateral-Directional Response to Lateral Control Input at 30-Degree Mast Angle at 120 Knots.

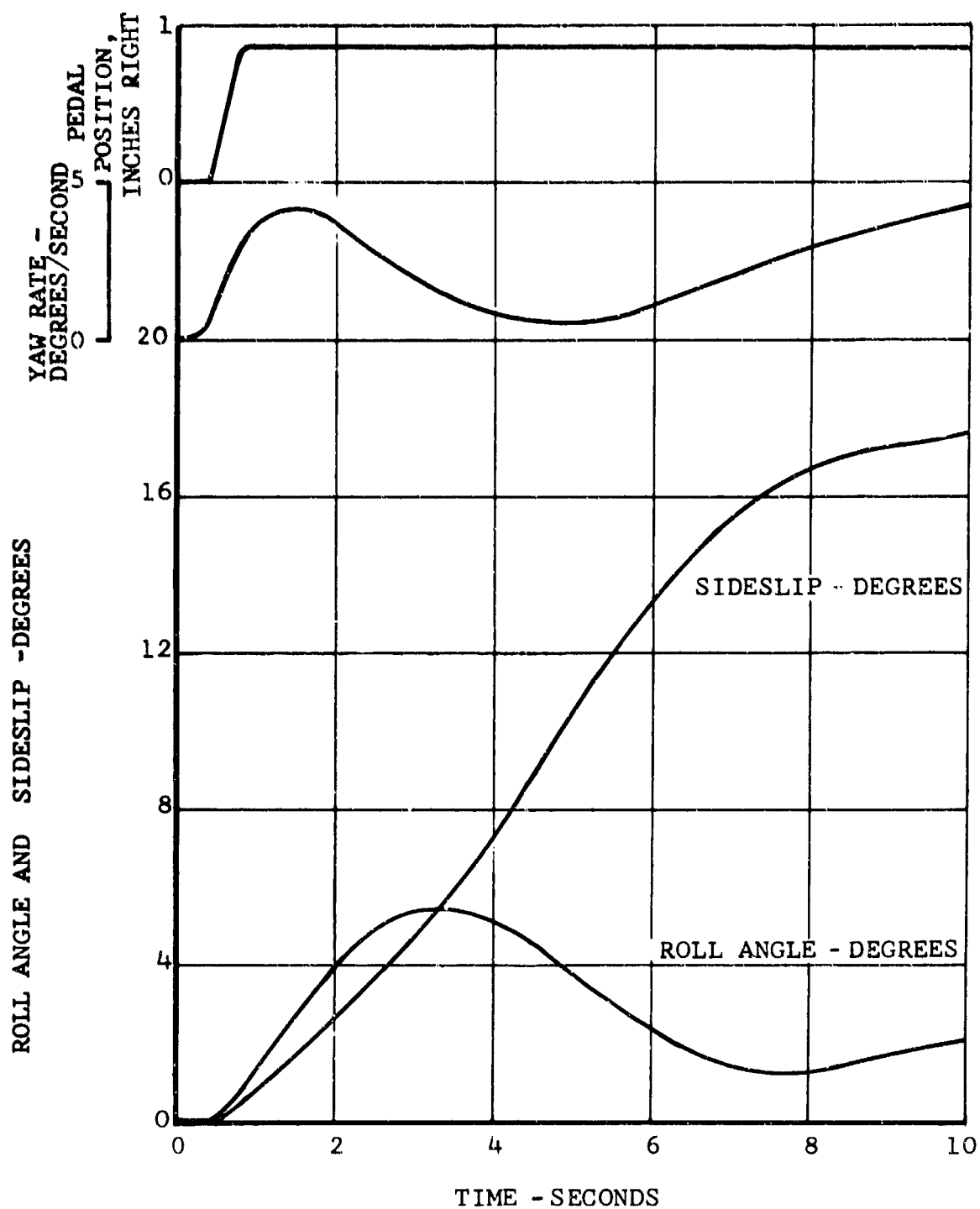


Figure 248. Lateral-Directional Response to Pedal Input at 60-Degree Mast Angle at 120 Knots.

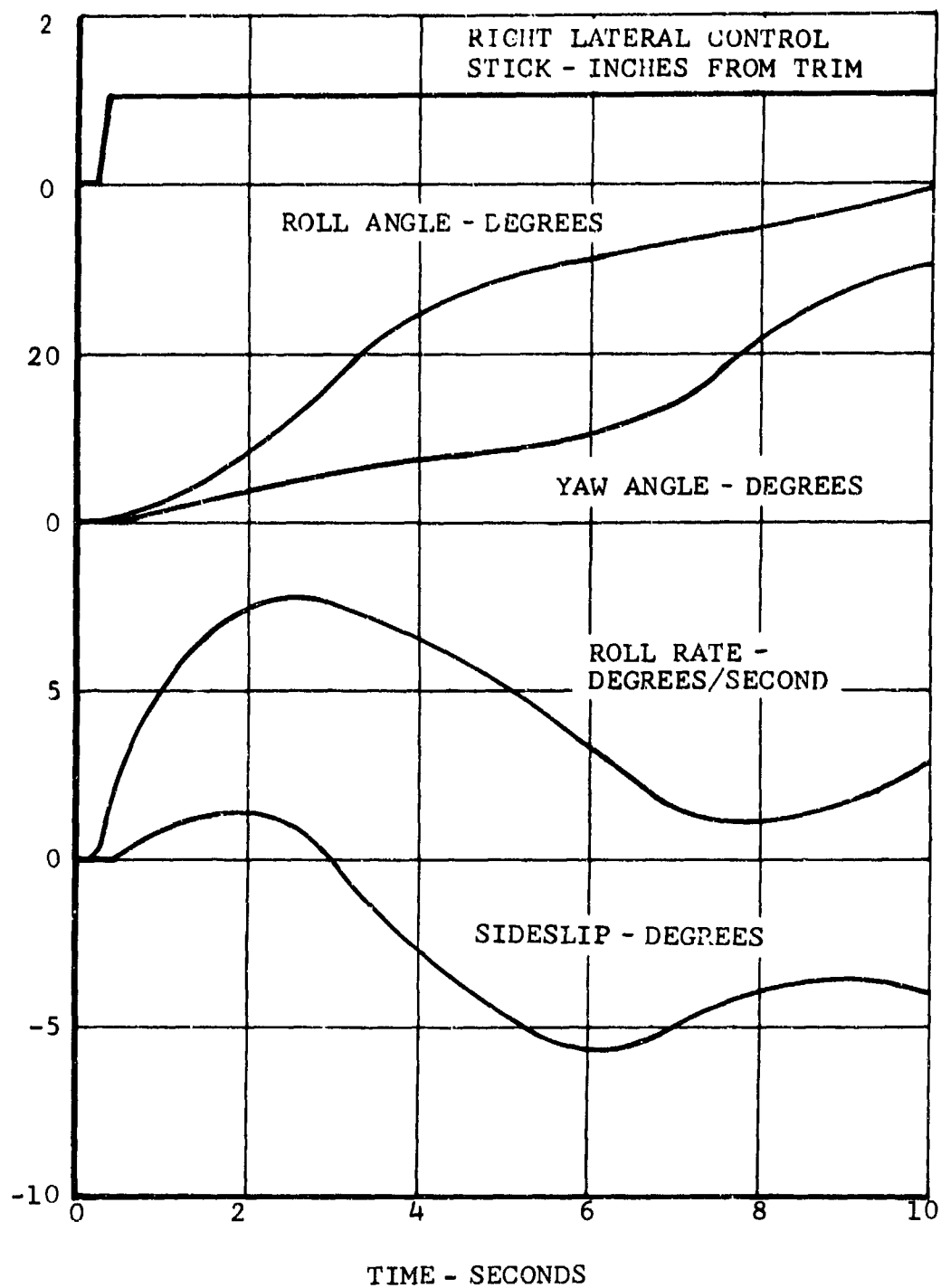


Figure 249. Lateral-Directional Response to Lateral Control Input at 60-Degree Mast Angle at 120 Knots.

SECTION VIII. COCKPIT ARRANGEMENT

The D266 cockpit has side-by-side crew seating, dual flight controls, excellent flight visibility, and ejection-seat emergency egress. The pilot, as aircraft commander, is seated on the right as in conventional helicopters. The cockpit arrangement is shown in Figure 256.

Normal access is through a center aisle from the aft cargo-passenger compartment. Emergency ground egress from (and external access to) the cockpit is through overhead escape panels above the pilots' heads.

A. SEATS

The Douglas Aircraft Company Escapac I-C-2 seats provide upward, zero-altitude, zero-speed, rocket-powered ejection. The seats conform to anthropometric requirements as defined in WADC TR-52-321. They are adjustable vertically (± 2.5 inches), but not horizontally. The rudder pedals, however, are adjustable forward and aft. The system utilizes the 28-foot NB-9 parachute and the Navy integrated torso harness. Ejection controls consist of both a D-handle on the front edge of the seat between the pilot's legs, and a face-screen handle. Either will initiate the ejection sequence. The shoulder harness and seat belt are released automatically during ejection, or manually for escape following nonejection emergencies such as ditching. The parachute and survival gear are integral parts of the ejection seat. The integrated torso harness attaches to the parachute and survival gear. The seat is attached to two ejection guide rails, which are secured to the main structure.

B. FLIGHT CONTROLS

The cockpit flight controls are in accordance with MIL-STD-250B and MIL-STD-203D, and they are conventional in location and actuation.

1. CONTROL STICKS

Control sticks are provided for both the pilot and the copilot. Both sticks are floor-mounted and are located at a pivot point in the medial vertical planes of the respective operators. The ranges of stick travel are ± 6 inches, longitudinally and laterally. The pilot's control stick is provided with a manual friction adjustment which is conventional for helicopter cyclic control sticks.

The secondary functions of the control sticks are to provide for force-gradient trim, SAS disconnect, engine start,

pylon conversion, and communications. These functions are accomplished through control switches on the stick grips.

2. COLLECTIVE LEVERS

Collective pitch controls are provided for the pilot and copilot. They are standard helicopter collective levers which control rotor-blade-pitch change during helicopter mode. During normal fixed-wing flight, the collective control lever is automatically controlled by the rotor-pitch governor. However, the pilot retains an override capability for emergency manual control in the event of rotor-pitch-governor failure.

The range of collective lever travel from the "full-down" position to the "full-up" position is 13.25 inches. This represents a ratio of 1.36 degrees of rotor-blade-pitch change per inch of collective input in helicopter mode. The amount of pressure required to operate the collective is determined by a manual friction adjustment located above the dual twist-grip controls.

Power management is controlled by two rotatable grips on the pilot's collective lever. The twist-grips are arranged so that they can be operated independently or together with the left hand. The total twist-grip travel is 240 degrees. An engine idle release switch permits either or both engines to be shut down. Depressing the switch electrically releases the idle detent.

3. PEDALS

Directional-control rudder pedals are provided for both the pilot and the copilot. Design and location of the controls are in compliance with MS 33575 for dimension and adjustment. The pedals may be adjusted ± 3 inches.

The pilot's pedals are also used to control the brakes for ground taxi control. Braking is accomplished through rotational depression of the pedals. To set the parking brake, the pilot's pedals are depressed and the parking-brake handle on his console is pulled. Depression of both brake pedals releases the brakes when the brake handle on the console is set.

4. FLAPS

The flap control is immediately forward of the power quadrant on the center pedestal. It is accessible to both the pilot and the copilot. Control motion corresponds to the actual flap movement and is marked UP and DOWN. The control is a toggle switch with an extended lever arm with an airfoil-shaped

handle. The switch permits any degree of flap setting from full up to 60 degrees down. The normal positions used are 60 degrees for takeoff and 30 degrees for conversion.

5. CONVERSION CONTROL

Rotation of the pylons for converting from one mode of flight to the other can be carried out by either pilot by actuation of the conversion switch located on the control-stick grip. Full actuation of the switch results in a 15-degree-per-second angular rotation of the pylons. An emergency reconversion handle on the center pedestal provides the means for manually positioning the hydraulic conversion valves. This handle is used only in the event of dual electrical failure.

6. LANDING GEAR

The landing-gear control lever is forward on the center pedestal and is marked UP and DOWN, corresponding to wheel position. The control lever is installed so that it is conveniently accessible to both the pilot and the copilot. The emergency gear handle on the landing-gear control panel may be operated by either pilot. It releases the landing-gear uplocks through a mechanical linkage and permits a gravity drop of the gear.

7. FLIGHT-ASSIST CONTROLS

The SAS control panel is located on the center pedestal immediately forward of the power-management panel. Both pilots' control-stick grips are equipped with SAS disengage, push-to-release buttons.

The force-gradient power switch is located on the hydraulic control panel in the center pedestal, and both pilots have trim switches on the stick grips.

Rotor trim control is provided to balance rotor thrust. In helicopter operation this provides roll trim, and in high-speed flight it provides yaw trim. The rotor trim switch is located in the hydraulic control panel.

Elevator trim-tab control is provided as a backup pitch-trim system. The switch is located on the hydraulic control panel and provides selection of either elevator trim or pitch force-gradient trim. Trim is activated with the trim switch on the stick grips.

C. POWER-MANAGEMENT CONTROLS

1. STARTING

Each engine is started independently with the power-management controls in the OFF position. A starter-select toggle switch on the fuel and engine panel, immediately aft of the power-management control panel, establishes which engine is to be started.

2. FUEL CONTROL

Two fuel systems, one in each wing, are normally used with the respective left and right engines. Low fuel is indicated by two quantity indicators on the instrument panel and a FUEL QUAN caution-panel light. In the event of failure of one of the dc fuel-boost pumps, the cross-feed valve is activated, and the single operative pump moves all usable fuel to the engines. Failure of either fuel-boost pump is noted by a warning light in the caution panel. A fuel-flow indicator for each engine is located with the engine instruments on the instrument panel.

Two fuel-cutoff toggle switches on the fuel and engine panel are placed in the ON position during the start procedure. Two fuel-boost pump switches are also located on this panel, as is the cross-feed fuel switch.

3. POWER CONTROL

a. Collective Lever

Power management in helicopter flight is through the conventional collective-pitch lever and the twin twist-grips on the lever. The operation and configuration of this control are standard, the only exception being the additional twist-grip control for twin-engine operation. The twist-grips are used in helicopter flight (with the power-turbine governors engaged) to select the desired rotor rpm between 95-100 percent.

b. Control Quadrant

A set of power-management levers on the center pedestal, accessible to both pilots, operates in conjunction with the twin twist-grips through a direct mechanical linkage. These are continuous lever-type controls, whose location, shape, and size assist nonvisual identification. During helicopter operations, these controls remain in the 95-100-percent rpm region, which is the most forward range. Throughout fixed-wing operations, the levers are utilized by the pilot as the primary power controls (below the 95-percent setting). The

design of these controls is consistent with the recommendations for controls for continuous operation as outlined in WADC Technical Report 56-172; it generally complies with MIL-STD-203D.

An rpm-select lever at the left of the power-management levers may be operated by either the pilot or the copilot. A control lever immediately to the right of the power-management levers sets the system friction for the power-management levers and the twist-grip controls.

4. ROTOR-PITCH GOVERNOR

The rotor-pitch-governor rpm-select lever, located on the pedestal, includes a press-to-disengage button. An offset detent aft of the OFF position precludes inadvertent activation of the rotor-pitch governor during helicopter operation. The governor rpm-select range is aft and left of the detent. The switch on the control lever knob allows the operator to select any rpm setting prior to governor engagement. It permits the lever to pass through the high-rpm range without engine follow-through and also permits immediate disengagement at any rpm setting. Two lights in the rotor-pitch-governor control section indicate when the rotor rpm is below 95 percent, when the rotor-pitch-governor circuitry is armed, and when the rotor-pitch governor is engaged. A rotor-pitch-governor malfunction is indicated by a light in the caution panel.

5. OPERATION

In helicopter operation the collective lever is used for power control, and the twist-grips are used for rotor-rpm setting. The power-turbine governing range and the selection range of the twist-grips are 95-100 percent of rotor rpm.

The power-management levers are used, with the rotor-pitch governor engaged, during normal fixed-wing flight. The rotor-pitch-governor rpm-select range is from below 95 percent to 48.5 percent. In normal fixed-wing flight, rotor rpm is between 48.5 and 73 percent.

The power-management levers and twist-grips are in the closed or OFF position during the start and are advanced to the idle position at approximately 20-percent engine speed. The start-ignite function is initiated by a switch on the control stick. The twist-grips are returned to OFF for shutdown. Electrical detent stops are released by depressing the engine idle release switch on the pilot's collective lever.

D. SUPPORT SYSTEM CONTROLS

1. HYDRAULIC

The hydraulic control panel is forward on the center pedestal. There are three toggle switches--one each for System I, System II, and System III--and one power-source-select switch for System III (normal or APU). A green light indicates the status of the select valve in System III. Also included is a force-gradient ON-OFF switch, a momentary rotor-trim toggle switch (activated laterally to the left or right position), and a two-position pitch-trim switch with normal and elevator trim-tab positions. Caution lights indicate low hydraulic pressure in any system and low fluid quantity in System III. The latter cautions the pilot that the power source is not the problem and that using the APU as an alternate power source will not provide system hydraulic pressure. In the event of failure of either System I or System II, a mechanical inter-connect feature allows the operative system to convert or re-convert both pylons.

2. ELECTRICAL

The electrical control panel on the overhead console is readily accessible to both pilots. On this panel are the five three-position toggle switches for the battery, the two dc generators, the ac generator, and the inverter. A "gang" bar is provided for simultaneous deactivation of all of these components in the event of an emergency. A dc bus rotary selector switch and an ac bus rotary selector switch are located aft on this panel. The NORMAL positions close the relays so that all buses are incorporated into the system. To investigate the failure of a bus, each bus may be isolated by selecting one of the alternate positions on the rotary control switch.

The pylon conversion actuators are controlled by power from the essential dc bus Number 1 to the left actuator and by power from the essential dc bus Number 2 to the right actuator. Both the pilot's and the copilot's conversion switches normally activate the pylon actuators on each side.

There are three panels which control the interior lighting. The lighting arrangement conforms to MIL-L-18276C. The overhead panel contains controls for cockpit dome lights and console lighting. The two side light-control panels give each pilot the capability of activating and adjusting his instrument-panel lights. Map lights are mounted on both pilots' side-canopy rails in such a manner as to be adjustable for directing light into their immediate areas. The map lights may be detached for use. Provision is made for both red and white lighting under separate control.

The exterior-lighting panel includes control switches for the navigation and anticollision lights. An intensity control and a FLASH-STEADY option are incorporated for the operation of the navigation lights. In addition, landing-light controls are located adjacent to the landing-gear panel on the center pedestal. The windshield wiper and washer control switches and the pitot-heat switch are in the overhead panel. They are conventional toggle switches.

3. AVIONICS

The center pedestal contains the VHF/FM control panel, the UHF control panel, and the pilot and copilot ICS control panels. The VOR/DME control panel is located on the center pedestal, forward of the communication panels.

4. AUXILIARY POWER UNIT

The APU control panel is on the center pedestal. A three-position OFF-RUN-START switch is located on the right side of the panel. Three red warning lights on this panel indicate the status of the APU engine. They are a LOW OIL pressure warning, an EXHAUST TEMP warning, and an engine OVERSPEED warning. There is also a green HYDRAULIC PRESS advisory light below the warning lights. It indicates that there is adequate hydraulic system pressure for starting the T64 engines and that the APU gas producer has reached operational speed.

E. ENVIRONMENTAL CONTROLS

Ventilating air enters through an intake above the cargo compartment, well forward of engine and APU exhaust areas. It is moved by a "vaneaxial" blower that is capable of approximately 1400 cfm. Bleed air is used to heat outside air supplied by the hydraulic-motor-driven ventilation fan. The cabin heating and ventilation outlets are located near the floor on the right and left side consoles and on the left and right sides of the instrument panel. Individual nozzles defrost the front windshield, lower panels, and side windows. The pilot and copilot both have manual controls to limit or to shut off the outlets. The cabin outlets may be shut off without disturbing the flow of air to the windshield and window area for defogging and defrosting. An overheat switch connected to the bleed air ON-OFF valves protects against overheat damage to the duct system or other structure such as the windshield.

F. INSTRUMENTS

Figure 256 in the Appendix illustrates the placement of the instrument panel, pedestal, side console, and overhead panel. Consideration has been given to the functional anthropometry

of the seated operator, including his biomechanical limitations and his basic visual skills. Flight and engine instruments are arranged in a simple, compact panel. Conventional, proven displays have been used uniformly. Where possible, all displays and controls pertinent to a sequence of activities have been placed in a common area. The most frequently used displays have been grouped in a central visual cone referenced about a mean line of sight. Non-critical or less frequently used displays are positioned peripherally to the optimum cone. Emergency warning displays (fire, rpm) demanding immediate attention are located at line-of-sight level.

1. FLIGHT INSTRUMENTS

Separate sets of flight instruments are provided for the pilot and copilot. They include airspeed, gyro horizon, bearing-distance-heading, turn-and-bank, barometric altitude, and vertical speed indicators. A course indicator and clock are provided in the pilot's group of flight instruments. The pilot's and copilot's pressure instruments are connected to separate pitot-static systems. The selection and arrangement of the instruments are in general compliance with MIL-STD-33572.

2. PROPULSION INSTRUMENTS

The propulsion instruments are located between the pilot's flight instruments and the copilot's flight instruments. The pilot and copilot are provided separate triple tachometers. The rotor rpm indication on the pilot's triple tachometer is driven by the rotor-pitch-governor tachometer generator, and the copilot's is driven by a separate tachometer generator. A dual torquemeter is located on the pilot's side. Gas-producer tachometer indicators, power-turbine inlet-temperature indicators, fuel-flow indicators, engine oil pressure indicators, and engine oil temperature indicators for each engine are vertically arranged. Two fuel-flow indicators, a fuel pressure indicator, and two fuel quantity gages are provided near the center of the instrument panel.

Transmission-oil temperature and pressure indicators are provided. In ECAN, the oil pressure and temperature indicators display the lowest system oil pressure and temperature. The temperature or pressure of each transmission or gearbox in the system can also be read individually.

3. NAVIGATION INSTRUMENTS

The pilot and copilot have separate bearing-distance-heading indicators (BDHI). The pilot's panel also contains a cross-pointer course indicator. A VOR DME navigation system is

provided for geographic position and azimuth indication. A magnetic standby compass is mounted above the instrument panel between the pilot and the copilot.

The avionics controls are located between the two pilots on the left side of a center pedestal. Included are the VOR DME, the VHF FM, and the UHF. Two intercom panels are side-by-side, aft of the other communications panels.

G. WARNING AND CAUTION SYSTEMS

The warning and caution systems are in compliance with MIL-STD-411A for such factors as color coding, shape coding, location, lighting, and intensity of lighting.

The caution panel is located in the center of the instrument panel, where it may be monitored by either pilot. It indicates the following malfunctions:

- Fuel-boost pump, left and right
- Fuel quantity
- Engine oil pressure, left and right
- Engine ice, left and right
- Chip, engine, left and right
- Chip, transmission, left and right
- Transmission oil pressure and temperature, left and right
- Force gradient
- Rotor-pitch governor
- Hydraulic pressure
- Hydraulic quantity, System III
- DC generator, left and right
- AC inverter
- External power
- Ejection seats
- Parking brake

Warning lights indicate unsafe rotor and engine rpm and unsafe landing-gear conditions. An audio signal is also included in the rpm warning system.

The engine fire-warning and -control system is in the upper center of the instrument panel. Three T-handles are for use with the APU unit, Engine One, and Engine Two. Each handle contains a fire-warning light which indicates that there is a fire in that particular unit. The extinguishing circuitry to the engine is armed by pulling the handle. The agent charge is released by either of two toggle switches. One charge is for the APU unit and two charges are for the main engines. Either or both engine charges may be directed to either engine.

H. VISIBILITY

The D266 has excellent interior exterior cockpit visibility. It may be noted from Figure 255 that the fields of vision provide a virtual 245-degree azimuth coverage through the extensive Plexiglas windshield and side panels. Forward-downward visibility over the nose exceeds 20 degrees below the horizontal viewing plane of the pilot, conforming to the recommendations of FAR 29. Forward-lateral-downward visibility is enhanced by the lower Plexiglas panels on either side of the cockpit. Upward visibility is effectively unrestricted, permitting a total of 196 degrees in the vertical plane. Laterally, each pilot has a 115-degree viewing angle on the near side and 38 degrees on the opposite side.

Projections from cockpit equipment have not been permitted to intrude into the pilots' fields of view. Frame members have been held to a recommended minimum without violating structural integrity. Thus, the effective binocular blind spot behind the frame is minimized.

The instrument panel was designed and located to accommodate the biomechanical and visual limitations of the human operator and to insure optimum visibility of instruments in accordance with standard human factors practice.

The cockpit is void of shiny metal or other high-reflectance objects, and all instrument cases are painted flat black to minimize reflectance.

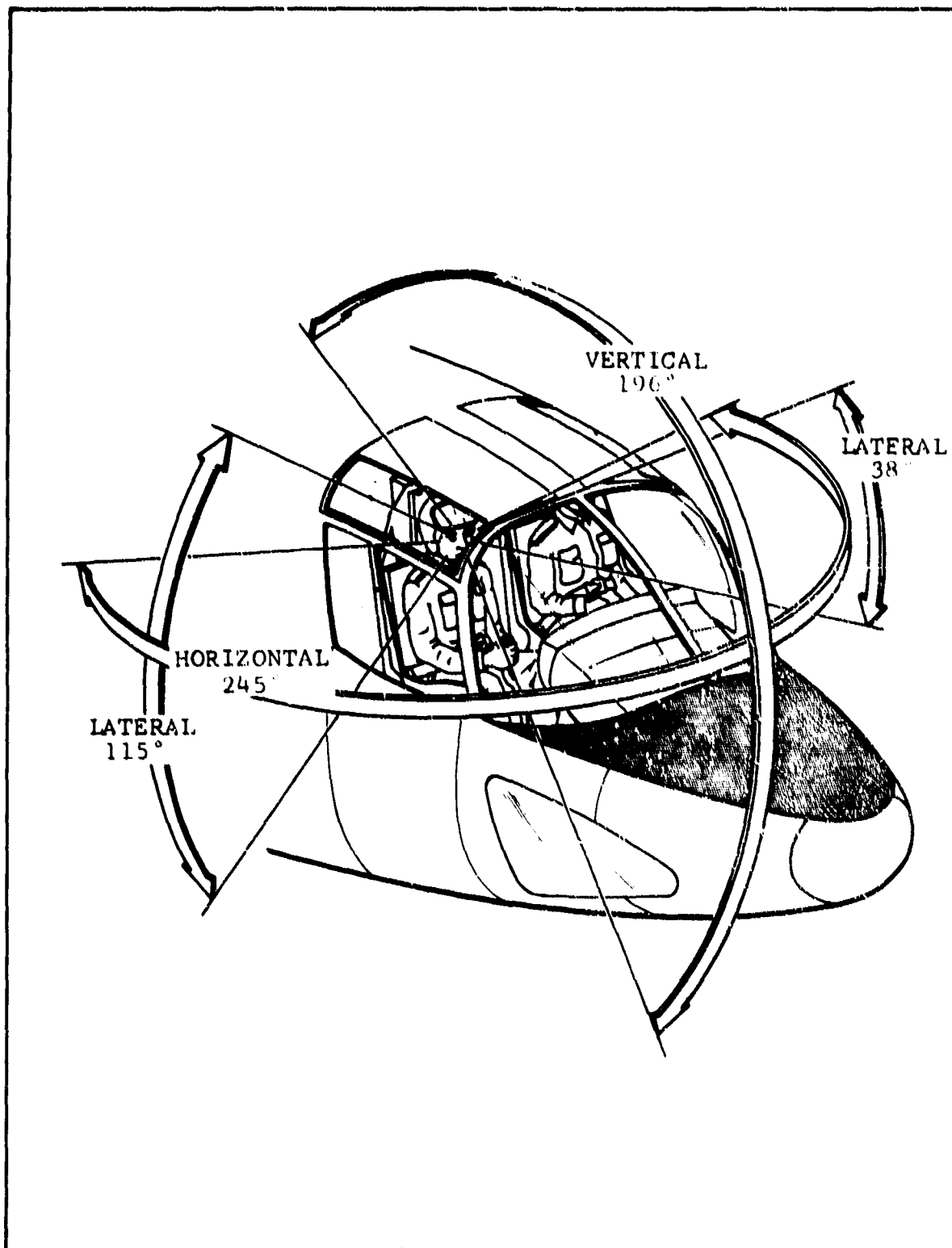


Figure 250. D266 Pilot Visibility.

SECTION IX. EMERGENCY SYSTEMS AND PROCEDURES

A. POWERPLANT

1. ENGINE FAILURE

The D266 can hover on one engine at design gross weight out of ground effect at altitudes up to 4400 feet on a standard day, or in ground effect above 1000 feet on a 95°F day. Therefore, a normal hovering landing can be accomplished under most conditions with a single operating engine. Forward flight is possible on a single engine at design gross weight (23,000 pounds). A true airspeed above 250 knots may be maintained under sea-level-standard conditions. Complete power loss is an extremely remote possibility; however, it is easily manageable in the D266, as landing can be accomplished in either STOL or helicopter mode.

The two engines normally use fuel from separate fuel systems; have separate oil systems, power-turbine governors, and ignition systems; and are independently managed. The fuel control schedules engine fuel flow and compressor-inlet guide-vane position so as to protect the engine from stall, to provide altitude and temperature compensation, and to maintain the selected power-turbine speed. Fuel control failure will normally necessitate shutting down the engine, but failure or loss of power on one engine during normal flight will result in the other engine's accelerating to accept the load. Either engine may be restarted in flight using normal starting procedures.

In the event that there is a complete loss of engine power during flight, several choices are available to the pilot, depending on airspeed, altitude, and mode of flight. Restarting of engines should be attempted if the flight conditions, the time, and the cause of power failure permit. In fixed-wing flight at high gross weight, a glide, reconversion to 30 degrees, and STOL landing may be made onto a prepared surface. At lower gross weights, reconversion to helicopter flight would give the most controllable power-off configuration.

Power-off reconversion from fixed-wing mode to helicopter flight is a simple, easy-to-accomplish maneuver. At high cruise speed, deceleration to reconversion speed range may be accomplished either by holding altitude and allowing the airspeed to decrease, or by initiating a climb. The rotor-rpm-select lever should be moved forward to the detent prior to reconversion. During reconversion and entry into autorotation, the rotor-pitch governor will automatically position the collective to maintain the proper rpm. As in a conventional helicopter, rate of descent may be controlled by the aircraft's

speed and attitude. All aircraft systems, including full hydraulic and electric power, are available during autorotation.

One of the noteworthy features of the D266 is its autorotational landing capability. As in any helicopter, airspeed and rate of descent must be monitored and controlled by the pilot. If time permits, the rotor speed select lever should be moved forward to the OFF position so that the pilot has more freedom to control rpm directly and to use collective control during the landing flare. If this is not done, he can override the rotor-pitch governor (with 30 pounds of force) to execute the landing. As wing lift must be considered at high airspeeds, the autorotational envelope must be observed in order not to unload the rotors excessively.

2. POWER-TURBINE-GOVERNOR FAILURE

Failure of a power-turbine governor may reduce power to a minimum setting or may increase it to a maximum power topping setting.

Failure of one governor resulting in minimum fuel flow will cause the other engine to accelerate to its maximum available power to accept the power requirement. Power control may be maintained by retarding the power-management lever of the normally operating engine or by decreasing the power required by lowering the collective lever.

Failure of one governor that causes it to go to the maximum setting will cause the other power-turbine governor to decrease power. Retarding the power-management lever or twist-grip on the high-power engine will result in the other engine's increasing speed to produce the power required. The engine with the malfunctioning governor may continue to be operated on open loop in the power control range. The governor on the normally operating engine will then schedule the flight transient power above the base-load setting of the malfunctioning engine.

3. ROTOR-PITCH-GOVERNOR FAILURE

A rotor-pitch-governor failure may be of two types: the governor may fail to maintain the control band (rpm tolerance), or it may lose control of either the upper or the lower limit. A light on the caution panel shows a rotor-pitch-governor malfunction of either type.

The rotor rpm will decrease when a governor failure occurs which drives rotor pitch to the maximum. Because the collective lever is connected to the governor, the collective position is an indication of the pitch and rpm settings. The pilot may manually override the governor by increasing or decreasing the collective pitch lever's position. A failure that

drives the rotor collective pitch to a minimum will cause a rotor overspeed which is controllable with the collective lever. The power-turbine governor will come into action (above 95-percent rpm) and will act as a topping governor to prevent engine overspeed.

Torsional oscillation of the governor will necessitate moving the rpm-select lever forward to the disengage position. Immediate disengagement may be made by pressing the disengage button on top of the lever.

4. ENGINE FIRE

The fire warning and control panel includes three T-handles which illuminate to indicate fire in the APU or in either engine. The fire extinguisher system includes the T-handles, which close fluid valves and open the fire-extinguishing-agent line to each engine, and the fire-extinguishing agent-discharge switches.

At the first illumination of a fire-warning light, the pilot should check engine instruments (temperature, and oil and fuel pressures) and, if possible, get a visual check for smoke and flame. Immediate power reduction on the affected engine should be made. If fire is present, the pilot should pull or direct the copilot to pull the appropriate T-handle.

Pulling the T-handle closes the fuel, oil, and hydraulic shut-off valves, turns off the ignition, closes the bleed-air line to the heating system, and opens the valve in the agent discharge line. The discharge switch is then moved forward to shoot the first charge into the engine. If the fire-warning light goes out, the circuitry should be checked by pushing the test button. If the appropriate T-handle then will not light, engine instruments and a visual check should be used to determine if the fire is out. Since only two shots of agent are available per flight, the second should not be unnecessarily discharged.

B. FUEL SYSTEM

Low-fuel-quantity indication by the caution light or the fuel gages presents a flight-termination warning to the pilot. A low-quantity indication on one gage with respect to the other normally indicates asymmetric fuel loading. The cross-feed valve should be opened, and the boost pump on the low-fuel side should be turned off until the tanks are equalized.

Other indicators for the fuel system include a fuel-manifold pressure gage, two fuel-flow meters, and caution lights for the left and right fuel-boost pumps. Illumination of a fuel-boost-

pump light is an indication of failure of either the boost pump or the ejector pump in that tank.

Fuel-boost failure, indicated by a caution light, can be classified as to boost-pump or ejector-pump failure by the following procedure:

- Turn off switch to failed boost pump.
- If the fuel-manifold pressure drops, the boost pump was operating and the ejector pump is clogged or inoperative.
- If the pressure remains the same, the boost pump has failed and the switch should remain off.

If the failure is in the ejector pump, the boost switch should be returned to the ON position. In the event of boost-pump failure, the fuel cross-feed line should be turned on to permit gravity flow between tanks. The remaining boost pump will supply fuel to the manifold for both engines. A back-flow check valve prevents fuel in the manifold from flowing into the tank with the inoperative boost pump. Failure of both fuel pumps does not inhibit flight below the altitude limit established by the suction capabilities of the engine-driven fuel pumps; however, flight at or near this engine critical altitude should not be attempted with both pumps inoperative.

Loss of fuel-manifold pressure without an indication of failure of both boost pumps is either a gage malfunction or an indication of fuel-line rupture. If a flowmeter indicates an abnormally high flow for the power setting, a line rupture has probably occurred between the flowmeter and the engine. The engine should be shut down and the firewall fuel-shutoff valve should be closed.

C. FLIGHT CONTROLS

1. HYDRAULIC SYSTEM

The three completely separate hydraulic systems are independent of engine operation. Each is designed to provide power for full-load operation.

Failure of System I or System II will in no way compromise the mission. Each supplies complete hydraulic power for conversion and for cyclic, collective, and aileron controls on its respective side. Complete power for operation of cyclic, collective, and aileron controls is also supplied by System III; and because the conversion actuators are interconnected, failure of either System I or System II will not restrict conversion or reconversion. Failure of System III will not compromise the functions powered by that system, as the APU may be used as an alternate power source.

2. STABILITY AUGMENTATION SYSTEM

The stability augmentation system (SAS) is not required for flight but is an added flight-assistance system. Both pilots have SAS disconnect buttons on the control-stick grips for fast or emergency shutoff of the system. When either button is depressed, power to the entire SAS is cut off. The master power switch must be turned off, then turned back on, to obtain power for the SAS system. Any of the three axes may be disengaged with the individual axis switches or the master power switch on the SAS panel.

3. FORCE-GRADIENT SYSTEM

The force gradient is not required for flight but is an added flight-assistance system. The pilot can override the force-gradient system in the event of failure or malfunction of the system. A malfunction of the force-gradient system is indicated by a light in the caution panel. The pitch-gradient force may be separately deactivated by moving the elevator-trim switch from the force-gradient position to the trim-tab position.

4. ELEVATOR TRIM

In the event of hydraulic failure in System III, malfunction of the elevator hydraulic cylinder, or malfunction of the pitch-force gradient, the elevator control switch in the hydraulic control panel should be moved from the force-gradient position to the trim-tab position. Fore-and-aft movement of the trim switch on the control-stick grip actuates either the force-gradient-pitch trim or the elevator trim, depending on which system is in operation.

5. FLAPS

The left and right flaps are interconnected: therefore, failure of either flap actuator will not disrupt operation. In the event of failure of the actuator, which is powered by System III, the APU should be started to supply power directly to the alternate actuator. If the interconnect fails, a split-flap condition will result which will be shown on the flap indicator (one flap up and the other down). The operating flap should be positioned to any symmetrical setting possible. Even if a symmetrical flap setting is not obtained, normal flight below 150 knots and a safe helicopter landing can be made without encountering control difficulty.

6. CONVERSION SYSTEM

Either conversion actuator will supply power for the complete conversion, as the actuators are mechanically interconnected.

Electrical power for conversion-actuator control is supplied from essential dc bus Number 1 to the left pylon actuator and from dc bus Number 2 to the right pylon actuator. Failure of either electrical system will not compromise normal conversion and reconversion.

A backup mechanical system for reconversion is operated by pulling the emergency reconversion T-handle in the cockpit. This process mechanically positions the hydraulic valves to allow the actuators to move to the "up" pylon position. It is used after complete dc power failure.

7. LANDING GEAR

Landing-gear position is shown by a three-position indicator for each of the three gears. The presentations are for a wheel "down and locked," a barber pole for "intermediate position," and an UP sign for "gear up and locked." The gear-actuating handle is clear plastic and contains a red light which is illuminated when the gear is unsafe. An audio signal also is activated by an unsafe gear condition. It may be silenced, however, with the horn cutout button.

The emergency gear-release handle is located on the center pedestal aft of the normal gear-control panel. The handle is pulled out to release the gear uplocks mechanically, and the wheels are free to drop into the down-and-locked position. The normal gear-down indication will then be shown.

D. EGRESS

1. FLIGHT

The D266 crew seats are Douglas Aircraft Company ESCAPAC I-C-2 seats which provide fully automatic, upward, zero-altitude, zero-speed, rocket-powered ejection. The seats are equipped with a 28-foot NB-9 parachute, a shoulder harness, an inertia reel, and seat belts. The pilot wears an integrated torso harness which attaches to the parachute. An ejection-seat light in the caution panel is illuminated when electrical power is on and when the integral safety control lever on the headrest is in the safe position. The safety lever, which protrudes forward and down from the headrest, also interferes with head motion until moved to the armed position.

The first action in a normal ejection is the release of the overhead panel. If a malfunction occurs in the overhead Plexiglas panel release, the seat will eject through the panel. An overhead section of the seat protects the pilot during this sequence. Each pilot initiates his upward rocket ejection sequence by a 20- to 40-pound upward force on the lower handle (D-ring) or by a similar force pulling the face-curtain down in front of his head.

A zero-delay lanyard initiates a 2-second delay in the parachute actuator as the seat moves up the rails. One second after ejection initiation, the attachment harness is released, the separation bladders inflate, and the pilot and seat are separated. The parachute pack opens approximately 2 seconds after ejection and is fully deployed less than 5 seconds after ejection has been initiated.

2. GROUND

Normal ground exit from the cockpit is through the door in the bulkhead aft of the pilot seats and through the cargo compartment exit. In the event of fire or other emergency that prohibits normal exit, the overhead escape panels may be used. A handle adjacent to each panel is pulled to fire the explosive bolts attaching the panel to the airframe. Standing in the seat, the pilot can easily step or crawl out of the aircraft.

E. CRASH PROTECTION

The engines of the D266 are aft of the wings, against the fuselage. They are mounted to the aft spar of the wing and are supported from the upper sides of the fuselage. Engine separation, even during an extremely hard landing, is quite unlikely. The engines are located far aft of the forward entrance door. Clear access to the cabin is thus available even after an engine explosion. The tailpipes are situated aft of the rear door; thus, the hot exhaust gas does not restrict entrance and exit through either the forward-right or the aft-left door.

All fuel is in the two tanks between the wing spars, and it is thus far removed from the cockpit area.

The auxiliary power unit is on the rear right side of the fuselage aft of the engine. Both the intake and the exhaust are well removed from cabin doors, and the location is such that noise or malfunction presents no problem to the crew.

The crew seats in the D266 are designed to withstand higher crash loads than the basic airframe structure, so they provide excellent aircrew crash protection. Both pilots are restrained in the seats by the shoulder harness, inertia takeup reel, and seat belts. Additional restraint is provided by the torso harness. A V-block-type headrest is attached to the seat and positions the head either for an ejection or for a crash.

REFERENCES

1. Brown, E. L., Edenborough, H. K., and Hampton, B. J., Results of Tilting-Rotor Dynamic Stability Model Tests, 599-063-904, Bell Helicopter Company, Fort Worth, Texas, 28 April 1966.
2. D266 Composite Research Aircraft, Test Plans - Follow On, D266-099-114, Bell Helicopter Company, Fort Worth, Texas, May 1966.
3. Ground Loads, ANC-2 Bulletin, Munitions Board Aircraft Committee, Washington, 1952.
4. Structural Design Requirements, Helicopters, MIL-S-8698(ASG), 28 February 1958.
5. Airplane Strength and Rigidity - Reliability Requirements, Repeated Loads and Fatigue, MIL-A-8866(ASG), 18 May 1960.
6. Fatigue Analysis Criteria for Typical Helicopter Dynamic Components, 299-099-076, Bell Helicopter Company, Fort Worth, Texas, 20 November 1957.
7. Hall, W. E., et. al., Rotor/Pylon Stability at High Advance Ratios, 599-063-903, Bell Helicopter Company, Fort Worth, Texas, 17 May 1966.
8. Airplane Strength and Rigidity - Vibration, Flutter, and Divergence, MIL-A-8870(ASG), 18 May 1960.
9. Cox, C. R., Analytical Development of Prop-Rotor Rotational Noise and Initial Parameter Studies, 8036-099-002, Bell Helicopter Company, Fort Worth, Texas, November 1964.
10. Rodden, W. P., Farkas, E. F., and Malcom, H. A., Flutter and Vibration Analysis by a Collocation Method: Analytical Development and Computational Procedure, TDR-169(3230-11) TN-14, Aerospace Corporation, Los Angeles, 31 July 1963.
11. Rodden, W. P., Farkas, E. F., and Malcom, H. A., Aerodynamic Influence Coefficients From Incompressible STRIP Theory, Analytical Development and Computational Procedure, TDR-169(3230-11) TN-5, Aerospace Corporation, Los Angeles, 3 September 1962.
12. D266 Composite Research Aircraft, Results of Analytical Studies, D266-099-110, Bell Helicopter Company, Fort Worth, Texas, May 1966.
13. Hall, W. E., "Prop-Rotor Stability at High Advance Ratios", Journal of the American Helicopter Society, April 1966.

14. Lynn, R. R., and Hall, W. E., Prop-Rotor Stability at High Advance Ratios - Analysis and Correlation, Bell Helicopter Company Report No. 599-063-903.
15. Hohenemser, K. H., "On a Type of Low-Advance-Ratio Blade Flapping Instability of Three or More Bladed Rotors Without Drag Hinges", Proceedings, Thirteenth National Forum, American Helicopter Society, May 1957.
16. Red, J. A., and Gean, J. A., Results of the Direct Analog Flutter Analysis of the XH-40 Three Bladed Rotor System, 204-099-662, Bell Helicopter Company, Fort Worth, Texas, 12 January 1959.
17. Hohenemser, K. H., and Perisho, C. H., Analysis of the Vertical Flight Dynamic Characteristics of the Rotor with Floating Hub and Off-Set Coning Hinges, Preprint 820, Institute of the Aeronautical Sciences, January 1958.
18. Hopton-Jones, F. C., A Practical Approach to the Problem of Structural Weight Estimation for Preliminary Design, Technical Paper 127, Society of Aeronautical Weight Engineers, May 1955.
19. Fuselage Weight Estimation by the Weight Penalty Evaluation Method, 10043, Chance Vought Aircraft Corporation, Dallas, Texas, 22 November 1955.
20. Helicopter Transmission Survey, BE83-12, General Tire and Rubber Company, Akron, Ohio, December 1953.
21. Abbott, I. H., von Doenhoff, A. E., and Stivers, L. S., Summary of Airfoil Data, TR 824, National Advisory Committee for Aeronautics, Washington, 1945.
22. Determination of Performance Parameters, TDR 02-981-009, Bell Aircraft Company, Buffalo, N. Y., February 1950.
23. Brown, E. L., and Red, J. A., Results of the Wind Tunnel Tests of the Quarter-Scale Semi-Span Model of the Bell XV-3 Tilting-Rotor Convertiplane, 200-094-270, Bell Helicopter Company, Fort Worth, Texas, 16 August 1958.
24. Curry, P. R., and Matthews, J. T., Suggested Requirements for V/STOL Flying Qualities, Technical Report 65-45, RTM 37, U. S. Army Aviation Materiel Laboratories, Fort Eustis, Virginia, June 1965.
25. Recommendations for V/STOL Handling Qualities, Report 408, NATO Advisory Group for Aeronautical Research and Development, Paris, October 1962.

26. Helicopter Flying and Ground Handling Qualities, General Requirements For, MIL-H-8501A, Amendment 1, 3 April 1962.
27. Flying Qualities for Piloted Airplanes, MIL-F-8785(ASG), Amendment 4, 17 April 1959.
28. Salmirs, S., and Tapscott, R. J., The Effects of Various Combinations of Damping and Control Power on Helicopter Handling Qualities During Both Instrument and Visual Flight, TND-58, National Aeronautics and Space Administration, Washington, October 1959.
29. Amer, K. B., and Gustafson, F. B., Charts for Estimation of Longitudinal-Stability Derivatives for a Helicopter Rotor in Forward Flight, TN-2309, National Aeronautics and Space Administration, Washington, March 1951.
30. Deckert, W. H., and Ferry, R. G., Limited Flight Evaluation of the XV-3 Aircraft, TR-60-4, U. S. Air Force Flight Test Center, Edwards AFB, California, May 1960.
31. Longhurst, W. S., A Report on Stability and Control Testing of a Tilt Wing V/STOL Aircraft, 660315, Society of Automotive Engineers, April 1966.
32. Simulation of Helicopter and V/STOL Aircraft, Volume 1, "Helicopter Analysis Report", NAVTRADEVCEEN 1205-1, U. S. Naval Training Device Center, Port Washington, N. Y., 1962.
33. Toll, T. A., Summary of Lateral-Control Research, TN-1245, National Advisory Committee for Aeronautics, Washington, March 1947.
34. Perkins, C. D., and Hage, R. E., Airplane Performance Stability and Control, Wiley and Sons, New York, 1949.
35. Etkin, P., Dynamics of Flight, Wiley and Sons, New York, 1959.

APPENDIX, DRAWINGS

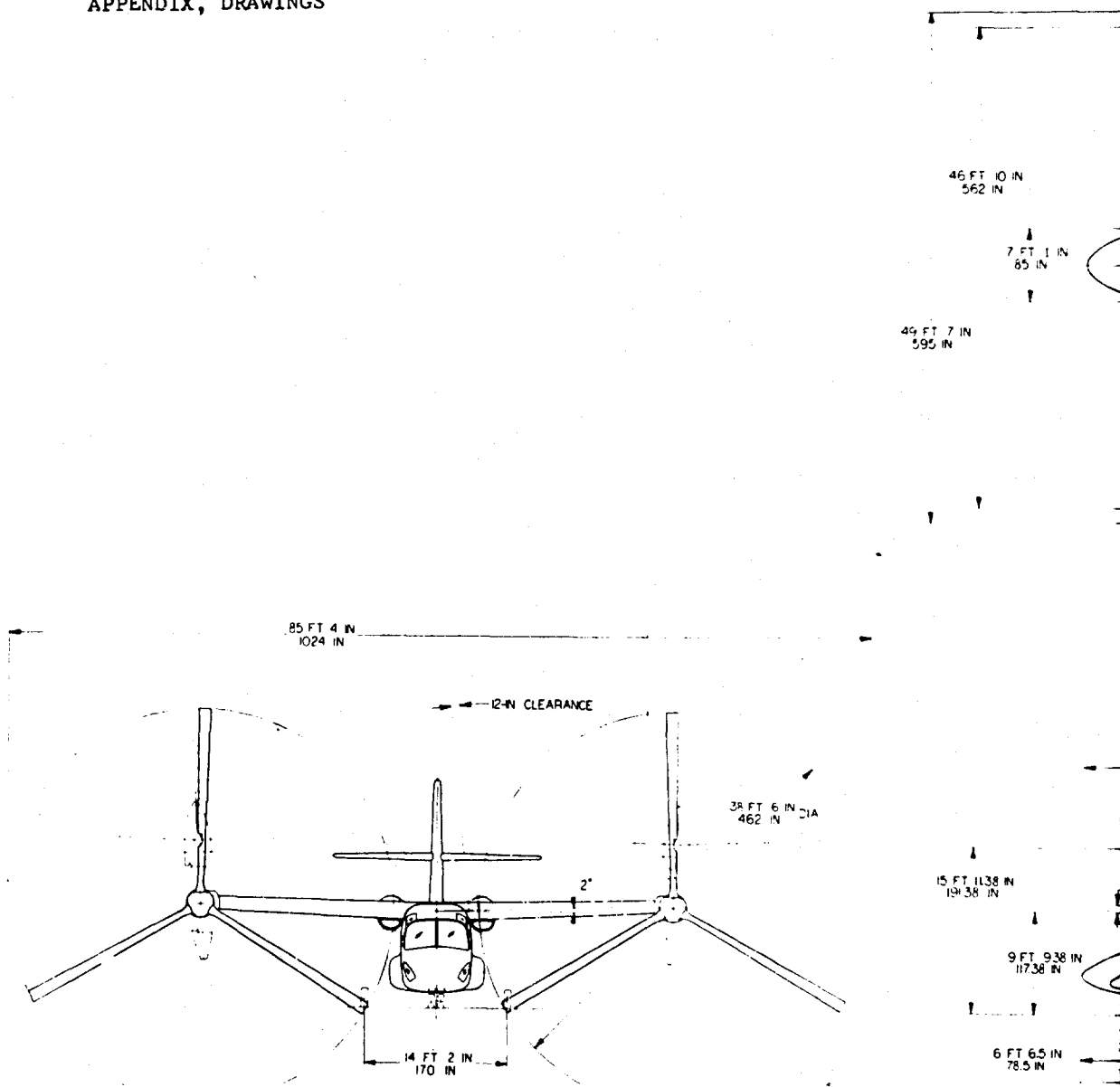
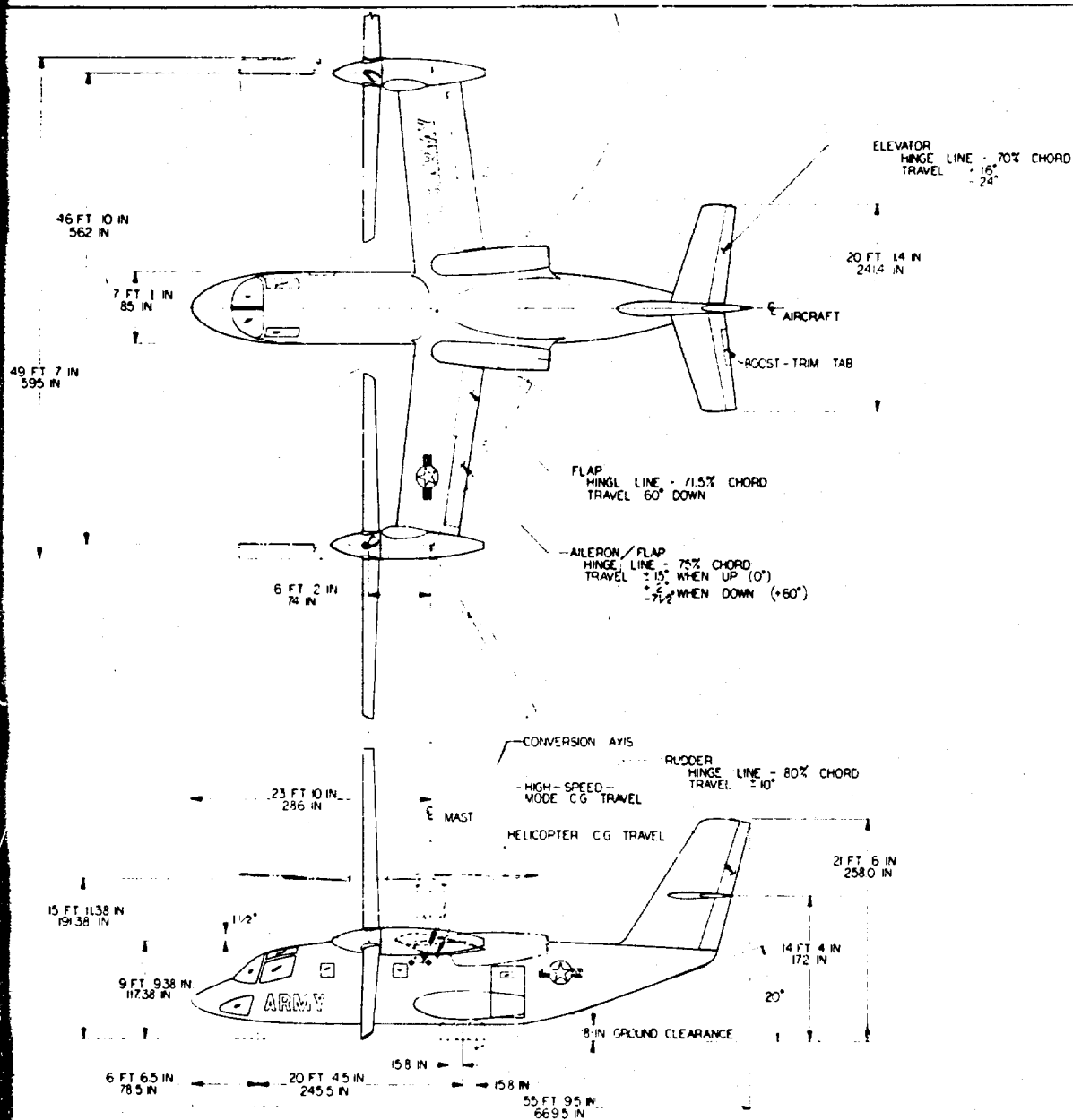


Figure 251. General Arrangement.



CHARACTERISTICS

WEIGHTS

DESIGN WEIGHT
OIL AND CREW
FUEL
PAYLOAD
GROWTH

POWER PLANT

MANUFACTURE
NORMAL
MILITARY
POWER

ROTOR

DIAMETER
NUMBER
DISC AREA
BLADE AREA
DISC LOAD
BLADE AREA

BLADE CHORD
SOLIDITY
BLADE TIP SPEED

WING

SPAN
AREA
WING LOADING
ASPECT RATIO
MEAN AIRFOIL

FLAP AREA
AILERON AREA

EMPELLAGE
HORIZONTAL

ELEVATOR
VERTICAL

RUDDER

B

CHARACTERISTICS:

WEIGHTS

DESIGN GROSS WEIGHT	23,000	LB
WEIGHT EMPTY	15,994	LB
OIL AND TRAPPED FUEL	166	LB
CREW	400	LB
FUEL	3,000	LB
PAYLOAD	3,000	LB
GROWTH POTENTIAL	440	LB

POWER PLANT

MANUFACTURER AND MODEL (2) -	GENERAL ELECTRIC	T64-GE-12	
NORMAL RATED POWER (2 x 3230)		6460	HP
MILITARY RATED POWER (2 x 3435)		6870	HP
POWER LOADING (MILITARY POWER)		3.35	LB/HP

ROTOR

DIAMETER	38.5	FT
NUMBER OF BLADES/ROTOR	3	
DISC AREA/ROTOR	1,164	SQ FT
BLADE AREA/ROTOR	96	SQ FT
DISC LOADING (DESIGN GROSS WEIGHT)	9.8P	LB/SQ FT
BLADE AIRFOIL	THEORETICAL ROOT, ξ	NACA 644030
	TIP	NACA 64A206, $\Delta : 3$
BLADE CHORD	20	IN
SOLIDITY	0.825	
BLADE TWIST (ξ TO TIP)	43 1/2	DEG
TIP SPEED	750-825	FT/SEC
	400-600	FT/SEC
	HELICOPTER MODE	
	HIGH SPEED MODE	

WING

SPAN	49.6	FT
AREA	330.5	SQ FT
WING LOADING	70	LB/SQ FT
ASPECT RATIO	7.44	
MEAN AERO DYNAMIC CHORD (AT BL M41)	80.2	IN
AIRFOIL	THEORETICAL ROOT (BL 0)	NACA 64A423 MODIFIED
	THEORETICAL TIP (BL 297.5)	NACA 64A419 MODIFIED
FLAP AREA (ONE SIDE)	13.75	SQ FT
AILERON AREA (ONE SIDE)	13.82	SQ FT

EMPENNAGE

HORIZONTAL TAIL	AREA	90	SQ FT
	ASPECT RATIO	4.5	
	AIRFOIL	NACA 64A012	
ELEVATOR AREA		25	SQ FT
VERTICAL TAIL	AREA	100	SQ FT
	ASPECT RATIO	1.73	
	AIRFOIL	NACA 64A015	
	ROOT	NACA 64A009	
	TIP	18	SQ FT
RUDDER AREA			

ELEVATOR
HINGE LINE - 70% CHORD
TRAVEL - 16"
24"

20 FT 14 IN
24 4 IN

RAFT

M TAB

CHORD

2 FT 6 IN
258.0 IN

4 IN

C

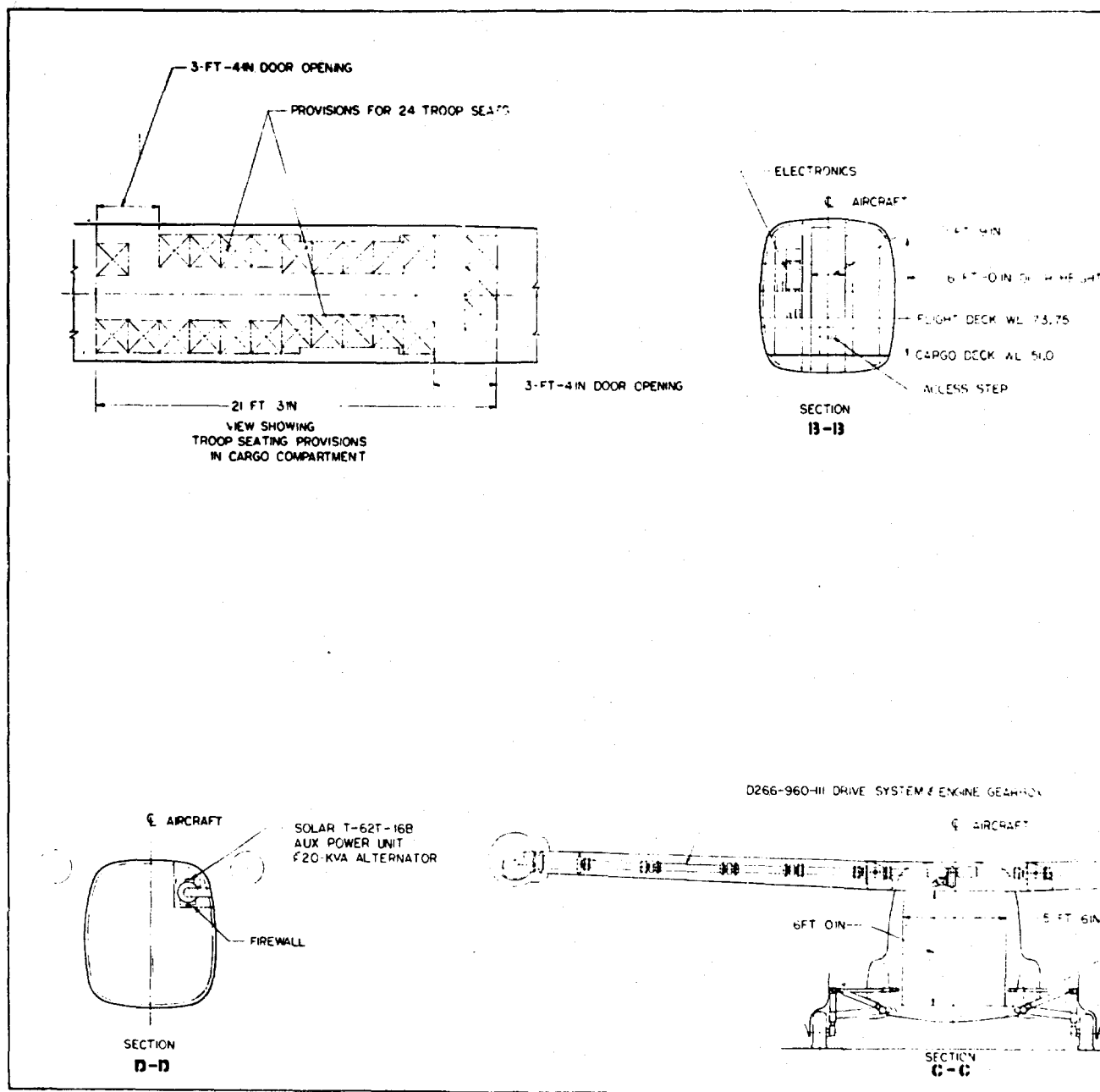
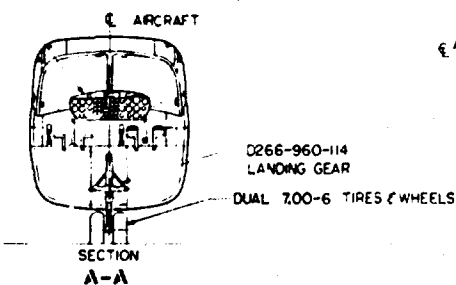


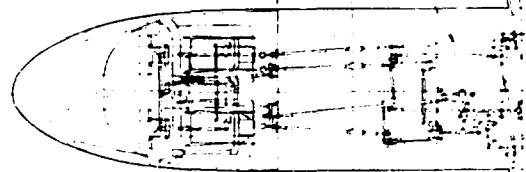
Figure 252. Inboard Profile.

D266-960-115 COCKPIT ARRANGEMENT



D266-960-106 FIXED CONTROLS FUSELAGE

DOOR OPENING 3 FT 4 IN



D266-960-112 FUSELAGE & ENGINE

D266-960-116 CONVERSION SYSTEM
D266-960-105 ROTATING CONTROLS

PYLON SHOWN IN HIGH-SPEED FLIGHT POSITION

EJECTION SEATS

SYSTEM & ENGINE GEARBOX

AIRCRAFT

WL 140.38
CONVERSION AXIS

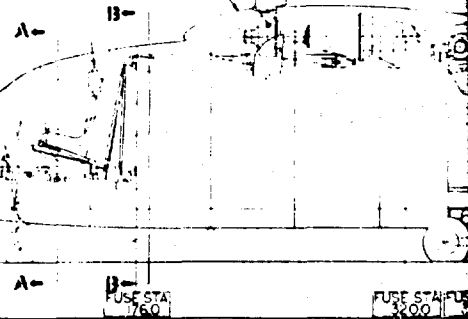
5 FT 6 IN

D266-960-114 LANDING GEAR

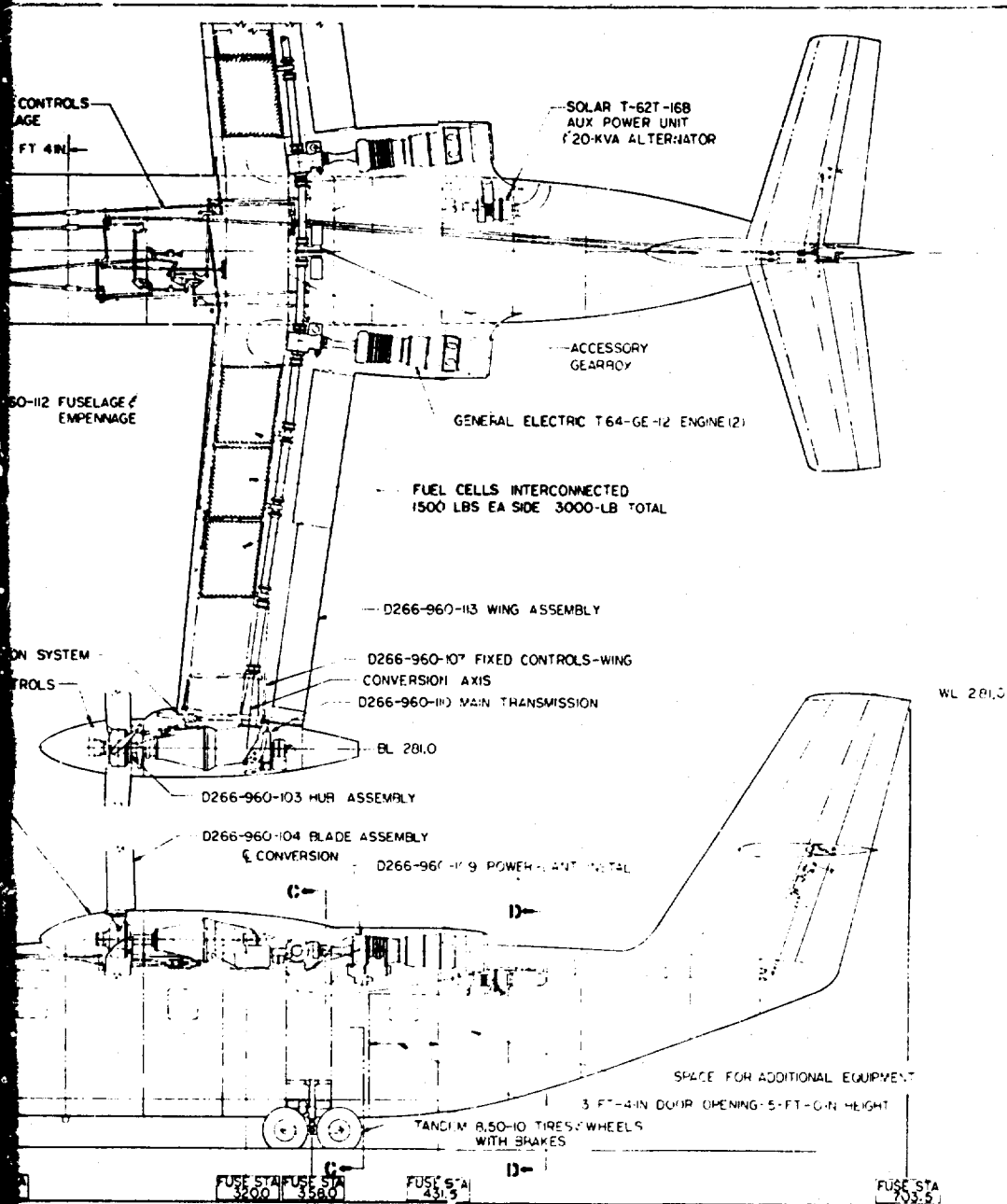
CARGO DECK WL 51.0

GROUND LINE WL 23

SECTION C-C



B



C

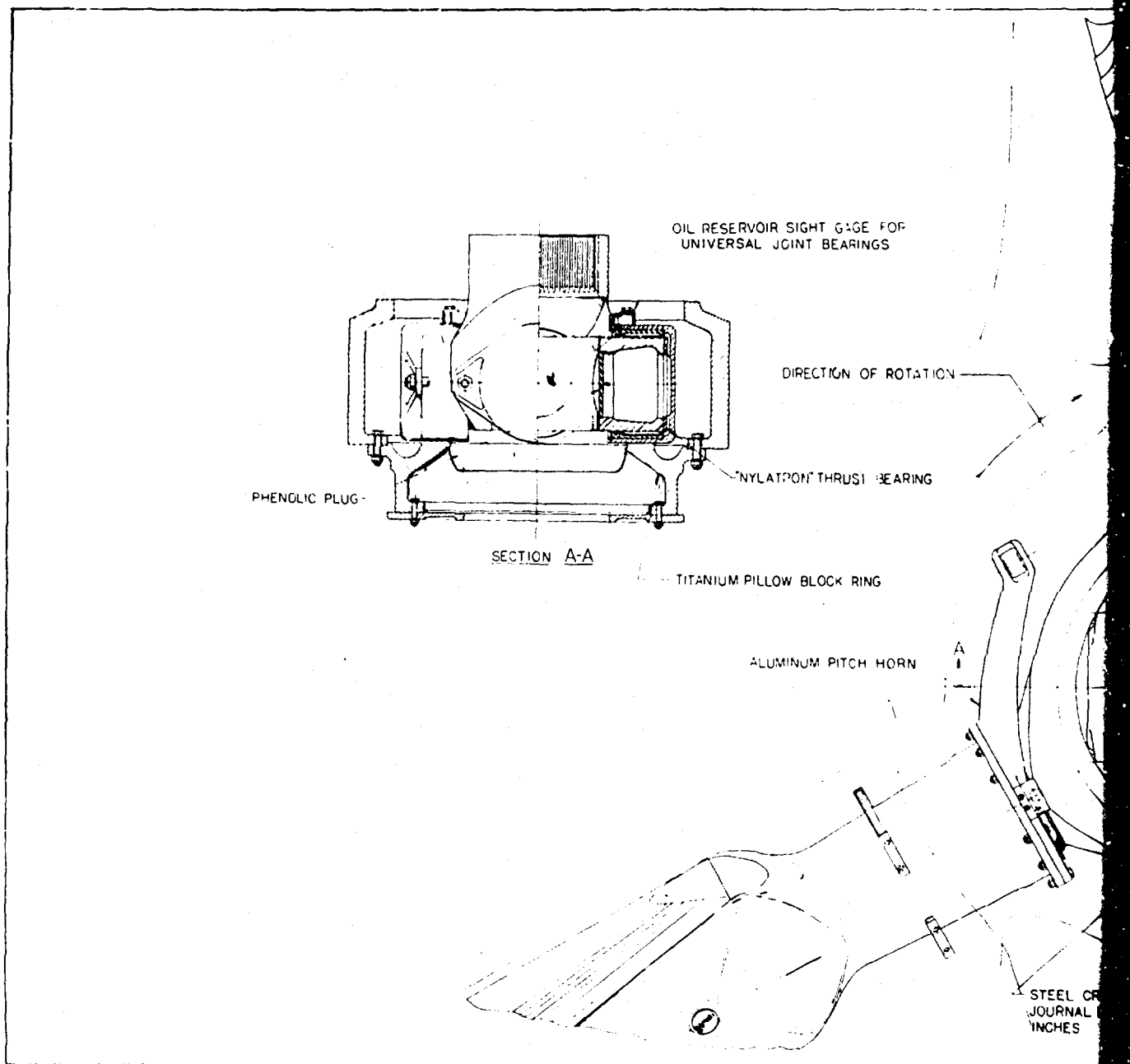


Figure 253. Hub Assembly.

22-50-260-104
ALUMINUM BLADE GRIP
INTEGRAL WITH BLADE

FAIRING SUPPORT BONDED
TO BLADE GRIP

UNIVERSAL JOINT NEEDLE
BEARING-SEPARATOR TYPE

ALUMINUM BEARING HOUSING

PROTECTIVE BOOT

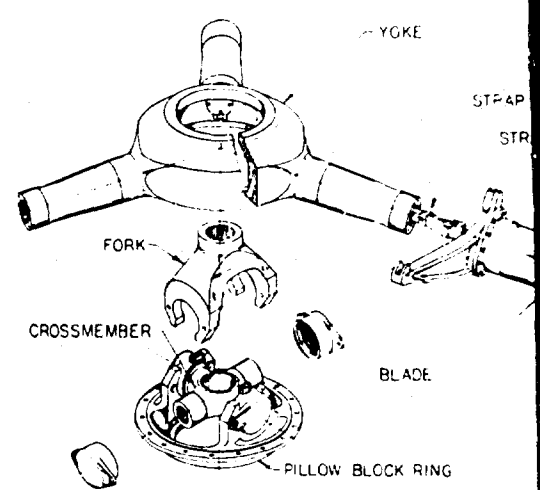
PITCH-CHANGE BEARINGS NEEDLE-
TYPE SPACER

TEFLON AND O-RING SEAL-TYPE

STEEL CROSSMEMBER-
JOURNAL DIAMETER: 5.000
INCHES

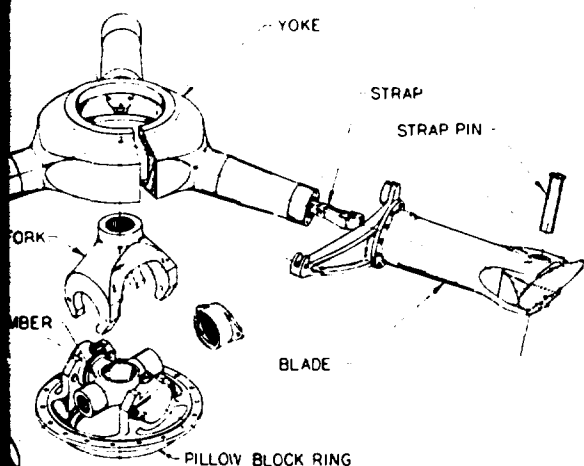
STEEL RETENTION
STRAP FITTING

LEFT-HAND ROTOR SHOWN
RIGHT HAND OPPOSITE



EXPLODED VIEW OF ROTOR
NO SCALE

B



EXPLODED VIEW OF ROTOR
NO SCALE

CHANGE BEARING'S NEEDLE
PULLER

TEFLON AND O-RING SEAL-TYP

BLADE-ROOT CUFF-REF
HELICOPTER RANGE -
HIGH-SPEED RANGE---

SPINDLE ROOT DIAMETER: 5.500 IN

OIL RESERVOIR SIGHT GAGE
PITCH-CHANGE BEARINGS

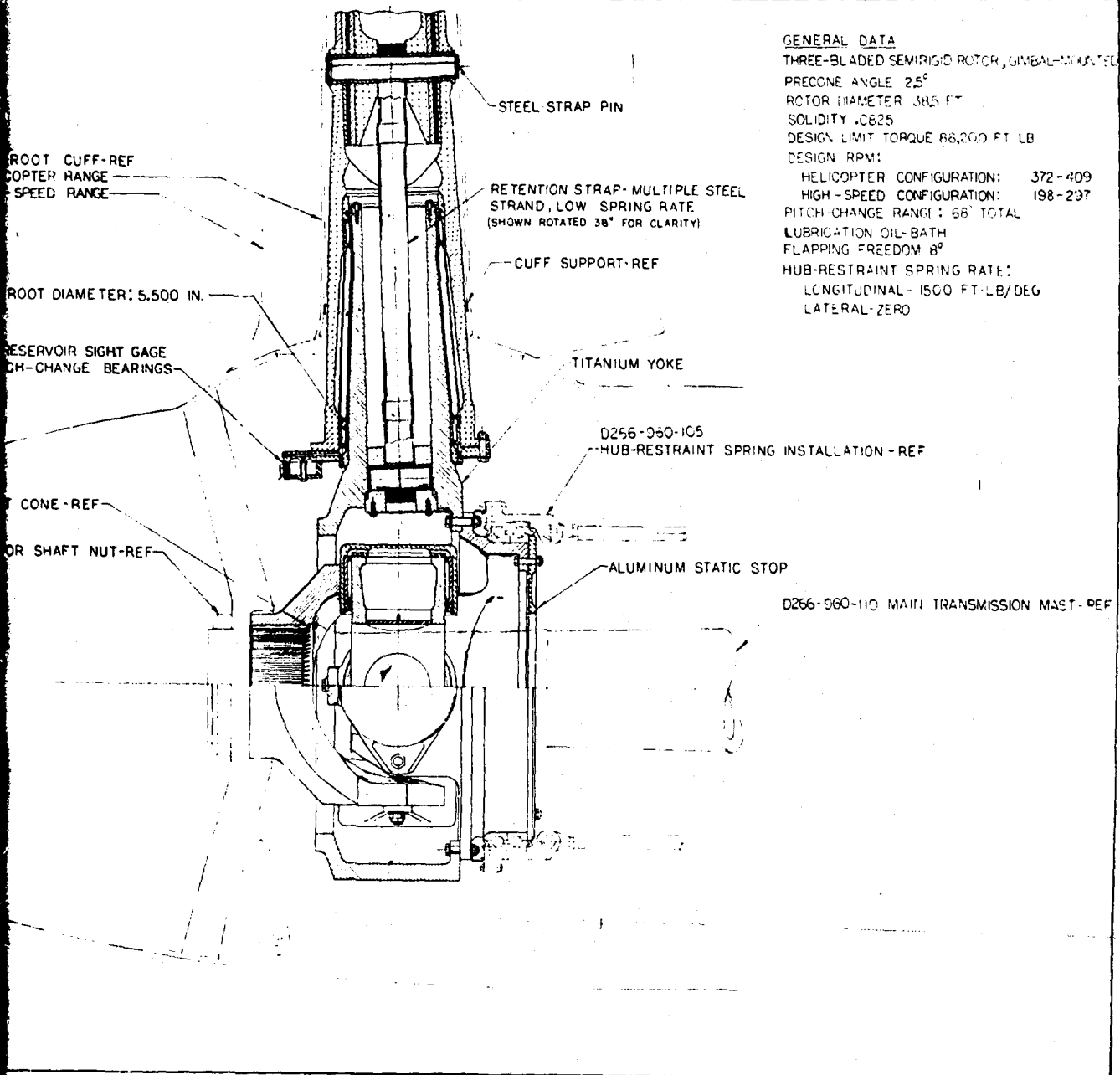
SPLIT CONE-REF

ROTOR SHAFT NUT REF

MAST

SPINNER-REF

c



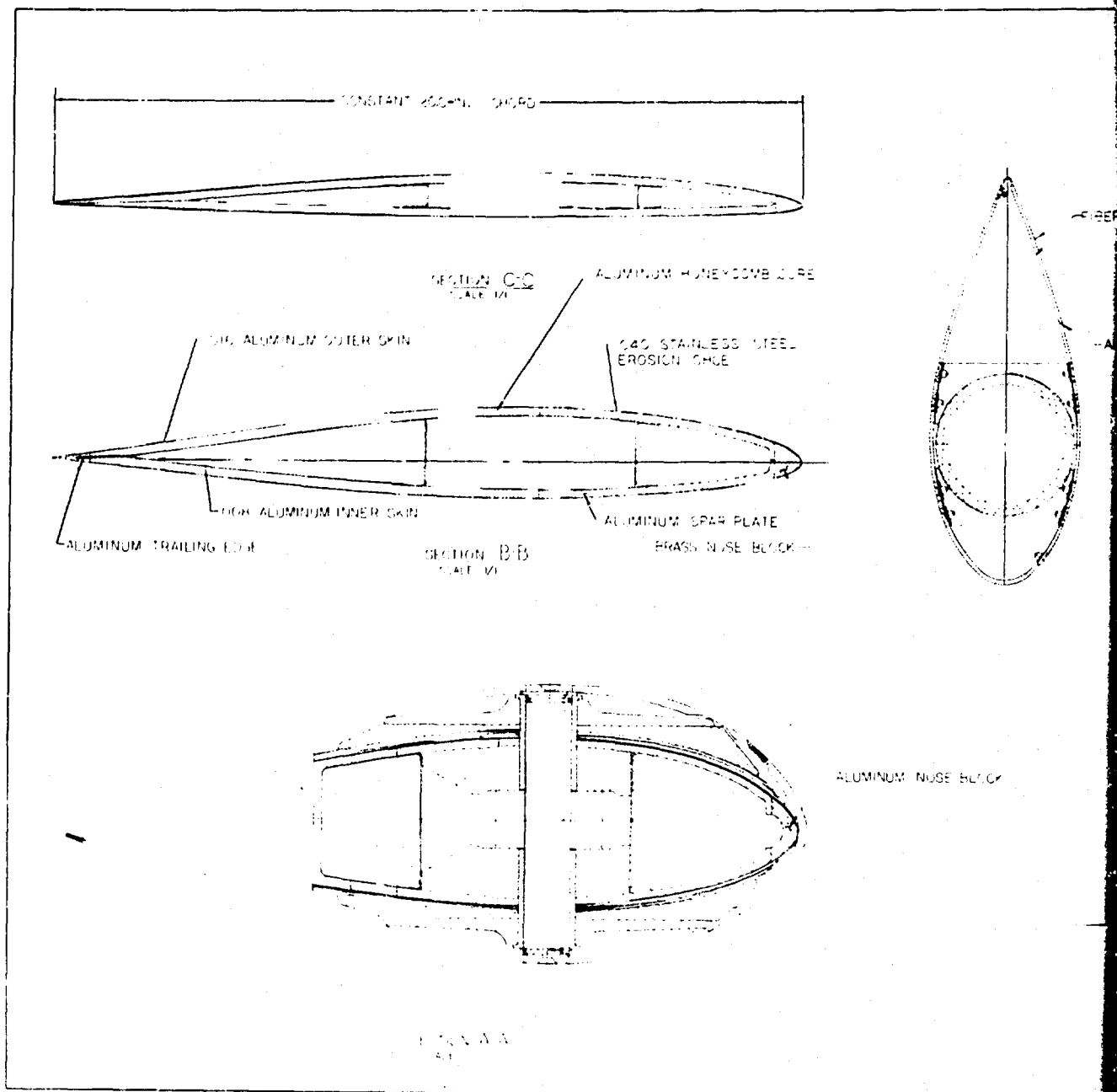
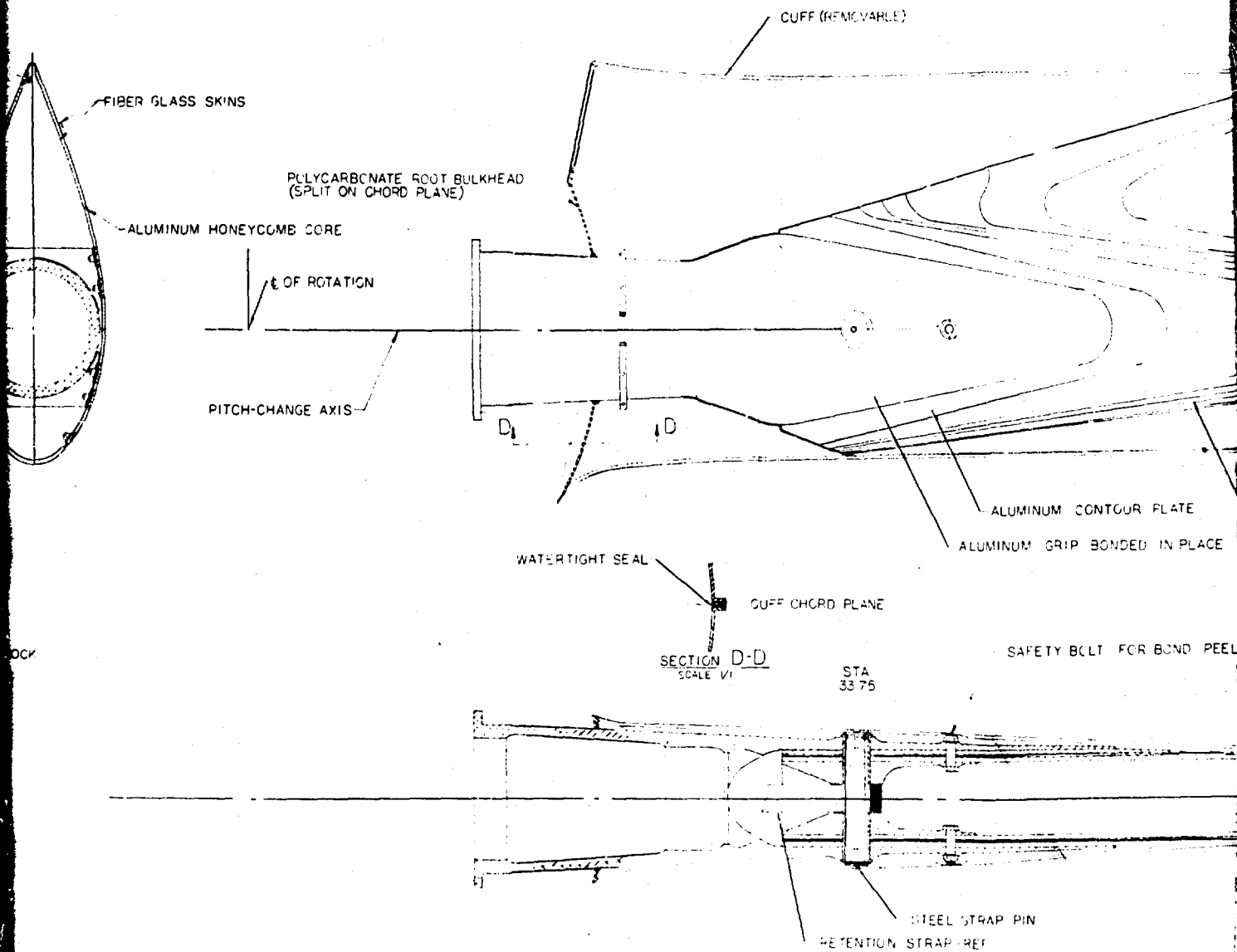
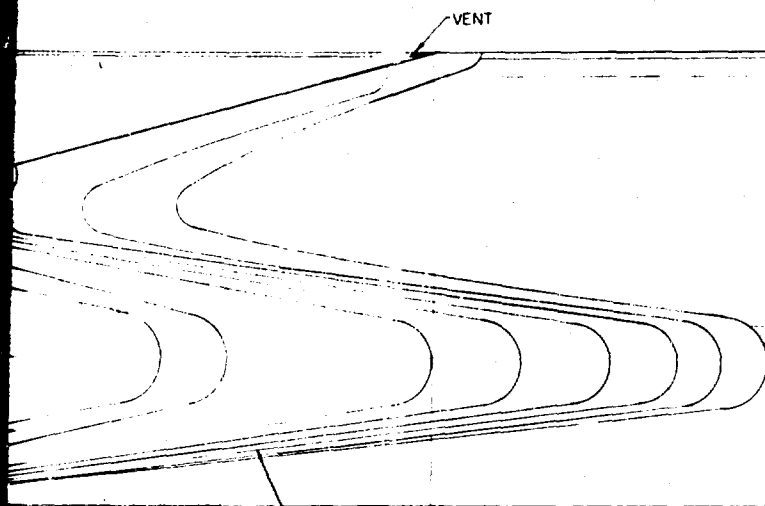


Figure 254. Blade Assembly.



B



VENT

FAIRED WITH SYNTACTIC FOAM

ALUMINUM CONTOUR PLATE

SHEET ALUMINUM DOUBLERS

MINUM GRIP BONDED IN PLACE

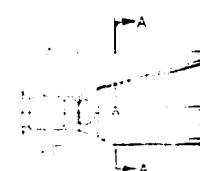
SAFETY BOLT FOR BOND PEEL PREVENTION

OF ROTATION

PITCH-CHANGE AXIS

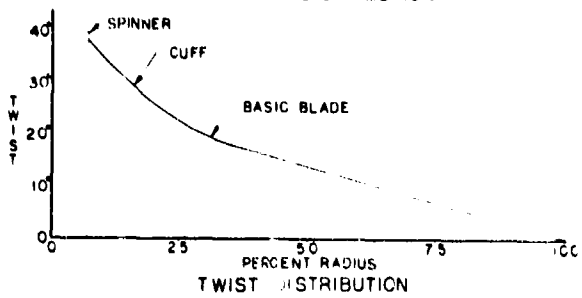
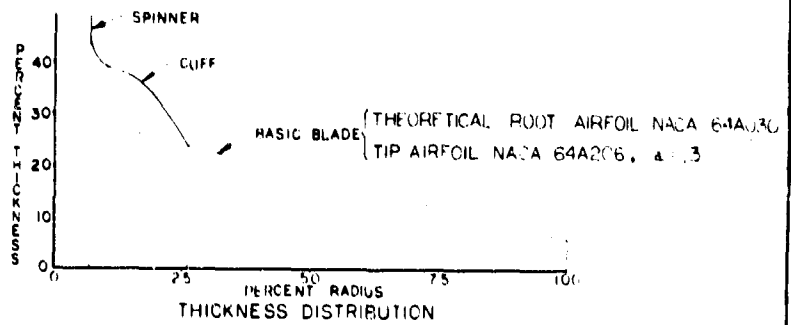
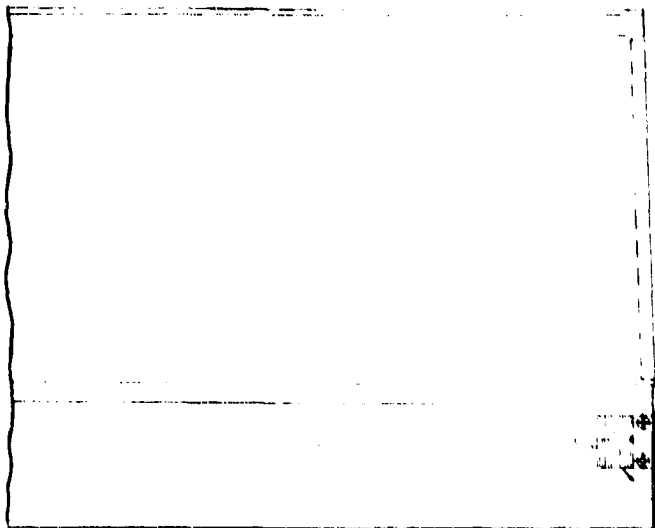
STA
00

STA
33.75

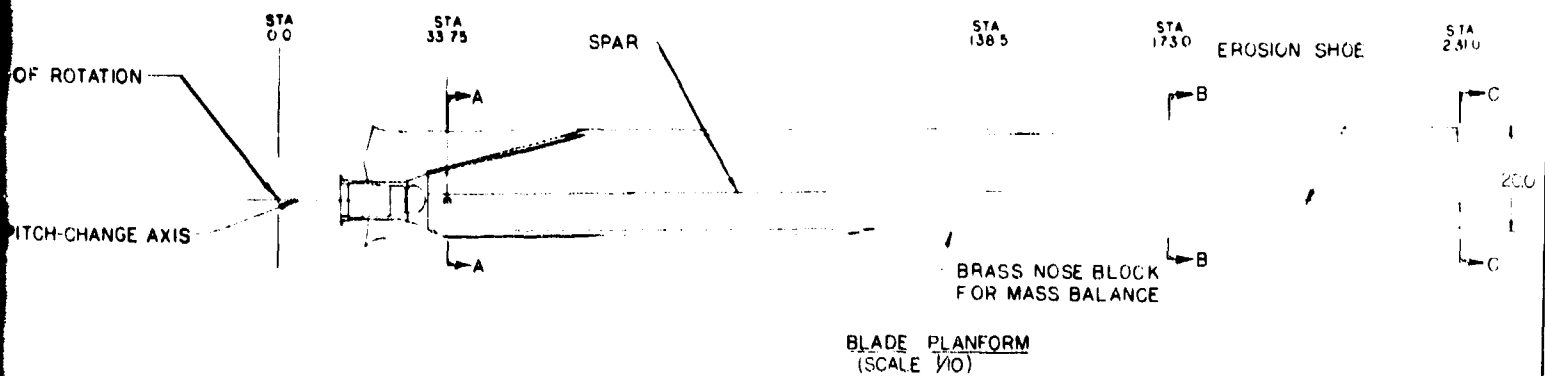


AP PIN

e



SPAN BALANCE WEIGHTS



D

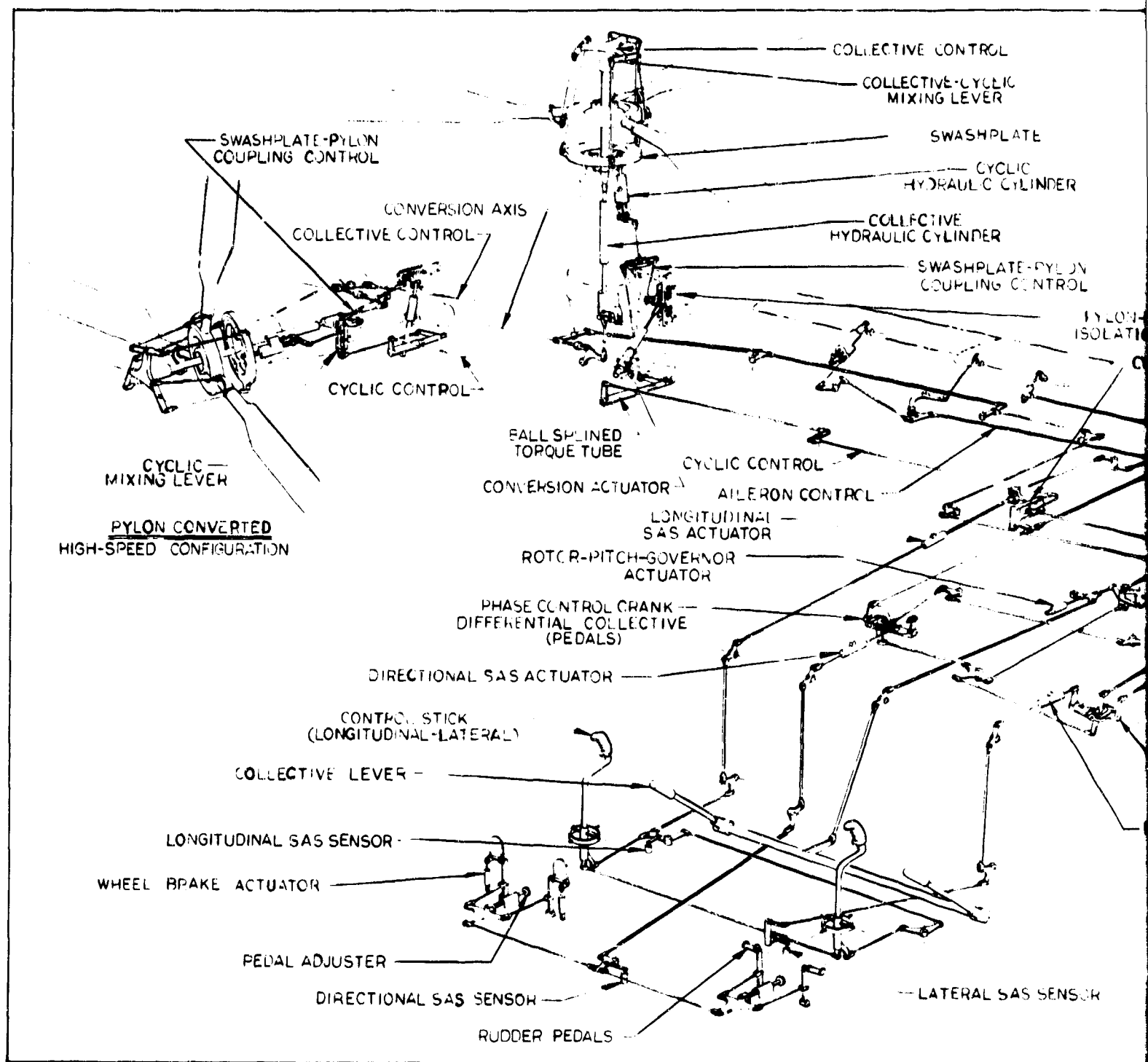


Figure 255. Control System Schematic.

VE CONTROL

LECTIVE-CYCLIC
MIXING LEVER

SWASHPLATE

CYCLIC
HYDRAULIC CYLINDER

LECTIVE
CYCLIC CYLINDER

SWASHPLATE-PYLON
COUPLING CONTROL

PYLON-PITCH-
ISOLATION MOUNT

CYCLIC-DIFFERENTIAL CYCLIC
MIXING LEVER

CONTROL PHASING
ACTUATOR

COLLECTIVE-
DIFFERENTIAL-COLLECTIVE
MIXING LEVER

FLAP-AILERON
INTERCONNECT

FLAP ACTUATOR

PHASE CONTROL CRANK
COLLECTIVE RANGE SHIFT

ROTOR-
TRIM ACTUATOR

DIFFERENTIAL COLLECTIVE
MIXING LEVER
(PEDALS/LATERAL STICK)

PHASE CONTROL CRANK
(LATERAL STICK)

LATERAL SAS ACTUATOR

FLAP-AILERON
MIXING LEVER

AILERON
HYDRAULIC CYLINDER

CONVERS

CONVERSION ACTUATOR
INTERCONNECT

COLLECTIVE CONTROL

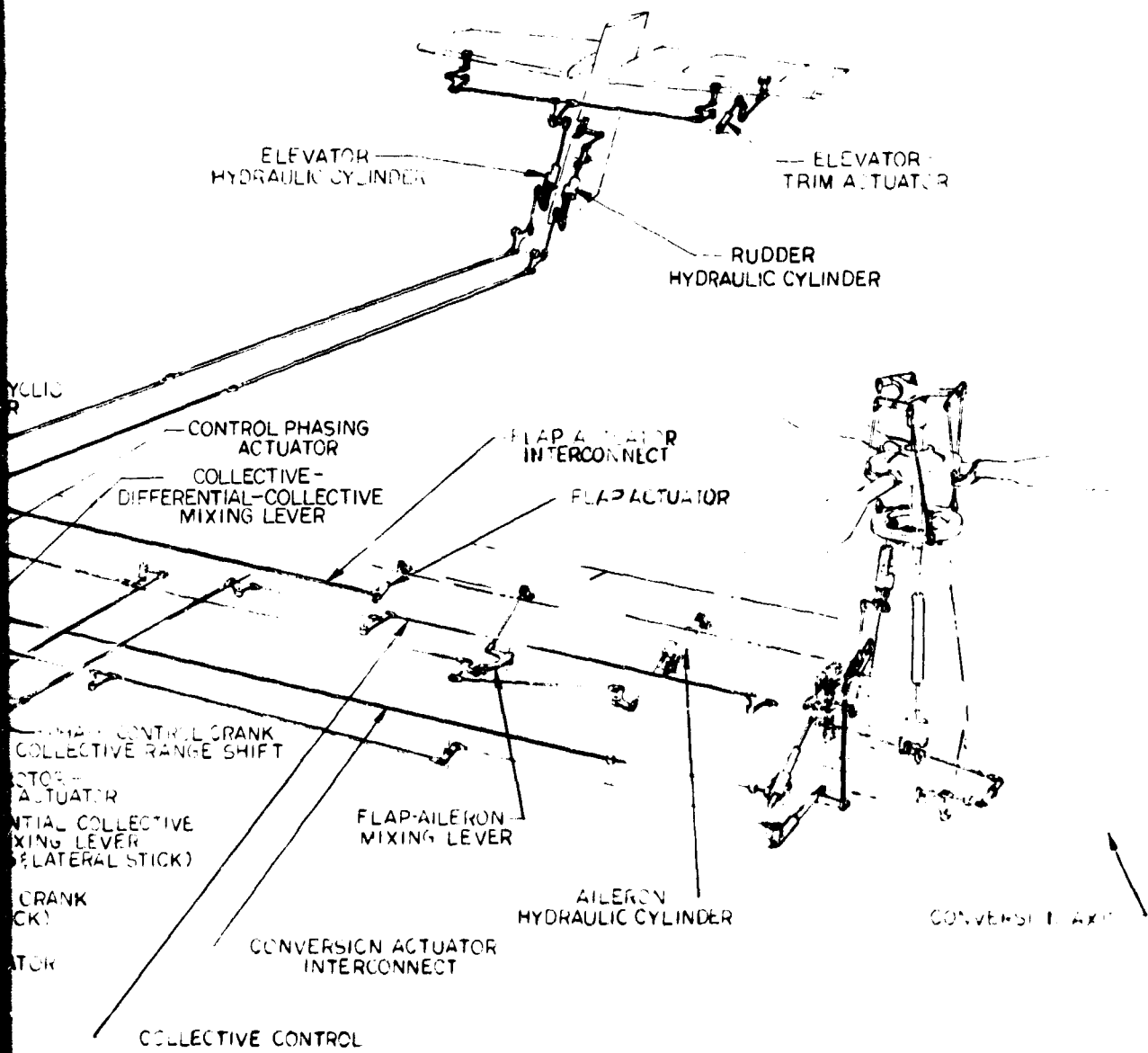
LATERAL SAS SENSOR

ELEVATOR
HYDRAULIC CYLINDER

ELEVATOR
TRIM ACTUATOR

RUDDER
HYDRAULIC CYLINDER

B



C

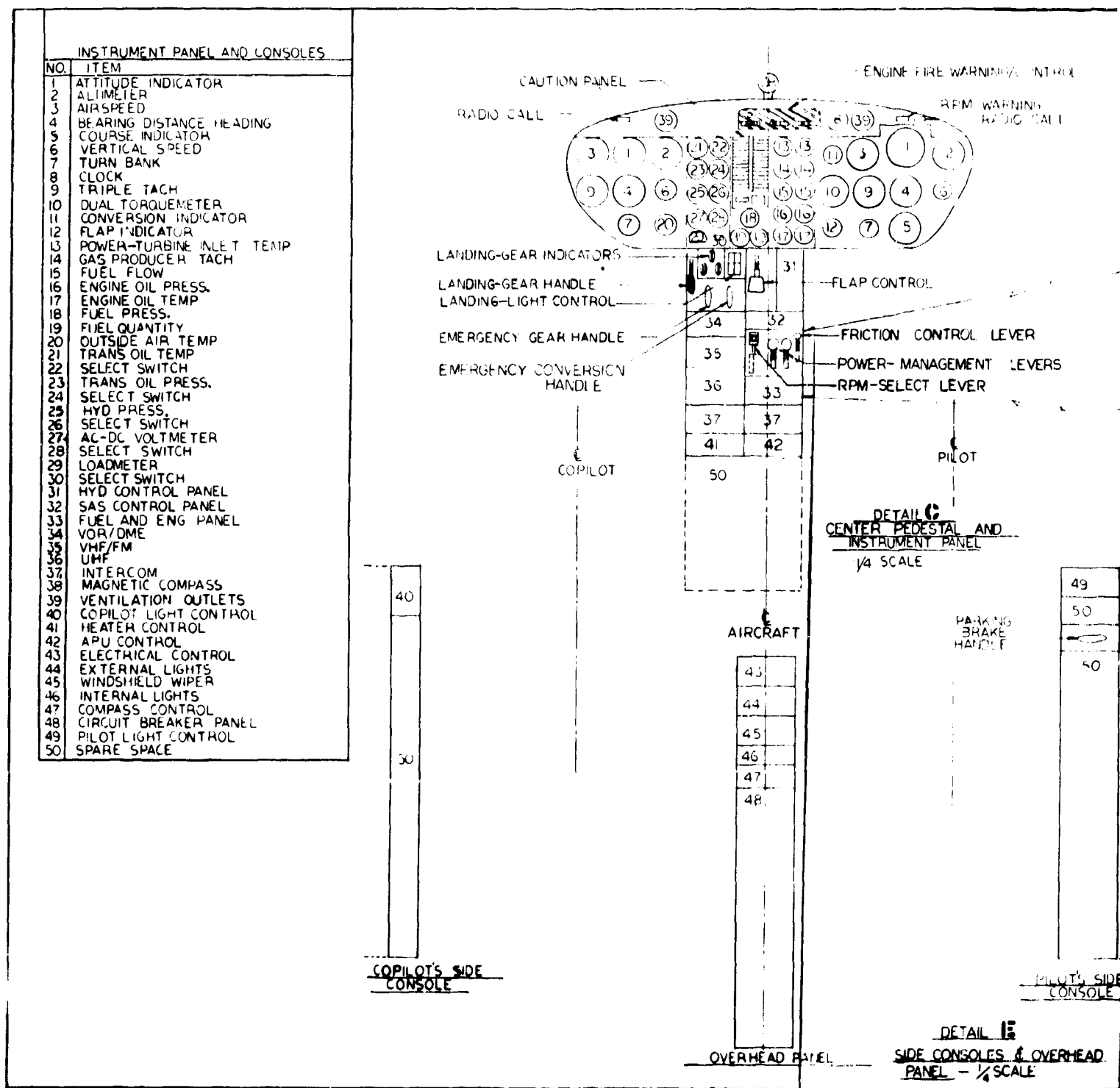


Figure 256. Cockpit Arrangement.

ENGINE FIRE WARNING CONTROL

RPM WARNING
RADIO CALL



CONTROL

ENGINE CONTROL LEVER

ENGINE MANAGEMENT LEVERS
ENGINE SELECT LEVER

PILOT

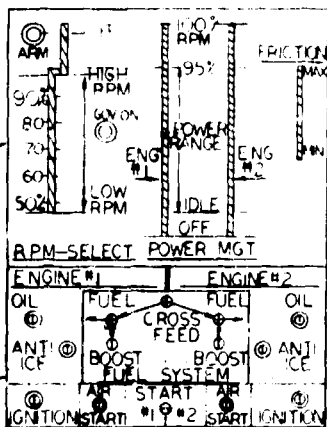
TAIL C
PEDESTAL AND
INSTRUMENT PANEL
SCALE

PARKING
BRAKE
HANDLE

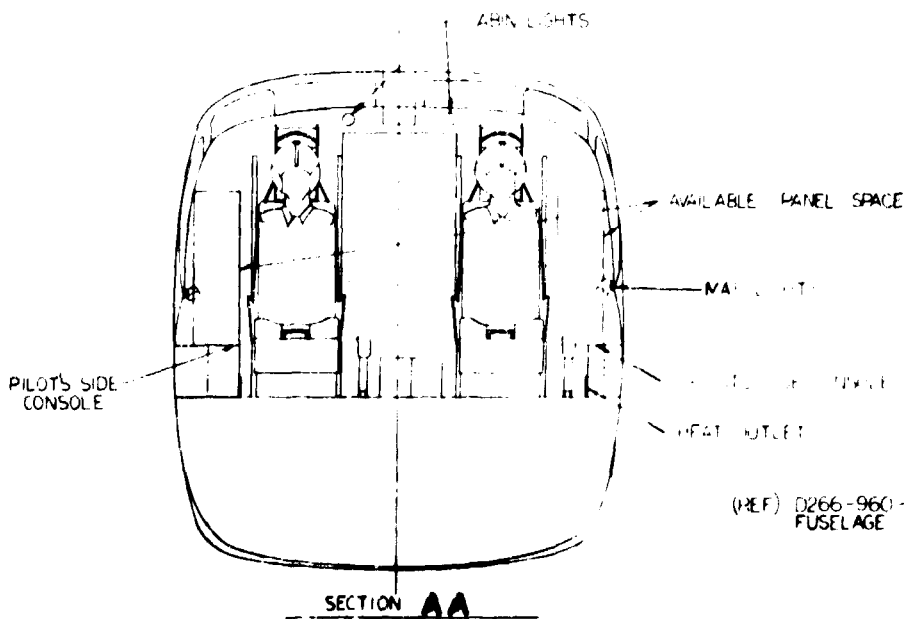


PILOT'S SIDE
CONSOLE

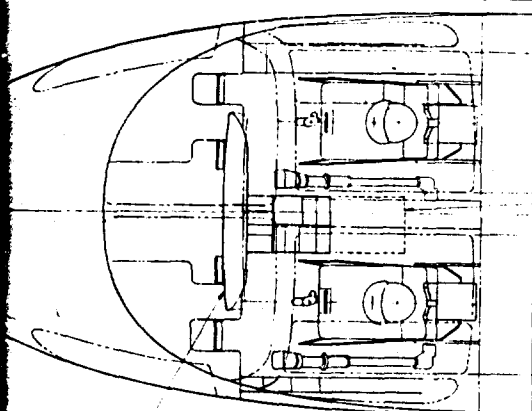
DETAIL 15
SIDE CONSOLES & OVERHEAD
PANEL - 1/4 SCALE



DETAIL 12
FUEL AND ENGINE PANEL
FULL SCALE



B



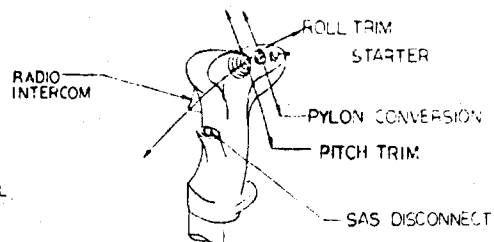
INSTRUMENT PANEL
AND GLARE SHIELD

30 IN.

CENTER PEDESTAL

EJECTION
ENVELOPE

30 IN.



DETAIL A
CONTROL-STICK GRIPS

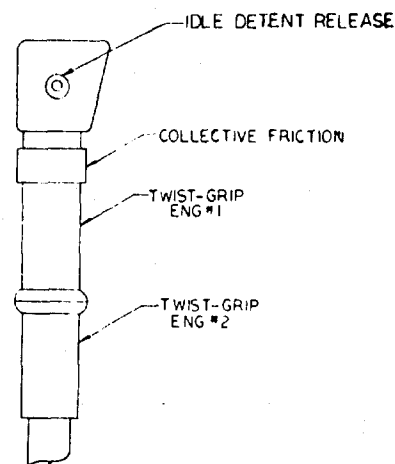
30-IN.
EJECTION
ENVELOPE

OVERHEAD PANEL

EJECTION SEATS - (DOUGLAS AIRCRAFT CO.)
ESCAPAC 1-C-2

(REF) D266-960-106
FIXED CONTROLS - FUSE.

DEFROSTING
NOZZLES



DETAIL B
PILOTS COLLECTIVE LEVER

2

Unclassified
Security Classification

DOCUMENT CONTROL DATA - R & D		
UNCLASSIFIED SECURITY CLASSIFICATION		
Bell Helicopter Company Fort Worth, Texas		Unclassified DA 44-177
TILT PROP-ROTOR COMPOSITE RESEARCH AIRCRAFT		
Final Technical Report		
Kenneth G. Wernicke		
REPORT DATE November 1968	DA FORM NO. 10-1 466	DA FORM NO. 10-1 33
DA CONTRACT NUMBER DA 44-177-AMC-373(T)	DA CONTRACT NUMBER USAAVLANS Technical Report 68-32	
PROJECT NO. Task 1F163204D15704	DA FORM NO. 10-1 D466-099-101 through 110	
This document has been approved for public release and sale; its distribution is unlimited.		
US Army Aviation Materiel Laboratories Fort Eustis, Virginia		
<p>A preliminary design study for a composite research aircraft has been conducted in accordance with Contract DA 44-177-AMC-373(T). The primary objectives were to define the optimum design and to prepare a program for the follow-on development of a VTOL rotary-wing composite research aircraft embodying the low disc loading and low-speed maneuverability of the helicopter and the high speed and lift/drag ratios of fixed-wing aircraft. The D466 Composite Research Aircraft design that has resulted is based on the demonstrated and proved tilting-rotor concept.</p> <p>Design gross weight of the D466 is 23,000 pounds. Power is provided by two General Electric T64-GE-12 free-turbine engines. Design complexity is no greater than that of a twin-engine dual-rotor helicopter. All flight procedures are simple and straightforward and may be performed by one pilot. The cargo compartment, which exceeds the requirements, provides space for 24 troops.</p>		

DD FORM 1473 1 NOV 68

Unclassified
Security Classification

Unclassified
Security Classification

16. KEY WORDS	LINE A		LINE B		LINE C	
	ROLE	WT	ROLE	WT	ROLE	WT
Tilt Prop-Rotor VTOL Aircraft Composite Research Aircraft (CRA)						

Unclassified
Security Classification

11960-68